THE ROLE OF NON-CODING RNAs IN GASTROINTESTINAL CANCERS, 3rd Edition

EDITED BY: Kanjoormana Aryan Manu, Divya P. Kumar and Muzafar Ahmad Macha

PUBLISHED IN: Frontiers in Oncology

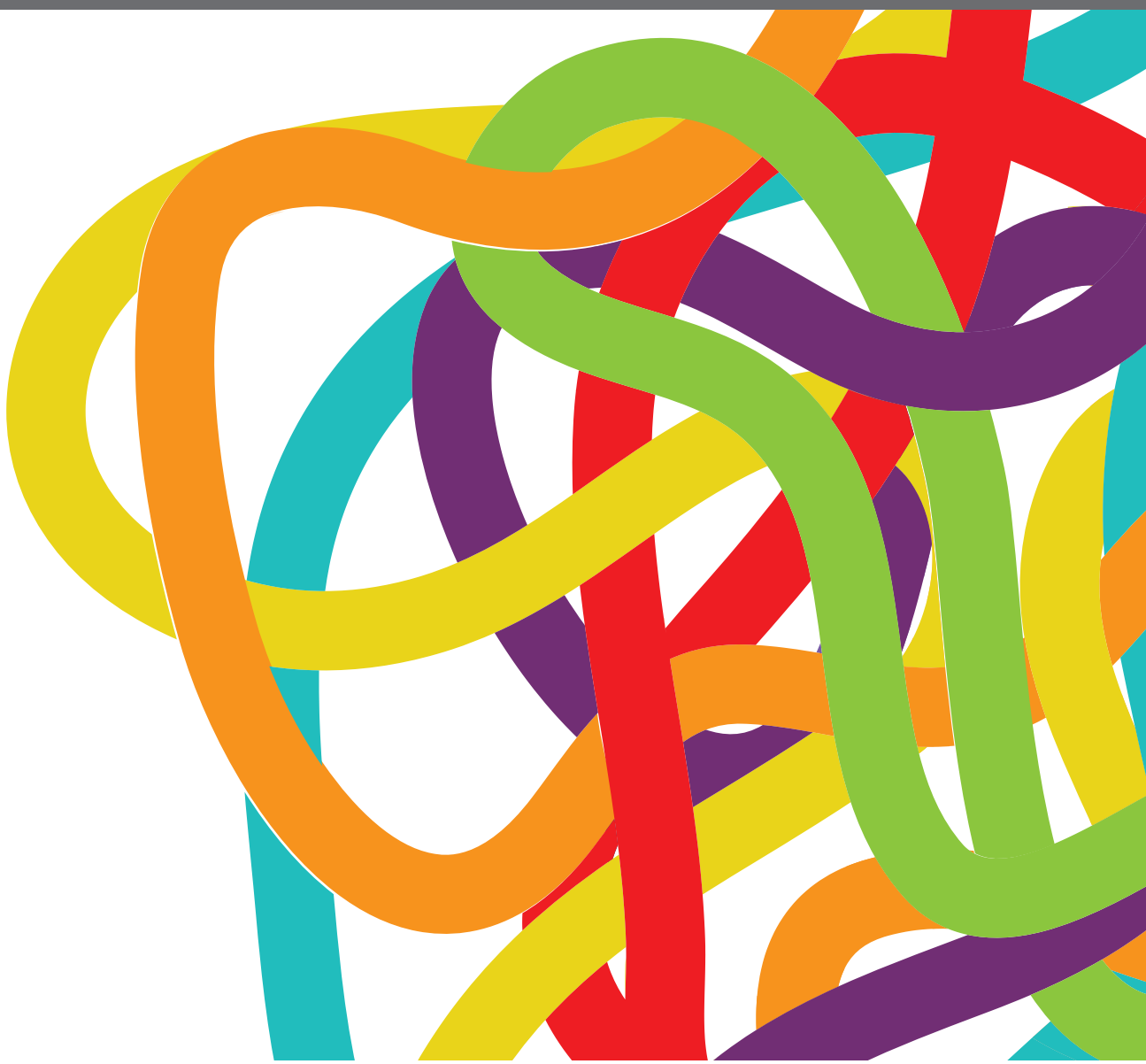

frontiers Research Topics

ISSN 1664-8714
ISBN 978-2-8325-4614-7
DOI 10.3389/978-2-8325-4614-7

About Frontiers

Frontiers is more than just an open-access publisher of scholarly articles: it is a pioneering approach to the world of academia, radically improving the way scholarly research is managed. The grand vision of Frontiers is a world where all people have an equal opportunity to seek, share and generate knowledge. Frontiers provides immediate and permanent online open access to all its publications, but this alone is not enough to realize our grand goals.

Frontiers Journal Series

The Frontiers Journal Series is a multi-tier and interdisciplinary set of open-access, online journals, promising a paradigm shift from the current review, selection and dissemination processes in academic publishing. All Frontiers journals are driven by researchers for researchers; therefore, they constitute a service to the scholarly community. At the same time, the Frontiers Journal Series operates on a revolutionary invention, the tiered publishing system, initially addressing specific communities of scholars, and gradually climbing up to broader public understanding, thus serving the interests of the lay society, too.

Dedication to Quality

Each Frontiers article is a landmark of the highest quality, thanks to genuinely collaborative interactions between authors and review editors, who include some of the world's best academicians. Research must be certified by peers before entering a stream of knowledge that may eventually reach the public - and shape society; therefore, Frontiers only applies the most rigorous and unbiased reviews.
Frontiers revolutionizes research publishing by freely delivering the most outstanding research, evaluated with no bias from both the academic and social point of view. By applying the most advanced information technologies, Frontiers is catapulting scholarly publishing into a new generation.

What are Frontiers Research Topics?

Frontiers Research Topics are very popular trademarks of the Frontiers Journals Series: they are collections of at least ten articles, all centered on a particular subject. With their unique mix of varied contributions from Original Research to Review Articles, Frontiers Research Topics unify the most influential researchers, the latest key findings and historical advances in a hot research area! Find out more on how to host your own Frontiers Research Topic or contribute to one as an author by contacting the Frontiers Editorial Office: frontiersin.org/about/contact

THE ROLE OF NON-CODING RNAs IN GASTROINTESTINAL CANCERS, 3rd Edition

Topic Editors:
Kanjoormana Aryan Manu, Amala Cancer Research Centre, India
Divya P. Kumar, JSS Medical College & Hospital, JSS Academy of Higher Education and Research, India
Muzafar Ahmad Macha, Islamic University of Science and Technology (IUST), India

Publisher's note: This is a 3rd edition due to an article retraction.

Citation: Manu, K. A., Kumar, D. P., Macha, M. A., eds. (2024). The Role of Non-coding RNAs in Gastrointestinal Cancers, 3rd Edition. Lausanne: Frontiers Media SA. doi: 10.3389/978-2-8325-4614-7

Table of Contents

frontiers | Frontiers in Oncology

TYPE Editorial
PUBLISHED 08 November 2022
DOI 10.3389/fonc.2022.1056897

OPEN ACCESS

EDITED AND REVIEWED BY
Liang Qiao,
Westmead Institute for Medical Research, Australia

*CORRESPONDENCE
Divya P. Kumar
divyapk243@gmail.com

SPECIALTY SECTION
This article was submitted to Gastrointestinal Cancers: Gastric and Esophageal Cancers, a section of the journal Frontiers in Oncology

RECEIVED 29 September 2022
ACCEPTED 21 October 2022
PUBLISHED 08 November 2022

CITATION
Kumar DP, Manu KA and Macha MA (2022) Editorial: The role of non-coding RNAs in gastrointestinal cancer. *Front. Oncol.* 12:1056897. doi: 10.3389/fonc.2022.1056897

Editorial: The role of non-coding RNAs in gastrointestinal cancer

Divya P. Kumar[1]*, Kanjoormana Aryan Manu[2] and Muzafar Ahmad Macha[3]

[1]Department of Biochemistry, JSS Medical College, Center of Excellence in Molecular Biology and Regenerative Medicine (CEMR), JSS Academy of Higher Education and Research, Mysore, Karnataka, India, [2]Department of Immunology, Amala Cancer Research Centre, Thrissur, Kerala, India, [3]Watson-Crick Center for Molecular Medicine, Islamic University of Science and Technology, Awantipora, Jammu & Kashmir, India

KEYWORDS

non-coding RNA, gastrointestinal cancer, biomarkers, gene regulation, tumorigenesis

Editorial on the Research Topic
The role of non-coding RNAs in gastrointestinal cancers

Gastrointestinal (GI) cancer including cancers of the colorectum, stomach, liver, oesophagus, pancreas, and gall bladder is a critical public health concern with high morbidity and mortality rates. According to Globocan 2020, GI malignancies account for 27% of the cancer incidence and 37% of all cancer-related deaths worldwide (1). The molecular pathogenesis of GI cancer is complex and the advancement in recent technology has led to the identification of non-coding RNAs (ncRNAs) that are critically involved in the regulation of cellular processes that promote tumor formation and development (2, 3).

Non-coding RNAs (ncRNAs) are RNA transcripts that do not encode proteins and are divided into two types based on the average length: small non-coding RNAs (sncRNAs, fewer than 200 nucleotides), and long non-coding RNAs (lncRNAs, >200 nucleotides). Small ncRNAs are classified into three types: micro RNA (miRNA), small interfering RNA (siRNA), and piwi-interacting RNA (piRNA). The other types of ncRNAs include promoter-associated transcripts (PATs), enhancer RNA (eRNA), circular RNA (circRNA), small nuclear ribonucleic acid (snRNA), small nucleolar RNA (snoRNA), and tRNA-derived fragments (tRF) (4). The ncRNAs are known to regulate the initiation and progression of various cancers, including GI cancers. The ncRNAs can act as tumor suppressors or oncogenic drivers by regulating processes such as proliferation, invasion, apoptosis, autophagy, and metastasis, thereby promoting malignant transformation and cancer progression (5–8). In addition, ncRNAs also control epigenetic processes and gene expression (9). The ncRNAs released by the cancer cells are used as diagnostic and prognostic markers for GI cancers (10).

This special issue entitled "The Role of non-coding RNAs in Gastrointestinal Cancer" features 4 review articles, 12 original research articles, and a systematic review and meta-analysis that provide insights on the regulatory roles of ncRNAs in GI tumor

development and progression. This topic had 60 manuscripts submitted, among which only 17 were accepted for publication.

In the review articles, He et al., describe the use of mRNA and non-coding RNAs as biomarkers for the diagnosis and prognosis of colorectal cancers (CRCs). These non-coding RNAs include miRNA, lncRNA, circRNA, SnoRNA, piRNA, and tRNA. Additionally, Jia et al. explain the clinical significance of ncRNAs in CRC. They summarize the most recent research on lncRNA, miRNA, and circRNAs that act as promoters or tumor suppressors in CRC, aiding in proliferation, apoptosis, invasion, metastasis, autophagy, angiogenesis, and chemo resistance. Yang et al., describe the different types of histone post-transcriptional modifications in gastric cancer (GC) with a special focus on the interaction between ncRNAs (lncRNA, miRNA, and circRNA) and histone acetylation and methylation. The review clearly explains how ncRNA-mediated histone modifications promote tumorigenesis in GC. Furthermore, Aishanjiang et al. discuss the potential role of circRNA as hepatocellular carcinoma (HCC) biomarkers. They also shed light on the challenges, limitations of circRNA research, and their therapeutic potential for the treatment of HCC.

Gao et al., provide experimental evidence of how circRNA protein tyrosine kinase 2 (circPTK2) inhibits cell proliferation, migration, and invasion in GC. CircPTK2 has been demonstrated to decrease tumor growth by specifically targeting the miR-196a-3p/AATK (apoptosis-associated tyrosine kinase) axis, raising the possibility that circPTK2 could be used as a therapeutic target for GC. Huang et al., elucidated that tRNA-derived small RNAs play a role in GC development and discovered that serum tRF-31-U5YKFN8DYDZDD can be used as a potential diagnostic biomarker. Huang et al. identified the biological processes and pathways associated with N6-methyladenosine-related lncRNAs in gastric adenocarcinoma. The study provides important evidence towards the development of predictive biomarkers and immunotherapy for gastric adenocarcinoma. Chen et al. demonstrated the upregulation of miR-199b-5p in GC and its role in promoting proliferation, migration, and metastasis by regulating the expression of hedgehog interacting protein (HHIP). These findings suggest the potential of miR-199b-5p/HHIP pathway axis as a promising therapeutic target for GC. Studies by Zou et al., showed that snRNA host gene 8 (SNHG8) promotes the progression of Epstein-Barr Virus (EBV)-associated GC *via* sponging miR-512-5p and targeting Tripartite Motif Containing 28 (TRIM28). Luo et al., have shown that A-kinase interacting protein 1 (AKIP1) promotes cell invasion and stemness in GC by regulating the HIF-1α and β-catenin pathways under hypoxic conditions. Moreover, Wu et al. identified a network of circRNAs, miRNAs, and immune-related mRNAs that regulate GC while researching the molecular mechanisms of GC at the immunological level. These studies provided evidence that tumor cells and the host immune system interact to regulate the pathogenesis and development of GC.

Du et al. have demonstrated the prognostic value of lncRNA LINC02474 and elucidated its role in regulating apoptosis and metastasis of CRC by suppressing the expression of granzyme B (GZMB). Similarly, Zhang et al., showed that lncRNA cancer susceptibility candidate 11 (CASC11) promote proliferation and migration of CRC cells by adsorbing miR646 and miR-381-3p to upregulate RAB11 family-interacting protein 2 (RAB11FIP2) *via* the PI3K/AKT pathway. These findings strongly suggest the therapeutic potential of CASC11 for CRC. Zhang et al. investigated the role of exosomal miR-15a-5p in the development of HCC. They demonstrated that miR-15a-5p derived from cancer cell exosomes inhibits PD1 expression in CD8+ T cells, thereby suppressing the development of HCC. Like wise, Zhang et al., demonstrated the involvement of miR-20a in the proliferation, invasion, and metastasis of HCC by targeting Enhancer of Zeste Homologue 1 (EZH1). Studies by Huang et al., filled the gap in predicting clinical prognosis based on m6A-related lncRNAs in pancreatic cancer. Furthermore, through a series of experiments, a robust m6A-related lncRNA prognostic model was developed for clinical workers to predict pancreatic ductal adenocarcinoma (PDAC) overall survival. The authors have looked into the potential biological mechanisms and signaling pathways of key m6A-related lncRNAs. They have also found a competitive endogenous RNA (ceRNA) network that connects lncRNAs and m6A-regulators *via* miRNAs.

In the study by Fang et al., the authors have performed a systematic review and meta-analysis of 25 studies that included 1260 patients to explore the prognostic role of microRNA 375, 133, 143, and 145 in esophageal carcinoma. The findings demonstrated a substantial correlation between high expression of miR-375, miR-133, miR-143, and miR-145 and a better prognosis in esophageal cancer.

Taken together, this special issue attempts to explore the diverse functions of ncRNAs in the control of gene expression at the epigenetic, transcriptional, and translational levels. The articles also provide evidence of the role of ncRNAs in the regulation of tumor formation, metastasis, immune response, and treatment resistance in GI cancers such as GC, CRC, HCC, and pancreatic cancer.

Author contributions

All authors listed have made a substantial, direct, and intellectual contribution to the work and approved it for publication.

Acknowledgments

We would like to deeply thank all the authors for their scientific contributions to this Research Topic, as well as all of the reviewers for their time, efforts, comments, and constructive criticism in refining the manuscript.

Conflict of interest

The authors declare that the research was conducted in the absence of any commercial or financial relationships that could be construed as a potential conflict of interest.

Publisher's note

References

1. Global Cancer Observatory. Available at: https://gco.iarc.fr/today/fact-sheets-cancers.

2. Arnold M, Abnet CC, Neale RE, Vignat J, Giovannucci EL, McGlynn KA, et al. Global burden of 5 major types of gastrointestinal cancer. *Gastroenterology* (2020) 159(1):335–49. doi: 10.1053/j.gastro.2020.02.068

3. Yan H, Bu P. Non-coding RNA in cancer. *Essays Biochem* (2021) 65(4):625–39. doi: 10.1042/EBC20200032

4. Diamantopoulos MA, Tsiakanikas P, Scorilas A. Non-coding RNAs: the riddle of the transcriptome and their perspectives in cancer. *Ann Transl Med* (2018) 6(12):241. doi: 10.21037/atm.2018.06.10

5. Slack FJ, Chinnaiyan AM. The role of non-coding RNAs in oncology. *Cell* (2019) 179(5):1033–55. doi: 10.1016/j.cell.2019.10.017

6. Yue Y, Lin X, Qiu X, Yang L, Wang R. The molecular roles and clinical implications of non-coding RNAs in gastric cancer. *Front Cell Dev Biol* (2021) 9:802745. doi: 10.3389/fcell.2021.802745

7. Wong CM, Tsang FC, Ng IL. Non-coding RNAs in hepatocellular carcinoma: molecular functions and pathological implications. *Nat Rev Gastroenterol Hepatol* (2018) 15:137–51. doi: 10.1038/nrgastro.2017.169

8. Wei L, Wang X, Lv L, Zheng Y., Zhang N., Yang M. The emerging role of noncoding RNAs in colorectal cancer chemoresistance. *Cell Oncol* (2019) 42:757–68. doi: 10.1007/s13402-019-00466-8

9. Kumar S, Gonzalez EA, Rameshwar P, Etchegaray JP. Non-coding RNAs as mediators of epigenetic changes in malignancies. *Cancers (Basel)* (2020) 12(12):3657. doi: 10.3390/cancers12123657

10. Happel C, Ganguly A, Tagle DA. Extracellular RNAs as potential biomarkers for cancer. *J Cancer Metastasis Treat* (2020) 6:32. doi: 10.20517/2394-4722.2020.71

frontiers in Oncology

ORIGINAL RESEARCH
published: 09 April 2021
doi: 10.3389/fonc.2021.651796

Long Non-coding RNA LINC02474 Affects Metastasis and Apoptosis of Colorectal Cancer by Inhibiting the Expression of GZMB

Tiantian Du[1†], Qinglun Gao[2†], Yinghui Zhao[1], Jie Gao[1], Juan Li[1], Lili Wang[3], Peilong Li[1], Yunshan Wang[1], Lutao Du[1,4,5] and Chuanxin Wang[1,4,5*]*

[1] Department of Clinical Laboratory, The Second Hospital, Cheeloo College of Medicine, Shandong University, Jinan, China, [2] Department of Hepatobiliary Surgery, Shandong Provincial Third Hospital, Cheeloo College of Medicine, Shandong University, Jinan, China, [3] Department of Clinical Laboratory, Qilu Hospital of Shandong University, Jinan, China, [4] Shandong Engineering & Technology Research Center for Tumor Marker Detection, The Second Hospital of Shandong University, Jinan, China, [5] Shandong Provincial Clinical Medicine Research Center for Clinical Laboratory, The Second Hospital of Shandong University, Jinan, China

OPEN ACCESS

Edited by:
Divya P. Kumar, JSS Academy of Higher Education and Research, India

Reviewed by:
Zhiyong Zhang, The State University of New Jersey, United States
Venugopal Reddy Bovilla, Public Health Research Institute of India, India

***Correspondence:**
Chuanxin Wang
cxwang@sdu.edu.cn
Lutao Du
lutaodu@sdu.edu.cn

[†]These authors have contributed equally to this work

Specialty section:
This article was submitted to Gastrointestinal Cancers, a section of the journal Frontiers in Oncology

Received: *11 January 2021*
Accepted: *12 March 2021*
Published: *09 April 2021*

Citation:
Du T, Gao Q, Zhao Y, Gao J, Li J, Wang L, Li P, Wang Y, Du L and Wang C (2021) Long Non-coding RNA LINC02474 Affects Metastasis and Apoptosis of Colorectal Cancer by Inhibiting the Expression of GZMB. Front. Oncol. 11:651796. doi: 10.3389/fonc.2021.651796

Background: Colorectal cancer (CRC) is one of the most frequently diagnosed malignancies. Metastasis is the main event that impedes the therapeutic effect on CRC, and its underlying mechanisms remain largely unclear. LINC02474 is a novel long noncoding RNA (lncRNA) associated with metastasis of CRC, while little is known about how LINC02474 regulates these malignant characteristics.

Methods: Expressions of LINC02474 and granzyme B (GZMB) were assessed by quantitative real-time polymerase chain reaction (qRT-PCR) or Western blotting analysis. Cell metastasis was detected by transwell assay and metastatic nude mouse model, and apoptosis was determined by Western blotting analysis and flow cytometry. Besides, the interaction between LINC02474 and GZMB was detected by dual-luciferase reporter assays.

Results: The expression of LINC02474 was significantly up-regulated in CRC tissues. Moreover, depletion of LINC02474 damaged the metastatic abilities of CRC cells *in vivo and in vitro* while boosting apoptosis. Besides, up-regulation of LINC02474 could promote migration and invasion, while apoptosis was inhibited in CRC cells. Besides, down-regulation of LINC02474 promoted the expression of GZMB, and interference of GZMB could increase the metastatic abilities of CRC cells while reducing apoptosis. Furthermore, LINC02474 was related to the transcriptional repression of GZMB in CRC cells determined by the dual-luciferase reporter assay.

Conclusions: The findings revealed that a novel lncRNA, LINC02474, as an oncogene, could promote metastasis, but limit apoptosis partly by impeding GZMB expression in

CRC. Besides, LINC02474 had the potential to be used as a biomarker in the prognosis of CRC.

Keywords: long non-coding RNA, colorectal cancer, migration, invasion, apoptosis

INTRODUCTION

The latest epidemiological investigation has shown that colorectal cancer (CRC) ranks as the third most common diseases of cancer-related deaths in the Western countries among both man and woman. It is considered to be the second among the general population. Even with advances in the screenings and therapeutic strategies of CRC in recent years, it is estimated that 53,200 CRC-related deaths will occur in 2020 (1, 2). The leading cause of patient death at advanced stages is metastasis of CRC cells to tissues and organs outside where the tumor developed, leading to increased overall mortality (3). Almost a quarter of CRC patients at an advanced level have metastasis at diagnosis, as there are sometimes no signs at the early stage of CRC before it enters the advanced stage (1). Current treatment regimens can only relieve CRC patients' symptoms at an advanced stage, 5-year survival rate of advanced CRC is only 10% to 20% (4–6). Therefore, it is urgently necessary to explore neo-biomarkers for CRC and understand their pathological mechanism to improve patients' survival with advanced CRC (7, 8).

Current evidence indicates that non-coding RNAs (ncRNAs) occupy more than 70% of the human genome (9). Among ncRNAs, those with a nucleotide chain longer than 200 are regarded as long non-coding RNAs (lncRNAs) (10). LncRNAs are attract increasing attention due to their influential regulatory roles in multiple biological processes, especially oncogenesis and cancer pathogenesis (11–16). Moreover, functional dysregulation of some lncRNAs affects cancer cells' progression and death (17–20). In facts, some researches have reported various dysregulated lncRNAs in CRC. For instance, RAMS11 have been reported associated with poor survival and aggressive phenotypes (21), and overexpression of CCAT2 promotes chromosomal instability (CIN) of CRC cells (22). Also, given the cancer-related characteristics of lncRNAs, some of the lncRNAs may serve as potential biomarkers in CRC.

Granzyme B (GZMB) is generally produced in the tumor microenvironment by cytotoxic T lymphocytes (CTLs) and natural killer (NK) cells as a toxic granule-secreted enzyme with killing activity (23–25). However, a few reports have recorded that low GZMB expression could be associated with early CRC metastasis (26). Moreover, as a serine protease, GZMB has hydrolytic activity and can cleave downstream caspase-3 and Bid to activate them, contributing to apoptosis of targeted cells (27, 28).

Here, we aimed to explore the possible biological function of a novel lncRNA, LINC02474, in the progression and metastasis of CRC. LINC02474 was highly expressed among cancerous areas. Moreover, depletion of LINC02474 inhibited the metastatic ability of CRC cells but intensified the apoptosis. Besides, LINC02474 might exert its effect by mediating transcriptional dysregulation of GZMB. Altogether, our current findings provided significant insights into the regulatory role of LINC02474 in the progression and metastasis of CRC.

MATERIALS AND METHODS

Human Specimens and Ethics Statement

A total of 80 paired CRC and adjacent non-tumor tissue specimens were obtained from CRC patients who underwent a surgical operation during 2016 and 2018 at the Second Hospital of Shandong University. All enrolled patients neither received preoperative chemotherapy or radiotherapy nor had other cancer at the specimen collection time. Histopathological grades were staged based on the 8th edition of the Cancer Staging Manual of the American Joint Committee on Cancer (AJCC). All collected tissue specimens were immediately snap-frozen in liquid nitrogen and stored at −80°C. The essential demographic characteristics and clinical information of these 80 CRC patients were obtained from medical records. All tissue specimens were collected in compliance with the informed consent policy, and this experiment was approved by the Committee for Ethical Review of Research involving Human Subjects of the Second Hospital, Cheeloo College of Medicine, Shandong University.

Cell Culture

The human CRC cell lines (DLD-1, SW480, HT-29, HCT116, SW1116, and LOVO), one standard colorectal epithelial cell line (FHC), and HEK293T cells were purchased from the cell bank of the Chinese Academy of Sciences (Shanghai, China). DLD-1, SW480, HT-29, HCT116, SW1116, FHC, and HEK293T cells were maintained in Dulbecco-modified essential medium (DMEM) (Gibco, Shanghai, China, Cat#11995500BT). Meanwhile, HCT116 cells were cultured in RPMI-1640 medium (Gibco, Shanghai, China, Cat#C11875500BT). All culture media contained 1% penicillin and streptomycin (Solarbio, Beijing, China, Cat#P1400) and 10% fetal bovine serum (FBS) (Sagecreation, Beijing, China). All cells were maintained at 37°C with 5% CO2, tested negative for mycoplasma contamination, and authenticated based on STR fingerprinting before use.

SiRNA, Plasmid Construction, and Cell Transfection

Three individual siRNAs specific for LINC02474 (si-LINC02474 1#, 2#, and 3#) and GZMB (si-GZMB 1#, 2#, and 3#), as well as a scrambled negative control siRNA, were acquired from GenePharma (Shanghai, China). Full-length cDNA of human

LINC02474 (441bp) was synthesized and cloned into the pcDNA3.1 plasmid vector (Obio Technology, Shanghai, China). The shRNA of LINC02474 was synthesized and cloned into the pLKD-shRNA plasmid vector (GeneCreat, China). All plasmid vectors were extracted by the Endo-Free Plasmid Mini Kit (Omega Bio-Tek, USA, Cat#D6950). The siRNAs or plasmid vectors were transfected into cells with Lipofectamine 2000 (Invitrogen, Cat#11668019) and OPTI-MEM (Gibco, Shanghai, China, Cat#31985062) mixture after a 20 min incubation following the manufacturer's instructions.

To establish stable LINC02474 depletion or overexpression cells, three-plasmid lentiviral packaging systems (plasmid vectors specific for LINC02474, PAX, and pMD2G) and HEK293T cells were used to produce supernatant containing viral particles after more than 48 h of cultivation. Then the supernatant was collected and incubated with the CRC cells for at least 48 h, and the positive cells were then selected by puromycin (2.5 μg/ml) (Solarbio, Beijing, China, Cat#P8230). The expression efficiency was examined by fluorescence microscope and qRT-PCR. All sequences of siRNA and shRNA are listed in **Supplementary Table 2**.

RNA Extraction and qRT-PCR Analysis

Total RNA was collected from tissues with TRIzol Reagent (Ambion, Invitrogen, Carlsbad, CA, USA, Cat#10296010), Simultaneously, it was purified from cultured cells by RNA fast 2000 Reagent (Fastagen, Shanghai, China, Cat#220011). Purified RNA was quantified with a NanoDrop spectrophotometer 2000 (Thermo Fisher Scientific, Waltham, MA, USA) and then reversely transcribed into cDNA using random primers with the PrimeScript™ RT Reagent Kit (TaKara, Dalian, China, Cat#RR037A). qRT-PCR was processed with TB Green™ Premix Ex Taq™ (TaKara, Dalian, China, Cat#RR420A) on a CFX-96 real-time PCR System (Bio-Rad, Shanghai, China). Briefly, after an initial denaturation at 95°C for 30 s, the amplifications were carried out with 42 cycles at a melting temperature of 95°C for 5 s and an annealing temperature at 58°C for 30 s. Glyceraldehyde-3-phosphate dehydrogenase (GAPDH) was served as an endogenous control. The $2^{-\Delta\Delta CT}$ method was used to calculate the relative expressions of target genes. The specific primers used for qRT-PCR are listed in **Supplementary Table 3**.

Western Blotting Analysis and Antibodies

Cells were washed with phosphate-buffered saline (PBS) and then lysed with a Western/IP lysis buffer (Beyotime, Shanghai, China, Cat#P0013) contained a protease inhibitor cocktail (Roche Applied Science, Indianapolis, IN, USA). After 30 min of lysis on ice, the whole lysates were centrifuged at 12,000 rpm for 30 min at 4°C. The proteins were then quantified with a bicinchoninic acid protein assay kit (Vazyme Biotech Co., Ltd., Nanjing, China, Cat#E112-01/02) after a 30 min incubation at 37°C. Subsequently, proteins were subjected to sodium dodecyl sulphate-polyacrylamide gel electrophoresis (SDS-PAGE) on 10% or 12% gels and electrotransferred onto 0.22-μm polyvinylidene difluoride membranes (Millipore, USA, Cat# SLGVR33RS). Then, the membranes were blocked with 5% bovine serum albumin (BSA) (Solarbio, Beijing, China, Cat#A8020) and 1% Tween-20 (Solarbio, Beijing, China, Cat#T8220) in PBS at room temperature for 1.5 to 2 h, followed by incubation with primary antibodies against GAPDH (CST, #5174S, 1:2,000), β-actin (CST, #8457, 1:2,000), GZMB (CST, #17215, 1:1,000), cleaved caspase substrate (CST, #8698, 1:1,000), cleaved caspase-3 (CST, #9664, 1:1,000), cleaved PARP (CST, #5625, 1:1,000), caspase-3 (CST, #9662, 1:1,000), PARP (CST, #9532, 1:1,000), and Bid (CST, #2002, 1:1,000) at 4°C overnight. Tris-buffered saline containing 1% Tween-20 was used to wash the membranes (four times, 5 min for each), followed by incubation with horseradish peroxidase-conjugated secondary antibodies (at a dilution of 1:2,000) at room temperature for 1 h. Next, the bands were visualized with the high-sensitivity ECL Chemiluminescence Detection Kit (Vazyme Biotech Co., Ltd., Nanjing, China, Cat#E412-01-AA) and an enhanced chemiluminescence analysis system (Bio-Rad, Shanghai, China). GAPDH and β-actin were used as controls. All images were quantified by ImageJ software. The assay was repeated at least three times.

Cell Migration and Invasion Assays

Cell migration and invasion assays were performed with 24-well transwell chambers (8-μm pore size, Corning). Briefly, for migration assays, single-cell suspension at appropriate densities (8×10^4 cells/per well for DLD-1, SW1116, and SW480 cells or 1×10^5 cells/per well for LOVO cells) was plated into the upper chamber with 300 μl serum-free medium. In comparison, the lower section was filled with a 600 μl medium containing 20% FBS. After 24 h (DLD-1, SW1116, and SW480) or 48 h (LOVO), the chamber was washed with PBS. Then cells trapped in the upper chamber were removed, and sections in the lower surface were fixed with methanol and stained with crystal violet (0.1%) (Solarbio, Beijing, China, Cat#G1064). The cell numbers were determined using a microscope from five randomly selected visual fields. For invasion assays, similar methods were performed except that the upper chamber was pre-coated with Matrigel (BD Biosciences, San Jose, CA, United States, Cat# 356234), the cell numbers were doubled, and the collection time was prolonged to 48 h for DLD-1, SW1116, and SW480 cells and 72 h for LOVO cells. These assays were repeated at least three times.

Flow Cytometry Analysis

The cells were digested with trypsin digestion solutions without EDTA (0.25%) (Solarbio, Beijing, China, Cat#T1350) and harvested. Centrifuging 5 min with 350g. The collected cells were washed with PBS two times, then stained with Annexin V-APC/propidium iodide (PI) apoptosis detection kit (BestBio, China, Cat#BB-41033) following the manual instruction. And finally analyzed with flow cytometry (BD Biosciences) according to the manufacturer's instructions. The assay was repeated at least three times.

RNA FISH

Fluorescence processed RNA FISH assay in Situ Hybridization Kit (GenePharma, Shanghai, China). Cy3-labeled LINC02474

and β-actin sense probe and Cy3-labeled LINC02474 antisense probe were acquired from RiboBio (China). DLD-1 cells were first fixed with 4% formaldehyde (Biosharp, Cat#BL539A) for 15 min and then permeabilized in PBS containing 0.1% Triton X-100 (Solarbio, Beijing, China, Cat#T8200) at room temperature for 15 min. After incubated with 2× SSC at 37 °C for 30 min, the cells were hybridized with labeled FISH probe pre-mixed solution at 37 °C overnight in the dark. Subsequently, the cells were washed with 0.1% Tween-20 for 5 min and then sequentially washed with 2× SSC and 1× SSC for 5 min. The three reagents mentioned above were warmed up to 42°C before use. Finally, 4,6-diamidino-2-phenylindole (DAPI) (Solarbio, Beijing, China, Cat#C0065) was used to stain the cell nucleus for 10 min. The images were produced by fluorescence microscopy (Carl Zeiss Microscopy, LLC, USA).

RNA-seq Analysis

Total RNA was isolated from DLD-1 cells, in which LINC02474 was stably depleted, and their control cells using the RNeasy mini kit (Qiagen, Germany, Cat#74104). Then the cDNA library was acquired and validated by Agilent 2100 bioanalyzer (Agilent Technologies, USA). Then sequencing was carried out by the Illumina NovaSeq 6000 (Illumina, USA). The library construction and sequencing were executed at Shanghai Sinomics Corporation. Cuffdiff was used to evaluate DEGs. $Log_2|$ fold change$|$ >1 and P< 0.05 were used to select DEGs.

Gene Expression and Analysis of the TCGA Database

The RNA sequencing data (647 CRC cases vs. 51 normal cases) were downloaded from the TCGA database. The R software was used to analyze the data, and the "DESeq2" R package was used to acquire differently expressed lncRNAs. $Log_2|$ fold change$|$ >1 and P value < 0.05 were used to pick statistically significant lncRNAs.

Dual-Luciferase Analysis

The GZMB promoter region was constructed and inserted downstream of the luciferase reporter gene of the pGL3 primary vector, which contained a modified coding region for firefly luciferase. The TK vector, which included an area for renilla luciferase, was used as the control. All vectors were purchased from Biosune. Lipofectamine 2000 was used to transfect the reporter gene into DLD-1 cells. After transfection for 48 h, the Dual-Luciferase Reporter System Kit (Promega, USA, Cat#E1910) was used to test firefly and luciferase activities. The assay was repeated three times.

Animal Experiments

For the *in vivo* metastasis experiments, 1×10^6 DLD-1 cells stably transfected with sh-LINC02474 and the corresponding control were resuspended in 0.2 ml PBS and then injected into 14 BALB/c female nude mice by tail intravenous. The mice were 5-week-old and divided into two groups randomly (n=7 for each group). The mice were dissected after 50 days of injection, and lung tissues were isolated, fixed with formalin, and then stained with hematoxylin and eosin. All animal experiments were received and approved by the Institutional Animal Care and Use Committee of The Second Hospital, Cheeloo College of Medicine, Shandong University.

Statistical Analysis

All data were presented as mean ± standard deviation (SD) from at least three independent experiments. The difference between the two groups was determined by two-tailed Student's t-test, and the variance among multiple groups was analyzed by one-way analysis of variance (ANOVA). Overall survival (OS) curves were produced by the Kaplan-Meier method. The correlation between the expression of LINC02474 and clinical parameters was explored by the non-parametric Mann-Whitney test. Statistical analyses were performed with R software (version 3.5.2), SPSS software (version 19.0) (IBM, SPSS, Chicago, IL, USA) and GraphPad Prism 6 (GraphPad, La Jolla, CA, USA). A P value < 0.05 was considered statistically significant.

RESULTS

Identification of Expression Profiles of LINC02474

We first accessed the raw RNA sequencing (RNA-seq) data of the CRC (TCGA-COAD and TCGA-READ) cohort study from The Cancer Genome Atlas (TCGA) database, including 51 normal tissues and 647 CRC tissues, to obtain the profiles of differentially expressed lncRNAs. Among the differentially expressed lncRNAs, we focused on a novel lncRNA, LINC02474, for further exploration. Analytical results from TCGA data suggested that LINC02474 was up-regulated in CRC tissues (**Figures 1A–C**). Moreover, receiver operating characteristic (ROC) analysis revealed that the expression of LINC02474 could be used to distinguish CRC tumor tissues from normal tissues (LINC02474: area under the curve [AUC] = 0.7915, 95% confidence interval [CI] = 0.7495–0.8335) (**Figure 1D**). Up-regulation of LINC02474 implied a poor survival although there was no statistical significance (**Figure 1E**). To validate the database results, we subsequently collected 80 pairs of tissue samples from CRC patients. By quantitative real-time polymerase chain reaction (qRT-PCR), LINC02474 was identified to be expressed at a higher level among human CRC tissues than adjacent normal tissues (P<0.05) (**Figure 1F**). ROC analysis confirmed that LINC02474 could also be used to distinguish tumor parts from adjacent regions in CRC patients (LINC02474: AUC = 0.6118, CI = 0.5243–0.6994) (**Figure 1G**). Besides, the clinical-pathological characterizations of CRC patients were analyzed by comparing with the expression of LINC02474; however, there was no significant correlation (**Supplementary Table 1**). Considering that recent studies have revealed that some lncRNAs can encode proteins, such as LINC00961 and lncRNA HOXB-AS3 (29–33), we also predicted the coding ability of LINC02474 in two web sites (http://lilab.research.bcm.edu/cpat/) (http://cnit.noncode.org/CNIT/) by definition of lncRNAs (34, 35). The site prediction results indeed revealed that LINC02474 did not have the protein-

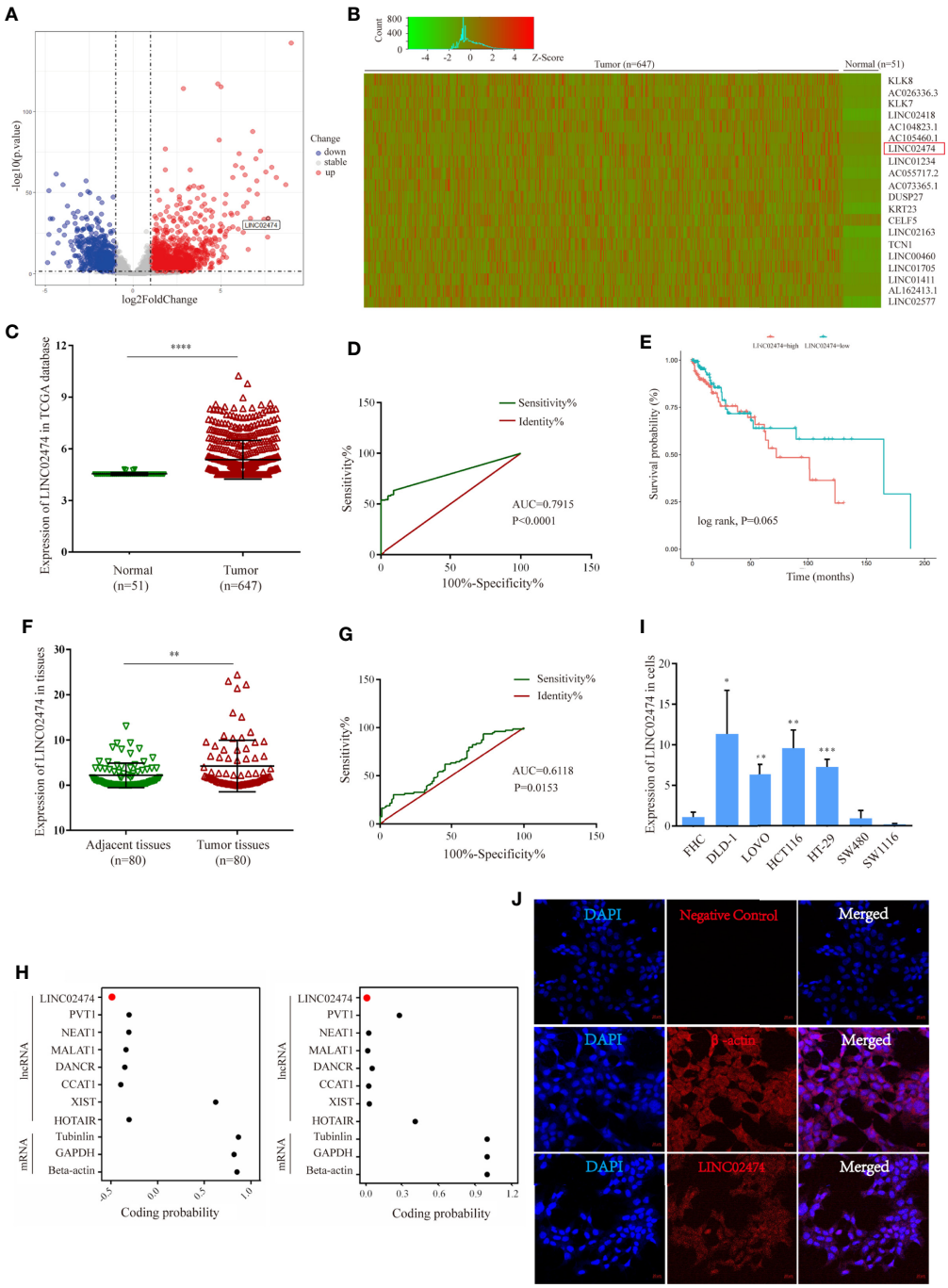

FIGURE 1 | Identification of expression profile characteristics of LINC02474. **(A–E)** Expression profile characteristics of LINC02474 from TCGA data sets (TCGA-COAD and TCGA-READ). **(A)** Volcano plot of DEGs. Red dots (right) represent up-regulated genes; gray dots (middle) represent genes excluded from the threshold ($|\log_2$ fold change$|$ >1, $p < 0.05$); and blue dots (left) represent down-regulated genes. **(B)** Heatmap of DEGs (http://shinyheatmap.com/). **(C)** Expression of LINC02474 in 51 normal tissues and 647 tumor tissues. **(D)** ROC curve of LINC02474 yielded an AUC value of 0.7915 (95% CI, 0.7495–0.8335) in distinguishing 647 CRC tissues from 51 normal tissues. **(E)** Survival analysis of LINC02474 from TCGA data sets. **(F)** Expression of LINC02474 in 80 pairs tissues from CRC patients. **(G)** ROC curve of LINC02474 yielded an AUC value of 0.6118 (95% CI, 0.5243–0.6994) in distinguishing tumor tissues from adjacent tissues in 80 CRC patients. **(H)** Coding probability prediction of LINC02474 (coding probability score<0 means no coding potential; coding probability score>0 means certain coding potential.) **(I)** Expression of LINC02474 in CRC cells (normalized to normal cell line, FHC.). **(J)** Subcellular localization of LINC02474 by RNA FISH. Red fluorescent probe: LINC02474 and β-actin (Cy3 labeled probes); blue fluorescent probe: DAPI. β-actin served as a positive control. Representative images (original magnification, ×200) are shown. Results are means ± SD. * represents $p < 0.05$; ** represents $p < 0.01$; *** represents $p < 0.001$; **** represents $p < 0.0001$.

coding ability (**Figure 1H**). Moreover, we checked the endogenous expression of LINC02474 among human CRC cell lines, including DLD-1, LOVO, HCT116, SW1116, SW480, and HT-29. We found that the highest expression of LINC02474 was detected in DLD-1, LOVO, and HCT116 cells, while its lowest expression was found in SW480 and SW1116 cells (**Figure 1I**). Besides, the cellular localization of LINC02474 was identified by RNA fluorescence *in situ* hybridization (FISH) in DLD-1 cells. We found that the molecule was more enriched in the cytoplasm than the nucleus (**Figure 1J**). Taken together, a novel lncRNA, LINC02474, was detected and significantly up-regulated in CRC patients, indicating its potentials to be a biomarker in CRC diagnosis.

Depletion of LINC02474 Represses Migration and Invasion but Accelerates the Apoptosis of CRC Cells

While we have shown that LINC02474 has a strong expression in CRC tissue, it remains uncertain if LINC02474 has any significant yet unexplained effect on CRC cells. Therefore, we depleted LINC02474 with short interfering RNAs (siRNAs) (**Figure 2A**). Compared with the negative control (scrambled), the migration and invasion abilities of DLD-1 cells treated by si-LINC02474#2 were affected (**Figures 2B, C**). Moreover, the expression of apoptosis-related proteins, including cleaved caspase-3, cleaved PARP, and cleaved caspase substrate, as well

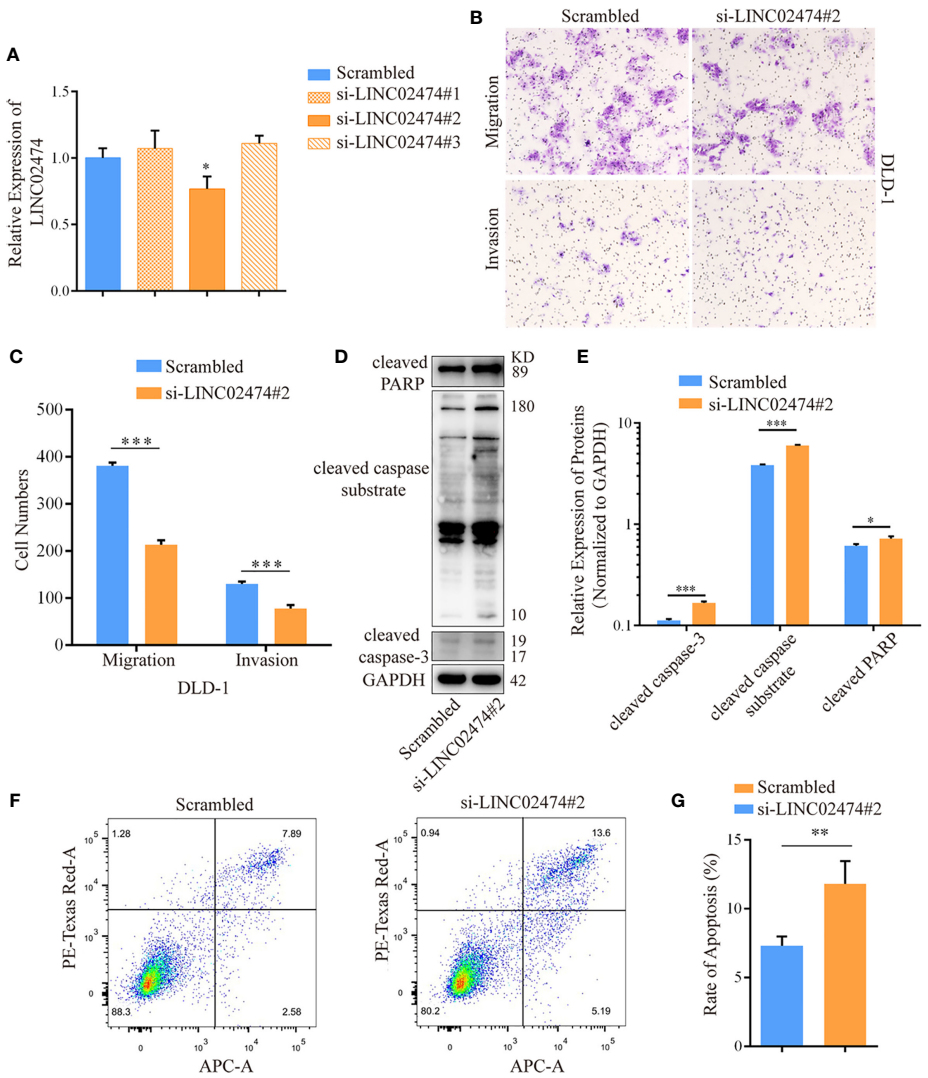

FIGURE 2 | Depletion of LINC02474 with siRNAs may impede metastasis and promote apoptosis of CRC cells. **(A)** qRT-PCR results of LINC02474 expression by siRNAs. **(B, C)** Migration and invasion abilities of DLD-1 cells by transwell assay. Representative images (original magnification, ×100) are shown. **(D, E)** Expressions of apoptosis-related proteins (cleaved PARP, cleaved caspase substrate, and cleaved caspase-3) in DLD-1 cells after LINC02474 were depleted. **(F, G)** Apoptosis after LINC02474 depletion by flow cytometry. Results are means ± SD. * represents $p < 0.05$; ** represents $p < 0.01$; *** represents $p < 0.001$.

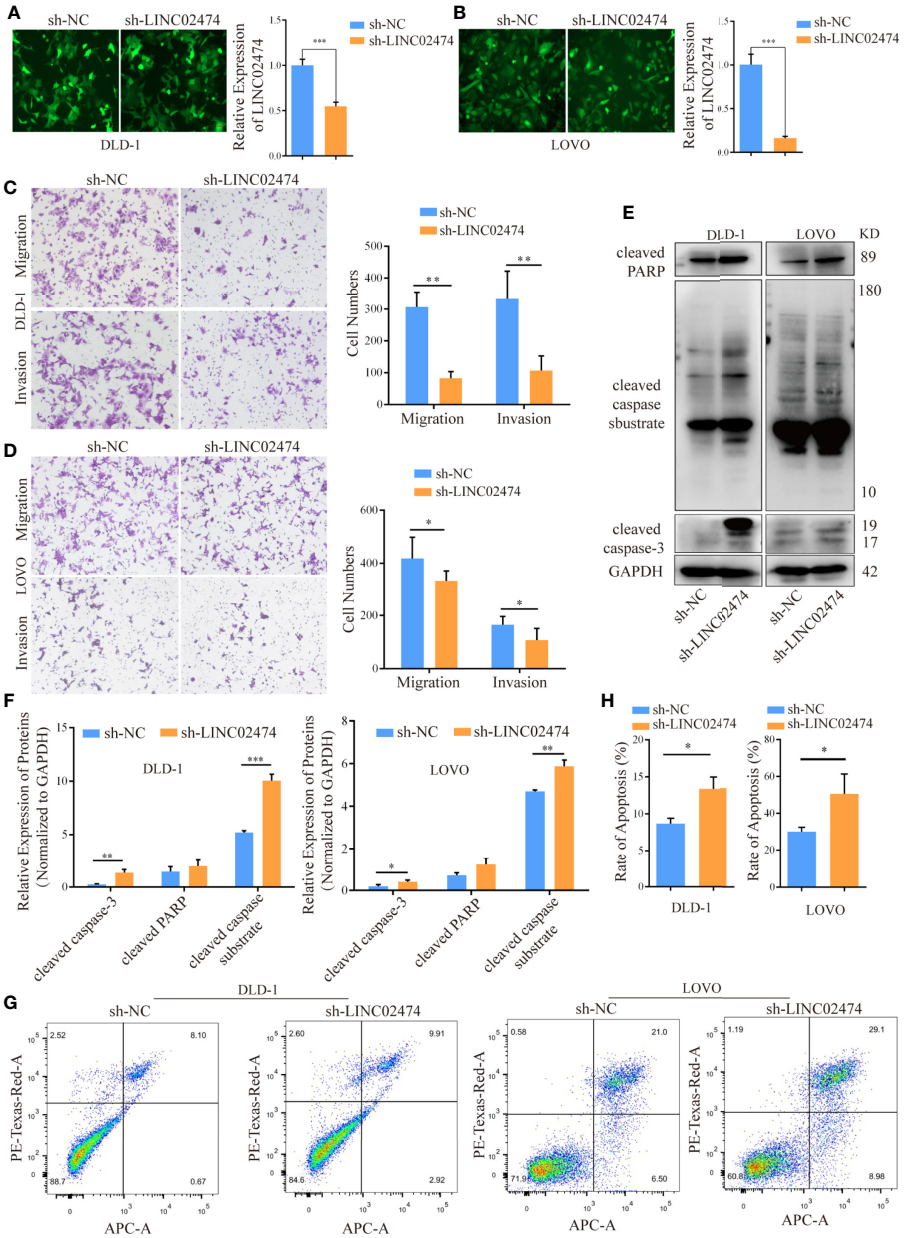

FIGURE 3 | LINC02474, as an oncogene, promotes the abilities of migration and invasion but inhibits the apoptosis of CRC cells. **(A, B)** qRT-PCR results for knockdown efficiency of LINC02474 in DLD-1 and LOVO cells by shRNAs. Representative images (original magnification, ×200) are shown. **(C, D)** Migration and invasion abilities of DLD-1 and LOVO cells after LINC02474 was stably depleted. Representative images (original magnification, ×100) are shown. **(E, F)** Expressions of apoptosis-related proteins (cleaved PARP, cleaved caspase substrate, and cleaved caspase-3) in DLD-1 and LOVO cells after LINC02474 was stably depleted. **(G, H)** Apoptosis in DLD-1 and LOVO cells after LINC02474 was stably depleted by flow cytometry. Results are means ± SD. * represents $p < 0.05$; ** represents $p < 0.01$; *** represents $p < 0.001$.

as apoptosis rate, were increased when LINC02474 was depleted, suggesting that LINC02474 also affected the apoptosis of CRC cells (**Figures 2D–G**). The results mentioned above implied that LINC02474 could mediate migration, invasion, and apoptosis of CRC cells.

To directly address whether LINC02474 affected metastasis and apoptosis of CRC cells, small hairpin RNA (shRNA) plasmid vectors were designed and transferred into HEK293T cells. Then supernatants of HEK293T cells containing viral particles were collected and incubated with CRC cells, such as DLD-1, LOVO, and HCT116 cells, for 48 h to generate cell lines with stable depletion of LINC02474 was stably depleted (**Figures 3A, B** and **Supplementary Figure 1A**). In line with the previous data, the transwell assay revealed that the three cell lines' migration and

invasion abilities in the sh-LINC02474 group were reduced compared with the negative control group (**Figures 3C, D** and **Supplementary Figure 1B**). The apoptosis was increased after LINC02474 was stably depleted, consistent with our previous findings (**Figures 3E–H** and **Supplementary Figures 1C, D**).

Similarly, we synthesized the exogenous LINC02474 plasmid vector and established LINC02474-overexpressing cell lines using SW1116 and SW480 cells (**Supplementary Figures 2A, B**). As expected, the invasion and migration abilities of LINC02474-overexpressing cells were significantly increased in comparison with those transfected by pcDNA3.1 empty vector (**Supplementary Figures 2C–F**). The apoptosis rate was decreased when LINC02474 was overexpressed in SW1116 and SW480 cells (**Supplementary Figures 2G–J**). Besides, to investigate whether LINC02474 also promoted CRC metastasis *in vivo*, we intravenously injected LINC02474-depleted DLD-1 cells into nude mice. In the metastatic nude mouse model by tail vein, sh-LINC02474 significantly prevented the formation of pulmonary metastatic nodules compared the control group after 50 days (**Figures 4A, B**). Altogether, the results as mentioned earlier suggested that LINC02474 was an oncogenic lncRNA, and promoted tumor metastasis both *in vivo* and *in vitro* but inhibited CRC cells' apoptosis.

Identification of Target Genes of LINC02474 by RNA-seq

This study showed that depletion of LINC02474 could damage metastasis but facilitate apoptosis of CRC cells. However, the underlying mechanism remained unknown. Therefore, we performed RNA-seq in DLD-1 cells by depletion of LINC02474 or not.

The RNA-seq data showed that hundreds of differentially expressed genes (DEGs) were identified between the LINC02474 depletion group and the negative control group (**Figures 5A, B**). Gene Ontology (GO) analysis showed that the most significantly overrepresented cellular component included an anchored part of the membrane and extracellular matrix (**Figure 5C**). Interestingly, the Kyoto Encyclopedia of Genes and Genomes (KEGG) analysis showed that most genes were enriched in the pathway named transcriptional misregulation in cancer (**Figure 5D**). The Gene Set Enrichment Analysis (GSEA) also revealed the gene markers between the sh-LINC02474 group and the control, and GZMB was ranked first (**Figure 5E**). Then genes involved in the transcriptional misregulation pathway, including GZMB, AMIGO3, L1CAM, FZD9, INHBA, RUNX2, ADAM12, FLT1, IGF1, and MMP20, were selected from DEG profiles and verified by qRT-PCR in DLD-1 cells (**Figure 5F**). GZMB was found to be significantly up-regulated among selected genes, which was consistent with our sequencing results. The other two CRC cell lines, LOVO, and HCT116, were examined for further identification, and found similar up-regulation was found in the sh-LINC02474 group. (**Figure 5G**). Besides, the protein expression of GZMB was also increased when LINC02474 was reduced (**Figure 5H**). Taken together, the data mentioned above implied that LINC02474 could suppress the expression of GZMB.

Influence of LINC02474 on CRC Cells Can Be Mediated by Restricting GZMB

Based on the above experiments, we hypothesized that the function of LINC02474 could be regulated by the expression of GZMB. Therefore, we designed siRNAs targeting GZMB and transferred them into LINC02474-depleted DLD-1 cells, and the expression of GZMB both in mRNA and protein levels was assessed (**Figures 6A, B**). Compared with the negative control, we found that the impaired migration and invasion abilities could be restored by siRNAs of GZMB (**Figures 6C–F** and **Supplementary Figures 3A, B**), implying that GZMB was involved in the metastatic process of CRC cells. On the other hand, the expressions of apoptosis-related proteins, including cleaved PARP and cleaved caspase-3, were reduced when GZMB was depleted. Besides, we found that the expression of another related protein, Bid, was decreased, which was the substrate of GZMB and functioned as a proteolytic enzyme (**Figures 6G, H**). Accordingly, some previous studies have shown that GZMB can cleave Bid and caspase-3 and induce apoptosis in cells.

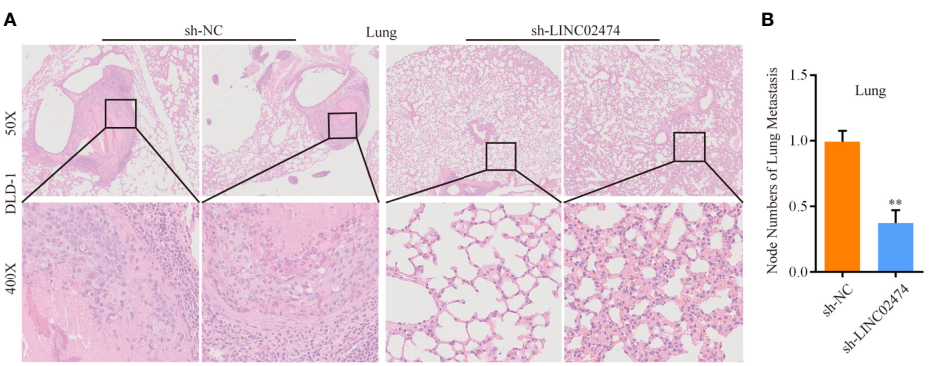

FIGURE 4 | LINC02474 promotes tumor metastasis *in vivo*. **(A)** Representative microscopic images of metastatic pulmonary lesions in two group nude mice (n = 7 for each group). Representative images (original magnification, ×50 [up] and ×400 [down]) are shown. **(B)** The number of metastatic nodules in the lung were counted. ** represents $p < 0.01$.

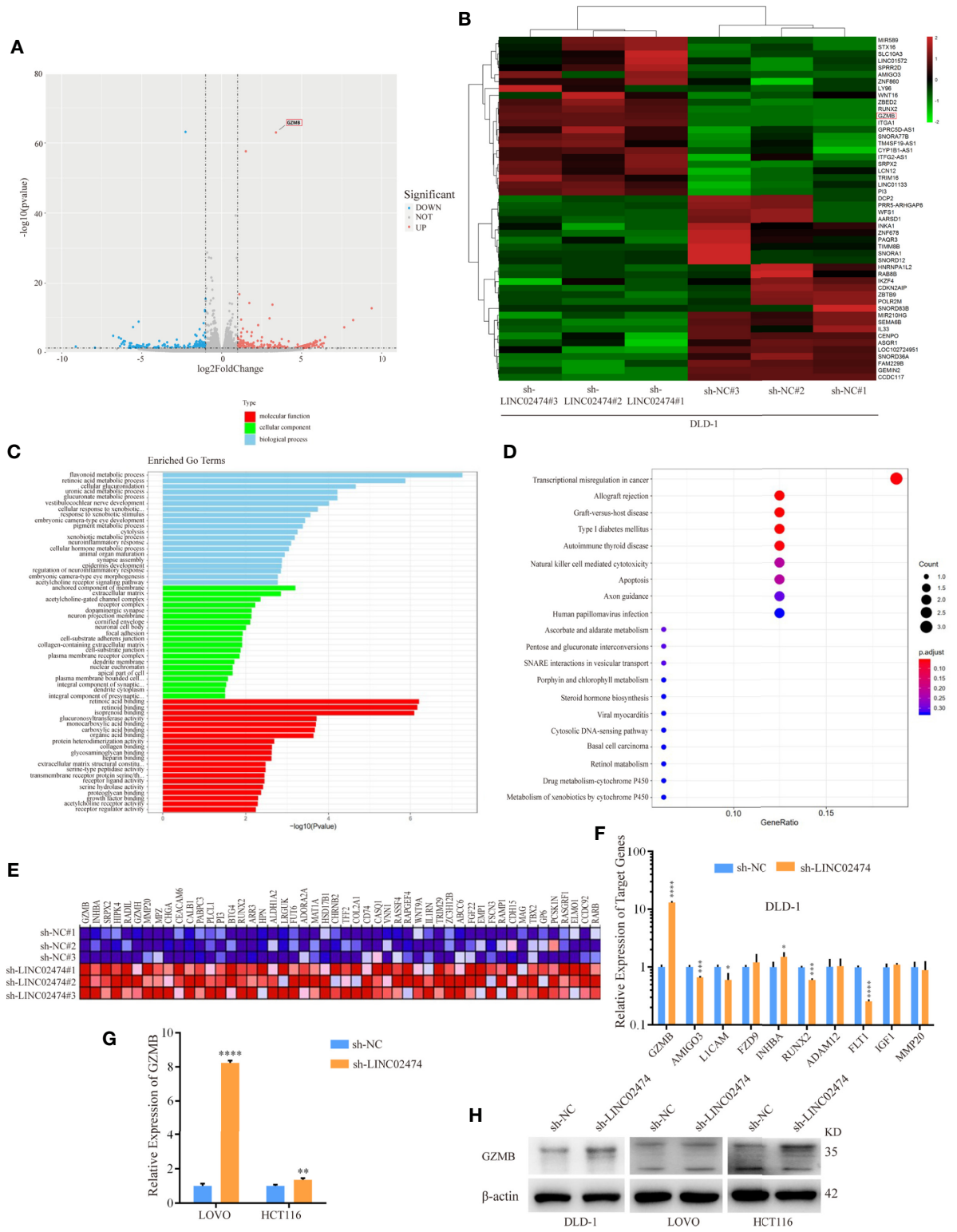

FIGURE 5 | Identification of target genes for LINC02474 with RNA-seq. **(A)** Volcano plot and **(B)** Heatmap after LINC02474 depletion in DLD-1 cells. **(C)** GO, **(D)** KEGG, and **(E)** GSEA gene markers after LINC02474 depletion in DLD-1 cells. **(F, G)** qRT-PCR results for expression identification of selected genes in DLD-1, LOVO, and HCT116 cells. **(H)** Protein expression of GZMB in DLD-1, LOVO, and HCT116 cells. Results are means ± SD. * represents $p < 0.05$; ** represents $p < 0.01$; *** represents $p < 0.001$; **** represents $p < 0.0001$.

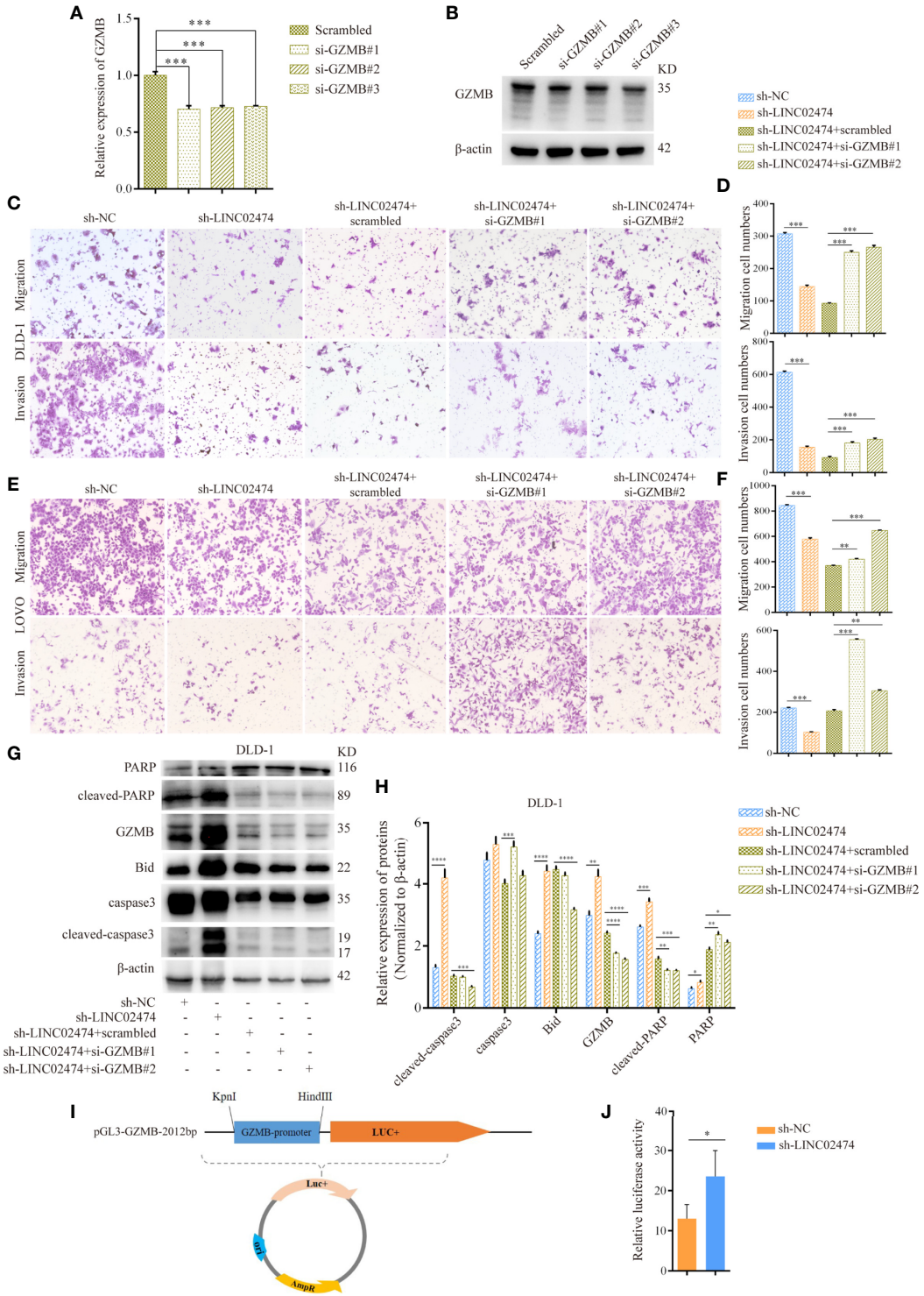

FIGURE 6 | The influence of LINC02474 on CRC cells can be mediated by restricting transcriptional regulation of GZMB. **(A)** qRT-PCR and **(B)** Western blotting analysis for the expression of GZMB by siRNAs. **(C–F)** Migration and invasion after GZMB depletion in DLD-1 and LOVO cells, in which LINC02474 was stably depleted. Representative images (original magnification, ×100) are shown. **(G, H)** Expressions of apoptosis-related proteins and GZMB after depleting GZMB in DLD-1 cells, in which LINC02474 was down-regulated. **(I)** Dual-luciferase reporter gene vector of GZMB gene promoter. **(J)** Relative luciferase activity of GZMB gene promoter after LINC02474 was depleted. Results are means ± SD. * represents $p < 0.05$; ** represents $p < 0.01$; *** represents $p < 0.001$; **** represents $p < 0.0001$.

These results supported that LINC02474 exerted an influence on metastasis and apoptosis of CRC cells mainly by suppressing the expression of GZMB.

Due to the effects of LINC02474 on GZMB, we further tested the mechanism underlying the GZMB-regulated inhibition. Since we showed that LINC02474 could suppress the expression of GZMB at the mRNA level, we assessed whether LINC02474 could impede the stability of GZMB mRNA. The LINC02474-depleted DLD-1 cells were treated with actinomycin D (ActD) for different durations, and the mRNA stability of GZMB was analyzed by qRT-PCR. Surprisingly, there were no effects of LINC0474 on stability (**Supplementary Figure 3C**). Next, to explore whether LINC02474 hindered the transcriptional regulation of GZMB, we designed a dual-luciferase reporter system, which included the promotor region of GZMB (**Figure 6I**). After the plasmid vector was transferred into DLD-1 cells, the fluorescence intensity was more vigorous in LINC02474-depleted cells (**Figure 6J**). These findings provided direct evidence that LINC02474 could contribute to the blocking of the transcriptional regulation of GZMB.

Collectively, the results mentioned above indicated that LINC02474 could affect metastasis and apoptosis in CRC cells by suppressing the transcriptional regulation of GZMB.

DISCUSSION

The previous studies have mainly focused on the roles of protein-coding genes. However, many ncRNAs have been recently found to influence on the cellular process and progression of human diseases significantly. In particular, the impact of lncRNAs on tumor progression has been a hot research spot (36–39). For instance, lncRNA SATB2-AS1 has specifically low CRC expression, and its down-regulation is related to poor survival (40). Moreover, lncRNA CGLL1, a functionally, mechanistically, and clinically active oncogene, can promote tumor carcinogenesis and glucose metabolism in CRC (41). Similarly, a novel lncRNA, named LINC02474, was identified to be localized on chromosome 1 by employing lncRNA expression profile data downloaded from public databases. Besides, we hypothesized that up-regulated LINC02474 was associated with a poor prognosis, and it could be used as a prognostic biomarker.

Depletion of LINC02474 could damage metastasis *in vitro* and *in vivo* but promote apoptosis of CRC cells. Subsequently, RNA-seq data showed that depletion of LINC02474 might affect the expressions of cancer-related genes, such as GZMB. Furthermore, LINC02474 could inhibit the expression of GZMB not only at the mRNA level but also at the protein aspect. To further identify the inhibition of LINC02474, we knocked down GZMB in LINC02474-depleted cells with siRNAs and found that the impaired migration, invasion, and apoptosis abilities caused by LINC02474 depletion could be restored by down-regulating GZMB. Therefore, we speculated that LINC02474 exerted its effect mainly by inhibiting GZMB. Finally, with more in-depth mechanism exploration, we found that LINC02474 might affect the transcription of GZMB to regulate its expression at the mRNA level, not through RNA stability.

Previous reports have shown that GZMB is usually expressed in immune cells, such as NK cells and CTLs, and it performs cell killing ability in the tumor microenvironment (42–44). However, only very few studies have focused on the role of GZMB in cancer cells, even less in CRC cells. It has been found that low expression of GZMB is related to early metastasis, indicating invasion of blood vessels and nerves (26). Furthermore, a recent study has proved that the expression of GZMB at the mRNA level is lower in early metastatic CRC (45). The present study found that GZMB could be expressed in CRC cells, and LINC02474 might inhibit its expression through transcriptional regulation.

Taken together, we identified a novel lncRNA, LINC02474, which could affect migration and invasion as well as apoptosis by inhibiting the expression of GZMB in CRC. Moreover, the high expression of LINC02474 might be associated with a poor prognosis. Therefore, LINC02474 could potentially be potential biomarker for CRC prognosis.

DATA AVAILABILITY STATEMENT

The raw and processed data of High-throughput Sequencing (Next Generation Sequencing) can been accessed with accession number GSE169722 (https://www.ncbi.nlm.nih.gov/geo/query/acc.cgi?acc=GSE169722) in the Gene Expression Omnibus (GEO) database.

ETHICS STATEMENT

The studies involving human participants were reviewed and approved by the Committee for Ethical Review of Research involving Human Subjects of the Second Hospital, Cheeloo College of Medicine, Shandong University. The patients/participants provided their written informed consent to participate in this study. The animal study was reviewed and approved by the Institutional Animal Care and Use Committee of The Second Hospital, Cheeloo College of Medicine, Shandong University.

AUTHOR CONTRIBUTIONS

CW and LD conceived and designed this study. TD and QG performed the experiments, conducted the data analysis, and prepared figures and tables. YZ, JG, JL, LW, PL, and YW provided technical support and revised the article. CW, LD, TD, and QG wrote the manuscript. All authors have read and approved the final version of the manuscript.

FUNDING

This research was supported by a grant from the National Natural Science Foundation of China (81972007 and 82002228), the National Key Research and Development Program of China

(2018YFC0114700), the Key Research and Development Program of Shandong Province (2019GHZ003, 2018YFJH0505 and 2019GSF108206), the Natural Science Foundation of Shandong Province (ZR201910250056), and the Fundamental Research Funds of Shandong University (2082018JC002).

ACKNOWLEDGMENTS

We thank all the staff who kindly provided technical support for this study.

SUPPLEMENTARY MATERIAL

The Supplementary Material for this article can be found online at: https://www.frontiersin.org/articles/10.3389/fonc.2021.651796/full#supplementary-material

Supplementary Figure 1 | LINC02474, as an oncogene, promotes the migration, and invasion but inhibits the apoptosis of CRC cells. **(A)** qRT-PCR results for knockdown efficiency of LINC02474 in HCT116 by shRNAs. Representative images (original magnification, ×200) are shown. **(B)** Migration and invasion abilities of HCT116 cells after LINC02474 was stably depleted. Representative images (original magnification, ×100) are shown. **(C)** Apoptosis in HCT116 cells after LINC02474 was stably depleted. **(D)** Expressions of apoptosis-related proteins (cleaved PARP, cleaved caspase substrate, and cleaved caspase-3) in HCT116 cells after LINC02474 being stably depleted. Results are means ± SD. ** represents $p<0.01$; *** represents $p<0.001$.

Supplementary Figure 2 | Overexpression of LINC02474 promotes the migration and invasion but reduces the apoptosis of CRC cells. **(A, B)** qRT-PCR results for overexpression efficiency of LINC02474 in SW1116 and SW480 cells. Representative images (original magnification, ×200) are shown. **(C–F)** Migration and invasion abilities of SW1116 and SW480 cells after LINC02474 was stably overexpressed. Representative images (original magnification, ×100) are shown. **(G–J)** Apoptosis in SW1116 and SW480 cells after LINC02474 was stably overexpressed. Results are means ± SD. ** represents $p<0.01$; **** represents $p<0.0001$.

Supplementary Figure 3 | The influence of LINC02474 on CRC cells is not associated with the RNA stability of GZMB. **(A, B)** Migration and invasion after GZMB knockdown in HCT116 cells, in which LINC02474 was stably depleted. Representative images (original magnification, ×100) are shown. **(C)** RNA stability of GZMB by ActD when LINC02474 was depleted, and c-myc served as a positive control. Results are means ± SD. ** represents $p<0.01$; *** represents $p<0.001$.

REFERENCES

1. Willauer AN, Liu Y, Pereira AAL, Lam M, Morris JS, Raghav KPS, et al. Clinical and molecular characterization of early-onset colorectal cancer. *Cancer* (2019) 125:2002–10. doi: 10.1002/cncr.31994
2. Siegel RL, Miller KD, Goding Sauer A, Fedewa SA, Butterly LF, Anderson JC, et al. Colorectal cancer statistics, 2020. *CA Cancer J Clin* (2020) 70:145–64. doi: 10.3322/caac.21601
3. La Vecchia S, Sebastián C. Metabolic pathways regulating colorectal cancer initiation and progression. *Semin Cell Dev Biol* (2020) 98:63–70. doi: 10.1016/j.semcdb.2019.05.018
4. Chen EX, Jonker DJ, Loree JM, Kennecke HF, Berry SR, Couture F, et al. Effect of Combined Immune Checkpoint Inhibition vs Best Supportive Care Alone in Patients With Advanced Colorectal Cancer: The Canadian Cancer Trials Group CO.26 Study. *JAMA Oncol* (2020) 6:831–8. doi: 10.1001/jamaoncol.2020.0910
5. Punt CJ, Koopman M, Vermeulen L. From tumour heterogeneity to advances in precision treatment of colorectal cancer. *Nat Rev Clin Oncol* (2017) 14:235–46. doi: 10.1038/nrclinonc.2016.171
6. Xie YH, Chen YX, Fang JY. Comprehensive review of targeted therapy for colorectal cancer. *Signal Transduct Target Ther* (2020) 5:22. doi: 10.1038/s41392-020-0116-z
7. Lenz HJ, Ou FS, Venook AP, Hochster HS, Niedzwiecki D, Goldberg RM, et al. Impact of Consensus Molecular Subtype on Survival in Patients With Metastatic Colorectal Cancer: Results From CALGB/SWOG 80405 (Alliance). *J Clin Oncol* (2019) 37:1876–85. doi: 10.1200/jco.18.02258
8. Alves Martins BA, de Bulhões GF, Cavalcanti IN, Martins MM, de Oliveira PG, Martins AMA. Biomarkers in Colorectal Cancer: The Role of Translational Proteomics Research. *Front Oncol* (2019) 9:1284. doi: 10.3389/fonc.2019.01284
9. Carninci P, Kasukawa T, Katayama S, Gough J, Frith MC, Maeda N, et al. The transcriptional landscape of the mammalian genome. *Science (New York N Y)* (2005) 309:1559–63. doi: 10.1126/science.1112014
10. Meng N, Chen M, Chen D, Chen XH, Wang JZ, Zhu S, et al. Small Protein Hidden in lncRNA LOC90024 Promotes "Cancerous" RNA Splicing and Tumorigenesis. *Adv Sci (Weinheim Baden-Wurttemberg Germany)* (2020) 7:1903233. doi: 10.1002/advs.201903233
11. Ponting CP, Oliver PL, Reik W. Evolution and functions of long noncoding RNAs. *Cell* (2009) 136:629–41. doi: 10.1016/j.cell.2009.02.006
12. Shi X, Sun M, Liu H, Yao Y, Song Y. Long non-coding RNAs: a new frontier in the study of human diseases. *Cancer Lett* (2013) 339:159–66. doi: 10.1016/j.canlet.2013.06.013
13. Yuan JH, Yang F, Wang F, Ma JZ, Guo YJ, Tao QF, et al. A long noncoding RNA activated by TGF-β promotes the invasion-metastasis cascade in hepatocellular carcinoma. *Cancer Cell* (2014) 25:666–81. doi: 10.1016/j.ccr.2014.03.010
14. Cesana M, Cacchiarelli D, Legnini I, Santini T, Sthandier O, Chinappi M, et al. A long noncoding RNA controls muscle differentiation by functioning as a competing endogenous RNA. *Cell* (2011) 147:358–69. doi: 10.1016/j.cell.2011.09.028
15. Rinn JL, Chang HY. Genome regulation by long noncoding RNAs. *Annu Rev Biochem* (2012) 81:145–66. doi: 10.1146/annurev-biochem-051410-092902
16. Schmitt AM, Chang HY. Long Noncoding RNAs in Cancer Pathways. *Cancer Cell* (2016) 29:452–63. doi: 10.1016/j.ccell.2016.03.010
17. Sang LJ, Ju HQ, Liu GP, Tian T, Ma GL, Lu YX, et al. LncRNA CamK-A Regulates Ca(2+)-Signaling-Mediated Tumor Microenvironment Remodeling. *Mol Cell* (2018) 72:71–83.e77. doi: 10.1016/j.molcel.2018.08.014
18. Gibb EA, Brown CJ, Lam WL. The functional role of long non-coding RNA in human carcinomas. *Mol Cancer* (2011) 10:38. doi: 10.1186/1476-4598-10-38
19. Ma Y, Yang Y, Wang F, Moyer MP, Wei Q, Zhang P, et al. Long non-coding RNA CCAL regulates colorectal cancer progression by activating Wnt/β-catenin signalling pathway via suppression of activator protein 2α. *Gut* (2016) 65:1494–504. doi: 10.1136/gutjnl-2014-308392
20. Ozawa T, Matsuyama T, Toiyama Y, Takahashi N, Ishikawa T, Uetake H, et al. CCAT1 and CCAT2 long noncoding RNAs, located within the 8q.24.21 'gene desert', serve as important prognostic biomarkers in colorectal cancer. *Ann Oncol* (2017) 28:1882–8. doi: 10.1093/annonc/mdx248
21. Silva-Fisher JM, Dang HX, White NM, Strand MS, Krasnick BA, Rozycki EB, et al. Long non-coding RNA RAMS11 promotes metastatic colorectal cancer progression. *Nat Commun* (2020) 11:2156. doi: 10.1038/s41467-020-15547-8
22. Chen B, Dragomir MP, Fabris L, Bayraktar R, Knutsen E, Liu X, et al. The Long Noncoding RNA CCAT2 induces chromosomal instability through BOP1 - AURKB signaling. *Gastroenterology* (2020) 159:2146–62. doi: 10.1053/j.gastro.2020.08.018
23. Multiprotein Particles from T Cells Deliver Cytotoxic Cargo to Targets. *Cancer Discov* (2020) 10:899. doi: 10.1158/2159-8290.Cd-rw2020-072
24. Konishi M, Erdem SS, Weissleder R, Lichtman AH, McCarthy JR, Libby P. Imaging Granzyme B Activity Assesses Immune-Mediated Myocarditis. *Circ Res* (2015) 117:502–12. doi: 10.1161/circresaha.115.306364

25. Wu CH, Li J, Li L, Sun J, Fabbri M, Wayne AS, et al. Extracellular vesicles derived from natural killer cells use multiple cytotoxic proteins and killing mechanisms to target cancer cells. *J Extracell Vesicles* (2019) 8:1588538. doi: 10.1080/20013078.2019.1588538
26. Salama P, Phillips M, Platell C, Iacopetta B. Low expression of Granzyme B in colorectal cancer is associated with signs of early metastastic invasion. *Histopathology* (2011) 59:207–15. doi: 10.1111/j.1365-2559.2011.03915.x
27. Chiusolo V, Jacquemin G, Yonca Bassoy E, Vinet L, Liguori L, Walch M, et al. Granzyme B enters the mitochondria in a Sam50-, Tim22- and mtHsp70-dependent manner to induce apoptosis. *Cell Death Differ* (2017) 24:747–58. doi: 10.1038/cdd.2017.3
28. Jacquemin G, Margiotta D, Kasahara A, Bassoy EY, Walch M, Thiery J, et al. Granzyme B-induced mitochondrial ROS are required for apoptosis. *Cell Death Differ* (2015) 22:862–74. doi: 10.1038/cdd.2014.180
29. Wang J, Zhu S, Meng N, He Y, Lu R, Yan GR. ncRNA-Encoded Peptides or Proteins and Cancer. *Mol Ther J Am Soc Gene Ther* (2019) 27:1718–25. doi: 10.1016/j.ymthe.2019.09.001
30. Matsumoto A, Pasut A, Matsumoto M, Yamashita R, Fung J, Monteleone E, et al. mTORC1 and muscle regeneration are regulated by the LINC00961-encoded SPAR polypeptide. *Nature* (2017) 541:228–32. doi: 10.1038/nature21034
31. Rion N, Rüegg MA. LncRNA-encoded peptides: More than translational noise? *Cell Res* (2017) 27:604–5. doi: 10.1038/cr.2017.35
32. Huang JZ, Chen M, Chen D, Gao XC, Zhu S, Huang H, et al. A Peptide Encoded by a Putative lncRNA HOXB-AS3 Suppresses Colon Cancer Growth. *Mol Cell* (2017) 68:171–84.e176. doi: 10.1016/j.molcel.2017.09.015
33. Anderson DM, Anderson KM, Chang CL, Makarewich CA, Nelson BR, McAnally JR, et al. A micropeptide encoded by a putative long noncoding RNA regulates muscle performance. *Cell* (2015) 160:595–606. doi: 10.1016/j.cell.2015.01.009
34. Bai Z, Wu Y, Bai S, Yan Y, Kang H, Ma W, et al. Long non-coding RNA SNGH7 Is activated by SP1 and exerts oncogenic properties by interacting with EZH2 in ovarian cancer. *J Cell Mol Med* (2020) 24:7479–89. doi: 10.1111/jcmm.15373
35. Guo JC, Fang SS, Wu Y, Zhang JH, Chen Y, Liu J, et al. CNIT: a fast and accurate web tool for identifying protein-coding and long non-coding transcripts based on intrinsic sequence composition. *Nucleic Acids Res* (2019) 47:W516–w22. doi: 10.1093/nar/gkz400
36. ICGC/TCGA Pan-Cancer Analysis of Whole Genomes Consortium. Pan-cancer analysis of whole genomes. *Nature* (2020) 578:82–93. doi: 10.1038/s41586-020-1969-6
37. Pandya-Jones A, Markaki Y, Serizay J, Chitiashvili T, Mancia Leon WR, Damianov A, et al. A protein assembly mediates Xist localization and gene silencing. *Nature* (2020) 587:145–51. doi: 10.1038/s41586-020-2703-0
38. Hu Q, Ye Y, Chan LC, Li Y, Liang K, Lin A, et al. Oncogenic lncRNA downregulates cancer cell antigen presentation and intrinsic tumor suppression. *Nat Immunol* (2019) 20:835–51. doi: 10.1038/s41590-019-0400-7
39. Chen F, Chen J, Yang L, Liu J, Zhang X, Zhang Y, et al. Extracellular vesicle-packaged HIF-1α-stabilizing lncRNA from tumour-associated macrophages regulates aerobic glycolysis of breast cancer cells. *Nat Cell Biol* (2019) 21:498–510. doi: 10.1038/s41556-019-0299-0
40. Xu M, Xu X, Pan B, Chen X, Lin K, Zeng K, et al. LncRNA SATB2-AS1 inhibits tumor metastasis and affects the tumor immune cell microenvironment in colorectal cancer by regulating SATB2. *Mol Cancer* (2019) 18:135. doi: 10.1186/s12943-019-1063-6
41. Tang J, Yan T, Bao Y, Shen C, Yu C, Zhu X, et al. LncRNA GLCC1 promotes colorectal carcinogenesis and glucose metabolism by stabilizing c-Myc. *Nat Commun* (2019) 10:3499. doi: 10.1038/s41467-019-11447-8
42. Lieberman J. The ABCs of granule-mediated cytotoxicity: new weapons in the arsenal. *Nat Rev Immunol* (2003) 3:361–70. doi: 10.1038/nri1083
43. Arias M, Martínez-Lostao L, Santiago L, Ferrandez A, Granville DJ, Pardo J. The Untold Story of Granzymes in Oncoimmunology: Novel Opportunities with Old Acquaintances. *Trends Cancer* (2017) 3:407–22. doi: 10.1016/j.trecan.2017.04.001
44. Zhang Z, Zhang Y, Xia S, Kong Q, Li S, Liu X, et al. Gasdermin E suppresses tumour growth by activating anti-tumour immunity. *Nature* (2020) 579:415–20. doi: 10.1038/s41586-020-2071-9
45. Pagès F, Berger A, Camus M, Sanchez-Cabo F, Costes A, Molidor R, et al. Effector memory T cells, early metastasis, and survival in colorectal cancer. *N Engl J Med* (2005) 353:2654–66. doi: 10.1056/NEJMoa051424

Conflict of Interest: The authors declare that the research was conducted in the absence of any commercial or financial relationships that could be construed as a potential conflict of interest.

frontiers in Oncology

ORIGINAL RESEARCH
published: 15 April 2021
doi: 10.3389/fonc.2021.657650

The LncRNA CASC11 Promotes Colorectal Cancer Cell Proliferation and Migration by Adsorbing miR-646 and miR-381-3p to Upregulate Their Target RAB11FIP2

Wei Zhang[1,2], *Xiaomin Li*[1], *Wenjuan Zhang*[1], *Yanxia Lu*[1], *Weihao Lin*[1], *Lawei Yang*[1], *Zheying Zhang*[3] *and Xuenong Li*[1]*

[1] Department of Pathology, School of Basic Medical Sciences, Southern Medical University, Guangzhou, China,
[2] Department of Pathology, The First Affiliated Hospital (Yijishan Hospital) of Wannan Medical College, Wuhu, China,
[3] Department of Pathology, Xinxiang Medical University, Xinxiang, China

Background: We previously reported that the long non-coding RNA (lncRNA) CASC11 promotes colorectal cancer (CRC) progression as an oncogene by binding to HNRNPK. However, it remains unknown whether CASC11 can act as a competitive endogenous RNA (ceRNA) in CRC. In this study, we focused on the role of CASC11 as a ceRNA in CRC by regulating miR-646 and miR-381-3p targeting of RAB11FIP2.

Methods: We identified the target microRNAs (miRNAs) of CASC11 and the target genes of miR-646 and miR-381-3p using bioinformatic methods. A dual-luciferase reporter assay was performed to validate the target relationship. Quantitative real-time PCR (qRT-PCR), western blotting (WB), and immunohistochemistry (IHC) were used to measure the RNA and protein expression levels. Rescue experiments *in vitro* and *in vivo* were performed to investigate the influence of the CASC11/miR-646 and miR-381-3p/RAB11FIP2 axis on CRC progression.

Results: We found that CASC11 binds to miR-646 and miR-381-3p in the cytoplasm of CRC cells. Moreover, miR-646 and miR-381-3p inhibitors reversed the suppressive effect of CASC11 silencing on CRC growth and metastasis *in vitro* and *in vivo*. We further confirmed that RAB11FIP2 is a mutual target of miR-646 and miR-381-3p. The expression levels of CASC11 and RAB11FIP2 in CRC were positively correlated and reciprocally regulated. Further study showed that CASC11 played an important role in regulating PI3K/AKT pathway by miR-646 and miR-381-3p/RAB11FIP2 axis.

Conclusion: Our study showed that CASC11 promotes the progression of CRC as a ceRNA by sponging miR-646 and miR-381-3p. Thus, CASC11 is a potential biomarker and a therapeutic target of CRC.

Keywords: CASC11, RAB11FIP2, colorectal cancer, miR-381-3p, miR-646

OPEN ACCESS

Edited by:
Muzafar Ahmad Macha, Islamic University of Science and Technology, India

Reviewed by:
Anju Kumari, National Cancer Institute, United States
Ravindra Deshpande, Wake Forest School of Medicine, United States
Devanjan Sinha, Banaras Hindu University, India
Arun Upadhyay, Northwestern University, United States
Allen Thayakumar Basanthakumar, Dana–Farber Cancer Institute, United States

***Correspondence:**
Xuenong Li
doctor_lixuenong@126.com

Specialty section:
This article was submitted to Gastrointestinal Cancers, a section of the journal Frontiers in Oncology

Received: *23 January 2021*
Accepted: *25 March 2021*
Published: *15 April 2021*

Citation:
Zhang W, Li X, Zhang W, Lu Y, Lin W, Yang L, Zhang Z and Li X (2021) The LncRNA CASC11 Promotes Colorectal Cancer Cell Proliferation and Migration by Adsorbing miR-646 and miR-381-3p to Upregulate Their Target RAB11FIP2. Front. Oncol. 11:657650. doi: 10.3389/fonc.2021.657650

INTRODUCTION

According to the World Cancer Report in 2018, colorectal cancer (CRC) is the third most frequent cancer and the second leading cause of cancer-related mortality (1). It is urgent to elucidate the critical molecular pathways involved in CRC and to develop effective therapeutic approaches for CRC. It has been established that non-coding genes occupy > 98% of the human genome, which far exceeds the proportion of coding genes (2, 3). Long non-coding RNAs (lncRNAs), RNA molecules longer than 200 nt in length have little or no protein-coding potential, and their functions are closely related to their subcellular localization (4, 5). In recent decades, an increasing number of lncRNAs have been found to be key regulators in tumour initiation and progression. Currently, the mechanisms of action of lncRNAs can be described by 4 modes: signal (functioning as indicators of transcriptional activity), decoy (acting as a "molecular sink" titrating away proteins and small regulatory RNAs), guide (directing the localization of ribonucleoprotein complex to specific targets), and scaffold (serving as central platforms upon which relevant molecular components are assembled) (6). Herein, lncRNAs acting as competitive endogenous RNAs (ceRNAs) of miRNAs are representative of the decoy mechanism (6). lncRNAs can crosstalk through their ability to compete for microRNA response elements (MREs), by which transcripts can actively communicate to each other to regulate their respective expression levels (7). The term "ceRNAs" refers to lncRNAs that share sequence identity and similarity with mRNA and can competitively bind to miRNAs to exert their function (7). Furthermore, extensive evidence has revealed that lncRNAs functioning as ceRNAs can bind to different miRNAs in different tumours. As reported, HOTAIR, a well-studied lncRNA, promotes non-small-cell lung cancer growth, invasion and metastasis by acting as a sponge of miR-149-5p (8) and facilitates CRC progression by sponging miR-214 (9).

We previously found that the lncRNA CASC11 plays an important role in the regulation of HNRNPK protein expression in CRC progression (10). CASC11 is located at the human chromosome 8q24 region, which is well known as a "genetic desert" because of the lack of any protein-coding oncogenes (10, 11). According to current studies, CASC11 can act as a critical tumour promoter in various tumours, such as gastric cancer (12), liver cancer (13) glioma (14) and CRC (10). The main functions of CASC11 are associated with binding to proteins or participating in ceRNA crosstalk. It has been reported that CASC11 acts as a ceRNA and promotes the proliferation and metastasis of gastric cancer by sponging miR-340-5p (12) Moreover, CASC11 facilitates the growth of glioma by adsorbing miR-498 (14). Given the versatile mechanisms of action of CASC11 in a variety of cancer types, we decided to explore the mechanisms of CASC11 as a ceRNA in CRC progression. To date, there has been no report regarding the ceRNA regulatory mechanism of CASC11 in CRC.

Abbreviations: CRC, Colorectal cancer; CASC11, Cancer susceptibility candidate 11; BSA, Albumin from bovine serum; qRT-PCR, Quantitative real-time PCR; WB, Western blotting; FISH, Fluorescence *in situ* hybridization; CCK-8, Cell counting kit-8; FBS, Fetal bovine serum; IF, Immunofluorescence; IHC, Immunohistochemistry; RAB11FIP2, RAB11 family-interacting protein 2; NC, Negative control.

MATERIALS AND METHODS

Cell Culture

FHC normal human colonic mucosal epithelial cells and SW480, LOVO, HCT116, RKO, Caco2, SW620, and LS174T human CRC cells were purchased from the American Type Culture Collection (ATCC, USA) and stored at 37°C in a 5% CO_2 atmosphere. FHC cells were cultured in Dulbecco's modified Eagle medium (DMEM, Gibco, USA) containing 20% foetal bovine serum (FBS, Gibco, USA), while the 7 CRC cell lines were grown in RPMI-1640 (Gibco, USA) supplemented with 10% FBS (Gibco, USA). We routinely tested for mycoplasma contamination by using the one-step Quickcolor Mycoplasma Detection Kit (Yise Medical Technology, Shanghai, China, #MD001), and all the cells used in our study were free of mycoplasma.

Tissue Samples and Animals

CRC tissues and adjacent normal tissues were collected from surgical specimens of patients from 2016 to 2018. Female BALB/c nude mice approximately 5-6 weeks old were purchased from the Guangdong Animal Center (Guangzhou, China) and housed in an SPF-grade animal experimental centre at Southern Medical University.

RNA Extraction and qRT-PCR

Total RNA was extracted with TRIzol (TaKaRa, Japan). RNA concentrations, and the 260/280 and 260/230 ratios were measured using a NanoDrop 2000 spectrophotometer (ThermoFisher, USA). Reverse transcription was performed using the PrimeScript RT reagent Kit (TaKaRa, Japan) and All-in-One miRNA qRT-PCR Kit (GeneCopoeia, USA). qRT-PCR was performed on an ABI 7500 Fluorescence Quantitative Detector with SYBR Green qPCR Mix (DBI Bioscience, Germany) and All-in-One miRNA qRT-PCR Kit (GeneCopoeia, USA). Fold changes=$2^{-\Delta\Delta Ct}$ represent the relative ratios between the groups, with GAPDH or U6 serving as the internal standard. The sequences of the qRT-PCR primers were as follows: CASC11 Forward, 5'-ACCCTATGGAGA ACCGAGAC-3' and Reverse, 5'-GAGGACCAACTCAGTAGG AAAT-3'; RAB11FIP2 Forward, 5'-TGTCCGAGCAAGCCCA AAAG-3' and Reverse, 5'- CTCCTTCCAAACTGGCTCAAG-3'; WEE1 Forward, 5'-AACAAGGATCTCCAGTCCACA-3' and Reverse, 5'- GGGCAAGCGCAAAAATATCTG-3'; RAB30 Forward, 5'- TGCCTCGTCCGAAGATTCAC-3' and Reverse, 5'- AGTAACTCTGGGTAATGGACCG-3'; GAPDH Forward, 5'-GGAGCGAGATCCCTCCAAAAT-3' and Reverse, 5'- GGC TGTTGTCATACTTCTCATGG-3'; and U6 Forward, 5'-CT CGCTTCGGCAGCACA-3' and Reverse, 5'-AACGCTTCAC GAATTTGCGT-3'.

Plasmid Construction and Transfection

The overexpression and interfering sequences of CASC11 reported previsouly (10) were used to construct the CASC11 overexpression plasmid and the intervention lentivirus (GeneChem, Shanghai, China). The miR-646 and miR-381-3p intervention viruses (LV-anti-miR-646 and LV-anti-miR-381-3p) were constructed by GeneChem (Shanghai, China). siRAB11FIP2 and its negative control siNC were purchased from RiboBio (Guangzhou, China); miRNA mimics and inhibitors were provided by GenePharma (Suzhou, China). Lipofectamine 3000 (Invitrogen, USA) was used for cell transfection according to the instructions of the manufacturer.

CCK-8 Cell Proliferation Assay

A CCK-8 assay (KeyGen Biotech, Nanjing, China) was used to detect the cell proliferation rates. Briefly, the transfected cells were seeded into 96-well plates (1000 cells/well). The cell proliferation assay was measured every 24 hours for 6 consecutive days. The spectrophotometric absorbance of each sample was read at 450 nm. Each sample was assayed in 5 replicates and repeated 3 times independently.

Plate Colony-Forming Assay

For colony formation assay, each well of a 6-well culture plate was seeded with 500 cells. After incubation at 37°C for 12 days, each well was washed three times with PBS, fixed with 4% paraformaldehyde for 30 min and stained with Giemsa solution for 10 min at room temperature. The number of colonies containing ≥ 50 cells was counted under a microscope and images were captured using a digital camera.

Flow Cytometry Cell Cycle Analysis

After 48h, the transfected cells were digested by trypsinization and fixed in cold 75% ethanol at 4 °C overnight. Subsequently, the Cell Cycle Detection Kit (KeyGen Biotech, Nanjing, China) was used according to the manufacturer's instruction. 1×10^6 cells were incubated with 100 ul RNase A at 37°C for 30 min and stained with 400ul propidium iodide (PI) staining solution for 15 min at 4 °C in the dark. Then, a flow cytometric analysis was performed, and the percentage of cells in G0–G1, S, and G2–M phases were calculated using ModFit LT software (version 3.0, Verity, USA).

Scratch Wound and Transwell Assays

The migratory capacity of cells was determined by scratch wound and Transwell assays. For the scratch wound assay, parallel lines were scratched on 6-well plates with 10-μl sterile tips when the transfected cells reached 90% confluence, followed by three washes with PBS to remove the cell debris. Images were then taken at 0, 24, and 48 h on an inverted microscope at 200× magnification. The scratch closure area was measured using ImageJ software (NIH, Bethesda, USA), and the equation for the healing rate was as follows: (% at 0 h) = (S0-ST)/S0 × 100%, where S0 and ST are the closure areas at 0 and T h, respectively. Next, 24-well plates with 8.0-μm pore membranes (Corning, NY, USA) were used for the Transwell assay. Transfected cells (1×10^5/well) were seeded into the upper chamber containing serum-free RPMI-1640 media, while 600 μl media supplemented with 20% FBS was added to the lower chamber. Other experimental procedures were performed as described elsewhere (15).

Western Blotting (WB)

Proteins were extracted with RIPA lysis buffer (KeyGen Biotech, Nanjing, China) and quantified by using a bicinchoninic acid protein quantification kit (KeyGen Biotech, Nanjing, China). Proteins were separated by SDS-PAGE and then transferred onto PVDF membranes (Millipore, Bedford, USA), followed by blocking with PBST solution containing 5% skim milk or 5% BSA for 1 h. Subsequently, the primary antibody was added, and the membranes were incubated at 4°C overnight, followed by a 1-h incubation with the corresponding secondary antibody at room temperature. Finally, Pierce ECL Western Blotting Substrate (FDbio Science, China) was used for the chemiluminescence assay. The following primary antibodies were used: anti-RAB11FIP2 (Abcam, UK, #ab180504), anti-AKT (Proteintech, USA, #10176–2-AP), anti-p-AKT (Ser473) (Proteintech, USA, #664441-Ig), anti-PI3K (Abcam, UK, #ab140307), anti-p-PI3K (Tyr607) (Abcam, UK, #ab182651) and anti-GAPDH (Proteintech, USA, #10494–1-AP). PI3K inhibitor LY294002 (Beyotime, Shanghai, China, #S1737) was used at a concentration (50 umol/L).

Fluorescence *In Situ* Hybridization (FISH)

The Cy3-labelled lncRNA CASC11 probe was synthesized by RiboBio (Guangzhou, China). FITC-labelled miR-646 and miR-381-3p probes were purchased from GENESEED (Guangzhou, China). The subcellular localization of CASC11 was detected using a FISH kit (RiboBio, China) with U6 as the nuclear control and 18S as the cytoplasmic control. Finally, the colocalization of CASC11 and miR-646 or miR-381-3p in CRC cells was detected as previously described (16).

Bioinformatics Predictions of miRNAs that Bind With CASC11 and Their Target Genes

The miRNA-binding sites of CASC11 were predicted by use of the bioinformatics databases LncTar (http://www.cuilab.cn/lnctar), LncBook (https://bigd.big.ac.cn/lncbook/index), RegRNA2.0 (http://regrna2.mbc.nctu.edu.tw/detection.html), and RNAhybrid (https://bibiserv.cebitec.uni-bielefeld.de/rnahybrid/). Filtering restrictions were as follows: total score, ≥140; normalized free energy, >1; and minimum free energy, < –20kcal/mol (17). The potential target genes of miR-646 and miR-381-3p were predicted by TargetScan Human (http://www.targetscan.org/vert_72/). In the results of Targetscan, miRNA binding sites of type "8mer" and "7mer-m8" were included, and the "context ++ score percentile" more than 80 was selected as the scoring cut-off (18).

Dual-Luciferase Reporter Assay

Full-length wild-type (Wt) or mutant (Mut) CASC11 oligonucleotides were inserted into the pmirGLO vector, and the dual-luciferase reporter plasmids were synthesized by Ruibiotech (Beijing, China). The length of the RAB11FIP2 3'UTR was 4182 bp, and the Wt and Mut psiCHECK2-

RAB11FIP2-3'UTR vectors were constructed by IGEbio (Guangzhou, China) to contain regions > 200 bp in length both downstream and upstream of each binding site. CRC cells were co-transfected with miRNA mimics or miR-NC and the aforementioned dual-luciferase plasmids using Lipofectamine 3000. After 48 h of transfection, the cells were lysed, and the luciferase activities were determined using the Promega Dual-Luciferase Reporter Assay System in accordance with the manufacturer's protocol.

Immunohistochemistry (IHC)

IHC staining and scoring were performed as described elsewhere (19). The primary antibodies anti-RAB11FIP2 (Abcam, UK, #ab180504) and anti-Ki67 (Abcam, UK, #ab94276) were used.

Immunofluorescence (IF)

The cells were fixed with 4% paraformaldehyde for 30 min and then treated with 0.5% Triton X-100 for 10 min, followed by 30 min of blocking with 1% BSA at room temperature. The primary antibodies anti-RAB11FIP2 (Abcam, UK, #ab180504), anti-AKT (Proteintech, USA, #10176–2-AP), and anti-p-AKT (Ser473) (Proteintech, USA, #664441-Ig) were added, and the wells were incubated overnight at 4°C. The next steps were the same as described previously (20).

In Vivo Xenograft Experiments

Stably transfected SW480 cells were used for the construction of nude mouse models bearing subcutaneous tumours or splenic capsule-injected metastatic tumours. A total of 1×10^7 SW480 cells were suspended in PBS and subcutaneously injected into the groin of nude mice (5-week-old female mice, n = 5 in each group). The tumour size was measured by a Vernier calliper from the 7th day of injection, and the tumour volume was calculated ($V = \text{length} \times \text{width}^2/2$). After 4 weeks, the tumour was removed and fixed with 10% neutral-buffered formalin, followed by haematoxylin and eosin (H&E) and IHC staining. SW480 cells (2×10^6) were injected into the splenic capsule of nude mice (6-week-old female mice, n = 4 in each group) to generate hepatic metastases. The mice were sacrificed after 8 weeks, and their spleens and livers were removed and subjected to histopathological examination.

Statistical Analyses

Statistical analyses were performed by using SPSS 21.0 (IBM, USA) and GraphPad Prism version 6.0 software (GraphPad Software, USA). Experimental data are represented as the mean ± SD. Intergroup differences were analysed by one-way analysis of variance (ANOVA) or the independent-samples *t-test*. Relationships between CASC11 or RAB11FIP2 expression and clinicopathologic parameters were determined by the χ^2 test. The linear correlation of gene expression was analysed with Spearman's correlation coefficient. WB images were quantified by a Gel-Pro Analyzer (Media Cybernetics, USA). IHC images were processed with Image-Pro Plus 6.0 (Media Cybernetics, USA). $p < 0.05$ was considered significant: *, $p < 0.05$; **, $p < 0.01$; ***, $p < 0.001$.

EXPERIMENTAL RESULTS

miR-646 and miR-381-3p Bind to CASC11 in the Cytoplasm

The subcellular localization of lncRNAs is closely related to their biological functions and molecular mechanisms (21). The endogenous expression of CASC11 was the highest in SW480 and the lowest in Caco2 cells among the 7 CRC cells, we chose these two cells for following experiment (**Additional File 1: Figure S1A**). We observed that CASC11 mainly resides in the cytoplasm of SW480 and Caco2 cells by performing FISH (**Figure 1A**). Then, we employed four bioinformatic databases to predict the target miRNAs of CASC11. The results showed that four candidate miRNAs, miR-646, miR-381-3p, miR-125b-5p, and miR-637, were predicted by more than three databases (**Additional File 1: Figure S1B**).

The binding relationship between CASC11 and miR-646, miR-381-3p, miR-125b-5p, or miR-637 was further validated by dual-luciferase reporter assays. The dual-luciferase reporter assay in SW480 and Caco2 cells showed that, compared with the those in control cells, the luciferase activities were reduced after co-transfection of miR-646 or miR-381-3p mimics and the CASC11-Wt plasmid, and there was no significant difference between the groups when miR-646 or miR-381-3p mimics and the CASC11-Mut plasmid were co-transfected. However, similar results were not obtained for miR-637 or miR-125b-5p (**Figure 1B**). In addition, RNA FISH revealed that CASC11 colocalized with miR-646 and miR-381-3p in the cytoplasm of HCT116 and Caco2 cells (**Figure 1C**). In summary, CASC11 binds to miR-646 and miR-381-3p in the cytoplasm of CRC cells.

miR-646 and miR-381-3p Reverse CASC11-Mediated Phenotypes of CRC Cell Proliferation and Migration *In Vitro* and *In Vivo*

According to the endogenous expression levels of CASC11, miR-646, and miR-381-3p in 7 CRC cells, we selected different cell lines for transfection. CASC11 was knocked down in SW480 and SW620 cells *via* shCASC11 lentiviral infection, with the empty lentivirus used as control (shNC). The reduced expression of CASC11 was confirmed by qRT-PCR. Treatment with miR-646 and miR-381-3p inhibitors successfully decreased the expression levels of miR-646 and miR-381-3p in SW620 and HCT116 (**Additional File 1: Figure S1C**). qRT-PCR analysis also indicated that CASC11, miR-646, and miR-381-3p expression was significantly increased after transfecting CASC11 overexpression plasmids, miR-646 and miR-381-3p mimics, respectively (**Additional File 1: Figure S1D**).

To confirm the effects of miR-646 and miR-381-3p on CASC11-mediated proliferation and migration of CRC cells, we conducted a series of *in vitro* functional assays. Both the CCK-8 assay and the plate colony-forming assay indicated that CASC11 interference restricted the growth of SW480 and SW620 cells, while this effect was reversed by the miR-646 and miR-381-3p inhibitors (**Figures 2A, B**). Flow cytometry cell cycle analysis revealed that CASC11 interference induced G1 phase arrest in

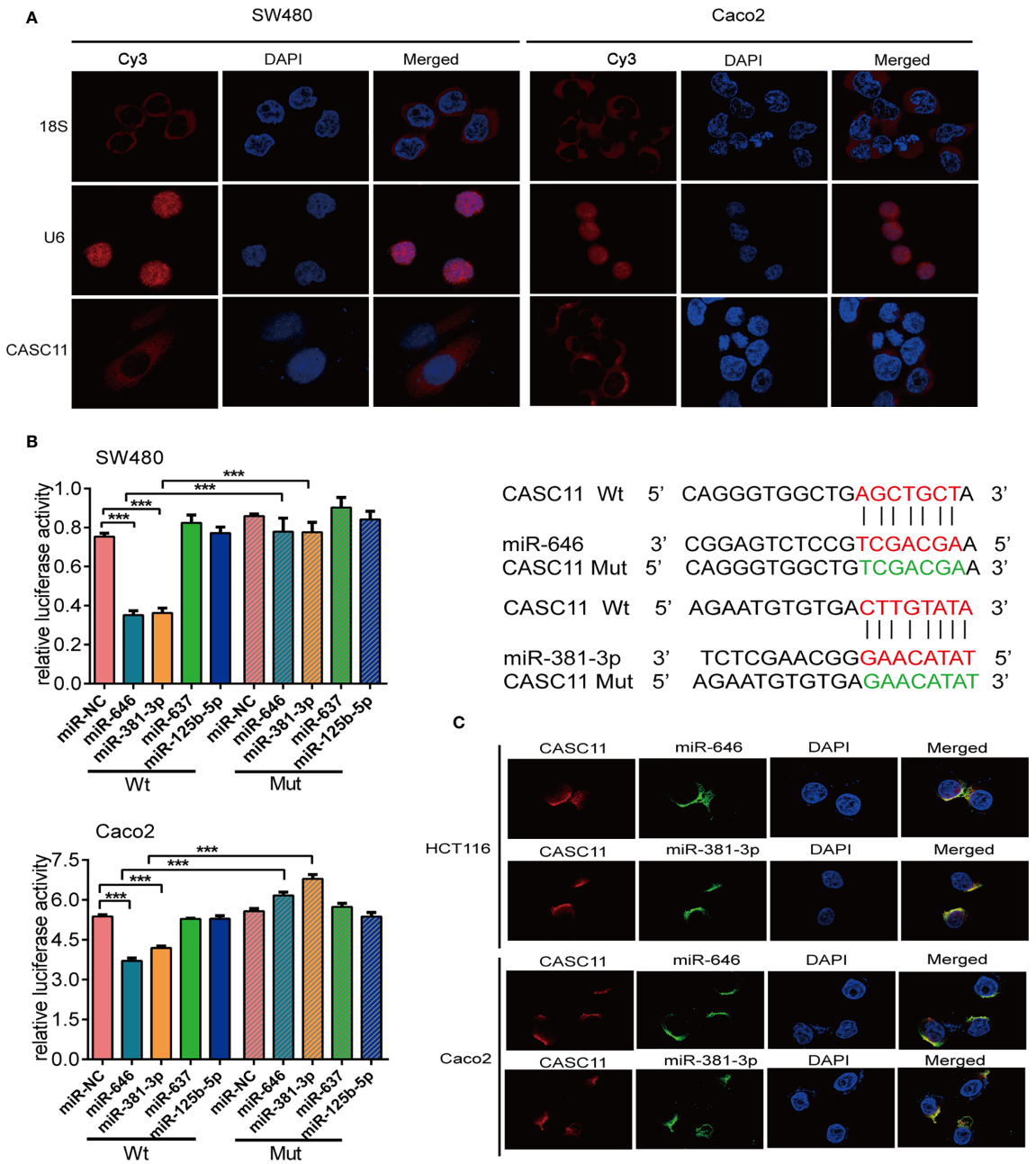

FIGURE 1 | miR-646 and miR-381-3p bind to CASC11 in the cytoplasm. **(A)** Representative fluorescence images of the subcellular localization of CASC11. U6 and 18S were used as positive controls for the nucleus and cytoplasm, respectively. **(B)** The relative luciferase activity of SW480 and Caco2 cells was tested after co-transfection with wild-type or mutant CASC11 and miRNA mimics. Sequence alignment of miR-646 and miR-381-3p with the binding sites in the wild-type and mutant regions of CASC11 were shown on the right side. Error bars represent the means ± SD of 3 independent experiments. ***p <0.001. **(C)** FISH demonstrated that CASC11 colocalized with miR-646 and miR-381-3p in the cytoplasm of HCT116 and Caco2 cells. Red: CASC11 probes were labelled with Cy3. Green: miR-646 and miR-381-3p probes were labelled with FITC. Blue: nuclei were stained with 4',6-diamidino-2-phenylindole (DAPI).

SW480 and SW620 cells, which in turn inhibited cell growth; this effect was also reversed by the miR-646 and miR-381-3p inhibitors, which increased the ratio of cells at G2 phase and accelerated cell growth (**Figure 2C**). Both the scratch wound assay and the Transwell migration assay confirmed that CASC11 interference suppressed the migration of CRC cells, while this effect was reversed by the miR-646 and miR-381-3p inhibitors, which in turn enhanced cell migration (**Figures 2D, E**). In addition, functional assays in RKO and SW620 cells confirmed that miR-646 and miR-381-3p mimics could cancel the promoting effects of CASC11 overexpression on cell proliferation and migration (**Additional File 2: Figure S2A–D**).

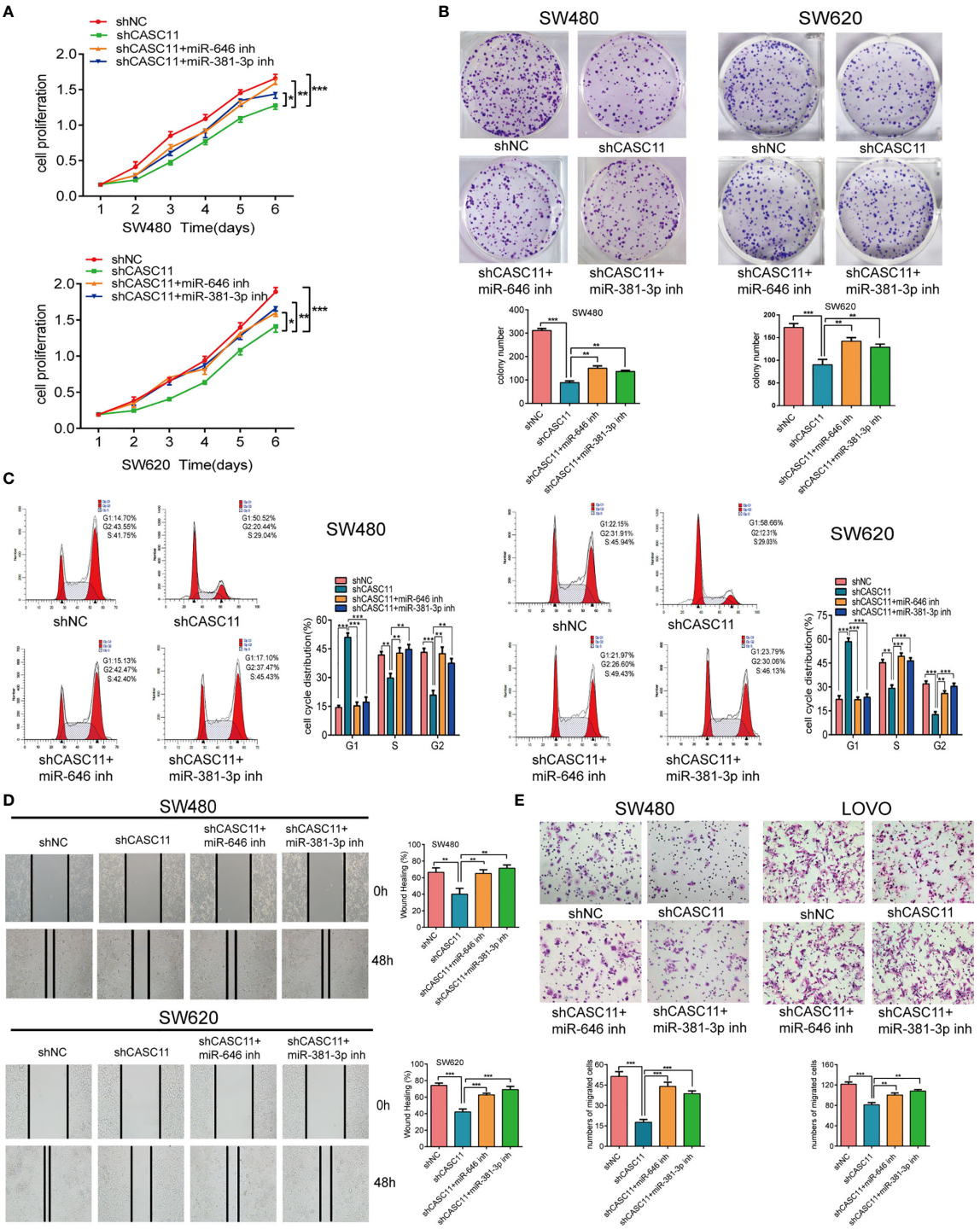

FIGURE 2 | miR-646 and miR-381-3p inhibitors reverse CASC11 interference -mediated phenotypes of CRC cell proliferation and migration *in vitro*. **(A–C)** Cell proliferation was assessed by CCK-8 assay, colony formation assay, and flow cytometry cell cycle analysis in CASC11-knockdown SW480 and SW620 cells. Error bars represent the means ± SD of 3 independent experiments. **(D)** Cell migration was analysed by scratch wound assay in CASC11-knockdown cells. The bar chart represents the percentage of distance at 48 h divided by the distance at 0 h. Error bars represent the means ± SD of 3 independent experiments. **(E)** Transwell migration assay used to evaluate the migration ability of cells with downregulated CASC11. Error bars represent the means ± SD of 5 different fields. $^{*}p < 0.05$; $^{**}p < 0.01$; $^{***}p < 0.001$.

The abovementioned results confirmed in different ways that miR-646 and miR-381-3p can reverse CASC11-mediated proliferation and migration of CRC cells *in vitro*.

To further demonstrate the role of miR-646 and miR-381-3p in CASC11-mediated proliferation and migration of CRC cells *in vivo*, we established SW480 nude mouse models bearing subcutaneous tumours or splenic capsule-injected liver metastatic tumours. SW480 cells transfected with shNC, shCASC11, shCASC11+LV-anti-miR-646, or shCASC11+LV-anti-miR-381-3p were injected. In the subcutaneous tumour mouse model, there was a notable reduction in the tumour growth rate in the shCASC11 group compared with the shNC group, while this growth reduction was reversed by LV-anti-miR-646 and LV-anti-miR-381-3p. After sacrificing the mice, we noted that LV-anti-miR-646 and LV-anti-miR-381-3p could partly counterbalance the effect of CASC11 knockdown on reducing the tumour volume and weight (**Figure 3A**). IHC confirmed that the Ki67 index was downregulated by shCASC11 and restored by LV-anti-miR-646 and LV-anti-miR-381-3p (**Figure 3B**). In the hepatic metastasis model, the average number of metastatic nodules in the shCASC11 group (0) was obviously reduced compared with that in the shNC group (3.0 ± 2.16), whereas suppressing the expression of miR-646 (1.25 ± 0.5) and miR-381-3p (3.5 ± 1.91) increased the number of metastatic nodules (**Figure 3C**). There were no metastatic nodules in any other organs in any group. In summary, we found that in nude mouse models of subcutaneous and splenic capsule-injected liver metastatic tumours, LV-anti-miR-646 and LV-anti-miR-381-3p could reverse the inhibitory effects of CASC11 knockdown on SW480 cells *in vivo*.

RAB11FIP2 Is a Mutual Target of miR-646 and miR-381-3p

The target genes of miR-646 and miR-381-3p were predicted by TargetScan. Venn diagrams showed that there were 9 mutual target genes of miR-646 and miR-381-3p (**Additional File 3: Figure S3A**). Among them, *RAB11FIP2, RAB30*, and *WEE1* were selected for further validation because they have been reported to play a key role in tumour development. qRT-PCR assays were performed on 8 different cell lines, and the expression levels of the above three target genes, miR-646, and miR-381-3p were determined. Correlation analyses revealed a clear negative correlation between RAB11FIP2 and miR-646 (r = -0.9696, p = 0.0003) or miR-381-3p (r = -0.7684, p = 0.036), whereas RAB30 (r = -0.2625, $p > 0.05$; r = 0.2328, $p > 0.05$) and WEE1 (r = -0.0260, $p > 0.05$; r = -0.3473, $p > 0.05$) were not inversely correlated with miR-646 or miR-381-3p in these cells (**Additional File 3: Figure S3B**). Hence, we chose *RAB11FIP2* as the mutual target gene for further validation. TargetScan predicted two high-scoring binding sites for miR-646 in the RAB11FIP2 3'UTR and three for miR-381-3p (**Figure 4A**). Luciferase reporter assays revealed that the overexpression of miR-646 obviously decreased the luciferase activity of RAB11FIP2-3'UTR-Wt but not RAB11FIP2-3'UTR-Mut in SW480 and SW620 cells (**Figure 4B**). Compared with miR-NC, miR-381-3p mimics significantly decreased the luciferase activity of RAB11FIP2-3'UTR-Wt1 and -Wt2 but not RAB11FIP2-3'UTR-Mut1 and -Mut2. The luciferase activity of RAB11FIP2-3'UTR-Wt3 was not significantly altered by miR-381-3p mimics compared to miR-NC (**Figure 4C**). Accordingly, it can be concluded that miR-646 and miR-381-3p can bind to the RAB11FIP2 3'UTR.

Considering that the binding of a miRNA to its target gene is followed by mRNA degradation or translational inhibition, qRT-PCR and WB were employed to probe the regulatory relationship between miR-646 or miR-381-3p and RAB11FIP2. Compared with the control transfection, transfection with miR-646 or miR-381-3p mimics led to a decrease in the mRNA and protein levels of RAB11FIP2, whereas transfection with the miR-646 or miR-381-3p inhibitor led to an increase in the mRNA and protein levels of RAB11FIP2 (**Figure 4D**). Therefore, it can be concluded that miR-646 and miR-381-3p negatively regulate RAB11FIP2. In summary, miR-646 and miR-381-3p bind to the RAB11FIP2 3'UTR and inhibit the translation of RAB11FIP2.

RAB11FIP2 and CASC11 Are Reciprocally Regulated by Sponging miR-646 and miR-381-3p

To further confirm whether CASC11 regulates the miR-646- and miR-381-3p-targeted gene RAB11FIP2, we increased CASC11 expression in CRC cells and found that it resulted in elevated expression of RAB11FIP2 at both the mRNA and protein levels (**Figures 5A, B**). In contrast, silencing CASC11 expression caused a decrease in RAB11FIP2 expression (**Figures 5C, D**). We also determined the expression of CASC11 and RAB11FIP2 in 27 pairs of CRC tissues by qRT-PCR. Our results revealed that the expression levels of both were higher in cancerous tissues than in normal adjacent tissues, indicating clear positive correlations (**Figure 5E**). Furthermore, to investigate the clinicopathologic significance of CASC11 and RAB11FIP2, the expression levels of CASC11 or RAB11FIP2 in 27 pairs of CRC tissues by qRT-PCR were divided into a high expression group and a low expression group by the median CASC11 or RAB11FIP2 expression. As summarized in Table S1 (**Additional File 6: Table S1**), the high expression level of CASC11 was significantly correlated with tumour size, lymph-vascular invasion, lymph metastasis, and T-stage. RAB11FIP2 expression was positively associated with tumour size and T-stage. We further evaluated the expression levels of miR-646 and miR-381-3p in 27 pairs of CRC tissues. The expression of miR-646 was lower in 23 of 27 CRC specimens compared to the adjacent normal tissues by qRT-PCR (p <0.001), as well as miR-381-3p (p <0.01) (**Additional File 5: Figure S5A**).

The successful construction of siRAB11FIP2-SW480 and siRAB11FIP2-SW620 cells was confirmed by qRT-PCR and WB (**Additional File 4: Figure S4A, B**). RAB11FIP2 interference led to a decrease in the expression of CASC11 compared to siNC (**Additional File 4: Figure S4C**). In addition, the WB results revealed that the miR-646 and miR-381-3p inhibitors could restore the decrease in RAB11FIP2 protein levels caused by CASC11 knockdown

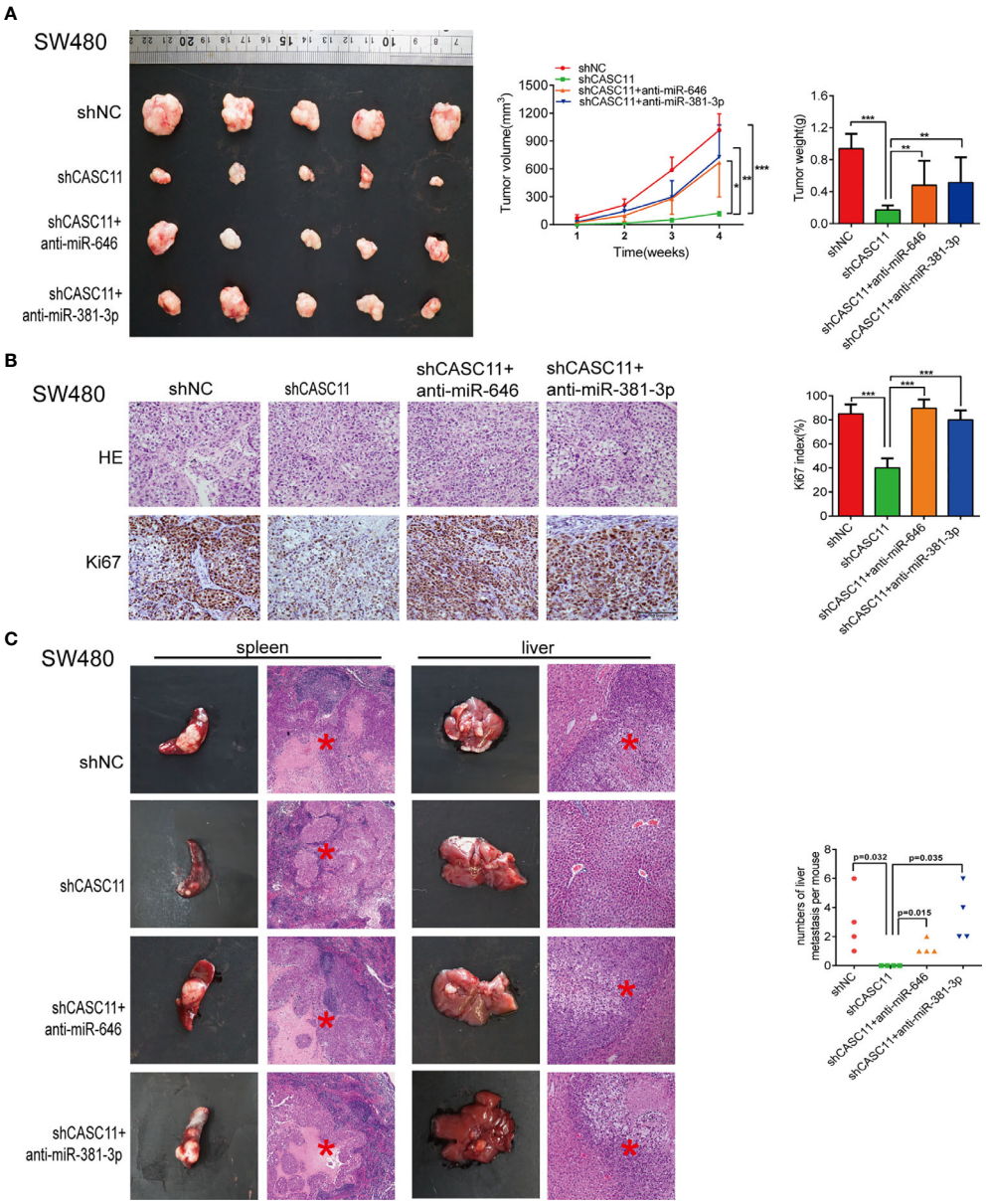

FIGURE 3 | miR-646 and miR-381-3p inhibitors reverse CASC11 interference -mediated phenotypes of CRC cell proliferation and migration *in vivo*. **(A)** Mouse models of subcutaneous tumours developed from CASC11-knockdown SW480 cells, which were treated with anti-miR-646 or anti-miR-381-3p (n=5). Left: Images of the tumour mass of each group at the endpoint of the experiment. Middle: tumour growth curves. The data were calculated as the mean tumour volumes ± SD for 5 samples. Right: Tumour weights of the xenografts upon euthanasia at day 28. **(B)** Representative images of Ki67-positive sections of subcutaneous tumours by IHC assay. The error bars in all graphs represent the means ± SD of 3 different fields. **(C)** Representative images of splenic tumours, hepatic metastases, and haematoxylin and eosin (H&E) staining. The numbers of hepatic metastases per mouse are indicated on the right side (n = 4). *$p < 0.05$; **$p < 0.01$; ***$p < 0.001$.

(**Additional File 4: Figure S4D**). The detection of 67 pairs of CRC tissues by IHC indicated that the positive rates of the RAB11FIP2 protein were significantly higher in the cancerous tissues than in the para-carcinoma tissues (**Additional File 4: Figure S4E**). The *in vitro* proliferation and migration assays in LOVO and RKO cells confirmed that siRAB11FIP2 could reverse the effect on the proliferation and migration of CRC cells caused by CASC11 overexpression (**Additional File 4: Figure S4F–H**). In summary, CASC11 and RAB11FIP2 are positively regulated by each other by sponging miR-646 and miR-381-3p.

CASC11 Is a PI3K/AKT Signaling Pathway Regulator in CRC Cells

According to a previous study, CASC11 can promote the progression and metastasis of liver cancer by activating the PI3K/AKT pathway (13), and RAB11FIP2 could facilitate the metastasis

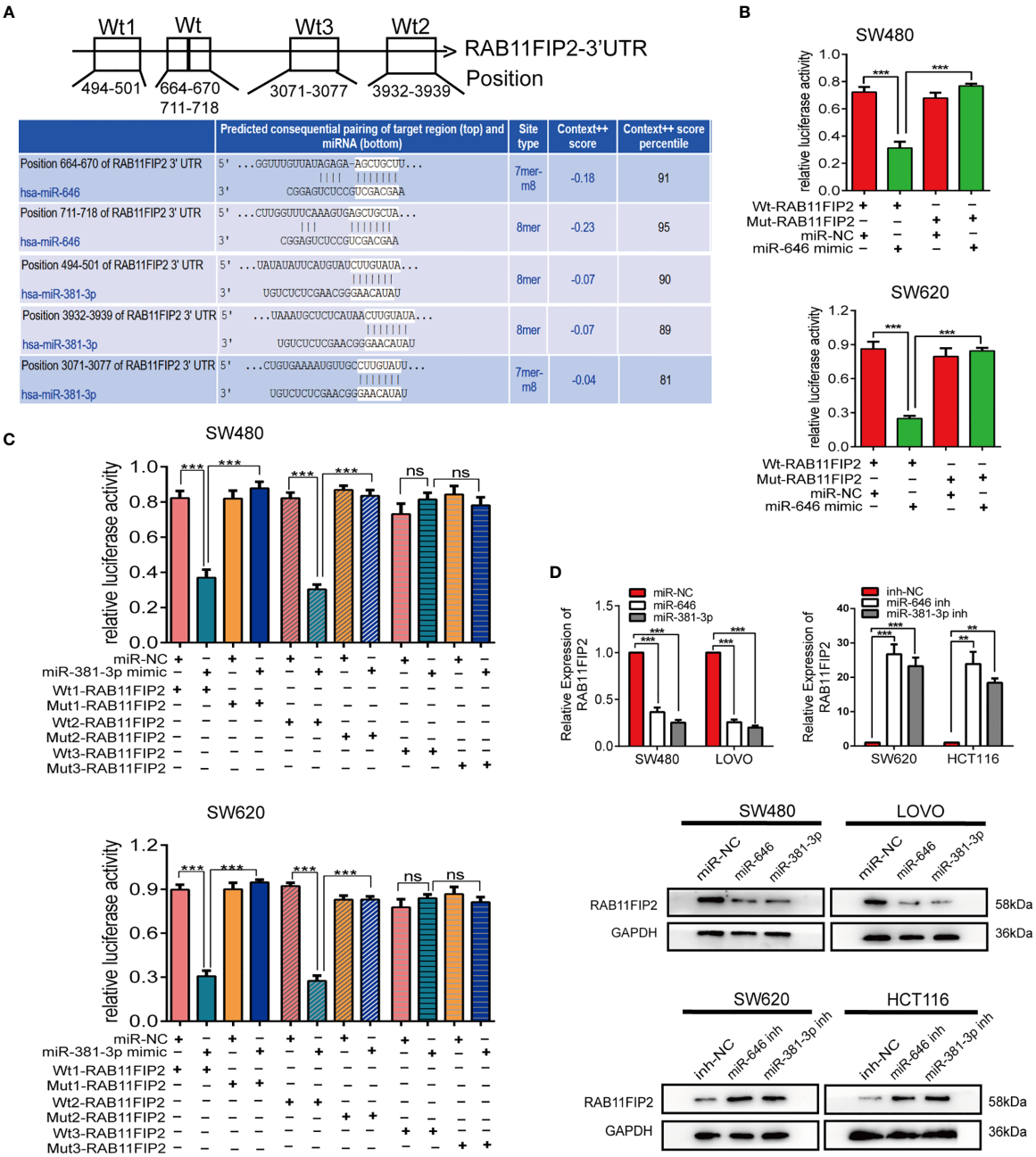

	Predicted consequential pairing of target region (top) and miRNA (bottom)	Site type	Context++ score	Context++ score percentile
Position 664-670 of RAB11FIP2 3' UTR hsa-miR-646	5' ...GGUUUGUUAUAGAGA-AGCUGCUU... 3' CGGAGUCUCCGUCGACGAA	7mer-m8	-0.18	91
Position 711-718 of RAB11FIP2 3' UTR hsa-miR-646	5' ...CUUGGUUUCAAAGUGAGCUGCUA... 3' CGGAGUCUCCGUCGACGAA	8mer	-0.23	95
Position 494-501 of RAB11FIP2 3' UTR hsa-miR-381-3p	5' ...UAUAUAUUCAUGUAUCUUGUAUA... 3' UGUCUCUCGAACGGGAACAUAU	8mer	-0.07	90
Position 3932-3939 of RAB11FIP2 3' UTR hsa-miR-381-3p	5' ...UAAAUGCUCUCAUAACUUGUAUA... 3' UGUCUCUCGAACGGGAACAUAU	8mer	-0.07	89
Position 3071-3077 of RAB11FIP2 3' UTR hsa-miR-381-3p	5' ...CUGUGAAAAUGUUGCCUUGUAUU... 3' UGUCUCUCGAACGGGAACAUAU	7mer-m8	-0.04	81

FIGURE 4 | miR-646 and miR-381-3p co-target and negatively regulate RAB11FIP2. **(A)** Predicted binding sites of miR-646 and miR-381-3p on the RAB11FIP2 3'UTR sequence. The white nucleotides are the seed sequences of miR-646 and miR-381-3p. **(B, C)** Luciferase activities were measured in CRC cells co-transfected with a luciferase reporter containing the wild-type RAB11FIP2 3'UTR and miR-646 and miR-381-3p mimics or the mutant RAB11FIP2 3'UTR. Data are presented as the relative ratio of Renilla luciferase activity and firefly luciferase activity. **(D)** The relative expression levels of RAB11FIP2 in CRC cells transfected with miR-646 and miR-381-3p mimics or inhibitors were determined by qRT-PCR and WB. Error bars represent the means ± SD of 3 independent experiments. ns, no significance; $^{**}p < 0.01$; $^{***}p < 0.001$.

and progression of CRC through the same pathway (22). For this reason, we wondered whether CASC11 involved in the growth and metastasis of CRC through the PI3K/AKT pathway. It was thus determined that, compared to the control vector, the CASC11 overexpression group promoted the phosphorylation of PI3K and AKT (p-PI3K and p-AKT), while treatment with the PI3K inhibitor LY294002 restrained the above effect of CASC11 overexpression (**Figure 6A**). CASC11 knockdown reduced p-PI3K and p-AKT, which could be restored by the miR-646 and miR-381-3p inhibitors (**Figure 6B**). Moreover, miR-646 and miR-381-3p mimics partly

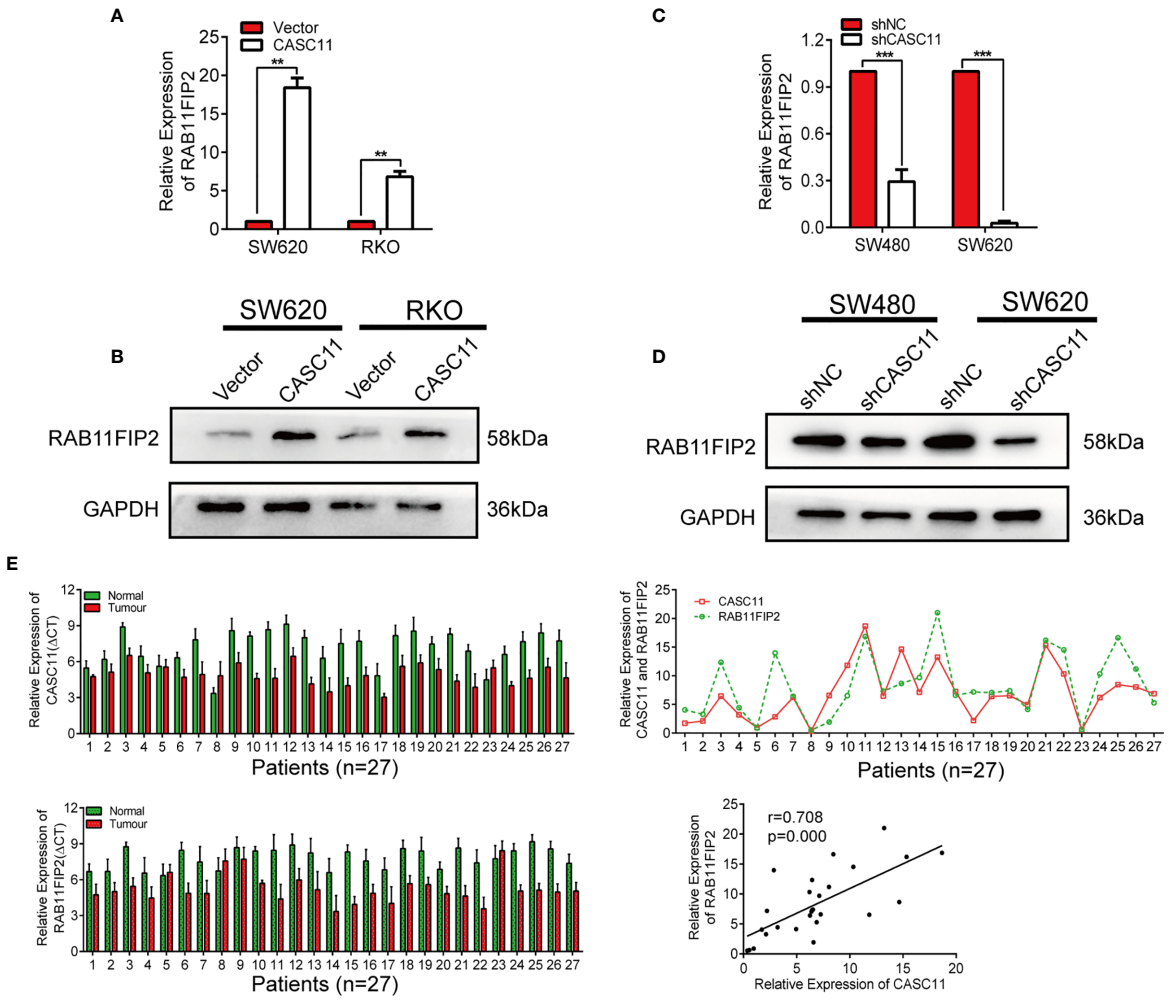

FIGURE 5 | CASC11 positively regulated RAB11FIP2 expression in CRC cells. **(A-D)** The relative expression levels of RAB11FIP2 in CRC cells transfected with CASC11 overexpression or interference reagents were determined by qRT-PCR and WB. **(E)** Expression of CASC11 and RAB11FIP2 in CRC tissues and the relationship between them (n=27). Left panel, qRT-PCR analysis of CASC11 and RAB11FIP2 expression in 27 paired human CRC tissues and adjacent normal tissues. Right panel, spearman correlation analysis showed a positive relationship between CASC11 expression levels and RAB11FIP2 mRNA levels in 27 CRC tissue samples. Error bars represent the means ± SD of 3 independent experiments. $^{**}p < 0.01$; $^{***}p < 0.001$.

reversed the increase in p-PI3K and p-AKT caused by CASC11 overexpression (**Figure 6C**). No significant change was noted in total PI3K and AKT (T-PI3K and T-AKT) under any condition. IF revealed that CASC11 interference reduced RAB11FIP2 and p-AKT levels compared with the control treatment, and this effect could be restored by the addition of the miR-646 and miR-381-3p inhibitors (**Figures 6D, E**). In summary, these data suggested that CASC11 played an important role in regulating PI3K/AKT pathway by miR-646 and miR-381-3p/RAB11FIP2 axis.

DISCUSSION

In this study, we found that miR-646 and miR-381-3p bind not only to CASC11 but also to the RAB11FIP2 3'UTR. The expression levels of CASC11 and RAB11FIP2 in CRC tissues were found to be higher than those in para-cancerous tissues and were positively correlated. miR-646 and miR-381-3p reversed CASC11-mediated phenotypes of CRC progression and restored the regulatory effects of CASC11 on RAB11FIP2 and the phosphorylation levels of the PI3K/AKT pathway.

Several past studies have reported that, as an oncogene, CASC11 participates in various biological processes of malignant tumours. For instance, CASC11 is highly expressed in gastric cancer tissues and is involved in the promotion of the growth, invasion, and metastasis of gastric cancer *via* the CASC11/miR-340-5p/CDK1 axis (12). In addition, CASC11 is highly expressed in liver cancer cells and promotes liver cancer progression by activating the PI3K/AKT pathway (13). Moreover, CASC11 targets the miR-498/FOXO3 axis and accelerates the proliferation and cell cycle progression of non-small-cell lung cancer (23). However, CASC11 is rarely reported

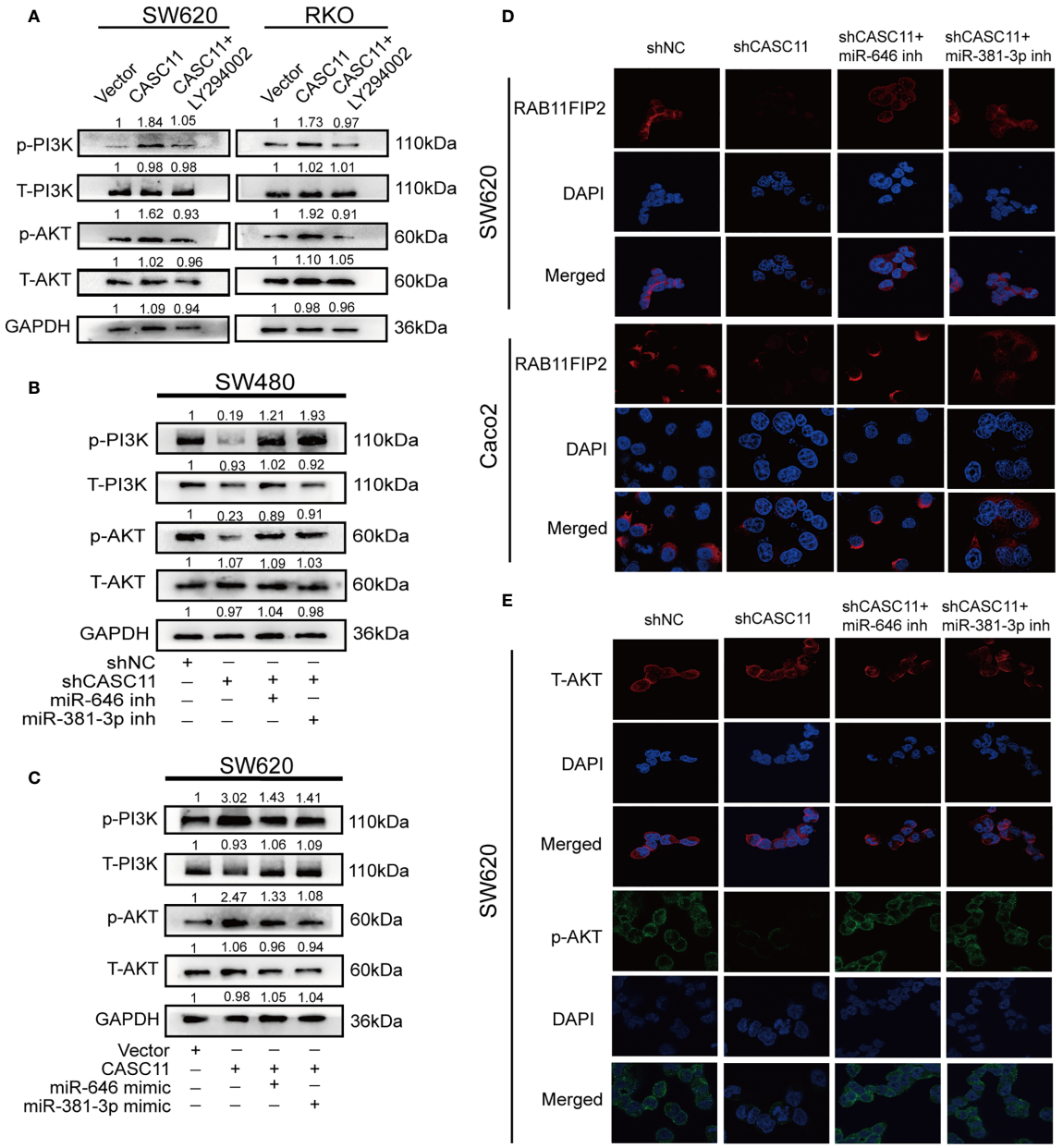

FIGURE 6 | CASC11 is a PI3K/AKT signalling pathway regulator in CRC cells. **(A)** The levels of the main molecules of the PI3K/AKT pathway in CRC cells transfected with CASC11 overexpression, followed by treatment with LY294002. **(B)** The main molecules of the PI3K/AKT pathway in CRC cells co-transfected with shCASC11 and the miR-646 or miR-381-3p inhibitor were analyzed. **(C)** The main molecules of the PI3K/AKT pathway in CRC cells co-transfected with CASC11 overexpression and miR-646 or miR-381-3p mimics were shown. **(D, E)** IF microscopy of the localization and expression of RAB11FIP2, AKT and p-AKT in CASC11-knockdown cells co-transfected with the miR-646 or miR-381-3p inhibitor.

in relation to CRC, with the only study reported by our group. We previously reported that CASC11 promotes CRC progression by binding to the HNRNPK protein and activating the Wnt/β-catenin pathway (10). The present study first discovered that CASC11 acts as a ceRNA and competes with RAB11FIP2 to bind to miR-646 and miR-381-3p and ultimately modulate CRC proliferation and metastasis.

ceRNAs refer to coding or non-coding RNAs that share sequence identity or similarity with mRNAs and competitively bind to miRNAs (7). The ceRNA mechanism was first reported by Poliseno et al., who showed that the pseudogene *PTENP1* is not translated into protein but rather acts as a molecular decoy of PTEN (24). LncRNAs are an important class of non-coding RNAs that function as ceRNAs. Linc-MD1 sponges miR-133

and miR-135 to regulate the transcription factors MAML1 and MEF2C, thus activating the expression of muscle differentiation-specific genes (25). LncRNA-KRTAP5-AS1 and lncRNA-TUBB2A can function as ceRNAs that bind miR-596 and miR-3620-3p and regulate Claudin-4 to promote the growth, metastasis, and epithelial-mesenchymal transition (EMT) of gastric cancer (26).

When acting as a ceRNA, one lncRNA molecule can bind with multiple miRNAs, and one miRNA can be targeted by multiple lncRNAs. miRNAs can be classified into cancer-promoting miRNAs, cancer-suppressing miRNAs, and dual-effect miRNAs (27, 28). This study confirmed that both miR-646 and miR-381-3p can site-specifically bind to CASC11. In addition, miR-646 and miR-381-3p are derived from human chromosomes 20 and 14, respectively, and their roles in tumours have been extensively reported. miR-646 has been indicated to function as a tumour suppressor in retinoblastoma (29), endometrial carcinoma (30), non-small-cell lung cancer (31), laryngeal squamous cell carcinoma (32), and CRC (33). miR-381-3p also functions as a tumour suppressor in non-small-cell lung cancer (34), oral squamous cell carcinoma (35), breast cancer (36), and cervical cancer (37). However, Zhao et al. (38) demonstrated that miR-381-3p can promote renal cell carcinoma by inhibiting apoptosis and necrosis. However, miR-381-3p has not been reported in CRC-related research. The present study revealed that miR-646 and miR-381-3p were significantly downregulated in CRC tissues and cells; subsequent functional assays *in vitro* and *in vivo* ascertained that the tumour-promoting effect of CASC11 could be cancelled by miR-646 and miR-381-3p in CRC; thus, miR-646 and miR-381-3p may function as tumour suppressors in CRC.

RAB11FIP2 is a member of the RAB11 family interacting proteins (RAB11-FIP) that plays crucial roles in tumour growth and metastasis (39). For example, Gidon et al. found that RAB11FIP2, acting as an element of the membrane platform, regulated the plasma membrane recycling of melanoma cells (40). It was reported that RAB11FIP2 was upregulated in gastric cancer tissues and that the overexpression of RAB11FIP2 facilitated the metastasis of gastric cancer (41). Dong et al. discovered that the overexpression of RAB11FIP2 may elevate the secretion of PAI-1, which results in the promotion of the proliferation, angiogenesis, and migration of CRC cells (42). Similarly, our study showed that RAB11FIP2, which is a mutual target of miR-646 and miR-381-3p, was highly expressed in CRC tissues and cells. CASC11 and RAB11FIP2 were positively regulated by each other. However, how RAB11FIP2 was causing an increase in CASC11 expression? After searching the relevant database, we found that there was no evidence that RAB11FIP2 could act as a transcription factor binding directly to CASC11 promoter. As RAB11FIP2 protein containing C2 domain and FIP domain has no DNA binding domain, it is impossible to bind directly to CASC11 promoter. In our work, RAB11FIP2 regulated PI3K/AKT signalling pathway. Our previous study found c-Myc directly bound to the promoter regions of CASC11 (10). Furthermore, it is widely accepted that the aberrant activation of PI3K/AKT signalling elevates c-Myc expression (43, 44). We speculated that RAB11FIP2 caused an increase in CASC11 expression by regulating PI3K/AKT/c-Myc signalling.

The PI3K/AKT pathway regulates cell proliferation, differentiation, apoptosis, and angiogenesis in CRC and various other tumour types (45). Han et al. reported that CASC11 can bind EZH2 and mediate PTEN silencing, which activates the PI3K/AKT pathway and promotes the progression of liver cancer (13). Xu et al. showed that RAB11FIP2 promotes CRC progression by upregulating MMP7 and activating the PI3K/AKT pathway (22). It could be inferred that CASC11 may play an important role in regulating PI3K/AKT pathway in CRC cells. We demonstrated in this study that interfering with CASC11 could reduce p-PI3K and p-AKT expression, which could be restored by the miR-646 and miR-381-3p inhibitors. Conversely, CASC11 overexpression increased p-PI3K and p-AKT levels, which could be restrained by

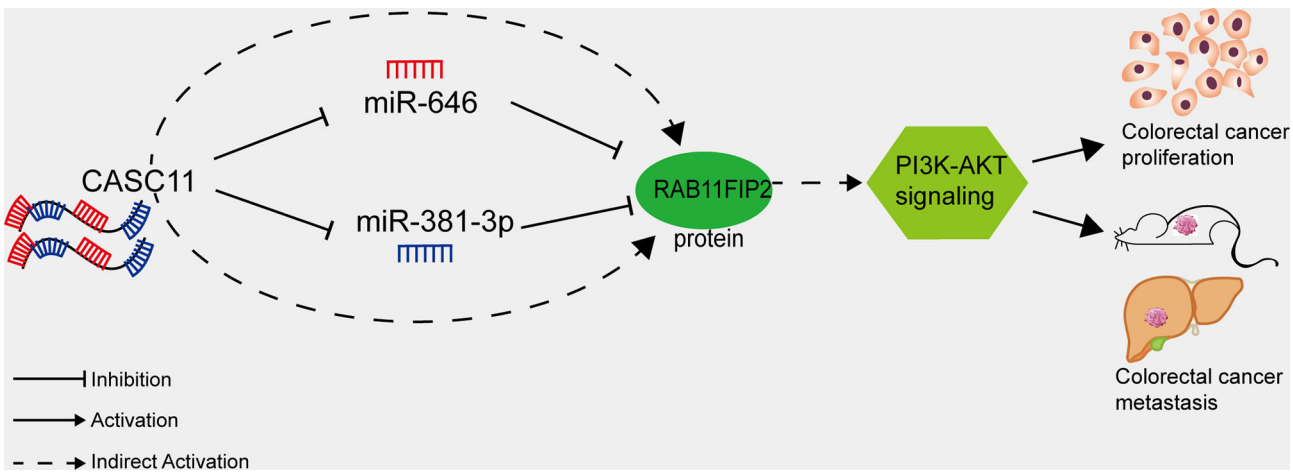

FIGURE 7 | Proposed model of how CASC11 regulates CRC proliferation and metastasis through the miR-646 and miR-381-3p/RAB11FIP2 axis.

miR-646 and miR-381-3p mimics. Our data thus suggest that CASC11 played an important role in regulating PI3K/AKT pathway by miR-646 and miR-381-3p/RAB11FIP2 axis in CRC cells (**Figure 7**).

CONCLUSION

In summary, in CRC, the lncRNA CASC11 acts not only as a tumour promoter that binds to related proteins and activates the Wnt/β-catenin pathway but also as a sponge of miR-646 and miR-381-3p to upregulate RAB11FIP2 and regulate the PI3K/AKT pathway, thus promoting CRC progression. Our previous and current research suggests that CASC11 is a potential biomarker and a promising therapeutic target of CRC. However, while our findings link CASC11 and RAB11FIP2 to the PI3K/AKT pathway, their mechanism in activating PI3K/AKT signalling needs to be further validated in depth.

DATA AVAILABILITY STATEMENT

The original contributions presented in the study are included in the article/**Supplementary Material**. Further inquiries can be directed to the corresponding author.

ETHICS STATEMENT

The studies involving human participants were reviewed and approved by the Ethics Agreement of Nanfang Hospital of Southern Medical University. The patients/participants provided their written informed consent to participate in this study. The animal study was reviewed and approved by the animal ethics committee of Southern Medical University. Written informed consent was obtained from the individual(s) for the publication of any potentially identifiable images or data included in this article.

AUTHOR CONTRIBUTIONS

XnL contributed to study design, obtaining funding, and study supervision. WZ carried out the experiments and wrote the manuscript. XmL contributed in data acquisition and statistics analysis. WjZ and YxL interpreted the results. WhL contributed in the collection of patient samples and data input. All authors contributed to the article and approved the submitted version.

FUNDING

This study was supported by the National Natural Science Foundation of China (grant numbers 81874074, 81672429, and 82072705).

ACKNOWLEDGMENTS

We sincerely thank the editor and the five reviewers for their valuable comments and suggestions.

SUPPLEMENTARY MATERIAL

The Supplementary Material for this article can be found online at: https://www.frontiersin.org/articles/10.3389/fonc.2021.657650/full#supplementary-material.

Supplementary Figure 1 | (A) qRT-PCR assay showed the expression of CASC11 in 8 cell lines. **(B)** Venn diagrams showing the intersection set of CASC11-binding miRNAs. **(C)** CASC11 in SW480 and SW620 cells after knockdown of CASC11 were detected by RT-qPCR. Treatment with miR-646 and miR-381-3p inhibitor successfully decreased the expression levels of miR-646 and miR-381-3p in SW620 and HCT116. **(D)** The overexpression of CASC11 in SW620 and RKO cells, miR-646 and miR-381-3p in SW480 and LOVO cells were confirmed by qRT-PCR. Error bars indicate the means ± SD of 3 independent experiments. $^{*}p < 0.05$; $^{**}p < 0.01$; $^{***}p < 0.001$.

Supplementary Figure 2 | miR-646 and miR-381-3p mimics reverse CASC11 overexpression-mediated phenotypes of CRC cell proliferation and migration *in vitro*. **(A, B)** Cell proliferation was assessed by CCK-8 assay and flow cytometry cell-cycle analysis in CASC11 overexpression RKO and SW620 cells. Error bars represent the means ± SD of 3 independent experiments. **(C, D)** Cell migration was analyzed by scratch wound assay and Transwell migration assay in CASC11 overexpression RKO and SW620 cells. Error bars represent the means ± SD of 3 independent experiments or 5 different fields, respectively. $^{*}p < 0.05$; $^{**}p < 0.01$; $^{***}p < 0.001$.

Supplementary Figure 3 | Selecting RAB11FIP2 as a mutual target gene of miR-646 and miR-381-3p. **(A)** Venn diagrams showing the intersection set of mutual target genes of miR-646 and miR-381-3p. **(B)** qRT-PCR assays showed expressions of RAB11FIP2, WEE1, RAB30, miR-646, and miR-381-3p in 8 cell lines. Spearman correlation analysis showed a negative relationship between RAB11FIP2 mRNA and the above two miRNAs. Error bars indicate the means ± SD of 3 independent experiments. $^{*}p < 0.05$; $^{**}p < 0.01$; $^{***}p < 0.001$.

Supplementary Figure 4 | RAB11FIP2 positively regulated CASC11 expression in CRC cells, and RAB11FIP2 knockdown can prohibit CRC cell proliferation and migration mediated by CASC11 overexpression. **(A, B)** The successful construction of siRAB11FIP2 cells was confirmed by qRT-PCR and WB. **(C)** The relative expressions of CASC11 in CRC cells transfected with siRAB11FIP2 by qRT-PCR. **(D)** miR-646 and miR-381-3p inhibitors rescued a decrease in RAB11FIP2 protein levels caused by CASC11 knockdown.**(E)** Immunohistochemical staining (IHC) evaluation of the expression of RAB11FIP2 in paraffin-embedded human CRC tissues and adjacent normal tissues (n=67). The error bars in all graphs represent the means ± SD of 3 different fields. **(F–H)** siRAB11FIP2 reverses CASC11 overexpression-mediated phenotypes of CRC cell proliferation and migration *in vitro*. Cell proliferation was assessed by CCK-8 assay, and cell migration was analyzed by scratch wound assay and Transwell migration assay. $^{*}p < 0.05$; $^{**}p < 0.01$; $^{***}p < 0.001$.

Supplementary Figure 5 | (A) qRT-PCR analysis of miR-646 and miR-381-3p expression in 27 paired CRC tissues. Left panel, the results were presented as the fold change in tumour tissues relative to the matched adjacent normal tissues. Right panel, comparison of miR-646 and miR-381-3p expression in 27 paired CRC tissues (T) and matched normal tissues (N). Error bars indicate the means ± SD of 3 independent experiments.

REFERENCES

1. Bray F, Ferlay J, Soerjomataram I, Siegel RL, Torre LA, Jemal A. Global cancer statistics 2018: GLOBOCAN estimates of incidence and mortality worldwide for 36 cancers in 185 countries. *CA Cancer J Clin* (2018) 68(6):394–424. doi: 10.3322/caac.21492
2. Esteller M. Non-coding RNAs in human disease. *Nat Rev Genet* (2011) 12 (12):861–74. doi: 10.1038/nrg3074
3. Carninci P, Kasukawa T, Katayama S, Gough J, Frith MC, Maeda N, et al. The transcriptional landscape of the mammalian genome. *Science* (2005) 309 (5740):1559–63. doi: 10.1126/science.1112014
4. Guttman M, Amit I, Garber M, French C, Lin MF, Feldser D, et al. Chromatin signature reveals over a thousand highly conserved large non-coding RNAs in mammals. *Nature.* (2009) 458(7235):223–7. doi: 10.1038/nature07672
5. Loayza-Puch F, Agami R. Lncing protein translation to metastasis. *EMBO J* (2013) 32(20):2657–8. doi: 10.1038/emboj.2013.210
6. Wang KC, Chang HY. Molecular mechanisms of long noncoding RNAs. *Mol Cell* (2011) 43(6):904–14. doi: 10.1016/j.molcel.2011.08.018
7. Salmena L, Poliseno L, Tay Y, Kats L, Pandolfi PP. A ceRNA hypothesis: the Rosetta stone of a hidden RNA language? *Cell* (2011) 146(3):353–8. doi: 10.1016/j.cell.2011.07.014
8. Li H, Cui Z, Lv X, Li J, Gao M, Yang Z, et al. Long Non-coding RNA HOTAIR Function as a Competing Endogenous RNA for miR-149-5p to Promote the Cell Growth, Migration, and Invasion in Non-small Cell Lung Cancer. *Front Oncol* (2020) 10:528520. doi: 10.3389/fonc.2020.528520
9. Liu B, Liu Q, Pan S, Huang Y, Qi Y, Li S, et al. The HOTAIR/miR-214/ST6GAL1 crosstalk modulates colorectal cancer procession through mediating sialylated c-Met via JAK2/STAT3 cascade. *J Exp Clin Cancer Res* (2019) 38(1):455. doi: 10.1186/s13046-019-1468-5
10. Zhang Z, Zhou C, Chang Y, Zhang Z, Hu Y, Zhang F, et al. Long non-coding RNA CASC11 interacts with hnRNP-K and activates the WNT/β-catenin pathway to promote growth and metastasis in colorectal cancer. *Cancer Lett* (2016) 376(1):62–73. doi: 10.1016/j.canlet.2016.03.022
11. Huppi K, Pitt JJ, Wahlberg BM, Caplen NJ. The 8q24 gene desert: an oasis of non-coding transcriptional activity. *Front Genet* (2012) 3:69. doi: 10.3389/fgene.2012.00069
12. Zhang L, Kang W, Lu X, Ma S, Dong L, Zou B. LncRNAs CASC11 promoted gastric cancer cell proliferation, migration and invasion in vitro by regulating cell cycle pathway. *Cell Cycle* (2018) 17(15):1886–900. doi: 10.1080/15384101.2018.1502574
13. Han Y, Chen M, Wang A, Fan X. STAT3-induced upregulation of lncRNAs CASC11 promotes the cell migration, invasion and epithelial-mesenchymal transition in hepatocellular carcinoma by epigenetically silencing PTEN and activating PI3K/AKT signaling pathway. *Biochem Biophys Res Commun* (2019) 508(2):472–9. doi: 10.1016/j.bbrc.2018.11.092
14. Jin J, Zhang S, Hu Y, Zhang Y, Guo C, Feng F. SP1 induced lncRNAs CASC11 accelerates the glioma tumorigenesis through targeting FOXK1 via sponging miR-498. *BioMed Pharmacother.* (2019) 116:108968. doi: 10.1016/j.biopha.2019.108968
15. Zhou C, Liu G, Wang L, Lu Y, Yuan L, Zheng L, et al. MiR-339–5p regulates the growth, colony formation and metastasis of colorectal cancer cells by targetizng PRL-1. *PloS One* (2013) 8(5):e63142. doi: 10.1371/journal.pone.0063142
16. Chen FB, Wu P, Zhou R, Yang QX, Zhang X, Wang RR, et al. LINC01315 Impairs microRNA-211-Dependent DLG3 Downregulation to Inhibit the Development of Oral Squamous Cell Carcinoma. *Front Oncol* (2020) 10:556084. doi: 10.3389/fonc.2020.556084
17. Li X, Wang J, Zhang C, Lin C, Zhang J, Zhang W, et al. Circular RNA circITGA7 inhibits colorectal cancer growth and metastasis by modulating the Ras pathway and upregulating transcription of its host gene ITGA7. *J Pathol* (2018) 246(2):166–79. doi: 10.1002/path.5125
18. Riffo-Campos ÁL, Riquelme I, Brebi-Mieville P. Tools for Sequence-Based miRNA Target Prediction: What to Choose? *Int J Mol Sci* (2016) 17(12):1987. doi: 10.3390/ijms17121987
19. Wang Y, Jiang Y, Chen L. Role of miR-218-GREM1 axis in epithelial-mesenchymal transition of oral squamous cell carcinoma: An in vivo and vitro study based on microarray data. *J Cell Mol Med* (2020) 24(23):13824–36. doi: 10.1111/jcmm.15972
20. Zhang W, Lu Y, Li X, Zhang J, Lin W, Zhang W, et al. IPO5 promotes the proliferation and tumourigenicity of colorectal cancer cells by mediating RASAL2 nuclear transportation. *J Exp Clin Cancer Res* (2019) 38(1):296. doi: 10.1186/s13046-019-1290-0
21. Chen F, Qi S, Zhang X, Wu J, Yang X, Wang R. lncRNAs PLAC2 activated by H3K27 acetylation promotes cell proliferation and invasion via the activation of Wnt/β – catenin pathway in oral squamous cell carcinoma. *Int J Oncol* (2019) 54(4):1183–94. doi: 10.3892/ijo.2019.4707
22. Xu CL, Wang JZ, Xia XP, Pan CW, Shao XX, Xia SL, et al. Rab11-FIP2 promotes colorectal cancer migration and invasion by regulating PI3K/AKT/MMP7 signaling pathway. *Biochem Biophys Res Commun* (2016) 470(2):397–404. doi: 10.1016/j.bbrc.2016.01.031
23. Yan R, Jiang Y, Lai B, Lin Y, Wen J. The positive feedback loop FOXO3/CASC11/miR-498 promotes the tumorigenesis of non-small cell lung cancer. *Biochem Biophys Res Commun* (2019) 519(3):518–24. doi: 10.1016/j.bbrc.2019.08.136
24. Poliseno L, Salmena L, Zhang J, Carver B, Haveman WJ, Pandolfi PP. A coding-independent function of gene and pseudogene mRNAs regulates tumour biology. *Nature* (2010) 465(7301):1033–8. doi: 10.1038/nature09144
25. Cesana M, Cacchiarelli D, Legnini I, Santini T, Sthandier O, Chinappi M, et al. A long noncoding RNA controls muscle differentiation by functioning as a competing endogenous RNA. *Cell.* (2011) 147(2):358–69. doi: 10.1016/j.cell.2011.09.028
26. Song YX, Sun JX, Zhao JH, Yang YC, Shi JX, Wu ZH, et al. Non-coding RNAs participate in the regulatory network of CLDN4 via ceRNA mediated miRNA evasion. *Nat Commun* (2017) 8(1):289. doi: 10.1038/s41467-017-00304-1
27. Yoon JH, Abdelmohsen K, Gorospe M. Functional interactions among microRNAs and long noncoding RNAs. *Semin Cell Dev Biol* (2014) 34:9–14. doi: 10.1016/j.semcdb.2014.05.015
28. Thomson DW, Dinger ME. Endogenous microRNA sponges: evidence and controversy. *Nat Rev Genet* (2016) 17(5):272–83. doi: 10.1038/nrg.2016.20
29. Zhang L, Wu J, Li Y, Jiang Y, Wang L, Chen Y, et al. Circ0000527 promotes the progression of retinoblastoma by regulating miR-646/LRP6 axis. *Cancer Cell Int* (2020) 20:301. doi: 10.1186/s12935-020-01396-4
30. Liu Y, Chen S, Zong ZH, Guan X, Zhao Y. CircRNA WHSC1 targets the miR-646/NPM1 pathway to promote the development of endometrial cancer. *J Cell Mol Med* (2020) 24(12):6898–907. doi: 10.1111/jcmm.15346
31. Wang J, Shu H, Guo S. MiR-646 suppresses proliferation and metastasis of non-small cell lung cancer by repressing FGF2 and CCND2. *Cancer Med* (2020) 9(12):4360–70. doi: 10.1002/cam4.3062
32. Zang Y, Li J, Wan B, Tai Y. circRNA circ-CCND1 promotes the proliferation of laryngeal squamous cell carcinoma through elevating CCND1 expression via interacting with HuR and miR-646. *J Cell Mol Med* (2020) 24(4):2423–33. doi: 10.1111/jcmm.14925
33. Dai H, Hou K, Cai Z, Zhou Q, Zhu S. Low-level miR-646 in colorectal cancer inhibits cell proliferation and migration by targeting NOB1 expression. *Oncol Lett* (2017) 14(6):6708–14. doi: 10.3892/ol.2017.7032
34. Zhang PF, Pei X, Li KS, Jin LN, Wang F, Wu J, et al. Correction to: Circular RNA circFGFR1 promotes progression and anti-PD-1 resistance by sponging miR-381-3p in non-small cell lung cancer cells. *Mol Cancer* (2020) 19(1):21. doi: 10.1186/s12943-020-1131-y
35. Yang X, Ruan H, Hu X, Cao A, Song L. miR-381-3p suppresses the proliferation of oral squamous cell carcinoma cells by directly targeting FGFR2. *Am J Cancer Res* (2017) 7(4):913–22.
36. Pan Z, Ding J, Yang Z, Li H, Ding H, Chen Q. LncRNAs FLVCR1-AS1 promotes proliferation, migration and activates Wnt/β-catenin pathway through miR-381-3p/CTNNB1 axis in breast cancer. *Cancer Cell Int* (2020) 20:214. doi: 10.1186/s12935-020-01247-2
37. Shang A, Zhou C, Bian G, Chen W, Lu W, Wang W, et al. miR-381-3p restrains cervical cancer progression by downregulating FGF7. *J Cell Biochem* (2019) 120(1):778–89. doi: 10.1002/jcb.27438
38. Zhao C, Zhou Y, Ran Q, Yao Y, Zhang H, Ju J, et al. MicroRNA-381-3p Functions as a Dual Suppressor of Apoptosis and Necroptosis and Promotes Proliferation of Renal Cancer Cells. *Front Cell Dev Biol* (2020) 8:290. doi: 10.3389/fcell.2020.00290

39. Hales CM, Vaerman JP, Goldenring JR. Rab11 family interacting protein 2 associates with Myosin Vb and regulates plasma membrane recycling. *J Biol Chem* (2002) 277(52):50415–21. doi: 10.1074/jbc.M209270200
40. Gidon A, Bardin S, Cinquin B, Boulanger J, Waharte F, Heliot L, et al. A Rab11A/myosin Vb/Rab11-FIP2 complex frames two late recycling steps of langerin from the ERC to the plasma membrane. *Traffic* (2012) 13(6):815–33. doi: 10.1111/j.1600-0854.2012.01354.x
41. Dong W, Qin G, Shen R. Rab11-FIP2 promotes the metastasis of gastric cancer cells. *Int J Cancer* (2016) 138(7):1680–8. doi: 10.1002/ijc.29899
42. Dong W, Wu X. Overexpression of Rab11-FIP2 in colorectal cancer cells promotes tumor migration and angiogenesis through increasing secretion of PAI-1. *Cancer Cell Int* (2018) 18:35. doi: 10.1186/s12935-018-0532-0
43. Welcker M, Orian A, Jin J, Grim JE, Harper JW, Eisenman RN, et al. The Fbw7 tumor suppressor regulates glycogen synthase kinase 3 phosphorylation-dependent c-Myc protein degradation. *Proc Natl Acad Sci USA* (2004) 101:9085–90. doi: 10.1073/pnas.0402770101
44. Tsai WB, Aiba I, Long Y, Lin HK, Feun L, Savaraj N, et al. Activation of Ras/PI3K/ERK pathway induces c-Myc stabilization to upregulate argininosuccinate synthetase, leading to arginine deiminase resistance in melanoma cells. *Cancer Res* (2012) 72:2622–33. doi: 10.1158/0008-5472.CAN-11-3605
45. Koveitypour Z, Panahi F, Vakilian M, Peymani M, Seyed Forootan F, Nasr Esfahani MH, et al. Signaling pathways involved in colorectal cancer progression. *Cell Biosci* (2019) 9:97. doi: 10.1186/s13578-019-0361-4

Conflict of Interest: The authors declare that the research was conducted in the absence of any commercial or financial relationships that could be construed as a potential conflict of interest.

frontiers in Oncology

REVIEW
published: 20 April 2021
doi: 10.3389/fonc.2021.653717

Circular RNAs and Hepatocellular Carcinoma: New Epigenetic Players With Diagnostic and Prognostic Roles

Kedeerya Aishanjiang[1,2†], Xin-dong Wei[3†], Yi Fu[1], Xinjie Lin[1], Yujie Ma[1], Jiamei Le[1], Qiuqin Han[1], Xuan Wang[3], Xiaoni Kong[4], Jinyang Gu[2*] and Hailong Wu[1,5,6*]*

[1] Shanghai University of Medicine and Health Sciences Affiliated Zhoupu Hospital, Department of Collaborative Innovation Center for Biomedicine, Shanghai, China, [2] Department of Transplantation, Xinhua Hospital Affiliated to Shanghai Jiao Tong University School of Medicine, Shanghai, China, [3] Department of General Surgery, The 81st Hospital Affiliated to Nanjing University of Traditional Chinese Medicine, Nanjing, China, [4] Institute of Clinical Immunology, Department of Liver Diseases, Central Laboratory, ShuGuang Hospital Affiliated to Shanghai University of Traditional Chinese Medicine, Shanghai, China, [5] Shanghai Key Laboratory of Molecular Imaging, Shanghai University of Medicine and Health Sciences, Shanghai, China, [6] Collaborative Innovation Center for Biomedicine, Shanghai University of Medicine & Health Sciences, Shanghai, China

Hepatocellular carcinoma (HCC) is one of the leading causes of cancer-related death worldwide. Due to the lack of potent diagnosis and prognosis biomarkers and effective therapeutic targets, the overall prognosis of survival is poor in HCC patients. Circular RNAs (circRNAs) are a class of novel endogenous non-coding RNAs with covalently closed loop structures and implicated in diverse physiological processes and pathological diseases. Recent studies have demonstrated the involvement of circRNAs in HCC diagnosis, prognosis, development, and drug resistance, suggesting that circRNAs may be a class of novel targets for improving HCC diagnosis, prognosis, and treatments. In fact, some artificial circRNAs have been engineered and showed their therapeutic potential in treating HCV infection and gastric cancer. In this review, we introduce the potential of circRNAs as biomarkers for HCC diagnosis and prognosis, as therapeutic targets for HCC treatments and discuss the challenges in circRNA research and chances of circRNA application.

Keywords: circular RNAs, hepatocellular carcinoma, biomarkers for diagnosis and prognosis, oncogenic circRNAs, tumor suppressive circRNAs, drug resistance

OPEN ACCESS

Edited by:
Rongxin Zhang, Guangdong Pharmaceutical University, China

Reviewed by:
Hamed Mirzaei, Kashan University of Medical Sciences, Iran
Aijuan Qu, Capital Medical University, China

***Correspondence:**
Hailong Wu
wuhl@sumhs.edu.cn
Jinyang Gu
gjynyd@126.com
Xiaoni Kong
xiaoni-kong@126.com

†These authors have contributed equally to this work

Specialty section:
This article was submitted to Gastrointestinal Cancers, a section of the journal Frontiers in Oncology

Received: *15 January 2021*
Accepted: *22 March 2021*
Published: *20 April 2021*

Citation:
Aishanjiang K, Wei X-d, Fu Y, Lin X, Ma Y, Le J, Han Q, Wang X, Kong X, Gu J and Wu H (2021) Circular RNAs and Hepatocellular Carcinoma: New Epigenetic Players With Diagnostic and Prognostic Roles. Front. Oncol. 11:653717. doi: 10.3389/fonc.2021.653717

Abbreviations: AFP, alpha-fetoprotein; AFP-L3, alpha-fetoprotein-L3; AJCC, the American Joint Committee on Cancer; ANL, adjacent noncancerous liver; AUC, Area Under Curve; BCLC, the Barcelona Clinic Liver Cancer; CCAR1, cell cycle and apoptosis regulator 1; CH, chronic hepatitis; CHC, chronic hepatitis C; circRNAs, Circular RNAs; CLIP, the Cancer of the Liver Italian Program; CSF-1, colony-stimulating factor 1; CXCL10, C-X-C motif chemokine ligand 10; DCP, Des-gamma-carboxy prothrombin; DECs, differentially expressed Circular RNAs; DPP4, SNAIL-mediated Dipeptidyl 4; FMBP, fragile X mental retardation protein; HCC, Hepatocellular carcinoma; HCV, Hepatitis C Virus; HNF4a, hepatocyte nuclear factor 4 alpha; LT, liver transplantation; MAPK1, mitogen-activated protein kinase 1; NOR1, Oxidored-nitro domain-containing protein 1; OS, Overall Survival; RFS, relapse-free survival; TMA, tissue microarray; Cdr1as, Cerebellar degeneration-related protein 1 antisense RNA; HUVECs, human umbilical vein endothelial cells; AKT3, AKT serine/threonine kinase 3.

INTRODUCTION

Hepatocellular carcinoma (HCC) is ranked as the sixth most common neoplasm and the third leading cause of cancer-related death worldwide (1). Curative treatments, including liver transplantation, liver resection, and ablation, are only available for early stage HCCs. But due to the absence of specific symptoms at early stages and the lack of early diagnostic biomarkers, most HCC patients are diagnosed at an advanced stage and not eligible for curative treatments (2). So far, the tyrosine kinase inhibitors (sorafenib and lenvatinib) and the combination of atezolizumab (an anti–PD-L1 antibody) with bevacizumab (a vascular endothelial growth factor inhibitor) are the only approved first-line systemic treatment for advanced HCCs (3–5). Moreover, although 5-year overall survival (OS) rate reaches up to 50%, recurrence occurs in more than 70% HCC patients after curative surgery (6), which severely impairs the prognosis of HCCs. Therefore, development of early diagnostic and/or prognostic biomarkers and identification of novel therapeutic targets are urgently required for improving HCC outcomes.

Circular RNAs (circRNAs) are a novel class of non-coding RNAs generated from back-splicing of pre-mature transcripts by forming covalently closed loop structures without 5′-caps or 3′-polyadenylated tails (7, 8) (**Figure 1**). Although most circRNAs were originally recognized as by-products of aberrant splicing (9), accumulating evidence has suggested their involvement in various physiological processes and pathological conditions, such as viral infection, sepsis, cardiovascular disease, diabetes, and aging and regenerative medicine (9–13). By functioning as miRNA sponges (14), acting as protein decoys, scaffolds and recruiters (15) or serving as RNA templates for short peptide synthesis (16), circRNAs play important roles in regulating gene expression and signaling transduction (8) (**Figure 1**).

Recent emerging evidence has demonstrated that circRNAs are closely associated with tumor initiation and progression (17–20). Firstly, deregulation of circRNAs has been confirmed in many types of cancers, including breast cancer (21, 22), lung cancer (23, 24), prostate cancer (25), colorectal cancer (26), gastrointestinal cancers (27), ovarian cancer (28), thyroid cancer (29), gynecologic cancers (30), and hepatocellular carcinoma (31); Secondly, some circRNAs have been demonstrated to play either oncogenic (32, 33) or tumor suppressive (34, 35) roles in affecting multiple cancer hallmarks, including deregulating cellular energetic, self-sufficiency in growth signals, insensitivity anti-growth signals, evading cell death, limitless replicative potential, substained angiogenesis, tissue invasion and metastasis (36, 37). Moreover, given the facts that circRNAs are more resistant to exoribonuclease degradation due to their lack of free 5′- and 3′-ends (38) and are abundant in body fluids, such as saliva, blood, and urine (39–41), they have been increasingly recognized as promising tumor biomarkers (42). This review introduces recently circRNAs identified with biomarker and therapeutic potentials for HCC diagnosis, prognosis and treatments, describes circRNAs related to drug resistance and discusses the challenges in circRNA research and chances of circRNA application.

CircRNAs AS NON-INVASIVE DIAGNOSIS BIOMARKERS OF HCCs

Early diagnosis is critical for the improvement of HCC prognosis and outcomes. The serum alpha-fetoprotein (AFP) (43), alpha-fetoprotein-L3 (AFP-L3) (44) and Des-gamma-carboxy prothrombin (DCP) (45) are the most commonly used non-invasive circulating biomarkers for HCC diagnosis in clinical practice, but limited evidence supports their contribution to HCC early detection or improvement in HCC outcomes (46). Therefore, identifying novel biomarkers for HCC early diagnosis is urgently required. CircRNAs are dysregulated in HCCs (47), and more resistant to nuclease degradation compared to linear RNAs due to their covalently closed loops (38), which make them potential biomarkers for HCC diagnosis. Here, we mainly introduce some recent studies indicating that circRNAs are promising non-invasive circulating diagnosis biomarkers of HCCs.

Zhang et al. demonstrated that circRNA_104075 was positively regulated by HNF4a, a HCC-promoting transcription factor, and highly expressed in HCC tissues and serum samples. CircRNA_104075 showed greater predictive performance (AUC: 0.973, sensitivity: 0.960; specificity: 0.983) for HCCs than AFP (AUC: 0.750, sensitivity: 0.693; specificity: 0.683), AFP-L3 (AUC: 0.766, sensitivity: 0.772; specificity: 0.633) and DCP (AUC: 0.771, sensitivity: 0.703; specificity: 0.750) (48).

By comparing the serum circRNA profiles between 36 healthy controls, 60 chronic hepatitis C (CHC) and 68 HCC patients, Matboli et al. found up-regulation of hsa_circ_000224 and down-regulation of hsa_circ_001565 and hsa_circ_000520 in the serum samples of HCC patients compared to those in healthy controls and CHC patients (49). The predictive performance for HCCs of hsa_circ_001565 (AUC: 0.839, sensitivity: 0.703; specificity: 0.750), hsa_circ_000520 (AUC: 0.943, sensitivity: 0.971; specificity: 0.896) and hsa_circ_000224 (AUC: 0.974, sensitivity: 0.956; specificity: 0.927) were better than that of serum AFP (AUC: 0.726, sensitivity: 0.779; specificity: 0.823) (49). Combing the three circRNAs showed remarkably high sensitivity (1.000) but did not improve the specificity (0.833). The authors failed to show the AUC value for the combined three circRNAs in diagnosing HCCs (49).

By analyzing differentially expressed circRNAs (DECs) in plasma between 40 healthy controls and 71 HCC patients, Sun et al. recently identified a three-circRNA signature, including hsa_circ_0004001, hsa_circ_0004123, and hsa_circ_0075792, which are highly expressed in HCC patients (50). This 3-circRNA signature showed a potent diagnosis value (AUC: 0.89, sensitivity: 0.905; specificity: 0.781) (50). In this study, the authors did not compared the diagnosis value of the 3-circRNA signature with that of AFP, but the AUC, sensitivity and specificity values of the 3-circRNA signature may slightly better than those of AFP from other studies (48, 49).

Comparison of circulating circRNAs, in 5 HCC patients before and after hepatectomy, 5 HBV-positive chronic hepatitis (CH) patients and 5 healthy controls, identified that the serum levels of hsa_circ_0009582, hsa_circ_0037120, and hsa_circ_0140117 were

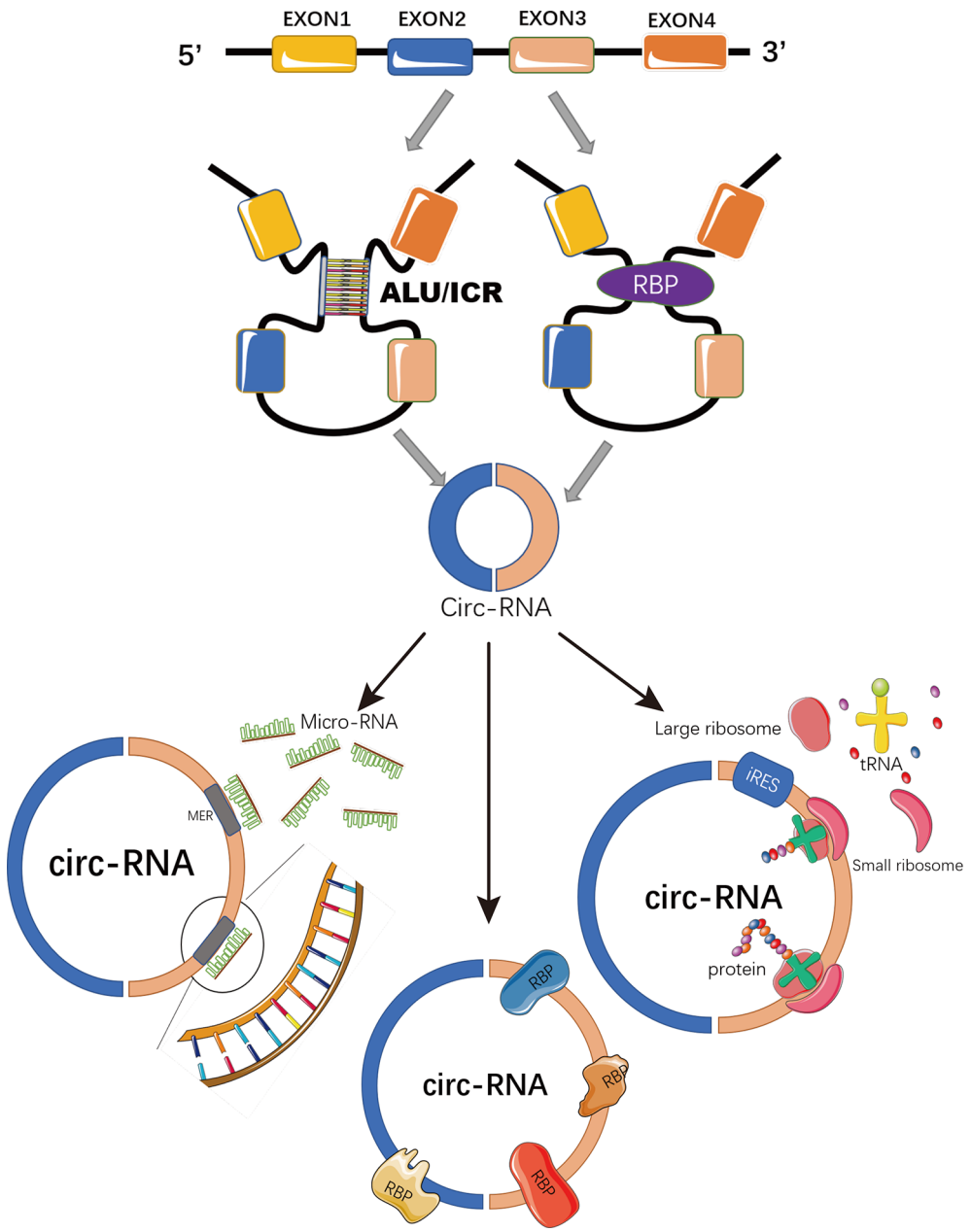

FIGURE 1 | Schematic representation of circRNA biogenesis and functions. CircRNAs are covalently closed loop structures generated by back-splicing of pre-mature transcripts mediated by either Alu repeats, inverted complementary repeats (ICR), or RNA binding proteins (RBP). CircRNAs could function as miRNA sponges to block miRNA-mediated inhibition on target genes; or as scaffolds, recruiters or decoys of some RNA binding proteins to regulate the function of the associated proteins. Some circRNAs containing IRES and ORFs serve as RNA template for translation.

high in HCCs and decreased after hepatectomy (51). Moreover, a combination of those three circRNAs with serum AFP greatly improved the diagnosis potential for HCC in a training set (20 HCCs vs. 20 CH patients; AUC: 0.988, sensitivity: 0.960; specificity: 1.015) and a validation set (180 HCCs vs. 180 CH patients; AUC: 0.955, sensitivity: 0.915; specificity: 0.994) (51).

Down-regulation of hsa_circ_0001445 (circSMARCA5) in HCCs was identified in 3 cohorts of 208 pairs of HCC and corresponding adjacent noncancerous liver (ANL) tissues, and circSMARCA5 overexpression inhibited HCC growth and metastasis *in vitro* and *in vivo* (52). By comparing plasma circSMARCA5 levels in 103 healthy controls, 117 hepatitis (hepatitis B and C), 143 cirrhosis and 135 HCC patients, Li et al. found that plasma circSMARCA5 decreases gradually but significantly from healthy controls, hepatitis, cirrhosis to HCC patients (53). It worth noting that, in patients whose AFP levels

were less than 200 ng/ml, circSMARCA5 showed satisfying accuracy in distinguishing HCCs from hepatitis (AUC = 0.847, sensitivity: 0.721; specificity: 0.882) and cirrhosis (AUC = 0.706, sensitivity: 0.721; specificity: 0.660) patients, suggesting circSMARCA5 as a putative biomarker for HCCs with low AFP levels (53).

Recently, a large-scale, multicenter study identified a plasma circRNA panel (CircPanel) containing three circRNAs (hsa_circ_0000976, hsa_circ_0007750, and hsa_circ_0139897), which had greater accuracy than AFP in distinguishing individuals with HCC from Non-HCC (54). The performance of CircPanel vs. AFP was AUC 0.863 *vs.* 0.790 (p=0.036) in the training set (53 healthy controls, 52 with CHB, 50 with liver cirrhosis and 158 with HCC), AUC 0.843 *vs.* 0.747 (p=0.011) in Validation Set 1 (152 HCC patients, 50 healthy controls, 54 CHB patients and 50 HBV-induced liver cirrhosis patients), and AUC 0.864 *vs.* 0.769 ($p<0.001$) in Validation Set 2 (290 HCC patients, 76 healthy controls, 80 CHB patients and 80 HBV-induced liver cirrhosis patients) (54). Moreover, CircPanel showed a higher accuracy than AFP in diagnosis of small-HCC (solitary, diameter ≤ 3 cm) (AUC of CircPanel *vs.* AFP: 0.862 *vs.* 0.680, $p=0.001$ in the training set; 0.838 *vs.* 0.699, $p=0.011$ in Validation Set 1 and 0.851 *vs.* 0.738, $p=0.009$ in Validation Set 2) (54). More significantly, CircPanel has been identified to be able to diagnose AFP-negative HCC and AFP-negative Small-HCC (54).

CircRNAs AS PROGNOSIS BIOMARKERS OF HCCs

Recurrence occurs in more than 70% HCC patients post curative surgery (6). Even for the most effective liver transplantation (LT), the recurrence rate is near 20% (55). Although the TNM staging system of the American Joint Committee on Cancer (AJCC), the Barcelona Clinic Liver Cancer (BCLC) classification, and the Cancer of the Liver Italian Program (CLIP) staging system, have been employed to evaluate the prognosis of HCC patients (56), their prognostic predictive performance was unsatisfactory partly because those assessments do not take the critical and complicated molecular pathogenesis of HCCs into account (57). Recent studies demonstrated that some circRNAs could serve as prognostic biomarkers for HCCs.

Hsa_circ_0000267 was up-regulated in HCC tumor tissues and positively associated aggressive clinicopathological features such as tumor size and TNM stage (58). Multivariable analysis identified enhanced hsa_circ_0000267 as an independent prognostic factor for the OS in HCC patients (58).

Chromosomal amplification at 7q21–7q31 was closely related to tumor recurrence in various types of cancers including HCCs (59–62). By assessing the expression of 43 putative circRNAs in this chromosomal region in 4 pairs of matched HCC and normal tissues, Huang et al. identified that hsa_circ_0082002 (circMET) was the most significantly and consistently up-regulated circRNA in HCCs (63). By evaluating circMET expression in 90 paired HCC and normal tissues and in a tissue microarray (TMA) consisting 209 HCC tissues, levels of circMET were significantly and positively correlated with microvascular invasion, absent tumor encapsulation, multiple tumors and late HCC stage. Multivariate analysis identified circMET as an independent predictor for both OS and postoperative recurrence in HCC patients (63).

Sun et al. have demonstrated that hsa_circ_0027345 (circLRIG3), a nucleus-enriched circRNA, was highly expressed in HCCs and positively associated with aggressive clinicopathological features, such as tumor size, vascular invasion, Edmondson's grade and later TNM stage, and was identified as an independent risk prognostic factor for OS in HCC patients (64).

The down-regulation of hsa_circ_0001727 (circZKSCAN1) in HCCs were determined by two independent groups (65, 66). Expression of circZKSCAN1 was associated with multiple clinicopathologic factors, such as tumor numbers, cirrhosis, vascular invasion, microscopic vascular invasion, or tumor grade (65), and was determined as an independent and significant factor affecting both OS and RFS in HCCs (66).

In addition to serving as a non-invasive biomarker, decreased expression of circSMARCA5 in HCC tumor tissues was significantly correlated with poorer tumor differentiation, more advanced tumor stage, larger tumor size and presence of microvascular invasion. Multivariate analysis demonstrated that circSMARCA5 expression level was an independent risk factor for OS and RFS in HCCs (52).

A recent study has demonstrated that an up-regulated plasma circRNA, hsa_cic_0005397, was positively correlated with tumor size (p = 0.020) and TNM stage (p = 0.006) (67). Meanwhile, a dynamic monitoring of plasma hsa_cic_0005397 in HCC patients who had undergone surgical resection revealed that plasma hsa_cic_0005397 level was drastically dropped in HCC patients after operation, but prominently elevated in recurrent or metastatic HCC patients, suggesting that plasma hsa_cic_0005397 could serve as a prognostic biomarker for post-operational recurrence and metastasis in HCC patients (67). Moreover, the plasma hsa_cic_0005397 level was negatively associated with OS in HCC patients (67).

However, due to the limited sample size and the lack of multicenter validation, the diagnosis and prognosis potential of those circRNAs should be further determined in the future.

ONCOGENIC AND TUMOR SUPPRESSIVE CircRNAs IN HCCs

Like many other non-coding RNAs, such as lncRNAs and miRNAs, circRNAs have been demonstrated to function as either oncogenes or tumor suppressors in HCCs.

By comparing circRNA expression profiles in primary HCCs with or without post-surgery pulmonary metastasis, Hu et al. identified that hsa_circ_0085616 (circASAP1) is highly expressed in HCCs with greater metastatic potential (31). Mechanistically, circASAP1 functions as a sponge for miR-326 and miR-532-5p and enhances the expression of CSF-1 and MAPK1, resulting in an increase in intra-tumor infiltration of tumor associated

macrophages and activation of the MAPK-ERK signaling pathway (31). Consistent with this study, Li et al. also demonstrated that circASAP1 plays an oncogenic role in HCCs possibly by activating the β-catenin, ERK and AKT signaling pathways (68).

Through bioinformatics analysis and experimental validation, Li et al. demonstrated that up-regulation of hsa_circ_0074854 (circMAT2B) in HCCs was correlated with poor prognosis and could serve as an independent prognostic factor (69). By functioning as a sponge of miR-338-3p, circMAT2B released miR-338-3p-mediated inhibition on PKM2, resulting in enhanced glycolysis, proliferation and metastasis in HCCs (69).

In addition to acting as a miRNA sponge, some circRNAs have been reported to function as protein decoys, scaffolds and recruiters to promote HCC progression. Wang et al. demonstrated that hsa_circ_102034 (circRHOT1) was highly expressed in HCCs and promoted proliferation, migration and invasion in HCC cells by acting as a protein recruiter to recruit TIP60 onto the promoter region of *NR2F6* to initiate *NR2F6* expression (70).

By performing a circRNA microarray assay specifically targeting human circRNA splicing sites in seven paired HCC tumor and normal samples, Han et al. demonstrated that hsa_circ_0007874 (circMTO1) was significantly decreased in HCCs and correlated with poor prognosis of HCC patients (71). CircMTO1 could serve as a miR-9 sponge to release miR-9–mediated inhibition on p21, resulting in inhibition on HCC growth both *in vitro* and *in vivo* (71).

Compared to oncogenic circRNAs, the tumor suppressive circRNAs are less studied probably due to their low expression in HCCs. Only countable circRNAs have been identified as tumor suppressors in HCCs. For example, circSMARCA5, a down-regulated circRNA in HCC, has been identified as a tumor suppressor for HCC progression. Over-expression of circSMARCA5 retained miR-17-3p and miR-181b-5p to release their common target, TIMP3, a well-known tumor suppressor in HCCs, resulting in enhanced HCC growth and metastasis both *in vitro* and *in vivo* (52, 72). By functioning as a decoy of fragile X mental retardation protein (*FMBP*), an RNA binding protein, circZKSCAN1 prevented the binding of FMBP with cell cycle and apoptosis regulator 1 (*CCAR1*) mRNA and in turn inhibited *CCAR1* expression and CCAR1-mediated activation of the Wnt/β-catenin signaling pathway, resulting in compromised stemness in HCC cells (66).

CircRNAs RELATED TO DRUG RESISTANCE IN HCCs

Advanced HCCs are not legible for curative treatments. Although chemotherapy, targeted therapy and immunotherapy are commonly employed for those advanced HCCs, the therapeutic efficacy is unsatisfied due to low objective response rate and acquired resistance (73–75). In addition to playing oncogenic or tumor suppressive roles in HCC progression, some circRNAs have been recently reported to be related to drug resistance in HCC treatments.

For HCC chemotherapy, hsa_circ_0001001 (circFBXO11), an up-regulated circRNA in HCCs, could serve as a sponge for miR-605 to induce FOXO3-mediated ABCB1 expression, resulting in HCC oxaliplatin resistance (76). CircRNA_101505 was down-regulated in cisplatin-resistant HCC tissues and cell lines, and over-expression of circRNA_101505 trapped miR-103 and relieved its target, oxidored-nitro domain-containing protein 1 (NOR1), a putative tumor suppressor in HCCs (77), consequently resulting in cisplatin sensitization (78).

For sorafenib-mediated targeted therapy, Wu et al. have identified thousands of deregulated circRNAs in sorafenib-resistant HCC cells compared to sorafenib-sensitive cells (79). Yang et al. have demonstrated that hsa_circ_0058124 (circFN1) was up-regulated in both sorafenib-resistant HCC tumor tissues and cell lines (80). Overexpression of circFN1 conferred HCC cell sorafenib resistance by restricting miR-1205–mediated E2F1 inhibition (80).

For PD1 antibody mediated immunotherapy, circMET has been demonstrated to confer HCC cells resistance to anti-PD1 treatment by enhancing the immunosuppressive tumor microenvironment (63). Mechanistically, circMET functions as a sponge of miR-30-5p to induce SNAIL-mediated Dipeptidyl 4 (DPP4) expression, resulting in degradation of CXCL10, an important chemokine promoting intra-tumor infiltration of effector T cells, and leading to subsequent resistance to anti-PD1 treatment (63).

EXOSOMAL CircRNAs IN HCC PROGRESSION

Exosome is a type of nano-sized secreted vesicles, which are present in all body fluids under both physiological and pathological conditions (81). By carrying various biomolecules, including proteins, nucleic acids, lipids, and transferring from one cell to another, exomes play an important role in mediating intercellular communication (81). In 2015, Li, et al. for the first time demonstrated the presence of abundant circRNAs in exosomes (82). By RNA-seq analysis, they demonstrated enrichment of circRNAs in exosome compared to producer cells (82). A number of exosomal circRNAs have been identified to function as either diagnosis/prognosis biomarkers or oncogenic/tumor suppressive factors in HCCs (83, 84). For example, an exosomal circRNA, hsa_circ_0070396, was identified as a better diagnostic biomarker than AFP in distinguishing HCCs from healthy controls (AUC: 0.8574 vs. 0.781), and differentiating early HCC patients (with BCLC are 0 or A) from advanced ones (with BCLC are B+C) (AUC: 0.7132 vs. 0.6535) (85). Higher circulating exosomal circAKT3 was identified in HCC patients compared to healthy controls, and positively correlated with tumor recurrence rates and mortality, suggesting that circAKT3 could serve as a prognostic biomarker of HCCs (86). A recent study has demonstrated that three exosomal circPTGR1 isoforms secreted from HCC cells with higher metastasis potential to promote the metastasis of HCC cells with lower metastasis potential *via* regulating the miR449a-

MET pathway (87). Su et al. have demonstrated that circRNA Cdr1as competitively bound to miR-1270 to upregulate AFP level, thereafter accelerating proliferative and migratory abilities of HCC cells (88). Meanwhile, exosome-transmitted circRNA Cdr1as stimulated malignant behaviors of surrounding normal cells and finally contributed to the progression of HCC (88). An interesting study showed that a pro-invasive exosomal circRNA-100338 secreted from HCC cells could transfer to HUVECs to affect cell proliferation, angiogenesis, permeability, and vasculogenic mimicry (VM) formation ability of HUVECs, and in turn promote HCC metastasis (89).

Instead of transporting exosomal circRNAs from HCC cells to surrounding normal cells, the exosomal circRNA can also be generated and transported from surrounding normal tissues to HCC cells, resulting in altered HCC progression. For example, an exosomal circRNA, circ-0051443, which was generated in normal cells and transferred to HCC cells, could inhibit HCC progression by competitive binding to miR-331-3p, resulting in enhanced apoptosis and cell cycle arrest in HCC cells (90).

It is clear that exosomal circular RNAs play a significant role in HCC progression. Therefore, identifying novel exosomal circRNAs and understanding their biological functions can not only help us better understand the new mechanisms of potential HCC development, but also improve the clinical diagnosis, prognosis and treatment of HCCs.

We have summarized all the circRNAs mentioned in this review in **Table 1**.

CHALLENGES AND CHANCES OF CircRNAs

With the advent of high-throughput sequencing and high-efficiency big data analysis, circular RNAs have been emerged as a novel class of non-coding RNAs in eukaryotes. Accumulating evidence indicates that circRNAs are novel non-coding players the involved in various biological processes and diseases. However, some fundamental questions regarding the function and regulation of circRNAs remain unknown.

First, the biological role of circRNAs is less defined. Only less than 3% (> 7000 circRNAs) of recorded circRNAs (295,526 circRNAs integrated from circBase, circNet, and circRNAdb) (91) were curated functional (92), which at least in part suggests that the most circRNAs may be the non-functional by-products of RNA splicing events. In a previous study, Guo et al. claimed that compared to mRNAs, most circRNAs are less abundant, less cell-type specific and less conserved (93). Moreover, ribosome profiling provides no evidence for their translation (93).

Second, serving as miRNA sponges may not be the general role of circRNAs. Although abundant studies support the role of circRNAs as miRNA sponges in regulating gene expression and executing their biological functions, the existence of numerous circRNAs in *P. falciparum* and *S. cerevisiae* (94, 95), who lack known siRNA and miRNA pathways, suggests that as miRNA sponges may not be a general role for most circRNAs. This is consistent with a previous study showing that there is no particular enrichment of AGO2 binding on exons involved in circRNAs compared to their neighboring linear exons (93).

Third, the *cis* and *trans* regulators for circRNAs remain illuminated. Some studies demonstrated that the significantly longer introns and the inverted repeat sequence bracketing the regions that produce circRNAs are essential *cis* regulators for circRNA formation in humans and flies (38, 96–98). Meanwhile, canonical splicing signals are required for the circularization of most circRNAs (93, 99), suggesting that canonical spliceosomal machinery may serve as *trans* regulators for circRNA formation. However, accumulating strong evidence indicates that the expression of circRNAs does not simply correlate with their linear host genes (100, 101), suggesting that circRNA formation is a complicated process which may be regulated by additional circRNA-specific *cis* and *trans* regulators.

Although it remains controversial on the general roles of circRNAs, most functional circRNAs identified so far have been demonstrated to serve as miRNA sponges in regulating gene expression. By employing this feature, some artificial circRNAs have been engineered to sequester miRNAs relevant in human disease and shown promising potential for application in molecular medicine and biology. For example, an artificial circRNA carrying an array of miRNA-122 binding sites could sequester liver specific miR-122 from HCV RNA, resulting in inhibition on HCV viral protein production and HCV replication (102). Liu et al. generated an artificial circRNA sponge for miR-21, an oncomiR in many types of cancers, to block miR-21–mediated proliferation in gastric carcinoma cells (103). Therefore, in companion of growing understanding of circRNAs, expended application of circRNAs could be established for both research and clinic purposes.

CONCLUSION AND PROSPECT

In summary, circRNAs are emerging as a class of novel non-coding RNAs participating diverse physiological processes and pathological conditions. Although it remains controversial on the general roles of circRNAs, accumulating evidence indicates that circRNAs are functional by serving as either miRNA sponges, protein decoys, or translational templates. Like other types of non-coding RNAs, deregulation of circRNAs has been demonstrated in HCCs. A number of deregulated circRNAs have been identified as either oncogenic or tumor suppressive regulators in HCC progression. Moreover, some deregulated circRNAs could serve as non-invasive circulating biomarkers for HCC early diagnosis with great specificity and sensitivity superior to clinically used serum AFP. Meanwhile, some circRNAs have been involved in drug resistance in HCC treatments. In this review, we summarized the recent findings of circRNAs in HCC diagnosis, prognosis, progression and drug resistance and proposed that circRNAs may have great potential to serve as novel biomarkers for HCC early diagnosis, prognosis and therapeutic targets for HCC treatments.

TABLE 1 | Summary of mentioned circRNAs with diagnosis, prognosis and therapeutic potential in HCCs.

Classification	CircRNA Symbols in Paper	Current circBase_ID	Host genes	Potential Application	Reference
Non-invasive diagnosis biomarkers	circRNA_104075	_	_	A serum biomarker for HCC diagnosis	(48)
	hsa_circ_001565	hsa_circ_0000064	*B4GALT2*	Serum biomarkers for HCC diagnosis	(49)
	hsa_circ_000520	hsa_circ_0000221	*VIM*		
	hsa_circ_000224	hsa_circ_0000737	*C17orf107*		
	_	hsa_circ_0004001, hsa_circ_0004123, hsa_circ_0075792	*CLK1* *ETV6* *KDM1B*	As a serum-derived three-circRNA signature for HCC diagnosis	(50)
	_	hsa_circ_0009582 hsa_circ_0037120 hsa_circ_0140117	*RERE* *RHBDF1* *CNKSR2*	As circulating biomarkers predicting the occurrence of HBV-related HCCs	(51)
	circSMARCA5	hsa_circ_0001445	*SMARCA5*	As a circulating biomarker to accurately distinguish HBV-related HCCs from hepatitis and cirrhosis patients with low AFP levels	(52, 53)
	CircPanel	hsa_circ_0000976 hsa_circ_0007750 hsa_circ_0139897	*HPCAL1* *RABGGTA* *MTM1*	Be able to diagnose AFP-negative HCC and AFP-negative Small-HCC	(54)
Prognosis Biomarkers	circSMARCA5	hsa_circ_0001445	*SMARCA5*	As an independent prognostic factor for the OS and RFS in HCC patients	(52)
	hsa_circ_0000267	hsa_circ_0000267	*FAM53B*	As an independent prognostic factor for the OS in HCC patients	(58)
	circMET	hsa_circ_0082002	*MET*	As an independent prognostic factor for the OS and RFS in HCC patients	(63)
	circLRIG3	hsa_circ_0027345	*LRIG3*	As an independent prognostic factor for the OS in HCC patients	(64)
	circZKSCAN1	hsa_circ_0001727	*ZKSCAN1*	As an independent prognostic factor for the OS and RFS in HCC patients	(65, 66)
	hsa_cic_0005397	hsa_cic_0005397	*RHOT1*	A prognostic biomarker for post-operational recurrence and metastasis in HCC patients	(67)
Oncogenic circRNAs	circASAP1	hsa_circ_0085616	*ASAP1*	Therapeutic target for HCC metastasis and immunotherapy	(31, 68)
	circMAT2B	hsa_circ_0074854	*MAT2B*	Therapeutic target for HCC progression	(69)
	circRHOT1	hsa_circ_102034	*RHOT1*	Therapeutic target for HCC progression	(70)
Tumor suppressive circRNAs	circMTO1	hsa_circ_0007874	*MTO1*	Therapeutic target for HCC progression	(71)
	circSMARCA5	hsa_circ_0001445	*SMARCA5*	Therapeutic target for HCC progression	(52, 72)
	circZKSCAN1	hsa_circ_0001727	*ZKSCAN1*	Therapeutic target for HCC progression	(66)
CircRNAs related to drug resistant	circMET	hsa_circ_0082002	*MET*	Therapeutic target for HCC anti-PD1 resistance	(63)
	circFBXO11	hsa_circ_0001001	*FBXO11*	Therapeutic target for HCC oxaliplatin resistance	(76)
	CircRNA_101505	hsa_circ_0002891	*PDIA3*	Therapeutic target for HCC cisplatin sensitization	(77)
	circFN1	hsa_circ_0058124	*FN1*	Therapeutic target for HCC sorafenib resistance	(80)
Exosomal CircRNAs	hsa_circ_0070396	hsa_circ_0070396,	*NUDT9*	A better diagnostic biomarker than AFP in distinguishing HCCs	(85)
	circAKT3	hsa_circ_0000199	*AKT3*	A prognostic biomarker of HCCs	(86)
	circPTGR1	hsa_circ_0008043 hsa_circ_0003731 hsa_circ_0088030	*PTGR1*	Promote the metastasis of HCC cells with lower metastasis potential	(87)
	CircRNA_Cdr1as	hsa_circ_0001946	*Cdr1as*	Accelerate proliferative and migratory abilities of HCC cells	(88)
	circRNA-100338	hsa_circ_0000130	*SNX27*	Promote HCC metastasis through regulating angiogenesis	(89)
	circ-0051443	hsa_circ_0051443	*TRAPPC6A*	Inhibit HCC progression by enhancing apoptosis and cell cycle arrest in HCC cells	(90)

Despite the advancements achieved in the circRNA field, several fundamental questions remain elusive. Given the fact that only a few percentage functional circRNAs (< 3%) were identified from the great circRNA popularity, whether circRNAs are a group of functional non-coding RNAs is still an open question. The existence of numerous circRNAs in species deficient with RNAi and miRNA pathways raises the question whether as miRNA sponges is the general role of circRNAs or just is an exception. Although some studies have demonstrated that the formation of circRNAs depends on the *cis* elements, such as the inverted repeats, and the *trans* regulators, such as spliceosomes, of linear host genes, the lack of correlation at expression levels and cell-type specificity between circRNAs and their linear host genes strongly suggests the existence of circRNA specific regulators. Therefore, novel techniques and concepts regarding those fundamental questions are warranted in the future to expand our understanding of circRNAs and improve our investigation on circRNAs.

AUTHOR CONTRIBUTIONS

KA, X-DW, YF, XL, YM, JL, XW, and QH performed extensive literature search and discussion. KA and X-DW drafted the manuscript. XK, JG, and HW edited the manuscript. All authors contributed to the article and approved the submitted version.

FUNDING

This work was supported by grants from the National Natural Science Foundation of China (31870905 to HW, 82072645 and 81772507 to JG, 82070633 and 81873582 to XK), the Scientific Program of Shanghai Municipal Health Commission (SHWJ2019211 to HW), the Shanghai Municipal Education Commission-Gaofeng Clinical Medicine Grant Support (No. 20191910), the Foundation for Shanghai Jiao Tong University

for SMC-morning Star Youth Scholars Program, the Clinical Research Plan of SHDC (SHDC2020CR3005A), the Program of Medical Engineering Cross Research Fund of Shanghai Jiao Tong University (YG2017MS50), Clinical innovation project of Xinhua Hospital Affiliated to Medical College of Shanghai Jiaotong University (19XHCR02A), "Teaching incentive plan" project of Xinhua Hospital Affiliated to Medical College of Shanghai Jiaotong University (XH001.006.010.020), National Health and Family Planning Commission medical and health science and technology development research center key projects (NHC2018RWS01007), the Construction project of Shanghai Key Laboratory of Molecular Imaging(18DZ2260400), Shanghai Municipal Education Commission (Class II Plateau Disciplinary Construction Program of Medical Technology of SUMHS, 2018-2020), and the Key Program of National Natural Science Foundation of China (grant 81830052).

REFERENCES

1. Bray F, Ferlay J, Soerjomataram I, Siegel RL, Torre LA, Jemal A. Global cancer statistics 2018: GLOBOCAN estimates of incidence and mortality worldwide for 36 cancers in 185 countries. *CA: Cancer J Clin* (2018) 68:394–424. doi: 10.3322/caac.21492
2. Ren Z, Li A, Jiang J, Zhou L, Yu Z, Lu H, et al. Gut microbiome analysis as a tool towards targeted non-invasive biomarkers for early hepatocellular carcinoma. *Gut* (2019) 68:1014–23. doi: 10.1136/gutjnl-2017-315084
3. Casak SJ, Donoghue M, Fashoyin-Aje L, Jiang X, Rodriguez L, Shen YL, et al. FDA Approval Summary: Atezolizumab plus bevacizumab for the treatment of patients with advanced unresectable or metastatic hepatocellular carcinoma. *Clin Cancer Res Off J Am Assoc Cancer Res* (2021) 27(7):1836–41. doi: 10.1158/1078-0432.CCR-20-3407
4. Cheng AL, Kang YK, Chen Z, Tsao CJ, Qin S, Kim JS, et al. Efficacy and safety of sorafenib in patients in the Asia-Pacific region with advanced hepatocellular carcinoma: a phase III randomised, double-blind, placebo-controlled trial. *Lancet Oncol* (2009) 10:25–34. doi: 10.1016/S1470-2045(08)70285-7
5. Llovet JM, Ricci S, Mazzaferro V, Hilgard P, Gane E, Blanc JF, et al. Sorafenib in advanced hepatocellular carcinoma. *New Engl J Med* (2008) 359:378–90. doi: 10.1056/NEJMoa0708857
6. Sherman M. Recurrence of hepatocellular carcinoma. *New Engl J Med* (2008) 359:2045–7. doi: 10.1056/NEJMe0807581
7. Chen L, Huang C, Wang X, Shan G. Circular RNAs in Eukaryotic Cells. *Curr Genomics* (2015) 16:312–8. doi: 10.2174/1389202916666150707161554
8. Salzman J. Circular RNA Expression: Its Potential Regulation and Function. *Trends Genet TIG* (2016) 32:309–16. doi: 10.1016/j.tig.2016.03.002
9. Han B, Chao J, Yao H, Circular RNA. and its mechanisms in disease: From the bench to the clinic. *Pharmacol Ther* (2018) 187:31–44. doi: 10.1016/j.pharmthera.2018.01.010
10. Braicu C, Zimta AA, Gulei D, Olariu A, Berindan-Neagoe I. Comprehensive analysis of circular RNAs in pathological states: biogenesis, cellular regulation, and therapeutic relevance. *Cell Mol Life Sci CMLS* (2019) 76:1559–77. doi: 10.1007/s00018-019-03016-5
11. Qu S, Zhong Y, Shang R, Zhang X, Song W, Kjems J, et al. The emerging landscape of circular RNA in life processes. *RNA Biol* (2017) 14:992–9. doi: 10.1080/15476286.2016.1220473
12. Hashemian SM, Pourhanifeh MH, Fadaei S, Velayati AA, Mirzaei H, Hamblin MR. Non-coding RNAs and Exosomes: Their Role in the Pathogenesis of Sepsis. *Mol Ther Nucleic Acids* (2020) 21:51–74. doi: 10.1016/j.omtn.2020.05.012
13. Nahand JS, Jamshidi S, Hamblin MR, Mahjoubin-Tehran M, Vosough M, Jamali M, et al. Circular RNAs: New Epigenetic Signatures in Viral Infections. *Front Microbiol* (2020) 11:1853:1853. doi: 10.3389/fmicb.2020.01853
14. Kulcheski FR, Christoff AP, Margis R. Circular RNAs are miRNA sponges and can be used as a new class of biomarker. *J Biotechnol* (2016) 238:42–51. doi: 10.1016/j.jbiotec.2016.09.011
15. Huang A, Zheng H, Wu Z, Chen M, Huang Y. Circular RNA-protein interactions: functions, mechanisms, and identification. *Theranostics* (2020) 10:3503–17. doi: 10.7150/thno.42174
16. Zhang M, Zhao K, Xu X, Yang Y, Yan S, Wei P, et al. A peptide encoded by circular form of LINC-PINT suppresses oncogenic transcriptional elongation in glioblastoma. *Nat Commun* (2018) 9:4475. doi: 10.1038/s41467-018-06862-2
17. Li J, Yang J, Zhou P, Le Y, Zhou C, Wang S, et al. Circular RNAs in cancer: novel insights into origins, properties, functions and implications. *Am J Cancer Res* (2015) 5:472–80.
18. Zhang X, Lu N, Wang L, Wang Y, Li M, Zhou Y, et al. Circular RNAs and esophageal cancer. *Cancer Cell Int* (2020) 20:362. doi: 10.1186/s12935-020-01451-0
19. Song H, Liu Q, Liao Q, Circular RNA. and tumor microenvironment. *Cancer Cell Int* (2020) 20:211. doi: 10.1186/s12935-020-01301-z
20. Yang X, Mei J, Wang H, Gu D, Ding J, Liu C. The emerging roles of circular RNAs in ovarian cancer. *Cancer Cell Int* (2020) 20:265. doi: 10.1186/s12935-020-01367-9
21. Zheng X, Huang M, Xing L, Yang R, Wang X, Jiang R, et al. The circRNA circSEPT9 mediated by E2F1 and EIF4A3 facilitates the carcinogenesis and development of triple-negative breast cancer. *Mol Cancer* (2020) 19:73. doi: 10.1186/s12943-020-01183-9
22. Liang G, Ling Y, Mehrpour M, Saw PE, Liu Z, Tan W, et al. Autophagy-associated circRNA circCDYL augments autophagy and promotes breast cancer progression. *Mol Cancer* (2020) 19:65. doi: 10.1186/s12943-020-01152-2
23. Wang C, Tan S, Liu WR, Lei Q, Qiao W, Wu Y, et al. RNA-Seq profiling of circular RNA in human lung adenocarcinoma and squamous cell carcinoma. *Mol Cancer* (2019) 18:134. doi: 10.1186/s12943-019-1061-8
24. Van Der Steen N, Lyu Y, Hitzler AK, Becker AC, Seiler J, Diederichs S. The Circular RNA Landscape of Non-Small Cell Lung Cancer Cells. *Cancers* (2020) 12(5):1091. doi: 10.3390/cancers12051091
25. Xia Q, Ding T, Zhang G, Li Z, Zeng L, Zhu Y, et al. Circular RNA Expression Profiling Identifies Prostate Cancer- Specific circRNAs in Prostate Cancer. *Cell Physiol Biochem Int J Exp Cell Physiol Biochem Pharmacol* (2018) 50:1903–15. doi: 10.1159/000494870
26. Artemaki PI, Scorilas A, Kontos CK. Circular RNAs: A New Piece in the Colorectal Cancer Puzzle. *Cancers* (2020) 12(9):2464. doi: 10.3390/cancers12092464
27. Naeli P, Pourhanifeh MH, Karimzadeh MR, Shabaninejad Z, Movahedpour A, Tarrahimofrad H, et al. Circular RNAs and gastrointestinal cancers: Epigenetic regulators with a prognostic and therapeutic role. *Crit Rev Oncol Hematol* (2020) 145:102854. doi: 10.1016/j.critrevonc.2019.102854
28. Shabaninejad Z, Vafadar A, Movahedpour A, Ghasemi Y, Namdar A, Fathizadeh H, et al. Circular RNAs in cancer: new insights into functions and implications in ovarian cancer. *J Ovarian Res* (2019) 12:84. doi: 10.1186/s13048-019-0558-5
29. Borran S, Ahmadi G, Rezaei S, Anari MM, Modabberi M, Azarash Z, et al. Circular RNAs: New players in thyroid cancer. *Pathol Res Pract* (2020) 216:153217. doi: 10.1016/j.prp.2020.153217
30. Razavi ZS, Tajiknia V, Majidi S, Ghandali M, Mirzaei HR, Rahimian N, et al. Gynecologic cancers and non-coding RNAs: Epigenetic regulators with emerging roles. *Crit Rev Oncol Hematol* (2021) 157:103192. doi: 10.1016/j.critrevonc.2020.103192
31. Hu ZQ, Zhou SL, Li J, Zhou ZJ, Wang PC, Xin HY, et al. Circular RNA Sequencing Identifies CircASAP1 as a Key Regulator in Hepatocellular Carcinoma Metastasis. *Hepatology* (2020) 72(3):906–22. doi: 10.1002/hep.31068
32. Guarnerio J, Bezzi M, Jeong JC, Paffenholz SV, Berry K, Naldini MM, et al. Oncogenic Role of Fusion-circRNAs Derived from Cancer-Associated Chromosomal Translocations. *Cell* (2016) 165:289–302. doi: 10.1016/j.cell.2016.03.020
33. Li L, Zhang Q, Lian K. Circular RNA circ_0000284 plays an oncogenic role in the progression of non-small cell lung cancer through the miR-377-3p-mediated PD-L1 promotion. *Cancer Cell Int* (2020) 20:247. doi: 10.1186/s12935-020-01310-y

34. Han D, Wang Y, Wang Y, Dai X, Zhou T, Chen J, et al. The Tumor-Suppressive Human Circular RNA CircITCH Sponges miR-330-5p to Ameliorate Doxorubicin-Induced Cardiotoxicity Through Upregulating SIRT6, Survivin, and SERCA2a. *Circ Res* (2020) 127:e108–25. doi: 10.1161/CIRCRESAHA.119.316061
35. Liu M, Luo C, Dong J, Guo J, Luo Q, Ye C, et al. CircRNA_103809 Suppresses the Proliferation and Metastasis of Breast Cancer Cells by Sponging MicroRNA-532-3p (miR-532-3p). *Front Genet* (2020) 11:485:485. doi: 10.3389/fgene.2020.00485
36. Mirzaei H, Hamblin MR. Regulation of Glycolysis by Non-coding RNAs in Cancer: Switching on the Warburg Effect. *Mol Ther Oncol* (2020) 19:218–39. doi: 10.1016/j.omto.2020.10.003
37. Su M, Xiao Y, Ma J, Tang Y, Tian B, Zhang Y, et al. Circular RNAs in Cancer: emerging functions in hallmarks, stemness, resistance and roles as potential biomarkers. *Mol Cancer* (2019) 18:90. doi: 10.1186/s12943-019-1002-6
38. Jeck WR, Sorrentino JA, Wang K, Slevin MK, Burd CE, Liu J, et al. Circular RNAs are abundant, conserved, and associated with ALU repeats. *Rna* (2013) 19:141–57. doi: 10.1261/rna.035667.112
39. Jafari Ghods F. Circular RNA in Saliva. *Adv Exp Med Biol* (2018) 1087:131–9. doi: 10.1007/978-981-13-1426-1_11
40. Vea A, Llorente-Cortes V, de Gonzalo-Calvo D. Circular RNAs in Blood. *Adv Exp Med Biol* (2018) 1087:119–30. doi: 10.1007/978-981-13-1426-1_10
41. Kölling M, Haddad G, Wegmann U, Kistler A, Bosakova A, Seeger H, et al. Circular RNAs in Urine of Kidney Transplant Patients with Acute T Cell-Mediated Allograft Rejection. *Clin Chem* (2019) 65:1287–94. doi: 10.1373/clinchem.2019.305854
42. Wang M, Yang Y, Xu J, Bai W, Ren X, Wu H. CircRNAs as biomarkers of cancer: a meta-analysis. *BMC Cancer* (2018) 18:303. doi: 10.1186/s12885-018-4213-0
43. Di Bisceglie AM, Sterling RK, Chung RT, Everhart JE, Dienstag JL, Bonkovsky HL, et al. Serum alpha-fetoprotein levels in patients with advanced hepatitis C: results from the HALT-C Trial. *J Hepatol* (2005) 43:434–41. doi: 10.1016/j.jhep.2005.03.019
44. Sterling RK, Jeffers L, Gordon F, Sherman M, Venook AP, Reddy KR, et al. Clinical utility of AFP-L3% measurement in North American patients with HCV-related cirrhosis. *Am J Gastroenterol* (2007) 102:2196–205. doi: 10.1111/j.1572-0241.2007.01405.x
45. Marrero JA, Su GL, Wei W, Emick D, Conjeevaram HS, Fontana RJ, et al. Des-gamma carboxyprothrombin can differentiate hepatocellular carcinoma from nonmalignant chronic liver disease in american patients. *Hepatology* (2003) 37:1114–21. doi: 10.1053/jhep.2003.50195
46. Bruix J, Reig M, Sherman M. Evidence-Based Diagnosis, Staging, and Treatment of Patients With Hepatocellular Carcinoma. *Gastroenterology* (2016) 150:835–53. doi: 10.1053/j.gastro.2015.12.041
47. Qiu L, Xu H, Ji M, Shang D, Lu Z, Wu Y, et al. Circular RNAs in hepatocellular carcinoma: Biomarkers, functions and mechanisms. *Life Sci* (2019) 231:116660. doi: 10.1016/j.lfs.2019.116660
48. Zhang X, Xu Y, Qian Z, Zheng W, Wu Q, Chen Y, et al. circRNA_104075 stimulates YAP-dependent tumorigenesis through the regulation of HNF4a and may serve as a diagnostic marker in hepatocellular carcinoma. *Cell Death Dis* (2018) 9:1091. doi: 10.1038/s41419-018-1132-6
49. Matboli M, Shafei AE, Ali MA, Ashry AM, Kamal KM, Agag MA, et al. circRNAs (hsa_circ_00156, hsa_circ _000224, and hsa_circ _000520) are novel potential biomarkers in hepatocellular carcinoma. *J Cell Biochem* (2019) 120:7711–24. doi: 10.1002/jcb.28045
50. Sun XH, Wang YT, Li GF, Zhang N, Fan L. Serum-derived three-circRNA signature as a diagnostic biomarker for hepatocellular carcinoma. *Cancer Cell Int* (2020) 20:226. doi: 10.1186/s12935-020-01302-y
51. Wu C, Deng L, Zhuo H, Chen X, Tan Z, Han S, et al. Circulating circRNA predicting the occurrence of hepatocellular carcinoma in patients with HBV infection. *J Cell Mol Med* (2020) 24(17):10216–22. doi: 10.1111/jcmm.15635
52. Yu J, Xu QG, Wang ZG, Yang Y, Zhang L, Ma JZ, et al. Circular RNA cSMARCA5 inhibits growth and metastasis in hepatocellular carcinoma. *J Hepatol* (2018) 68:1214–27. doi: 10.1016/j.jhep.2018.01.012
53. Li Z, Zhou Y, Yang G, He S, Qiu X, Zhang L, et al. Using circular RNA SMARCA5 as a potential novel biomarker for hepatocellular carcinoma. *Clin Chim Acta Int J Clin Chem* (2019) 492:37–44. doi: 10.1016/j.cca.2019.02.001
54. Yu J, Ding WB, Wang MC, Guo XG, Xu J, Xu QG, et al. Plasma circular RNA panel to diagnose hepatitis B virus-related hepatocellular carcinoma: A large-scale, multicenter study. *Int J Cancer* (2020) 146:1754–63. doi: 10.1002/ijc.32647
55. Maccali C, Chagas AL, Boin I, Quiñonez E, Marciano S, Vilatobá M, et al. Recurrence of hepatocellular carcinoma after liver transplantation: Prognostic and predictive factors of survival in a Latin American cohort. *Liver Int Off J Int Assoc Study Liver* (2021) 41(4):851–62. doi: 10.1111/liv.14736
56. Liu PH, Hsu CY, Hsia CY, Lee YH, Su CW, Huang YH,, et al. Prognosis of hepatocellular carcinoma: Assessment of eleven staging systems. *J Hepatol* (2016) 64:601–8. doi: 10.1016/j.jhep.2015.10.029
57. Zhu J, Tang B, Li J, Shi Y, Chen M, Lv X, et al. Identification and validation of the angiogenic genes for constructing diagnostic, prognostic, and recurrence models for hepatocellular carcinoma. *Aging* (2020) 12:7848–73. doi: 10.18632/aging.103107
58. Pan H, Tang L, Jiang H, Li X, Wang R, Gao J, et al. Enhanced expression of circ_0000267 in hepatocellular carcinoma indicates poor prognosis and facilitates cell progression by sponging miR-646. *J Cell Biochem* (2019) 120:11350–7. doi: 10.1002/jcb.28411
59. Rao UN, Gollin SM, Beaves S, Cieply K, Nalesnik M, Michalopoulos GK. Comparative genomic hybridization of hepatocellular carcinoma: correlation with fluorescence in situ hybridization in paraffin-embedded tissue. *Mol Diagn J Devoted Underst Hum Dis Clin Appl Mol Biol* (2001) 6:27–37. doi: 10.1054/modi.2001.22021
60. Glukhova L, Lavialle C, Fauvet D, Chudoba I, Danglot G, Angevin E, et al. Mapping of the 7q31 subregion common to the small chromosome 7 derivatives from two sporadic papillary renal cell carcinomas: increased copy number and overexpression of the MET proto-oncogene. *Oncogene* (2000) 19:754–61. doi: 10.1038/sj.onc.1203397
61. Jenkins R, Takahashi S, DeLacey K, Bergstralh E, Lieber M. Prognostic significance of allelic imbalance of chromosome arms 7q, 8p, 16q, and 18q in stage T3N0M0 prostate cancer. *Genes Chromosomes Cancer* (1998) 21:131–43. doi: 10.1002/(SICI)1098-2264(199802)21:2<131::AID-GCC9>3.0.CO;2-1
62. Li Y, Zhai Y, Song Q, Zhang H, Cao P, Ping J, et al. Genome-Wide Association Study Identifies a New Locus at 7q21.13 Associated with Hepatitis B Virus-Related Hepatocellular Carcinoma. *Clin Cancer Res Off J Am Assoc Cancer Res* (2018) 24:906–15. doi: 10.1158/1078-0432.CCR-17-2537
63. Huang XY, Zhang PF, Wei CY, Peng R, Lu JC, Gao C, et al. Circular RNA circMET drives immunosuppression and anti-PD1 therapy resistance in hepatocellular carcinoma via the miR-30-5p/snail/DPP4 axis. *Mol Cancer* (2020) 19:92. doi: 10.1186/s12943-020-01213-6
64. Sun S, Gao J, Zhou S, Li Y, Wang Y, Jin L, et al. A novel circular RNA circ-LRIG3 facilitates the malignant progression of hepatocellular carcinoma by modulating the EZH2/STAT3 signaling. *J Exp Clin Cancer Res CR* (2020) 39:252. doi: 10.1186/s13046-020-01779-5
65. Yao Z, Luo J, Hu K, Lin J, Huang H, Wang Q, et al. ZKSCAN1 gene and its related circular RNA (circZKSCAN1) both inhibit hepatocellular carcinoma cell growth, migration, and invasion but through different signaling pathways. *Mol Oncol* (2017) 11:422–37. doi: 10.1002/1878-0261.12045
66. Zhu YJ, Zheng B, Luo GJ, Ma XK, Lu XY, Lin XM, et al. Circular RNAs negatively regulate cancer stem cells by physically binding FMRP against CCAR1 complex in hepatocellular carcinoma. *Theranostics* (2019) 9:3526–40. doi: 10.7150/thno.32796
67. Liu R, Li Y, Wu A, Kong M, Ding W, Hu Z, et al. Identification of Plasma hsa_circ_0005397 and Combined With Serum AFP, AFP-L3 as Potential Biomarkers for Hepatocellular Carcinoma. *Front Pharmacol* (2021) 12:639963:639963. doi: 10.3389/fphar.2021.639963
68. Li W, Zhou X, Wu X, Wei J, Huang Z. The role of circular RNA hsa_circ_0085616 in proliferation and migration of hepatocellular carcinoma cells. *Cancer Manage Res* (2019) 11:7369–76. doi: 10.2147/CMAR.S211020
69. Li Q, Pan X, Zhu D, Deng Z, Jiang R, Wang X. Circular RNA MAT2B Promotes Glycolysis and Malignancy of Hepatocellular Carcinoma Through the miR-338-3p/PKM2 Axis Under Hypoxic Stress. *Hepatology* (2019) 70:1298–316. doi: 10.1002/hep.30671
70. Wang L, Long H, Zheng Q, Bo X, Xiao X, Li. Circular RNA circRHOT1 promotes hepatocellular carcinoma progression by initiation of NR2F6 expression. *Mol Cancer* (2019) 18:119. doi: 10.1186/s12943-019-1046-7

71. Han D, Li J, Wang H, Su X, Hou J, Gu Y, et al. Circular RNA circMTO1 acts as the sponge of microRNA-9 to suppress hepatocellular carcinoma progression. *Hepatology* (2017) 66:1151–64. doi: 10.1002/hep.29270
72. Gu X, Fu M, Ding Y, Ni H, Zhang W, Zhu Y, et al. TIMP-3 expression associates with malignant behaviors and predicts favorable survival in HCC. *PloS One* (2014) 9:e106161. doi: 10.1371/journal.pone.0106161
73. Ikeda M, Mitsunaga S, Ohno I, Hashimoto Y, Takahashi H, Watanabe K, et al. Systemic Chemotherapy for Advanced Hepatocellular Carcinoma: Past, Present, and Future. *Diseases* (2015) 3:360–81. doi: 10.3390/diseases3040360
74. Chen S, Cao Q, Wen W, Wang H. Targeted therapy for hepatocellular carcinoma: Challenges and opportunities. *Cancer Lett* (2019) 460:1–9. doi: 10.1016/j.canlet.2019.114428
75. Yarchoan M, Hopkins A, Jaffee EM. Tumor Mutational Burden and Response Rate to PD-1 Inhibition. *New Engl J Med* (2017) 377:2500–1. doi: 10.1056/NEJMc1713444
76. Li J, Qin X, Wu R, Wan L, Zhang L, Liu R. Circular RNA circFBXO11 modulates hepatocellular carcinoma progress and oxaliplatin resistance through miR-605/FOXO3/ABCB1 axis. *J Cell Mol Med* (2020) 24:5152–61. doi: 10.1111/jcmm.15162
77. Li DQ, Qiu M, Nie XM, Gui R, Huang MZ. Oxidored-nitro domain-containing protein 1 expression is associated with the progression of hepatocellular carcinoma. *Oncol Lett* (2016) 11:3003–8. doi: 10.3892/ol.2016.4362
78. Luo Y, Fu Y, Huang R, Gao M, Liu F, Gui R, et al. CircRNA_101505 sensitizes hepatocellular carcinoma cells to cisplatin by sponging miR-103 and promotes oxidored-nitro domain-containing protein 1 expression. *Cell Death Discovery* (2019) 5:121. doi: 10.1038/s41420-019-0202-6
79. Wu MY, Tang YP, Liu JJ, Liang R, Luo XL. Global transcriptomic study of circRNAs expression profile in sorafenib resistant hepatocellular carcinoma cells. *J Cancer* (2020) 11:2993–3001. doi: 10.7150/jca.39854
80. Yang C, Dong Z, Hong H, Dai B, Song F, Geng L, et al. circFN1 Mediates Sorafenib Resistance of Hepatocellular Carcinoma Cells by Sponging miR-1205 and Regulating E2F1 Expression. *Mol Ther Nucleic Acids* (2020) 22:421–33. doi: 10.1016/j.omtn.2020.08.039
81. Pegtel DM, Gould SJ. Exosomes. *Annu Rev Biochem* (2019) 88:487–514. doi: 10.1146/annurev-biochem-013118-111902
82. Li Y, Zheng Q, Bao C, Li S, Guo W, Zhao J,, et al. Circular RNA is enriched and stable in exosomes: a promising biomarker for cancer diagnosis. *Cell Res* (2015) 25:981–4. doi: 10.1038/cr.2015.82
83. Sukowati CHC, Cabral LKD, Tiribelli C, Pascut D. Circulating Long and Circular Noncoding RNA as Non-Invasive Diagnostic Tools of Hepatocellular Carcinoma. *Biomedicines* (2021) 9(1):90. doi: 10.3390/biomedicines9010090
84. Li LM, Liu ZX, Cheng QY. Exosome plays an important role in the development of hepatocellular carcinoma. *Pathol Res Pract* (2019) 215:152468. doi: 10.1016/j.prp.2019.152468
85. Lyu L, Yang W, Yao J, Wang H, Zhu J, Jin A, et al. The diagnostic value of plasma exosomal hsa_circ_0070396 for hepatocellular carcinoma. *Biomarkers Med* (2021) 15(5):359–71. doi: 10.2217/bmm-2020-0476
86. Luo Y, Liu F, Gui R. High expression of circulating exosomal circAKT3 is associated with higher recurrence in HCC patients undergoing surgical treatment. *Surg Oncol* (2020) 33:276–81. doi: 10.1016/j.suronc.2020.04.021
87. Wang G, Liu W, Zou Y, Wang G, Deng Y, Luo J, et al. Three isoforms of exosomal circPTGR1 promote hepatocellular carcinoma metastasis via the miR449a-MET pathway. *EBioMedicine* (2019) 40:432–45. doi: 10.1016/j.ebiom.2018.12.062
88. Su Y, Lv X, Yin W, Zhou L, Hu Y, Zhou A, et al. CircRNA Cdr1as functions as a competitive endogenous RNA to promote hepatocellular carcinoma progression. *Aging* (2019) 11:8183–203. doi: 10.18632/aging.102312
89. Huang XY, Huang ZL, Huang J, Xu B, Huang XY, Xu YH, et al. Exosomal circRNA-100338 promotes hepatocellular carcinoma metastasis via enhancing invasiveness and angiogenesis. *J Exp Clin Cancer Res CR* (2020) 39:20. doi: 10.1186/s13046-020-1529-9
90. Chen W, Quan Y, Fan S, Wang H, Liang J, Huang L, et al. Exosome-transmitted circular RNA hsa_circ_0051443 suppresses hepatocellular carcinoma progression. *Cancer Lett* (2020) 475:119–28. doi: 10.1016/j.canlet.2020.01.022
91. Zhao M, Qu H. circVAR database: genome-wide archive of genetic variants for human circular RNAs. *BMC Genomics* (2020) 21:750. doi: 10.1186/s12864-020-07172-y
92. Meng X, Hu D, Zhang P, Chen Q, Chen M. CircFunBase: a database for functional circular RNAs. *Database J Biol Database Curation* (2019) 2019: baz003. doi: 10.1093/database/baz003
93. Guo JU, Agarwal V, Guo H, Bartel DP. Expanded identification and characterization of mammalian circular RNAs. *Genome Biol* (2014) 15:409. doi: 10.1186/s13059-014-0409-z
94. Drinnenberg IA, Weinberg DE, Xie KT, Mower JP, Wolfe KH, Fink GR, et al. RNAi in budding yeast. *Science* (2009) 326:544–50. doi: 10.1126/science.1176945
95. Baum J, Papenfuss AT, Mair GR, Janse CJ, Vlachou D, Waters AP, et al. Molecular genetics and comparative genomics reveal RNAi is not functional in malaria parasites. *Nucleic Acids Res* (2009) 37:3788–98. doi: 10.1093/nar/gkp239
96. Zhang Y, Zhang XO, Chen T, Xiang JF, Yin QF, Xing YH, et al. Circular intronic long noncoding RNAs. *Mol Cell* (2013) 51:792–806. doi: 10.1016/j.molcel.2013.08.017
97. Westholm JO, Miura P, Olson S, Shenker S, Joseph B, Sanfilippo P, et al. Genome-wide analysis of drosophila circular RNAs reveals their structural and sequence properties and age-dependent neural accumulation. *Cell Rep* (2014) 9:1966–80. doi: 10.1016/j.celrep.2014.10.062
98. Ivanov A, Memczak S, Wyler E, Torti F, Porath HT, Orejuela MR, et al. Analysis of intron sequences reveals hallmarks of circular RNA biogenesis in animals. *Cell Rep* (2015) 10:170–7. doi: 10.1016/j.celrep.2014.12.019
99. Starke S, Jost I, Rossbach O, Schneider T, Schreiner S, Hung LH, et al. Exon circularization requires canonical splice signals. *Cell Rep* (2015) 10:103–11. doi: 10.1016/j.celrep.2014.12.002
100. Salzman J, Chen RE, Olsen MN, Wang PL, Brown PO. Cell-type specific features of circular RNA expression. *PloS Genet* (2013) 9:e1003777. doi: 10.1371/journal.pgen.1003777
101. Barrett SP, Wang PL, Salzman J. Circular RNA biogenesis can proceed through an exon-containing lariat precursor. *eLife* (2015) 4:e07540. doi: 10.7554/eLife.07540
102. Jost I, Shalamova LA, Gerresheim GK, Niepmann M, Bindereif A, Rossbach O. Functional sequestration of microRNA-122 from Hepatitis C Virus by circular RNA sponges. *RNA Biol* (2018) 15:1032–9. doi: 10.1080/15476286.2018.1435248
103. Liu X, Abraham JM, Cheng Y, Wang Z, Wang Z, Zhang G, et al. Synthetic Circular RNA Functions as a miR-21 Sponge to Suppress Gastric Carcinoma Cell Proliferation. *Mol Ther Nucleic Acids* (2018) 13:312–21. doi: 10.1016/j.omtn.2018.09.010

Conflict of Interest: The authors declare that the research was conducted in the absence of any commercial or financial relationships that could be construed as a potential conflict of interest.

frontiers in Oncology

REVIEW
published: 29 April 2021
doi: 10.3389/fonc.2021.632834

Biomarkers (mRNAs and Non-Coding RNAs) for the Diagnosis and Prognosis of Colorectal Cancer – From the Body Fluid to Tissue Level

Jinhua He[1†], Feifeng Wu[2†], Zeping Han[1†], Min Hu[2], Weida Lin[2], Yuguang Li[1] and Mingrong Cao[2*]*

[1] Department of Laboratory Medicine, Central Hospital of Panyu District, Guangzhou, China, [2] Department of Hepatobiliary Surgery, The First Affiliated Hospital of Jinan University, Guangzhou, China

OPEN ACCESS

Edited by:
Divya P. Kumar, JSS Academy of Higher Education and Research, India

Reviewed by:
Ashwini Kumar, Indian Institute of Technology Delhi, India
Anjali Devi, JSS Academy of Higher Education and Research, India

***Correspondence:**
Mingrong Cao
tcaomr@163.com
Yuguang Li
lyg_py@126.com

[†]These authors have contributed equally to this work

Specialty section:
This article was submitted to Gastrointestinal Cancers, a section of the journal Frontiers in Oncology

Received: *24 November 2020*
Accepted: *09 April 2021*
Published: *29 April 2021*

Citation:
He J, Wu F, Han Z, Hu M, Lin W, Li Y and Cao M (2021) Biomarkers (mRNAs and Non-Coding RNAs) for the Diagnosis and Prognosis of Colorectal Cancer – From the Body Fluid to Tissue Level. Front. Oncol. 11:632834. doi: 10.3389/fonc.2021.632834

In recent years, the diagnosis and treatment of colorectal cancer (CRC) have been continuously improved, but the mortality rate continues to be high, especially in advanced patients. CRC patients usually have no obvious symptoms in the early stage and are already in the advanced stage when they are diagnosed. The 5-year survival rate is only 10%. The blood markers currently used to screen for CRC, such as carcinoembryonic antigen and carbohydrate antigen 19-9, have low sensitivity and specificity, whereas other methods are invasive or too expensive. As a result, recent research has shifted to the development of minimally invasive or noninvasive biomarkers in the form of body fluid biopsies. Non-coding RNA molecules are composed of microRNAs, long non-coding RNAs, small nucleolar RNAs, and circular RNAs, which have important roles in the occurrence and development of diseases and can be utilized for the early diagnosis and prognosis of tumors. In this review, we focus on the latest findings of mRNA-ncRNA as biomarkers for the diagnosis and prognosis of CRC, from fluid to tissue level.

Keywords: colorectal cancer, biomarkers, mRNA, ncRNA, diagnosis, prognosis

INTRODUCTION

Colorectal cancer (CRC) has the third highest incidence of all types of cancer worldwide, but the second highest mortality rate, with more than 1 million cases diagnosed and half a million deaths each year (1). The prognosis of CRC is related to the stage at the time of diagnosis. A quarter of patients present with lymph node-negative disease (American Joint Committee on Cancer stages I and II), and more than 50% of stage III patients have local recurrence and/or metastasis. The 5-year survival rate of patients with early CRC is 90%, whereas the 5-year survival rate of patients with distant metastasis is less than 10% (2, 3). The lack of early detection can affect the survival of CRC patients.

Reliable biomarkers that can detect CRC at an early stage could improve the prognosis, treatment response prediction, and risk of recurrence. These markers may identify susceptibility or early stages of the disease, and could also accurately identify patients at risk of disease recurrence and spread, as well as those patients who have failed systemic therapy. These patients may benefit

from early active treatment, replacement therapy, and/or frequent monitoring and early detection of disease recurrence (4, 5).

Molecular Pathogenesis of CRC

CRC develops through the gradual accumulation of genetic and epigenetic changes, leading to the transformation of normal colonic mucosa into invasive cancer. Most CRC develops from adenoma (adenoma-carcinoma sequence), and tumor transformation is deemed to take more than 10 years. Hyperplastic adenoma is the most common precancerous lesion in CRC (6). It is estimated that 20%–25% of cases have an associated genetic component, which is called familial CRC (7). Sporadic CRC is the result of a complex multi-factor process, which can lead to changes in the cell cycle of normal colonic epithelial cells.

At present, three principal molecular mechanisms are considered to lead to the onset of CRC: microsatellite instability, chromosomal instability, and CpG island methylation (8, 9). These pathways lead to the pathological transition and development of malignant tumors, accompanied by oncogenes suppressing the expression of tumor suppressor genes. This heterogeneity in the molecular pathogenesis of CRC is very important to clinical practice given that the identification of these subtypes with different subtype-specific gene markers can guide the "personalized" treatment of CRC patients (10).

CURRENT DIAGNOSIS, PROGNOSIS, AND PREDICTION METHODS OF CRC

CRC is diagnosed by colonoscopy and radiography before surgery and is confirmed by biopsy or histopathological examination of surgically removed specimens (11). However, these diagnostic methods are highly invasive and costly, and cumbersome bowel preparations usually result in pain, discomfort, and financial pressure for patients. In addition, the success of colonoscopy depends on the skills and experience of the operator. Accordingly, the widespread application of colonoscopy for large-scale CRC screening has been hindered (12).

Other less invasive tests, such as the stool occult blood test and serum tests for tumor markers such as carcinoembryonic antigen (CEA) and carbohydrate antigen 19-9 (CA19-9) are commonly used in clinical practice, but their sensitivity and specificity are poor and their value is limited (13). Therefore, innovative large-scale screening programs have been established using feces or body fluids targeting mRNA expression, gene mutations (such as KRAS, adenomatous polyposis coli [APC], and p53), microsatellite instability, or methylated promoter regions (14). At present, a large amount of research has been carried out worldwide to identify molecular markers based on DNA, RNA, or proteins to develop novel, non-invasive blood and stool CRC biomarker detection methods (15–20).

The APC gene is mutated in CRC, and its inactivation is considered to be a key early genetic change in CRC (21). DNA sequencing and RT-PCR analysis of APC gene expression and APC gene mutations in tumor tissues of 195 CRC patients found that 66 (33.8%) of 195 tumor tissues contained APC gene mutations, and indicated that APC gene mutations can be used as a marker for the clinical prognosis of CRC.

p53 (encoded by TP53) is involved in DNA damage repair, cell cycle regulation, apoptosis, and cellular senescence (22). The role of p53 inactivation in the progression and prognosis of CRC has been studied extensively, but still remains unclear. Loss of this gene is associated with a poor prognosis in CRC patients (23).

Epidermal growth factor receptor (EGFR) is a protein found on cells that plays a vital role in promoting cell growth. In gastric, breast, endometrial cancer and CRC,.EGFR overexpression is associated with reduced recurrence-free or overall survival rates (24). Cetuximab inhibits EGFR-mediated signaling by blocking its binding to endogenous ligands, and patient resistance to cetuximab is also associated with the EGFR pathway. In conclusion, EGFR is a key prognostic factor for CRC patients (25).

At present, for anti-EGFR antibody-based treatments, as well as the response to cetuximab and panitumumab, mutations in the KRAS gene are the most commonly used marker (26). The KRAS proto-oncogene encodes a small G protein (guanosine triphosphate-/guanosine diphosphate-binding protein) in the PI3K/PTEN/AKT and RAF/MEK/ERK signaling pathways downstream of EGFR. Most KRAS-activating mutations (~90%) are found in codons 12 and 13 of exon 1, and nearly 5% of mutations occur in codon 16 of exon 2 (27, 28). It has been suggested that KRAS gene mutation analysis combined with phosphatidylinositol-4,5-bisphosphate 3-kinase catalytic subunit alpha mutation analysis can be used as a prognostic marker for CRC before anti-EGFR treatment is given (8). At present, the diagnostic test markers for CRC also include circulating tumor cells, CEA and CA19-9, cell-free nucleic acid, serum DNA, and other circulating DNA methylation biomarkers (vimentin, nerve growth factor receptor, septin 9 and transmembrane protein with EGF-like and two follistatin-like domains 2, p16, APC, mutL homolog 1, helicase-like transcription factor, and death-associated protein kinase 1), mRNA, and non-coding RNA (ncRNA) (8).

CANDIDATE RNA MOLECULES AS BIOMARKERS FOR CRC

mRNAs as Biomarkers for CRC

mRNAs are single-stranded ribonucleic acid molecules that are transcribed from a strand of DNA as a template, carry genetic information, and can guide protein synthesis (29, 30). The levels of free baculoviral IAP repeat-containing 5 (BIRC5) mRNA are significantly increased in the serum of CRC patients, with a sensitivity of 84.8% and a specificity of 80.0%. In addition, when BIRC5 mRNA is combined with CEA, its diagnostic performance is significantly improved. Patients with high levels of BIRC5 mRNA have a worse prognosis than those with low

levels. BIRC5 mRNA is a non-invasive molecular biomarker used in the diagnosis of CRC and has a higher diagnostic efficacy compared with CEA (31). B-lymphoma Moloney murine leukemia virus insertion region-1 (BMI1), a member of the Polycomb group family of proteins, is involved in axial patterning, hematopoiesis, regulation of proliferation, and senescence, BMI1 can be utilized as a non-invasive biomarker for monitoring occult metastasis and predicting the occurrence of distant metastases in CRC (32).

Hereditary non-polyposis CRC (HNPCC) is caused by functional defects of mismatch repair genes, including MLH1 and mut S homolog 2. MLH1 mRNA levels in peripheral blood have a high diagnostic value for HNPCC (33). The sensitivity of MLH1 mRNA levels to distinguish HNPCC from a control group is 81.3%, with a specificity of 86.7%.

The expression of cytokeratin 19, cytokeratin 20, and coronary cell cyclase C mRNAs in peripheral blood can be used for the diagnosis of non-metastatic CRC; when used in combination, their expression has a sensitivity and specificity of 88% and 68%, respectively. Coronary cell cyclase C, with a specificity of 100%, is considered a specific marker for the detection of CRC (34). The detection of cytokeratin 20 mRNA expression in the serum of CRC patients has extremely high specificity as a marker for the diagnosis of CRC (35). The expression of organic anion transporting polypeptide 1B3 (Ct-OATP1B3) mRNA in CRC tissue and adjacent tissue is related to the overall survival rate of CRC patients. At the same time, Ct-OATP1B3 mRNA is present in extracellular vesicles derived from CRC patients and can be detected in serum samples. The detection of Ct-OATP1B3 mRNA in CRC-derived extracellular vesicles as a diagnostic biomarker is worthy of further study (36).

The expression of related genes detected in platelets of CRC patients can also be used in the diagnosis of CRC. An increase in expression of TIMP metallopeptidase inhibitor 1 mRNA in platelets of CRC patients has a much higher receiver operating characteristic curve (0.958; 95% confidence interval [CI], 0.936–0.980) than CEA (0.765; 95% CI, N/A) and CA19-9 (0.612; 95% CI, N/A), indicating that the expression of TIMP metallopeptidase inhibitor 1 mRNA in platelets could be used as a non-invasive biomarker (37).

The newly discovered prognostic biomarker solute carrier family 35 member D3 is highly expressed in the cancerous tissue of CRC patients. It is associated with CEA cell adhesion molecule 5, kallikrein-related peptidase 6, and mucin 2, and a combined construction formula can be used to identify people at risk. CEA cell adhesion molecule 5 is suggested to be the common denominator of three biomarkers (kallikrein-related peptidase 6, solute carrier family 35 member D3, and mucin 2). This formula produces 5 categories (-1, 0, 1, 2, and 3). Categories -1 and 0 suggest a good prognosis, categories 1 and 2 suggest a relatively poor prognosis, and category 3 suggests a poor prognosis. This approach, which converts data into a simple formulation based on the ratio of several biomarkers, could provide useful tools for the postoperative treatment of CRC patients and for the future development of new therapies (38).

MicroRNAs (miRNAs) as Biomarkers for CRC

Approximately 70%–90% of the human genome is transcribed into RNA, but most RNA transcripts are non-coding, and only 2% of the genome encodes proteins (39). ncRNAs are important molecules that regulate the expression of genes at different stages such as the epigenetic, transcription, and post-transcription levels (40, 41). ncRNAs are divided into three main categories: short/small ncRNAs, long ncRNAs (lncRNAs), and circular RNAs (circRNAs). Short/small ncRNAs are also divided into three main sub-categories: miRNAs, short interfering RNAs, and PIWI-interacting RNAs (piRNAs). Other types of ncRNAs are found universally in all cell types, which may be considered as housekeeping RNAs, including transfer RNAs (tRNAs) and small nucleolar RNAs (snoRNAs) (1).

miRNAs are a class of endogenous ncRNAs of 20–25 nucleotides in length that are found in eukaryotes and have regulatory functions. Mature miRNAs are produced from long primary transcripts by a series of nucleases and then assembled into an RNA-induced silencing complex, which recognizes target mRNAs through base complementary pairing and guides the silencing complex to degrade target mRNAs or inhibit the translation of target mRNAs according to different degrees of complementation (42, 43). In the past 5 years, extensive research has been conducted on miRNAs as clinically relevant biomarkers for CRC (**Table 1**).

miRNAs are present in CRC tumor tissue, feces, and various body fluids (plasma, serum, exosomes, and urine). miR-143 and miR-145 expression is significantly downregulated in CRC tissue and both have a role in the pathogenesis of CRC (44). miR-143 overexpression can reduce the expression of KRAS protein and inhibit cell proliferation (45). The inhibitory effect of miR-143 on KRAS expression represses the phosphorylation of extracellular regulatory protein kinase 1/2 and then stimulates cell proliferation. miR-143 downregulation may promote tumor development (46). miR-143 can enhance the sensitivity of KRAS mutant CRC cells to paclitaxel treatment (47). miR-145 inhibits cell viability, migration, and invasion by targeting the tumor suppressor candidate gene 3 in CRC cells (48). miR-145 expression is significantly higher in CRC patients with lymph node metastasis compared with patients without lymph node metastasis, and it plays an important role in advanced CRC (49). Low miR-145 expression is linked to poor prognosis; patients with low miR-145 expression have a 1.92-fold higher short-term overall survival risk than patients with high expression (45). Given the lack of abundant miR-143 and miR-145 expression data in the global population, further large-scale, well-designed, multicenter prospective studies are needed to confirm these findings before miR-143 and miR-145 can be used as disease progression biomarkers to predict CRC survival outcomes.

miR-21 is an oncogene that is upregulated in almost all malignant tumors, including CRC tumor tissue (50), and it is steadily upregulated in CRC patient serum (51). High serum levels of miR-21 and miR-92a may be potential biomarkers for the early detection of CRC and advanced adenoma (52). Programmed cell death 4 and phosphatase and tension

TABLE 1 | MicroRNAs as potential biomarkers for colorectal cancer.

MicroRNA	Expression	Sample	Biomarker	Reference
miR-21	↑	Tissue/Plasma exosomes	Diagnostic/Prognostic	(1–4)
miR-23a	↑	Serum/Plasma exosomes	Diagnostic	(3, 5)
miR-17-5p	↑	Plasma/Tissue/Exosomes	Diagnostic/Prognostic	(6, 7)
miR-150-5p	↓	Serum	Diagnostic	(8, 9)
miR-92a	↑	Plasma exosomes	Diagnostic	(3, 4)
miR-29a	↑	Serum/Exosomes/Stool	Diagnostic	(4, 10)
miR-122	↑	Serum	Diagnostic/Prognostic	(11)
miR-199a/b-3p	↑	Serum	Prognostic	(12)
miR-199a-5p	↑	Serum	Prognostic	(12)
miR-199b-5p	↑	Serum	Prognostic	(12)
miR-99b-5p	↓	Serum	Diagnostic	(8)
miR-4461	↓	Serum	Diagnostic/Therapeutic	(13)
miR-92b	↓	Serum	Diagnostic	(14)
miR-320d	↑	Serum	Diagnostic	(15)
miR-301a	↑	Serum	Diagnostic	(5)
miR-181a-5p	↑	Plasma/Tissue/Exosomes	Diagnostic	(6)
miR-18a-5p	↑	Plasma/Tissue/Exosomes	Diagnostic	(6)
miR-18b-5p	↑	Plasma/Tissue/Exosomes	Diagnostic	(6)
miR-548c-5p	↓	Plasma exosomes	Diagnostic/Prognostic	(16)
miR-27a	↑	Plasma exosomes	Diagnostic/Prognostic	(17)
miR-130a	↑	Plasma exosomes	Diagnostic/Prognostic	(17)
miR-92a-3p	↑	Plasma exosomes	Prognostic	(7)
miR-6803-5p	↑	Plasma exosomes	Diagnostic/Prognostic	(18)
miR-6869-5p	↓	Plasma exosomes	Prognostic	(19)
miR-125a-3p	↑	Plasma exosomes	Diagnostic	(20)
miR-96-5p	↓	Tissue/Plasma exosomes	Diagnostic/Therapeutic	(21)
miR-149	↓	Tissue/Plasma exosomes	Diagnostic/Therapeutic	(21)
miR-19a-3p	↑	Tissue/Plasma exosomes	Diagnostic	(22)
miR-21-5p	↑	Tissue/Plasma exosomes	Diagnostic	(22)
miR-425-5p	↑	Tissue/Plasma exosomes	Diagnostic	(22)
miR-1246	↑	Plasma exosomes	Diagnostic	(3)
miR-4772-3p	↓	Plasma exosomes	Prognostic	(23)
miR-19a	↑	Serum/Exosomes	Prognostic	(24)
miR-34a-5p	↓	Tissue	Prognostic	(25)
miR-132	↓	Tissue	Prognostic	(26)
miR-199b	↓	Tissue	Prognostic	(27)
miR-145	↓	Tissue/Serum	Prognostic	(1)
miR-223	↓	Stool	Diagnostic	(10)
miR-224	↓	Stool	Diagnostic	(10)
miR-195-5p	↓	Tissue/Cell lines	Prognostic	(28)
miR-145-5p	↓	Tissue	Diagnostic/Therapeutic	(29)

References showed in ***Supplementary Material 1****.*

homolog (PTEN) levels are negatively correlated with the expression of miR-21 in CRC tissue and cells (53). In serum samples from 200 CRC patients, 50 advanced adenoma patients, and 80 healthy controls, the area under the receiver operating characteristic curve (AUC) of miR-21 was 0.802, and that of miR-92a was 0.786 (54). miR-92a plays a role in CRC by targeting the tumor suppressor PTEN, and high miR-92a expression is significantly correlated with tumor, node, metastasis (TNM) staging, lymph node metastasis, and distant metastasis (55).

Exosomes are lipid vesicles with a diameter of 40-100 nm that were first discovered in sheep reticulocytes in 1983 (56). Exosomal miR-21 levels are an independent prognostic factor of overall survival and disease-free survival in TNM stage II/III CRC patients and overall survival in TNM stage IV patients (51). The growth rate of CRC is related to the concentration of miRNAs in exosomes. miR-21, miR-92a, and miR-1246 overexpression in exosomes promotes the proliferation of cancer cells, whereas miR-23a and miR-92a overexpression inhibits apoptosis in cancer cells (57).

miRNAs are sufficiently stable to be detected in stool samples because they are protected in exosomes (58). miR-21 is not only highly expressed in the serum of patients with CRC but can also be detected at high levels in stool samples. High levels of miR-92a are found in the stool samples from CRC patients (59). Twelve upregulated miRNAs (miR-7, miR-17, miR-20a, miR-21, miR-92a, miR-96, miR-106a, miR-134, miR-183, miR-196a, miR-199a-3p, and miR-214) and eight downregulated miRNAs (miR-9, miR-29b, miR-127-5p, miR-138, miR-143, miR-146a, miR-222, and miR-938) can distinguish different TNM stages with high sensitivity and specificity (60). miR-135b and miR-31 were found to be significantly upregulated in CRC and advanced adenoma as compared with their adjacent normal tissues. the expression of miR-135b correlated positively with stages of lesions, with more advanced lesions having the highest miRNA level. The expression levels of miR-135b in feces can be used to

distinguish different stages of CRC (61). In extracellular vesicles isolated from peritoneal lavage fluid, 210 miRNAs were found to be significantly dysregulated; the top 10 miRNAs with an AUC value higher than 0.95 were miR-199b-5p, miR-150-5p, miR-29c-5p, miR-218-5p, miR-99a-3p, miR-383-5p, miR-199a-3p, miR-193a-5p, miR-10b-5p, and miR-181c-5p (62).

lncRNAs as Biomarkers for CRC

lncRNAs are special ncRNA molecules of more than 200 nucleotides in length (63). lncRNAs exert regulatory functions at different levels of gene expression, including chromatin modification, transcription, and post-transcription (64). In cancer, lncRNAs may promote cell proliferation, invasion, and development, induce angiogenesis, and promote cell resistance to apoptosis (65). lncRNAs are abnormally expressed in various types of cancer cells and play vital roles in common cancer characteristics (66). In recent years, numerous reports have indicated that dysregulation of lncRNA expression has been found in the tumor tissue, blood, and exosomes of CRC patients (67–69). These dysregulated lncRNAs can be used as new biomarkers for the diagnosis, treatment, and prognosis of CRC patients (**Table 2**).

CRC-related transcription-1 (CCAT1) is a newly discovered lncRNA with a length of 2628 nucleotides (70). CCAT1 expression is upregulated in CRC (71), with CCAT1 levels on average 235 times higher in CRC tissue than in normal mucosa. In CRC patients, CCAT1 overexpression is detected in all hematoxylin and eosin-positive lymph nodes, and its detection rate in hematoxylin and eosin- and immunohistochemical-negative lymph nodes reaches 40.0%. CCAT1 is also highly expressed in peripheral blood samples from CRC patients. High CCAT1 expression indicates that CCAT1 can be utilized for the screening, diagnosis, and assessment of staging and overall prognosis of CRC patients (71). CCAT1 expression is significant in the progression of colonic adenoma to cancer, suggesting that it plays an important role in tumor genesis and metastasis (72). The combination of CCAT1 with another lncRNA (HOTAIR) provides higher diagnostic performance (73). CCAT1 alone or in combination with CCAT2 can be utilized as an important prognostic biomarker in CRC (74).

lncRNAs and miRNAs play mutual regulation roles, acting as competitive endogenous RNAs (ceRNAs) (75). Highly expressed CCAT1 targets and regulates miR-181a-5p, and is negatively correlated with its expression. CCAT1 and miR-181a-5p may act as ceRNAs, which can affect the growth of CRC tumors by regulating the p53 signaling pathway (76). The upregulation of CCAT1 expression increases sensitivity to fluorouracil chemotherapy, whereas its downregulation effectively reverses the resistance of colon cancer cell lines to fluorouracil, thereby opening up a new approach for the treatment of colon cancer (77).

Metastatic lung adenocarcinoma transcript 1 (MALAT1), also known as nuclear-enriched transcript 2, is a highly conserved nuclear-enriched lncRNA of ~8,000 nucleotides, which was the first marker for the independent prognosis of early non-small cell lung cancer (78, 79). MALAT1 is upregulated in lung, breast, pancreatic, liver, prostate cancer and CRC, suggesting that it plays an important role in the pathogenesis and progression of cancer (80). MALAT1 can promote the growth and migration of CRC cells by competitively binding to the splicing factor proline- and glutamine-rich (SFPQ) tumor suppressor gene and releasing SFPQ from the SFPQ/polypyrimidine tract-binding protein 2 (PTBP2) complex, resulting in an increase in free proto-oncogene PTBP2, suggesting that MALAT1 can be a potential therapeutic target for CRC (81). MALAT1 binds to miR-15, inhibits the regulation of LDL receptor-related protein 6 expression by miR-15, and enhances β-catenin signaling, resulting in the downregulation of RUNX family transcription factor 2 (RUNX2) gene expression. Secondly, MALAT1 binds to SFPQ and dissociates SFPQ/PTBP2 dimers to release PTBP2, thereby increasing the translation of RUNX2 by interacting with the IRES domain in the 5′-untranslated region (UTR) of RUNX2 mRNA (82). The prognosis of patients with CRC tumors with high MALAT1 expression is significantly worse than those with low expression, suggesting that high MALAT1 expression may be a negative prognostic marker for patients with stage II/III CRC (83).

The lncRNA H19 is a maternally expressed imprinted gene that plays an important role in mammalian development (84, 85). H19 is substantially upregulated in CRC and has a carcinogenic effect (86). H19 combines with eukaryotic translation initiation factor 4A3 (eIF4A3) to prevent the recruitment of eIF4A3 to mRNAs encoding cell cycle genes, and then influences the expression of cell cycle regulation genes at the translation or post-translation level. High H19 expression in CRC is significantly correlated with the degree of tumor differentiation and advanced TNM stage, indicating its potential as a prognostic biomarker (87). Four selected single nucleotide polymorphisms in H19 (RS2839698, RS3024270, RS217727, and RS2735971) were genotyped and evaluated for their association with CRC risk in the Chinese population. The results showed that RS2839698 is associated with increased CRC risk, indicating its potential as a biomarker for predicting CRC susceptibility (88). The H19/miR-29b-3p/granulin precursor axis promotes epithelial-mesenchymal transition in CRC cells by acting on the Wnt/β-catenin signaling pathway, which suggests a direction for targeted gene therapy for CRC (89).

Pvt1 oncogene (PVT1) is an lncRNA that is greater than 30 kb in size (90) and is upregulated in cancers (especially various cancers of the digestive system, including esophageal, gastric, primary liver, and pancreatic cancer and CRC) and can promote tumor cell proliferation, migration, and invasion (91). PVT1 upregulation is usually associated with poor prognosis. High PVT1 expression helps to predict early metastasis or recurrence of CRC after radical resection, and is a prospective prognostic marker (92). PVT1 overexpression may promote multidrug resistance in CRC cells, and PVT1 knockdown can reverse the resistance of CRC cells to fluorouracil. These observations indicate that PVT1 is a potential target for the treatment of multidrug resistance in CRC (93). The diagnostic sensitivity and specificity of PVT1 in CRC patients are 72.5% and 87.5%, respectively, and the AUC value is 0.856. It has high diagnostic performance, indicating that it has good clinical value for the early diagnosis of CRC (94).

TABLE 2 | Potential long non-coding RNAs as biomarkers for the diagnosis and prognosis of colorectal cancer.

LncRNA	Expression	Sample	Biomarker	Reference
CCAT1	↑	Tissue/Plasma	Diagnostic/Prognostic	(1–4)
HOTAIR	↑	Tissue/Cell lines	Diagnostic/Therapeutic	(5–7)
NEAT1	↑	Cell lines	Diagnostic/Therapeutic	(8–10)
PVT1	↑	Tissue	Diagnostic/Prognostic	(11–13)
MALAT1	↑	Tissue/Cell lines		(3, 14)
UAC1	↑	Tissue/Cell lines/Exosomes	Diagnostic/Prognostic	(11, 15)
BCYRN1	↑	Tissue/Cell lines	Prognostic/Therapeutic	(16, 17)
CCAT2	↑	Tissue	Diagnostic/Prognostic	(1, 18)
XIST	↑	Tissue/Cell lines	Prognostic/Therapeutic	(19, 20)
PANDAR	↑	Tissue/Cell lines	Prognostic	(21, 22)
H19	↑	Tissue/Cell lines	Diagnostic/Prognostic/Therapeutic	(23, 24)
SNHG6	↑	Tissue/Cell lines	Prognostic/Therapeutic	(25, 26)
LINC01510	↑	Tissue/Cell lines	Prognostic	(27, 28)
MIR4435-2HG	↑	Tissue	Diagnostic/Prognostic	(29, 30)
SLCO4A1-AS1	↑	Tissue/Cell lines	Prognostic/Therapeutic	(31, 32)
RP11-59H7.3	↑	Tissue/Serum/Cell lines	Diagnostic/Therapeutic	(33)
GACAT3	↑	Tissue	Diagnostic/Prognostic	(34)
LINC00152	↑	Tissue	Diagnostic/Prognostic	(34)
TRERNA1	↑	Tissue/Cell lines	Prognostic	(35)
LEF1-AS1	↑	Tissue/Cell lines	Therapeutic/Prognostic	(36)
B3GALT5-AS1	↓	Serum	Diagnostic	(37)
DANCR	↑	Serum	Diagnostic	(38)
HANR	↑	Tissue	Diagnostic/Prognostic	(39)
MFI2-AS1	↑	Tissue	Prognostic/Therapeutic	(40)
treRNA	↑	Tissue	Prognostic	(41)
LINC00461	↑	Tissue/Cell lines	Prognostic/Therapeutic	(42)
AP003555.2	↑	Tissue	Prognostic	(43)
AP006284.1	↑	Tissue	Prognostic	(43)
LINC01602	↑	Tissue	Prognostic	(43)
LINRIS	↑	Tissue/Cell lines	Prognostic/Therapeutic	(44)
cCSC1	↑	Tissue/Cell lines	Prognostic/Therapeutic	(45)
LINC01234	↑	Tissue	Prognostic	(46)
SNHG11	↑	Plasma	Diagnostic/Prognostic	(47)
AK001058	↑	Cell lines	Diagnostic/Therapeutic	(48)
DNAH17-AS1	↑	Tissue	Prognostic/Therapeutic	(49)
RP11-400N13.2	↑	Tissue	Prognostic/Therapeutic	(49)
LINC00957	↑	Tissue/Cell lines	Prognostic/Therapeutic	(50)
NKILA	↓	Tissue/Cell lines	Diagnostic/Prognostic	(51)
MEG3	↓	Tissue/Cell lines/Serum	Diagnostic/Prognostic	(52)
XIRP2-AS1	↓	Tissue/Cell lines	Prognostic/Therapeutic	(53)
CTA-941F9.9	↓	Tissue	Diagnostic	(54)
ZFAS1	↑	Tissue/Cell lines	Diagnostic/Therapeutic	(55)
LNRRIL6	↑	Tissue/Cell lines	Prognostic/Therapeutic	(56)
KIAA0125	↓	Tissue/Cell lines	Diagnostic	(57)
IQCJ-SCHIP1	↓	Tissue	Prognostic/Therapeutic	(58)
DILC	↓	Tissue	Diagnostic/Prognostic	(59)
CRCAL-3	↑	Tissue/Cell lines	Diagnostic/Prognostic/Therapeutic	(60)
CASC19	↑	Tissue/Cell lines	Diagnostic/Therapeutic	(61)
HOTTIP	↑	Tissue	Diagnostic	(11)
PVT1	↑	Tissue	Diagnostic	(11)
UCA1	↑	Tissue	Diagnostic	(11)
RP11	↑	Tissue	Therapeutic	(62)
KAT7	↓	Tissue/Cell lines	Diagnostic/Therapeutic	(63)
TINCR	↑	Tissue/Cell lines	Diagnostic/Prognostic	(64)
GIHCG	↑	Tissue/Cell lines	Prognostic/Therapeutic	(65)
LUCAT1	↑	Tissue/Cell lines	Prognostic/Therapeutic	(66)
ENST00000547547	↓	Tissue/Cell lines	Prognostic/Diagnostic	(67)
MLK7–AS1	↑	Tissue/Cell lines	Diagnostic/Therapeutic	(68)
MAPKAPK5-AS1	↑	Tissue/Cell lines	Prognostic/Therapeutic	(69)
SNHG15	↑	Tissue	Prognostic	(70)
RP1–85F18.6	↑	Tissue/Cell lines	Diagnostic/Prognostic	(71)
NONHSAT074176.2	↓	Tissue	Diagnostic/Therapeutic	(72)
DLEU1	↑	Tissue/Cell lines	Therapeutic	(73)

(Continued)

TABLE 2 | Continued

LncRNA	Expression	Sample	Biomarker	Reference
CYTOR	↑	Tissue	Prognostic/Therapeutic	(74)
SPINT1-AS1	↑	Tissue/Serum exosomes	Prognostic/Therapeutic	(75)
u50535	↑	Tissue/Cell lines	Diagnostic/Prognostic	(76)
RP11-909B2.1	↓	Tissue/Cell lines	Diagnostic/Prognostic	(77)
AK098783	↑	Tissue	Prognostic	(78)
XLOC_010588	↑	Tissue/Cell lines	Diagnostic/Prognostic/Therapeutic	(79)
91H	↑	Serum exosomes	Diagnostic/Prognostic/Therapeutic	(80)
SNHG1	↑	Tissue/Cell lines	Diagnostic/Therapeutic	(81)
LINC00959	↓	Tissue/Cell lines	Prognostic	(82)
GHRLOS	↓	Tissue	Prognostic/Therapeutic	(83)
CPS1-IT1	↓	Tissue/Cell lines	Prognostic/Therapeutic	(84)
HNF1A-AS1	↑	Tissue/Cell lines	Prognostic/Therapeutic	(85)
HOXA-AS2	↑	Tissue/Cell lines	Diagnostic/Therapeutic	(86)
HEIH	↑	Tissue/Cell lines	Prognostic/Therapeutic	(87)
NONHSAT062994	↓	Tissue/Cell lines	Prognostic/Therapeutic	(88)
BANCR	↑	Tissue	Prognostic	(89)
LL22NC03-N64E9.1	↑	Tissue/Cell lines	Prognostic/Therapeutic	(90)
ZEB1-AS1	↑	Tissue/Cell lines	Prognostic	(20)
BCAT1	↓	Tissue/Cell lines	Prognostic	(91)
BLACAT1	↑	Tissue/Cell lines	Diagnostic/Therapeutic	(92)
UBC1	↑	Tissue/Cell lines	Diagnostic	(93)
SNHG12	↑	Tissue/Cell lines	Diagnostic/Prognostic	(94)
SPRY4-IT1	↑	Tissue	Prognostic	(95)
HOXA11-AS	↓	Tissue/Cell lines	Prognostic/Therapeutic	(96)
CRNDE-h	↑	Serum exosomes	Diagnostic/Prognostic	(97)
Loc554202	↓	Tissue	Prognostic	(98)
FOXP4-AS1	↑	Tissue/Cell lines	Prognostic/Therapeutic	(99)
HOTAIRM1	↓	Tissue/Cell lines	Diagnostic	(100)
CTNNAP1	↓	Tissue	Diagnostic	(101)
LINC01133	↓	Tissue/Cell lines	Prognostic/Therapeutic	(102)
CASC11	↑	Tissue/Cell lines	Diagnostic/Therapeutic	(103)
TUG1	↑	Tissue/Cell lines	Diagnostic/Prognostic/Therapeutic	(104)
PRNCR1	↑	Tissue/Cell lines	Diagnostic	(105)
ATB	↑	Plasma	Diagnostic/Prognostic	(2)

References showed in ***Supplementary Material 2***.

circRNAs as Biomarkers for the Diagnosis and Prognosis of CRC

circRNAs are endogenous molecules formed by the reverse splicing of exons, introns, or both exons and introns, resulting in exonic or intronic circRNAs (95). Compared with their linear counterparts, they are highly stable, abundant, and evolutionarily conserved, indicating that they may have important regulatory roles in the development of human tumors (96). circRNAs have a covalently closed loop structure with no 5′-cap or 3′-polyadenylic acid tail, and they are not sensitive to digestion by RNase enzymes (97). Due to the stability of circRNAs, they are abundant in the cytoplasm, and their cellular level can be adjusted by exosome removal or core activity (98).

Although the biological functions of circRNAs are largely not known, previous reports have confirmed that their functions can be divided into roughly four aspects: acting as miRNA sponges, interacting with RNA-binding proteins, encoding proteins, and regulating transcription (99). First, the most researched circRNA molecules are effective miRNA sponges for the regulation of gene expression (100–103). circRNAs may act as miRNA sponges through ceRNA networks, leading to the upregulation or downregulation of target miRNA expression. A single circRNA can bind one or more miRNAs, affecting the translation of dozens or even hundreds of ceRNA transcripts (104). Second, circRNAs have been described as "scaffolds" that interact with many RNA-binding proteins to regulate gene expression. Third, some circRNAs can code for proteins. SHPRH-146aa is a new protein produced by the SNF2 histone linker PHD helicase (SHPRH) gene. The SHPRH circRNA uses overlapping genetic codes to produce a UGA termination codon, resulting in the translation of 17-kDa SHPRH-146aa (105). Fourth, circRNAs may regulate transcription. Studies have shown that circ-ANKRD52 is a circRNA derived from an intron in ankyrin repeat domain 52 (ANKRD52). The combination of circ-ANKRD52 and RNA Pol II knockdown reduces the expression of the parental genes, suggesting that circRNAs may be positive regulators of RNA Pol II transcription (106). circRNAs have a wide range of expression patterns and have unique characteristics such as tissue specificity, stability, and evolutionary conservation, so they may become ideal biomarkers (107). Importantly, circRNAs are stably expressed in saliva, blood, and exosomes, which further increases their potential as biomarkers for disease diagnosis and prognosis (108).

In the past 5 years, with the development of high-throughput sequencing technology, studies of circRNAs as CRC biomarkers

have become ever more extensive. circRNAs are differentially expressed in many cancers, including CRC. The expression of hsa_circ_001988 is significantly downregulated in CRC tissue. The sensitivity and specificity of hsa_circ_001988 for diagnosing CRC are 68% and 73%, respectively, with an AUC value of 0.788. These results indicate that hsa_circ_001988 is a potential biomarker for the diagnosis of CRC (109). circLMNB1, encoded by lamin B1 (LMNB1), is highly expressed in CRC tissue and in 5 CRC cell lines (HT29, LoVo, HCT116, SW480, and RKO). Knockout of circLMNB1 upregulates the expression of E-cadherin, Bax, and caspase-3 in LoVo cells and downregulates the expression of matrix metallopeptidase 2, matrix metallopeptidase 9, and N-cadherin to inhibit the proliferation, migration, and invasion of LoVo cells and to promote cell cycle arrest and apoptosis, indicating that circLMNB1 can be a potential therapeutic target for CRC patients (110). circHIPK3 (hsa_circ_0000284) is derived from exon 2 of the homeodomain-interacting protein kinase 3 (HIPK3) gene, and its spliced mature sequence length is 1099 nucleotides. circHIPK3 is also highly expressed in CRC tissues (111). Elevated circHIPK3 expression is an independent prognostic factor for low overall survival in CRC, which means that circHIPK3 may be a promising prognostic biomarker in CRC. circHIPK3 acts as a miRNA sponge for miR-7 in CRC. Overexpression of circHIPK3 effectively reverses miR-7-induced inhibition of CRC cells progression, and circHIPK3 is regulated by the upstream transcription factor c-Myb. The signaling pathway formed by the c-Myb/circHIPK3/miR-7 axis can also be used as a potential target for the treatment of CRC (111).

Research on circRNAs is still in its infancy, and there are still many challenges to be faced. The mechanisms by which circRNAs participate in the progression of CRC are very complicated. Studies that have determined the partial functions of circRNAs in CRC are shown in **Table 3**. However, there are more circRNAs for CRC that need to be studied. Their functions, mechanisms of action, and clinical application need to be further clarified.

Small Nucleolar RNAs (snoRNAs) as Biomarkers for the Diagnosis and Prognosis of CRC

snoRNAs are a type of generally recognized ncRNA molecule with a length of 60-300 nucleotides that are located mainly in the nucleolus (112, 113). There are two major types of snoRNAs, namely, C/D box snoRNAs and H/ACA box snoRNAs. They differ in their sequence, structure, binding partners, and the nature of post-transcriptional modifications they induce (114). Traditionally, snoRNAs have been considered housekeeping genes because they promote the modification, maturation, and stabilization of pre-ribosomal RNAs by inducing 2′-o-methylation or pseudo-nuclear modifications at specific pre-ribosomal RNA sites with the help of small nucleolar ribonucleoproteins (115). However, more recently, there has been some evidence that they have carcinogenic or anticancer roles (116–118). snoRNAs exist in a stable form in plasma, sputum, and urine samples (118); therefore, they have the potential to be fluid-based biomarkers for cancer (**Table 4**).

The high SNORA42 expression is significantly correlated with a reduction of overall survival and disease-free survival in CRC patients, suggesting that high SNORA42 expression can be used as a prognostic biomarker for CRC (119). The expression of SNORA21 is significantly higher in adenoma and CRC tissues than in adjacent tissue. Receiver operating characteristic curve analysis showed that SNORA21 expression could distinguish CRC tissue from adjacent tissue and that SNORA21 could be used as a diagnostic biomarker for colorectal tumors. Elevated SNORA21 expression also significantly correlates with TNM staging and distant metastasis of CRC, and these results indicate that SNORA21 is also a putative prognostic biomarker for CRC (120). SNORD126 is remarkably highly expressed in tissue samples from CRC patients. SNORD126 promotes the growth of CRC cells by activating the PI3K-Akt pathway *via* the upregulation of fibroblast growth factor receptor 2 expression, and SNORD126 may be a potential therapeutic biomarker for CRC (121).

Transfer RNAs (tRNAs), tRNA-Derived Fragments (tRFs), and tRNA Stress-Induced Small RNAs (tiRNAs) as Biomarkers for CRC

tRNAs are ncRNAs with a length of 76–90 nucleotides (122). tRNAs deliver amino acids to ribosomes and play a key role in protein synthesis (123). According to the length and cutting site of tRNAs, tRNA-derived small RNAs can be divided into two main types (1): tRFs, 14-30 nucleotides in length, derived from mature or precursor tRNAs; and (2) tiRNAs, 29-50 nucleotides in length, induced by stress and produced by specific cleavage of the anticodon loop of mature tRNAs (124). tRF/miR-1280 (derived from both pre-miRNA and tRNA-Leu) levels are significantly reduced in CRC tissue compared with adjacent tissue (125). tRF/miR-1280 is a fundamental regulator of cancer stem cell growth and function in CRC cells. tRF/miR-1280 inhibits Notch/GATA and miR-200b signal transduction through its direct interaction with the 3′-UTR of Jagged canonical Notch ligand 2 (125). According to whether they contain a 5′- or 3′-sequence, tiRNAs can be divided into two subtypes: 5′-tiRNAs and 3′-tiRNAs (126). The expression of 5′-tiRNA-Val is significantly higher in the serum of CRC patients compared with healthy controls, and the average relative level of 5′-tiRNA-Val is higher in CRC tissues with metastasis than in CRC tissues without metastasis, indicating that 5′-tiRNA-Val is a potential biomarker for assessing the progression of CRC (127). However, very little research has been conducted on the application of tRNAs, tRFs, and tiRNAs as CRC biomarkers.

piRNAs as Biomarkers for CRC

piRNAs are a newly discovered class of small RNA molecules that are expressed mainly in germ cell lines and play important roles in maintaining the DNA integrity of germ lines, inhibiting transposon transcription, inhibiting translation, participating in the formation of heterochromatin, epigenetic regulation, and germ cell maturation (128, 129). In addition, some studies have

TABLE 3 | circRNAs as biomarkers for the diagnosis and prognosis of CRC.

CircRNAs	Targeted miRNA	Regulatory Role of circRNA on miRNA	The expression of circRNA	Potential biomarkers	Reference
circSMARCC1	miR-140-3p	Negative	↑	Therapeutic	(1)
	hsa-miR-6833-				(2)
circ-PNN	3p/hsa-let-7i-3p/hsa-miR-1301-3p	Negative	↑	Diagnostic	
circRNA_101951	/	/	↑	Prognostic/Therapeutic	(3)
circPTK2	/	/	↑	Diagnostic/Therapeutic	(4)
circCAMSAP1	miR-328-5p	Negative	↑	Prognostic/Diagnostic/ Therapeutic	(5)
circ-0004771	/	/	↑	Diagnostic	(6)
circ_0000338	/	/	↑	Therapeutic	(7)
hsa_circ_0082182			↑		
				Diagnostic	(8)
hsa_circ_0000370	/	/	↑↓		
hsa_circ_0035445					
circ-CCDC66			↓		(9)
circ-ABCC1 circ-STIL	/	/	↓↓	Diagnostic	
circ-ITGA7	miR-3187-3p	Negative	↓	Diagnostic/Therapeutic	(10)
hsa_circ_0004585	Multiple	/	↑	Diagnostic/Therapeutic	(11)
hsa_circ_0142527	/	/	↓	Diagnostic	(12)
circVAPA	miR-101	Negative	↑	Diagnostic/Therapeutic	(13)
circDDX17	hsa-miR-21-5p	Negative	↓	Diagnostic/Therapeutic	(14)
circ_0026344	miR-21/miR-31	Negative	↓	Prognostic	(15)
circHIPK3	miR-7	Negative	↑	Prognostic/Therapeutic	(16)
hsa_circ_0007534	/	/	↑	Diagnostic/Prognostic	(17)
circRNA0003906	/	/	↓	Diagnostic/Therapeutic	(18)
hsa_circRNA_103809	/	/	↓	Diagnostic	(19)
hsa_circRNA_104700			↓		
circRNA_001569	miR-145	Negative	↑	Therapeutic	(20)
hsa_circ_0005075	/	/	↑	Diagnostic/Therapeutic	(21)
hsa_circ_0020397	miR-138	Negative	↑	Therapeutic	(22)
hsa_circ_0136666	miR-136	Negative	↑	Therapeutic	(23)
hsa_circ_0000523	miR-31	Negative	↓	Therapeutic	(24)
has_circ_0055625	miR-106b-5p	Negative	↑	Therapeutic/Prognostic	(25)
circ_104916	/	/	↓	Therapeutic/Prognostic	(26)
hsa_circ_0000423	/	/	↑	Therapeutic/Prognostic	(27)
hsa_circ_0001649	/	/	↓	Diagnostic	(28)
hsa_circ_0000567	/	/	↓	Diagnostic/Prognostic	(29)
hsa_circ_0000826	/	/	↓	Diagnostic/Therapeutic	(30)
circ-FBXW7	/	/	↓	Therapeutic	(31)
circMTO1	/	/	↓	Therapeutic/Prognostic	(32)
circ_0002138	/	/	↓	Diagnostic/Therapeutic	(33)
hsa_circ_0002320	/	/	↓	Diagnostic/Prognostic	(34)
hsa_circ_0000711	/	/	↓	Diagnostic/Prognostic	(35)
circLMNB1	/	/	↑	Therapeutic	(36)
circFADS2	/	/	↑	Therapeutic/Prognostic	(37)
circUBAP2	miR-199a	Negative	↑	Therapeutic	(38)
hsa_circ_0044556	hsa-mir-214-3p	Negative	↑	Diagnostic/Therapeutic/ Prognostic	(39)
circVAPA	miR-125a	Negative	↑	Therapeutic	(40)
circHUWE1	miR-486	Negative	↑	Diagnostic/Therapeutic	(41)
circMBOAT2	miR-519d-3p	Negative	↑	Diagnostic/Prognostic	(42)

References showed in ***Supplementary Material 3****.*

shown that piRNAs regulate mRNA expression by binding to the 3′-UTR of mRNAs (130, 131). More than 30,000 piRNAs have been identified in humans (132) and are believed to be related to the biological behavior of cancer and participate in the occurrence and development of cancer (129). piRNAs have recently been shown to be potential prognostic biomarkers for CRC (133). The expression of piR-1245 is significantly higher in CRC tissue than in paracancerous tissue. piR-1245 is not only highly expressed in CRC tissue but is also upregulated in other types of cancer (including lung, breast, stomach, bladder, kidney, and prostate cancer), highlighting its important role in carcinogenesis. Meanwhile, high piR-1245 expression is an independent predictor of poor prognosis in CRC (133). The expression of 5 piRNAs (piR-001311, piR-004153, piR-017723, piR-017724, and piR-020365) is markedly downregulated in CRC patients (134). The AUC value of these 5 piRNAs is 0.867

TABLE 4 | snoRNA as potential biomarker for colorectal cancer.

Cancer	snoRNA	Expression	Sample	Potential biomarker	Function of RNA	Reference
Colorectal cancer	SNORA42	↑	Tissue/Cell lines	Prognostic	Oncogene	(1)
Colorectal cancer	SNORA21	↑	Tissue/Cell lines	Diagnostic/Prognostic/Therapeutic	Oncogene	(2)
Hepatocellular carcinoma/Colorectal cancer	SNORD126	↑	Tissue	Therapeutic	Oncogene	(3)
Hepatocellular carcinoma	SNORACA11	↑	Tissue/Cell lines	Prognostic/Therapeutic	Oncogene	(4)
Lung carcinoma	SNORA71A	↑	Tissue	Prognostic/Therapeutic	Oncogene	(5)
Gastric carcinoma	SNORD105b	↑	Tissue	Prognostic/Therapeutic	Oncogene	(6)
Breast carcinoma	SNORA7B	↑	Tissue/Cell lines	Diagnostic/Prognostic	Oncogene	(7)
Prostate cancer	SNORA42	↑	Tissue/Cell lines	Diagnostic/Prognostic	Oncogene	(8)

References showed in ***Supplementary Material 4****.*

(95%CI, 0.817-0.907), with a sensitivity of 78.3% and specificity of 74.2%. These findings suggest that these 5 serum piRNAs may be potential diagnostic biomarkers for CRC (134). Other putative piRNA biomarkers of CRC are shown in **Table 5**.

CONCLUSION AND FUTURE OUTLOOK

CRC is one of the most common malignant tumors in humans, with more than half a million deaths each year, and a delayed

TABLE 5 | piRNAs as potential biomarker for colorectal cancer.

piRNA	Expression	Sample	Biomarker	Reference
piR-1245	↑	Tissue	Prognostic	(1)
piR-001311				
piR-004153				
piR-017723	↓	Serum	Diagnostic/Prognostic	(2)
piR-017724				
piR-020365				
piR-823	↑	Tissue	Prognostic/Therapeutic	(3)
piR-020619	↑	Serum	Diagnostic	(4)
piR-020450				
piR-24000	↑	Tissue	Diagnostic/Therapeutic	(5)
piR-54265	↑	Tissue/Cell lines	Therapeutic/Prognostic	(6)

References showed in ***Supplementary Material 5****.*

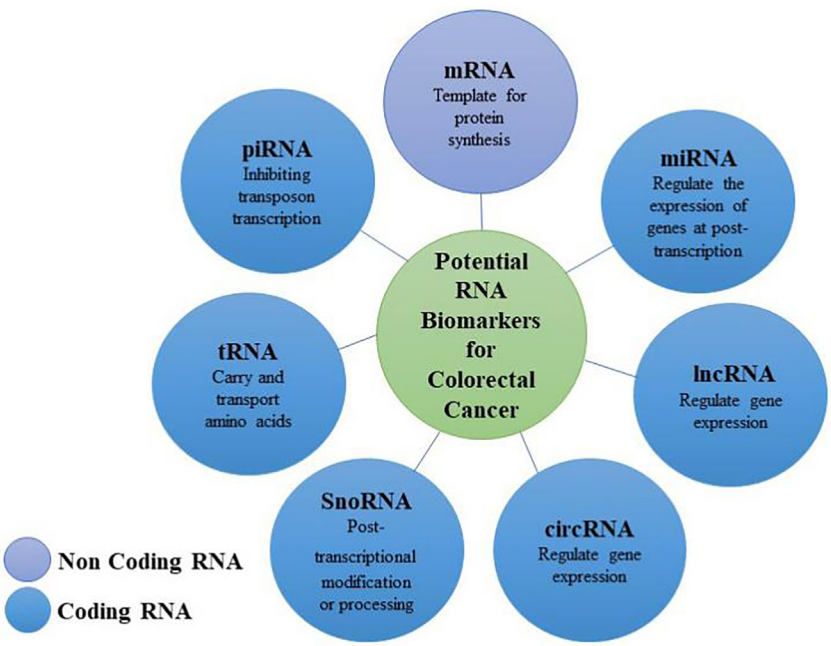

FIGURE 1 | Biomarkers (mRNAs and non-coding RNAs) for the diagnosis and prognosis of colorectal cancer.

diagnosis is one of the most critical problems of CRC. Despite significant efforts and progress in improving the treatment of CRC through surgery and chemotherapy, its prognosis remains poor. In addition, recurrence and metastasis often occur after surgery. However, it is encouraging that screening has become routine in many countries, and newer, less invasive techniques are being developed to replace highly invasive colonoscopies. In these less invasive or non-invasive methods, further progress is needed to achieve early diagnosis, preoperative and postoperative staging, and to predict the clinical prognosis of CRC. Increasing evidence shows that ncRNAs play vital roles in the occurrence and development of CRC. The emergence of high-throughput sequencing technology and the study of epigenetics and transcriptomics have also further promoted our understanding of CRC. In this review, we described the performance of various RNAs as potential biomarkers for CRC, including the transition from tissue samples and cell line models to body fluid biopsies. In addition to the diagnostic performance and prognostic value of a single RNA biomarker, a variety of RNA biomarker combinations can improve the sensitivity and specificity of diagnosis and prognosis. Being able to detect RNAs in various body fluids is their main advantage as biomarkers so that a non-invasive diagnosis can be made. There are numerous studies on RNA biomarkers of CRC, but there are few unified opinions at present. The goal of current and future studies is to determine which non-invasive CRC diagnostic biomarkers are feasible, to understand which biomarkers can better predict patient prognosis, and to seek more personalized therapeutic targets (**Figure 1**).

AUTHOR CONTRIBUTIONS

JH and FW wrote the manuscript. All authors contributed to the article and approved the submitted version.

FUNDING

This work was supported by grants from the Medical and Health Science and Technology Project of Panyu District, Guangzhou (No. 2017-Z04-18, 2018-Z04-59, 2018-Z04-50, 2019-Z04-02), Science and Technology Planning Project of Guangdong Province (No. 2017ZC0372), Guangzhou Health and Family Planning Commission Program (No. 20181A011118, 20192A011027, 20191A011119, 20201A010085), Project of Guangdong Administration of Traditional Chinese Medicine (No. 20192073), Natural Science Foundation of Guangdong Province (No. 2018A0303130191), Guangzhou Science and Technology Plan Project (No.201904010044, 202002030032), and Medical Science and Technology Research Foundation of Guangdong Province (No. A2020304).

SUPPLEMENTARY MATERIAL

The Supplementary Material for this article can be found online at: https://www.frontiersin.org/articles/10.3389/fonc.2021.632834/full#supplementary-material

REFERENCES

1. Bray F, Ferlay J, Soerjomataram I, Siegel RL, Torre LA, Jemal A. Global Cancer Statistics 2018: GLOBOCAN Estimates of Incidence and Mortality Worldwide for 36 Cancers in 185 Countries. *CA Cancer J Clin* (2018) 68 (6):394–424. doi: 10.3322/caac.21492
2. Coppede F, Lopomo A, Spisni R, Migliore L. Genetic and Epigenetic Biomarkers for Diagnosis, Prognosis and Treatment of Colorectal Cancer. *World J Gastroenterol* (2014) 20(4):943–56. doi: 10.3748/wjg.v20.i4.943
3. Manfredi S, Bouvier AM, Lepage C, Hatem C, Dancourt V, Faivre J. Incidence and Patterns of Recurrence After Resection for Cure of Colonic Cancer in a Well Defined Population. *Br J Surg* (2006) 93(9):1115–22. doi: 10.1002/bjs.5349
4. Langan RC, Mullinax JE, Raiji MT, Upham T, Summers T, Stojadinovic A, et al. Colorectal Cancer Biomarkers and the Potential Role of Cancer Stem Cells. *J Cancer* (2013) 4(3):241–50. doi: 10.7150/jca.5832
5. Lech G, Slotwinski R, Slodkowski M, Krasnodebski IW. Colorectal Cancer Tumour Markers and Biomarkers: Recent Therapeutic Advances. *World J Gastroenterol* (2016) 22(5):1745–55. doi: 10.3748/wjg.v22.i5.1745
6. Jass JR. Classification of Colorectal Cancer Based on Correlation of Clinical, Morphological and Molecular Features. *Histopathology* (2007) 50(1):113–30. doi: 10.1111/j.1365-2559.2006.02549.x
7. Piñol V, Castells A, Andreu M, Castellví-Bel S, Alenda C, Llor X, et al. Accuracy of Revised Bethesda Guidelines, Microsatellite Instability, and Immunohistochemistry for the Identification of Patients With Hereditary Nonpolyposis Colorectal Cancer. *JAMA* (2005) 293(16):1986–94. doi: 10.1001/jama.293.16.1986
8. Gonzalez-Pons M, Cruz-Correa M. Colorectal Cancer Biomarkers: Where are We Now? *BioMed Res Int* (2015) 2015:149014. doi: 10.1155/2015/149014
9. De Sousa EMF, Wang X, Jansen M, Fessler E, Trinh A, de Rooij LP, et al. Poor-Prognosis Colon Cancer is Defined by a Molecularly Distinct Subtype and Develops From Serrated Precursor Lesions. *Nat Med* (2013) 19(5):614–8. doi: 10.1038/nm.3174
10. Sadanandam A, Lyssiotis CA, Homicsko K, Collisson EA, Gibb WJ, Wullschleger S, et al. A Colorectal Cancer Classification System That Associates Cellular Phenotype and Responses to Therapy. *Nat Med* (2013) 19(5):619–25. doi: 10.1038/nm.3175
11. Ni Y, Xie G, Jia W. Metabonomics of Human Colorectal Cancer: New Approaches for Early Diagnosis and Biomarker Discovery. *J Proteome Res* (2014) 13(9):3857–70. doi: 10.1021/pr500443c
12. Lieberman D. Colorectal Cancer Screening With Colonoscopy. *JAMA Intern Med* (2016) 176(7):903–4. doi: 10.1001/jamainternmed.2016.1333
13. Knudsen AB, Zauber AG, Rutter CM, Naber SK, Doria-Rose VP, Pabiniak C, et al. Estimation of Benefits, Burden, and Harms of Colorectal Cancer Screening Strategies: Modeling Study for the US Preventive Services Task Force. *JAMA* (2016) 315(23):2595–609. doi: 10.1001/jama.2016.6828
14. Villeger R, Lopes A, Veziant J, Gagniere J, Barnich N, Billard E, et al. Microbial Markers in Colorectal Cancer Detection and/or Prognosis. *World J Gastroenterol* (2018) 24(22):2327–47. doi: 10.3748/wjg.v24.i22.2327
15. De Mattos-Arruda L, Weigelt B, Cortes J, Won HH, Ng CKY, Nuciforo P, et al. Capturing Intra-Tumor Genetic Heterogeneity by De Novo Mutation Profiling of Circulating Cell-Free Tumor DNA: A Proof-of-Principle. *Ann Oncol* (2014) 25(9):1729–35. doi: 10.1093/annonc/mdu239
16. Murtaza M, Dawson SJ, Pogrebniak K, Rueda OM, Provenzano E, Grant J, et al. Multifocal Clonal Evolution Characterized Using Circulating Tumour DNA in a Case of Metastatic Breast Cancer. *Nat Commun* (2015) 6:8760. doi: 10.1038/ncomms9760
17. Thierry AR, El Messaoudi S, Gahan PB, Anker P, Stroun M. Origins, Structures, and Functions of Circulating DNA in Oncology. *Cancer Metastasis Rev* (2016) 35(3):347–76. doi: 10.1007/s10555-016-9629-x
18. Zhang X, Sun XF, Shen B, Zhang H. Potential Applications of DNA, RNA and Protein Biomarkers in Diagnosis, Therapy and Prognosis for Colorectal

Cancer: A Study From Databases to AI-Assisted Verification. *Cancers (Basel)* (2019) 11(2):172. doi: 10.3390/cancers11020172
19. Das V, Kalita J, Pal M. Predictive and Prognostic Biomarkers in Colorectal Cancer: A Systematic Review of Recent Advances and Challenges. *BioMed Pharmacother* (2017) 87:8–19. doi: 10.1016/j.biopha.2016.12.064
20. Cheshomi H, Matin MM. Exosomes and Their Importance in Metastasis, Diagnosis, and Therapy of Colorectal Cancer. *J Cell Biochem* (2019) 120 (2):2671–86. doi: 10.1002/jcb.27582
21. Kulendran M, Stebbing JF, Marks CG, Rockall TA. Predictive and Prognostic Factors in Colorectal Cancer: A Personalized Approach. *Cancers (Basel)* (2011) 3(2):1622–38. doi: 10.3390/cancers3021622
22. Chen TH, Chang SW, Huang CC, Wang KL, Yeh KT, Liu CN, et al. The Prognostic Significance of APC Gene Mutation and miR-21 Expression in Advanced-Stage Colorectal Cancer. *Colorectal Dis* (2013) 15(11):1367–74. doi: 10.1111/codi.12318
23. Sarasqueta AF, Forte G, Corver WE, Miranda NFD, Ruano D, Eijk RV, et al. Integral Analysis of p53 and its Value as Prognostic Factor in Sporadic Colon Cancer. *BMC Cancer* (2013) 2013(13):277. doi: 10.1186/1471-2407-13-277
24. Nicholson RI, Gee JM, Harper ME. EGFR and Cancer Prognosis. *Eur J Cancer* (2001) 37:9–15. doi: 10.1016/s0959-8049(01)00231-3
25. De Robertis M, Loiacono L, Fusilli C, Poeta ML, Mazza T, Sanchez M, et al. Dysregulation of EGFR Pathway in EphA2 Cell Subpopulation Significantly Associates With Poor Prognosis in Colorectal Cancer. *Clin Cancer Res* (2017) 23(1):159–70. doi: 10.1158/1078-0432.CCR-16-0709
26. Cunningham D, Humblet Y, Siena S, Khayat D, Bleiberg H, Santoro A, et al. Cetuximab Monotherapy and Cetuximab Plus Irinotecan in Irinotecan-Refractory Metastatic Colorectal Cancer. *N Engl J Med* (2004) 351(4):337–45. doi: 10.1056/NEJMoa033025
27. Roth AD, Tejpar S, Delorenzi M, Yan P, Fiocca R, Klingbiel D, et al. Prognostic Role of KRAS and BRAF in Stage II and III Resected Colon Cancer: Results of the Translational Study on the PETACC-3, Eortc 40993, SAKK 60-00 Trial. *J Clin Oncol* (2010) 28(3):466–74. doi: 10.1200/JCO.2009.23.3452
28. Kislitsin D, Lerner A, Rennert G, Lev Z. K-Ras Mutations in Sporadic Colorectal Tumors in Israel: Unusual High Frequency of Codon 13 Mutations and Evidence for Nonhomogeneous Representation of Mutation Subtypes. *Dig Dis Sci* (2002) 47(5):1073–9. doi: 10.1023/a:1015090124153
29. Best MG, Sol N, Kooi I, Tannous J, Westerman BA, Rustenburg F, et al. Rna-Seq of Tumor-Educated Platelets Enables Blood-Based Pan-Cancer, Multiclass, and Molecular Pathway Cancer Diagnostics. *Cancer Cell* (2015) 28(5):666–76. doi: 10.1016/j.ccell.2015.09.018
30. Garcia V, Garcia JM, Pena C, Silva J, Dominguez G, Lorenzo Y, et al. Free Circulating mRNA in Plasma From Breast Cancer Patients and Clinical Outcome. *Cancer Lett* (2008) 263(2):312–20. doi: 10.1016/j.canlet.2008.01.008
31. Wang H, Zhang X, Wang L, Zheng G, Du L, Yang Y, et al. Investigation of Cell Free BIRC5 mRNA as a Serum Diagnostic and Prognostic Biomarker for Colorectal Cancer. *J Surg Oncol* (2014) 109(6):574–9. doi: 10.1002/jso.23526
32. Pun JC, Chan JY, Chun BK, Ng KW, Tsui SY, Wan TM, et al. Plasma Bmi1 mRNA as a Potential Prognostic Biomarker for Distant Metastasis in Colorectal Cancer Patients. *Mol Clin Oncol* (2014) 2(5):817–20. doi: 10.3892/mco.2014.321
33. Yu H, Li H, Cui YG, Xiao W, Dai GH, Huang JX, et al. The mRNA Level of MLH1 in Peripheral Blood is a Biomarker for the Diagnosis of Hereditary Nonpolyposis Colorectal Cancer. *Am J Cancer Res* (2016) 6(5):1135–40.
34. Mohammadi P, Saidijam M, Kaki A, Etemadi K, Shabab N, Yadegarazari R. A Pilot Study of CK19, CK20 and GCC mRNA in the Peripheral Blood as a Colorectal Cancer Biomarker Panel. *Int J Mol Cell Med* (2016) 5(1):30–6.
35. Ji B, Cheng X, Cai X, Kong C, Yang Q, Fu T, et al. CK20 Mrna Expression in Serum as a Biomarker for Colorectal Cancer Diagnosis: A Meta-Analysis. *Open Med (Wars)* (2017) 12:347–53. doi: 10.1515/med-2017-0050
36. Morio H, Sun YC, Harada M, Ide H, Shimozato O, Zhou XJ, et al. Cancer-Type OATP1B3 mRNA in Extracellular Vesicles as a Promising Candidate for a Serum-Based Colorectal Cancer Biomarker. *Biol Pharm Bull* (2018) 41 (3):445–9. doi: 10.1248/bpb.b17-00743
37. Yang L, Jiang Q, Li DZ, Zhou X, Yu DS, Zhong J. Timp1 mRNA in Tumor-Educated Platelets is Diagnostic Biomarker for Colorectal Cancer. *Aging (Albany NY)* (2019) 11(20):8998–9012. doi: 10.18632/aging.102366
38. Olsson L, Hammarstrom ML, Israelsson A, Lindmark G, Hammarstrom S. Allocating Colorectal Cancer Patients to Different Risk Categories by Using a Five-Biomarker mRNA Combination in Lymph Node Analysis. *PloS One* (2020) 15(2):e0229007. doi: 10.1371/journal.pone.0229007
39. Kung JT, Colognori D, Lee JT. Long Noncoding RNAs: Past, Present, and Future. *Genetics* (2013) 193(3):651–69. doi: 10.1534/genetics.112.146704
40. Quan M, Chen J, Zhang D. Exploring the Secrets of Long Noncoding Rnas. *Int J Mol Sci* (2015) 16(3):5467–96. doi: 10.3390/ijms16035467
41. Zeng X, Lin W, Guo M, Zou Q. A Comprehensive Overview and Evaluation of Circular RNA Detection Tools. *PloS Comput Biol* (2017) 13(6):e1005420. doi: 10.1371/journal.pcbi.1005420
42. Esquela-Kerscher A, Slack FJ. Oncomirs - microRNAs With a Role in Cancer. *Nat Rev Cancer* (2006) 6(4):259–69. doi: 10.1038/nrc1840
43. Malumbres M. miRNAs and Cancer: An Epigenetics View. *Mol Aspects Med* (2013) 34(4):863–74. doi: 10.1016/j.mam.2012.06.005
44. Michael MZ, Connor SMO, Pellekaan NGVH, Young GP, James RJ. Reduced Accumulation of Specific microRNAs in Colorectal Neoplasia. *Mol Cancer Res* (2003) 1(12):882–91.
45. Li C, Yan G, Yin L, Liu T, Li C, Wang L. Prognostic Roles of microRNA 143 and microRNA 145 in Colorectal Cancer: A Meta-Analysis. *Int J Biol Markers* (2019) 34(1):6–14. doi: 10.1177/1724600818807492
46. Chen X, Guo X, Zhang H, Xiang Y, Chen J, Yin Y, et al. Role of miR-143 Targeting KRAS in Colorectal Tumorigenesis. *Oncogene* (2009) 28 (10):1385–92. doi: 10.1038/onc.2008.474
47. Fei BY, Wang XY, Fang XD. MicroRNA-143 Replenishment Re-Sensitizes Colorectal Cancer Cells Harboring Mutant, But Not Wild-Type, KRAS to Paclitaxel Treatment. *Tumour Biol* (2016) 37(5):5829–35. doi: 10.1007/s13277-015-4354-6
48. Tang H, Li K, Zheng J, Dou X, Zhao Y, Wang L. microRNA-145 Regulates Tumor Suppressor Candidate 3 and Mitogen-Activated Protein Kinase Pathway to Inhibit the Progression of Colorectal Cancer. *J Cell Biochem* (2019) 120(5):8376–84. doi: 10.1002/jcb.28122
49. Yuan W, Sui C, Liu Q, Tang W, An H, Ma J. Up-Regulation of microRNA-145 Associates With Lymph Node Metastasis in Colorectal Cancer. *PloS One* (2014) 9(7):e102017. doi: 10.1371/journal.pone.0102017
50. Krichevsky AM, Gabriely G. miR-21: A Small Multi-Faceted RNA. *J Cell Mol Med* (2009) 13(1):39–53. doi: 10.1111/j.1582-4934.2008.00556.x
51. Tsukamoto M, Iinuma H, Yagi T, Matsuda K, Hashiguchi Y. Circulating Exosomal MicroRNA-21 as a Biomarker in Each Tumor Stage of Colorectal Cancer. *Oncology* (2017) 92(6):360–70. doi: 10.1159/000463387
52. Xu K, Liang X, Cui D, Wu Y, Shi W, Liu J. miR-1915 Inhibits Bcl-2 to Modulate Multidrug Resistance by Increasing Drug-Sensitivity in Human Colorectal Carcinoma Cells. *Mol Carcinog* (2013) 52(1):70–8. doi: 10.1002/mc.21832
53. Xu F, Xu L, Wang M, An G, Feng G. The Accuracy of Circulating microRNA-21 in the Diagnosis of Colorectal Cancer: A Systematic Review and Meta-Analysis. *Colorectal Dis* (2015) 17(5):O100–7. doi: 10.1111/codi.12917
54. Liu GH, Zhou ZG, Chen R, Wang MJ, Zhou B, Li Y, et al. Serum miR-21 and miR-92a as Biomarkers in the Diagnosis and Prognosis of Colorectal Cancer. *Tumour Biol* (2013) 34(4):2175–81. doi: 10.1007/s13277-013-0753-8
55. Zhang G, Zhou H, Xiao H, Liu Z, Tian H, Zhou T. MicroRNA-92a Functions as an Oncogene in Colorectal Cancer by Targeting PTEN. *Dig Dis Sci* (2014) 59(1):98–107. doi: 10.1007/s10620-013-2858-8
56. Pan BP, Johnstone RM. Fate of the Transferrin Receptor During Maturation of Sheep Reticulocytes In Vitro: Selective Externalization of the Receptor. *Cell* (1983) 33(3):967–78. doi: 10.1016/0092-8674(83)90040-5
57. Lai X, Friedman A. Exosomal microRNA Concentrations in Colorectal Cancer: A Mathematical Model. *J Theor Biol* (2017) 415:70–83. doi: 10.1016/j.jtbi.2016.12.006
58. Ahmed FE, Jeffries CD, Vos PW, Flake G, Nuovo GJ, Sinar DR, et al. Diagnostic microRNA Markers for Screening Sporadic Human Colon Cancer and Active Ulcerative Colitis in Stool and Tissue. *Cancer Genomics Proteomics* (2009) 6(5):281–95.
59. Wu CW, Ng SSM, Dong YJ, Ng SC, Leung WW, Lee CW, et al. Detection of miR-92a and miR-21 in Stool Samples as Potential Screening Biomarkers for

Colorectal Cancer and Polyps. *Controlled Clin Trial* (2012) 61(5):739–45. doi: 10.1136/gut.2011.239236
60. Ahmed FE, Ahmed NC, Vos PW, Bonnerup C, Atkins JN, Casey M, et al. Diagnostic microRNA Markers to Screen for Sporadic Human Colon Cancer in Stool: I. *Proof principle. Cancer Genomics Proteomics* (2013) 10(3):93–113.
61. Wu CW, Ng SC, Dong Y, Tian L, Ng SS, Leung WW, et al. Identification of microRNA-135b in Stool as a Potential Noninvasive Biomarker for Colorectal Cancer and Adenoma. *Clin Cancer Res* (2014) 20(11):2994–3002. doi: 10.1158/1078-0432.CCR-13-1750
62. Roman-Canal B, Tarragona J, Moiola CP, Gatius S, Bonnin S, Ruiz-Miro M, et al. EV-Associated miRNAs From Peritoneal Lavage as Potential Diagnostic Biomarkers in Colorectal Cancer. *J Transl Med* (2019) 17 (1):208. doi: 10.1186/s12967-019-1954-8
63. Cabili MN, Trapnell C, Goff L, Koziol M, Tazon-Vega B, Regev A, et al. Integrative Annotation of Human Large Intergenic Noncoding RNAs Reveals Global Properties and Specific Subclasses. *Genes Dev* (2011) 25 (18):1915–27. doi: 10.1101/gad.17446611
64. Orom UA, Derrien T, Beringer M, Gumireddy K, Gardini A, Bussotti G, et al. Long Noncoding RNAs With Enhancer-Like Function in Human Cells. *Cell* (2010) 143(1):46–58. doi: 10.1016/j.cell.2010.09.001
65. Gutschner T, Diederichs S. The Hallmarks of Cancer: A Long non-Coding RNA Point of View. *RNA Biol* (2012) 9(6):703–19. doi: 10.4161/rna.20481
66. Hanahan D, Weinberg RA. The Hallmarks of Cancer. *Cell* (2000) 100(1):57–70. doi: 10.1016/s0092-8674(00)81683-9
67. Shen X, Xue Y, Cong H, Wang X, Fan Z, Cui X, et al. Circulating Lncrna DANCR as a Potential Auxillary Biomarker for the Diagnosis and Prognostic Prediction of Colorectal Cancer. *Biosci Rep* (2020) 40(3): BSR20191481. doi: 10.1042/BSR20191481
68. Chen S, Shan T, Chen X, Yang WB, Wu T, Sun XL, et al. Association of treRNA With Lymphatic Metastasis and Poor Prognosis in Colorectal Cancer. *Int J Clin Exp Pathol* (2019) 12(5):1770–4.
69. Li C, Li W, Zhang Y, Zhang X, Liu T, Zhang Y, et al. Increased Expression of Antisense Lncrna SPINT1-AS1 Predicts a Poor Prognosis in Colorectal Cancer and is Negatively Correlated With its Sense Transcript. *Onco Targets Ther* (2018) 11:3969–78. doi: 10.2147/OTT.S163883
70. Xin Y, Li Z, Shen J, Chan MT, Wu WK. CCAT1: A Pivotal Oncogenic Long non-Coding RNA in Human Cancers. *Cell Prolif* (2016) 49(3):255–60. doi: 10.1111/cpr.12252
71. Nissan A, Stojadinovic A, Mitrani-Rosenbaum S, Halle D, Grinbaum R, Roistacher M, et al. Colon Cancer Associated transcript-1: A Novel RNA Expressed in Malignant and Pre-Malignant Human Tissues. *Int J Cancer* (2012) 130(7):1598–606. doi: 10.1002/ijc.26170
72. Alaiyan B, Ilyayev N, Stojadinovic A, Izadjoo M, Roistacher M, Pavlov V, et al. Differential Expression of Colon Cancer Associated Transcript1 (CCAT1) Along the Colonic Adenoma-Carcinoma Sequence. *BMC Cancer* (2013) 13:196. doi: 10.1186/1471-2407-13-196
73. Zhao W, Song M, Zhang J, Kuerban M, Wang H. Combined Identification of Long non-Coding RNA CCAT1 and HOTAIR in Serum as an Effective Screening for Colorectal Carcinoma. *Int J Clin Exp Pathol* (2015) 8 (11):14131–40.
74. Ozawa T, Matsuyama T, Toiyama Y, Takahashi N, Ishikawa T, Uetake H, et al. CCAT1 and CCAT2 Long Noncoding RNAs, Located Within the 8q.24.21 'Gene Desert', Serve as Important Prognostic Biomarkers in Colorectal Cancer. *Ann Oncol* (2017) 28(8):1882–8. doi: 10.1093/annonc/mdx248
75. Chen L, Hu N, Wang C, Zhao H, Gu Y. Long non-Coding RNA CCAT1 Promotes Multiple Myeloma Progression by Acting as a Molecular Sponge of miR-181a-5p to Modulate HOXA1 Expression. *Cell Cycle* (2018) 17 (3):319–29. doi: 10.1080/15384101.2017.1407893
76. Shang A, Wang W, Gu C, Chen W, Lu W, Sun Z, et al. Long non-Coding RNA CCAT1 Promotes Colorectal Cancer Progression by Regulating miR-181a-5p Expression. *Aging (Albany NY)* (2020) 12(9):8301–20. doi: 10.18632/aging.103139
77. Yang C, Pan Y, Deng SP. Downregulation of Lncrna CCAT1 Enhances 5-Fluorouracil Sensitivity in Human Colon Cancer Cells. *BMC Mol Cell Biol* (2019) 20(1):9. doi: 10.1186/s12860-019-0188-1
78. Tripathi V, Ellis JD, Shen Z, Song DY, Pan Q, Watt AT, et al. The Nuclear-Retained Noncoding RNA MALAT1 Regulates Alternative Splicing by Modulating SR Splicing Factor Phosphorylation. *Mol Cell* (2010) 39 (6):925–38. doi: 10.1016/j.molcel.2010.08.011
79. Wilusz JE, Freier SM, Spector DL. 3' End Processing of a Long Nuclear-Retained Noncoding RNA Yields a tRNA-like Cytoplasmic RNA. *Cell* (2008) 135(5):919–32. doi: 10.1016/j.cell.2008.10.012
80. Wu Y, Lu W, Xu J, Shi Y, Zhang H, Xia D. Prognostic Value of Long non-Coding RNA MALAT1 in Cancer Patients. *Tumour Biol* (2016) 37(1):897–903. doi: 10.1007/s13277-015-3870-8
81. Ji Q, Zhang L, Liu X, Zhou L, Wang W, Han Z, et al. Long non-Coding RNA MALAT1 Promotes Tumour Growth and Metastasis in Colorectal Cancer Through Binding to SFPQ and Releasing Oncogene PTBP2 From SFPQ/PTBP2 Complex. *Br J Cancer* (2014) 111(4):736–48. doi: 10.1038/bjc.2014.383
82. Ji Q, Cai G, Liu X, Zhang Y, Wang Y, Zhou L, et al. MALAT1 Regulates the Transcriptional and Translational Levels of Proto-Oncogene RUNX2 in Colorectal Cancer Metastasis. *Cell Death Dis* (2019) 10(6):378. doi: 10.1038/s41419-019-1598-x
83. Zheng HT, Shi DB, Wang YW, Li XX, Xu Y, Tripathi P, et al. High Expression of Lncrna MALAT1 Suggests a Biomarker of Poor Prognosis in Colorectal Cancer. *Int J Clin Exp Pathol* (2014) 7(6):3174–81.
84. Steinhoff C, Paulsen M, Kielbasa S, Walter J, Vingron M. Expression Profile and Transcription Factor Binding Site Exploration of Imprinted Genes in Human and Mouse. *BMC Genomics* (2009) 10:144. doi: 10.1186/1471-2164-10-144
85. Engemann S, Strödicke M, Paulsen M, Franck O, Reinhardt R, Lane N, et al. Sequence and Functional Comparison in the Beckwith-Wiedemann Region: Implications for a Novel Imprinting Centre and Extended Imprinting. *Hum Mol Genet* (2000) 9(18):2691–706. doi: 10.1093/hmg/9.18.2691
86. Tsang WP, Ng EKO, Ng SSM, Jin H, Yu J, Sung JJY, et al. Oncofetal H19-derived miR-675 Regulates Tumor Suppressor RB in Human Colorectal Cancer. *Carcinogenesis* (2010) 31(3):350–8. doi: 10.1093/carcin/bgp181
87. Han D, Gao X, Wang M, Qiao Y, Xu Y, Yang J, et al. Long Noncoding RNA H19 Indicates a Poor Prognosis of Colorectal Cancer and Promotes Tumor Growth by Recruiting and Binding to Eif4a3. *Oncotarget* (2016) 7 (16):22159–73. doi: 10.18632/oncotarget.8063
88. Li S, Hua Y, Jin J, Wang H, Du M, Zhu L, et al. Association of Genetic Variants in Lncrna H19 With Risk of Colorectal Cancer in a Chinese Population. *Oncotarget* (20116) 7(18):25470–7. doi: 10.18632/oncotarget.8330
89. Ding D, Li C, Zhao T, Li D, Yang L, Zhang B. Lncrna H19/miR-29b-3p/PGRN Axis Promoted Epithelial-Mesenchymal Transition of Colorectal Cancer Cells by Acting on Wnt Signaling. *Mol Cells* (2018) 41(5):423–35. doi: 10.14348/molcells.2018.2258
90. Shtivelman E, Bishop JM. Effects of Translocations on Transcription From PVT. *Mol Cell Biol* (1990) 10(4):1835–9. doi: 10.1128/mcb.10.4.1835
91. Wang C, Zhu X, Pu C, Song X. Upregulated Plasmacytoma Variant Translocation 1 Promotes Cell Proliferation, Invasion and Metastasis in Colorectal Cancer. *Mol Med Rep* (2018) 17(5):6598–604. doi: 10.3892/mmr.2018.8669
92. Fan H, Zhu JH, Yao XQ. Long non-Coding RNA PVT1 as a Novel Potential Biomarker for Predicting the Prognosis of Colorectal Cancer. *Int J Biol Markers* (2018) 33(4):415–22. doi: 10.1177/1724600818777242
93. Fan H, Zhu JH, Yao XQ. Knockdown of Long Noncoding RNA PVT1 Reverses Multidrug Resistance in Colorectal Cancer Cells. *Mol Med* (2018) Rep17(6):8309–15. doi: 10.3892/mmr.2018.8907
94. Gharib E, Anaraki F, Baghdar K, Ghavidel P, Sadeghi H, Nasrabadi PN, et al. Investigating the Diagnostic Performance of HOTTIP, PVT1, and UCA1 Long Noncoding RNAs as a Predictive Panel for the Screening of Colorectal Cancer Patients With Lymph Node Metastasis. *J Cell Biochem* (2019) 120 (9):14780–90. doi: 10.1002/jcb.28739
95. Jeck WR, Sorrentino JA, Wang K, Slevin MK, Burd CE, Liu J, et al. Circular RNAs are Abundant, Conserved, and Associated With ALU Repeats. *RNA* (2013) 19(2):141–57. doi: 10.1261/rna.035667.112
96. Jeck WR, Sharpless NE. Detecting and Characterizing Circular Rnas. *Nat Biotechnol* (2014) 32(5):453–61. doi: 10.1038/nbt.2890
97. Yao R, Zou H, Liao W. Prospect of Circular RNA in Hepatocellular Carcinoma: A Novel Potential Biomarker and Therapeutic Target. *Front Oncol* (2018) 8:332. doi: 10.3389/fonc.2018.00332

98. Lasda E, Parker R. Circular RNAs Co-Precipitate With Extracellular Vesicles: A Possible Mechanism for circRNA Clearance. *PloS One* (2016) 11(2):e0148407. doi: 10.1371/journal.pone.0148407
99. Zhang H, Shen Y, Li Z, Ruan Y, Li T, Xiao B, et al. The Biogenesis and Biological Functions of Circular RNAs and Their Molecular Diagnostic Values in Cancers. *J Clin Lab Anal* (2020) 34(1):e23049. doi: 10.1002/jcla.23049
100. Zhang XL, Xu LL, Wang F. Hsa_Circ_0020397 Regulates Colorectal Cancer Cell Viability, Apoptosis and Invasion by Promoting the Expression of the miR-138 Targets TERT and PD-L1. *Cell Biol Int* (2017) 41(9):1056–64. doi: 10.1002/cbin.10826
101. Jin C, Wang A, Liu L, Wang G, Li G. Hsa_Circ_0136666 Promotes the Proliferation and Invasion of Colorectal Cancer Through miR-136/SH2B1 Axis. *J Cell Physiol* (2019) 234(5):7247–56. doi: 10.1002/jcp.27482
102. Jin Y, Yu LL, Zhang B, Liu CF, Chen Y. Circular RNA Hsa_Circ_0000523 Regulates the Proliferation and Apoptosis of Colorectal Cancer Cells as miRNA Sponge. *Braz J Med Biol Res* (2018) 51(12):e7811. doi: 10.1590/1414-431X20187811
103. Hansen TB, Jensen TI, Clausen BH, Bramsen JB, Finsen B, Damgaard CK, et al. Natural RNA Circles Function as Efficient microRNA Sponges. *Nature* (2013) 495(7441):384–8. doi: 10.1038/nature11993
104. Taulli R, Loretelli C, Pandolfi PP. From pseudo-ceRNAs to circ-ceRNAs: A Tale of Cross-Talk and Competition. *Nat Struct Mol Biol* (2013) 20(5):541–3. doi: 10.1038/nsmb.2580
105. Zhang M, Huang N, Yang X, Luo J, Yan S, Xiao F, et al. A Novel Protein Encoded by the Circular Form of the SHPRH Gene Suppresses Glioma Tumorigenesis. *Oncogene* (2018) 37(13):1805–14. doi: 10.1038/s41388-017-0019-9
106. Zhang Y, Zhang X, Chen T, Xiang J, Yin Q, Xing Y, et al. Circular Intronic Long Noncoding Rnas. *Mol Cell* (2013) 51(6):792–806. doi: 10.1016/j.molcel.2013.08.017
107. Salzman J, Chen RE, Olsen MN, Wang PL, Brown PO. Cell-Type Specific Features of Circular RNA Expression. *PloS Genet* (2013) 9(9):e1003777. doi: 10.1371/journal.pgen.1003777
108. Zhang M, Xin Y. Circular RNAs: A New Frontier for Cancer Diagnosis and Therapy. *J Hematol Oncol* (2018) 11(1):21. doi: 10.1186/s13045-018-0569-5
109. Wang X, Zhang Y, Huang L, Zhang J, Pan F, Li B, et al. Decreased Expression of Hsa_Circ_001988 in Colorectal Cancer and its Clinical Significances. *Int J Clin Exp Pathol* (2015) 8(12):16020–5.
110. He C, Huang C, Zhou R, Yu H. CircLMNB1 Promotes Colorectal Cancer by Regulating Cell Proliferation, Apoptosis and Epithelial-Mesenchymal Transition. *OncoTargets Ther* (2019) 12:6349–59. doi: 10.2147/ott.S204741
111. Zeng K, Chen X, Xu M, Liu X, Hu X, Xu T, et al. CircHIPK3 Promotes Colorectal Cancer Growth and Metastasis by Sponging Mir-7. *Cell Death Dis* (2018) 9(4):417. doi: 10.1038/s41419-018-0454-8
112. Kiss-László Z, Henry Y, Bachellerie JP, Caizergues-Ferrer M, Kiss T. Site-Specific Ribose Methylation of Preribosomal RNA: A Novel Function for Small Nucleolar Rnas. *Cell* (1996) 85(7):1077–88. doi: 10.1016/s0092-8674(00)81308-2
113. Ferreira HJ, Heyn H, Moutinho C, Esteller M. Cpg Island Hypermethylation-Associated Silencing of Small Nucleolar RNAs in Human Cancer. *RNA Biol* (2012) 9(6):881–90. doi: 10.4161/rna.19353
114. Brameier M, Herwig A, Reinhardt R, Walter L, Gruber J. Human Box C/D snoRNAs With miRNA Like Functions: Expanding the Range of Regulatory Rnas. *Nucleic Acids Res* (2011) 39(2):675–86. doi: 10.1093/nar/gkq776
115. Reichow SL, Hamma T, Ferre-D'Amare AR, Varani G. The Structure and Function of Small Nucleolar Ribonucleoproteins. *Nucleic Acids Res* (2007) 35(5):1452–64. doi: 10.1093/nar/gkl1172
116. Mei YP, Liao JP, Shen J, Yu L, Liu BL, Liu L, et al. Small Nucleolar RNA 42 Acts as an Oncogene in Lung Tumorigenesis. *Oncogene* (2012) 31(22):2794–804. doi: 10.1038/onc.2011.449
117. Dong XY, Rodriguez C, Guo P, Sun X, Talbot JT, Zhou W, et al. Snorna U50 is a Candidate Tumor-Suppressor Gene At 6q14.3 With a Mutation Associated With Clinically Significant Prostate Cancer. *Hum Mol Genet* (2008) 17(7):1031–42. doi: 10.1093/hmg/ddm375
118. Mannoor K, Liao J, Jiang F. Small Nucleolar RNAs in Cancer. *Biochim Biophys Acta* (2012) 1826(1):121–8. doi: 10.1016/j.bbcan.2012.03.005
119. Okugawa Y, Toiyama Y, Toden S, Mitoma H, Nagasaka T, Tanaka K, et al. Clinical Significance of SNORA42 as an Oncogene and a Prognostic Biomarker in Colorectal Cancer. *Gut* (2017) 66(1):107–17. doi: 10.1136/gutjnl-2015-309359
120. Yoshida K, Toden S, Weng W, Shigeyasu K, Miyoshi J, Turner J, et al. Snora21 - An Oncogenic Small Nucleolar RNA, With a Prognostic Biomarker Potential in Human Colorectal Cancer. *EBioMedicine* (2017) 22:68–77. doi: 10.1016/j.ebiom.2017.07.009
121. Fang X, Yang D, Luo H, Wu S, Dong W, Xiao J, et al. SNORD126 Promotes HCC and CRC Cell Growth by Activating the PI3K-AKT Pathway Through FGFR2. *J Mol Cell Biol* (2017) 9(3):243–55. doi: 10.1093/jmcb/mjw048
122. Sharp SJ, Schaack J, Cooley L, Burke DJ, Söll D. Structure and Transcription of Eukaryotic tRNA Genes. *CRC Crit Rev Biochem* (1985) 19(2):107–44. doi: 10.3109/10409238509082541
123. Banerjee R, Chen S, Dare K, Gilreath M, Praetorius-Ibba M, Raina M, et al. tRNAs: Cellular Barcodes for Amino Acids. *FEBS Lett* (2010) 584(2):387–95. doi: 10.1016/j.febslet.2009.11.013
124. Zhu L, Ge J, Li T, Shen Y, Guo J. tRNA-derived Fragments and tRNA Halves: The New Players in Cancers. *Cancer Lett* (2019) 452:31–7. doi: 10.1016/j.canlet.2019.03.012
125. Huang B, Yang H, Cheng X, Wang D, Fu S, Shen W, et al. Trf/Mir-1280 Suppresses Stem Cell-like Cells and Metastasis in Colorectal Cancer. *Cancer Res* (2017) 77(12):3194–206. doi: 10.1158/0008-5472.CAN-16-3146
126. Li S, Hu GF. Emerging Role of Angiogenin in Stress Response and Cell Survival Under Adverse Conditions. *J Cell Physiol* (2012) 227(7):2822–6. doi: 10.1002/jcp.23051
127. Li S, Shi X, Chen M, Xu N, Sun D, Bai R, et al. Angiogenin Promotes Colorectal Cancer Metastasis Via tiRNA Production. *Int J Cancer* (2019) 145(5):1395–407. doi: 10.1002/ijc.32245
128. Ishizu H, Siomi H, Siomi MC. Biology of PIWI-interacting Rnas: New Insights Into Biogenesis and Function Inside and Outside of Germlines. *Genes Dev* (2012) 26(21):2361–73. doi: 10.1101/gad.203786.112
129. Chalbatani GM, Dana H, Memari F, Gharagozlou E, Ashjaei S, Kheirandish P, et al. Biological Function and Molecular Mechanism of piRNA in Cancer. *Pract Lab Med* (2019) 13:e00113. doi: 10.1016/j.plabm.2018.e00113
130. Chu H, Hui G, Yuan L, Shi D, Wang Y, Du M, et al. Identification of Novel piRNAs in Bladder Cancer. *Cancer Lett* (2015) 356(2 Pt B):561–7. doi: 10.1016/j.canlet.2014.10.004
131. Peng L, Song L, Liu C, Lv X, Li X, Jie J, et al. piR-55490 Inhibits the Growth of Lung Carcinoma by Suppressing mTOR Signaling. *Tumour Biol* (2016) 37(2):2749–56. doi: 10.1007/s13277-015-4056-0
132. Ku HY, Lin H. PIWI Proteins and Their Interactors in piRNA Biogenesis, Germline Development and Gene Expression. *Natl Sci Rev* (2014) 1(2):205–18. doi: 10.1093/nsr/nwu014
133. Weng W, Liu N, Toiyama Y, Kusunoki M, Nagasaka T, Fujiwara T, et al. Novel Evidence for a PIWI-interacting Rna (piRNA) as an Oncogenic Mediator of Disease Progression, and a Potential Prognostic Biomarker in Colorectal Cancer. *Mol Cancer* (2018) 17(1):16. doi: 10.1186/s12943-018-0767-3
134. Qu A, Wang W, Yang Y, Zhang X, Dong Y, Zheng G, et al. A Serum piRNA Signature as Promising non-Invasive Diagnostic and Prognostic Biomarkers for Colorectal Cancer. *Cancer Manag Res* (2019) 11:3703–20. doi: 10.2147/CMAR.S193266

Conflict of Interest: The authors declare that the research was conducted in the absence of any commercial or financial relationships that could be construed as a potential conflict of interest.

frontiers in Oncology

ORIGINAL RESEARCH
published: 23 August 2021
doi: 10.3389/fonc.2021.723753

Elucidating the Role of Serum tRF-31-U5YKFN8DYDZDD as a Novel Diagnostic Biomarker in Gastric Cancer (GC)

Yuejiao Huang[1,2†], Haiyan Zhang[2,3†], Xinliang Gu[2,4], Shiyi Qin[2,4], Ming Zheng[2,4], Xiangrong Shi[5], Chunlei Peng[5] and Shaoqing Ju[2,4*]*

[1] Department of Medical Oncology, Affiliated Hospital of Nantong University, Nantong, China, [2] Medical School of Nantong University, Nantong, China, [3] Department of Pathology, Affiliated Nantong Third Hospital of Nantong University, Nantong, China, [4] Department of Laboratory Medicine, Affiliated Hospital of Nantong University, Nantong, China, [5] Department of Medical Oncology, Affiliated Tumor Hospital of Nantong University, Nantong, China

OPEN ACCESS

Edited by:
Muzafar Ahmad Macha, Islamic University of Science and Technology, India

Reviewed by:
Ravindra Deshpande, Wake Forest School of Medicine, United States
Priyanka Sharma, University of Texas MD Anderson Cancer Center, United States

***Correspondence:**
Shaoqing Ju
jsq814@hotmail.com
Chunlei Peng
sword226@163.com

[†]These authors have contributed equally to this work

Specialty section:
This article was submitted to Gastrointestinal Cancers, a section of the journal Frontiers in Oncology

Received: *11 June 2021*
Accepted: *29 July 2021*
Published: *23 August 2021*

Citation:
Huang Y, Zhang H, Gu X, Qin S, Zheng M, Shi X, Peng C and Ju S (2021) Elucidating the Role of Serum tRF-31-U5YKFN8DYDZDD as a Novel Diagnostic Biomarker in Gastric Cancer (GC). Front. Oncol. 11:723753. doi: 10.3389/fonc.2021.723753

Background: Gastric cancer (GC) is one of the malignant tumors with the highest morbidity and mortality in the world. Early diagnosis combined with surgical treatment can significantly improve the prognosis of patients. Therefore, it is urgent to seek higher sensitivity and specificity biomarkers in GC. tRNA-derived small RNAs are a new non-coding small RNA that widely exists in tumor cells and body fluids. In this study, we explore the expression and biological significance of tRNA-derived small RNAs in GC.

Materials and Methods: First of all, we screened the differentially expressed tRNA-derived small RNAs in tumor tissues by high-throughput sequencing. Agarose gel electrophoresis (AGE), Sanger sequencing, and Nuclear and Cytoplasmic RNA Separation Assay were used to screen tRF-31-U5YKFN8DYDZDD as a potential tumor biomarker for the diagnosis of GC. Then, we detected the different expressions of tRF-31-U5YKFN8DYDZDD in 24 pairs of GC and paracancerous tissues, the serum of 111 GC patients at first diagnosis, 89 normal subjects, 48 superficial gastritis patients, and 28 postoperative GC patients by quantitative real-time PCR (qRT-PCR). Finally, we used the receiver operating characteristic (ROC) curve to analyze its diagnostic efficacy.

Results: The expression of tRF-31-U5YKFN8DYDZDD has good stability and easy detection. tRF-31-U5YKFN8DYDZDD was highly expressed in tumor tissue, serum, and cell lines of GC, and the expression was significantly related to TNM stage, depth of tumor invasion, lymph node metastasis, and vascular invasion. The expression of serum tRF-31-U5YKFN8DYDZDD in the GC patients decreased after the operation ($P = 0.0003$). Combined with ROC curve analysis, tRF-31-U5YKFN8DYDZDD has better detection efficiency than conventional markers.

Conclusions: The expressions of tRF-31-U5YKFN8DYDZDD in the tumor and paracancerous tissues, the serum of GC patients and healthy people, and the serum of

GC patients before and after operation were different. tRF-31-U5YKFN8DYDZDD is not only a diagnostic biomarker of GC but also a predictor of poor prognosis.

Keywords: tRNA-derived small RNAs, tRF-31-U5YKFN8DYDZDD, diagnosis biomarker, gastric cancer, prognosis

HIGHLIGHTS

- The expression of tRF-31-U5YKFN8DYDZDD was high in GC cells, tissues, and serum.
- tRF-31-U5YKFN8DYDZDD may serve as a potential biomarker for GC.
- High expression of tRF-31-U5YKFN8DYDZDD was associated with clinical prognostic factors.
- tRF-31-U5YKFN8DYDZDD combined with other markers can improve the diagnostic efficiency.

INTRODUCTION

There are nearly one million new cases of gastric cancer (GC) in the world every year, and China accounts for about 40% of all, with the morbidity and mortality ranking among the top three malignancies in China (1, 2). GC is derived from the malignant transformation of gastric epithelial cells, and its pathological type is mainly adenocarcinoma (3). Because it is a hollow organ, the clinical symptoms in the early stage of malignant transformation are not obvious, mainly nausea, which is difficult to distinguish from diseases such as gastritis. Approximately 70% of the patients were already in the local progressive stage when diagnosed. It is of great clinical significance to improve the prognosis of patients with GC by early diagnosis and treatments (4). The early diagnosis of GC mainly depends on the pathology of gastroscopy, while the early screening mainly depends on the tumor biomarkers. Compared with gastroscopic diagnosis, hematological screening has the advantages of convenient, economical, and non-invasive detection and is easy to popularize (5). Carcinoembryonic antigen (CEA), carbohydrate antigen 199 (CA199), and carbohydrate antigen 724 (CA724) are relatively mature tumor biomarkers in clinical use at present, but their specificity and sensitivity are not high (6). Yu et al. demonstrated that the sensitivity of CEA in the diagnosis of gastric cancer is about 13–35%, while the specificity is only about 65%, and the CA199 is about 40 and 70%, respectively (7, 8). Therefore, new diagnostic biomarkers for GC are urgently needed in the clinic.

Non-coding RNA (ncRNAs) is the largest component of human transcriptome (9). There are many kinds of ncRNAs, which play important roles in the physiological and pathological processes of humans. Among them, the roles of microRNAs (miRNAs), long non-coding RNAs (lncRNAs), and circular RNAs (circRNAs) in the occurrence and development of cancers have been relatively thoroughly studied (10). Previous studies have shown that the ncRNAs above can be used as biomarkers for tumor diagnosis and prognosis evaluation (11, 12). Transfer RNA (tRNA) is also a kind of ubiquitously expressed and conservative ncRNAs. They account for about 10% of the entire cellular RNA and play a fundamental role in maintaining normal homeostasis, cell stress, stem cell differentiation, tumorigenesis, and cancer cell viability (13, 14).

The earliest reports of products derived from tRNAs can be traced back to the late 1970s, wherein fragments of tRNAs were observed in cancer patients (15). tRNA-derived small RNAs (tsRNAs) can be classified based on their cleavage sites of tRNA from which they are derived. tsRNAs are mainly divided into two subgroups: tRNA-derived fragments (tRFs) with lengths of 14–36 nt and tRNA halves (tiRNAs) with lengths of 30–40 nt (16, 17). tRFs are derived into 1-tRFs, 2-tRFs, 3-tRFs, 5-tRFs, and i-tRFs according to the different digesting positions of Angiogenin, Dicer, or other RNases on the mature tRNA or pre-tRNA, while tiRNAs including 5'- and 3'- fragments, named 5'-tiRNAs and 3'-tiRNAs, respectively (18, 19).

In recent years, as a new type of ncRNAs, the role of tsRNAs has gradually attracted people's attention in cancers. There is a growing interest in whether tsRNAs can be used as a promising new biomarker. Numerous studies have indicated that tsRNAs may be potential biomarkers in breast cancer (20–22), ovarian cancer (23), lung cancer (24), prostate cancer (25–27), colorectal cancer (28, 29), renal cell carcinoma (30, 31), and others (18, 32). Huang Y et al. demonstrated that the expression of tDR-7816 could promote the occurrence of early non-triple-negative breast cancer and has been proved to be a biomarker for the diagnosis (33). Pekarsky et al. identified two new tiRNAs, ts-4521 and ts-3676, which were downregulated in lung cancer and chronic lymphocytic leukemia, exhibiting antitumor functions (34). In digestive tract tumors, 16 tRFs were identified as being significantly changed in colon cancer and paracancerous tissues (35). In GC, tRF-3019a regulates cell proliferation, migration, and invasion by targeting FBXO47, which may be a potential diagnosis biomarker (36). tRF-3017A was highly expressed in tissues and cell lines of GC and was positively correlated with lymph node metastasis. It may be that tRF-3017A promotes the migration and invasion of GC cells by silencing the

Abbreviations: GC, Gastric cancer; AGE, Agarose gel electrophoresis; qRT-PCR, quantitative real-time PCR; ROC, Receiver operating characteristic; CEA, Carcinoembryonic antigen; CA199, Carbohydrate antigen 199; CA724, Carbohydrate antigen 724; ncRNAs, non-coding RNA; tRNAs, transfer RNA; tsRNAs, tRNA-derived small RNAs; tRFs, tRNA-derived fragments; tiRNAs, tRNA halves; U6, RNU6B; AUC, Area under the curve; CI, Confidence interval; SD, Standard deviation; CV, Coefficient of variation; SEN, Sensitivity; SPE, Specificity; ACCU, Overall accuracy; PPV, Positive predictive value; NPV, Negative predictive value; EMT, epithelial to mesenchymal transformation; Runx 1, runt-related transcription factor 1.

tumor suppressor NELL2 (37). In the previous study, our team also found that serum hsa_tsr016141 has good stability and specificity and could be used for dynamic monitoring of patients with GC (38).

Based on the previous studies, we further explored the clinical significance of tsRNAs in GC. In this study, high-throughput sequencing was used to screen the high expression of tsRNAs in GC tissues, including tRF-31-U5YKFN8DYDZDD. The expression of serum tRF-31-U5YKFN8DYDZDD in the patients with GC diagnosed for the first time was detected, and the correlations with clinicopathological features were analyzed. Then, we evaluated the diagnostic efficacy of tRF-31-U5YKFN8DYDZDD in GC by receiver operating characteristic (ROC) analysis in an attempt to provide a novel biomarker.

MATERIALS AND METHODS

Tissue Specimens and Serum Samples

In this study, the collections of serum and tissue samples of patients who signed informed consent were approved by the Ethics Committee of the Affiliated Hospital of Nantong University (approval No. 2018-L055). From 2016 to 2020, we collected sera of GC from 111 patients with newly diagnosed and 28 postoperative patients. We also collected sera from 89 healthy volunteers and 48 patients with gastritis. With the assistance of the department of gastrointestinal surgery and pathology of our hospital, we accumulated 24 pairs of GC and paracancerous tissues ($T_{1\text{-}4}N_{1\text{-}0}M_0$, stage I–III). All the patients of GC were diagnosed by two different pathologists, and the patients did not receive neoadjuvant radiotherapy and chemotherapy. The paracancerous tissue, which had a distance of 3 cm from the tumor tissue, obtained from GC patients was confirmed to be free of tumor infiltration using H&E staining. After resection, the samples were put into the RNA fixator Bioteke (Nantong, China) immediately and stored in the refrigerator at −80°C.

High-Throughput Sequencing

The total RNA or purified sRNA fragment of the sample was extracted, ligated at the 3' end and 5' end successively, reverse transcribed into cDNA, and then amplified by PCR. Then cut the glue to recover the target fragment library, and the qualified library was sequenced on Agilent 2100 Bioanalyzer (Agilent, USA). The raw reads obtained from Illumina HiSeqTM2500 (Illumina, USA) sequencing were filtered firstly, including removing the connectors at both ends of the reads, removing the reads with fragment length <15 nt, low-quality reads, etc., and obtaining the clean reads after preliminary filtering of the data. The whole-genome reads distribution map was obtained by comparing clean reads with the reference genome, and clean reads were classified and annotated by ncRNAs. The expression quantity calculation, expression clustering, and the difference among samples were carried out on the identified tRFs. tRFs were defined as the differentially expressed tRFs when log2FC > 1 or < −1 and Q value <0.05 using the DESeq2.0 algorithm.

Cell Culture

The human GC cell lines MKN-1, MKN-45, AGS, BGC-823, MGC803, HGC-27, and SGC-7901 and normal gastric mucosal epithelial cell line GES-1 were purchased from the Shanghai Institutes for Biological Sciences, China Academy of Science (Shanghai, China). All cell lines were cultured with RPMI 1640 medium (REF.10-013-CV, Corning, Manassas, VA, USA) containing 10% fetal bovine serum (REF.10100-147, FBS, Gibco, Grand Island, NY, USA) and 100 U/ml penicillin-streptomycin mixture (REF.15140-122, GibCo BRL, Grand Island, NY, USA) in an atmosphere containing 5% CO2 at 37°C (Thermo, Waltham, MA, USA).

Total RNA Extraction and cDNA Synthesis

Serum total RNA was extracted by Total RNA Pure and Isolation Kit with Spin Column (39–41) (Cat.RP4002, BioTeke, Beijing, China), while the tissue and cell total RNA was extracted using TRIzol reagent (Cat.15596018, Invitrogen, Karlsruhe, Germany). cDNA was amplified by Revert Aid RT Reverse Transcription Kit (Cat.K1622, Thermo Fisher Scientific, USA) at 42°C for 1 h and inactivated at 70°C for 5 min. The reverse transcription system was 10 μl. All steps were performed following the manufacturer's instructions.

qRT -PCR

All qRT-PCR assays were performed with the FastStart Universal SYBR Green Master Mix (Cat.Q711-02, Roche, Mannheim, Germany) on the QuantStudio 5 (Thermo, Waltham, MA, USA) for a total value of 20 μl. The reaction system included 10 μl of SYBR Green I Mix, 5 μl of cDNA, 1 μl of primer, and 3 μl of enzyme-free Water. To quantify the amount of tRFs, cDNA was synthesized from 500 ng of RNA. RNU6B (U6) was used as an internal control. All primers used in this study were synthesized by RiboBio Corporation (Suzhou, China). After the reaction, the $2^{-\Delta\Delta CT}$ method was used to analyze the data results of relative expression level, and the ΔΔCt value was presented as the difference between the experimental group ($Ct_{(target)}$ – $Ct_{(reference)}$) and the control group ($Ct_{(target)}$ – $Ct_{(reference)}$). The relative expression level of each sample was divided by the mean of the expression levels of the references.

Nuclear and Cytoplasmic RNA Separation Assay

The nuclear and cytoplasmic RNA was isolated from MKN-45 and HGC-27 cells using a PARIS™ Kit (Cat.AM1921, Thermo Fisher Scientific, USA) following the manufacturer's instructions and subjected to qRT-PCR analysis. Up to 5×10^6 GC cells were digested by trypsin and collected in a small centrifuge tube for the next steps. The experimental procedures have been provided in our previous study (42). The samples were tested by the RNA quality inspection before the next experiments.

Actinomycin D Assay

The concentration of actinomycin D was 2.5 μg/ml (43, 44). The time points of total RNA extraction were 0, 2, 4, 8, 12, and 24 h after treatment with actinomycin D, respectively.

Statistical Analysis

All data were analyzed by SPSS version 20.0 (IBM SPSS Statistics, Chicago, USA), GraphPad Prism v8.0 (Graphpad Software, La Jolla, CA, USA). The scatter plot drawn according to $-\triangle\triangle$Ct and paired t-test was used to describe the relative expression of tRF-31-U5YKFN8DYDZDD in preoperative *vs* postoperative and GC *vs* paracancerous tissues. Two-sided unpaired test was adopted for the comparison of two independent samples, while one-way analysis of variance was used to compare multiple independent samples. The relative expression of tRF-31-U5YKFN8DYDZDD and clinicopathological parameters was analyzed by chi-square test. The cutoff value of serum tRF-31-U5YKFN8DYDZDD expression to dichotomize as low and high was the median of relative expression. If the expression level was higher than the median, it was considered to be high expression of tRF-31-U5YKFN8DYDZDD; on the contrary, it was recognized as low expression (21, 38). For the analysis of survival data, Kaplan–Meier curves were constructed, and the log-rank test was performed. ROC curve and area under the curve (AUC) were used to evaluate the diagnostic performance of tRF-31-U5YKFN8DYDZDD in GC. Before plotting the ROC curve, we performed binomial logistic regression. Multivariate analysis was performed using Cox's proportional hazards model. The risk ratio and its 95% confidence interval (CI) were recorded for each marker. All experiments were repeated independently at least three times. Mean value ± standard deviation (SD) was used to list Data. $P < 0.05$ was considered statistically significant.

RESULTS

Expression of tRFs in GC Tissues and Cell Lines

To study the expression of tRFs in GC, we used a high-throughput sequencing technique to determine differential expression of tRFs in three pairs of GC patients and matched paracancerous specimens. There were about 5,512 different expression tRFs detected in total. According to the tRF-Seq data, we identified the tRFs between the two groups, of which seven were upregulated (fold change >2.0, $P < 0.05$) and six were downregulated (fold change <−2.0, $P < 0.05$) in GC tissues relative to paracancerous tissues (**Figure 1A**). According to the results of high-throughput sequencing, we verified the expression of tRF in another three pairs of GC and paracancerous tissues (**Figure 1B**) and found that the results were basically consistent with the results of sequencing. The difference in the expression of tRF-31-U5YKFN8DYDZDD between GC and paracancerous tissues was the most significant, which is the key molecule of this study. To validate the results of tRF-Seq data, we further collected 24 pairs of GC samples and detected the expression of tRF-31-U5YKFN8DYDZDD. Intriguingly, significantly higher levels of tRF-31-U5YKFN8DYDZDD were detected in carcinomas than paracancerous specimens ($P = 0.0011$, **Figure 1C**). Meanwhile, we detected the expression of tRF-31-U5YKFN8DYDZDD in different GC cell lines and found that tRF-31-U5YKFN8DYDZDD was significantly increased in GC cells as compared to normal gastric mucosal epithelial cell line GES-1 ($P < 0.01$, **Figure 1D**).

tRF-31-U5YKFN8DYDZDD Is a Type of i-tRF

According to the human genome build (GRCh37/hg19) from the UCSC Genome Browser database (https://genome.ucsc.edu/), tRF-31-U5YKFN8DYDZDD was mapped to ChrMT with coordinates of 1,602–1,670, and the length was 69 bp (**Figure 2A**). To verify the accuracy of the product of qRT-PCR, we detected the amplification procedure by agarose gel electrophoresis (AGE) assay and showed a single electrophoresis band about 80 bp in size (**Figure 2B**). After recovering and cloning, they were confirmed by Sanger sequencing that the product contained the full-length sequence of tRF-31-U5YKFN8DYDZDD (**Figure 2C**). In the MINTbase v2.0 (http://cm.jefferson.edu/MINTbase/), tRF-31-U5YKFN8DYDZDD was an i-tRF with a length of 31nt (5'- TACACTTAGGAGATTTCAACTTAACTTGACC -3') (**Figure 2D**). According to the basic information of tRF-31-U5YKFN8DYDZDD in Transfer RNA Database (http://trna.bioinf.uni-leipzig.de/), the cleavage site was located on the anticodon loop (CTTACAC) (**Figure 2E**).

Characteristics of the tRF-31-U5YKFN8DYDZDD as a Biomarker for GC

To further clarify the possibility of tRF-31-U5YKFN8DYDZDD as a biomarker for GC, we studied its characteristics. First of all, we used the Nuclear and Cytoplasmic RNA Separation Assay to test the expression of tRF-31-U5YKFN8DYDZDD in HGC-27 and MKN-45cell lines. The RNA quality inspection of RNA Separation Assay is shown in **Figure 3A**. It is mainly located in the cytoplasm and can be further secreted into the extracellular fluid (**Figure 3B**). The expression trend was consistent with that in cell lines and tissues. It can be inferred that tRF-31-U5YKFN8DYDZDD is secreted from the cytoplasm to the extracellular fluid, and its expression can be determined directly. Next, we placed the mixed serum samples at room temperature for 0, 6, 12, 18, and 24 h and repeated freeze-thaw for 0, 1, 3, 5, and 10 times. There is no statistical difference in the relative expression of tRF-31-U5YKFN8DYDZDD in the above two experiments ($P > 0.05$), which indicated that its detection would not be easily affected (**Figures 3C, D**). Meanwhile, to explore whether the detection of tRF-31-U5YKFN8DYDZDD can be applied in clinical practice, we conducted the repeatability of its detection methods. We selected mixed serum for precision determination of tRF-31-U5YKFN8DYDZDD and found that the coefficient of variation (CV) performed well. The results showed that the CV of tRF-31-U5YKFN8DYDZDD in intra-assay was 3.76% and in the inter-assay it was 3.19% (**Table 1**). Finally, the stable expression of tRF-31-U5YKFN8DYDZDD was further verified by actinomycin D assay. After treatment with actinomycin D for 24 h, the expression of tRF-31-U5YKFN8DYDZDD in BGC-823 and MKN-45 cell lines did not decrease significantly (**Figure 3E**). tRF-31-

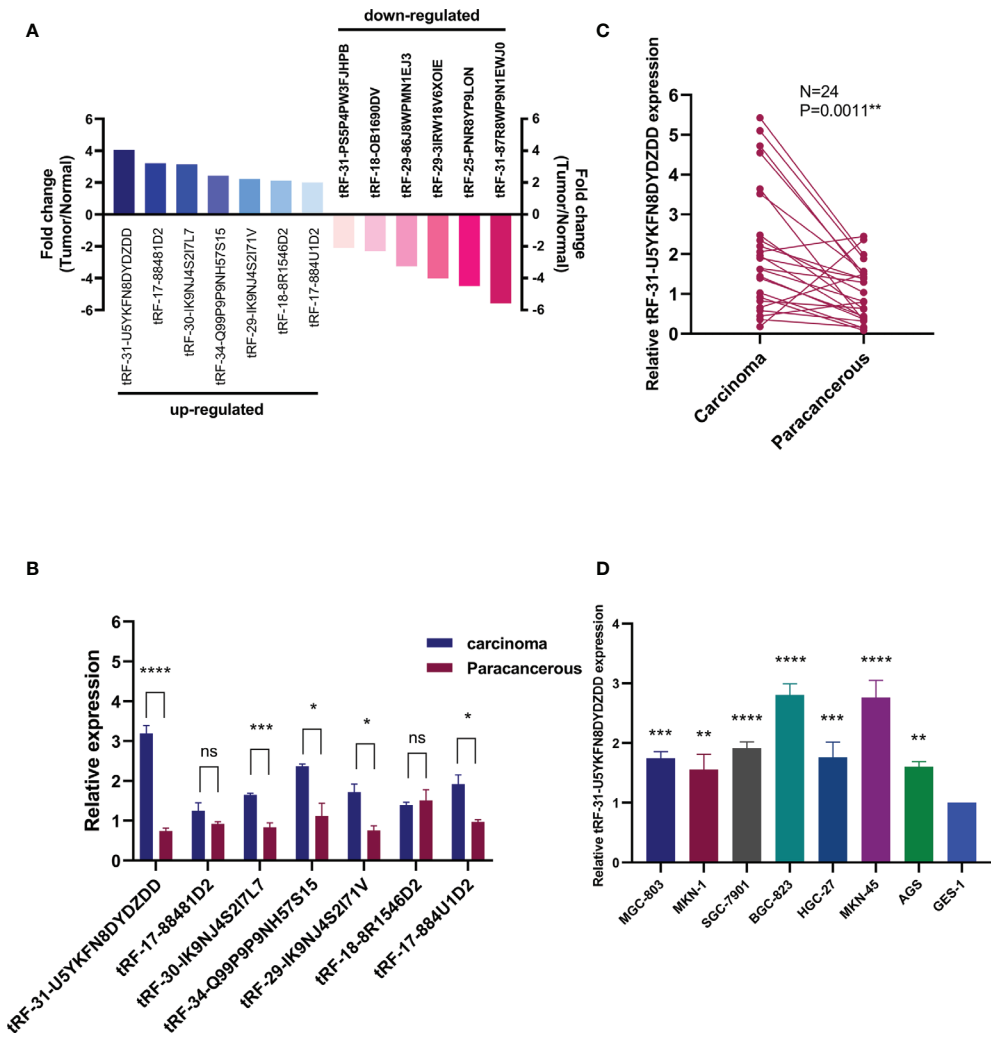

FIGURE 1 | *Expression of tRFs in GC tissues and cell lines.* **(A)** Differential expression results of tRFs-seq for GC *vs.* matched paracancerous tissues, including seven upregulated and six downregulated (fold change > 2.0, $P < 0.05$). **(B)** The expression levels of tRFs in GC tissues and their paired adjacent paracancerous tissues. **(C)** Expression of tRF-31-U5YKFN8DYDZDD was quantified by qRT-PCR in tissues, and its expression is normalized by U6 RNA in each sample. **(D)** Expression of tRF-31-U5YKFN8DYDZDD in GC cells and normal gastric mucosal epithelial cell line (GES-1). U6 was used for normalization. *Indicated statistical significance (****P < 0.0001, ***P < 0.001, **P < 0.01, *P < 0.05); NS, no significance.

U5YKFN8DYDZDD was stable with the effect of actinomycin D and had a longer half-life. The above experiments can preliminarily determine that tRF-31-U5YKFN8DYDZDD can be detected as a biomarker in GC serum, and the detection method of tRF-31-U5YKFN8DYDZDD had high stability and repeatability.

Expression of tRF-31-U5YKFN8DYDZDD in GC Serum and the Correlation With the Clinicopathological Parameter

tRF-31-U5YKFN8DYDZDD already has the basic characteristics as a biomarker, and the specificity of tRF-31-U5YKFN8D YDZDD in GC diagnosis and its correlation with clinicopathological data would be further studied. Firstly, the expressions of tRF-31-U5YKFN8DYDZDD in 111 GC patients, 48 gastritis patients, and 89 healthy donors' serum samples were evaluated by qRT-PCR (**Figure 4A**). We found the expression of tRF-31-U5YKFN8DYDZDD in serum from 111 GC patients was significantly increased as compared to healthy controls ($P < 0.0001$) and gastritis patients ($P = 0.0003$). Chi-square test was used to analyze the clinicopathologic parameter of 111 GC patients to further explore the potential clinical value of tRF-31-U5YKFN8DYDZDD expression level and clinicopathologic features (**Table 2**). As shown, we found that higher tRF-31-U5YKFN8DYDZDD expression was significantly associated with depth of tumor invasion ($P = 0.016$), lymph node metastasis ($P = 0.010$), higher TNM stage ($P = 0.003$), and positive vascular invasion ($P = 0.033$), but no significant relationship with age, gender, differentiation grade, tumor size, Lauren classification, nerve invasion, and the expression

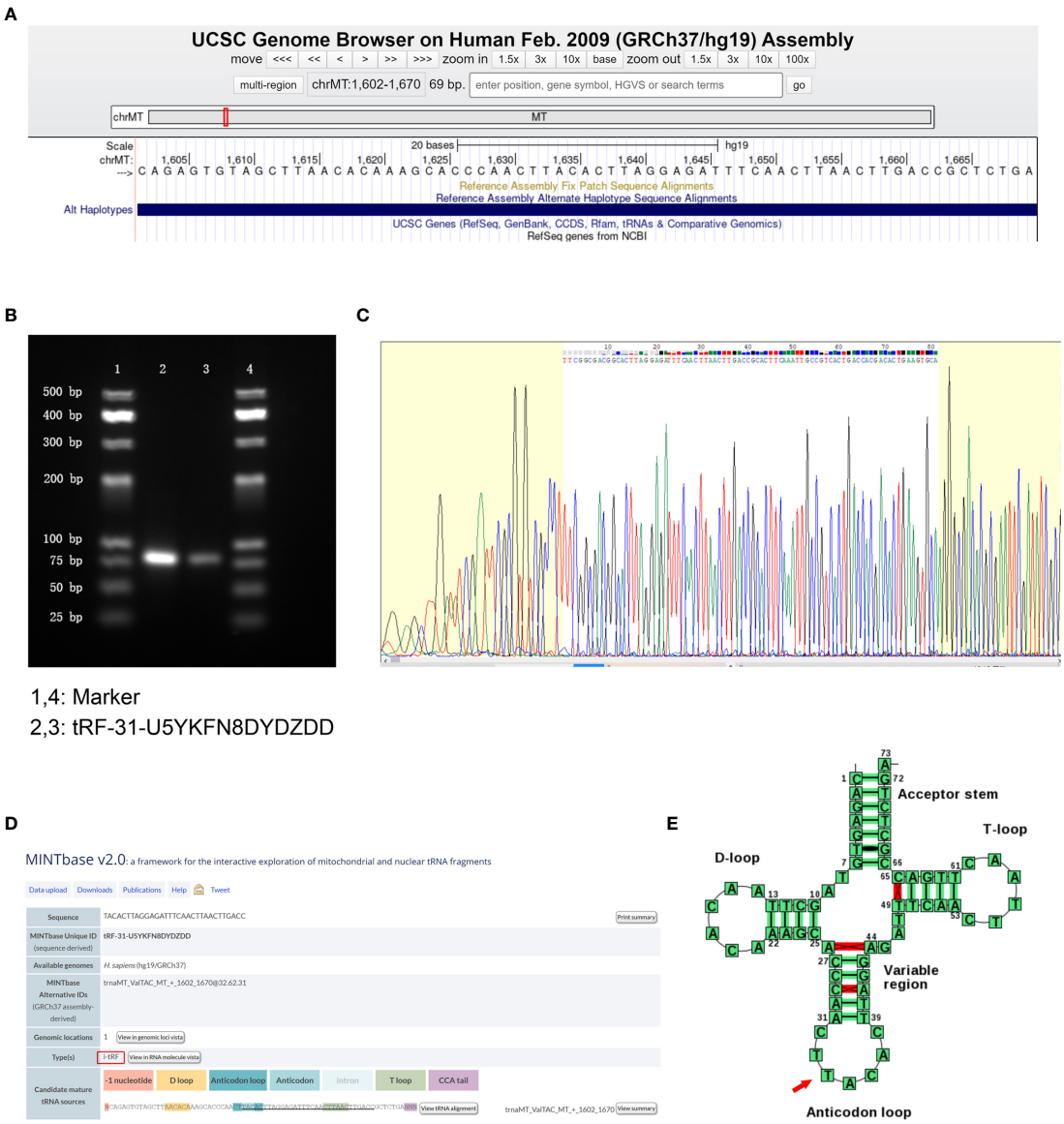

FIGURE 2 | *tRF-31-U5YKFN8DYDZDD is a type of i-tRF.* **(A)** tRF-31-U5YKFN8DYDZDD is located on ChrMT with coordinates of 1,602–1,670 and the length of 69 bp using the UCSC Genome Browser database (human genome build GRCh37/hg19). Search the relevant database for details. **(B)** The product of qRT-PCR was run on 2.5% agarose gel showing a single electrophoresis band about 80 bp in size. **(C)** The product of qRT-PCR was confirmed by Sanger sequencing, which contained the full-length sequence of tRF-31-U5YKFN8DYDZDD. **(D)** tRF-31-U5YKFN8DYDZDD was an i-tRF with a length of 31 nt (5'- TACACTTAGGAGATTTCAACTTAACTTGACC-3') in the MINTbase v2.0. **(E)** The cleavage site of tRF-31-U5YKFN8DYDZDD was located above the anticodon loop (CTTACAC) in Transfer RNA Database.

of C-erbB-2, CEA, CA199, CA724. Secondly, increased tRF-31-U5YKFN8DYDZDD expression in GC was significantly correlated with in different stage GC (**Figure 4B**, $P = 0.0452$), which is consistent with the results in **Table 2**. Besides, the expression of tRF-31-U5YKFN8DYDZD in 28 pairs of preoperative and postoperative GC specimens was confirmed using qRT-PCR assay (**Figure 4C**). The statistical analysis results showed that the tRF-31-U5YKFN8DYDZDD expression had a close correlation with tumor burden ($P = 0.0003$). Kaplan–Meier analysis revealed that high tRF-31-U5YKFN8DYDZDD expression was significantly correlated with shorter overall survival ($P < 0.0001$, log-rank test; **Figure 4D**). Furthermore, multivariate Cox regression analysis indicated that tRF-31-U5YKFN8DYDZDD expression was an independent prognostic factor (HR = 4.179, 95% CI 2.143–8.149, P < 0.001; **Table 3**). Given that no studies have reported this novel tRNA derivative, we reasoned that tRF-31-U5YKFN8DYDZDD may act as a biomarker for the diagnosis of GC, to judge the tumor load, and as a tumor correlation factor associated with poor prognosis.

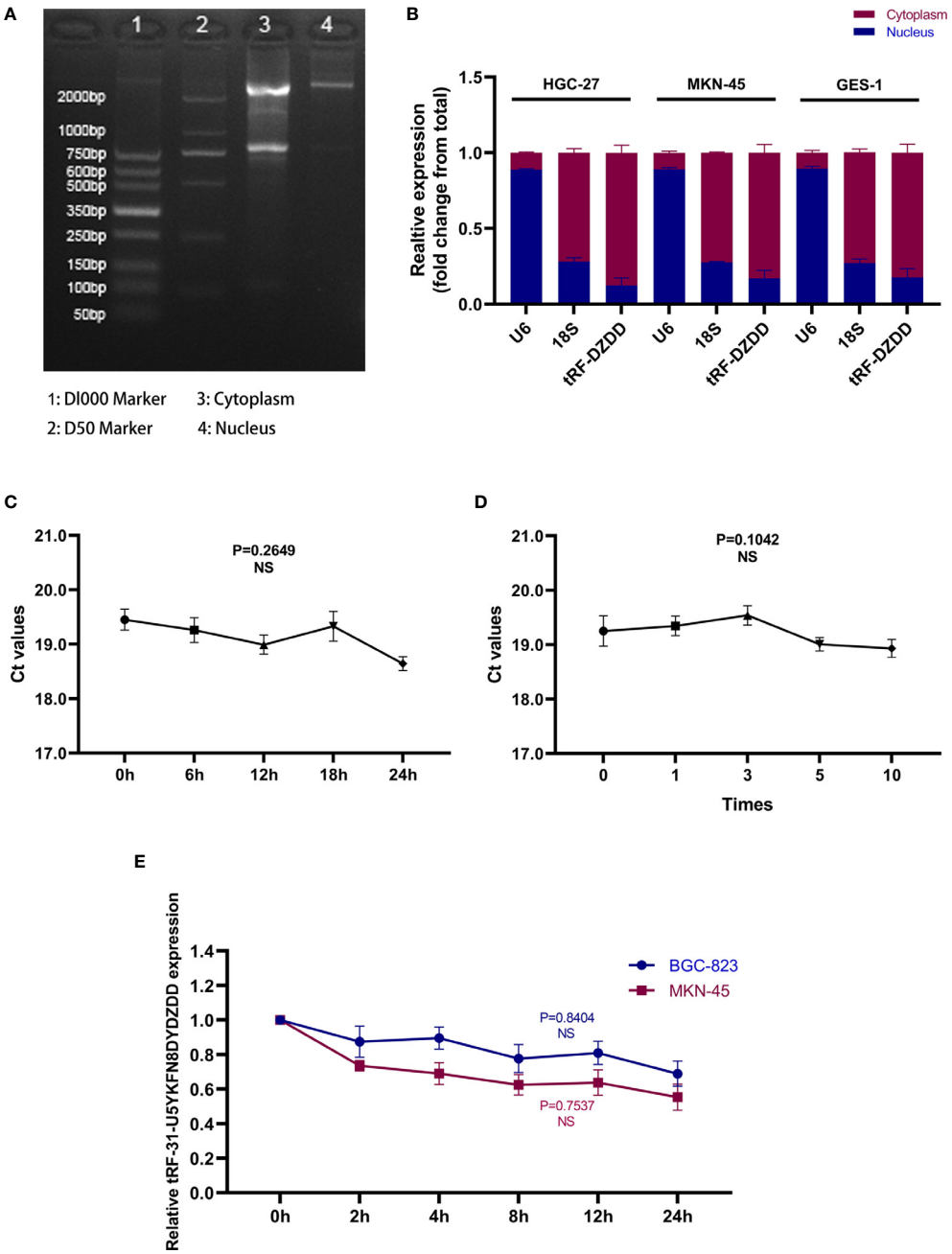

FIGURE 3 | *Characteristics of the tRF-31-U5YKFN8DYDZDD as a biomarker for GC.* ***(A)*** The RNA quality inspection of RNA Separation Assay of HGC-27 cells was detected by agarose gel electrophoresis. **(B)** Detection of tRF-31-U5YKFN8DYDZDD location in HGC-27, MKN-45, and GES-1 cell lines by Nuclear and Cytoplasmic RNA Separation Assay. **(C, D)** The good stability and repeatability of tRF-31-U5YKFN8DYDZDD were confirmed by qRT-PCR. **(E)** qRT-PCR for abundance of tRF-31-U5YKFN8DYDZDD in in BGC-823 and MKN-45 cell lines treated with Actinomycin D at the indicated time point.

Evaluation of the Diagnostic Accuracy of Serum tRF-31-U5YKFN8DYDZDD and Combined Diagnostic Model in GC

Compared with mature GC biomarkers such as CEA, CA199, and CA724, the diagnostic efficiency of tRF-31-U5YKFN8DYDZDD is the key factor to evaluate. The ROC curve showed that the AUC of tRF-31-U5YKFN8DYDZDD was 0.740 (95% CI: 0.6720–0.808), which was higher than 0.696 of CEA (95% CI: 0.624–0.768), 0.600 of CA199 (95% CI: 0.521–0.678), and 0.639 of CA724 (95% CI: 0.561–0.718) (**Figure 5A**). And the level of tRF-31-U5YKFN8DYDZDD presented a 60.36% sensitivity (SEN) and 80.90% specificity (SPE) in separating GC

TABLE 1 | The intra-assay coefficient of variation and the inter-assay coefficient of variation of tRF-31-U5YKFN8DYDZDD.

	tRF-31-U5YKFN8DYDZDD	U6
Intra-assay CV, %	3.76	1.61
Inter-assay CV, %	3.19	2.35

CV (coefficient of variance) = SD/Mean × 100%.

patients from healthy controls. As for CEA, CA199, and CA724, the SEN was 57.66, 36.04, and 42.34%; and the SPE was 67.42, 82.02, and 74.16%, respectively (**Table 4**). Using the healthy group as the control, some diagnostic test evaluation indicators were also calculated in the two-combination group, three-combination group, or four-combination group to assess their SEN, SPE, overall accuracy (ACCU), positive predictive value (PPV), and negative predictive value (NPV). The efficacy of joint diagnosis of AUC increased to 0.783 after the combination of tRF-31-U5YKFN8DYDZDD and CEA, 0.769 after combining with CA199, and 0.771 after combining with CA724 (**Figure 5B**). As shown in **Figures 5B, C**, the model combining four indicators yielded a good diagnostic efficacy for GC patients with an AUC of 0.813 (95% CI: 0.754–0.873), which was higher than that of the two-/three-combination group or either of the four indicators alone. Interestingly, it was found that the SEN, ACCU, and NPV values of the four-combination group were 81.98, 76.50, and 75.61%, respectively, which were the highest of the 11 groups (**Table 4**). The above findings indicate that tRF-31-U5YKFN8DYDZDD may be a potential biomarker of GC and, combined with other tumor markers, can improve the diagnostic efficiency.

In serum samples, the expression of tRF-31-U5YKFN8 DYDZDD is also different in GC and gastritis, so it is very important to further study the efficacy of tRF-31-U5YKFN8DYDZDD in the distinction between GC and

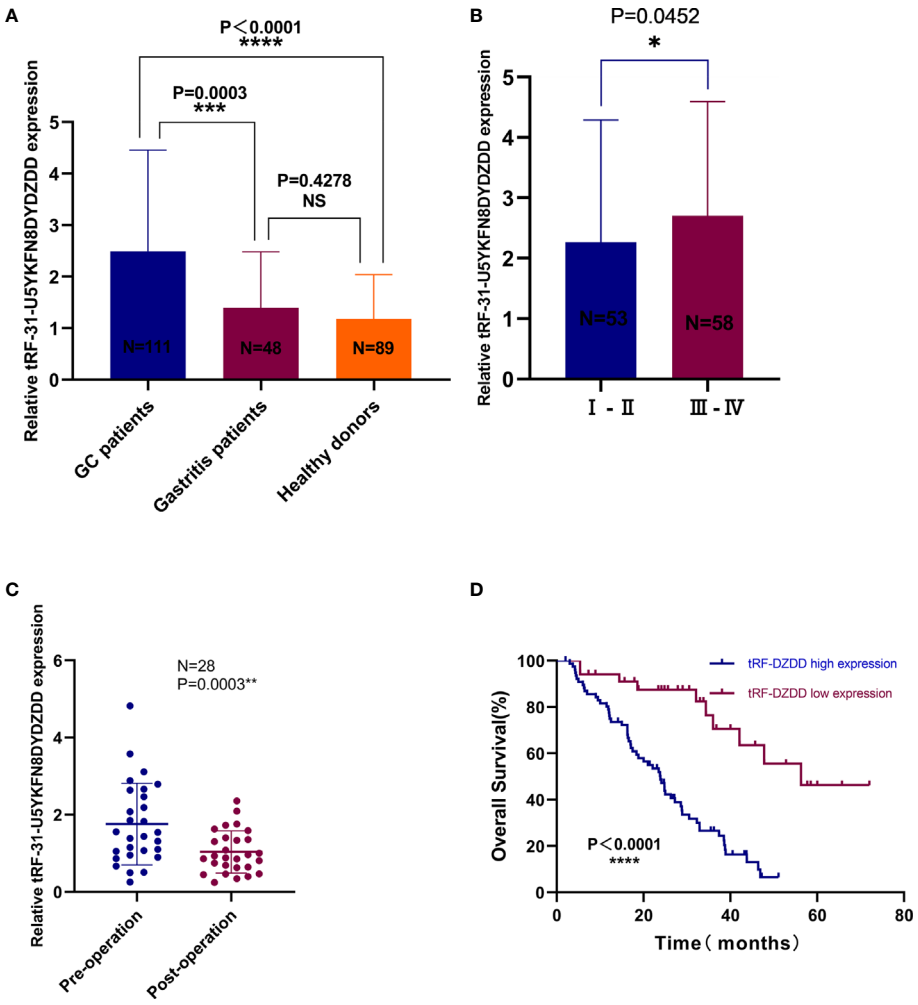

FIGURE 4 | *Expression of tRF-31-U5YKFN8DYDZDD in GC serum.* **(A)** The expression of tRF-31-U5YKFN8DYDZDD expression levels between GC (n = 111), gastritis patients (n = 48), and healthy volunteers (n = 89). **(B)** The expression levels of tRF-31-U5YKFN8DYDZDD in different pathologic stages of GC patients (stage I–II, n = 53; stage III–IV, n = 58). **(C)** Paired comparison of tRF-31-U5YKFN8DYDZDD in 28 pairs of preoperative and postoperative patients' serums was determined using qRT-PCR. **(D)** Kaplan–Meier survival curves for 111 GC patients according to tRF-31-U5YKFN8DYDZDD expression status (log-rank test, $P < 0.001$).

TABLE 2 | The association between tRF-31-U5YKFN8DYDZDD expression and clinicopathologic parameters in 111 GC specimens.

Parameters	Total	tRf-DZDD expression		*P* value
		Low (<median)	High (≥median)	
Age				0.504
<60	37	12	25	
≥60	74	19	55	
Gender				0.518
Male	70	18	52	
Female	41	13	28	
Differentiation grade				0.527
Well-moderate	49	12	37	
Poor-undifferentiation	62	19	43	
Tumor size				0.078
<5 cm	70	24	46	
≥5 cm	41	7	34	
Depth of invasion				0.016*
T1–T2	43	18	25	
T3–T4	68	13	55	
Lymph node metastasis				0.010*
Negative	46	19	27	
Positive	65	12	53	
TNM stage				0.003**
I–II	53	22	31	
III–IV	58	9	49	
Lauren classification				0.907
Intestinal type	32	8	24	
Diffuse type	34	10	24	
Mixed type	45	13	32	
Nerve invasion				0.668
Negative	67	20	47	
Positive	44	11	33	
Vascular invasion				0.033*
Negative	46	18	28	
Positive	65	13	52	
C-erbB-2				0.113
Negative	102	26	76	
Positive	9	5	4	
CEA				0.833
Negative (<5 ng/ml)	48	14	34	
Positive (≥5 ng/ml)	63	17	46	
CA199				0.385
Negative (<37 U/ml)	71	22	49	
Positive (≥37 U/ml)	40	9	31	
CA724				0.831
Negative (<10 U/ml)	46	19	46	
Positive (≥10 U/ml)	65	12	34	

Statistical analyses were performed by the Pearson χ^2 test.
**P < 0.05, **P < 0.01 was considered significant.*

gastritis. We compared the four indicators and found that the related sensitivity and specificity of tRF-31-U5YKFN8DYDZD were 58.56 and 72.92%, respectively, with the AUC of 0.680 (95% CI:0.591–0.769) *vs.* 0.651 for CEA (95% CI: 0.547–0.755) *vs.* 0.568 for CA199 (95% CI: 0.471–0.666) and 0.602 for CA724 (95% CI: 0.503–0.701) (**Table 5** and **Figure 5C**). Similar to the results of tRF-31-U5YKFN8DYDZD expression in normal serum, the combination of tRF-31-U5YKFN8DYDZDD and other tumor markers was the highest value for diagnosis between GC and gastritis. Both **Figures 5D–F** and **Table 5** show that the combined detection of serum tRF-31-U5YKFN8DYDZDD, CEA, CA199, and CA724 is superior to any of the biomarkers detected separately in the diagnosis of GC patients (AUC = 0.713). Besides, the combination of tRF-31-U5YKFN8DYDZDD, CEA, CA199, and CA724 could improve the diagnostic SEN (86.49%), ACCU (74.84%), and NPV (60.53%), which were better than these in the two-/three-combination group or any of the four indicators alone. All these results suggest that tRF-31-U5YKFN8DYDZD seemed better than CEA, CA199, and CA724 in terms of the diagnostic value for GC.

Target Prediction of tRF-31-U5YKFN8DYDZDD

We next want to investigate the molecular mechanism of tRF-31-U5YKFN8DYDZDD in cell biological behavior regulation. We predict downstream target genes of tRF-31-U5YKFN8DYDZDD using online databases. As shown in **Figure 6A**, overlapped between miRanda and TargetSca prediction tools were 514 potential target genes that are most likely to bind to tRF-31-U5YKFN8DYDZDD. Next, enrichment analysis of the KEGG signaling pathway suggested that cell cycle, pathways in cancer, and drug metabolism were significantly enriched in the signaling pathways (**Figure 6B**). GO functional enrichment analysis of the target genes indicated that tRF-31-U5YKFN8DYDZDD (**Figure 6C**) may have the potential role in signal transduction, cell division, and regulation of transcription. The mechanisms of tRF-31-U5YKFN8DYDZDD expression in cell biological behavior regulation in GC need to be further investigated.

DISCUSSION

As a common malignant tumor of the digestive tract, the incidence and mortality of GC are among the highest, which is mainly related to the late course of the disease and poor response to treatment (45). Although the prognosis of GC has improved with the continuous updating and development of surgical methods, chemotherapeutic drugs, and targeted drugs, the 5-year survival rate is still not high, and the incidence rate is stable without significant decline (46). In conclusion, improving the early diagnosis and treatment of GC is the key to improve the prognosis of patients. However, the specificity and sensitivity of clinical tumor biomarkers are low, so it is particularly urgent to look for new GC screening markers. The occurrence and development of GC is a multistage and multifactor process. Now the multiple genetic and epigenetic changes of coding genes in the complex regulatory interaction network have become the focus of oncology research, including GC (47, 48). With the development of microarray and RNA sequencing technology, more and more ncRNAs have been identified. Their roles and functions have also been gradually studied in depth. This paper focuses on the role of ncRNA in the early diagnosis and prognosis of GC.

Different from common ncRNAs, the function and study of tRNAs are not as thorough as microRNAs, lncRNAs, and circRNAs. tRNAs routinely play a role in translation, and tRNA(~72 nt) can be processed into smaller bioactive tRNA-derived fragments, ranging in size from 18 to 50 nt, which play a

TABLE 3 | Multivariate Cox regression analysis of tRF-31-U5YKFN8DYDZDD and clinical variables predicting survival from 111 GC specimens.

Parameter	Relative ratio	95% CI	*P* Value
Age (<60 *vs.* ≥60)	0.608	0.355–1.042	.070
Gender (Male *vs.* Female)	1.204	0.720–2.015	.479
Differentiation grade (Well-moderate *vs.* Poor-undifferentiation)	0.806	0.449–1.447	.470
Tumor size (<5 *vs.* ≥5 cm)	0.814	0.471–1.405	.459
Depth of invasion (T1–T2 *vs.* T3–T4)	1.429	1.032–1.979	.032*
Lymph node metastasis (Negative *vs.* Positive)	1.459	0.671–3.171	.340
TNM stage (I–II *vs.* III–IV)	0.399	0.162–.984	.046*
Lauren classification (Intestinal type *vs.* Diffuse type *vs.* Mixed type)	0.897	0.457–1.760	.752
Nerve invasion (Negative *vs.* Positive)	1.719	0.915–3.230	.092
Vascular invasion (Negative *vs.* Positive)	0.574	0.308–1.068	.080
C-erbB-2 (Negative *vs.* Positive)	1.329	0.430–4.107	.621
CEA (<5 *vs.* ≥5 ng/ml)	0.690	0.406–1.173	.171
CA199 (<37 *vs.* ≥37 U/ml)	0.865	0.507–1.476	.595
CA724 (<10 *vs.* ≥10 U/ml)	1.381	0.813–2.347	.232
tRF-31-U5YKFN8DYDZDD (Negative *vs.* Positive)	4.179	2.143–8.149	.001**

**P < 0.05, **P < 0.01 was considered significant.*

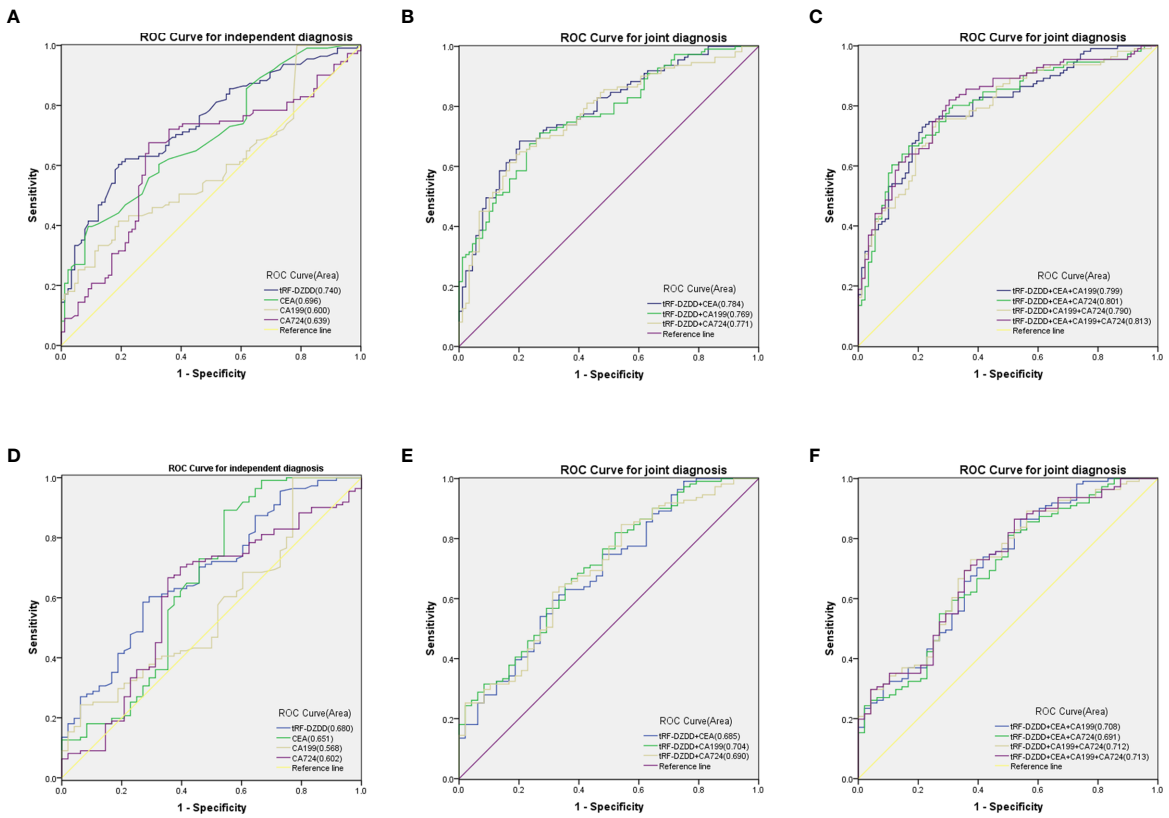

FIGURE 5 | *Evaluation of the diagnostic accuracy of serum tRF-31-U5YKFN8DYDZDD and combined diagnostic model in GC.* **(A–C)** ROC curves for GC diagnosis using serum tRF-31-U5YKFN8DYDZDD, CEA, CA199, and CA724 between GC patients and healthy controls. **(D–F)** ROC curves for GC diagnosis using serum tRF-31-U5YKFN8DYDZDD, CEA, CA199, and CA724 between GC and gastritis patients. **(B, C, E, F)** Combined diagnostic efficacy of serum tRF-31-U5YKFN8DYDZDD, CEA, CA199, and CA724 exerted the best diagnostic efficacy in distinguishing GC patients and non-malignant disease.

role in the occurrence and progression of tumors (15, 49). tRNAs can give rise to different types of tRNA-derived fragments, including tRFs with lengths of 14–36 nt and tiRNAs with lengths of 30–40 nt (50). tRNAs can also produce other kinds of small RNAs, in which the start or end position does not match the 5' or 3' end of the parent tRNA. These small RNAs are generally called i-tRFs, which belong to tRFs. The number of i-tRF is usually small compared with other types (14). The biological functions of tRFs include acting as a miRNA, regulating translation, regulating the expression and silencing

TABLE 4 | Use the expression levels of tRF-31-U5YKFN8DYDZDD, CEA, CA199, and CA724 to distinguish GC patients from healthy donors.

	SEN, %	SPE, %	ACCU, %	PPV, %	NPV, %
tRF-DZDD	60.36 (67/111)	80.90 (72/89)	69.50 (139/200)	79.76 (67/84)	62.07 (72/116)
CEA	57.66 (64/111)	67.42 (60/89)	62.00 (124/200)	68.82 (64/93)	56.07 (60/107)
CA199	36.04 (40/111)	82.02 (73/89)	56.50 (113/200)	71.43 (40/56)	50.69 (73/144)
CA724	42.34 (47/111)	74.16 (66/89)	56.50 (113/200)	67.14 (47/70)	50.77 (66/130)
tRF-DZDD+CEA	68.47 (76/111)	79.78 (71/89)	73.50 (147/200)	80.85 (76/94)	66.98 (71/106)
tRF-DZDD+CA199	71.17 (79/111)	73.03 (65/89)	72.00 (144/200)	76.70 (79/103)	67.01 (65/97)
tRF-DZDD+CA724	63.96 (71/111)	80.90 (72/89)	71.50 (143/200)	80.68 (71/88)	64.29 (72/112)
tRF-DZDD+CEA+CA199	72.97 (81/111)	78.65 (70/89)	75.50 (151/200)	81.00 (81/100)	70.00 (70/100)
tRF-DZDD+CEA+CA724	66.67 (74/111)	83.15 (74/89)	74.00 (148/200)	83.15 (74/89)	66.67 (74/111)
tRF-DZDD+ CA199+CA724	74.77 (83/111)	74.16 (66/89)	74.50 (149/200)	78.30 (83/106)	70.21 (66/94)
tRF-DZDD+CEA+ CA199+CA724	81.98 (91/111)	69.66 (62/89)	76.50 (153/200)	77.12 (91/118)	75.61 (62/82)

SEN, sensitivity; SPE, specificity; ACCU, overall accuracy; PPV, positive predictive value; NPV, negative predictive value.

TABLE 5 | Use the expression levels of tRF-31-U5YKFN8DYDZDD, CEA, CA199, and CA724 to distinguish GC patients from gastritis patients.

	SEN, %	SPE, %	ACCU, %	PPV, %	NPV, %
tRF-DZDD	58.56 (65/111)	72.92 (35/48)	62.89 (100/159)	83.33 (65/78)	43.21 (35/81)
CEA	57.66 (64/111)	62.50 (30/48)	59.12 (94/159)	78.05 (64/82)	38.96 (30/77)
CA199	36.04 (40/111)	70.83 (34/48)	46.54 (74/159)	74.07 (40/54)	32.38 (34/105)
CA724	42.34 (47/111)	68.75 (33/48)	50.31 (/15980)	75.81 (47/62)	34.02 (33/97)
tRF-DZDD+CEA	59.46 (66/111)	68.75 (33/48)	62.26 (99/159)	81.48 (66/81)	42.31 (33/78)
tRF-DZDD+CA199	81.98 (91/111)	47.92 (23/48)	71.70 (114/159)	78.45 (91/116)	53.49 (23/43)
tRF-DZDD+CA724	62.16 (69/111)	68.75 (33/48)	64.15 (102/159)	82.14 (69/84)	44.00 (33/75)
tRF-DZDD+CEA+CA199	86.49 (96/111)	45.83 (22/48)	74.21 (118/159)	78.69 (96/122)	59.46 (22/37)
tRF-DZDD+CEA+CA724	81.08 (90/111)	50.00 (24/48)	71.70 (114/159)	78.95 (90/114)	53.33 (24/45)
tRF-DZDD+ CA199+CA724	72.97 (81/111)	62.50 (30/48)	69.81 (111/159)	81.82 (81/99)	50.00 (30/60)
tRF-DZDD+CEA+ CA199+CA724	86.49 (96/111)	47.92 (23/48)	74.84 (119/159)	79.34 (96/121)	60.53 (23/38)

SEN, sensitivity; SPE, specificity; ACCU, overall accuracy; PPV, positive predictive value; NPV, negative predictive value.

of target genes, and participating in cellular stress response. The understanding of tRF-mediated cancer progression is still in the initial stage. Previous studies have shown that tRF is involved in various cellular stages, such as differentiation, proliferation and apoptosis, chromatin remodeling, RNA editing, and RNA splicing, which lead to cancer (17, 28). Fei Zhang et al. demonstrated that tRF-3019a enhanced cell proliferation, migration, and invasion by targeting FBXO47, and it might serve as a potential diagnostic biomarker for GC (36). Similar results were found that tRF-3017A might play an important role in promoting migration and invasion by silencing NELL2 in GC (37). In this study, tRFs were screened from GC tissues by high-throughput sequencing. The results showed that the expression of tRF-31-U5YKFN8DYDZDD in GC was significantly higher than that in normal control or cancer after *in vitro* verification in cell lines, serums, and tissues. After further analysis, it was found that tRF-31-U5YKFN8DYDZDD belonged to i-tRF. Its stable structure and high expression in body fluids make it relatively easy to detect, which makes it possible to become a new potential biomarker for tumors. Currently, most studies on tsRNAs have described the effects on proliferation, invasion, and migration of tumor cells and the mechanisms involved in hypoxia and epithelial to mesenchymal transformation (EMT) (10, 21, 51, 52). However, there are few studies on whether tsRNAs can be used as a biomarker for tumors (18, 24, 53). Therefore, this study explored the possibility of tRF-31-U5YKFN8DYDZDD as a tumor biomarker for GC, which was highly innovative.

In the present study, it was proved that the expression of tRF-31-U5YKFN8DYDZDD in GC tissues was significantly higher than that in paracancerous tissues, the expression in GC cell lines was also higher than that in normal gastric epithelial cells, and the expression in GC serum was significantly higher than that in normal physical examination population and gastritis patients, with statistically significant differences. The results of qRT-PCR detection were consistent with those of high-throughput sequencing, indicating that the high expression of tRF-31-U5YKFN8DYDZDD was closely related to tumorigenesis. After the detection of serum tRF-31-U5YKFN8DYDZDD expression in patients before and after the operation, it was found that the tumor load reduced and the expression of tRF decreased significantly after the operation, which can be used as an index for dynamic monitoring of tumor load, and may also be an important indication of tumor recurrence. Statistical analysis of large samples showed that the high expression of tRF-31-U5YKFN8DYDZDD was positively correlated with late-stage, deep tumor invasion, lymph node metastasis, and vascular invasion in patients with GC, and was a related factor of poor prognosis. The survival time of patients with high expression of tRF-31-U5YKFN8DYDZDD is significantly lower than that of patients with low expression, which is an independent prognostic factor. For the related experiments of the molecular characteristics of tRF-31-U5YKFN8DYDZDD itself, chromosome location, and PCR amplification sequencing, it is clear that it has the basic conditions to become a biomarker. Further ROC curve analysis

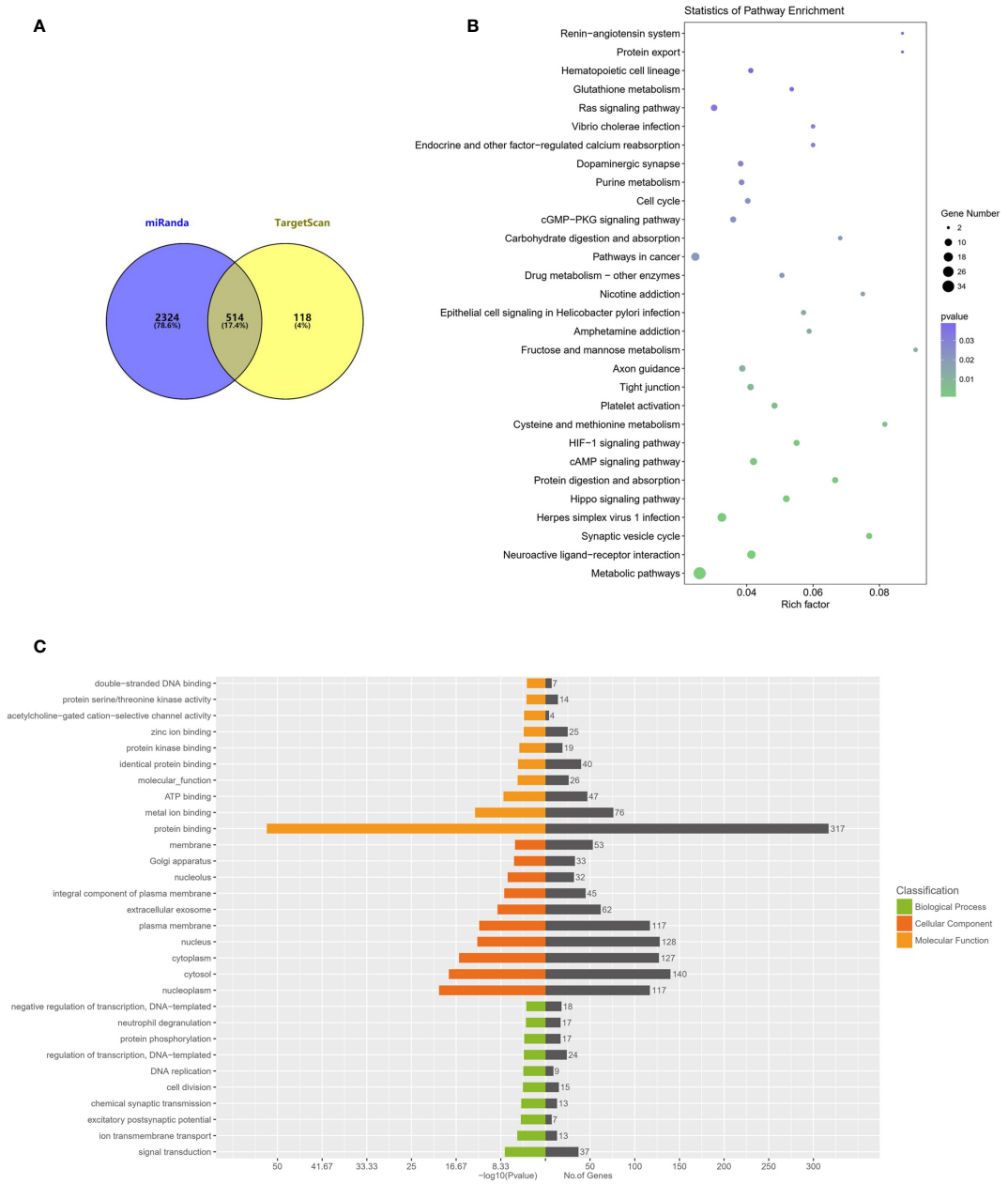

FIGURE 6 | *GO and KEGG enrichment analyses of tRF-31-U5YKFN8DYDZDD target genes.* **(A)** Schematic diagram of tRF-31-U5YKFN8DYDZDD target prediction. Venn diagram evaluated the overlapped genes between miRandan and TargetScan predictions. **(B)** Bubble chart of KEGG analysis of candidate tRF-31-U5YKFN8DYDZDD different target genes expressed of enriched pathways. **(C)** GO analysis of the tRF-31-U5YKFN8DYDZDD target genes enriched in biological process, cellular component, and molecular function.

showed that tRF-31-U5YKFN8DYDZDD had high sensitivity and specificity, which was superior to conventional markers such as CEA in differentiating diagnosis of benign and malignant gastric tumors. What is more exciting is that the combined diagnosis of tRF-31-U5YKFN8DYDZDD with CEA, CA199, and CA724 has more diagnostic potency and good clinical application potential.

High-throughput sequencing revealed tsRNA signatures in cancers, indicating that like microRNAs, tsRNAs may have an oncogenic or tumor-suppressor function in tumors (34, 54). In the study of cellular function, it has been found that tRF-33-P4R8YP9LON4VDP could proliferate GC cells *in vitro* and might be a potential site for targeted therapy (55). In breast cancer research, it was also found that the runt-related transcription factor 1 (Runx 1) can reverse the excessive proliferation of tumor cells induced by ts-112 (56). tsRNA-26576 can not only promote the proliferation of tumor cells but also promote invasion and

migration in breast cancer (57). In this study, we demonstrated the existence of tRF-31-U5YKFN8DYDZDD in GC cells, tissues, and serum. Moreover, tRF-31-U5YKFN8DYDZDD in GC patients have significantly higher tsRNA levels than that in healthy donors, indicating their great potential as a novel "liquid biopsy" biomarker for GC diagnosis. Notably, it was statistically found that the high expression of tRF-31-U5YKFN8DYDZDD was associated with late-stage, deep tumor invasion, lymph node metastasis, and vascular invasion, and these indicators were closely related to the invasion and migration ability of tumor cells. Of course, the proliferation ability of GC cells cannot be ignored. These laid a theoretical foundation for our further study of the functional role of tRF-31-U5YKFN8DYDZDD in patients with GC, which is also the focus of our next research. In conclusion, the findings provided in this study of tRF-31-U5YKFN8DYDZDD could provide new insights for novel types of diagnostic biomarkers and predictors of poor prognosis. The tRF-31-U5YKFN8DYDZDD, as a representative GC-associated tsRNA, may play a tumor promoter role in GC and could serve as a potential therapeutic target.

DATA AVAILABILITY STATEMENT

The datasets presented in this study can be found in online repositories. The names of the repository/repositories and accession number(s) can be found in the article/supplementary material.

ETHICS STATEMENT

The studies involving human participants were reviewed and approved by the ethics committee of the Affiliated Hospital of Nantong University (ethical review report number: 2018-L055). The patients/participants provided their written informed consent to participate in this study.

AUTHOR CONTRIBUTIONS

YH and SJ conceived the study. SJ and CP gave constructive guidance and made critical revisions. XS and CP provided the clinical knowledge and data collection of GC. YH, SQ, and MZ performed experiments. XG and HZ arranged the data and performed the statistical analysis. YH finished the manuscript and figures. All authors contributed to the article and approved the submitted version.

FUNDING

This project was supported by grants from the National Natural Science Foundation of China (No. 81600158, No. 81871720, No. 82072363) and Nantong Municipal Health Commission (QA2020027).

REFERENCES

1. Smyth EC, Nilsson M, Grabsch HI, van Grieken NC, Lordick F. Gastric Cancer. *Lancet* (2020) 396(10251):635–48. doi: 10.1016/S0140-6736(20)31288-5
2. Wang FH, Shen L, Li J, Zhou ZW, Liang H, Zhang XT, et al. The Chinese Society of Clinical Oncology (CSCO): Clinical Guidelines for the Diagnosis and Treatment of Gastric Cancer. *Cancer Commun (Lond)* (2019) 39(1):10. doi: 10.1186/s40880-019-0349-9
3. Baretton GB, Aust DE. Current Biomarkers for Gastric Cancer. *Pathologe* (2017) 38(2):93–7. doi: 10.1007/s00292-017-0271-3
4. 5Cainap C, Vlad C, Seicean A, Balacescu O, Seicean R, Constantin AM, et al. Gastric Cancer: Adjuvant Chemotherapy Versus Chemoradiation. A Clinical Point of View. *J BUON* (2019) 24(6):2209–19.
5. Wu D, Zhang P, Ma J, Xu J, Yang L, Xu W, et al. Serum Biomarker Panels for the Diagnosis of Gastric Cancer. *Cancer Med* (2019) 8(4):1576–83. doi: 10.1002/cam4.2055
6. Li Y, Yang Y, Lu M, Shen L. Predictive Value of Serum CEA, CA19-9 and CA72.4 in Early Diagnosis of Recurrence After Radical Resection of Gastric Cancer. *Hepatogastroenterology* (2011) 58(112):2166–70. doi: 10.5754/hge11753
7. Yu J, Zhang S, Zhao B. Differences and Correlation of Serum CEA, CA19-9 and CA72-4 in Gastric Cancer. *Mol Clin Oncol* (2016) 4(3):441–9. doi: 10.3892/mco.2015.712
8. Yang AP, Liu J, Lei HY, Zhang QW, Zhao L, Yang GH. CA72-4 Combined With CEA, CA125 and CAl9-9 Improves the Sensitivity for the Early Diagnosis of Gastric Cancer. *Clin Chim Acta* (2014) 437:183–6. doi: 10.1016/j.cca.2014.07.034
9. Hanly DJ, Esteller M, Berdasco M. Interplay Between Long non-Coding RNAs and Epigenetic Machinery: Emerging Targets in Cancer? *Philos Trans R Soc Lond B Biol Sci* (2018) 373(1748):20170074. doi: 10.1098/rstb.2017.0074
10. Landeros N, Santoro PM, Carrasco-Avino G, Corvalan AH. Competing Endogenous RNA Networks in the Epithelial to Mesenchymal Transition in Diffuse-Type of Gastric Cancer. *Cancers (Basel)* (2020) 12(10):2741. doi: 10.3390/cancers12102741
11. Shekari N, Asghari F, Haghnavaz N, Shanehbandi D, Khaze V, Baradaran B, et al. Let-7a Could Serve as A Biomarker for Chemo-Responsiveness to Docetaxel in Gastric Cancer. *Anticancer Agents Med Chem* (2019) 19(3):304–9. doi: 10.2174/1871520619666181213110258
12. Gao Y, Wang JW, Ren JY, Guo M, Guo CW, Ning SW, et al. Long Noncoding RNAs in Gastric Cancer: From Molecular Dissection to Clinical Application. *World J Gastroenterol* (2020) 26(24):3401–12. doi: 10.3748/wjg.v26.i24.3401
13. Krishna S, Raghavan S, DasGupta R, Palakodeti D. tRNA-Derived Fragments (tRFs): Establishing Their Turf in Post-Transcriptional Gene Regulation. *Cell Mol Life Sci* (2021) 78(6):2607–19. doi: 10.1007/s00018-020-03720-7
14. Kim HK, Yeom JH, Kay MA. Transfer RNA-Derived Small RNAs: Another Layer of Gene Regulation and Novel Targets for Disease Therapeutics. *Mol Ther* (2020) 28(11):2340–57. doi: 10.1016/j.ymthe.2020.09.013
15. Speer J, Gehrke CW, Kuo KC, Waalkes TP, Borek E. tRNA Breakdown Products as Markers for Cancer. *Cancer* (1979) 44(6):2120–3. doi: 10.1002/1097-0142(197912)44:6<2120::aid-cncr2820440623>3.0.co;2-6
16. Li S, Xu Z, Sheng J. tRNA-Derived Small RNA: A Novel Regulatory Small Non-Coding RNA. *Genes (Basel)* (2018) 9(5):246. doi: 10.3390/genes9050246
17. Shen Y, Yu X, Zhu L, Li T, Yan Z, Guo J. Transfer RNA-Derived Fragments and tRNA Halves: Biogenesis, Biological Functions and Their Roles in Diseases. *J Mol Med (Berl)* (2018) 96(11):1167–76. doi: 10.1007/s00109-018-1693-y
18. Jia Y, Tan W, Zhou Y. Transfer RNA-Derived Small RNAs: Potential Applications as Novel Biomarkers for Disease Diagnosis and Prognosis. *Ann Transl Med* (2020) 8(17):1092. doi: 10.21037/atm-20-2797
19. Zhu L, Ge J, Li T, Shen Y, Guo J. tRNA-Derived Fragments and tRNA Halves: The New Players in Cancers. *Cancer Lett* (2019) 452:31–7. doi: 10.1016/j.canlet.2019.03.012
20. Sun C, Yang F, Zhang Y, Chu J, Wang J, Wang Y, et al. tRNA-Derived Fragments as Novel Predictive Biomarkers for Trastuzumab-Resistant Breast Cancer. *Cell Physiol Biochem* (2018) 49(2):419–31. doi: 10.1159/000492977

21. Mo D, Jiang P, Yang Y, Mao X, Tan X, Tang X, et al. A tRNA Fragment, 5'-tiRNA(Val), Suppresses the Wnt/beta-Catenin Signaling Pathway by Targeting FZD3 in Breast Cancer. *Cancer Lett* (2019) 457:60–73. doi: 10.1016/j.canlet.2019.05.007
22. Cui Y, Huang Y, Wu X, Zheng M, Xia Y, Fu Z, et al. Hypoxia-Induced tRNA-Derived Fragments, Novel Regulatory Factor for Doxorubicin Resistance in Triple-Negative Breast Cancer. *J Cell Physiol* (2019) 234(6):8740–51. doi: 10.1002/jcp.27533
23. Zhou K, Diebel KW, Holy J, Skildum A, Odean E, Hicks DA, et al. A tRNA Fragment, Trf5-Glu, Regulates BCAR3 Expression and Proliferation in Ovarian Cancer Cells. *Oncotarget* (2017) 8(56):95377–91. doi: 10.18632/oncotarget.20709
24. Gu W, Shi J, Liu H, Zhang X, Zhou JJ, Li M, et al. Peripheral Blood non-Canonical Small Non-Coding RNAs as Novel Biomarkers in Lung Cancer. *Mol Cancer* (2020) 19(1):159. doi: 10.1186/s12943-020-01280-9
25. Martens-Uzunova ES, Jalava SE, Dits NF, van Leenders GJ, Moller S, Trapman J, et al. Diagnostic and Prognostic Signatures From the Small Non-Coding RNA Transcriptome in Prostate Cancer. *Oncogene* (2012) 31(8):978–91. doi: 10.1038/onc.2011.304
26. Olvedy M, Scaravilli M, Hoogstrate Y, Visakorpi T, Jenster G, Martens-Uzunova ES. A Comprehensive Repertoire of tRNA-Derived Fragments in Prostate Cancer. *Oncotarget* (2016) 7(17):24766–77. doi: 10.18632/oncotarget.8293
27. Zhao C, Tolkach Y, Schmidt D, Muders M, Kristiansen G, Muller SC, et al. tRNA-Halves Are Prognostic Biomarkers for Patients With Prostate Cancer. *Urol Oncol* (2018) 36(11):503.e1–e7. doi: 10.1016/j.urolonc.2018.08.003
28. Huang B, Yang H, Cheng X, Wang D, Fu S, Shen W, et al. tRF/miR-1280 Suppresses Stem Cell-Like Cells and Metastasis in Colorectal Cancer. *Cancer Res* (2017) 77(12):3194–206. doi: 10.1158/0008-5472.CAN-16-3146
29. Li S, Shi X, Chen M, Xu N, Sun D, Bai R, et al. Angiogenin Promotes Colorectal Cancer Metastasis *via* tiRNA Production. *Int J Cancer* (2019) 145 (5):1395–407. doi: 10.1002/ijc.32245
30. Nientiedt M, Deng M, Schmidt D, Perner S, Muller SC, Ellinger J. Identification of Aberrant tRNA-Halves Expression Patterns in Clear Cell Renal Cell Carcinoma. *Sci Rep* (2016) 6:37158. doi: 10.1038/srep37158
31. Zhao C, Tolkach Y, Schmidt D, Kristiansen G, Muller SC, Ellinger J. 5'-tRNA Halves Are Dysregulated in Clear Cell Renal Cell Carcinoma. *J Urol* (2018) 199(2):378–83. doi: 10.1016/j.juro.2017.07.082
32. Pepe F, Balatti V. Role of Non-Coding RNAs in the Development of Targeted Therapy and Immunotherapy Approaches for Chronic Lymphocytic Leukemia. *J Clin Med* (2020) 9(2):593. doi: 10.3390/jcm9020593
33. Huang Y, Ge H, Zheng M, Cui Y, Fu Z, Wu X, et al. Serum tRNA-Derived Fragments (tRFs) as Potential Candidates for Diagnosis of Nontriple Negative Breast Cancer. *J Cell Physiol* (2020) 235(3):2809–24. doi: 10.1002/jcp.29185
34. Pekarsky Y, Balatti V, Palamarchuk A, Rizzotto L, Veneziano D, Nigita G, et al. Dysregulation of a Family of Short Noncoding RNAs, tsRNAs, in Human Cancer. *Proc Natl Acad Sci USA* (2016) 113(18):5071–6. doi: 10.1073/pnas.1604266113
35. Xiong W, Wang X, Cai X, Liu Y, Li C, Liu Q, et al. Identification of Trnaderived Fragments in Colon Cancer by Comprehensive Small RNA Sequencing. *Oncol Rep* (2019) 42(2):735–44. doi: 10.3892/or.2019.7178
36. Zhang F, Shi J, Wu Z, Gao P, Zhang W, Qu B, et al. A 3'-tRNA-Derived Fragment Enhances Cell Proliferation, Migration and Invasion in Gastric Cancer by Targeting FBXO47. *Arch Biochem Biophys* (2020) 690:108467. doi: 10.1016/j.abb.2020.108467
37. Tong L, Zhang W, Qu B, Zhang F, Wu Z, Shi J, et al. The tRNA-Derived Fragment-3017a Promotes Metastasis by Inhibiting NELL2 in Human Gastric Cancer. *Front Oncol* (2020) 10:570916. doi: 10.3389/fonc.2020.570916
38. Gu X, Ma S, Liang B, Ju S. Serum Hsa_Tsr016141 as a Kind of tRNA-Derived Fragments Is a Novel Biomarker in Gastric Cancer. *Front Oncol* (2021) 11:679366. doi: 10.3389/fonc.2021.679366
39. Usman T, Yu Y, Liu C, Wang X, Zhang Q, Wang Y. Genetic Effects of Single Nucleotide Polymorphisms in JAK2 and STAT5A Genes on Susceptibility of Chinese Holsteins to Mastitis. *Mol Biol Rep* (2014) 41(12):8293–301. doi: 10.1007/s11033-014-3730-4
40. Dong L, Qi P, Xu MD, Ni SJ, Huang D, Xu QH, et al. Circulating CUDR, LSINCT-5 and PTENP1 Long Noncoding RNAs in Sera Distinguish Patients With Gastric Cancer From Healthy Controls. *Int J Cancer* (2015) 137 (5):1128–35. doi: 10.1002/ijc.29484
41. Luo T, Zhao J, Lu Z, Bi J, Pang T, Cui H, et al. Characterization of Long non-Coding RNAs and MEF2C-AS1 Identified as a Novel Biomarker in Diffuse Gastric Cancer. *Transl Oncol* (2018) 11(5):1080–9. doi: 10.1016/j.tranon.2018.06.007
42. Xu Y, Kong S, Qin X, Ju S. Comprehensive Assessment of Plasma Circ_0004771 as a Novel Diagnostic and Dynamic Monitoring Biomarker in Gastric Cancer. *Onco Targets Ther* (2020) 13:10063–74. doi: 10.2147/OTT.S263536
43. Zheng Q, Bao C, Guo W, Li S, Chen J, Chen B, et al. Circular RNA Profiling Reveals an Abundant Circhipk3 That Regulates Cell Growth by Sponging Multiple miRNAs. *Nat Commun* (2016) 7:11215. doi: 10.1038/ncomms11215
44. Li XN, Wang ZJ, Ye CX, Zhao BC, Huang XX, Yang L. Circular RNA circVAPA Is Up-Regulated and Exerts Oncogenic Properties by Sponging miR-101 in Colorectal Cancer. *BioMed Pharmacother* (2019) 112:108611. doi: 10.1016/j.biopha.2019.108611
45. Poonyam P, Aumpan N, Vilaichone RK. Prognostic Factors for Survival in Patients With Gastric Adenocarcinoma. *Cancer Rep (Hoboken)* (2021) 4(1): e1305. doi: 10.1002/cnr2.1305
46. Uno Y. Prevention of Gastric Cancer by Helicobacter Pylori Eradication: A Review From Japan. *Cancer Med* (2019) 8(8):3992–4000. doi: 10.1002/cam4.2277
47. Wadhwa R, Song S, Lee JS, Yao Y, Wei Q, Ajani JA. Gastric Cancer-Molecular and Clinical Dimensions. *Nat Rev Clin Oncol* (2013) 10(11):643–55. doi: 10.1038/nrclinonc.2013.170
48. Figueiredo C, Camargo MC, Leite M, Fuentes-Panana EM, Rabkin CS, Machado JC. Pathogenesis of Gastric Cancer: Genetics and Molecular Classification. *Curr Top Microbiol Immunol* (2017) 400:277–304. doi: 10.1007/978-3-319-50520-6_12
49. Ma Z, Zhou J, Shao Y, Jafari FA, Qi P, Li Y. Biochemical Properties and Progress in Cancers of tRNA-Derived Fragments. *J Cell Biochem* (2020) 121 (3):2058–63. doi: 10.1002/jcb.29492
50. Kim HK. Transfer RNA-Derived Small Non-Coding RNA: Dual Regulator of Protein Synthesis. *Mol Cells* (2019) 42(10):687–92. doi: 10.14348/molcells.2019.0214
51. Luan N, Mu Y, Mu J, Chen Y, Ye X, Zhou Q, et al. Dicer1 Promotes Colon Cancer Cell Invasion and Migration Through Modulation of tRF-20-MEJB5Y13 Expression Under Hypoxia. *Front Genet* (2021) 12:638244. doi: 10.3389/fgene.2021.638244
52. Tao EW, Wang HL, Cheng WY, Liu QQ, Chen YX, Gao QY. A Specific tRNA Half, 5'tiRNA-His-GTG, Responds to Hypoxia *via* the HIF1alpha/ANG Axis and Promotes Colorectal Cancer Progression by Regulating LATS2. *J Exp Clin Cancer Res* (2021) 40(1):67. doi: 10.1186/s13046-021-01836-7
53. Zhu L, Li J, Gong Y, Wu Q, Tan S, Sun D, et al. Exosomal tRNA-Derived Small RNA as a Promising Biomarker for Cancer Diagnosis. *Mol Cancer* (2019) 18 (1):74. doi: 10.1186/s12943-019-1000-8
54. Balatti V, Nigita G, Veneziano D, Drusco A, Stein GS, Messier TL, et al. tsRNA Signatures in Cancer. *Proc Natl Acad Sci USA* (2017) 114(30):8071–6. doi: 10.1073/pnas.1706908114
55. Shen Y, Yu X, Ruan Y, Li Z, Xie Y, Yan Z, et al. Global Profile of tRNA-Derived Small RNAs in Gastric Cancer Patient Plasma and Identification of tRF-33-P4R8YP9LON4VDP as a New Tumor Suppressor. *Int J Med Sci* (2021) 18(7):1570–9. doi: 10.7150/ijms.53220
56. Farina NH, Scalia S, Adams CE, Hong D, Fritz AJ, Messier TL, et al. Identification of tRNA-Derived Small RNA (tsRNA) Responsive to the Tumor Suppressor, RUNX1, in Breast Cancer. *J Cell Physiol* (2020) 235 (6):5318–27. doi: 10.1002/jcp.29419
57. Zhou J, Wan F, Wang Y, Long J, Zhu X. Small RNA Sequencing Reveals a Novel tsRNA-26576 Mediating Tumorigenesis of Breast Cancer. *Cancer Manag Res* (2019) 11:3945–56. doi: 10.2147/CMAR.S199281

Conflict of Interest: The authors declare that the research was conducted in the absence of any commercial or financial relationships that could be construed as a potential conflict of interest.

this article, or claim that may be made by its manufacturer, is not guaranteed or endorsed by the publisher.

frontiers in Oncology

ORIGINAL RESEARCH
published: 31 August 2021
doi: 10.3389/fonc.2021.728393

MiR-199b-5p Promotes Gastric Cancer Progression by Regulating HHIP Expression

*Songda Chen[1], Huijie Wu[1], Lingyu Zhu[1], Mengjie Jiang[1], Shuli Wei[2], Jinhua Luo[2] and Aiqun Liu[1]**

[1] Department of Endoscopy, Guangxi Medical University Cancer Hospital, Nanning, China, [2] Department of Gastroenterology, The 10th Affiliated Hospital of Guangxi Medical University, Qinzhou, China

Objectives: Gastric cancer (GC) is one of the most common malignant tumors. More and more evidences support the role of microRNAs (miRNAs) in tumor progression. However, the role of miRNAs in human GC remains largely unknown.

Methods: Based on the published gastric cancer expression profile data, combined with bioinformatics analysis, potential miRNAs in the process of GC were screened. The expression of miR-199b-5p in GC cells and patients' plasma was detected by RT-PCR. The effects of miR-199b-5p on GC *in vitro* were detected by EdU proliferation assay, colony formation assay, Transwell assay and wound healing assay. Western blot was used to detect epithelial-mesenchymal transition (EMT) related proteins. The subcutaneous tumorigenesis model and metastatic tumor model of mice were used to study its effect *in vivo*. Bioinformatics and Dual luciferase reporter assay were used to verify the effect of miR-199b-5p and its target gene.

Results: Through bioinformatics analysis, we screened a novel miRNA miR-199b-5p that was significantly up-regulated in GC tissue and associated with poor prognosis of GC patients. RT-PCR results showed that its expression was also up-regulated in GC cell lines and patients' plasma. MiR-199b-5p can significantly promote GC cell proliferation and migration *in vitro* and *in vivo*. Western blot showed that miR-199b-5p could promote the EMT process of GC. HHIP has been proved to be a target of miR-199b-5p, and the recovery of HHIP can weaken the effect of miR-199b-5p.

Conclusion: MiR-199b-5p may play an oncogene role in GC by targeting *HHIP*, suggesting that miR-199b-5p may be a potential therapeutic target for GC.

Keywords: miR-199b-5p, *HHIP*, GC, bioinformatics, maker

OPEN ACCESS

Edited by:
Kanjoormana Aryan Manu, Amala Cancer Research Centre, India

Reviewed by:
Nisha Padmanabhan, Duke-NUS Medical School, Singapore
Wafaa M. Rashed, Children's Cancer Hospital, Egypt

***Correspondence:**
Aiqun Liu
liuaiqun_2004@163.com

Specialty section:
This article was submitted to Gastrointestinal Cancers, a section of the journal Frontiers in Oncology

Received: *21 June 2021*
Accepted: *03 August 2021*
Published: *31 August 2021*

Citation:
Chen S, Wu H, Zhu L, Jiang M, Wei S, Luo J and Liu A (2021) MiR-199b-5p Promotes Gastric Cancer Progression by Regulating HHIP Expression. Front. Oncol. 11:728393. doi: 10.3389/fonc.2021.728393

INTRODUCTION

Although the incidence of gastric cancer (GC) has declined in the past few decades, it is still one of the most common malignant tumors, especially in East Asia, where its incidence and mortality rank fourth and third in the world, respectively (1, 2). GC patients are often in the advanced stage after diagnosis, and one of the reasons for their high mortality is the lack of specific diagnosis. Although

early diagnosis, surgical techniques, and postoperative radiotherapy and chemotherapy have gradually improved the clinical prognosis of GC, the 5-year survival rate of patients with advanced GC is still relatively low (3).The poor prognosis of patients with advanced GC is mainly attributed to invasion and metastasis, among which lymph node metastasis exceeds 50% (4). Therefore, it is extremely necessary to explore the molecular mechanism of GC progression, which may provide a basis for new therapeutic targets for GC.

miRNA is a type of non-coding RNA composed of 20-24 nucleotides, which plays an important role in human health and disease by regulating gene expression (5, 6). MiRNA was first discovered in 1993, and it regulates more than 50% of the known genes in humans (7, 8). It has been reported that miRNAs can have multiple target genes, and multiple miRNAs can also regulate the same target gene (9). Mature miRNAs can play a bidirectional regulatory function by degrading or inhibiting the translation of target mRNAs, that is, miRNAs actually assume at least two functions of oncogene or tumor suppressor gene in life activities. Study has found that miR-199b-5p is highly expressed in osteosarcoma and promotes the malignant development of osteosarcoma (10). However, miR-199b-5p is under-expressed in prostate cancer and breast cancer and inhibits tumor cell growth (11, 12). These studies show that miR-199b-5p plays a two-way regulatory role in different cancer cells. However, the related functions of miR-199b-5p in GC have not been reported yet. Through bioinformatics, we found that miR-199b-5p is significantly highly expressed in gastric cancer tissues, and the highly expressed miR-199b is related to the poor prognosis of gastric cancer patients. Therefore, we were very interested in the role of miR-199b-5p produced from the 5,arm in gastric cancer. In this study, we found that miR-199b-5p can promote the progress of GC both *in vivo* and *in vitro*.

Hedgehog interacting protein (*HHIP*) gene is located on chromosome 4q31.21–31.3 and encodes the production of *HHIP*. As an evolutionarily conserved protein, HHIP is a key mediator of many basic processes in embryonic development (13). *HHIP* is an endogenous antagonist of the hedgehog signaling pathway, and its loss of function or mutation may lead to the up-regulation of this signal and promote tumorigenesis (14, 15). Scholars have found that the expression of *HHIP* in gastric cancer tissues is reduced, and the overexpression of *HHIP* reduces the migration and invasion of GC (16). We have confirmed that *HHIP* is the direct target of miR-199b-5p and plays an important role in human GC through bioinformatics analysis and related functional analysis.

In this study, we aimed to explore the biological role of miR-199b-5p and its relationship with *HHIP*. Our research results show that over-expression of miR-199b-5p can promote the progress of GC *in vivo* and *in vitro*, and on the contrary, it can inhibit the malignant development of GC. *HHIP* is the direct target gene of miR-199b-5p. Overexpression of HHIP can partially reverse the role of miR-199b-5p in GC, that is, the related role of miR-199b-5p in GC was partly caused by regulating *HHIP*. These findings also provided a basis for miR-199b-5p as a potential therapeutic target for GC.

MATERIALS AND METHODS

Microarray Data

Three GC datasets (GSE93415, GSE78091,GSE23739) were downloaded from GEO database. Among them, GSE93415 includes 20 pairs of GC tissues and 20 pairs of normal tissues, GSE78091 includes 3 pairs of GC tissues and 3 pairs of normal tissues, and GSE23739 includes 40 pairs of GC tissues and 40 pairs of normal tissues. $P < 0.05$ and [logFC] > 1 as screening conditions

Tissue Samples and GC Cell Lines

The specimens were collected in the Department of Pathology, Affiliated Guangxi Medical University Cancer Hospital. No radiotherapy or chemotherapy was performed before the operation, and the patients or their relatives signed informed consent form. This study was approved by the Ethics Committee of the Guangxi Medical University Cancer Hospital. Human GC cell lines, AGS, MGC803, SGC7901 and rumen-free epithelial cells GES1 were purchased from the Shanghai Institute of Biological Sciences Center. All cell lines were cultured in DMEM medium (Gibico, USA) supplemented with 10% fetal bovine serum (Gibico, USA) and 1% penicillin/streptomycin (Gibico, USA) in a cell incubator at 37°C and 5% CO_2.

RNA Extraction and PCR

Total RNA was extracted from GC cells using TRIzol reagent (Beyotime, China), according to the manufacturer's agreement. U6 and β-actin were used as endogenous controls to quantify miRNA and mRNA, respectively. All primers(Shangon Biotech, China) used in our research are as follows: β-actin forward, 5, -GCATCGTCACCAACTGGGAC-3, andβ-actin reverse, 5, -ACCTGGCCGTCAGGCAGCTC-3,; U6 forward, 5'-CTCGC TTCGGCAGCACA-3' and U6 reverse, 5'-AACGCTTCAC GAATTTGCGT-3'; HHIP forward, 5'-TCTCAAAGCCTGTT CCACTCA-3' and HHIP reverse 5'-GCCTCGGCAAGTGT AAAAGAA-3'; miR-199b-5p:5'-CCCAGTGTTTAGACTATCTGT T-3'. The relative expression is quantified by the $2^{-\Delta\Delta C\ T}$ method. Each sample was repeated three times for PCR.

Cell Transfection

According to the experimental design, commercial lentiviral vectors (GenePharma, China)were used to construct LV-hsa-miR-199b-5p-mimic vector (miR-mimic), LV-miR-199b-5p-inhibitor vector (miR-inhibitor) and Lv-HHIP vector, and then cell transfection was carried out according to the reagent instructions. Finally, 5μg/mL puromycin (Beyotime, China) was used for about a week to obtain stable transfected cell lines.

Colony Formation Assay

Stably transfected GC cells were placed in a 6-well plate (500 cells/well) and cultured in DMEM medium for about 2 weeks。 The colonies were stained with 0.1% crystal violet (Beyotime, China) after washing away with PBS. All procedures were performed in triplicate.

5-Ethynyl-2-Deoxyuridine (EdU) Assay

EdU assay kit (RiboBio, China) was used to detect cell proliferation. First, the cells were seeded into a 96-well plate (2×10^4cells/well) and cultured in complete medium for 24 hours. On the second day, cells were incubated with 50μM EdU about 2h at 37°C and fixed in 4% formaldehyde for 20min. And then 0.5% TritonX-100 was permeabilized for 10 minutes at room temperature. After washing with PBS, 200μL 1×ApolloR reaction cocktail was added to react with the EdU for 30 minutes. Then add 200μL hoechst33342 for 10min to observe the nucleus. Images of cells were captured under a fluorescence microscope (Olympus Corp, Japan).

Migration Assay

The migratory ability of cells were assayed by using a 6.5mm chamber with 8μm pores (Corning, USA). 2×10^4 stably transfected GC cells were suspended in 200μL serum-free DMEM medium and placed on the top of the chamber, and then complete medium (500μL)was added into lower chamber. After the cells were cultured in a 37°C incubator for 24 hours, the cells in the upper layer of the chamber were removed with cotton swabs. Staining with 1% crystal violet for 30min after washing with PBS. We imaged and counted the cells on the bottom surface of membrane by microscope (Olympus Corp. Japan). All procedures were performed in triplicate.

Wound Healing Assay

Stably transfected GC cells (5×10^5) were seeded in six-well plates. After the cells adhere to the wall, 200μL sterile pipette tips were used to form linear scratches. Then the plate was washed several times with PBS to remove the suspended cells, and the cells were cultured in serum-free medium. After 0 and 24h, we imaged the wounds at the same position under the microscope (Olympus Corp. Japan) and the distance between the wound sides was calculated. All procedures were performed in triplicate.

Western Blot Assay

Proteins were extracted from GC cells with RIPA lysis buffer (Beyotime, China), separated by sodium dodecyl sulfate polyacrylamide gel electrophoresis (SDS-PAGE), and then transferred to polyvinylidene fluoride (PVDF) membrane. The PVDF membrane was blocked with 5% skim milk at room temperature for 1.5 hours, and incubated with specific antibodies overnight at 4°C. On the second day, the membrane was incubated with the secondary antibody for 1 hour at room temperature. After washing with TBST, proteins were detected with enhanced chemiluminescence (ECL) detection system. β-actin was used as an internal control.

Cell Immunofluorescence Assay

Cells in each group were sliced in six-well plate. The cells were fixed with 4% paraformaldehyde for 15 minutes and then sealed with 5% BSA at room temperature for 1 hour. Then, the primary antibody HHIP (affinity. USA) was dripped and incubated overnight at 4°C. After cleaning with PBS, Cy3 labeled secondary antibody (beyotime, China) was dropped and incubated at room temperature for 1 hour. Then the cell nucleus were labeled with Hoechst 33342. Finally, the film was sealed with anti-fluorescence quenching agent and observed with fluorescence microscope immediately.

Immunohistochemistry

All samples were fixed with 4% paraformaldehyde solution and embedded in paraffin. Then, paraffin embedded sections were dewaxed in xylene and then rehydrated in graded ethanol. After antigen repair, endogenous catalase was blocked by 3% hydrogen peroxide. Then the primary antibody for HHIP (affinity. USA) and Ki-67 (Servicebio,China)was incubated on the slices overnight at 4°C. After PBS washing, the sections were incubated with HRP-polymer-conjugated secondary antibody at 37°C for 1 h, and then stained with 3,3-diaminobenzidine (DAB) solution for 3min. The nucleus were stained with hematoxylin. We randomly selected three observation fields to observe.

Animal Experiment

4-week-old female BALB/c nude mice were purchased from the animal center of Guangxi Medical University. The experimental animals all conform to the regulations of the animal nursing and use Committee of Guangxi Medical University. In the subcutaneous tumorigenesis experiment, 15 female nude mice were randomly divided into three groups. The stably transfected cells (2×10^6 cells/200μL PBS) were injected into the lateral abdomen of each group. The tumor volume was measured with Vernier caliper every 4 days, and the formula was: volume = (length × width ^{2})/2. The mice were euthanized after 3 weeks. We injected stable transfected cells (1×10^6 cells/100μL PBS) into the tail vein of mice to observe lung metastases. Six weeks later, the nude mice were dissected to observe the lung metastasis.

Dual Luciferase Reporter Assay

The 3 '- UTR sequence of *HHIP* containing mutants (MUT) or wild type (WT) miR - 199b - 5p binding sites was constructed by Genscript (Nanjing, China), and cloned into PGL - 3 luciferase reporting vector. After incubation in 24-well plates for 24 hours, *pGL3 - WT - HHIP or pGL3 - MUT - HHIP 3 '- UTR* reporter plasmids were cotransfected with miR -199b-5p mimic or miR-NC with Lipofectamine 3000 (Invitrogen). The luciferase activity of firefly and renal was evaluated by Dual-Luciferase Assay System (Promega, USA). The relative expression of luciferase activity of firefly was normalized to luciferase activity of Renilla kidney. All procedures were performed in triplicate.

Statistical Analysis

Each experiment was repeated three times. Difference between two groups were analyzed by t-test, and all data were expressed as mean ± SD. All of the data were analyzed using SPSS17.0 software (SPSS, USA) and were considered to be statistically significant when p values were <0.05.

RESULTS

Differentially Expressed miRNAS (DE miRNAS) Identification

With $P < 0.05$ and [logFC] > 1 as screening conditions, five DE miRNAS were screened by R limma package (**Figure 1A**). MiR-199b-5p, miR-331-3p and miR-142-3p were up-regulated in GC, while miR-665 and miR-375 were down regulated in GC (**Figure 1B**). The specific change thresholds of miRNAs in the three chips are shown in **Table 1**. In order to identify the potential molecules in these miRNAs, we used Kaplan-Meier plotter to analyze the overall survival of all DE miRNAs. The results showed that the high expression of miR-199b and miR-331 was associated with poor prognosis of GC, while the low expression of miR-375 was associated with poor prognosis of GC (**Figure 1C**). However, miR-331-3p and miR-375 have been studied in GC (17, 18). Therefore, we aimed to investigate the related role of miR-199b-5p produced from the 5 'arm in GC.

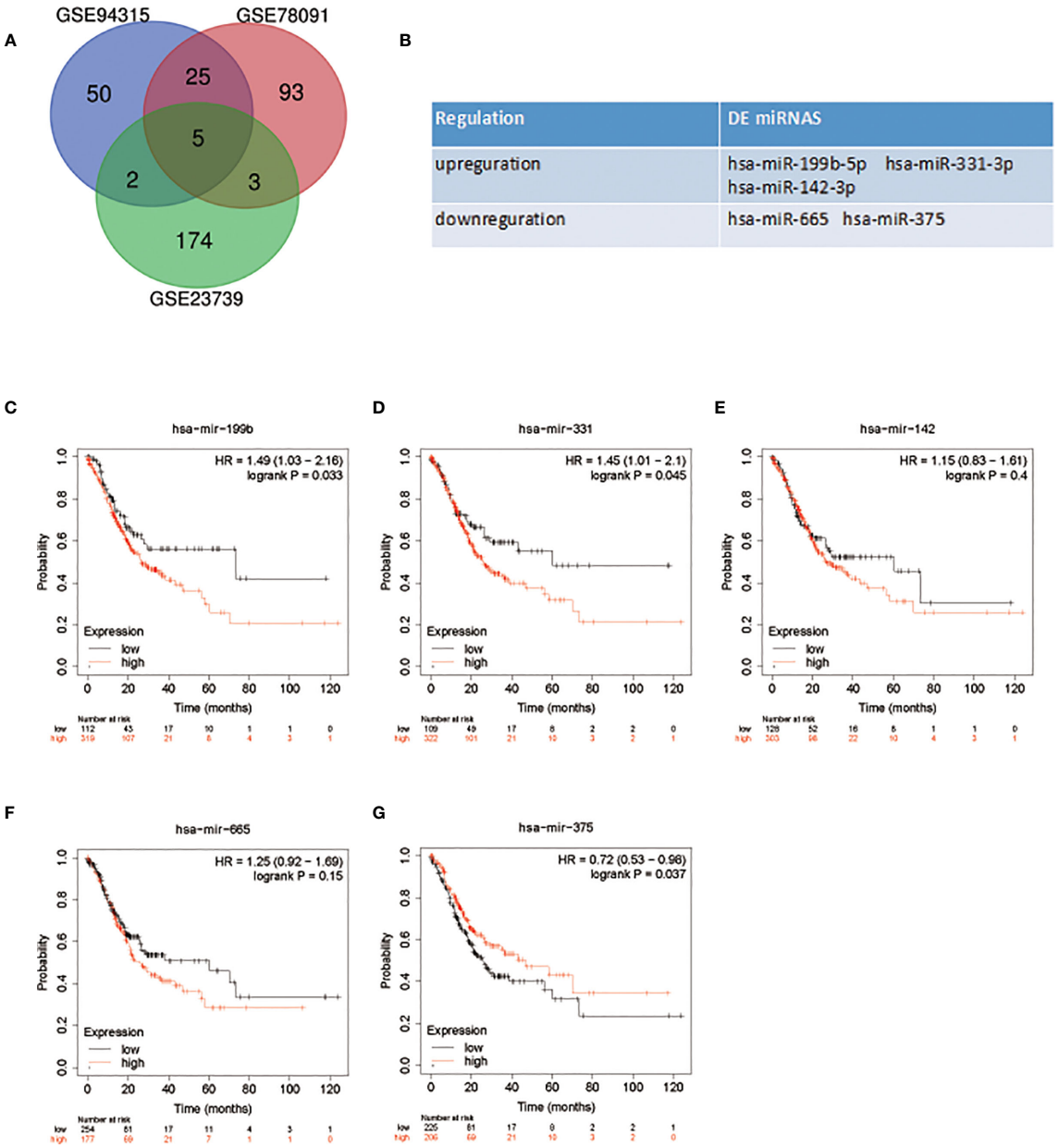

FIGURE 1 | DE miRNAs selection and survival analysis. **(A)** Venn diagram of DE miRNAs in GC. **(B)** The name of DE miRNAs. **(C–G)** Survival analysis of DE miRNAs in patients with GC.

TABLE 1 | Differential expression of miRNAs in each dataset.

Genes	GSE78091		GSE93415		GSE23739	
	logFC	*P*.Value	logFC	*P*.Value	logFC	*P*.Value
hsa-miR-199b-5p	1.87	0.001	1.30	0.001	175.52	0.001
hsa-miR-331-3p	1.07	0.001	1.01	0.001	78.45	0.001
hsa-miR-142-3p	1.33	0.002	1.05	0.005	1028.20	0.002
hsa-miR-665	-1.3	0.02	-1.10	0.001	-63.50	0.01
hsa-miR-375	-2.29	0.001	-1.15	0.001	-824.05	0.001

miR-199b-5p Is Up-Regulated in GC Cells and GC Patients and Promotes GC Cell Proliferation

We detected the expression of miR-199b-5p in normal gastric epithelial cells (GES1) and GC cell lines (SGC7901, MGC803, AGS) by RT-PCR. Compared with GES1, the expression of miR-199b-5p in SGC7901 and MGC803 was significantly higher, which was consistent with GEO database, but there was no difference in the expression of miR-199b-5p in AGS (**Figure 2A**). At the same time, we found that miR-199b-5p was also highly expressed in the plasma of GC patients (**Figure 2B**). To investigate the biological role of miR-199b-5p in GC, we chose SGC7901 and MGC803 for further study. Then miR-199b-5p mimic and inhibitor lentivirus were constructed and transfected into MGC803 and SGC7901 cells respectively. Then RT-PCR was used to verify the transfection efficiency. Compared with the control group, the expression level of miR-199b-5p was significantly increased in the mimic group and decreased in the inhibitor group (**Figures 2C, D**). Edu proliferation assay and clone formation assay were used to detect the proliferation function of miR-199b-5p in GC (**Figures 2E, F**). The results showed that overexpression of miR-199b-5p could promote the proliferation of SGC7901 and MGC803 Cells, while inhibition of miR-199b-5p had the opposite effect (**Figures 2G, H**). In conclusion, the above results showed that overexpression of miR-199b-5p could promote the proliferation of GC cells *in vitro*.

miR -199b - 5p Enhances Migration and the EMT Processing in GC Cells

Further study on the effect of miR-199b-5p on GC cells. The effect of miR-199b-5p on the migration of GC cells was detected by wound healing assay and Transwell assay. In wound healing assay, overexpression of miR-199b-5p promoted the migration rate of GC cells. On the contrary, inhibition of miR-199b-5p significantly inhibited the migration of GC cells (**Figures 3A–D**). Consistent with the results of wound healing assay, we found the same results in Transwell assay. The overexpression of miR-199b-5p in SGC7901 and MGC803 Cells promoted the cell migration, while inhibition of miR-199b-5p was lower than that of the control group (**Figures 3E, F**).

In order to clarify whether miR-199b-5p affects the EMT process of GC cells, we detected the EMT related markers by Western blot assay. The analysis showed that the up regulation of miR-199b-5p could reduce the level of E-cadherin and increase the level of vimentin, N-cadherin. However, after inhibiting miR-199b-5p expression, E-cadherin increased in SGC7901 and MGC803, but vimentin and N-cadherin decreased (**Figure 3G**).

These results suggested that miR-199b-5p may play a key role in the EMT process, thus promoting the migration of GC cells *in vitro*.

miR -199b - 5p Contributes to Tumor Progression and Metastasis *In Vivo*

In order to verify the effect of miR-199b-5p on tumor growth *in vivo*, SGC7901 cells stably transfected with miR-199b-5p mimic or miR-199b-5p inhibitors were injected into the flank of nude mice, and SGC7901 cells transfected with miR-NC served as negative control. As shown in **Figures 4A–C**, compared with miR-NC group, the tumor volume and weight in miR-199b-5p mimic group were significantly increased, while those in miR-199b-5p inhibitor group were decreased. The effect of miR-199b-5p on tumorigenesis was further verified by Ki67 staining. The expression of Ki67 in miR-199b-5p mimic group was higher than that in miR-NC group, while the expression of Ki67 in miR-199b-5p inhibitor group was weaker than that in miR-NC group (**Figure 4D**). To further verify the effect of miR-199b-5p on tumor metastasis *in vivo*, stably transfected cells were injected into the tail vein of BALB/C nude mice. After 7 weeks, we found that miR-199b-5p group significantly promoted lung metastasis than miR-NC group. We also found that the miR-199b-5p inhibitor group had a alleviating effect on lung metastasis compared with the miR-NC group (**Figures 4E, G**). Then the lung tissue of mice was stained with H&E assay, and the results were consistent (**Figure 4F**). In conclusion, our results *in vivo* were consistent with those *in vitro*.

HHIP Is a Direct Target of miR- 199b - 5p and Down-Regulated in GC Tissues and Cells

In order to better predict the target gene of miR-199b-5p in GC, we screened the differentially expressed genes(DEGs) in GC tissue through GEO database(**Figure 5A**). Then, the potential target genes of miR-199b-5p were predicted by TargetScan database, and these potential target genes were intersected with the differentially expressed mRNA in GC (**Figure 5B**). The result showed that there were 27 potential target genes with altered expression in GC (**Figure 5C**). *HHIP* was chosen as a candidate gene because it has a potential miR-199b-5p binding site in its 3'UTR, and study have found that *HHIP* plays an anti-cancer role in GC (16).

In our experiments, our results showed that *HHIP* expression in GC cell lines were lower than GES1(**Figure 5D**). The results of

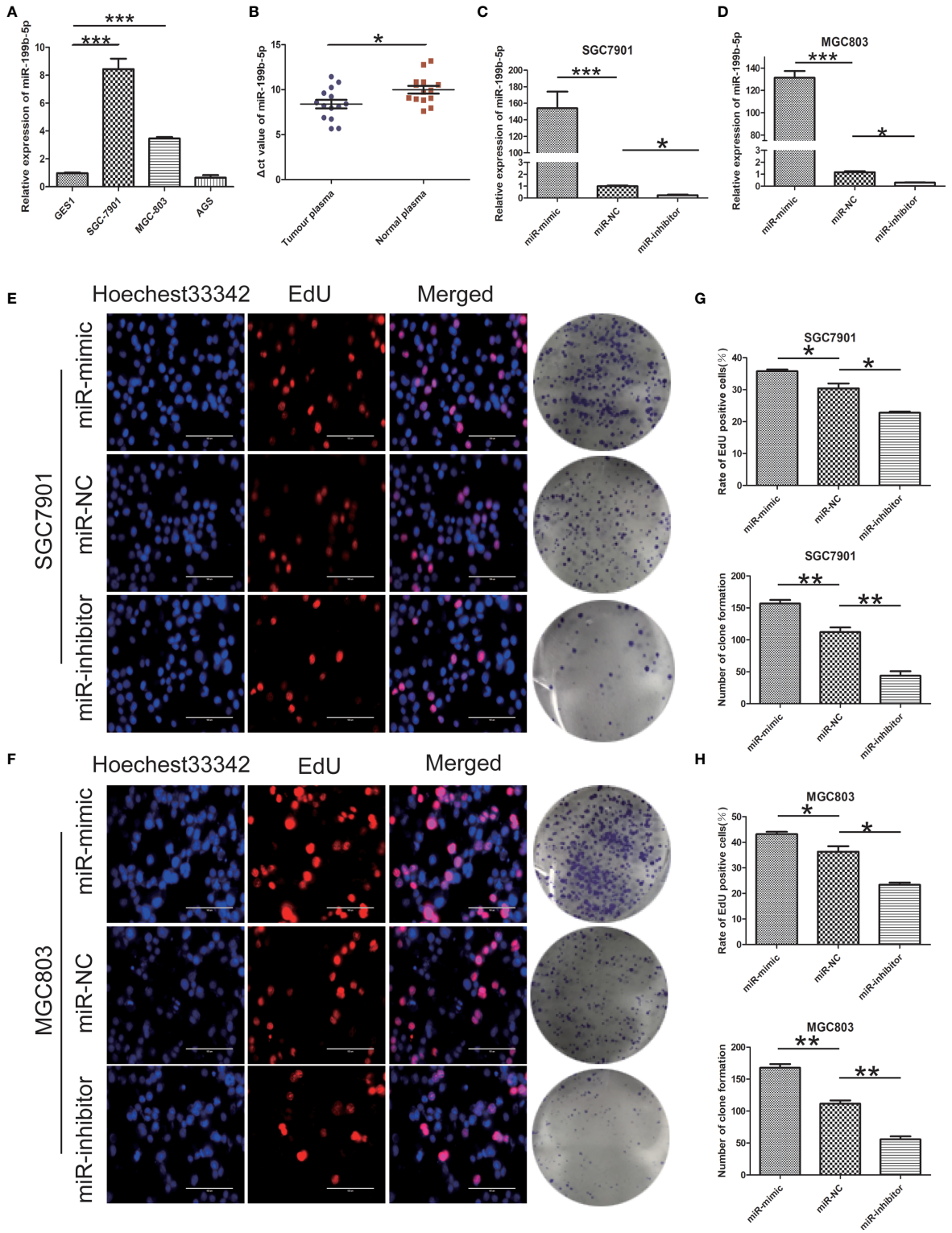

FIGURE 2 | miR - 199b - 5p is upregulated in GC and promotes GC cell proliferation. **(A)** The relative expression of miR-199b-5p in GC cells and GES1. **(B)** Expression of miR-199b-5p in plasma of 14 patients with GC and 14 normal controls. **(C, D)** The relative expression of miR-199b-5p in cells after transfection of miR-199b-5p mimic, NC and inhibitor lentivirus, respectively, in SGC7901 and MGC803. **(E, F)** Representative profiles of EdU assay and colony formation assay in miR-199b-5p mimic and inhibitor groups in SGC7901 and MGC803. **(G, H)** The rate of EdU positive cells and number of colony formation were counted in miR-199b-5p mimic and inhibitor groups. $^{*}p < 0.05$, $^{**}p < 0.01$, $^{***}p < 0.001$. The data expressed as the mean ± SD.

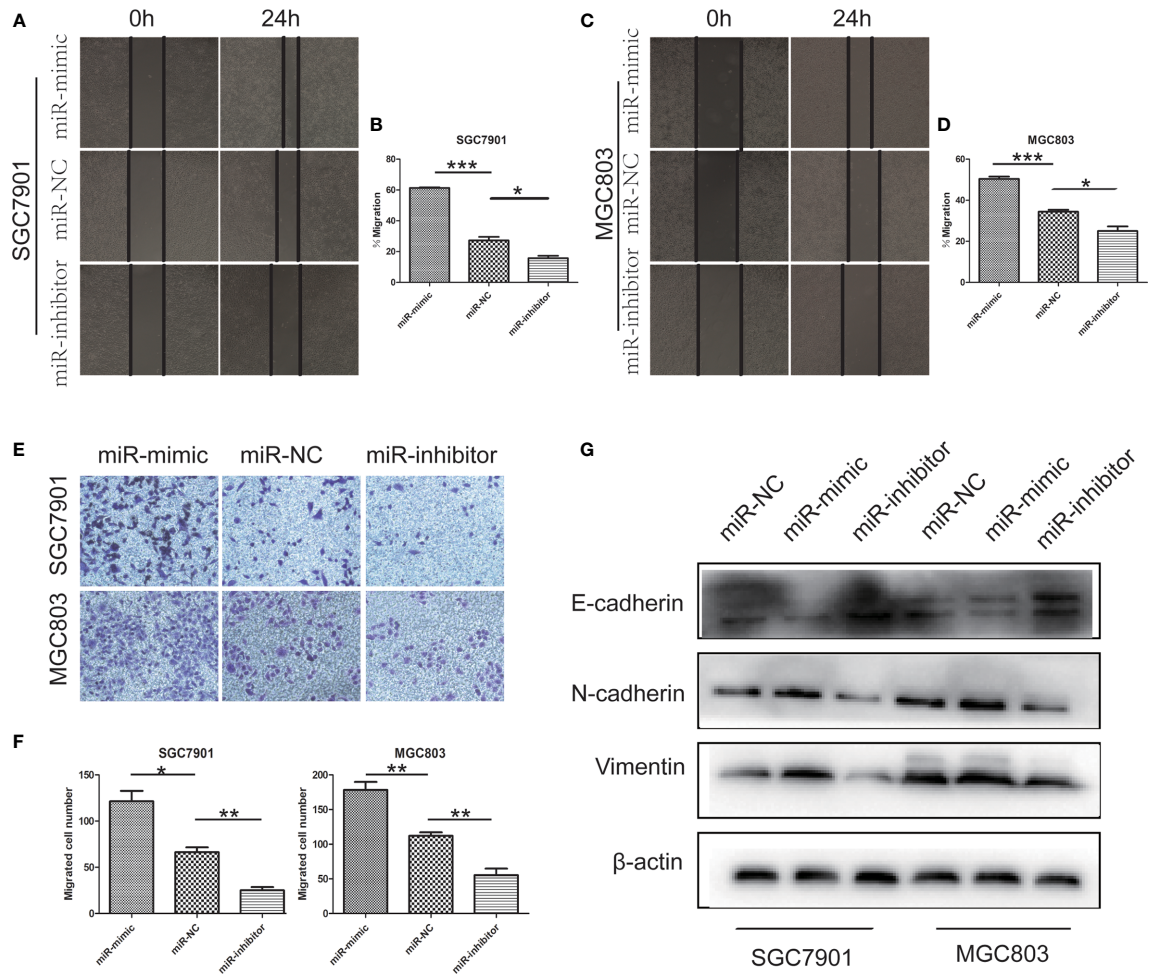

FIGURE 3 | miR -199b - 5p facilitates migration and the EMT processing in GC cells. **(A–D)** Wound-healing assay was used to determine the migration of GC cells after transfection of miR-199b-5p mimic, NC and inhibitor lentivirus, respectively, in SGC7901 and MGC803. **(E, F)** Effects of miR-199b-5p alteration on migration by transwell assay *in vitro*. **(G)** The expression of EMT-associated proteins detected by Western blot when expression of miR-199b-5p was altered in SGC7901 and MGC803. *$p < 0.05$, **$p < 0.01$, ***$p < 0.001$. The data expressed as the mean± SD.

immunohistochemistry showed that *HHIP* was mainly expressed in the cytoplasm of GC, and the expression of *HHIP* was lower than that of normal gastric tissue(**Figure 5E**). We further verified whether miR-199b-5p could directly target 3 '- UTR of *HHIP* mRNA through Dual luciferase reporter assay. In 293T cells, the *HHIP* 3'UTR sequences of WT and MUT were subcloned into *pGL3* luciferase reporter vector. We noted that Co-transfection of miR-199b-5p mimic and *pGL3-WT- HHIP* 3'UTR resulted in decreased luciferase activity compared with the control group. In contrast, overexpression of miR-199b-5p did not affect luciferase activity in *pGL3-MUT- HHIP* 3'UTR transfected cells (**Figure 5F**). In addition, we found that overexpression of miR-199b-5p could reduce the mRNA and protein levels of HHIP, but it was the opposite after inhibiting the expression of miR-199b-5p(**Figures 5G–J**). Overall, our results suggested that *HHIP* is a direct target of miR-199b-5p and is frequently down regulated in GC tissues and cells.

miR -199b - 5p Enhances Proliferation, Migration, and EMT in GC Cells by Targeting HHIP

To further confirm whether mir-199b-5p promotes proliferation, migration and EMT in GC by regulating *HHIP*, we first constructed *lv-HHIP* vector to allow *HHIP* expression. Then, *miR- NC+ lv-NC, miR-mimic + lv-NC, miR-NC + lv-HHIP*, and *miR- mimic + lv-HHIP* were co-transfected into SGC7901 and MGC803 Cells. The expression of *HHIP* was confirmed by RT-PCR and Western blot (**Figures 6A, B**, **7H, I**). Our results show that co-transfection of *lv-HHIP* into miR-199b-5p-mimic cells reversed the proliferation of miR-199b-5p-mimic in EdU assay and clone formation assay(**Figures 6C–F**). Similarly, we found similar results in Transwell assay, wound healing assay and EMT marker detection, that is, overexpression of *HHIP* can partially reversed the migration of miR-199b-5p in GC cells and EMT process(**Figures 7A–I**).These results suggested that miR-

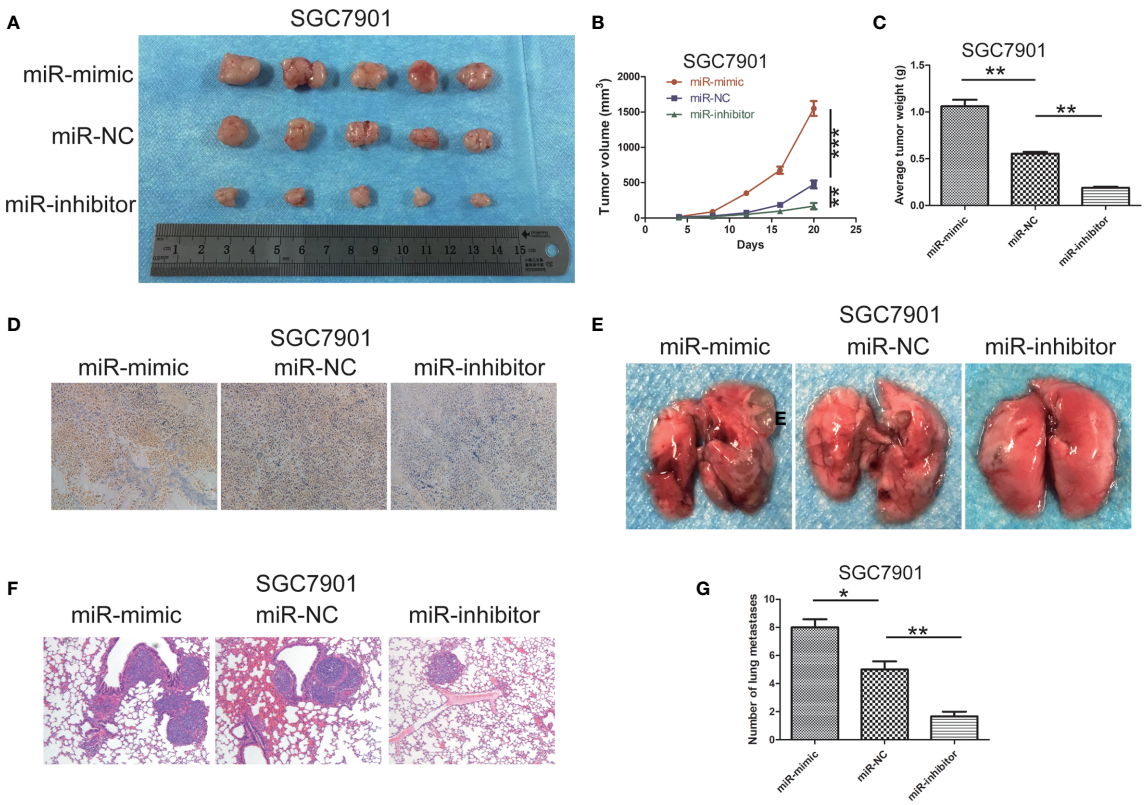

FIGURE 4 | miR -199b - 5p contributes to tumor progression and metastasis *in vivo*. **(A)** photographs of tumors obtained from mice in miR-199b-5p mimic and inhibitor groups. **(B, C)** Tumor volume and weight were calculated in miR-199b-5p mimic and inhibitor groups in SGC7901. volume=(length×width ^{2})/2. **(D)** Ki67 staining assay was used to further verify that miR-199b-5p promoted tumorigenicity. **(E)** Representative images of different groups of lung metastases. **(F)** Representative HE-stained sections of lung from mice in different groups. **(G)** Number of lung metastases in each group. $^*p < 0.05$, $^{**}p < 0.01$, $^{***}p < 0.001$. The data expressed as the mean± SD.

199b-5p promoted the proliferation, migration and EMT process of GC cells by directly targeting *HHIP*.

DISCUSSION

Numerous evidences showed that miRNAs can regulate gene expression by binding to the 3 '- untranslated region of downstream genes, and play different roles in cancer progression as carcinogens or tumor suppressors (19–21). Du et al. studies have shown that miR-95 can inhibit GC by regulating dusp5 (22).Li et al. found that miR-20a-5p can promote the progress of GC by inhibiting the expression of WTX (23). Deng et al. also showed that miR-192 and miR-215 could simultaneously target APC and promote the progression of GC (24). Therefore, it is of great significance to explore the biological role of miRNA in the discovery of carcinogenic mechanism and treatment of cancer. It has been found that miR-199b-5p plays a role as a cancer promoting factor in osteosarcoma by regulating cell proliferation, migration, invasion and EMT (10).Li et al. found that miR-199b-5p was highly expressed in cervical cancer and promoted tumor growth and metastasis by down regulating KLK10 (25). At the same time, miR-199b-5p is low expressed in oral cancer cells and promotes oral cancer cell apoptosis (26). However, the potential molecular mechanism of miR-199b-5p in GC remains to be elucidated. In this study, we found that miR-199b-5p was highly expressed in GC through GEO database. Survival analysis also showed that miR-199b was associated with poor prognosis of GC patients. Therefore, we were very interested in the role of miR-199b-5p produced from 5,end arm in GC. Compared with GES1 cells, we found that miR-199b-5p was also highly expressed in SGC7901 and MGC803 Cells. Interestingly, we found that miR-199b-5p was highly expressed in the plasma of GC patients, and we speculated that miR-199b-5p might be an effective molecule for liquid biopsies of GC patients. But this needs to be verified with a large number of samples. Through a series of proliferation and migration experiments, our results showed that overexpression of miR-199b-5p can promote the occurrence of tumor, and the opposite result was obtained after inhibition of miR-199b-5p. *In vivo*, the results are consistent with those *in vitro*. These results suggest that miR-199b-5p may be a potential therapeutic target for GC. It is worth noting that compared with GES1 cells, the expression of miR-199b-5p in AGS cells has no significant difference. It was found that miR-96-5p was

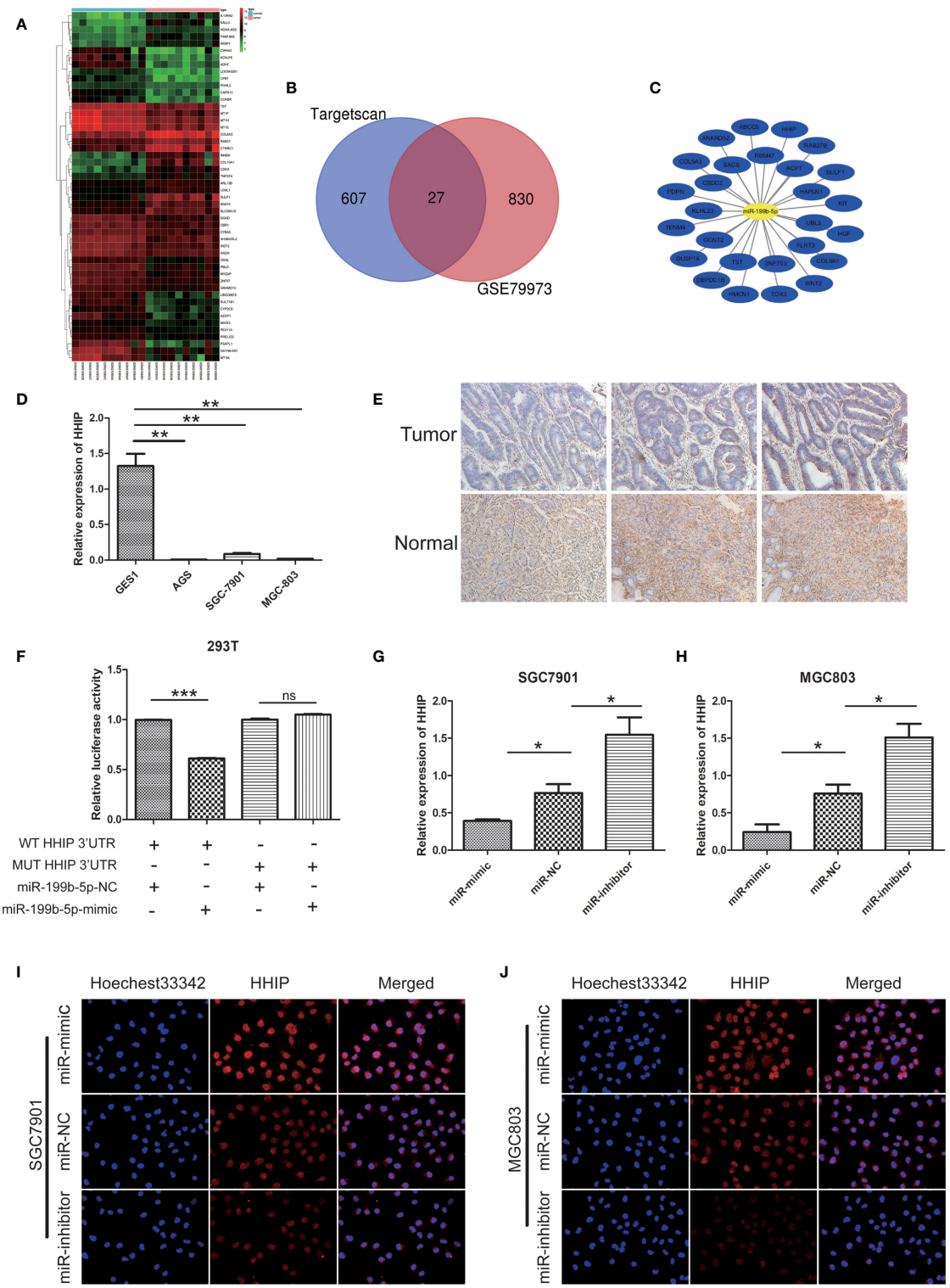

FIGURE 5 | HHIP is a direct target of miR - 199b - 5p and downregulated in GC tissues and cells. **(A)** The heat map of the top 50 genes of DEGs. The vertical axis represents samples. The horizontal axis represents DEGs. **(B)** Venn diagram of DEGs. **(C)** miRNA-DEGs regulatory network. **(D)** The relative expression of miR-199b-5p in GC cells. **(E)** Representative IHC staining of HHIP in five pairs of GC and normal specimens. **(F)** Relative luciferase activity was analyzed in 293T cells co-transfected miR-199b-5p mimics or NC with HHIP-WT or HHIP-MUT, respectively. **(G, H)** The relative expression of HHIP after transfection of miR-199b-5p mimic, NC and inhibitor lentivirus. **(I, J)** The level of HHIP protein was detected by immunofluorescence. *$p < 0.05$, **$p < 0.01$, ***$p < 0.001$. The data expressed as the mean± SD. ns, no significance.

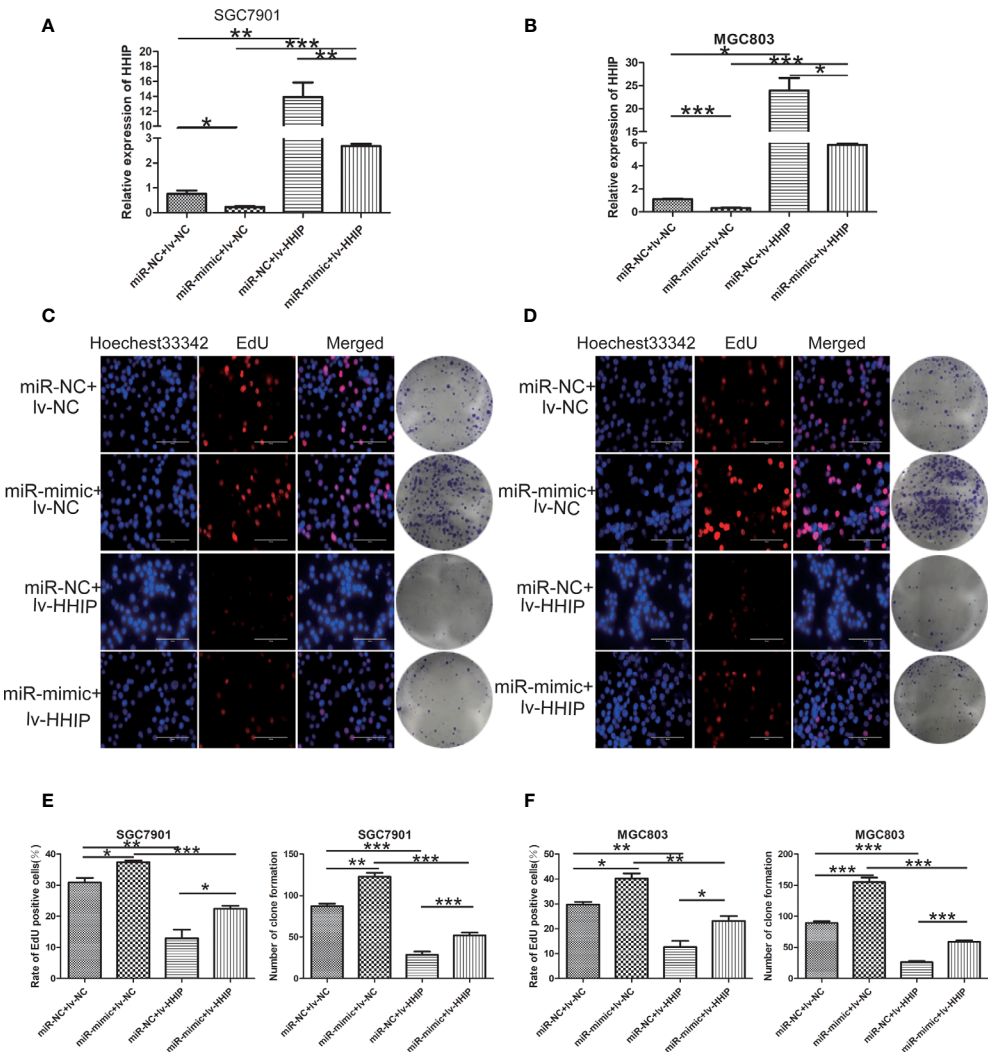

FIGURE 6 | Overexpressed HHIP could partially reverse the effects of miR-199b-5p on GC cells. **(A, B)** RT-PCR was used to verify the expression of HHIP in each group. **(C–F)** EdU incorporation assay and colony formation assay were conducted to verify that ectopic HHIP expression could reverse proliferation induced by miR-199b-5p overexpression in GC cells. *$p < 0.05$, **$p < 0.01$, ***$p < 0.001$. The data expressed as the mean± SD.

significantly up-regulated from liver cirrhosis to dysplastic nodules to advanced liver cancer, but there was no difference in the expression of miR-96-5p between well-differentiated liver cancer and advanced liver cancer (27). We speculate that the expression level of miR-199b-5p may be the same as that of miR-96-5p, and it may be regulated by other potential factors in AGS cells, which needs further study.

To elucidate the mechanism of miR-199b-5p on cell proliferation and migration. We further used bioinformatics analysis to predict the possible target genes of miR-199b-5p in GC cells. Among the candidate target genes, we focused on *HHIP*. *HHIP*, as a member of Hedgehog (*Hh*) family, can compete with *PTCH* gene to bind to *Hh* protein, thus blocking the *Hh* signaling pathway, which has extremely important anti-tumor significance (15, 28, 29). Many studies have shown that *HHIP* plays an anti-tumor role in GC, liver cancer and glioblastoma (16, 30, 31). In our study, compared with GES1 cells, *HHIP* expression was significantly lower in GC cell lines, and our Immunohistochemistry results also suggested that *HHIP* expression was also lower in GC tissues. In addition, Dual luciferase reporter assay confirmed that miR-199b-5p directly combined with *HHIP*, and overexpression of miR-199b-5p could inhibit the expression of *HHIP*. At the same time, overexpression of *HHIP* partially counteracted the effect of miR-199b-5p on cell proliferation and migration. In conclusion, our results show that miR-199b-5p plays a role in GC by down regulating *HHIP*. However, it is worth noting that the expression of HHIP is significantly reduced in AGS cells where miR-199b-5p is not significantly expressed. Studies have shown that HHIP is the target gene of miR-25-3p in hepatocellular carcinoma (32). We speculate that the connection between miR-199b-5p and *HHIP* is regulated by potential factors in AGS cells, but this requires further mechanism research to explore.

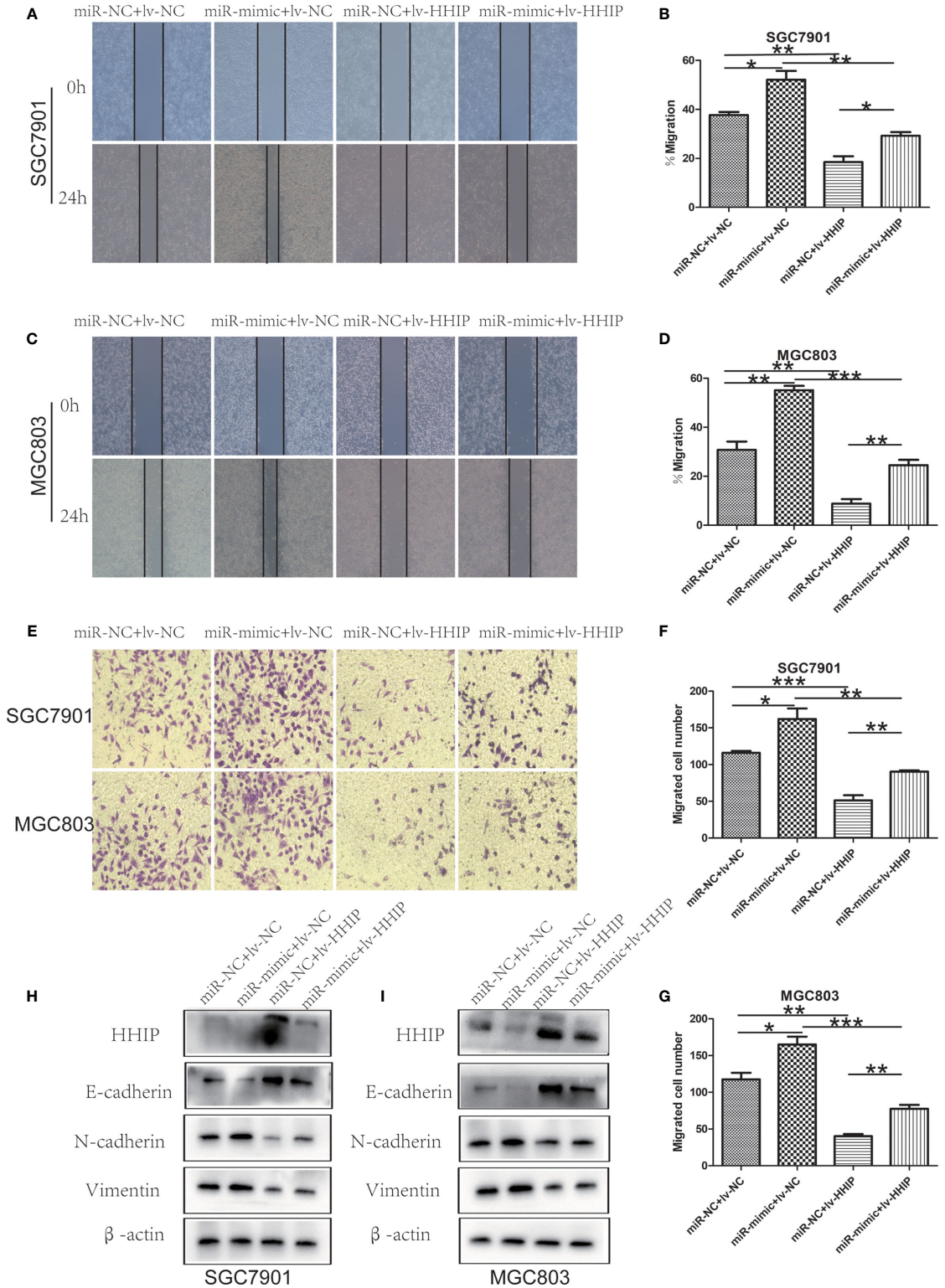

FIGURE 7 | Overexpressed HHIP could partially reverse the effects of miR-199b-5p on GC cells. **(A–D)** The change of cell migration was examined by wound healing assay in SGC7901 and MGC803 cells. **(E–G)** Transwell assay was carried out to confirm the effects of HHIP alteration in migration of GC cells. **(H, I)**, The expression of EMT-associated proteins was detected when HHIP alteration in SGC7901 and MGC803 cells. *$p < 0.05$, **$p < 0.01$, ***$p < 0.001$. The data expressed as the mean± SD.

EMT refers to the biological process that epithelial cells transform into specific mesenchymal phenotype cells through a specific process (33). In cancer, EMT is associated with tumor metastasis and treatment resistance (34, 35). The typical feature of EMT is that the expression of cell adhesion protein (*E-cadherin*) is decreased, while the expression of interstitial related molecules (*N-cadherin* and *Vimentin*) is increased (36, 37). Therefore, EMT plays an important role in tumor migration and invasion. Recently, more and more studies have confirmed that miRNAs are associated with EMT in malignant tumors. Jaca et al. showed that high expression of miR-21 was associated with *E-cadherin* positive cases (38).Shi et al. also suggested that miR-106a is involved in the progression of oral cancer by regulating *E-cadherin, N-cadherin* and *Vimentin* (39).In this study, we confirmed that overexpression of miR-199b-5p can promote EMT process by significantly reducing the level of *E-cadherin* and up regulating the expression of *N-cadherin* and *Vimentin*. These results were consistent with our *in vivo* and *in vitro* migration results.

With the deepening of miRNA research, they may provide potential and effective choices for clinical diagnosis and treatment of specific malignant tumors (40, 41). According to relevant reports, the drug therapy targeting miRNA has entered the clinical development stage, in which the tumor suppressor miR-34 has entered the phase I clinical trial, and the drug targeting miR-122 has entered the phase II clinical trial for the treatment of hepatitis (42–44). In this study, we found that miR-199b-5p can promote the proliferation, migration and EMT process of GC. It may become a new potential target for the treatment of GC in the future. However, we still need a large number of clinical samples and more related pathways to further study the role of miR-199b-5p in GC.

In short, our data demonstrated that miR-199b-5p is up-regulated in GC. Overexpression of miR-199b-5p could promote GC proliferation, migration and EMT, and this role is played by directly regulating the expression of *HHIP*. In conclusion, our results suggested that miR-199b-5p/*HHIP* pathway axis may be a potential therapeutic target for GC.

DATA AVAILABILITY STATEMENT

The datasets presented in this study can be found in online repositories. The names of the repository/repositories and accession number(s) can be found in the article/supplementary material.

ETHICS STATEMENT

The studies involving human participants were reviewed and approved by Guangxi Medical University Cancer Hospital Institutional Ethics Committee. The patients/participants provided their written informed consent to participate in this study. The animal study was reviewed and approved by Guangxi Medical University Cancer Hospital Institutional Ethics Committee. Written informed consent was obtained from the owners for the participation of their animals in this study.

AUTHOR CONTRIBUTIONS

SC was in charge of the overall experiment. HW, LZ, and MJ were responsible for animal experiments. SW and JL were responsible for the collection of experimental specimens. AL was responsible for the design and management of the experiment. All authors contributed to the article and approved the submitted version.

FUNDING

This project was supported by Guangxi Natural Science Foundation(No. 2017GXNSFAA198065),Guangxi Medical High-level Backbone Talent “139” Plan (No. G201903015), Guangxi Key R & D Plan (AB18221084),and Funding for the development and promotion of suitable medical and health technologies in Guangxi (S2018059).

REFERENCES

1. Sung H, Ferlay J, Siegel RL, Laversanne M, Soerjomataram I, Jemal A, et al. Global Cancer Statistics 2020: GLOBOCAN Estimates of Incidence and Mortality Worldwide for 36 Cancers in 185 Countries. *CA Cancer J Clin* (2021) 71(3):209–49. doi: 10.3322/caac.21660
2. Chen W, Zheng R, Baade PD, Zhang S, Zeng H, Bray F, et al. Cancer Statistics in China, 2015. *CA Cancer J Clin* (2016) 66(2):115–32. doi: 10.3322/caac.21338
3. Smyth EC, Nilsson M, Grabsch HI, van Grieken NCT, Lordick F. Gastric Cancer. *Lancet* (2020) 396(10251):635–48. doi: 10.1016/S0140-6736(20)31288-5
4. Ikoma N, Blum M, Chiang YJ, Estrella JS, Chowdhuri SR, Foumier K, et al. Race Is a Risk for Lymph Node Metastasis in Patients With Gastric Cancer. *Ann Surg Oncol* (2017) 24(4):960–5. doi: 10.1245/s10434-016-5645-x
5. Wang B, You Z, Ren D. Target-Assisted FRET Signal Amplification for Ultrasensitive Detection of microRNA. *Anal* (2019) 144(7):2304–11. doi: 10.1039/C8AN02266F
6. Zhao C, Zhang Y, Popel AS. Mechanistic Computational Models of MicroRNA-Mediated Signaling Networks in Human Diseases. *Int J Mol Sci* (2019) 20(2):421. doi: 10.3390/ijms20020421
7. Lee RC, Feinbaum RL, Ambros V. The C. Elegans Heterochronic Gene Lin-4 Encodes Small RNAs With Antisense Complementarity to Lin-14. *Cell* (1993) 75(5):843–54. doi: 10.1016/0092-8674(93)90529-Y
8. Rodriguez A, Griffiths-Jones S, Ashurst JL, Bradley A. Identification of Mammalian microRNA Host Genes and Transcription Units. *Genome Res* (2004) 14(10a):1902–10. doi: 10.1101/gr.2722704
9. Yu J, Peng J, Luan Z, et al. MicroRNAs as a Novel Tool in the Diagnosis of Liver Lipid Dysregulation and Fatty Liver Disease. *Molecules* (2019) 24 (2):230. doi: 10.3390/molecules24020230
10. Chen Z, Zhao G, Zhang Y, Ma Y, Ding Y, Xu N, et al. MiR-199b-5p Promotes Malignant Progression of Osteosarcoma by Regulating HER2. *J buon* (2018) 23(6):1816–24.
11. Zhao Z, Zhao S, Luo L, Xange Q, Zhu Z, Wang J, et al. miR-199b-5p-DDR1-ERK Signalling Axis Suppresses Prostate Cancer Metastasis *via* Inhibiting Epithelial-Mesenchymal Transition. *Br J Cancer* (2021) 124(5):982–94. doi: 10.1038/s41416-020-01187-8
12. Lin X, Qiu W, Xiao Y, Ma J, Xu F, Zhang K, et al. MiR-199b-5p Suppresses Tumor Angiogenesis Mediated by Vascular Endothelial Cells in Breast Cancer by Targeting Alk1. *Front Genet* (2019) 10:1397. doi: 10.3389/fgene.2019.01397

13. Ingham PW, McMahon AP. Hedgehog Signaling in Animal Development: Paradigms and Principles. *Genes Dev* (2001) 15(23):3059–87. doi: 10.1101/gad.938601
14. Zhao JG, Wang JF, Feng JF, Jin XY, Ye WL. HHIP Overexpression Inhibits the Proliferation, Migration and Invasion of Non-Small Cell Lung Cancer. *PloS One* (2019) 14(11):e0225755. doi: 10.1371/journal.pone.0225755
15. Chang L, Zhang P, Zhao D, Liu H, Wang Q, Li C, et al. The Hedgehog Antagonist HHIP as a Favorable Prognosticator in Glioblastoma. *Tumour Biol* (2016) 37(3):3979–86. doi: 10.1007/s13277-015-3442-y
16. Sun H, Ni SJ, Ye M, Weng W, Zhang Q, Zhang M, et al. Hedgehog Interacting Protein 1 Is a Prognostic Marker and Suppresses Cell Metastasis in Gastric Cancer. *J Cancer* (2018) 9(24):4642–9. doi: 10.7150/jca.27686
17. Guo X, Guo L, Ji J, Zhang J, Zhang J, Chen X, et al. miRNA-331-3p Directly Targets E2F1 and Induces Growth Arrest in Human Gastric Cancer. *Biochem Biophys Res Commun* (2010) 398(1):1–6. doi: 10.1016/j.bbrc.2010.05.082
18. Shen ZY, Zhang ZZ, Liu H, Zhao EH, Cao H. miR-375 Inhibits the Proliferation of Gastric Cancer Cells by Repressing ERBB2 Expression. *Exp Ther Med* (2014) 7(6):1757–61. doi: 10.3892/etm.2014.1627
19. Yang YB, Tan H, Wang Q. MiRNA-300 Suppresses Proliferation, Migration and Invasion of Non-Small Cell Lung Cancer *via* Targeting ETS1. *Eur Rev Med Pharmacol Sci* (2019) 23(24):10827–34. doi: 10.26355/eurrev_201912_19786
20. Yu Y, Wang Y, Xiao X, Cheng W, Hu L, Yao W, et al. MiR-204 Inhibits Hepatocellular Cancer Drug Resistance and Metastasis Through Targeting NUAK1. *Biochem Cell Biol = Biochimie Biol Cell* (2019) 97(5):563–70. doi: 10.1139/bcb-2018-0354
21. Zhang W, Liao K, Liu D. MiRNA-12129 Suppresses Cell Proliferation and Block Cell Cycle Progression by Targeting SIRT1 in GASTRIC Cancer. *Technol Cancer Res Treat* (2020) 19:1533033820928144. doi: 10.1177/1533033820928144
22. Du M, Zhuang Y, Tan P, Yu Z, Zhang X, Wang A, et al. microRNA-95 Knockdown Inhibits Epithelial-Mesenchymal Transition and Cancer Stem Cell Phenotype in Gastric Cancer Cells Through MAPK Pathway by Upregulating DUSP5. *J Cell Physiol* (2020) 235(2):944–56. doi: 10.1002/jcp.29010
23. Li J, Ye D, Shen P, Liu X, Zhou P, Zhu G, et al. Mir-20a-5p Induced WTX Deficiency Promotes Gastric Cancer Progressions Through Regulating PI3K/AKT Signaling Pathway. *J Exp Clin Cancer Res: CR* (2020) 39(1):212. doi: 10.1186/s13046-020-01718-4
24. Deng S, Zhang X, Qin Y, Chen W, Fan H, Feng X, et al. miRNA-192 and -215 Activate Wnt/β-Catenin Signaling Pathway in Gastric Cancer *via* APC. *J Cell Physiol* (2020) 235(9):6218–29. doi: 10.1002/jcp.29550
25. Xu LJ, Duan Y, Wang P, Yin HQ. MiR-199b-5p Promotes Tumor Growth and Metastasis in Cervical Cancer by Down-Regulating KLK10. *Biochem Biophys Res Commun* (2018) 503(2):556–63. doi: 10.1016/j.bbrc.2018.05.165
26. Wang H, Guo Y, Mi N, Zhou L. miR-101-3p and miR-199b-5p Promote Cell Apoptosis in Oral Cancer by Targeting BICC1. *Mol Cell Probes* (2020) 52:101567. doi: 10.1016/j.mcp.2020.101567
27. Zhang H, Xing AY, Ma RR, Wang YW, Liu YH, Gao P, et al. Diagnostic Value of miRNA-96-5p/3p in Dysplastic Nodules and Well-Differentiated Small Hepatocellular Carcinoma. *Hepatol Res* (2016) 46(8):784–93. doi: 10.1111/hepr.12628
28. Büller NV, Rosekrans SL, Westerlund J, van den Brink GR. Hedgehog Signaling and Maintenance of Homeostasis in the Intestinal Epithelium. *Physiol (Bethesda Md)* (2012) 27(3):148–55. doi: 10.1152/physiol.00003.2012
29. Wei H, Li J, Shi S, Zhang L, Xiang A, Shi X, et al. Hhip Inhibits Proliferation and Promotes Differentiation of Adipocytes Through Suppressing Hedgehog Signaling Pathway. *Biochem Biophys Res Commun* (2019) 514(1):148–56. doi: 10.1016/j.bbrc.2019.04.047
30. Wang X, Ma W, Yin J, Chen M, Jin H. HHIP Gene Overexpression Inhibits the Growth, Migration and Invasion of Human Liver Cancer Cells. *J Buon* (2020) 25(5):2424–9.
31. Shahi MH, Zazpe I, Afzal M, Sinha S, Rebhun RB, Melendez B, et al. Epigenetic Regulation of Human Hedgehog Interacting Protein in Glioma Cell Lines and Primary Tumor Samples. *Tumour Biol* (2015) 36(4):2383–91. doi: 10.1007/s13277-014-2846-4
32. Ouyang Y, Tang Y, Fu L, Peng S, Wu W, Tan D, et al. Exosomes Secreted by Chronic Hepatitis B Patients With PNALT and Liver Inflammation Grade ≥ A2 Promoted the Progression of Liver Cancer by Transferring miR-25-3p to Inhibit the Co-Expression of TCF21 and HHIP. *Cell Proliferation* (2020) 53(7):e12833. doi: 10.1111/cpr.12833
33. Saitoh M. Involvement of Partial EMT in Cancer Progression. *J Biochem* (2018) 164(4):257–64. doi: 10.1093/jb/mvy047
34. Cho ES, Kang HE, Kim NH, Yook JI. Therapeutic Implications of Cancer Epithelial-Mesenchymal Transition (EMT). *Arch Pharmacal Res* (2019) 42(1):14–24. doi: 10.1007/s12272-018-01108-7
35. Yeung KT, Yang J. Epithelial-Mesenchymal Transition in Tumor Metastasis. *Mol Oncol* (2017) 11(1):28–39. doi: 10.1002/1878-0261.12017
36. Wang L, Li B, Zhang L, Li Q, He Z, Huang X, et al. miR-664a-3p Functions as an Oncogene by Targeting Hippo Pathway in the Development of Gastric Cancer. *Cell Proliferation* (2019) 52(3):e12567. doi: 10.1111/cpr.12567
37. Lei H, Gao Y, Xu X. LncRNA TUG1 Influences Papillary Thyroid Cancer Cell Proliferation, Migration and EMT Formation Through Targeting miR-145. *Acta Biochim Biophys Sin* (2017) 49(7):588–97. doi: 10.1093/abbs/gmx047
38. Jaca A, Govender P, Locketz M, et al. The Role of miRNA-21 and Epithelial Mesenchymal Transition (EMT) Process in Colorectal Cancer. *J Clin Pathol* (2017) 70(4):331–56. doi: 10.1136/jclinpath-2016-204031
39. Shi B, Ma C, Liu G, Guo Y. MiR-106a Directly Targets LIMK1 to Inhibit Proliferation and EMT of Oral Carcinoma Cells. *Cell Mol Biol Lett* (2019) 24:1. doi: 10.1186/s11658-018-0127-8
40. Mishra S, Yadav T, Rani V. Exploring miRNA Based Approaches in Cancer Diagnostics and Therapeutics. *Crit Rev Oncol/Hematol* (2016) 98:12–23. doi: 10.1016/j.critrevonc.2015.10.003
41. Link A, Kupcinskas J. MicroRNAs as non-Invasive Diagnostic Biomarkers for Gastric Cancer: Current Insights and Future Perspectives. *World J Gastroenterol* (2018) 24(30):3313–29. doi: 10.3748/wjg.v24.i30.3313
42. Rupaimoole R, Slack FJ. MicroRNA Therapeutics: Towards a New Era for the Management of Cancer and Other Diseases. *Nat Rev Drug Discov* (2017) 16(3):203–22. doi: 10.1038/nrd.2016.246
43. Gibson NW. Engineered microRNA Therapeutics. *J R Coll Phys Edinburgh* (2014) 44(3):196–200. doi: 10.4997/JRCPE.2014.302
44. Zhang L, Liao Y, Tang L. MicroRNA-34 Family: A Potential Tumor Suppressor and Therapeutic Candidate in Cancer. *J Exp Clin Cancer Res: CR* (2019) 38(1):53. doi: 10.1186/s13046-019-1059-5

Conflict of Interest: The authors declare that the research was conducted in the absence of any commercial or financial relationships that could be construed as a potential conflict of interest.

Publisher's Note: All claims expressed in this article are solely those of the authors and do not necessarily represent those of their affiliated organizations, or those of the publisher, the editors and the reviewers. Any product that may be evaluated in this article, or claim that may be made by its manufacturer, is not guaranteed or endorsed by the publisher.

frontiers in Oncology

ORIGINAL RESEARCH
published: 15 September 2021
doi: 10.3389/fonc.2021.706415

CircPTK2 Suppresses the Progression of Gastric Cancer by Targeting the MiR-196a-3p/AATK Axis

Ling Gao[1†], Tingting Xia[2†], Mingde Qin[3], Xiaofeng Xue[1], Linhua Jiang[1] and Xinguo Zhu[1]*

[1] Department of General Surgery, The First Affiliated Hospital of Soochow University, Suzhou, China, [2] Department of Gastroenterology, The First Affiliated Hospital of Soochow University, Suzhou, China, [3] Department of the Stem Cell and Biomedical Material Key Laboratory of Jiangsu Province (the State Key Laboratory Incubation Base), Soochow University, Suzhou, China

Background: Gastric cancer is a type of malignant tumor with high morbidity and mortality. It has been shown that circular RNAs (circRNAs) exert critical roles in gastric cancer progression *via* working as microRNA (miRNA) sponges to regulate gene expression. However, the role and potential molecular mechanism of circRNAs in gastric cancer remain largely unknown.

Methods: CircPTK2 (hsa_circ_0005273) was identified by bioinformatics analysis and validated by RT-qPCR assay. Bioinformatics prediction, dual-luciferase reporter, and RNA pull-down assays were used to determine the interaction between circPTK2, miR-196a-3p, and apoptosis-associated tyrosine kinase 1 (AATK).

Results: The level of circPTK2 was markedly downregulated in gastric cancer tissues and gastric cancer cells. Upregulation of circPTK2 significantly suppressed the proliferation, migration, and invasion of gastric cancer cells, while circPTK2 knockdown exhibited opposite effects. Mechanically, circPTK2 could competitively bind to miR-196a-3p and prevent miR-196a-3p to reduce the expression of AATK. In addition, overexpression of circPTK2 inhibited tumorigenesis in a xenograft mouse model of gastric cancer.

Conclusion: Collectively, circPTK2 functions as a tumor suppressor to suppress gastric cancer cell proliferation, migration, and invasion through regulating the miR-196a-3p/AATK axis, suggesting that circPTK2 may serve as a novel therapeutic target for gastric cancer.

Keywords: gastric cancer, circPTK2, miR-196a-3p, AATK, proliferation

OPEN ACCESS

Edited by:
Kanjoormana Aryan Manu, Amala Cancer Research Centre, India

Reviewed by:
Chenyu Lin, The Ohio State University, United States
Arun Upadhyay, Northwestern University, United States

****Correspondence:***
Xinguo Zhu
zhuxinguo2017@126.com

[†]These authors have contributed equally to this work and share first authorship

Specialty section:
This article was submitted to Gastrointestinal Cancers, a section of the journal Frontiers in Oncology

Received: *27 May 2021*
Accepted: *26 August 2021*
Published: *15 September 2021*

Citation:
Gao L, Xia T, Qin M, Xue X, Jiang L and Zhu X (2021) CircPTK2 Suppresses the Progression of Gastric Cancer by Targeting the MiR-196a-3p/AATK Axis. Front. Oncol. 11:706415. doi: 10.3389/fonc.2021.706415

INTRODUCTION

Gastric cancer is the fifth most common malignancy worldwide and is the third leading cause of cancer-related deaths (1–3). Although the current clinical diagnosis and treatment for gastric cancer are continuously improving, the 5-year survival rate of patients with gastric cancer is less than 30% (4, 5). Gastric cancer is a complex cellular network (6, 7). Currently, the etiology and pathogenesis are not yet clear, which brings corresponding difficulties to its early diagnosis and treatment (6, 7).

Circular RNAs (circRNAs) are a class of non-coding RNAs derived from back-spliced exons (8, 9). Unlike linear RNA, circRNAs are covalently closed continuous loops that lack 5′ (cap) and 3′

(polyadenylation) ends (10). Meanwhile, circRNAs are found to be relatively stable and evolutionally conserved in the cytoplasm (10, 11). CircRNAs have been found to be implicated in the progression of cancers (12, 13). Significantly, circRNAs are aberrantly expressed in multiform types of cancer, including gastric cancer (14, 15). However, the biological function of circRNAs in gastric cancer remains largely unclear.

MicroRNAs (miRNAs) are a kind of non-coding RNAs with 19–25 nucleotides in length (16, 17). It has been shown that miRNA can regulate gene expression at the post-transcriptional level (18, 19). Considerable studies reported that circRNAs could exhibit their biological roles through acting as "miRNA sponges" to regulate gene expressions (20, 21). For instance, Zhang et al. reported that circNRIP1 could promote gastric cancer progression through sponging miR-149-5p (22). Luo et al. found that circCCDC9 could inhibit the proliferation of gastric cancer cells *via* targeting the miR-6792-3p/CAV1 axis (23).

In this study, we screened differentially expressed circRNAs (DEcircRNAs) between gastric cancer tissues and normal tissues and found that circPTK2 was significantly downregulated in gastric cancer tissues. In addition, circPTK2 could inhibit the proliferation, migration, and invasion of gastric cancer cells through functioning as a miRNA sponge to upregulate the expression of the tumor-suppressor gene AATK. These data indicated that circPTK2 may be used as a potential target in gastric cancer therapy.

MATERIALS AND METHODS

Identification of Differentially Expressed CircRNAs

Gastric cancer-related datasets (GSE93541, GSE89143, and GSE78092) were downloaded from the GEO database. For the GSE93541 dataset, R language was utilized to analyze the DEcircRNAs in plasma samples from gastric cancer patients and healthy controls. For the GSE89143 and GSE78092 datasets, R language was utilized to analyze the DEcircRNAs between gastric cancer tissues and adjacent normal tissues. The threshold value of differentially expressed genes was set at two times of different multiple and $p < 0.05$. The intersection of DEcircRNAs from three datasets was performed using the Venn diagram package.

Specimen Collection

Gastric cancer tissues and matched adjacent normal tissues were obtained from the First Affiliated Hospital of Soochow University. Written consent was obtained from each patient with gastric cancer. All samples were frozen in liquid nitrogen and stored at −80°C. This study was approved by the Ethics Committee of The First Affiliated Hospital of Soochow University.

Cell Culture

Human gastric epithelial cell line GES-1 and human AGS, MKN45, and SNU-5 cell lines were obtained from ATCC (Manassas, VA, USA). Cells were maintained in DMEM medium (Thermo Fisher Scientific, Waltham, MA, USA) containing 10% fetal bovine serum (FBS) and cultured in a 5% CO_2 incubator at 37°C.

Cell Transfection

MiR-196a-3p mimics and miR-196a-3p inhibitor were designed and synthesized by RiboBio (Guangzhou, China). After that, AGS and MKN45 cells were transfected with miR-196a-3p mimics or miR-196a-3p inhibitor using the Lipofectamine 2000 kit (Thermo Fisher Scientific).

Human circPTK2 or AATK cDNA was synthesized and cloned into pcDNA3.1 vector. After that, AGS and MKN45 cells were transfected with the pcDNA3.1 control plasmid, pcDNA3.1-circPTK2 (circPTK2-OE) or pcDNA3.1 AATK (AATK-OE) using Lipofectamine 2000, followed by selection with G418.

Lentivirus-containing short hairpin RNA (shRNA) targeting circPTK2 or AATK plasmids was purchased from Hanbio (Shanghai, China). After that, 293T cells were transfected with the abovementioned lentiviral plasmids and were transduced into 293T cells to package lentivirus to infect AGS and MKN45 cells. Subsequently, the infected cells were selected by 2 μg/ml of puromycin.

RT-PCR and RT-qPCR

A TRIzol reagent (Thermo Fisher Scientific) was used to extract total RNA. Meanwhile, genomic DNA (gDNA) was isolated using the Genomic DNA Isolation Kit (Sangon Biotech, Shanghai, China). After that, cDNA was synthesized using EntiLink™ 1st Strand cDNA Synthesis Kit (ELK Biotechnology). In addition, qPCR was performed using the EnTurbo™ SYBR Green PCR SuperMix on a Verse flow cytometry system (BD Biosciences, NJ, USA). The DreamTaq DNA Polymerase (Thermo Fisher Scientific) was used for PCR. Then, the cDNA and gDNA PCR products were analyzed by 2% agarose gel electrophoresis. β-Actin and U6 were used as internal controls. The primers are listed in **Table 1**.

Actinomycin D and RNase R Treatment

AGS and MKN45 cells were incubated with actinomycin D (2 μg/ml; Sigma) for 0, 6, 12, 18, and 24 h to assess the stability of circPTK2 and its linear isoform. In addition, total RNA (10 μg) was treated with RNase R (5 U/μg; Epicenter Technologies) for 30 min at 37°C, then the level of circPTK2 was detected using RT-qPCR assay.

TABLE 1 | Primer sequences.

Name		Primer sequences
U6	Forward	5′-CTCGCTTCGGCAGCACAT-3′
	Reverse	5′-AACGCTTCACGAATTTGCGT-3′
MiR-196a-3p	Forward	5′-CGGCAACAAGAAACUGCCUGAG-3′
	Reverse	5′-CAGGCAGUUUCUUGUUGCCGUU-3′
Actin	Forward	5′-GTCCACCGCAAATGCTTCTA-3′
	Reverse	5′-TGCTGTCACCTTCACCGTTC-3′
CircPTK2	Forward	5′-GAAAGATTTCTGCCCAGCAGA-3′
	Reverse	5′-GTGATTCCATGTGAACCAGGG-3′
AATK	Forward	5′-ATGCTGGCCTGCCTGTGTTGT-3′
	Reverse	5′-AGGGGCAGGACATACACATCGG-3′

Cell Viability Assay

Cell viability was measured using a Cell Counting Kit-8 (CCK-8, Dojindo Laboratories, Kumamoto, Japan). Transfected AGS and MKN45 cells (5×10^3 cells/well) were seeded onto 96-well plates and cultured for the indicated times. Later on, 10 μl of CCK-8 reagent was added into each well, and cells were incubated for another 2 h. Subsequently, the absorbance was measured at a wavelength of 450 nm.

Colony Formation Assay

Transfected AGS and MKN45 cells (5×10^3 cells/well) were plated onto six-well plates. After 2 weeks of incubation, cells were fixed with 4% paraformaldehyde for 20 min and then stained with 0.1% crystal violet at room temperature. After that, cell colonies were imaged and counted using a light microscope.

Transwell Assay

Transfected AGS and MKN45 cells were suspended in 200 μl serum-free medium and placed into the upper chambers (Corning, NY, USA). Later on, the lower chambers were loaded with DMEM medium (600 μl) containing 10% FBS. After 24 h of incubation, the cells on the lower surface were fixed with 4% formaldehyde, and then stained with 0.1% crystal violet solution. After that, the stained cells were imaged using a light microscope. Transwell chambers that were coated with Matrigel (BD Biosciences) were used for the cell invasion assay.

Animal Study

BALB/c nude mice (5–6 weeks old) were purchased from the Jingda Experimental Animal Co., Ltd. (Changsha, China). This study was approved by the First Affiliated Hospital of Soochow University and conducted according to institutional guidelines. Animals were divided into eight groups (six mice per group): group I (AGS cell)—shRNA NC, circPTK2 shRNA2, OE NC, and circPTK2 OE groups; group II (MKN45 cell)—shRNA NC, circPTK2 shRNA2, OE NC, and circPTK2 OE groups. AGS or MKN45 cells (5×10^6 cells/mouse) were subcutaneously injected into the right flank of each mouse. The size of the tumor was measured every 5 days. The tumor volume was calculated by the formula: (length × width^2)/2. At the end of the experiment, the tumor was removed, and tumor weight was measured.

Luciferase Reporter Assay

The sequences including miR-196a-3p binding sites in the circPTK2 3′ UTRs and AATK 3′ UTR were cloned into the luciferase reporter vector pGL6-miR (Beyotime). After that, AGS or MKN45 cells were co-transfected with the luciferase plasmids and miR-196a-3p mimics for 48 h. Later on, the firefly and Renilla luciferase activities were measured by a dual-luciferase reporter assay system (Promega, Madison, USA).

RNA Pull-Down Assay

The biotinylated circPTK2 or biotinylated miR-196a-3p probe was incubated with streptavidin magnetic beads (Thermo Fisher Scientific) for 2 h at room temperature. Later on, AGS or MKN45 cells were incubated with the magnetic beads at 4°C overnight. After that, the complex was pulled down and analyzed by RT-qPCR assay.

Immunohistochemistry

The tumor tissues were fixed in 4% paraformaldehyde and then embedded in paraffin. Later on, tissues were sectioned (5 μm thick) and then stained with primary antibody specific for AATK (Abcam) overnight at 4°C. Images were captured by a fluorescence microscope.

Western Blot Assay

Protein concentration was determined by the BCA kit (Pierce, Rockford, USA). After that, equal amounts of proteins (30 μg) were separated by 10% SDS-PAGE and transferred onto a PVDF membrane. Later on, the membrane was incubated with primary antibodies against STK39 (1:1,000, Abcam), AATK (1:1,000, Abcam), p-STK39 (1:1,000, Abcam), p-p38 (1:1,000, Abcam), p38 (1:1,000, Abcam), Bax (1:1,000, Abcam), Bcl-2 (1:1,000, Abcam), cleaved caspase 3 (1:1,000, Abcam), CD81 (1:1,000, Abcam), CD63 (1:1,000, Abcam), and GAPDH (1:1,000, Abcam) at 4°C overnight. Then, the membrane was incubated with horseradish peroxidase (HRP)-labeled secondary antibodies at room temperature and then visualized using the enhanced chemiluminescence reagent (Thermo Fisher Scientific).

Co-Immunoprecipitation

Cells were transfected with pcDNA3.1-AATK or pcDNA3.1-STK39 plasmids. After that, the transfected cells were lysed using RIPA buffer, and then the cell lysates were treated with anti-AATK, anti-STK39, or anti-IgG antibodies. Later on, the samples were incubated with protein A and G Sepharose beads for 4 h at 4°C. Then, the protein binding complex was isolated and subjected to Western blot assay.

Statistical Analysis

Data were presented as mean ± standard deviation (SD). Student's *t*-test was applied to determine the statistical significance between two groups. Differences between three or more groups were analyzed by one-way analysis of variance (ANOVA) and Tukey's tests. $p < 0.05$ was considered statistically significant. All data were repeated in triplicate.

RESULTS

Differential Expression of CircRNAs in Gastric Cancer

To identify DEcircRNAs in gastric cancer, R language was performed to analyze the circRNA expression profiles from three gastric cancer-related datasets (GSE93541, GSE89143, and GSE78092). As shown in **Figure 1A**, the heatmap showed that 538, 268, and 211 DEcircRNAs were identified in the GSE93541, GSE89143, and GSE78092 datasets, respectively. Using a Venn diagram, 12 overlapping DEcircRNAs (4 were upregulated, while 8 were downregulated) were identified in these three datasets (**Figure 1B**). To verify these results, all of

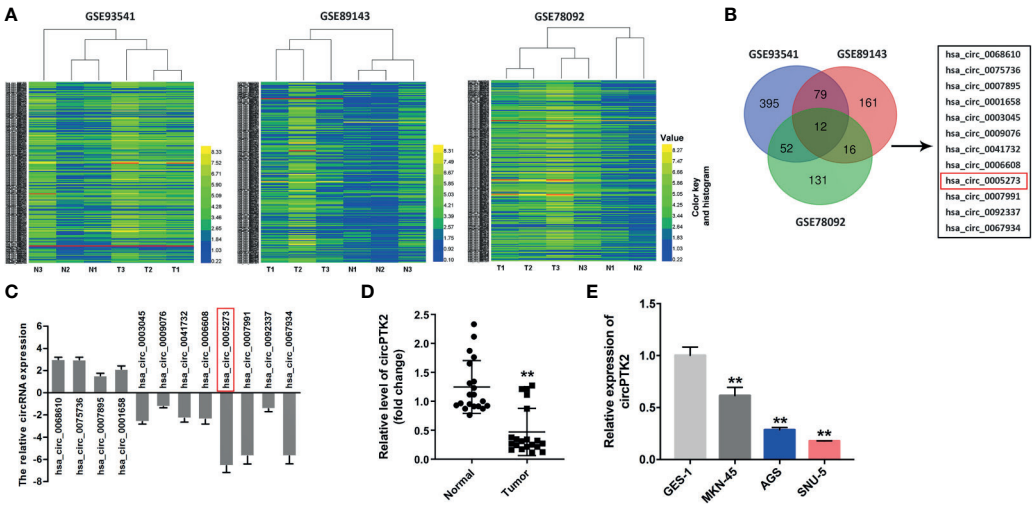

FIGURE 1 | Differential expression of circular RNAs (circRNAs) in gastric cancer. **(A)** The heatmaps of the DEcircRNA profiles in gastric cancer and compared normal tissues in GSE93541, GSE89143, and GSE78092. CircRNAs in yellow indicate overexpression; circRNAs in blue indicate reduced expression. **(B)** Venn diagram of overlapping DEcircRNAs from intersection of GSE93541, GSE89143, and GSE78092 datasets. **(C)** The expressions of circRNAs in tumor tissues (n = 5) and normal tissues (n = 5) were detected with RT-qPCR. **(D)** RT-qPCR analysis of circPTK2 level in tumor tissues (n = 20) and normal tissues (n = 20). **(E)** RT-qPCR analysis of circPTK2 level in AGS, MKN45, and SNU-5 cells. $^{**}p < 0.01$. The significance between two or more groups was analyzed by Student's t-test or one-way ANOVA, respectively.

these circRNAs were chosen for further confirmation in gastric cancer tissues and normal tissues using RT-qPCR (**Figure 1C**). RT-qPCR results showed that hsa_circ_0005273 (circPTK2) significantly decreased in gastric cancer tissues compared with that in normal tissues and exhibited the most significant difference between gastric cancer tissues and normal tissues (**Figures 1C, D**). Meanwhile, 95% of the total 20 of patients expressed a lower level of circPTK2 in gastric cancer tissues compared with normal tissues (**Figure 1D**). As shown in **Figure 1E**, circPTK2 expression was markedly decreased in MKN45, AGS, and SNU-5 cells compared with GES-1 cells. Thus, hsa_circ_0005273 (circPTK2) was chosen for further experiments.

Furthermore, we found that circPTK2 is derived from exons 27, 28, and 29 of the PTK2 gene (**Figure 2A**). In addition, Sanger sequencing verified the head-to-tail splicing in the RT-qPCR product of circPTK2 (**Figure 2A**). Next, RNase R digestion assay showed that the linear form of PTK2 was markedly decreased under the RNase R treatment, while the circular isoform was resistant to RNase R digestion, suggesting that circPTK2 harbors a loop structure (**Figures 2B, C**). Meanwhile, the stability of circPTK2 in AGS and MKN45 cells was detected using the actinomycin D assay. The data showed that the linear PTK2 mRNA transcript was less stable than circPTK2 transcript in AGS and MKN45 cells under treatment with actinomycin D (**Figures 2D, E**). Furthermore, to confirm the existence of circPTK2, we designed convergent primers to amplify PTK2 mRNA and divergent primers to amplify circPTK2. The results of PCR showed that circPTK2 was only amplified by cDNA templates from AGS and MKN45 cells using divergent primers (**Figure 2F**). To sum up, circPTK2 is decreased in gastric cancer tissues and is a stable circRNA from PTK2.

Overexpression of CircPTK2 Inhibits Gastric Cancer Cell Proliferation and Tumor Growth

To explore the biological role of circPTK2 in gastric cancer cells, we used shRNAs to downregulate the level of circPTK2 in gastric cancer cells (**Figure 3A**). Meanwhile, we established circPTK2 stably overexpressing gastric cancer cells *via* transfecting with circPTK2 OE plasmids (**Figure 3A**). Additionally, downregulation of circPTK2 notably promoted the viability, proliferation, migration, and invasion of AGS, MKN45, and SNU-5 cells, while circPTK2 overexpression exhibited opposite effects (**Figures 3B–E** and **Supplementary Figures S1A–C**). We further investigated the effect of circPTK2 on tumor growth *in vivo*. As shown in **Figures 4A–C**, silencing of circPTK2 markedly increased the tumor volume weight in mouse xenografts, whereas overexpression of circPTK2 obviously inhibited the tumor growth of AGS and MKN45 cells. Collectively, circPTK2 may play a tumor-suppressive role in gastric cancer *in vitro* and *in vivo*.

CircPTK2 Acts as the Sponge of MiR-196a-3p

It has been shown that circRNAs can regulate gene expression *via* acting as miRNA sponges (24). Thus, we predicted the potential miRNAs binding to circPTK2 using the CircInteractome dataset. The data showed that miR-196a-3p functioned as the target of circPTK2 with complementary binding sites (**Figure 5A**). In addition, miR-196a-3p mimics notably reduced the luciferase activity in AGS and MKN45 cells co-transfected with circPTK2-WT; however, miR-196a-3p

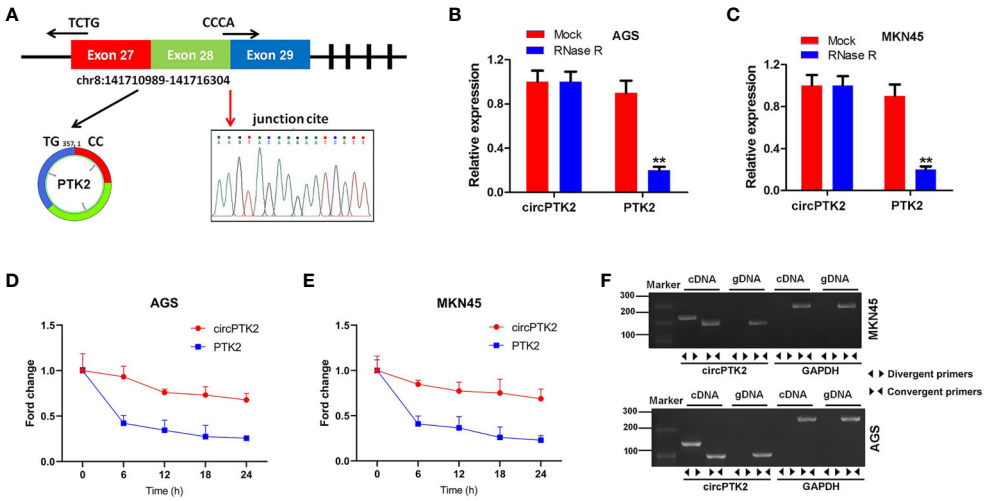

FIGURE 2 | CircPTK2 is a stable circRNA from PTK2. **(A)** Schematic diagram showed the formation of circPTK2. Sanger sequencing showed the joint site of circPTK2 (red arrow). **(B, C)** The expression of linear and circRNA linear was detected with RT-qPCR, after RNase R treatment. $^{**}p < 0.05$ *vs.* Mock. **(D, E)** After actinomycin treatment, the half-lives of linear and circRNAs were detected. **(F)** The existence of circPTK2 was detected in AGS and MKN45 cells by RT-qPCR with divergent or convergent primers and confirmed by gel electrophoresis.

mimics had no effect on luciferase activity in AGS and MKN45 cells co-transfected with circPTK2-MT, suggesting that miR-196a-3p is a direct binding target of circPTK2 (**Figure 5B**). The RNA pull-down assay results showed that miR-196a-3p was pulled down by biotin-labeled circPTK2 probe in both AGS and MKN45 cells and circPTK2 was pulled down by biotin-labeled miR-196a-3p probe, indicating that miR-196a-3p directly interacted with circPTK2 (**Figures 5C, D**). Meanwhile, RT-qPCR results showed that the level miR-196a-3p was significantly increased in gastric cancer tissues (**Figure 5E**). To sum up, circPTK2 could act as a miRNA sponge for miR-196a-3p in gastric cancer.

AATK Is a Direct Binding Target of MiR–196a-3p

Two datasets miRDB and TargetScan were used to predict the potential binding targets of miR-196a-3p, and it was found that AATK might be a potential target of miR-196a-3p (**Figures 6A, B**). Additionally, miR-196a-3p mimics decreased the luciferase activity in cells co-transfected with AATK-WT (**Figure 6C**). In addition, miR-196a-3p mimics significantly downregulated the expression of AATK in AGS and MKN45 cells, while the miR-196a-3p inhibitor displayed opposite results (**Figures 6D, E**). Moreover, RNA pull-down assay showed that AATK was pulled down by biotin-labeled miR-196a-3p probe, indicating that miR-196a-3p directly interacted with AATK (**Figure 6F**). Moreover, AATK expression was negatively correlated with the expression of miR-196a-3p ($r = -0.674$, $p < 0.05$), and its expression was positively correlated with circPTK2 expression ($r = -0.793$, $p < 0.05$) (**Figures 6G, H**). Furthermore, the expression of AATK was notably downregulated in gastric cancer tissues (**Figures 6I, J**). Regarding prognosis, Kaplan–Meier curves showed that low AATK expression correlated with poor survival rate of patients of gastric cancer (**Figure 6K**). Collectively, AATK is a direct target gene of miR-196a-3p and is downregulated in gastric cancer tissues.

Knockdown of AATK Reverses the Tumor-Suppressing Effect of CircPTK2

Next, to further confirm the interaction among circPTK2, miR-196a-3p, and AATK, rescue experiments were performed. We found that upregulation of circPTK2 notably increased the expression of AATK in AGS and MKN45 cells; however, these phenomena were reversed by miR-196a-3p mimics or by AATK knockdown (**Figure 7A**). In addition, the data of CCK-8 and colony formation showed that overexpression of circPTK2 significantly inhibited the viability and proliferation of AGS and MKN45 cells; however, these changes were reversed by miR-196a-3p mimics or AATK knockdown (**Figures 7B, C**). Meanwhile, upregulation of circPTK2 markedly suppressed the migration and invasion and triggered the apoptosis of AGS and MKN45 cells; however, these changes were reversed by miR-196a-3p mimics or AATK knockdown (**Figures 7D–F**). These data indicated that circPTK2 inhibited gastric cancer tumorigenesis by sponging miR-196a-3p, thus increasing AATK expression.

Interaction of AATK With STK39 in Gastric Cancer

We further elucidated the anti-tumor mechanism of circPTK2 in gastric cancer. The protein–protein interaction network showed that AATK might interact with STK39, CDK5, and CDK5R1, respectively (**Figure 8A**). Serine/threonine kinase 39 (STK39) has been found to function as a tumor oncogene in human cancers (25, 26). In addition, Zhao et al. found that downregulation of STK39 could induce the

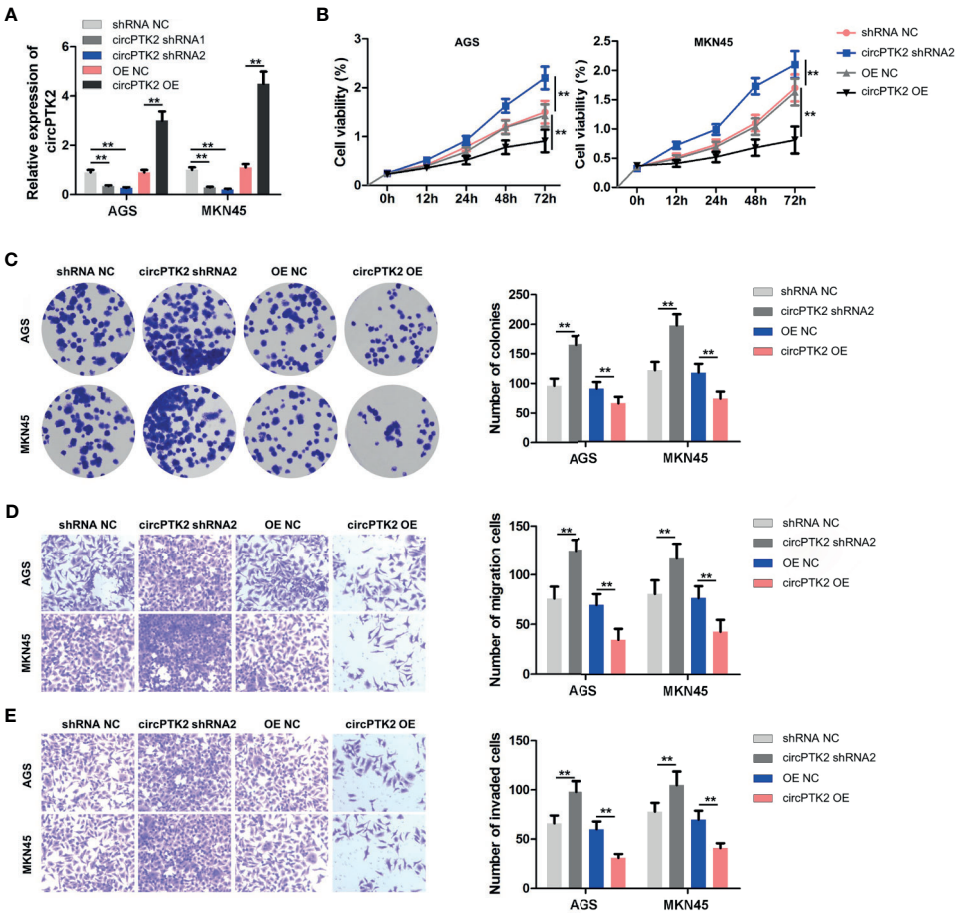

FIGURE 3 | Overexpression of circPTK2 inhibits gastric cancer cell proliferation, migration, and invasion. **(A)** RT-qPCR analysis of circPTK2 level in AGS and MKN45 cells treated with circPTK2 shRNA1, circPTK2 shRNA2, or circPTK2-OE. **(B)** AGS and MKN45 cells were treated with circPTK2 shRNA2 or circPTK2-OE. Cell viability was measured by CCK-8 assay. **(C)** Cell proliferation was determined by colony formation staining assay. **(D)** Cell migration and **(E)** cell invasion were measured by transwell assays. $^{**}p < 0.01$. The significance between the four groups was analyzed by one-way ANOVA.

apoptosis of renal cell carcinoma cells *via* inactivating the p38 signaling pathway (27). Thus, among the candidates for AATK-interacting proteins, STK39 was selected for further study. To explore the protein interactions between AATK and STK39, co-immunoprecipitation (co-IP) experiments were performed. The results showed that AATK could bind with STK39 in gastric cancer cell contexts (**Figure 8B**). Moreover, overexpression of AATK reduced the expressions of p-STK39, p-p38, and Bcl-2 and increased the expressions of Bax and cleaved caspase 3 in AGS and MKN45 cells (**Figures 8C, D**). Collectively, circPTK2 could induce the apoptosis of gastric cancer cells by regulating the miR-196a-3p/AATK/STK39/p39 pathways (**Figure 8E**).

DISCUSSION

CircRNAs have been identified as novel non-coding RNAs, which play key roles in tumor progression and affect the hallmarks of cancer (22, 28). However, the functions of circRNAs in gastric cancer remain largely unclear. In this study, we identified a cancer-associated circRNA, circPTK2, originating from exons 27, 28, and 29 of its host gene PTK2, and found that circPTK2 was significantly downregulated in gastric cancer tissues. In addition, upregulation of circPTK2 could inhibit gastric cancer cell proliferation, migration, and invasion by targeting the miR-196a-3p/AATK axis. In contrast, Yu et al. found that circPTK2 could promote gastric cancer cell proliferation by sponging miR-139-3p (29). These results suggested that circPTK2 might function as an oncogene or tumor-suppressor gene in gastric cancer.

Recently, circRNAs have been proven to exert various biological functions *via* acting as miRNA sponges (30). To determine whether circPTK2 could regulate gastric cancer progression *via* sponging miRNAs, the CircInteractome dataset was used to predict the potential miRNAs. We found that miR-196a-3p might be sponged by circPTK2, which was verified by luciferase reporter assay and RNA pull-down assay. Rescue experiments revealed that overexpression of miR-196a-3p

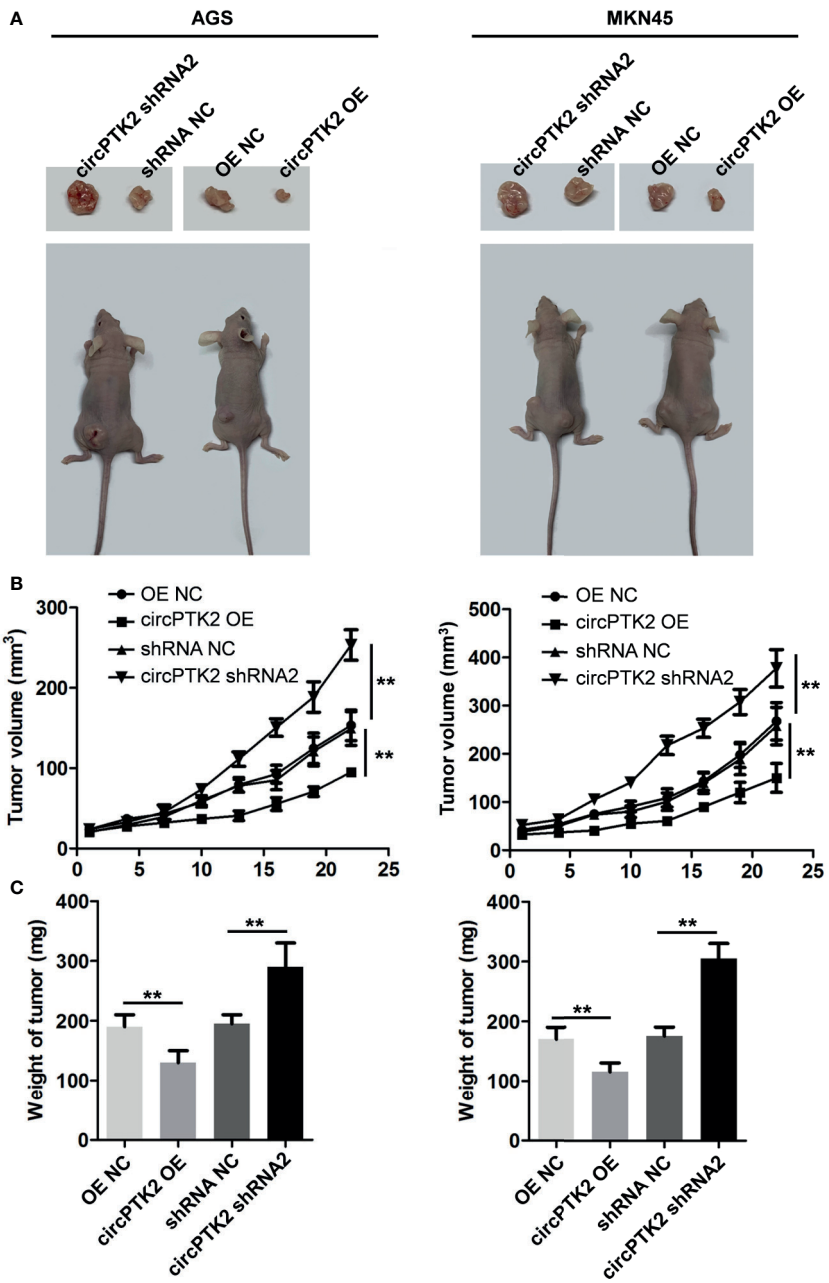

FIGURE 4 | Overexpression of circPTK2 inhibits gastric cancer cell growth *in vivo*. **(A–C)** Tumor volume and tumor weight of xenograft tumors. $^{**}p < 0.01$. The significance between the four groups was analyzed by one-way ANOVA.

significantly attenuated the anti-cancer role of circPTK2 in gastric cancer, suggesting that circPTK2 regulated the progression of gastric cancer *via* sponging miR-196a-3p. Besides, circRNAs could sponge miRNAs and prevent them from interacting with target mRNA, which in turn upregulate target gene expression (31). In this study, we found that AATK is a downstream target gene of miR-196a-3p. Ma et al. showed that the expression of AATK was downregulated in metastatic melanoma cells, and overexpression of AATK could suppress the migration and trigger the apoptosis of melanoma cells (32). In agreement with a previous study, we found that AATK was downregulated in gastric cancer cells. In addition, overexpression of circPTK2 markedly upregulated the expression of AATK in gastric cancer cells, suggesting that circPTK2 could interact with miR-196a-3p and function as a miRNA sponge to regulate AATK expression.

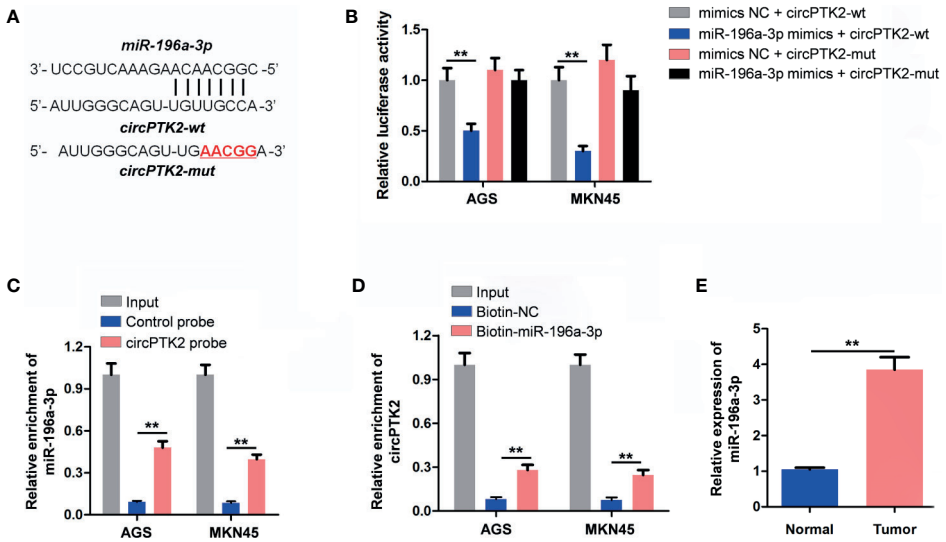

FIGURE 5 | CircPTK2 acts as the sponge of miR-196a-3p. **(A)** Schematic diagram of binding sites between circPTK2 and miR-196a-3p. **(B)** Luciferase activity analysis in AGS and MKN45 cells co-transfected with the circPTK2-wt/mut vectors together with miR-196a-3p mimics or mimics control. **(C, D)** RNA pull-down assay was performed in AGS and MKN45 cells to verify the binding between circPTK2 and miR-196a-3p. **(E)** RT-qPCR analysis of miR-196a-3p level in tumor tissues and in normal tissue. $^{**}p < 0.01$. The significance between two or more groups was analyzed by Student's *t*-test or one-way ANOVA, respectively.

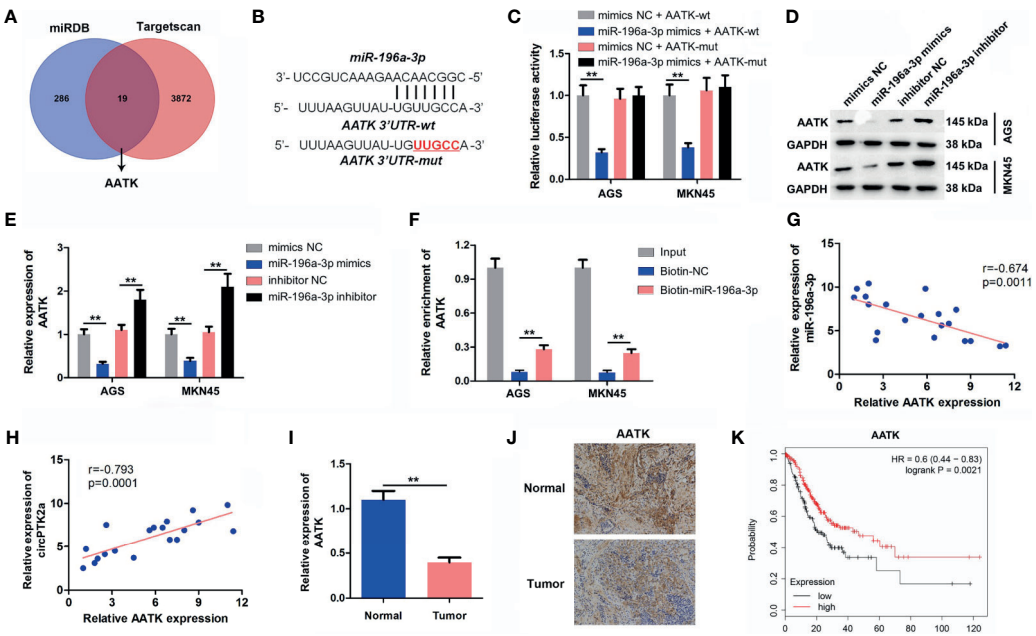

FIGURE 6 | AATK is a direct binding target of miR–196a-3p. **(A)** Screen of the candidate genes that target miR-196a-3p predicted by miRDB and TargetScan. **(B)** Schematic diagram of binding sites between AATK and miR-196a-3p. **(C)** Luciferase activity analysis in AGS and MKN45 cells co-transfected with the AATK-wt/mut vectors together with miR-196a-3p mimics or mimics control. **(D, E)** Western blot analysis of AATK expression in AGS and MKN45 cells transfected with miR-196a-3p mimics or miR-196a-3p inhibitor. **(F)** RNA pull-down assay was performed in AGS and MKN45 cells to verify the binding between AATK and miR-196a-3p. **(G, H)** The Pearson's correlation coefficients showed the correlation between AATK and miR-196a-3p or between AATK and circPTK2 in gastric cancer tissues. **(I)** RT-qPCR and **(J)** IHC analysis of AATK level in tumor tissues and in normal tissue. **(K)** Survival analysis of the correlation between AATK levels and survival rates in gastric cancer patients. $^{**}p < 0.01$. The significance between two or more groups was analyzed by Student's *t*-test or one-way ANOVA, respectively.

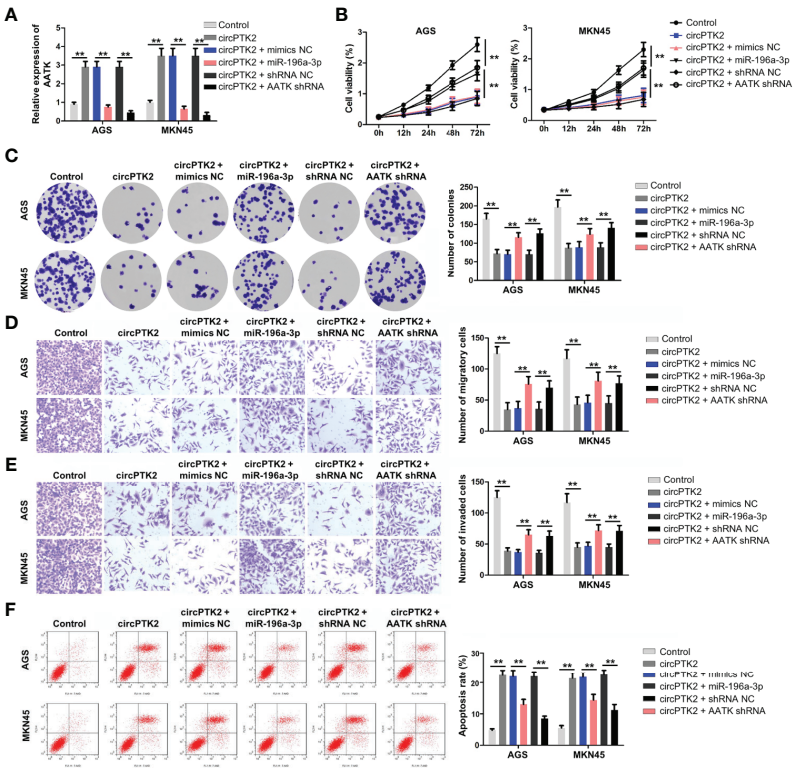

FIGURE 7 | Knockdown of AATK reverses the tumor-suppressing effect of circPTK2. AGS and MKN45 cells were treated with circPTK2, circPTK2 plus miR-196a-3p mimics, or circPTK2 plus AATK shRNA. **(A)** RT-qPCR was used to detect the level of AATK in AGS and MKN45 cells. **(B)** Cell viability was measured by CCK-8 assay. **(C)** Cell proliferation was determined by colony formation staining assay. **(D)** Cell migration and **(E)** cell invasion were measured by transwell assays. **(F)** Cell apoptosis was measured by flow cytometry. $^{**}p < 0.01$. The significance between five groups was analyzed by one-way ANOVA.

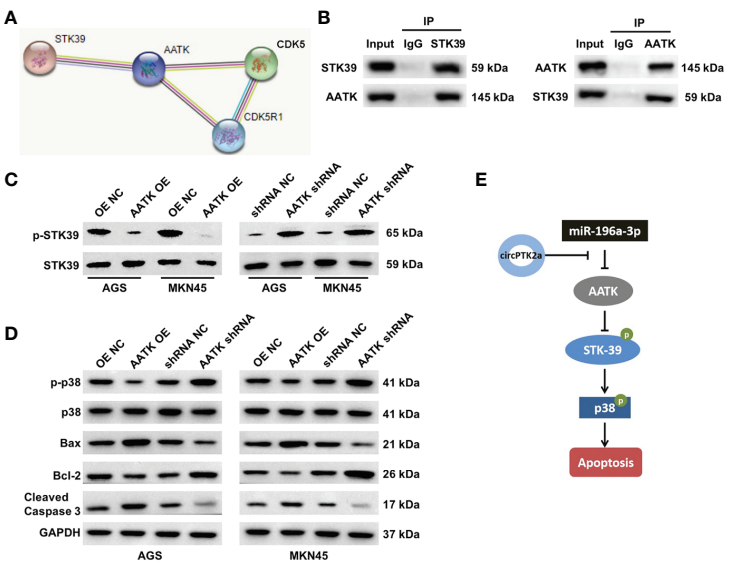

FIGURE 8 | AATK interacts with STK39 and modulates the phosphorylation of p38. **(A)** Protein–protein interaction network of AATK. **(B)** Co-IP was performed to evaluate the interaction between AATK and STK39. **(C)** Western blot analysis of p-STK39 and STK39 protein expressions in AGS and MKN45 cells transfected with AATK-OE or AATK shRNA. **(D)** Western blot analysis of p-p38, p38, Bax, Bcl-2, and cleaved caspase 3 protein expressions in AGS and MKN45 cells transfected with AATK-OE or AATK shRNA. **(E)** The potential mechanism by which circPTK2 regulated the progression of gastric cancer was presented.

Importantly, the association of AATK with the development of gastric cancer has not been described. Bioinformatics analysis indicated that AATK might interact with STK39 (also known as SPAK), which was verified by co-IP assay. Evidence has shown that STK39 could promote cervical cancer progression *via* the NF-κB/p38 MAPK/MMP2 pathway (33). Our data indicated that overexpression of AATK notably downregulated the expressions of p-STK39 and p-p38 in gastric cancer cells, suggesting that AATK might inhibit gastric cancer progression *via* inactivating the STK39/p38 signaling pathway. These data indicated that circPTK2 can sponge miR-196a-3p and upregulate miR-196a-3p targeting gene AATK, thereby inactivating the STK39/p38 signaling pathway.

CONCLUSION

In summary, we found that circPTK2 might serve as a tumor-suppressive circRNA. Mechanistically, circPTK2 could suppress the proliferation, migration, and invasion of gastric cancer cells through directly binding to miR-196a-3p and subsequently decrease the inhibiting ability of miR-196a-3p on AATK. These data indicated that exosomal circPTK2 may be a therapeutic target in gastric cancer.

DATA AVAILABILITY STATEMENT

The raw data supporting the conclusions of this article will be made available by the authors, without undue reservation.

ETHICS STATEMENT

The studies involving human participants were reviewed and approved by the First Affiliated Hospital of Soochow University. The patients/participants provided their written informed consent to participate in this study. The animal study was reviewed and approved by the First Affiliated Hospital of Soochow University and conducted according to institutional guidelines.

AUTHOR CONTRIBUTIONS

LG and TX made major contributions to the conception, design, and manuscript drafting of this study. MQ, XX, and LJ were responsible for data acquisition, data analysis, data interpretation, and manuscript revision. XZ made substantial contributions to the conception and design of the study and revised the manuscript. All authors agreed to be accountable for all aspects of the work. All authors contributed to the article and approved the submitted version.

FUNDING

This study received funding from the National Natural Science Foundation of China (Grant No. 81974375).

SUPPLEMENTARY MATERIAL

The Supplementary Material for this article can be found online at: https://www.frontiersin.org/articles/10.3389/fonc.2021.706415/full#supplementary-material

Supplementary Figure 1 | Overexpression of circPTK2 inhibits SNU-5 cell proliferation, migration and invasion. **(A)** SNU-5 cells were treated with circPTK2 shRNA2 or circPTK2-OE. Cell viability was measured by CCK-8 assay. **(B)** Cell proliferation was determined by colony formation staining assay. **(C)** Cell migration and cell invasion were measured by transwell assays. $^{**}p < 0.01$. The significance between four groups was analyzed by one-way ANOVA.

REFERENCES

1. Kang YK, Cho H. Perioperative FLOT: New Standard for Gastric Cancer? *Lancet* (2019) 393(10184):1914–6. doi: 10.1016/s0140-6736(18)33189-1
2. Yang HK, Berlth F. Gastric Cancer Surgery: The Importance of Technique and Not Only the Extent of Lymph Node Dissection. *Lancet Oncol* (2019) 20 (3):329–31. doi: 10.1016/s1470-2045(19)30073-7
3. McCaw ZR, Kim DH, Tian L, Fu H, Wei LJ. Trifluridine/tipiracil in Metastatic Gastric Cancer. *Lancet Oncol* (2019) 20(1):e8. doi: 10.1016/s1470-2045(18) 30908-2
4. Zeraati H, Amiri Z. Estimating Postoperative Survival of Gastric Cancer Patients and Factors Affecting it in Iran: Based on a TNM-7 Staging System. *Acta Med Iran* (2016) 54(2):114–8.
5. Katai H, Mizusawa J, Katayama H, Morita S, Yamada T, Bando E, et al. Survival Outcomes After Laparoscopy-Assisted Distal Gastrectomy *Versus* Open Distal Gastrectomy With Nodal Dissection for Clinical Stage IA or IB Gastric Cancer (JCOG0912): A Multicentre, Non-Inferiority, Phase 3 Randomised Controlled Trial. *Lancet Gastroenterol Hepatol* (2020) 5 (2):142–51. doi: 10.1016/s2468-1253(19)30332-2
6. Roviello G, Generali D. Pertuzumab Therapy for HER2-Positive Metastatic Gastric or Gastro-Oesophageal Junction Cancer. *Lancet Oncol* (2018) 19 (10):1270–2. doi: 10.1016/s1470-2045(18)30512-6
7. Song Z, Wu Y, Yang J, Yang D, Fang X. Progress in the Treatment of Advanced Gastric Cancer. *Tumour Biol* (2017) 39(7):1010428317714626. doi: 10.1177/1010428317714626
8. Patop IL, Wüst S, Kadener S. Past, Present, and Future of circRNAs. *EMBO J* (2019) 38(16):e100836. doi: 10.15252/embj.2018100836
9. Li X, Yang L, Chen LL. The Biogenesis, Functions, and Challenges of Circular RNAs. *Mol Cell* (2018) 71(3):428–42. doi: 10.1016/j.molcel.2018.06.034
10. Greene J, Baird AM, Brady L, Lim M, Gray SG, McDermott R, et al. Circular RNAs: Biogenesis, Function and Role in Human Diseases. *Front Mol Biosci* (2017) 4:38. doi: 10.3389/fmolb.2017.00038
11. Li J, Yang J, Zhou P, Le Y, Zhou C, Wang S, et al. Circular RNAs in Cancer: Novel Insights Into Origins, Properties, Functions and Implications. *Am J Cancer Res* (2015) 5(2):472–80.
12. Kristensen LS, Hansen TB, Venø MT, Kjems J. Circular RNAs in Cancer: Opportunities and Challenges in the Field. *Oncogene* (2018) 37(5):555–65. doi: 10.1038/onc.2017.361
13. Verduci L, Strano S, Yarden Y, Blandino G. The circRNA-microRNA Code: Emerging Implications for Cancer Diagnosis and Treatment. *Mol Oncol* (2019) 13(4):669–80. doi: 10.1002/1878-0261.12468
14. Li R, Jiang J, Shi H, Qian H, Zhang X, Xu W. CircRNA: A Rising Star in Gastric Cancer. *Cell Mol Life Sci* (2020) 77(9):1661–80. doi: 10.1007/s00018-019-03345-5

15. Zeng K, Chen X, Xu M, Liu X, Hu X, Xu T, et al. CircHIPK3 Promotes Colorectal Cancer Growth and Metastasis by Sponging miR-7. *Cell Death Dis* (2018) 9(4):417. doi: 10.1038/s41419-018-0454-8
16. Qadir MI, Faheem A. miRNA: A Diagnostic and Therapeutic Tool for Pancreatic Cancer. *Crit Rev Eukaryot Gene Expr* (2017) 27(3):197–204. doi: 10.1615/CritRevEukaryotGeneExpr.2017019494
17. García-Sancha N, Corchado-Cobos R, Pérez-Losada J, Cañueto J. MicroRNA Dysregulation in Cutaneous Squamous Cell Carcinoma. *Int J Mol Sci* (2019) 20(9):2181. doi: 10.3390/ijms20092181
18. Pfeffer SR, Yang CH, Pfeffer LM. The Role of miR-21 in Cancer. *Drug Dev Res* (2015) 76(6):270–7. doi: 10.1002/ddr.21257
19. Ali Syeda Z, Langden SSS, Munkhzul C, Lee M, Song SJ. Regulatory Mechanism of MicroRNA Expression in Cancer. *Int J Mol Sci* (2020) 21 (5):1723. doi: 10.3390/ijms21051723
20. Dong W, Bi J, Liu H, Yan D, He Q, Zhou Q, et al. Circular RNA ACVR2A Suppresses Bladder Cancer Cells Proliferation and Metastasis Through miR-626/EYA4 Axis. *Mol Cancer* (2019) 18(1):95. doi: 10.1186/s12943-019-1025-z
21. Lu Q, Liu T, Feng H, Yang R, Zhao X, Chen W, et al. Circular RNA Circslc8a1 Acts as a Sponge of miR-130b/miR-494 in Suppressing Bladder Cancer Progression *via* Regulating PTEN. *Mol Cancer* (2019) 18(1):111. doi: 10.1186/s12943-019-1040-0
22. Zhang X, Wang S, Wang H, Cao J, Huang X, Chen Z, et al. Circular RNA Circnrip1 Acts as a microRNA-149-5p Sponge to Promote Gastric Cancer Progression *via* the AKT1/mTOR Pathway. *Mol Cancer* (2019) 18(1):20. doi: 10.1186/s12943-018-0935-5
23. Luo Z, Rong Z, Zhang J, Zhu Z, Yu Z, Li T, et al. Circular RNA Circccdc9 Acts as a miR-6792-3p Sponge to Suppress the Progression of Gastric Cancer Through Regulating CAV1 Expression. *Mol Cancer* (2020) 19(1):86. doi: 10.1186/s12943-020-01203-8
24. Dudekula DB, Panda AC, Grammatikakis I, De S, Abdelmohsen K, Gorospe M. CircInteractome: A Web Tool for Exploring Circular RNAs and Their Interacting Proteins and microRNAs. *RNA Biol* (2016) 13(1):34–42. doi: 10.1080/15476286.2015.1128065
25. Li Z, Zhu W, Xiong L, Yu X, Chen X, Lin Q. Role of High Expression Levels of STK39 in the Growth, Migration and Invasion of Non-Small Cell Type Lung Cancer Cells. *Oncotarget* (2016) 7(38):61366–77. doi: 10.18632/oncotarget.11351
26. Huang T, Zhou Y, Cao Y, Tao J, Zhou ZH, Hang DH. STK39, Overexpressed in Osteosarcoma, Regulates Osteosarcoma Cell Invasion and Proliferation. *Oncol Lett* (2017) 14(4):4599–604. doi: 10.3892/ol.2017.6728
27. Zhao Q, Zhu Y, Liu L, Wang H, Jiang S, Hu X, et al. STK39 Blockage by RNA Interference Inhibits the Proliferation and Induces the Apoptosis of Renal Cell Carcinoma. *Onco Targets Ther* (2018) 11:1511–9. doi: 10.2147/ott.S153806
28. Shan C, Zhang Y, Hao X, Gao J, Chen X, Wang K. Biogenesis, Functions and Clinical Significance of circRNAs in Gastric Cancer. *Mol Cancer* (2019) 18 (1):136. doi: 10.1186/s12943-019-1069-0
29. Yu D, Zhang C. Circular RNA PTK2 Accelerates Cell Proliferation and Inhibits Cell Apoptosis in Gastric Carcinoma *via* miR-139-3p. *Dig Dis Sci* (2021) 66(5):1499–509. doi: 10.1007/s10620-020-06358-4
30. Panda AC. Circular RNAs Act as miRNA Sponges. *Adv Exp Med Biol* (2018) 1087:67–79. doi: 10.1007/978-981-13-1426-1_6
31. Zheng Q, Bao C, Guo W, Li S, Chen J, Chen B, et al. Circular RNA Profiling Reveals an Abundant Circhipk3 That Regulates Cell Growth by Sponging Multiple miRNAs. *Nat Commun* (2016) 7:11215. doi: 10.1038/ncomms11215
32. Ma S, Rubin BP. Apoptosis-Associated Tyrosine Kinase 1 Inhibits Growth and Migration and Promotes Apoptosis in Melanoma. *Lab Invest* (2014) 94 (4):430–8. doi: 10.1038/labinvest.2014.13
33. Chiu MH, Liu HS, Wu YH, Shen MR, Chou CY. SPAK Mediates KCC3-Enhanced Cervical Cancer Tumorigenesis. *FEBS J* (2014) 281(10):2353–65. doi: 10.1111/febs.12787

Conflict of Interest: The authors declare that the research was conducted in the absence of any commercial or financial relationships that could be construed as a potential conflict of interest.

Publisher's Note: All claims expressed in this article are solely those of the authors and do not necessarily represent those of their affiliated organizations, or those of the publisher, the editors and the reviewers. Any product that may be evaluated in this article, or claim that may be made by its manufacturer, is not guaranteed or endorsed by the publisher.

frontiers in Oncology

ORIGINAL RESEARCH
published: 27 September 2021
doi: 10.3389/fonc.2021.725181

Identification of N6-Methylandenosine-Related lncRNAs for Subtype Identification and Risk Stratification in Gastric Adenocarcinoma

Yuancheng Huang[1], Zehong Yang[1], Chaoyuan Huang[1], Xiaotao Jiang[1], Yanhua Yan[1], Kunhai Zhuang[2], Yi Wen[3], Fengbin Liu[2]* and Peiwu Li[3]**

[1] First Clinical Medical College, Guangzhou University of Chinese Medicine, Guangzhou, China, [2] Department of Gastroenterology, Baiyun Branch of the First Affiliated Hospital of Guangzhou University of Chinese Medicine, Guangzhou, China, [3] Department of Gastroenterology, The First Affiliated Hospital of Guangzhou University of Chinese Medicine, Guangzhou, China

Objectives: The purpose of this study was to investigate the role of m^{6}A-related lncRNAs in gastric adenocarcinoma (STAD) and to determine their prognostic value.

Methods: Gene expression and clinicopathological data were obtained from The Cancer Genome Atlas (TCGA) database. Correlation analysis and univariate Cox regression analysis were conducted to identify m^{6}A-related prognostic lncRNAs. Subsequently, different clusters of patients with STAD were identified *via* consensus clustering analysis, and a prognostic signature was established by least absolute shrinkage and selection operator (LASSO) Cox regression analyses. The clinicopathological characteristics, tumor microenvironment (TME), immune checkpoint genes (ICGs) expression, and the response to immune checkpoint inhibitors (ICIs) in different clusters and subgroups were explored. The prognostic value of the prognostic signature was evaluated using the Kaplan-Meier method, receiver operating characteristic curves, and univariate and multivariate regression analyses. Additionally, Gene Set Enrichment Analysis (GSEA), Kyoto Encyclopedia of Genes and Genomes (KEGG) pathway, and Gene Ontology (GO) analysis were performed for biological functional analysis.

Results: Two clusters based on 19 m^{6}A-related lncRNAs were identified, and a prognostic signature comprising 14 m^{6}A-related lncRNAs was constructed, which had significant value in predicting the OS of patients with STAD, clinicopathological characteristics, TME, ICGs expression, and the response to ICIs. Biological processes and pathways associated with cancer and immune response were identified.

OPEN ACCESS

Edited by:
Kanjoormana Aryan Manu, Amala Cancer Research Centre, India

Reviewed by:
Zhijun Dai, Zhejiang University, China
Piyush Khandelia, Birla Institute of Technology and Science, India

***Correspondence:**
Yi Wen
20172101031@stu.gzucm.edu.cn
Fengbin Liu
liufengbin163@163.com
Peiwu Li
doctorlipw@gzucm.edu.cn

Specialty section:
This article was submitted to Gastrointestinal Cancers, a section of the journal Frontiers in Oncology

Received: *15 June 2021*
Accepted: *02 September 2021*
Published: *27 September 2021*

Citation:
Huang Y, Yang Z, Huang C, Jiang X, Yan Y, Zhuang K, Wen Y, Liu F and Li P (2021) Identification of N6-Methylandenosine-Related lncRNAs for Subtype Identification and Risk Stratification in Gastric Adenocarcinoma. Front. Oncol. 11:725181. doi: 10.3389/fonc.2021.725181

Conclusions: We revealed the role and prognostic value of m^{6}A-related lncRNAs in STAD. Together, our finding refreshed the understanding of m^{6}A-related lncRNAs and provided novel insights to identify predictive biomarkers and immunotherapy targets for STAD.

Keywords: gastric adenocarcinoma, N6-methyladenosine, long noncoding RNAs, prognostic signature, tumor microenvironment, immunotherapy

INTRODUCTION

Globally, gastric cancer (GC) is the fifth most common cancer and the third most deadly neoplasm (1). Gastric adenocarcinoma (STAD) is the most common pathological type of GC, and despite considerable progress in the diagnosis and therapeutic strategies for STAD, the prognosis of patients with STAD remains poor due to advanced stage and postsurgical recurrence (2, 3). Therefore, the identification of novel biomarkers for early detection and effective therapeutic targets for treating patients with STAD is critical and urgent.

Accumulating evidence has shown that long noncoding RNAs (lncRNAs) had various biological functions and played a crucial role in the oncogenesis and progression of GC (4). For example, lncRNA IGF2-AS functions as a competing endogenous RNA (ceRNA) to miR-503 and promotes the pathogenicity of STAD by regulating SHOX2 (5). LINC00707 acts as an oncogene in GC by interacting with RNA-binding protein HuR and increasing the stability of VAV3/F11R mRNAs (6). LncRNA CRNDE could bind to splicing protein SRSF6 to reduce its stability and thus regulate alternative splicing events and affect autophagy regulation in GC (7).

Increasing evidence suggests that RNA modifications play a critical role in tumorigenesis and progression of different cancers, including GC (8, 9). N6-methyladenosine (m^{6}A), which introduces a methyl group in the nitrogen-6 position of adenosine, is found to be the most frequent internal RNA modification in mammals (10). As a dynamic and reversible process, m^{6}A RNA modification is primarily regulated by "writers" (adenosine methyltransferases) and "erasers" (demethylases) and performs different functions by interacting with "readers" (m^{6}A-binding proteins). As identified to distribute extensively in a variety of RNAs, such as messenger RNAs (mRNAs), pri-microRNAs (pri-miRNAs), circular RNAs (circRNAs), and lncRNAs, m^{6}A is involved in various biological processes related to the occurrence and progression of tumors, including GC (11–13). For instance, the m^{6}A writer METTL3 stimulates m^{6}A modification of HDGF mRNA, and the m^{6}A reader IGF2BP3 recognizes and binds to the m^{6}A site and enhances its stability, which promotes tumor angiogenesis and glycolysis in GC (14). Overexpression METTL3 facilitates the processing of pri-miR-17 into the miR-17 through an m^{6}A DGCR8-dependent method, which activates the AKT/mTOR pathway and the progression of GC (15). LINC00470 promotes the degradation of PTEN mRNA to facilitate malignant behavior in GC cells by interacting with METTL3 (16). Additionally, extensive literature has demonstrated that m^{6}A plays an important role in immune recognition, immune responses, and tumor microenvironment (TME) (17–19). However, the specific role and prognostic value of m^{6}A-related lncRNAs in STAD remain unclear.

Here, we analyzed the Cancer Genome Atlas (TCGA) database for m^{6}A-related lncRNAs involved in STAD, identified two clusters based on m^{6}A-related lncRNAs, and constructed an m^{6}A-related lncRNA prognostic signature. Then, we estimated its predictive value and diagnostic effectiveness, as well as the correlation of m^{6}A-related lncRNAs with TME and immunotherapy. Furthermore, the molecular mechanisms associated with m^{6}A-related prognostic lncRNAs were explored. The finding in this study revealed the critical role of m^{6}A-related lncRNAs and shed light on the latent relationship and the underlying mechanism between m^{6}A-related lncRNAs and tumor-immune interactions.

MATERIAL AND METHODS

Acquisition of Datasets

The RNA-seq transcriptome data [fragments per kilobase million (FPKM)] (20) from 373 samples and clinical information from 406 patients with STAD in the TCGA database (http://cancergenome.nih.gov/) were downloaded for our study. Patients with complete clinicopathological and survival information were included for further assessment.

Selection of m^{6}A-Related Regulators

Based on published data (21–23), 24 m^{6}A-related regulators, including METTL3, METTL14, METTL16, WTAP, VIRMA, KIAA1429, ZC3H13 RBM15, RBM15B, YTHDC1, YTHDC2, YTHDF1, YTHDF2, YTHDF3, HNRNPC, FMR1, LRPPRC, HNRNPA2B1, IGFBP1, IGFBP2, IGFBP3, RBMX, FTO, and ALKBH5, were used in our study.

Bioinformatic Analysis

Primarily, the correlation analysis was performed between m^{6}A-related regulators and all lncRNAs in STAD. m^{6}A-related lncRNAs were identified based on the following classification parameters (1): correlation coefficients more than 0.4 and (2) *p*-value less than 0.001. Then, to filtrate the m^{6}A-related lncRNAs that were highly correlated with overall survival (OS), univariate Cox regression analysis was performed. Additionally, the correlation analysis of m^{6}A-related prognostic lncRNAs was implemented using the "corrplot" package in R. Next, to explore the potential function of m^{6}A-related lncRNAs in STAD, two different clusters (clusters I and II) were identified using the "Consensus ClusterPlus" R package (24) based on the expression of m^{6}A-related prognostic lncRNAs with a resample rate of 80%, 50 iterations, and Pearson's correlation. The

different clinicopathological characteristics and OS were compared between clusters I and II. Furthermore, the differences in the content of immune infiltrating cells, TME scores, and the expression of immune checkpoint genes (ICGs) between different clusters were explored (25). The content of immune infiltrating cells was identified by CIBERSORT (26), and the immune/stromal scores and tumor purity were calculated through the "ESTIMATE" package in R (27).

Then, we randomly divided the patients with STAD into two groups: the training group and the testing group. Subsequently, based on m^{6}A-related prognostic lncRNAs identified by univariate Cox regression analysis, the least absolute shrinkage and selection operator (LASSO) Cox regression algorithm was used to identify m^{6}A-related lncRNAs with powerful prognostic significance and construct the prognostic risk model from the training group data. According to the best penalty parameter λ, the coefficients of the m^{6}A-related lncRNAs were calculated. The risk score (RS) was estimated using the following formula:

$$\mathrm{RS} = \sum_{i=1}^{n} \mathrm{Coef}(i) X(i)$$

where Coef(i) is the coefficient and $X(i)$ represents the expression levels of m^{6}A-related lncRNAs. Using the median RS obtained as the demarcation value, patients with STAD were classified into two groups: high-risk and low-risk groups. Kaplan-Meier analysis and the receiver operating characteristic (ROC) curves were used to validate the predictive efficiency (28). Then, the accuracy of the model was validated from the test group and the combined group using the same method. Furthermore, the differences in clinicopathological features, the content of immune infiltrating cells, TME scores, and ICGs expression between high-risk and low-risk groups were also explored. Moreover, we further predicted the response to immune checkpoint inhibitors (ICIs) in subgroups based on the immunophenoscores (IPS) of patients with STAD obtained from The Cancer Immunome Atlas (TCIA) (https://tcia.at/home). Additionally, the prognostic value of the RS was verified using univariate and multivariate Cox regression analyses. The hazard ratio (HR) with 95% confidence intervals and log-rank p-value were calculated using the "glmnet" and "survival" R packages (29).

To explore the biological functions associated with m^{6}A-related lncRNAs, Gene Set Enrichment Analysis (GSEA), Kyoto Encyclopedia of Genes and Genomes (KEGG) pathway, and Gene Ontology (GO) analysis were performed. Genes that were significantly upregulated (fold change >1 and $p < 0.05$) or downregulated (fold change <−1 and $p < 0.05$) between clusters I and II or between the high-risk and low-risk groups were identified using the "edgeR" package in R, which were used for GO and KEGG pathway analysis. Additionally, genes in different clusters and different risk groups were functionally annotated using GSEA. Based on the m^{6}A-related prognostic lncRNAs, the target miRNAs were predicted *via* miRcode database and target mRNAs of these miRNAs were found in different databases, such as TargetScan, miRTarBase, and miRDB. Target mRNAs in the ceRNA network were also functionally annotated using GO and KEGG pathway analyses. The flow chart of bioinformatic analysis was shown in **Figure 1**.

Cell Culture

The GC cell line MGC-803 and the normal human gastric epithelial cell line GES-1 were purchased from the American Type Culture Collection (ATCC, Manassas, VA, USA). All cells were cultured in RPMI-1640 medium (Life Technologies, Grand Island, NY, USA) supplemented with 10% fetal bovine serum (Life Technologies) at 37°C in a humidified atmosphere with 5% CO_2.

Quantitative Reverse Transcription-Polymerase Chain Reaction

Total RNA was extracted from cells with TRIzol reagent (Invitrogen, China) according to manufacturer's instruction. Reverse transcription was carried out according to the manufacturer's instructions using the PrimeScript RT Reagent Kit (Takara, China). The SYBR PrimeScript RT-PCR Kit (Takara) was applied for the analysis of quantitative reverse transcription-polymerase chain reaction (qRT-PCR). Related lncRNAs expression levels were calculated using the 2-ΔΔCT method and the related GAPDH mRNA expression was used as an endogenous control. Primers sequences used in our study were as follows: GAPDH forward 5′-GGACCTGACCTGCC GTCTAG-3′, and reverse 5′-GTAGCCCAGGATGCCCTTGA-3′; SREBF2-AS1 forward 5′-TAGTGCCGCTGCTGGAAA-3′, and reverse 5′-TGTGGGAGTCGTGCTGGT-3′; LINC00106 forward 5′-AAGCATTTGGCAAGCACA-3′, and reverse 5′-GCCTGAAGTCTTCCCGTTA-3′; SENCR forward 5′-CCAC GCTTTGGACTTGCT-3′, and reverse 5′-GCGGGTTT CTGGTGAGGT-3′; LINC01537 forward 5′-GTCGGGATAC ATCTTGGT-3′, and reverse 5′-TTGAGTTGTTCTGCCTTT-3′; MAGI2-AS3 forward 5′-CCTTACTTCTAGGCTTCT-3′, and reverse 5′-GTTTACTTTGCTGGTGTC-3′; STARD4-AS1 forward 5′-TCAAACAAGTATTCACCCTA-3′, and reverse 5′-ATCACCCATTCTCCACAT-3′.

Statistical Analysis

The expression data of m^{6}A-related regulators and all lncRNAs in tumor tissues and adjacent mucosa of STAD obtained from TCGA was compared using one-way analysis of variance (ANOVA); the clinical characteristics of different groups were compared using the Chi-square test; the Kaplan-Meier method was used to perform a bilateral logarithmic rank test in overall survival analysis; p-value <0.05 were regarded as statistically significant. All statistical analyses were implemented using R v4.0.3 (https://www.r-project.org/) or GraphPad Prism software (Version 8.0).

RESULTS

Identification of m^{6}A-Related Prognostic lncRNAs

Firstly, the expression levels of 24 m^{6}A-related genes and all lncRNAs from the TCGA were extracted respectively. Through coexpression analysis, we identified 471 m^{6}A-related lncRNAs

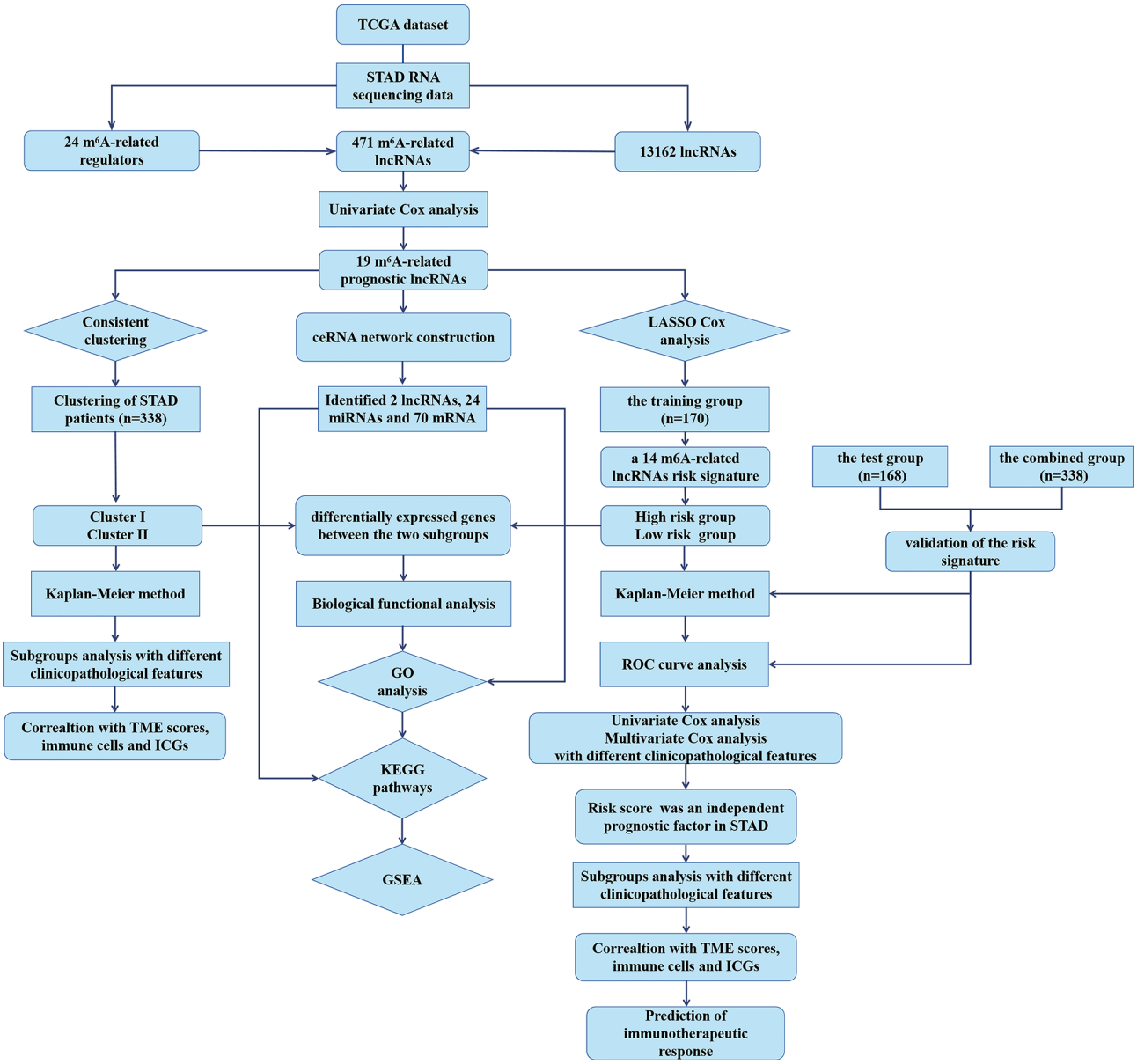

FIGURE 1 | The flow chart of the study design and analysis.

(|cor| > 0.4, *p*-value <0.05). The gene co-expression network of 24 m^{6}A-related genes and 471 m^{6}A-related lncRNAs was shown in **Figure 2A**. After conducting univariate Cox analysis, 19 candidate lncRNAs that were highly correlated with OS were identified ($p < 0.05$) (**Figure 2B**). The expression of 19 m^{6}A-related prognostic lncRNAs was compared between tumor tissues and adjacent mucosa (**Figures 2C, D**). Among these lncRNAs, seven (AL139147.1, AC022031.2, AC036103.1, MAGI2-AS3, STARD4-AS1, SENCR, LINC01537) were prognostic risk factors, and 12 (RHPN1-AS1, AL512506.1, SREBF2-AS1, AC026740.1, LINC00106, AL139289.1, AC005586.1, AL139089.1, AC093752.3, AL033527.3, AP000873.4, AL355574.1) were prognostic protective factors. The 19 m^{6}A-related lncRNAs were closely correlated with each other (**Figure 2E**).

Consensus Clustering of m^{6}A-Related Prognostic lncRNAs Identified Two Clusters of STAD With Different Clinicopathological Features and Immune Landscape

Based on the expression levels of 19 m^{6}A-related prognostic lncRNAs, consistent clustering analysis of patients with STAD was implemented. Patients were clustered into two clusters due to

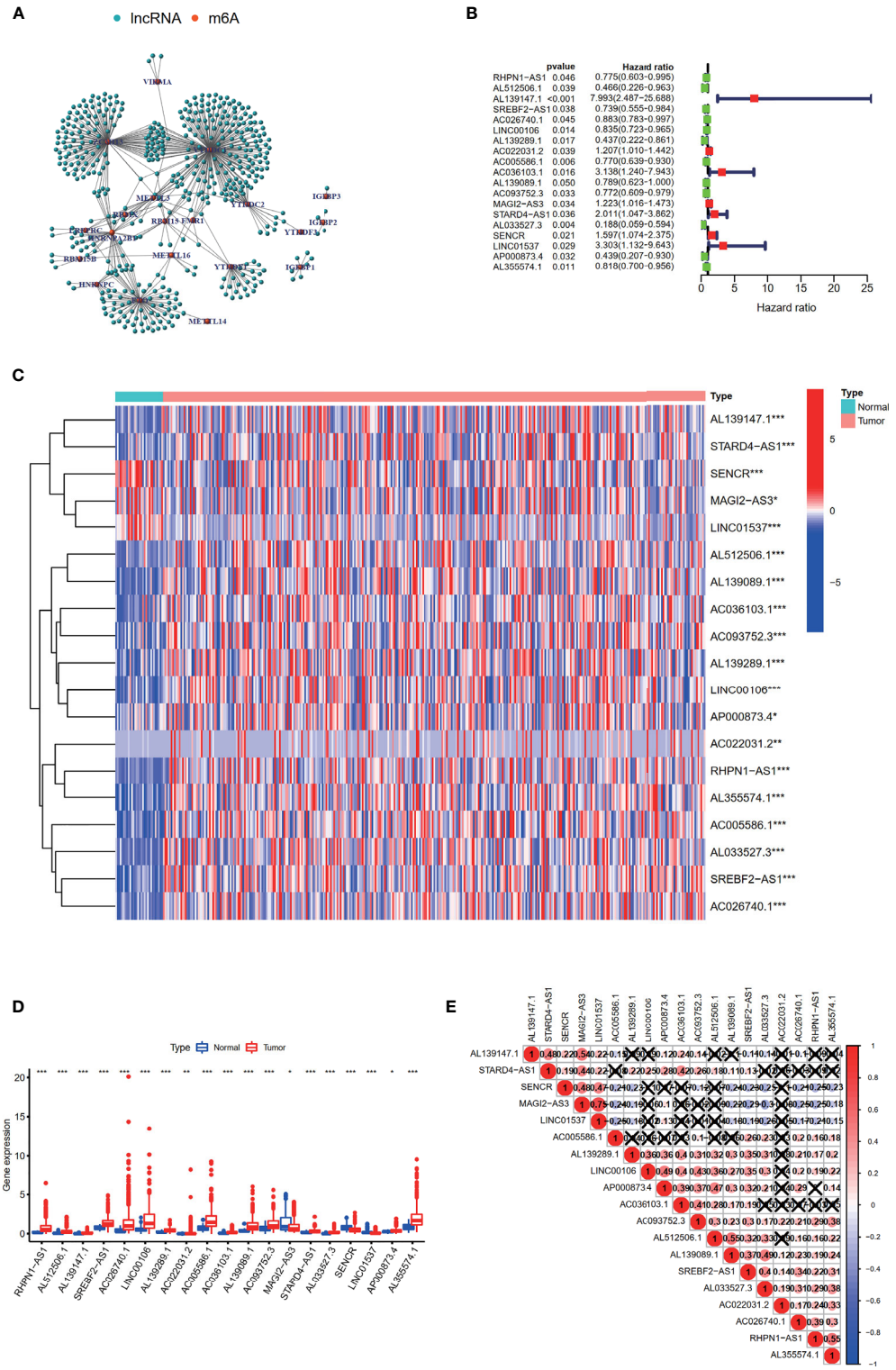

FIGURE 2 | Identification of m^{6}A-related prognostic lncRNAs in STAD patients. **(A)** The network of the 24 m^{6}A-related regulators and 471 m^{6}A-related lncRNAs. **(B)** The hazard ratio (HR) and 95% confidence interval (CI) of 19 m^{6}A-related lncRNAs estimated by univariate Cox regression. **(C, D)** The expression of 19 prognostic m^{6}A-related lncRNAs in TCGA database between the tumor group and the normal group. **(E)** Spearman's correlation analysis of the 19 m^{6}A-related prognostic lncRNAs. *$p < 0.05$, **$p < 0.01$, and ***$p < 0.001$.

the minimal interference between the two subgroups (**Figures 3A–D**).

The distribution of the clinicopathological characteristics in clusters I and II were displayed as a heat map (**Figure 3E**). Evident differences between the two clusters according to tumor grade ($p < 0.01$) were observed. Notably, the OS rate of clusters I and II were significantly different based on the Kaplan-Meier method and cluster II was associated with poorer OS (**Figure 3F**).

In terms of TME scores, it was found that ESTIMATE, immune, and stromal scores significantly increased in cluster II, while tumor purity increased in cluster I. In addition, the content of 22 immune cells in clusters I and II was compared (**Figure 4A**). As a result, cluster I contained more follicular helper T cells ($p < 0.001$) and M0 macrophages ($p < 0.01$), and cluster II had more monocytes ($p < 0.01$), M2 macrophages ($p < 0.05$), resting dendritic cells (DC) ($p < 0.001$) and resting

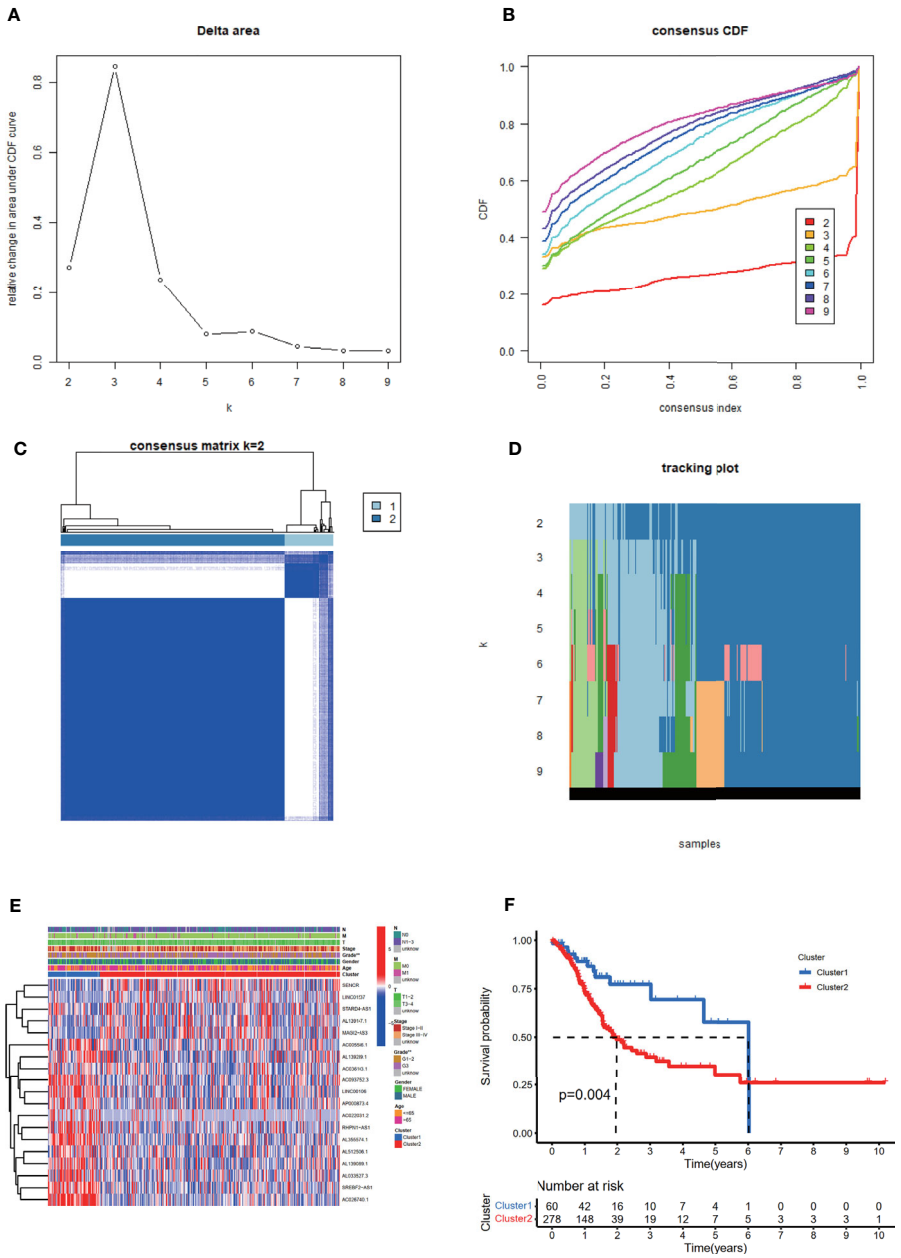

FIGURE 3 | Consistent cluster analysis of patients with STAD based on 19 prognostic m^{6}A-related lncRNAs. **(A)** The consistency clustering cumulative distribution function (CDF) when *k* is between 2 and 10. **(B)** The relative change of the area under the CDF curve from 2 to 10 of *k* **(C)** At $k = 2$, the correlation between groups. **(D)** The distribution of the sample when *k* is between 2 and 10. **(E)** The distribution of clinicopathological characteristics and the expression of 19 prognostic m^{6}A-related lncRNAs in clusters I and II. $^{**}p < 0.01$. **(F)** Comparison of Kaplan-Meier overall survival (OS) curve for STAD patients in clusters I and II.

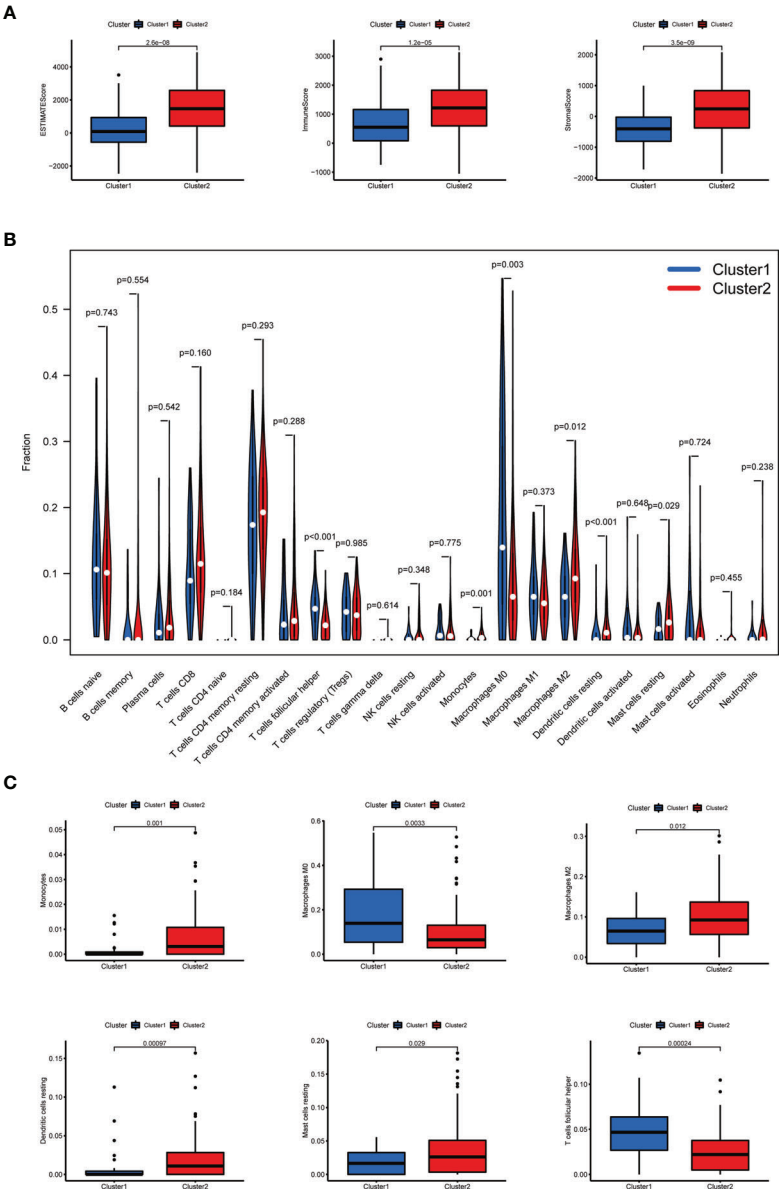

FIGURE 4 | The TME scores and the content of 22 immune cells in clusters I and II. **(A)** The ESTIMATE, immune, and stromal scores significantly increased in cluster II. **(B)** The content of 22 immune cells between clusters I and II. **(C)** The infiltration status of follicular helper T cells, M0 macrophages, M2 macrophages, monocytes, resting dendritic cells, and resting mast cells between cluster I and cluster II was significantly different.

mast cells($p < 0.05$). Differential analysis of immune infiltration cells was displayed in **Figures 4B, C**.

Regarding the expression of ICGs, we investigated the distribution of 38 ICGs obtained from previous studies in different clusters (30–34). Through differential expression analysis, we found that 22 ICGs in the tumor tissues differentially expressed compared with the adjacent mucosa **(Figure 5A)**, and 11 of 22 ICGs in cluster I differentially expressed compared with cluster II **(Figure 5B)**. Moreover, we observed three ICGs (namely, YTHDF1, IL23A, LDHC) were significantly overexpressed in cluster I and eight ICGs (namely, PDCD1LG2, CD86, HAVCR2, LAMA3, TNFSF4, IL12B, LDHA, ICOS) were significantly overexpressed in cluster II.

Construction and Verification of the m^{6}A-Related lncRNAs Prognostic Signature

Based on 19 candidate lncRNAs that were highly correlated with OS, we used the LASSO method in the training group to construct an m^{6}A-related lncRNA signature for evaluating the prognosis of patients with STAD. Finally, 14 lncRNAs were chosen to establish a prognostic signature and the risk score was calculated **(Figures 6A, B)**. Using the median risk score as the

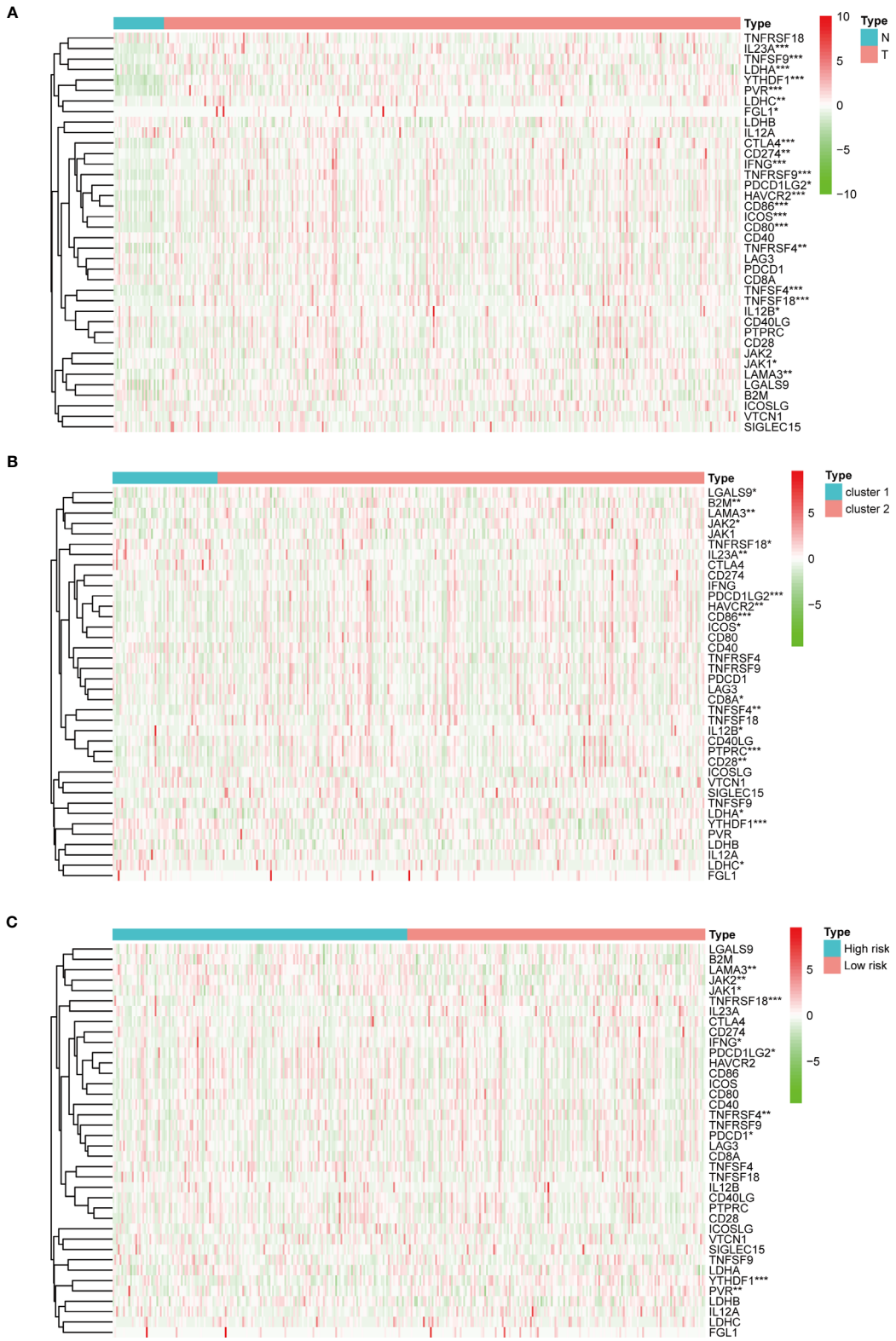

FIGURE 5 | The expression of immune checkpoint genes. **(A)** The expression of immune checkpoint genes between the normal and the tumor groups. **(B)** The expression of immune checkpoint genes between cluster I and cluster II. **(C)** The expression of immune checkpoint genes between the high-risk and the low-risk groups. *$p < 0.05$, **$p < 0.01$, and ***$p < 0.001$.

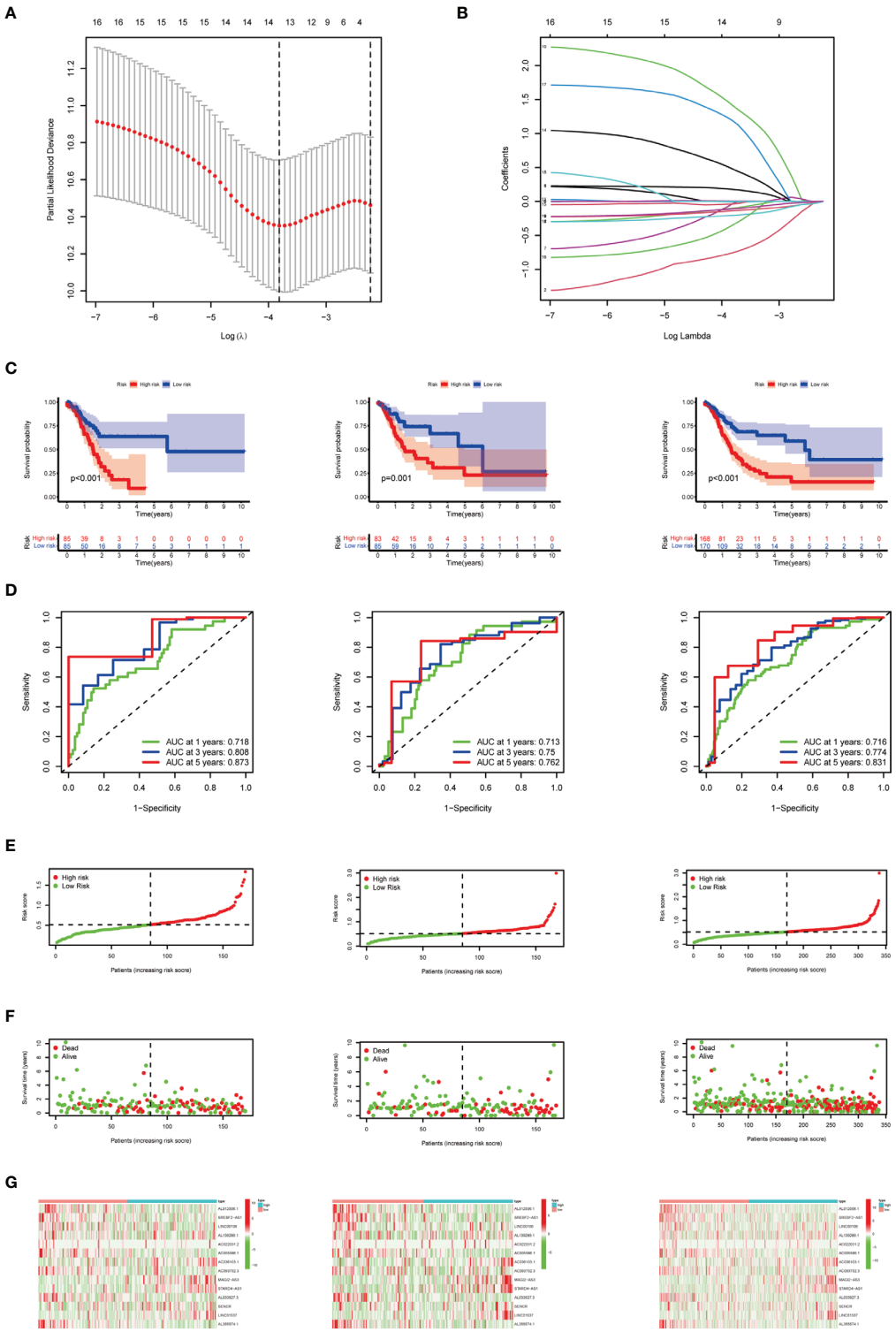

FIGURE 6 | Construction and verification of the m^{6}A-related lncRNA prognostic signature. **(A)** The point with the smallest cross-verification error corresponds to the number of factors included in the LASSO regression model. **(B)** The lines of different colors represent the trajectory of the correlation coefficient of different factors in the model with the increase of Log Lamda. **(C)** Kaplan-Meier analysis of patients in the high-risk and low-risk groups in the training group, the test group, and the combined group. **(D)** ROC analysis of 1, 3, and 5 years in the training group, the test group, and the combined group. **(E)** Distribution of patients with different risk scores in the training group, the test group, and the combined group. **(F)** OS status of patients with different risk scores in the training group, the test group, and the combined group. **(G)** Heat map of the prognostic signature scores in the training group, the test group, and the combined group.

demarcation value, the patients in the training group (n = 170) were classified into two groups, namely, the high-risk and low-risk groups. To test the efficacy of the prognostic model, survival and ROC curve analyses were conducted. Kaplan-Meier analysis showed that the low-risk group had a significantly longer survival time than the high-risk group ($p < 0.001$) **(Figure 6C)**. The value of the area under the curve (AUC) in the time-dependent ROC curve of 1, 3, and 5 years was 0.718, 0.808, and 0.873 severally **(Figure 6D)**, suggesting good prediction performance of the survival model. To further validate this 14 lncRNA prognostic signature, verification analysis in the test group (n = 168) and the combined group (n = 338) was implemented. As a result, the high-risk group in the test group and the combined group had significantly shorter survival time compared with the low-risk group, which was previously observed in the training group **(Figure 6C)**. The time-dependent ROC curve of the test group and the combined group also had well-prediction performances, and the AUC value of 1, 3, and 5 years is shown in **Figure 6D**. The distribution plot of the risk score and survival status showed that the higher the risk score, the more deaths of patients with STAD (**Figures 6E, F**).The expression of 14 m^{6}A-related prognostic lncRNAs in the training group, the test group and the combined group, was displayed as a heat map (**Figures 6G**).

To examine whether the risk score was an independent prognostic factor, univariate and multivariate Cox regression analyses were conducted. In the training group, the risk score was significantly associated with OS both in univariate and multivariate Cox regression analyses ($p < 0.001$), in addition to age at diagnosis and pathological stage ($p < 0.05$). It should be noted that the risk score was also closely related with OS in the test group ($p < 0.05$) and the combined group ($p < 0.001$) by the same analysis, which indicated that the risk score was an independent powerful prognostic factor for the prognosis of OS in STAD **(Figures 7A, B)**.

Subgroup Analysis With Different Clinicopathological Features and Immune Landscape

The expression of 14 m^{6}A-related prognostic lncRNAs and the distribution of clinicopathological characteristics, the immune scores of TME, and the clustering of patients in the high-risk and low-risk groups were displayed as a heat map **(Figure 7C)**. Evident differences between the two groups according to different clusters ($p < 0.001$) were observed. Significant differences of risk score were found between (1): different tumor grades ($p < 0.01$) (2), different immune scores of TME ($p < 0.05$), and (3) different clusters ($p < 0.01$) **(Figure 7D)**.

To evaluate whether the m^{6}A-related lncRNAs prognostic model could serve as a prognostic indicator for OS in subgroups of patients with different clinical characteristics, we stratified subgroups by age (age ≤65 and age >65), gender (female and male), grade (G1–G2 and G3), clinical stage (stages I–II and III–IV), stage T (T1–T2 and T3–T4), stage M (M0 and M1), and stage N (N0 and N1). As the result shown in **Figure 8**, the OS of the low-risk patients based on age ($p = 0.004$ in age ≤65 and $p < 0.001$ in age >65), sex ($p = 0.004$ in female and $p < 0.001$ in male), grade ($p = 0.006$ in G1–G2 and $p < 0.001$ in G3), clinical stage ($p = 0.017$ in stages I–II and $p < 0.001$ in stages III–IV), stage T3–T4 ($p < 0.001$), stage M0 ($p < 0.001$), and stage N ($p = 0.014$ in N0 and $p < 0.001$ in N1) was significantly higher than those of the high-risk patients.

Furthermore, we analyzed the association between immune cells and ICGs and subgroups. As a result, we found that the high-risk group had significant positive correlations with infiltrating levels of resting DC ($r = 0.17$, $p = 0.025$), eosinophils ($r = 0.23$, $p = 0.0026$), M2 macrophages ($r = 0.23$, $p = 0.0022$), resting mast cells ($r = 0.18$, $p = 0.015$), monocytes ($r = 0.27$, $p = 0.00035$), memory resting CD4 T cells ($r = 0.28$, $p = 0.00015$) **(Figures 9A–F)**, and the low-risk group had significant positive correlations with infiltrating levels of M0 macrophages ($r = -0.25$, $p = 0.00086$), plasma cells ($r = -0.18$, $p = 0.017$), follicular helper T cells ($r = -0.23$, $p = 0.0026$), regulatory T cells ($r = -0.18$, $p = 0.017$) **(Figures 9G–J)**. Next, we observed that four ICGs (namely, JAK2, LAMA3, PDCD1LG2, JAK1) were significantly high expression in high-risk group and six ICGs (namely, YTHDF1, TNFRSF18, TNFRSF4, PVR, PDCD1, IFNG) were significantly high expression in low-risk group **(Figure 5C)**. Furthermore, the difference in the response of ICIs between high-risk and low-risk groups was explored. As a result, the low-risk group was more likely to respond to immunotherapy than the high-risk group whether they were compared in IPS-PD1(+)/CTLA4(+), IPS-PD1(+)/CTLA4(−), IPS-PD1(−)/CTLA4(+), and IPS-PD1(−)/CTLA4(−) **(Figure 10)**.

Construction of the ceRNA Network and Functional Enrichment Analysis

To explore the biological function of 19 m^{6}A-related prognostic lncRNAs, a ceRNA network was constructed based on the mechanism of lncRNAs regulating mRNAs expression by sponging miRNAs. Two lncRNAs were extracted from the miRcode database and 28 pairs of interaction between the Two lncRNAs and 24 miRNAs were identified. Based on three mRNA predicting databases mentioned previously and differentially expressed mRNA between the normal and tumor groups of STAD in TCGA, we identified 70 target mRNA. Finally, two lncRNAs, 24 miRNAs, and 70 mRNAs were included to construct ceRNA by Cytoscape software 3.7.1 **(Figure 11A)**. KEGG pathways and GO analysis were performed to annotate the function of 70 target mRNAs, and we found that these target mRNAs were enriched in transcription coactivator activity and tubulin binding (GO analysis); microRNAs in cancer, MAPK signaling pathway, proteoglycans in cancer, PI3K-Akt signaling pathway, focal adhesion, Rap1 signaling pathway, and Ras signaling pathway (KEGG pathways) **(Figures 11B, C)**.

As we stratified the patients with STAD into clusters I and II or high-risk and low-risk groups, genes that were significantly upregulated (fold change >1 and $p < 0.05$) or downregulated (fold change <−1 and $p < 0.05$) between the different clusters or different subgroups were identified using the "edgeR" package in R. GO and KEGG pathways analysis were used for biological functional analysis. Concerning the differentially expressed genes between different clusters, these genes were associated with immune-related biological processes, such as "antigen binding" and "immunoglobulin receptor binding," and malignancy-associated pathways, including "focal adhesion" and "Wnt signaling pathway." The differentially expressed genes between the high-risk and the low-risk groups were enriched in

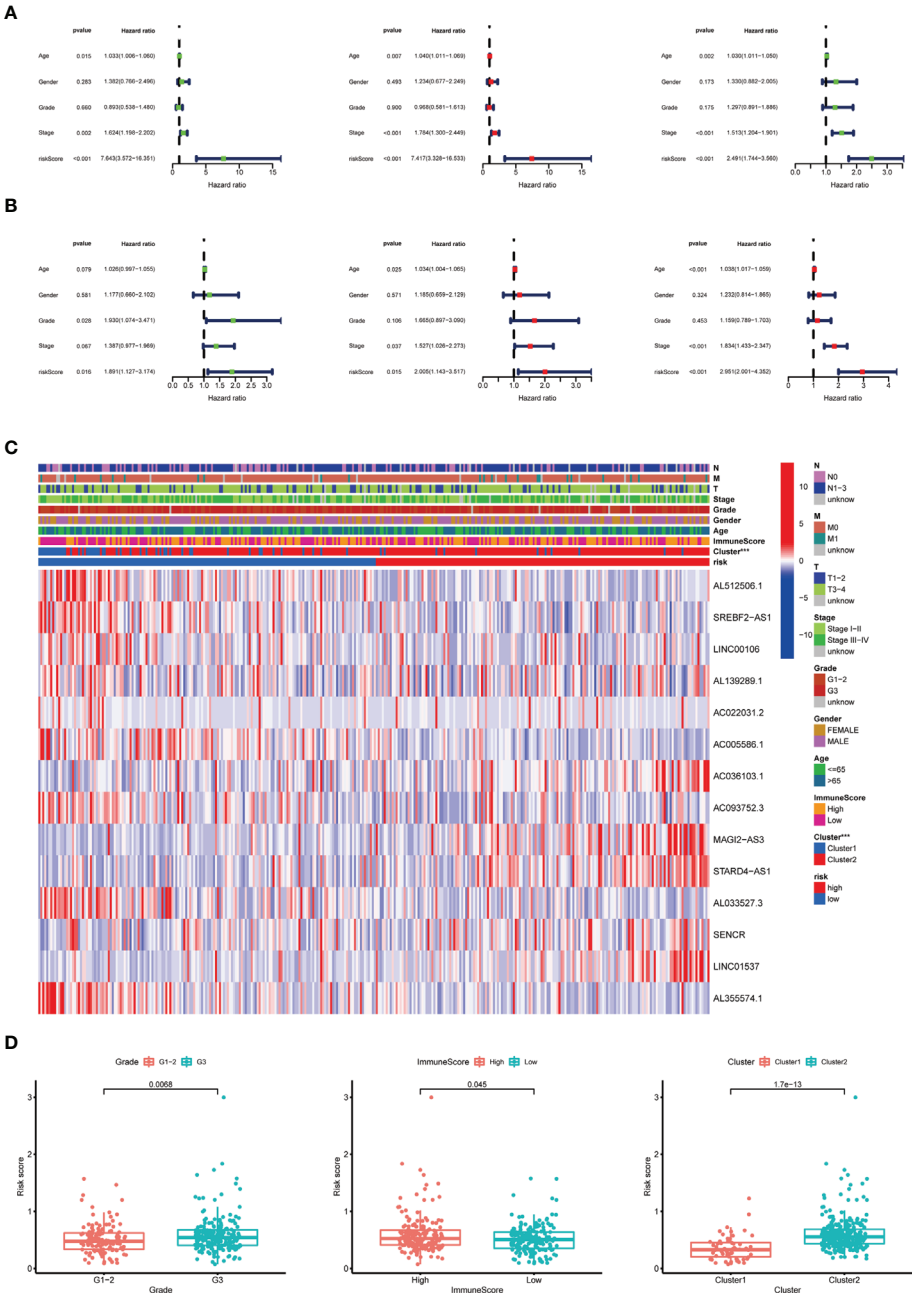

FIGURE 7 | Relationship between the risk score and clinicopathological characteristics. **(A)** Univariate Cox regression analysis of the association between clinicopathological factors (including risk score) and OS of patients in the training group, the test group, and the combined group. **(B)** Multivariate Cox regression analysis of the association between clinicopathological factors (including risk score) and OS of patients in the training group, the test group, and the combined group. **(C)** The heat map showed the expression of 14 m^{6}A-related prognostic lncRNAs, the distribution of clinicopathological characteristics, the immune scores of TME, and the clustering of patients in the high-risk and low-risk groups. ***$p < 0.001$. **(D)** The risk score was significantly higher in patients with higher-grade tumors ($p < 0.01$), higher immune scores of TME ($p < 0.05$), and cluster II ($p < 0.01$).

malignancy-associated biological processes and pathways, containing "chemokine receptor binding", "chemokine activity (GO analysis)", and "focal adhesion" and "Wnt signaling pathway (KEGG pathway) **(Figures 11B, C)**".

Furthermore, we used GSEA to predict the functional difference between clusters I and II or between the high-risk and the low-risk groups. The results showed that cluster II had a worse OS and a lower 5-year survival rate was closely related with

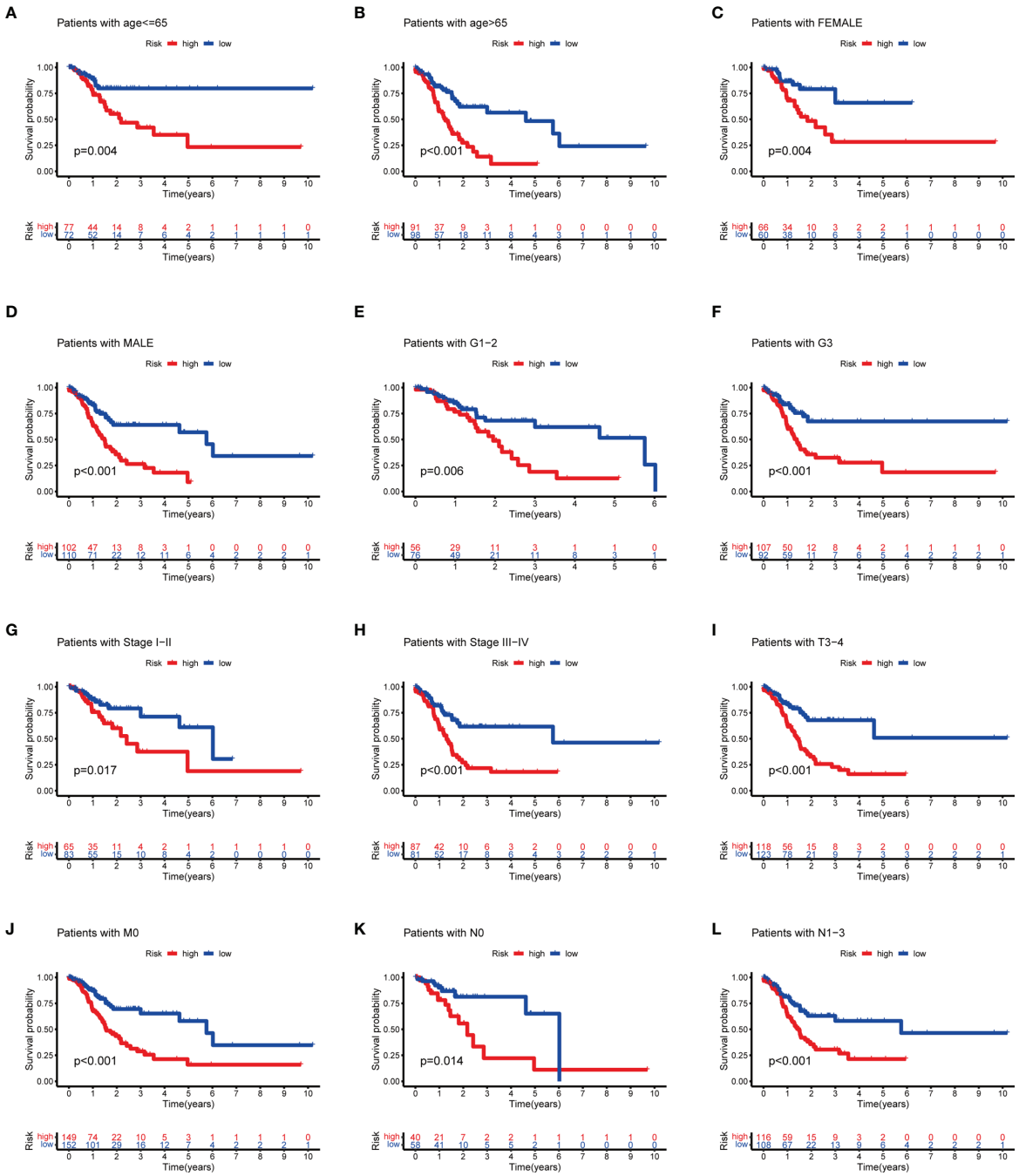

FIGURE 8 | Subgroup analysis with different clinicopathological features in STAD: **(A)** age ≤65; **(B)** age >65; **(C)** female; **(D)** male; **(E)** G1–G2; **(F)** G3; **(G)** stages I–II; **(H)** stage III–IV; **(I)** T3–T4; **(J)** M0; **(K)** N0; and **(L)** N1.

the malignant hallmarks of cancer, such as "focal adhesion", "ECM-receptor interaction", and "cell adhesion molecules (CAMs)" and immune-related pathway, such as, "complement and coagulation cascades". The high-risk group was also associated with cancer-related pathways, which were similar to cluster II (**Figure 12**).

Validation of the Expression Levels of the m^{6}A-Related lncRNA in Cell Lines

For validating the expression levels of the m^{6}A-related prognostic lncRNAs from prognostic signature, we detected six m^{6}A-related prognostic lncRNA expression levels in GC cell line MGC-803 and normal human gastric epithelial cell line GES-1.

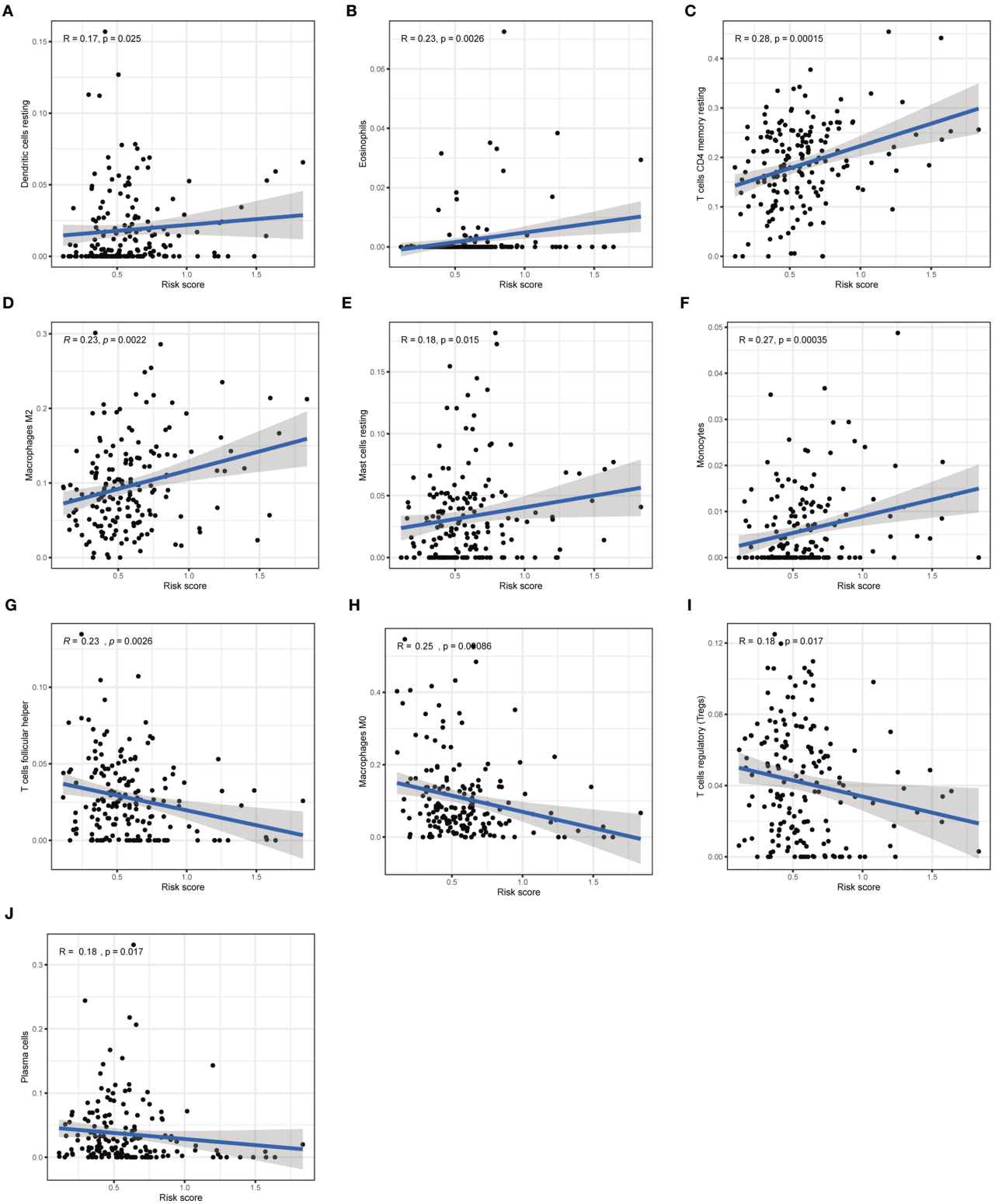

FIGURE 9 | Correlation of subgroup with immune infiltration level in STAD. **(A–F)** The high-risk group has significant positive correlations with resting DC, eosinophils, memory resting CD4 T cells, M2 macrophages, resting mast cells, and monocytes. **(G–J)** The high-risk group has significant negative correlations with M0 macrophages, plasma cells, follicular helper T cells, and regulatory T cells.

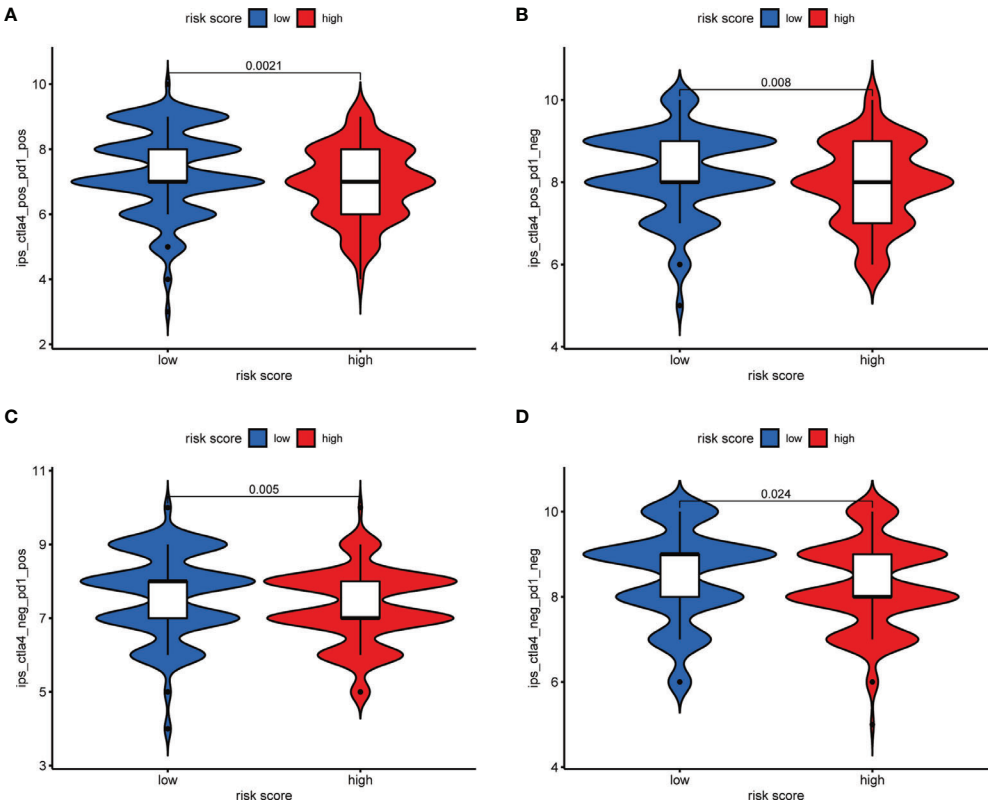

FIGURE 10 | The relative probabilities to respond to anti-PD-1/PD-L1 and anti-CTLA-4 treatment in the low-risk score and high-risk score group. **(A)** IPS-PD1(+)/CTLA4(+). **(B)** IPS-PD1(–)/CTLA4(+). **(C)** IPS-PD1(+)/CTLA4(–). **(D)** IPS-PD1(–)/CTLA4(–).

Our results showed that LINC01537 and MAGI2-AS3 were significantly downregulated in MGC-803 compared with GES-1 while LINC00106 and STARD4-AS1 were significantly upregulated. SREBF2-AS1 was highly expressed in MGC-803 and SENCR was lowly expressed in MGC-803, but they had no significant difference in cells (**Figure 13**).

DISCUSSION

Recently, an increasing number of studies focusing on the role of lncRNAs in GC proved that lncRNAs exerted a critical oncogenic role based on their dysregulated expression and localization (35). Additionally, as the most abundant posttranscriptional modification in eukaryotic noncoding RNAs (ncRNAs), m^{6}A has a huge effect on its stability and transport (36–38). Previous studies have shown that m^{6}A "writers" and "erasers" could adjust the levels of m^{6}A modification in mRNAs and ncRNAs to regulate binding sites to m^{6}A "reader" proteins. Different m^{6}A reader proteins recognize and bind to methylated ncRNAs to perform different functions. For instance, YTHDF3 recognizes and binds to m^{6}A-modified lncRNA GAS5 and promotes its degradation, which elevates YAP expression and promotes colorectal cancer (CRC) progression (39). The m^{6}A mark increases the stability of lncRNA FAM225A, which promotes the progression of nasopharyngeal carcinoma by acting as ceRNA to sponge miR-590-3p/miR-1275 (40). IGF2BP2 recognizes and binds to m^{6}A-modified circRNA NSUN2 and increases its export to the cytoplasm (41). Overexpression METTL3 can significantly increase the nuclear localization of lncRNA RP11 in CRC cells (42). Additionally, copious studies have shown that m^{6}A RNA modification affects the maturation and response function of immune cells in tumor immunity and could remodel TME (43, 44). For example, durable neoantigen-specific immunity is regulated by m^{6}A-modified mRNA through YTHDF1 (45). METTL3-mediated m^{6}A of CD40, CD80, and TLR4 signaling adaptor Tirap transcripts could enhance their translation in DC for stimulating T-cell activation (46). Moreover, some studies have indicated that m^{6}A-modified lncRNAs participate in the immune response. As DC migration is critical for the protective immunity and immune homeostasis, m^{6}A modification promotes the degradation of lncRNA Dpf3, which is associated with DC migration (47). Thus, in consideration of the crucial role of lncRNAs, m^{6}A RNA modification, and immunity response in STAD, these researches call our attention to investigate the gene profile of m^{6}A-related lncRNAs in STAD, explore whether m^{6}A-related lncRNAs could serve as ideal biomarkers for STAD prognosis and participate in STAD initiation, progression, TME, and immunotherapy.

In our study, a total of 373 samples, 406 patients with STAD, 24 m^{6}A-related regulators, and 13,162 lncRNAs were included to

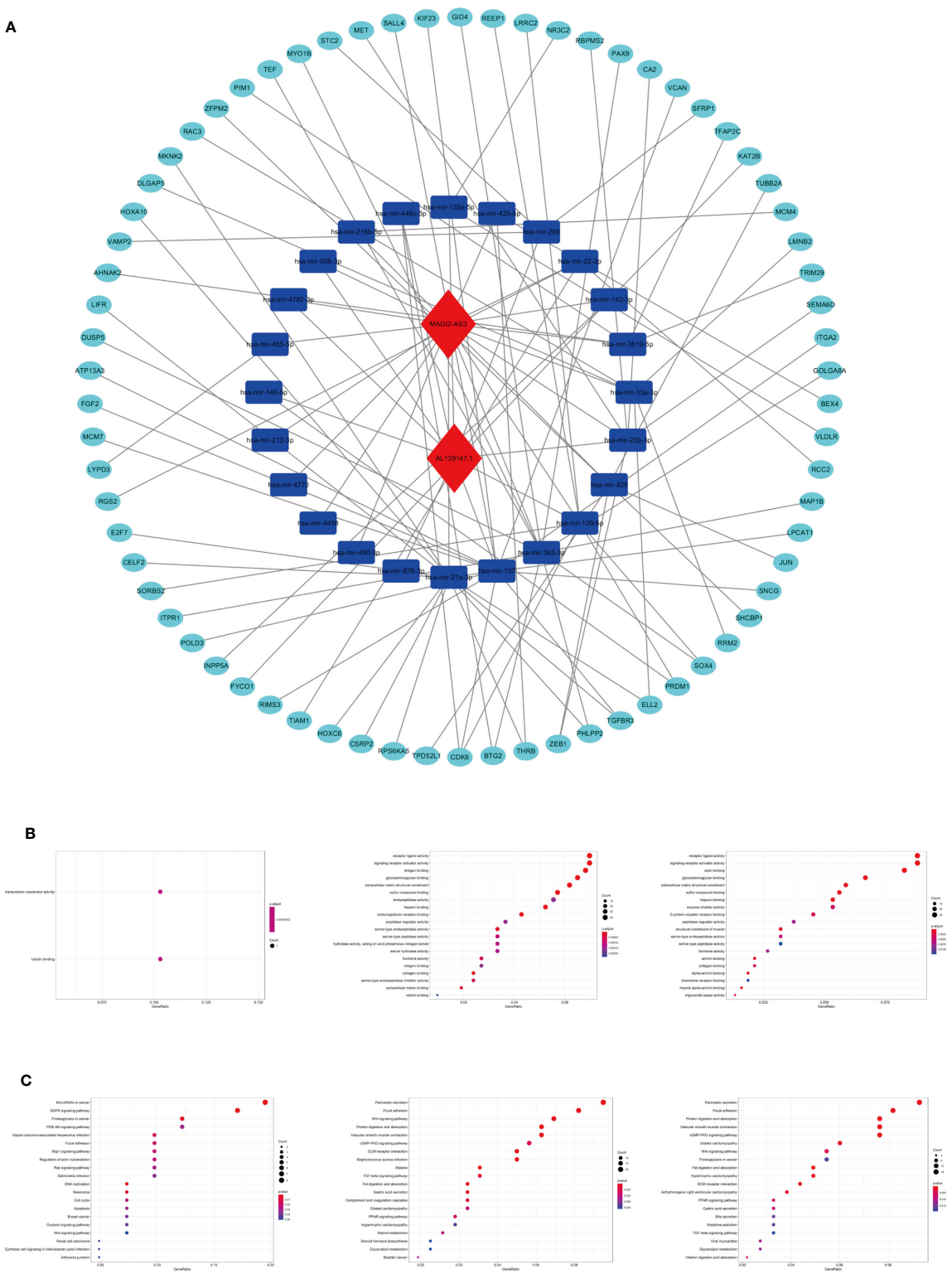

FIGURE 11 | The ceRNA network construction and biological function analysis. **(A)** The ceRNA network of two lncRNAs (red) and their target miRNAs (blue) and mRNAs (green). **(B)** GO analysis in 70 target mRNAs, differentially expressed genes between cluster I and cluster II, differentially expressed genes between the high-riska and the low-risk group. **(C)** KEGG pathway analysis in 70 target mRNAs, differentially expressed genes between cluster I and cluster II, differentially expressed genes between the high-risk group and the low-risk group.

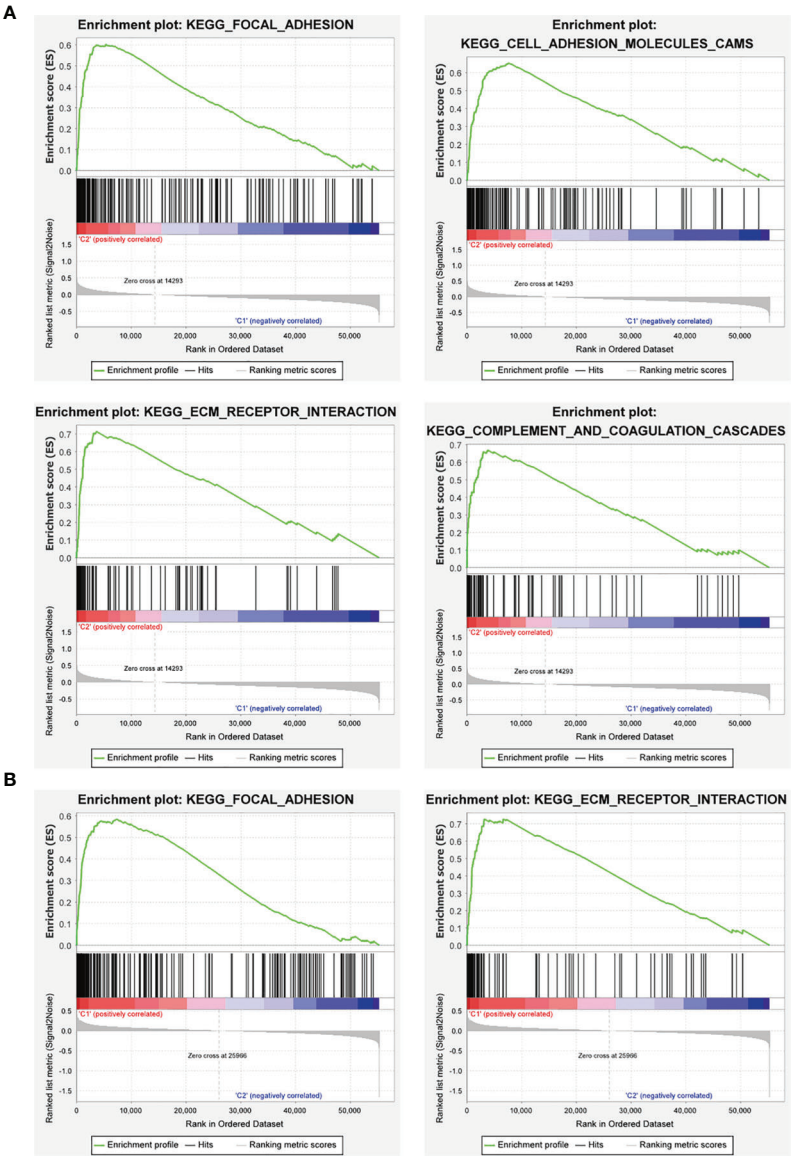

FIGURE 12 | GSEA analysis of the cluster II and the high-risk group. **(A)** The cluster II was mainly enriched in "focal adhesion", "ECM-receptor interaction", and "cell adhesion molecules (CAMs)", and "complement and coagulation cascades". **(B)** The high-risk group was mainly enriched in "focal adhesion" and "ECM-receptor interaction".

exploit the specific role of m^{6}A-related lncRNAs in STAD. Nineteen candidate lncRNAs that were highly correlated with OS were identified. Based on the expression of 19 m^{6}A-related prognostic lncRNAs, patients with STAD were clustered into two clusters (clusters I and II), which had significant differences in the OS rate and tumor grade. Then, 14 of 19 m^{6}A-related prognostic lncRNAs were used to establish a prognostic signature with the LASSO method in the training group. Kaplan-Meier analysis showed that the OS of patients with low-risk scores was longer than those of patients with high-risk scores. Additionally, the result of ROC curve analysis indicated that the 14-lncRNAs signature could serve as a highly specific and sensitive prognostic survival model in STAD. Moreover, the results were further validated in the test groups and in the combined group. This signature can be used as an independent prognostic factor for STAD, suggesting that these 14 lncRNAs may be vital m^{6}A-related lncRNAs and significant prognostic factors for patients with STAD. Furthermore, this m^{6}A-related lncRNA prognostic model could serve as a prognostic indicator for OS in subgroups of patients with different clinical characteristics, especially age, sex, tumor grade, clinical stage, stages T3–T4, stage M0, and stage N.

Moreover, different clusters or subgroups were correlated with diverse TME scores, immune infiltration cells, and ICGs

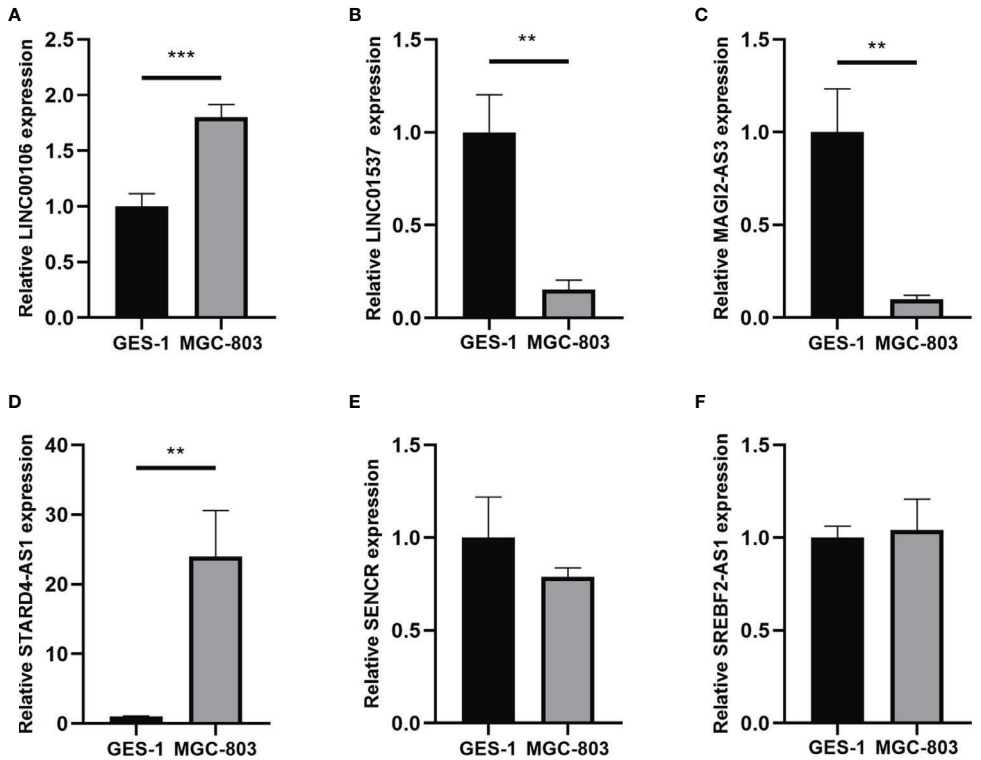

FIGURE 13 | **(A–F)** Expression of six lncRNAs from the prognostic signature in GC cell line MGC-803 and normal human gastric epithelial cell line GES-1. $^{**}p < 0.01$, and $^{***}p < 0.001$.

expression, which suggested that m^{6}A-related lncRNAs may play a critical regulatory role in the TME and immune exhaustion of STAD. The tumor purity of cluster II that was associated with poorer OS and the high-risk group decreased, which indicated the promotion role of stromal cells and the dysfunction of immune infiltration cells in STAD. Fibroblasts, the most abundant stromal cell, could promote tumor proliferation and metastasis by secreting cytokines, growth factors, and chemokines and the remodeling of extracellular matrix (ECM) (48). Concerning immune infiltration cells, there is a significant positive correlation between M2 macrophages and cluster II and the high-risk group, which implicated the potential regulatory role of m^{6}A-related lncRNAs in the polarization of tumor-associated macrophages. M2 macrophages could facilitate tumor occurrence and metastasis through the inhibition of T-cell-mediated antitumor immune response and the promotion of tumor angiogenesis (49). Although abundant immune cells infiltrated in TME, they could not lead to the antitumor immune response because of immune checkpoints blockade and the effects of hypoxia and metabolic alternation. To be more specific, hypoxia is strongly linked to immunosuppression *via* immune trafficking, angiogenesis, and alteration of molecular markers, which has hugely detrimental effects on T-cell function (50). Similarly, metabolic alternation also can lead to T-cell suppression, which was related to a host of metabolic byproducts (51). Moreover, as our results showed, some prominent ICGs, such as PDCD1LG2, HAVCR2, and ICOS, were significantly overexpressed in cluster II and the high-risk group, which resulted in immune exhaustion in TME. In addition, we discovered the difference in the response to ICIs between subgroups. Together, these findings suggest that the m^{6}A-related lncRNAs may play a potential influence on the dysfunction of immune infiltration cells and the response to immunotherapy in STAD.

To provide a comprehensive analysis of m^{6}A-related lncRNAs, a ceRNA network consisting of two lncRNAs, 24 miRNAs, and 70 mRNAs was constructed, and differentially expressed genes between different clusters or subgroups were identified for viewing the latent functions of m^{6}A-related lncRNAs. With the two key m^{6}A-related lncRNAs found in STAD, lncRNA MAGI2-AS3 has been reported to be associated with patient clinical characteristics in different tumors and can regulate a variety of biological processes (52). MAGI2-AS3 significantly promoted GC progression and migration *via* maintaining ZEB1 overexpression by sponging miR-141/200a (53). KEGG pathway and GO analysis shows that 70 target mRNAs and differentially expressed genes between different clusters or subgroups were enriched in several biological processes and pathways associated with the occurrence and progression of STAD (54–56), including "MAPK signaling pathway," "PI3K-Akt signaling pathway," "Wnt signaling pathway," "focal adhesion," and so on. Genes in different clusters or subgroups were functionally annotated using GSEA.

Genes in cluster II and the high-risk group were also enriched in the cancer-related pathways. In addition, it should be noted that several biological processes and pathways associated with immune response were identified, such as "antigen binding", "immunoglobulin receptor binding", and "complement and coagulation cascades". Previous studies have demonstrated that the activation of the complement system and coagulation cascades plays an important role in cancer malignant biological behavior (57–59).

CONCLUSION

In this study, we identified two clusters based on 19 m^{6}A-related lncRNAs and constructed a prognostic signature comprising 14 m^{6}A-related lncRNAs in STAD, which had significant value in predicting the OS of patients with STAD, clinicopathological characteristics, TME, ICGs expression, and the response to ICIs. Additionally, biological processes and pathways associated with m^{6}A-related lncRNAs were identified, which improved our understanding of the role of m^{6}A-related lncRNAs in the occurrence and progression of STAD. This work also provides important evidence for the development of predictive biomarkers and immunotherapy for STAD.

DATA AVAILABILITY STATEMENT

Publicly available datasets were analyzed in this study, which can be found in the Cancer Genome Atlas (TCGA) database.

ETHICS STATEMENT

This study met the publication guidelines stated by TCGA (https://cancergenome.nih.Gov/publications/publicationguidelines). All data used in the study were obtained from TCGA. Ethics approval and informed consent were not required.

AUTHOR CONTRIBUTIONS

YH, PL, and FL conceived and designed the study. YH, ZY, CH, XJ, and YY organized the database and performed statistical analyses. YH and YW wrote the first draft of the manuscript. ZY, CH, and XJ prepared the figures and tables and were involved in manuscript writing. KZ, YW, PL, and FL revised and proofread the manuscript. All authors contributed to the article and approved the submitted version.

FUNDING

This study was supported by The National Natural Science Foundation (No. 81904139, No. 81973819, and No. 81904145), Collaborative Innovation Team Project of First-Rate Universities and Disciplines and High-level University Discipline of Guangzhou University of Chinese Medicine (No. 2021xk47), The Natural Science Foundation of Guangdong Province (No. 2019A1515011145), Guangdong Medical Science and Technology Research Fund (No. B2021089, No. A2020186), Clinical Research Project of Innovation Hospital in the First Affiliated Hospital of Guangzhou University of Chinese Medicine (No. 2019IIT19), and High-level Hospital Construction project of the First Affiliated Hospital of Guangzhou University of Chinese Medicine (No. 2019QN01).

ACKNOWLEDGMENTS

This study benefited from the Cancer Genome Atlas (TCGA) databases. We appreciate the data platform and the authors uploaded their data.

REFERENCES

1. Bray F, Ferlay J, Soerjomataram I, Siegel RL, Torre LA, Jemal A. Global Cancer Statistics 2018: GLOBOCAN Estimates of Incidence and Mortality Worldwide for 36 Cancers in 185 Countries. *CA Cancer J Clin* (2018) 68:394–424. doi: 10.3322/caac.21492
2. Rugge M, Meggio A, Pravadelli C, Barbareschi M, Fassan M, Gentilini M, et al. Gastritis Staging in the Endoscopic Follow-Up for the Secondary Prevention of Gastric Cancer: A 5-Year Prospective Study of 1755 Patients. *GUT* (2019) 68:11–7. doi: 10.1136/gutjnl-2017-314600
3. Digklia A, Wagner AD. Advanced Gastric Cancer: Current Treatment Landscape and Future Perspectives. *World J Gastroenterol* (2016) 22:2403–14. doi: 10.3748/wjg.v22.i8.2403
4. Sexton RE, Al HM, Diab M, Azmi AS. Gastric Cancer: A Comprehensive Review of Current and Future Treatment Strategies. *Cancer Metastasis Rev* (2020) 39:1179–203. doi: 10.1007/s10555-020-09925-3
5. Huang J, Chen YX, Zhang B. IGF2-AS Affects the Prognosis and Metastasis of Gastric Adenocarcinoma *via* Acting as a ceRNA of miR-503 to Regulate SHOX2. *Gastric Cancer* (2020) 23:23–38. doi: 10.1007/s10120-019-00976-2
6. Xie M, Ma T, Xue J, Ma H, Sun M, Zhang Z, et al. The Long Intergenic non-Protein Coding RNA 707 Promotes Proliferation and Metastasis of Gastric Cancer by Interacting With mRNA Stabilizing Protein HuR. *Cancer Lett* (2019) 443:67–79. doi: 10.1016/j.canlet.2018.11.032
7. Zhang F, Wang H, Yu J, Yao X, Yang S, Li W, et al. LncRNA CRNDE Attenuates Chemoresistance in Gastric Cancer *via* SRSF6-Regulated Alternative Splicing of PICALM. *Mol Cancer* (2021) 20:6. doi: 10.1186/s12943-020-01299-y
8. Begik O, Lucas MC, Liu H, Ramirez JM, Mattick JS, Novoa EM. Integrative Analyses of the RNA Modification Machinery Reveal Tissue- and Cancer-Specific Signatures. *Genome Biol* (2020) 21:97. doi: 10.1186/s13059-020-02009-z
9. Barbieri I, Kouzarides T. Role of RNA Modifications in Cancer. *Nat Rev Cancer* (2020) 20:303–22. doi: 10.1038/s41568-020-0253-2
10. Nombela P, Miguel-López B, Blanco S. The Role of M(6)A, M(5)C and Ψ RNA Modifications in Cancer: Novel Therapeutic Opportunities. *Mol Cancer* (2021) 20:18. doi: 10.1186/s12943-020-01263-w
11. Xie S, Chen W, Chen K, Chang Y, Yang F, Lin A, et al. Emerging Roles of RNA Methylation in Gastrointestinal Cancers. *Cancer Cell Int* (2020) 20:585. doi: 10.1186/s12935-020-01679-w
12. He PC, He C. M(6) A RNA Methylation: From Mechanisms to Therapeutic Potential. *EMBO J* (2021) 40:e105977. doi: 10.15252/embj.2020105977
13. Karthiya R, Khandelia P. M6a RNA Methylation: Ramifications for Gene Expression and Human Health. *Mol Biotechnol* (2020) 62:467–84. doi: 10.1007/s12033-020-00269-5

14. Wang Q, Chen C, Ding Q, Zhao Y, Wang Z, Chen J, et al. METTL3-Mediated M(6)A Modification of HDGF mRNA Promotes Gastric Cancer Progression and has Prognostic Significance. *Gut* (2020) 69:1193–205. doi: 10.1136/gutjnl-2019-319639
15. Sun Y, Li S, Yu W, Zhao Z, Gao J, Chen C, et al. N(6)-Methyladenosine-Dependent pri-miR-17-92 Maturation Suppresses PTEN/TMEM127 and Promotes Sensitivity to Everolimus in Gastric Cancer. *Cell Death Dis* (2020) 11:836. doi: 10.1038/s41419-020-03049-w
16. Yan J, Huang X, Zhang X, Chen Z, Ye C, Xiang W, et al. LncRNA LINC00470 Promotes the Degradation of PTEN mRNA to Facilitate Malignant Behavior in Gastric Cancer Cells. *Biochem Biophys Res Commun* (2020) 521:887–93. doi: 10.1016/j.bbrc.2019.11.016
17. Lou X, Wang JJ, Wei YQ, Sun JJ. Emerging Role of RNA Modification N6-Methyladenosine in Immune Evasion. *Cell Death Dis* (2021) 12:300. doi: 10.1038/s41419-021-03585-z
18. Shulman Z, Stern-Ginossar N. The RNA Modification N(6)-Methyladenosine as a Novel Regulator of the Immune System. *Nat Immunol* (2020) 21:501–12. doi: 10.1038/s41590-020-0650-4
19. Li M, Zha X, Wang S. The Role of N6-Methyladenosine mRNA in the Tumor Microenvironment. *Biochim Biophys Acta Rev Cancer* (2021) 1875:188522. doi: 10.1016/j.bbcan.2021.188522
20. Mortazavi A, Williams BA, McCue K, Schaeffer L, Wold B. Mapping and Quantifying Mammalian Transcriptomes by RNA-Seq. *Nat Methods* (2008) 5:621–8. doi: 10.1038/nmeth.1226
21. Jiang X, Liu B, Nie Z, Duan L, Xiong Q, Jin Z, et al. The Role of M6a Modification in the Biological Functions and Diseases. *Signal transduction targeted Ther* (2021) 6:74–4. doi: 10.1038/s41392-020-00450-x
22. Zhou KI, Shi H, Lyu R, Wylder AC, Matuszek Ż, Pan JN, et al. Regulation of Co-Transcriptional Pre-mRNA Splicing by M(6)A Through the Low-Complexity Protein hnRNPG. *Mol Cell* (2019) 76:70–81.e9. doi: 10.1016/j.molcel.2019.07.005
23. Yang Y, Hsu PJ, Chen YS, Yang YG. Dynamic Transcriptomic M(6)A Decoration: Writers, Erasers, Readers and Functions in RNA Metabolism. *Cell Res* (2018) 28:616–24. doi: 10.1038/s41422-018-0040-8
24. Wilkerson MD, Hayes DN. ConsensusClusterPlus: A Class Discovery Tool With Confidence Assessments and Item Tracking. *Bioinformatics* (2010) 26:1572–3. doi: 10.1093/bioinformatics/btq170
25. Yang S, Wu Y, Deng Y, Zhou L, Yang P, Zheng Y, et al. Identification of a Prognostic Immune Signature for Cervical Cancer to Predict Survival and Response to Immune Checkpoint Inhibitors. *Oncoimmunology* (2019) 8: e1659094. doi: 10.1080/2162402X.2019.1659094
26. Newman AM, Steen CB, Liu CL, Gentles AJ, Chaudhuri AA, Scherer F, et al. Determining Cell Type Abundance and Expression From Bulk Tissues With Digital Cytometry. *Nat Biotechnol* (2019) 37:773–82. doi: 10.1038/s41587-019-0114-2
27. Yoshihara K, Shahmoradgoli M, Martínez E, Vegesna R, Kim H, Torres-Garcia W, et al. Inferring Tumour Purity and Stromal and Immune Cell Admixture From Expression Data. *Nat Commun* (2013) 4:2612. doi: 10.1038/ncomms3612
28. Hanley JA, McNeil BJ. The Meaning and Use of the Area Under a Receiver Operating Characteristic (ROC) Curve. *Radiology* (1982) 143:29–36. doi: 10.1148/radiology.143.1.7063747
29. Simon N, Friedman J, Hastie T, Tibshirani R. Regularization Paths for Cox's Proportional Hazards Model *via* Coordinate Descent. *J Stat Softw* (2011) 39:1–13. doi: 10.18637/jss.v039.i05
30. Patel SJ, Sanjana NE, Kishton RJ, Eidizadeh A, Vodnala SK, Cam M, et al. Identification of Essential Genes for Cancer Immunotherapy. *Nature* (2017) 548:537–42. doi: 10.1038/nature23477
31. Nishino M, Ramaiya NH, Hatabu H, Hodi FS. Monitoring Immune-Checkpoint Blockade: Response Evaluation and Biomarker Development. *Nat Rev Clin Oncol* (2017) 14:655–68. doi: 10.1038/nrclinonc.2017.88
32. Wang J, Sanmamed MF, Datar I, Su TT, Ji L, Sun J, et al. Fibrinogen-Like Protein 1 Is a Major Immune Inhibitory Ligand of LAG-3. *Cell* (2019) 176:334–47.e12. doi: 10.1016/j.cell.2018.11.010
33. Zhang Q, Bi J, Zheng X, Chen Y, Wang H, Wu W, et al. Blockade of the Checkpoint Receptor TIGIT Prevents NK Cell Exhaustion and Elicits Potent Anti-Tumor Immunity. *Nat Immunol* (2018) 19:723–32. doi: 10.1038/s41590-018-0132-0
34. Han D, Liu J, Chen C, Dong L, Liu Y, Chang R, et al. Anti-Tumour Immunity Controlled Through mRNA M(6)A Methylation and YTHDF1 in Dendritic Cells. *Nature* (2019) 566:270–4. doi: 10.1038/s41586-019-0916-x
35. Xie S, Chang Y, Jin H, Yang F, Xu Y, Yan X, et al. Non-Coding RNAs in Gastric Cancer. *Cancer Lett* (2020) 493:55–70. doi: 10.1016/j.canlet.2020.06.022
36. He RZ, Jiang J, Luo DX. The Functions of N6-Methyladenosine Modification in lncRNAs. *Genes Dis* (2020) 7:598–605. doi: 10.1016/j.gendis.2020.03.005
37. Zhang L, Hou C, Chen C, Guo Y, Yuan W, Yin D, et al. The Role of N(6)-Methyladenosine (M(6)A) Modification in the Regulation of circRNAs. *Mol Cancer* (2020) 19:105. doi: 10.1186/s12943-020-01224-3
38. Chen Y, Lin Y, Shu Y, He J, Gao W. Interaction Between N(6)-Methyladenosine (M(6)A) Modification and Noncoding RNAs in Cancer. *Mol Cancer* (2020) 19:94. doi: 10.1186/s12943-020-01207-4
39. Ni W, Yao S, Zhou Y, Liu Y, Huang P, Zhou A, et al. Long Noncoding RNA GAS5 Inhibits Progression of Colorectal Cancer by Interacting With and Triggering YAP Phosphorylation and Degradation and is Negatively Regulated by the M(6)A Reader YTHDF3. *Mol Cancer* (2019) 18:143. doi: 10.1186/s12943-019-1079-y
40. Zheng ZQ, Li ZX, Zhou GQ, Lin L, Zhang LL, Lv JW, et al. Long Noncoding RNA FAM225A Promotes Nasopharyngeal Carcinoma Tumorigenesis and Metastasis by Acting as ceRNA to Sponge miR-590-3p/miR-1275 and Upregulate Itgb3. *Cancer Res* (2019) 79:4612–26. doi: 10.1158/0008-5472.CAN-19-0799
41. Chen RX, Chen X, Xia LP, Zhang JX, Pan ZZ, Ma XD, et al. N(6)-Methyladenosine Modification of Circnsun2 Facilitates Cytoplasmic Export and Stabilizes HMGA2 to Promote Colorectal Liver Metastasis. *Nat Commun* (2019) 10:4695. doi: 10.1038/s41467-019-12651-2
42. Wu Y, Yang X, Chen Z, Tian L, Jiang G, Chen F, et al. M(6)A-Induced lncRNA RP11 Triggers the Dissemination of Colorectal Cancer Cells *via* Upregulation of Zeb1. *Mol Cancer* (2019) 18:87. doi: 10.1186/s12943-019-1014-2
43. Gu Y, Wu X, Zhang J, Fang Y, Pan Y, Shu Y, et al. The Evolving Landscape of N(6)-Methyladenosine Modification in the Tumor Microenvironment. *Mol Ther* (2021) 29:1703–15. doi: 10.1016/j.ymthe.2021.04.009
44. Zhang M, Song J, Yuan W, Zhang W, Sun Z. Roles of RNA Methylation on Tumor Immunity and Clinical Implications. *Front Immunol* (2021) 12:641507. doi: 10.3389/fimmu.2021.641507
45. Han D, Liu J, Chen C, Dong L, Liu Y, Chang R, et al. Anti-Tumour Immunity Controlled Through mRNA M(6)A Methylation and YTHDF1 in Dendritic Cells. *Nature* (2019) 566:270–4. doi: 10.1038/s41586-019-0916-x
46. Wang H, Hu X, Huang M, Liu J, Gu Y, Ma L, et al. Mettl3-Mediated mRNA M(6)A Methylation Promotes Dendritic Cell Activation. *Nat Commun* (2019) 10:1898. doi: 10.1038/s41467-019-09903-6
47. Liu J, Zhang X, Chen K, Cheng Y, Liu S, Xia M, et al. CCR7 Chemokine Receptor-Inducible lnc-Dpf3 Restrains Dendritic Cell Migration by Inhibiting HIF-1α-Mediated Glycolysis. *Immunity* (2019) 50:600–615.e15. doi: 10.1016/j.immuni.2019.01.021
48. Joshi RS, Kanugula SS, Sudhir S, Pereira MP, Jain S, Aghi MK. The Role of Cancer-Associated Fibroblasts in Tumor Progression. *Cancers* (2021) 13:1399. doi: 10.3390/cancers13061399
49. Pan Y, Yu Y, Wang X, Zhang T. Tumor-Associated Macrophages in Tumor Immunity. *Front Immunol* (2020) 11:583084. doi: 10.3389/fimmu.2020.583084
50. Augustin RC, Delgoffe GM, Najjar YG. Characteristics of the Tumor Microenvironment That Influence Immune Cell Functions: Hypoxia, Oxidative Stress, Metabolic Alterations. *Cancers* (2020) 12:3802. doi: 10.3390/cancers12123802
51. Kazemi MH, Najafi A, Karami J, Ghazizadeh F, Yousefi H, Falak R, et al. Immune and Metabolic Checkpoints Blockade: Dual Wielding Against Tumors. *Int Immunopharmacol* (2021) 94:107461. doi: 10.1016/j.intimp.2021.107461
52. Xue C, Li G, Lu J, Luo J, Jia J. Novel Insights for lncRNA MAGI2-AS3 in Solid Tumors. *BioMed Pharmacother* (2021) 137:111429. doi: 10.1016/j.biopha.2021.111429
53. Li D, Wang J, Zhang M, Hu X, She J, Qiu X, et al. LncRNA MAGI2-AS3 Is Regulated by BRD4 and Promotes Gastric Cancer Progression *via* Maintaining ZEB1 Overexpression by Sponging miR-141/200a. *Mol Ther Nucleic Acids* (2020) 19:109–23. doi: 10.1016/j.omtn.2019.11.003

54. Baghery SKA, Pourbagheri-Sigaroodi A, Pirsalehi A, Safaroghli-Azar A, Zali MR, Bashash D. The PI3K/Akt/mTOR Signaling Pathway in Gastric Cancer; From Oncogenic Variations to the Possibilities for Pharmacologic Interventions. *Eur J Pharmacol* (2021) 898:173983. doi: 10.1016/j.ejphar.2021.173983
55. Flanagan DJ, Vincan E, Phesse TJ. Winding Back Wnt Signalling: Potential Therapeutic Targets for Treating Gastric Cancers. *Br J Pharmacol* (2017) 174:4666–83. doi: 10.1111/bph.13890
56. Shi J. Pathogenetic Mechanisms in Gastric Cancer. *World J Gastroentero* (2014) 20:13804. doi: 10.3748/wjg.v20.i38.13804
57. Afshar-Kharghan V. The Role of the Complement System in Cancer. *J Clin Invest* (2017) 127:780–9. doi: 10.1172/JCI90962
58. Wang X, Wang E, Kavanagh JJ, Freedman RS. Ovarian Cancer, the Coagulation Pathway, and Inflammation. *J Transl Med* (2005) 3:25. doi: 10.1186/1479-5876-3-25
59. Richichi C, Fornasari L, Melloni G, Brescia P, Patanè M, Del BM, et al. Mutations Targeting the Coagulation Pathway are Enriched in Brain Metastases. *Sci Rep* (2017) 7:6573. doi: 10.1038/s41598-017-06811-x

Conflict of Interest: The authors declare that the research was conducted in the absence of any commercial or financial relationships that could be construed as a potential conflict of interest.

Publisher's Note: All claims expressed in this article are solely those of the authors and do not necessarily represent those of their affiliated organizations, or those of the publisher, the editors and the reviewers. Any product that may be evaluated in this article, or claim that may be made by its manufacturer, is not guaranteed or endorsed by the publisher.

frontiers in Oncology

ORIGINAL RESEARCH
published: 15 October 2021
doi: 10.3389/fonc.2021.734694

SNHG8 Promotes the Progression of Epstein–Barr Virus-Associated Gastric Cancer *via* Sponging miR-512-5p and Targeting TRIM28

Changyan Zou[1†], Jinrong Liao[1†], Dan Hu[2†], Ying Su[1], Huamei Lin[1], Keyu Lin[1], Xingguan Luo[3], Xiongwei Zheng[2], Lurong Zhang[1], Tao Huang[4*] and Xiandong Lin[1,5*]*

[1] Laboratory of Radiation Oncology and Radiobiology, Fujian Medical University Cancer Hospital and Fujian Cancer Hospital, Fuzhou, China, [2] Department of Pathology, Fujian Medical University Cancer Hospital and Fujian Cancer Hospital, Fuzhou, China, [3] Department of Genetics, Yale University School of Medicine, New Haven, CT, United States, [4] Bio-Med Big Data Center, Chinese Academy of Sciences (CAS) Key Laboratory of Computational Biology, Shanghai Institute of Nutrition and Health, Chinese Academy of Sciences, Shanghai, China, [5] Fujian Provincial Key Laboratory of Translational Cancer Medicine, Fuzhou, China

OPEN ACCESS

Edited by:
Kanjoormana Aryan Manu, Amala Cancer Research Centre, India

Reviewed by:
Kin Israel Notarte, University of Santo Tomas, Philippines
Wenliang Li, University of Texas Health Science Center at Houston, United States

***Correspondence:**
Xiandong Lin
linxdong1970@yeah.net
Tao Huang
tohuangtao@126.com
Lurong Zhang
lz8506@163.com

†These authors have contributed equally to this work

Specialty section:
This article was submitted to Gastrointestinal Cancers: Gastric & Esophageal Cancers, a section of the journal Frontiers in Oncology

Received: *01 July 2021*
Accepted: *23 September 2021*
Published: *15 October 2021*

Citation:
Zou C, Liao J, Hu D, Su Y, Lin H, Lin K, Luo X, Zheng X, Zhang L, Huang T and Lin X (2021) SNHG8 Promotes the Progression of Epstein–Barr Virus-Associated Gastric Cancer via Sponging miR-512-5p and Targeting TRIM28. Front. Oncol. 11:734694. doi: 10.3389/fonc.2021.734694

SNHG8, a family member of small nucleolar RNA host genes (SNHG), has been reported to act as an oncogene in gastric carcinoma (GC). However, its biological function in Epstein–Barr virus (EBV)-associated gastric cancer (EBVaGC) remains unclear. This study investigated the role of SNHG8 in EBVaGC. Sixty-one cases of EBVaGC, 20 cases of non-EBV-infected gastric cancer (EBVnGC), and relative cell lines were studied for the expression of SNHG8 and BHRF1 (BCL2 homolog reading frame 1) encoded by EBV with Western blot and qRT-PCR assays. The relationship between the expression levels of SNHG8 and the clinical outcome in 61 EBVaGC cases was analyzed. Effects of overexpression or knockdown of *BHRF1*, SNHG8, or *TRIM28* on cell proliferation, migration, invasion, and cell cycle and the related molecules were determined by several assays, including cell proliferation, colony assay, wound healing assay, transwell invasion assay, cell circle with flow cytometry, qRT-PCR, and Western blot for expression levels. The interactions among SNHG8, miR-512-5p, and *TRIM28* were determined with Luciferase reporter assay, RNA immunoprecipitation (RIP), pull-down assays, and Western blot assay. The *in vivo* activity of SNHG8 was assessed with SNHG8 knockdown tumor xenografts in zebrafish. Results demonstrated that the following. (1) *BHRF1* and SNHG8 were overexpressed in EBV-encoded RNA 1-positive EBVaGC tissues and cell lines. *BHRF1* upregulated the expressions of SNHG8 and TRIM28 in AGS. (2) SNHG8 overexpression had a significant correlation with tumor size and vascular tumor thrombus. Patients with high SNHG8 expression had poorer overall survival (OS) compared to those with low SNHG8 expression. (3) SNHG8 overexpression promoted EBVaGC cell proliferation, migration, and invasion *in vitro* and *in vivo*, cell cycle arrested at the G2/M phase *via* the activation of *BCL-2*, *CCND1*, *PCNA*, *PARP1*, *CDH1*, *CDH2 VIM*, and *Snail*. (4) Results of dual-luciferase reporter assay, RNA immunoprecipitation, and pull-down assays indicated that SNHG8 sponged miR-512-5p, which targeted on *TRIM28* and promoted cancer malignant behaviors of EBVaGC cells. Our data suggest

that BHRF1 triggered the expression of SNHG8, which sponged miR-512-5p and upregulated *TRIM28* and a set of effectors (such as *BCL-2*, *CCND1*, *CDH1*, *CDH2 Snail*, and VIM) to promote EBVaGC tumorigenesis and invasion. SNHG8 could be an independent prognostic factor for EBVaGC and sever as target for EBVaGC therapy.

Keywords: EBVaGC, SNHG8, miR-512-5p, *TRIM28*, cell proliferation, migration, invasion

INTRODUCTION

Epstein–Barr virus (EBV), belonging to the herpes virus family (1, 2), is a causative virus for many malignancies including nasopharyngeal carcinoma (NPC) and Burkitt lymphoma (3–5). The existence of the EBV genome in gastric cancer (GC) was first detected using a polymerase chain reaction (PCR) in 1990 (5, 6). So far, EBV has been detected in approximately 10% of gastric cancers worldwide (6, 7).

EBVaGC is a distinct subset of GC determined by comprehensive molecular analyses, which has unique clinical pathological features, including *PIK3CA* mutations, DNA hypermethylation, amplification of *JAK2* and *PD-L1*/*PD-L2* (1, 7). However, the underlying molecular mechanism of the development and progression of EBVaGC is unclear.

LncRNAs, non-coding RNAs with their sizes longer than 200 nucleic acids, were initially considered as "junk" or "genomic dark matter" without function (8, 9). However, recently, lncRNAs have been found to participate widely in various physiological and pathological processes, including cancer progression (9–12). Dysregulations of lncRNAs are associated with a variety of cancer malignant behaviors, such as cell migration, invasion, metastasis, gene transcription, and tumorigenesis (13, 14). For example, SNHG8, located on 4q26 and encoding small nucleolar RNAs (snoRNAs), was detected in multiple malignant tumors, including non-small-cell lung cancer, hepatocellular carcinoma (10, 15), and pancreatic adenocarcinoma (11, 16). LncRNAs, as oncogenes or tumor suppressors, are directly involved in tumorigenesis, cell cycle arrest, apoptosis, epithelial to mesenchymal transition (EMT), cell migration, invasion metastasis, and chemoresistance *via* activating the JAK2/STAT3 pathway or Wnt/β-catenin signaling (17–20). Therefore, lncRNAs might be excellent candidates for individualized treatments and monitoring the prognosis of gastric cancer.

We have reported that SNHG8 was a key regulator of EBVaGC by an integrative analysis of lncRNA and mRNA expression (21). This study was to explore the molecular mechanisms of SNHG8 contributing to the progression of EBVaGC *via* sponging miR-512-5p and targeting TRIM28 and a set of effectors.

Abbreviations: EBV, Epstein–Barr virus; GC, gastric carcinoma; EBVaGC, EBV-positive GC; EBVnGC, non-EBV-infected gastric cancer; RIP, RNA immunoprecipitation; OS, overall survival; ISH, *in situ* hybridization; EMT, epithelial–mesenchymal transition; TCGA, The Cancer Genome Atlas; SNHG8, small nucleolar RNA host gene 8; BHRF1, EBV-encoded small ribonucleic acid 1; TRIM28, tripartite motif-containing 28; RIP, RNA immunoprecipitation; EBER-1, Epstein–Barr encoding region 1; FFPE, formalin-fixed and paraffin-embedded; MTS, (4,5-dimethylthiazol)-3-(4-sulfophenyl)tetrazolium, inner salt; HBLV-SNHG8, pHBLV-CMV-mcs-3flag-EF1-ZsGReen-T2A-PURO inserted with SNHG8 gene; AGS-BX1/NC, empty vector of AGS-BX1 cell infection; AGS-BX1/SNHG8-OE, SNHG8 overexpression AGS-BX1 cell; AGS-BX1/SNHG8-SH, SNHG8 knockdown AGS-BX1 cell; AGS/BHRF1-OE, BHRF1 overexpression AGS cell; SNHG8-wt, SNHG8/miR-512-5p-binding site wild-type cells; SNHG8-mut, SNHG8/miR-512-5p-binding site mutant cells; TRIM28-wt, TRIM28/miR-512-5p-binding site wild-type cells; TRIM28-mut, TRIM28/miR-512-5p-binding site mutant cells; AGS-BX1/SNHG8-OE/TRIM28-SH, SNHG8 overexpression/TRIM28 knockdown AGS-BX1 cell.

METHODS

Collection of Tissue Specimens

After GCs were surgically resected, tissues from 61 patients with EBER-1-positive EBVaGC and 20 patients with EBER-1-negative EBVnGC were identified by *in situ* hybridization (22) and used in this study. All GC tissue adjacent normal tissues were quickly frozen in liquid nitrogen and stored at −80°C until use. The study protocol was approved by the Ethics Committee of the Fujian University Cancer Hospital, Fujian Cancer Hospital (Fuzhou, China), and the written informed consents from all the participators were obtained. All protocols are consistent with the Helsinki declaration.

In Situ Hybridization

EBER1 *in-situ* hybridization (ISH) was carried out with the EBER1 probe ISH kit (ZsBio, Beijing, China) on FFPE (formalin-fixed and paraffin-embedded) tissue slides. The tumor cells with clear nuclear staining of EBER1 were considered EBV positive.

Cell Lines and Cell Culture

AGS-BX1 [EBV-infected GC cell line (23)] was obtained from Dr. HL Chen (The University of Hong Kong); MKN-28 (GC cell line) and GES-1 (normal epithelial cell line of gastric mucosa) were purchased from ATCC. Cells were cultured in DMEM/F-12 containing 10% (v/v) heat-inactivated fetal bovine serum (FBS) and 100 U/ml of streptomycin/penicillin mixture (Gibco; Thermo Fisher Scientific, Inc., Waltham, MA, USA) in a humidified 37°C incubator with 5% of CO_2.

Construction of Overexpression or Knockdown SNHG8 Cell Lines

For the overexpression or knockdown SNHG8 in cell lines, the virus vectors were constructed by Hanheng Biotechnology Co Ltd (Beijing, China). To create cell lines with SNHG8 overexpression, HBLV-SNHG8-OE (pHBLV-CMV-mcs-3flag-EF1-ZsGReen-T2A-PURO inserted with SNHG8 gene) was

used. The original vector was used as vector alone control (HBLV-NC). For SNHG8 knockdown in cells, HBLV-SNHG8-shrna1, HBLV-SNHG8-shrna2, and HBLV-SNHG8-shrna3 were used and their parental vector pHBLV-U6-MCS-CMV-Zs/m cherry was used as vector alone control. AGS-BX1 cells cultured in six-well plates(5×10^5/well) were infected with 10 MOI of viral vectors in the presence of 6 μg/ml of polyamine. After 48 h, the cells were selected with 2 μg/ml of puromycin for 2 weeks to obtain stable infected cells. Newly established cells were named as AGS-BX1/NC, AGS-BX1/SNHG8-OE, or AGS-BX1/SNHG8-SH. The symbols -OE and –SH mean overexpression and knockdown, respectively.

Construction of Overexpression BHRF1 AGS Cell

The plasmids pCDNA3.1-flag-N-humanized-BHRF1 and pCDNA3.1-flag-NC were purchased from Hanheng Biotechnology Co. Ltd. (Beijing, China); AGS cells in six-well plates(5×10^5/well) were transfected with 2 μg plasmid. After 48 h of transfection, the cells with overexpression of BHRF1 or with empty vector were named as AGS/BHRF1-OE or AGS-NC.

Reverse-Transcription Quantitative Polymerase Chain Reaction

Total RNAs were isolated using the RNeasy Mini Kit (Qiagen, Valencia, CA, USA). To reversely transcribe total RNAs into complementary DNA (cDNA) of SNHG8, hsa-miR-512-5p, *TRIM28*, *BCL-2*, *CCND1*, *PCNA*, *PARP1*, *CDH1*, *CDH2 VIM*, and *Snail* in AGS-BX1 cells, the RevertAid First Strand cDNA Synthesis Kit (Thermo Fisher Scientific; Waltham, MA, USA) and miScript Reverse Transcription Kit were used. The generated cDNAs were used as templates for assessing gene expressions with miScript SYBR Green PCR Kit (Qiagen GmbH, Hilden, Germany) and LightCycler 480 SYBR Green I Master (Roche Applied Science; Indianapolis, IN, USA). The housekeeping gene glyceraldehyde phosphate dehydrogenase (GAPDH) served as the internal control of *TRIM28*, *BCL-2*, *CCND1*, *PCNA*, *PARP1*, *CDH1*, *CDH2 VIM*, and *Snail*, whereas U6 small nuclear RNA served as the internal reference for the expression of hsa-miR-512-5p. Relative gene expression was calculated with the $2^{-\Delta\Delta Ct}$ method.

Relative mRNA expression levels of SNHG8 were quantified in all EBVaGC samples using the comparative $2^{-\Delta\Delta Ct}$ method. *GAPDH* was used to normalize expression levels of SNHG8.

MTT Assay and Cell Cycle Analysis

Twenty-four hours after infection, the cells were collected, resuspended in the medium, and inoculated into 96-well plates (5,000 cells in 100 μl/well). The cell proliferation was assessed at 24, 48, 72, and 96 h later. At every time point, 20 μl of the MTT solution (Promega; Madison, WI, USA) was added into each well, followed by incubation at 37°C for another 4 h. One hundred fifty microliters of dimethyl sulfoxide was added into each well and shaken for 10 min to fully dissolve the MTT. The absorbance of each well was detected at OD_{490} nm by Model 680 reader (Bio-Rad Laboratories, Inc., Hercules, CA, USA). Cell cycle analysis was done using Muse™ Cell Cycle Kit™ Cell Analyzer (Millipore, USA) in accordance with the manufacturer's instructions (24).

Transwell Invasion Assays

The transwell chambers (8 μm diameter; Corning Inc., Corning, NY, USA) were used for cell migration assessment, while the upper chambers precoated with Matrigel (BD Biosciences, USA) were used for the invasion assay. Cells were harvested, washed with PBS, and resuspended in DMEM/F-12 without FBS. One hundred microliters of 2×10^4 cells were added into the upper chambers of a 24-well plate with 500 μl of media. At 24 h after seeding, the cells in the upper chambers were gently removed, and the migrated or invaded cells in the bottom side were fixed with 100% methanol, stained with 0.5% crystal violet, washed with PBS, and observed under inverted microscope (Olympus Corporation, Tokyo, Japan).

Colony Formation Assays

For colony-formation assay, about 200 cells/well were seeded in six-well plates and cultured for 14 days, then the cells were fixed in methanol and stained with 0.2% crystal violet. The colonies with >50 cells were pictured with ImageScanner (GE, USA) and counted using ImageJ (NIH, MD, USA).

Wound Healing Assay

Cells infected with lentiviral constructors were detached with trypsin and then seeded with DMEM/F12-10% FBS in a six-well plate in triplicates. After 24 h, the middle cells of each well were scratched with a 10-μl sterile pipette tip to make an empty line *via* washing off the detached cell twice with PBS. After 48 h, the pictures of cells that migrated into the empty line were taken under microscope and analyzed by ImageJ.

Prediction of Target Genes of SNHG8 and hsa-miR-512-5p

The lncRNASNP2 database (http://bioinfo.life.hust.edu.cn/lncRNASNP#!/) was utilized for the prediction of the binding site in SNHG8 for hsa-miR-512-5p and analyzed with inmiRDB (http://mirdb.org/) and TargetScan (http://www.targetscan.org/vert_72/).

Dual-Luciferase Reporter, RNA Immunoprecipitation (RIP), and Pull-Down Assays

The wild-type (wt) SNHG8 and mutant (mut) SNHG8 that had the predicted hsa-miR-512-5p-binding site were chemically synthesized by Hanheng Biotechnology Co. Ltd. (Beijing, China) and inserted into pSI-check2 luciferase reporter plasmids (Promega Corporation, Madison, WI, USA) to make the pMIR-SNHG8-wt (SNHG8-wt) and pMIR-SNHG8-mut (SNHG8-mut) reporter plasmids. Similarly, the reporter plasmids, TRIM28-wt and TRIM28-mut, were also made. For the reporter assay, when cells in 24-well plates grew to 70% confluence, the reporter plasmids were co-transfected with hsa-miR-512-5p mimics or miR-NC into the cells using

Lipofectamine 2000 reagent. After 48 h, the luciferase activity in the transfected cells was detected with Dual-Luciferase Reporter Assay System (Promega Corporation, Madison, WI, USA) on a Synergy H4 reader. The relative luciferase activity was normalized with Renilla luciferase activity.

For the RIP assay, the EZ-Magna RIP Kit (Sigma, St. Louis, MO, USA) was used. In brief, the lysate of 1 × 107 AGS/BX-1 cells in RIP lysis buffer was incubated with Anti-IgG or Anti-Ago2-coated magnetic beads for 6 h. RNAs of SNHG8 and miR-512-5p enriched on the beads was extracted and quantified by reverse-transcription quantitative polymerase chain reaction (qRT-PCR).

RNA pull-down assay was carried out to assess the interaction of miR-512-5p with SNHG8 using a Magnetic RNA Pull-Down Kit (Thermo Fisher Scientific). The miR-512-5p mimic (Bio-miR-512-5p) and negative control (Bio-miR-NC) were biotinylated by RiboBio Inc. (Guangzhou, China). AGS/BX-1 cells were transfected with 100-nm biotinylated probes for 48 h; then, the cell lysates were incubated with streptavidin-coated magnetic beads overnight. The RNA enriched on the beads was separated, and the content of SNHG8 was detected by qRT-PCR.

Western Blot Analysis

Cells were harvested and lysed with RIPA buffer (50 mM Tris–Cl, pH 8.0, 150 mM NaCl, 5 mM EDTA, 0.1% SDS, 1% NP-40) containing protease inhibitor cocktail (Abcam, Cat No. ab65621). The lysates were centrifuged at 12,000 rpm for 30 min at 4°C. The protein concentrations of supernatants were determined by BCA protein assay (Thermo Scientific, Rockford, IL, USA). The protein extract of each sample (25 μg) was electrophoresed on 10%–12% polyacrylamide gel with sodium dodecyl sulfate and then transferred onto nitrocellulose membrane (Millipore A) at 100 V for 1.5 h. After being blocked with 3% BSA in TBST (TBS-1% Tween 20) for 1 h, the membranes were incubated with 1:1,000 primary antibodies (purchased from CST, Danvers, MA, USA) of TRIM28 (Cat No. #4124), VIM (Cat No. 5741S), CCND1 (Cat No. 55506s), PCNA (Cat No. D3H8P), Bcl-2 (Cat No. 5071S), CDH1 (Cat No. 3195s), CDH2 (Cat No. 13116s), Snail (Cat No. 3879S), or PARP (Cat No. 46D11) overnight at 4°C, respectively, then washed and further incubated with secondary horseradish peroxidase-conjugated anti-rabbit IgG. Finally, protein bands were detected by developing the blots with Immobilon ECL Ultra Western HRP Substrate (Millipore, Cat No. WBULS0500) and pictured on Image Station 4000MM Pro (Carestream, Canada). ImageJ was used to quantify protein levels relative to load control β-actin.

Transplantation of Zebrafish With SNHG8 Knockout Gastric Cancer EBV-Positive Cells AGS/BX-1

Transgenic zebrafish TG (apo14-GFP) was provided by the Institute of Hydrobiology, Chinese Academy of Sciences. The culture condition of adult fish was 26.5°C, and the light dark ratio was 12 h:12 h. AGS-BX-1/SNHG8-SH cells and AGS-BX-1/NC cells were injected with a Pico-liter injector. Under a microscope, 1,500 cells were injected into the IVF Development Zone of apo14-EGFP zebrafish yolk sac on the second day after fertilization. After injection, the embryos were cultured in a 33°C incubator and transferred to a 35°C incubator 24 h later. The distribution and expression of red fluorescence in the abdominal cavity of zebra were observed under a laser scanning confocal microscope (LSM 710, Carl Zeiss AG, Oberkochen, Germany). The expression level of red fluorescence in the abdominal cavity was analyzed by ImageJ 1.48v. Imaging and quantification of the results were performed with an inverted SP5 STED confocal microscope (Leica, Germany). At least 40 zebrafishes in each group were analyzed, and three representative images were used. All the experiments were repeated three times.

Statistical Analysis

All data were processed by SPSS 19.0 software (SPSS Company, Chicago, USA). Pearson correlation analysis was used. The two-tailed *t test* was used to test the difference between groups. *Paired or nonparametric Kruskal–Wallis test* was used to evaluate the relationship between SNHG8 level and other characteristics. The survival curve was calculated by the *Kaplan–Meier* method. A p value less than 0.05 ($*p < 0.05$, $**p < 0.01$, $***p < 0.001$, and $****p < 0.0001$) was statistically significant.

RESULTS

Expression of EBV-Related Protein BFRF1 in GC and Its Upregulation of the Expressions of SNHG8 and TRIM28

BHRF1 (EBV-encoded small ribonucleic acid 1) is an EBV oncogene confirmed recently. **Figures 1A, B** show that BHRF1 was expressed in EBVaGC cases, but not expressed in EBVnGC (EBV-negative GC) tissues. In addition, the BHRF1 expression was significantly higher in AGS-BX (EBV infected GC cell line) than that in non-EBV-infected GC cell lines (AGS and MKN28) (**Figure 1D**). Besides, SNHG8 expression was also much higher in EBVaGC and AGS-BX than in EBVnGC- and in non-EBV-infected GC cell lines (AGS, MKN28) (**Figures 1C, D**).

To determine the relationship between BHRF1 and SNHG8, we constructed a vector pcdna3.1-flag-BHRF1 to stably express human BHRF1 protein in EBV-negative AGS cells. Western blot assays (WB) show that the expression levels of BFRF1 and TRIM28 were much higher in AGS/BHRF1 cells than those in AGS/NC cells (**Figure 1E**). qRT-PCR assays revealed that the expression of BHRF1, SNHG8, and TRIM28 was much higher in the AGS/BHRF1 group than in the AGS/NC group (**Figure 1F**). These results indicated that the over-expression of EBV-related protein BFRF1 in EBV-negative AGS cells upregulated the expression of SNHG8 and TRIM28.

Association of SNHG8 With Clinicopathological Features and Prognosis of EBVaGC

With *in situ* hybridization, EBVaGC was recognized by the expression of EBER1 in nuclei of cancer cells; EBVaGC is a group of lymphoepithelioma-like diffuse-type carcinoma with dense lymphocytic infiltration. As shown in **Figure 2A**, EBVaGC had EBER1-positive nuclei and surrounded with lymphoid stroma.

To determine the expression of SNHG8 in EBVaGC, qRT-PCR assays were performed in 61 cancer tissues and paired

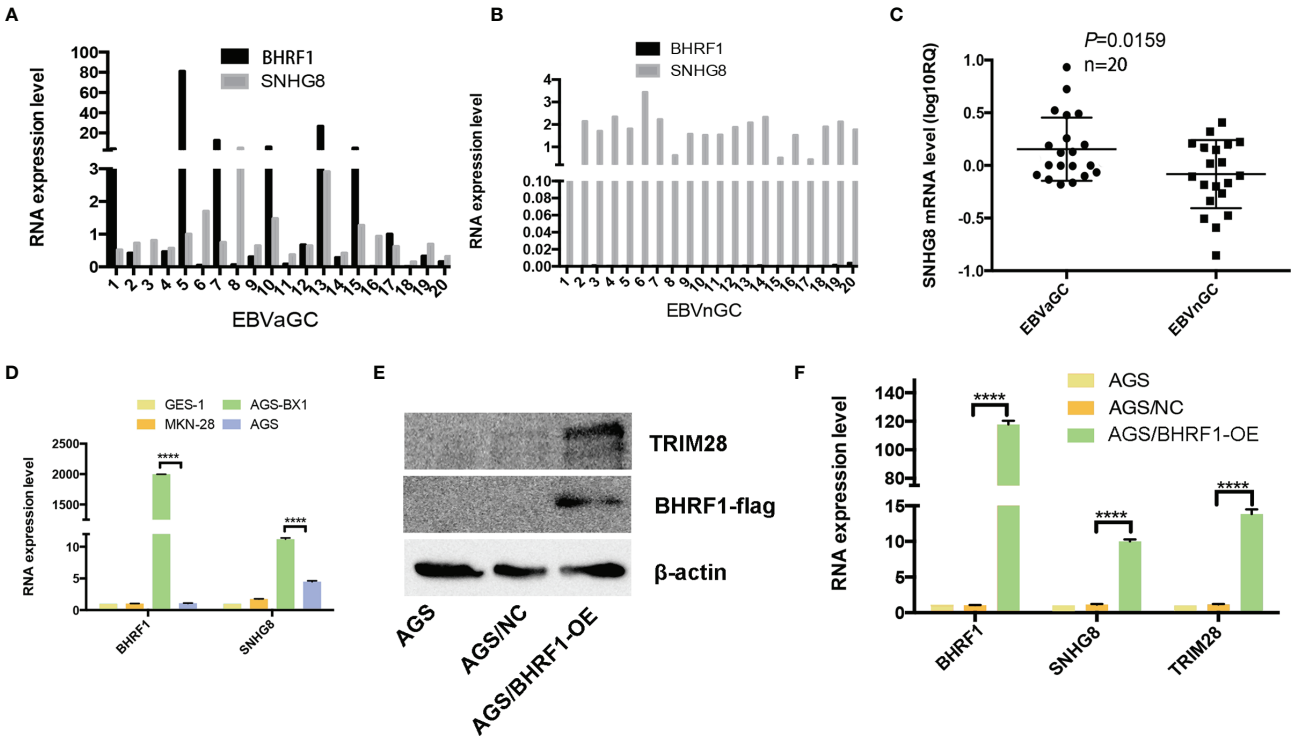

FIGURE 1 | Expression of *BFRF1* in GC and GC cell lines and its regulation with SNHG8 and *TRIM28*. **(A, B)** *BHRF1* was expressed in EBVaGC tissues at different levels, while it was almost not expressed on EBVnGC. **(C)** The SNHG8 expression was much higher in EBVaGC tissues than that in EBVnGC tissues ($p = 0.0159$). RQ = $2^{-\Delta\Delta Ct}$, where Ct values were generated from qPCR. **(D)** The expression of *BHRF1* and SNHG8 was much higher in EBV$^+$ AGS-BX cells than in EBV$^-$ GC cell lines (AGS, MKN28). **(E)** Overexpression of EBV protein BFRF1 resulted in an increased TRIM28 demonstrated by Western blot analysis. **(F)** Overexpression of EBV protein *BFRF1* enhanced the transcription of SNHG8 and *TRIM28* demonstrated by qRT-PCR. ****$p < 0.0001$.

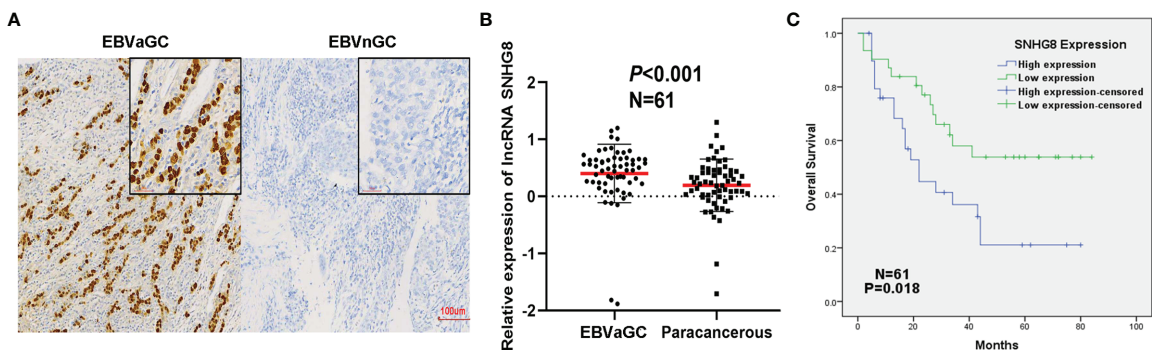

FIGURE 2 | Poor prognosis of EBVaGC was associated with the upregulation of SNHG8. **(A)** EBER in gastric cancer detected by *in situ* hybridization. Left: EBER is positive in EBV-associated gastric cancer (EBVaGC). Right: EBER is negative in non-EBV-associated gastric cancer (EBVnGC). **(B)** The expression of SNHG8 was higher in 61 cases of EBVaGC than that in their paracancerous tissues ($p < 0.001$). **(C)** Kaplan–Meier curves showed that patients with a high level of SNHG8 had a poor OS ($p = 0.018$).

paracancerous tissues. SNHG8 was expressed at significantly higher levels in EBVaGC compared to the level in paracancerous tissues (**Figure 2B**). The average log10 relative expression levels in cancer tissues were ~0.41, a two-fold increase compared to that in paracancerous tissues (~0.20). Furthermore, EBVaGC tissue samples were divided into two groups (SNHG8 high- and low-expression groups) using the median mRNA level of SNHG8 as the cutoff value. As shown in **Table 1**, the overexpression of SNHG8 had a significant correlation with tumor size ($p = 0.036$) and vascular tumor thrombus ($p = 0.024$). Moreover, the overexpression of SNHG8 correlated with the poor prognosis in EBVaGC. Patients with the high levels of SNHG8 had

significantly shorter overall survival (OS) than those with low SNHG8 expression (p = 0.018; **Figure 2C**). The results suggested that the expression of SNHG8 was positively correlated with tumor size and poor prognosis in EBVaGC.

Overexpression of SNHG8 Promotes the Proliferation, Migration, and Invasiveness of EBVaGC

To assess the effects of SNHG8 on the malignant behaviors of EBVaGC, EBV-positive gastric carcinoma cell lines AGS-BX1 were infected with HBLV-NC or HBLV-SNHG8-OE lentivirus. RT-qPCR analysis revealed that SNHG8 expression was efficiently increased in AGS-BX1/SNHG8-OE as compared with AGS-BX1/NC (**Figure 3A**). The effect of SNHG8 overexpression on the enhanced proliferation and colony formation of AGS-BX1 cells was demonstrated in MTT assay (**Figure 3B**) and colony assay (**Figure 3C**). In addition, SNHG8 overexpression markedly promoted cell cycle arrest at the G2/M phase of AGS-BX1 compared with control cell AGS-BX1/NC (**Figure 3D**). Furthermore, results of RT-qPCR and WB showed that the expression of proliferation-related genes *CCND1*, *PCNA*, and anti-apoptotic *BCL-2*, metastasis-related genes *Snai1VIM* and *CDH2* were upregulated, while *PARP1* and *CDH1* were downregulated in AGS-BX1/SNHG8-OE cells (**Figures 3E, F, J, K**). Besides, the results of wound healing and transwell invasion assays showed that the upregulation of SNHG8 resulted in an increased abilities of wound healing (**Figures 3G, H**) and transwell invasiveness (**Figure 3I**). These findings suggested that SNHG8 might exert oncogenic effects on the aggressiveness of EBVaGC cell *in vitro*.

Silence of SNHG8 Inhibits the Proliferation, Migration, and Invasiveness of EBVaGC

To assess if downregulation of SNHG8 could reduce the malignant behaviors of EBVaGC, AGS-BX1 was infected with HBLV-NC or HBLV-SNHG8-SH lentivirus. RT-qPCR analysis showed that the SNHG8 expression was significantly reduced in AGS-BX1/SNHG8-SH as compared with AGS-BX1/NC (**Figure 4A**). SNHG8 silencing markedly inhibited the proliferation and colony formation of AGS-BX1 (**Figures 4B, C**). In addition, compared with AGS-BX1/NC, there was a significant amount of cells arrested at the GO/G1 phase in AGS-BX1/SNHG8-SH as measured by a Muse cell analyzer (**Figure 4D**). RT-qPCR and WB results showed that the expressions of proliferation-related genes *BCL-2*, *CCND1*, *PCNA*, and metastasis-related genes *Snai1VIM* and *CDH1* were downregulated, while *PARP1* and *CDH1 were* upregulated in AGS-BX1/SNHG8-SH cells (**Figures 4E, F, J, K**). Furthermore, the wound healing migratory ability and transwell invasive abilities were inhibited after the downregulation of SNHG8 (**Figures 4G–I**). These findings suggested that silencing of SNHG8 inhibited the proliferation, migration, and invasiveness of EBVaGC cells *in vitro*.

SNHG8 Sponges hsa-miR-512-5p and Regulates *TRIM28*

Potential miRNAs associated with SNHG8 in EBVaGC cells were examined since lncRNAs mainly functioned as miRNA spongers. Analyzed with the lncRNASNP2 database, hsa-miR-512-5p turned out to be a possible target of SNHG8. Further analyzed with the TargetScan and miRDB databases, TRIM28 turned out to be a possible target of hsa-miR-512-5p. Putative binding sites of hsa-miR-512-5p and wild-type regions of SNHG8 and *TRIM28* are shown in **Figures 5A, B**. RT-qPCR analysis showed that the overexpression or silencing of SNHG8 significantly decreased or increased hsa-miR-512-5p expression (**Figures 5C, D**), respectively. In parallel, the overexpression of hsa-miR-512-5p decreased the functions of SNGH8 and *TRIM28* expression, knockdown of hsa-miR-512-5p increased the functions of SNGH8 and *TRIM28* expression (**Figures 5E, F**).

To explore whether SNHG8 and *TRIM28* were functional targets of hsa-miR-512-5p, dual-luciferase reporter assay was

TABLE 1 | Relationship of SNHG8 expression with clinicopathologic characteristics in EBVaGC.

Characteristics	Number of patients	SNHG8 expression		*p*-value
		Low	High	
All patients	61	30	31	
Gender				0.479
Male	49	23	26	
Female	12	7	5	
Age				0.252
<60	35	15	20	
≥60	26	15	11	
Lauren's type				0.221
Intestinal type	49	26	23	
Diffuse type	12	4	8	
Size(cm)				0.036*
<5	41	24	17	
≥5	20	6	14	
Vascular tumor thrombus				0.024*
Absent	45	26	19	
Present	16	4	12	

*$p < 0.05$.

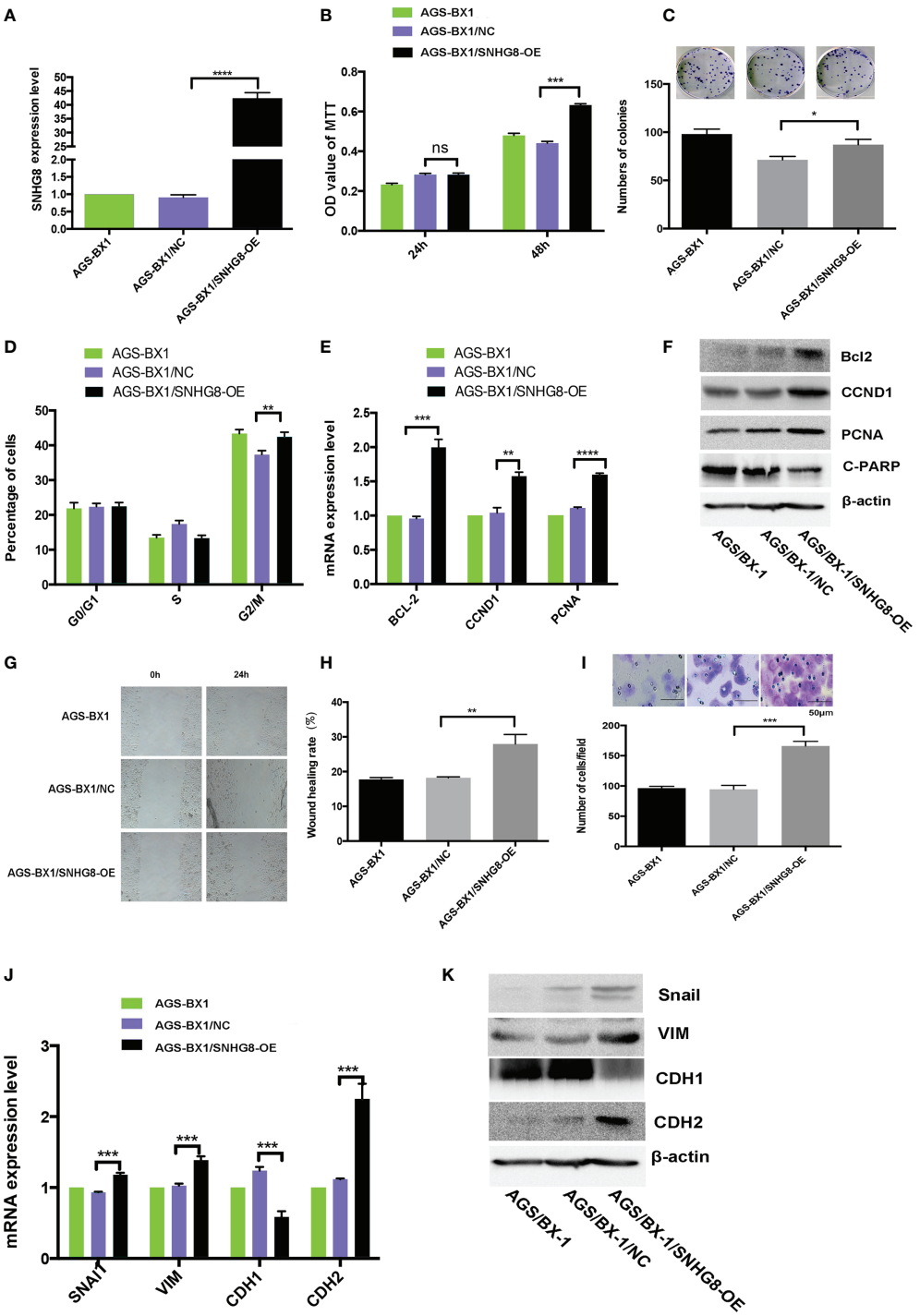

FIGURE 3 | Overexpression of SNHG8 promoted the proliferation, migration, and invasion of EBVaGC. **(A)** AGS-BX1 cells with SNHG8 gene overexpression (AGS-BX1/SNHG8-OE)had a high level of the expression of SNHG8 demonstrated by qPCR as compared to vector alone control (AGS-BX1/NC) and wild-type cells (AGS-BX1). The overexpression of SNHG8 promoted the malignant behaviors of AGS-BX1/SNHG8-OE cells in the following aspects: **(B)** increasing cell proliferation as measured with MTS assay; **(C)** enhancing colony formation; **(D)** stopping cells at G2/M; **(E, F)** increasing the expression of proliferation-related genes of *BCL-2*, *CCND1*, *C-PARP*, and *PCNA*, confirmed by qRT-PCR and Western blot; **(G, H)** promoting the migration measured with the wound healing assay and the invasion measured with the transwell invasive assay; **(I)** and enhancing the expression of invasion/metastasis-related-genes, *Snai1*, *VIM*, CDH1, and *CDH2* as demonstrated by qRT-PCR and Western blot **(J, K)**. $^{*}p < 0.05$; $^{**}p < 0.01$; $^{***}p < 0.001$; $^{****}p < 0.0001$. ns mean not statistical significance.

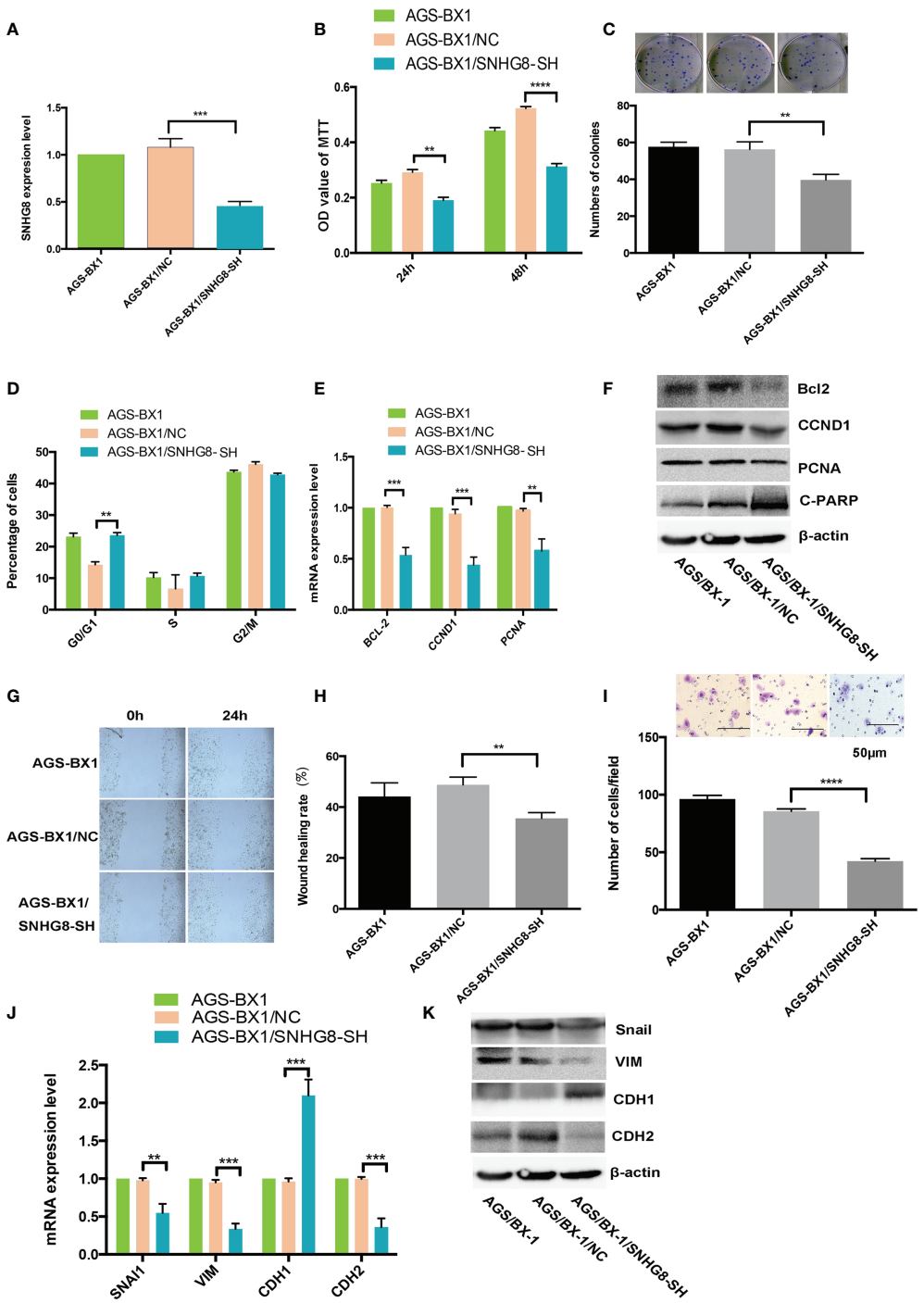

FIGURE 4 | Silencing SNHG8 inhibited the proliferation, migration, and invasion of EBVaGC. **(A)** SNHG8 gene knockdown in AGS-BX1 cells (AGS-BX1/SNHG8-SH) had a low expression of SNHG8 quantified by qPCR as compared to vector alone control (AGS-BX1/NC) and wild-type cells (AGS-BX1). SNHG8 silencing reduced the malignant behaviors of AGS-BX1/SNHG8-SH cells in following aspects: the cell proliferation as measured with MTT assay **(B)**; colony formation **(C)**; cells in G0/1 **(D)**; the expressions of proliferation-related-genes of *BCL-2*, *CCND1*, *C=PARP*, and *PCNA* demonstrated by qRT-PCR and Western blot **(E, F)**; the migration measured with the wound healing assay **(G, H)**; the invasion measured with the transwell invasive assay **(I)**; and the expressions of invasion/metastasis-related-genes of *Snail*, *VIM*, CDH1, and *CDH2* demonstrated by qRT-PCR and Western blotting **(J, K)**. $^{**}p < 0.01$; $^{***}p < 0.001$; $^{****}p < 0.0001$.

performed. The luciferase activity was significantly reduced when hsa-miR-512-5p mimics were added into cultured SNHG8-Wt or TRIM28-Wt-co-transfected HEK293T and AGS-BX1 cells, while there was no effect on the same cell transfected with SNHG8-Mut or TRIM28-Mut vector (**Figures 5G–J**).

As expected, knocking down of SNHG8 with lentivirus significantly suppressed the expression of *TRIM28* in AGS-BX1 cells (**Figures 5K, M**). In contrast, the overexpression of SNHG8 significantly increased the expression of *TRIM28* in AGS-BX1 cells (**Figures 5K, L**). RNA pull-down analysis presented that SNHG8 could bind to hsa-miR-512-5p (**Figure 5N**). In addition, the result of the NA immunoprecipitation (RIP) assay showed that SNHG8 and hsa-miR-512-5p could be co-enriched in an Ago2-dependent manner (**Figure 5O**).

Taken together, these results demonstrated that SNHG8 and TRIM28's 3 ′UTR had hsa-miR-512-5p-binding sites. Hsa-miR-512-5p was an inhibitor of SNHG8 and a blocker of TRIM28 in the EBVaGC progression.

Enhancement of *TRIM28* Is Critical for SNHG8-Mediated Malignant Behaviors

To test our hypothesis that *TRIM28* might contribute to SNHG8-mediated malignant behaviors, the effects of SNHG8 on the *TRIM28* expression in AGS-BX1 cells were studied. A rescue assay by silencing *TRIM28* in AGS-BX1/SNHG8-OE was performed. Results of qPCR and WB revealed that the expression level of *TRIM28* in AGS-BX1/SNHG8-OE/TRIM28-SH was significantly lower than that in AGS-BX1/SNHG8-OE (**Figures 6A, B**). Silencing of *TRIM28* reduced the proliferation and colony formation of AGS-BX1/SNHG8-OE cell as determined by MTT assay (**Figure 6C**) and colony assay (**Figure 6D**). The silencing *TRIM28* markedly reduced the cell cycle arrest at the G2/M phase of AGS-BX1 compared with AGS-BX1/SNHG8-OE (**Figure 6E**). In addition, results of qRT-PCR and WB assay showed that the expression of a panel of proliferation or apoptosis-related genes, such as *BCL-2*, *CCND1*, and *PCNA*, was reduced after *TRIM28* was silenced in AGS-BX1/SNHG8-OE cells (**Figures 6F, G**). Furthermore, the migratory and invasive abilities of AGS-BX1/SNHG8-OE cell lines greatly reduced after the silencing of *TRIM28*, as demonstrated in wound healing (**Figures 6H, I**) and transwell invasion assays (**Figure 6J**). The expressions of downstream molecules (*Snai1*, *VIM*, and *CDH2*) related with metastasis were downregulated as determined by qRT-PCR and WB, while CDH1 was upregulated silencing TRIM28 in AGS-BX1/SNHG8-OE cells (**Figures 6K, L**).

These findings suggest that the enhancement of *TRIM28* is critical for SNHG8-mediated malignant behaviors in EBVaGC cells *in vitro*.

SNHG8 Promotes Growth of EBVaGC Tumor in Zebrafish

To explore the role of *SNHG8* in tumor growth of EBVaGC *in vivo*, the zebrafish EBVaGC tumor xenograft model was used. Injection of AGS-BX1 cells did not affect the normal development of zebrafish (**Figure 7A**). However, the growth of SNHG8-knocked-down mCherry-expressing AGS-BX1 cells significantly decreased compared to the vector-alone control group on 3 days after injection of the same number of cells into the circulation of zebrafish embryos, as demonstrated by the low intensity of red fluorescence (**Figures 7B, C**) and low proliferation rate (**Figure 7D**) in the AGS/BX-1/SNHG8-SH group.

Taken together, these data show that SNHG8 could sponge hsa-miR-512-5p and regulate the expression of *TRIM28* in EBVaGC to enhance malignant behaviors.

DISCUSSION

In this study, several facts were revealed for the first time for EBVaGC, a distinct subtype of GC: (**1**) the existence of BHRF1 was correlated with the expression of SNHG8; (**2**) BHRF1^{+}/SNHG8 ^{high} had a poor prognosis; (**3**) there was a coexistence of BHRF1^{+}/SNHG8 ^{high}/miR-512-5p ^{low}/TRIM28^{high} in EBVaGC; (**4**) the chain reaction was that *BHRF1* triggered the high expression of SNHG8, which sponged hsa-miR-512-5p and upregulated *TRIM28*; (**5**) the malignant behaviors of BHRF1^{+}/SNHG8 ^{high}/miR-512-5p ^{low}/TRIM28^{high} EBVaGC were exerted by a set of proliferation-related genes, such as *BCL-2*, *CCND1*, *PCNA*, and *PARP1* and metastasis-related genes, such as *Snail*, *VIM*, *CDH1*, and *CDH2*. This study further explored the molecular mechanism of our previous finding that BHRF1-SNHG8 was a key regulator of EBVaGC (21).

EBV is an oncogenic virus, associated with tumors from epithelia and hematopoietic cells (2, 25). Most studies have focused on genomes of EBV, such as EBER, EBNA-1, and BART (2, 26, 27), while this study further studied the role of *BHRF1* in the development and progression of EBVaGC. The upregulation of *BHRF1* resulted in over-expression of SNHG8, connecting the viral component to the human oncogene, possibly leading to this unique subtype of GC.

Cellular lncRNAs can be differentially induced by EBV infection. The dysregulated lncRNAs probably modulate tumorigenesis and other biological functions (28–30). Our result is consistent with others' reports that SNHG8 is associated with the progression in multiple types of cancer in the liver, colon, lung, ovary, prostate, esophagus, and so on (15, 31–35). Our data support that the acting mechanism of SNHG8 could be multiple: (**1**) it activated *BCL-2*, preventing GC cells from apoptosis; (**2**) it activated *CCND1*, regulating the cell cycle; and (**3**) it activated *CDH1*, *CDH2Snai1*, and *VIM*, enhancing the epithelial–mesenchymal transition, thus promoting the migration, invasion, and metastasis of GC cells.

LncRNAs are involved in the regulation of gene transcription, post-transcription, and epigenetic modulation (12, 36). Since lncRNAs and mRNAs share miRNAs' response elements, they compete for binding to these miRNAs, regulating the expression of each other. The interaction between these RNA molecules forms a network of complex posttranscriptional regulation (21, 37–40). Bioinformatics analyses revealed that miR-512-5p shared common binding sites with SNHG8 and *TRIM28*. Our

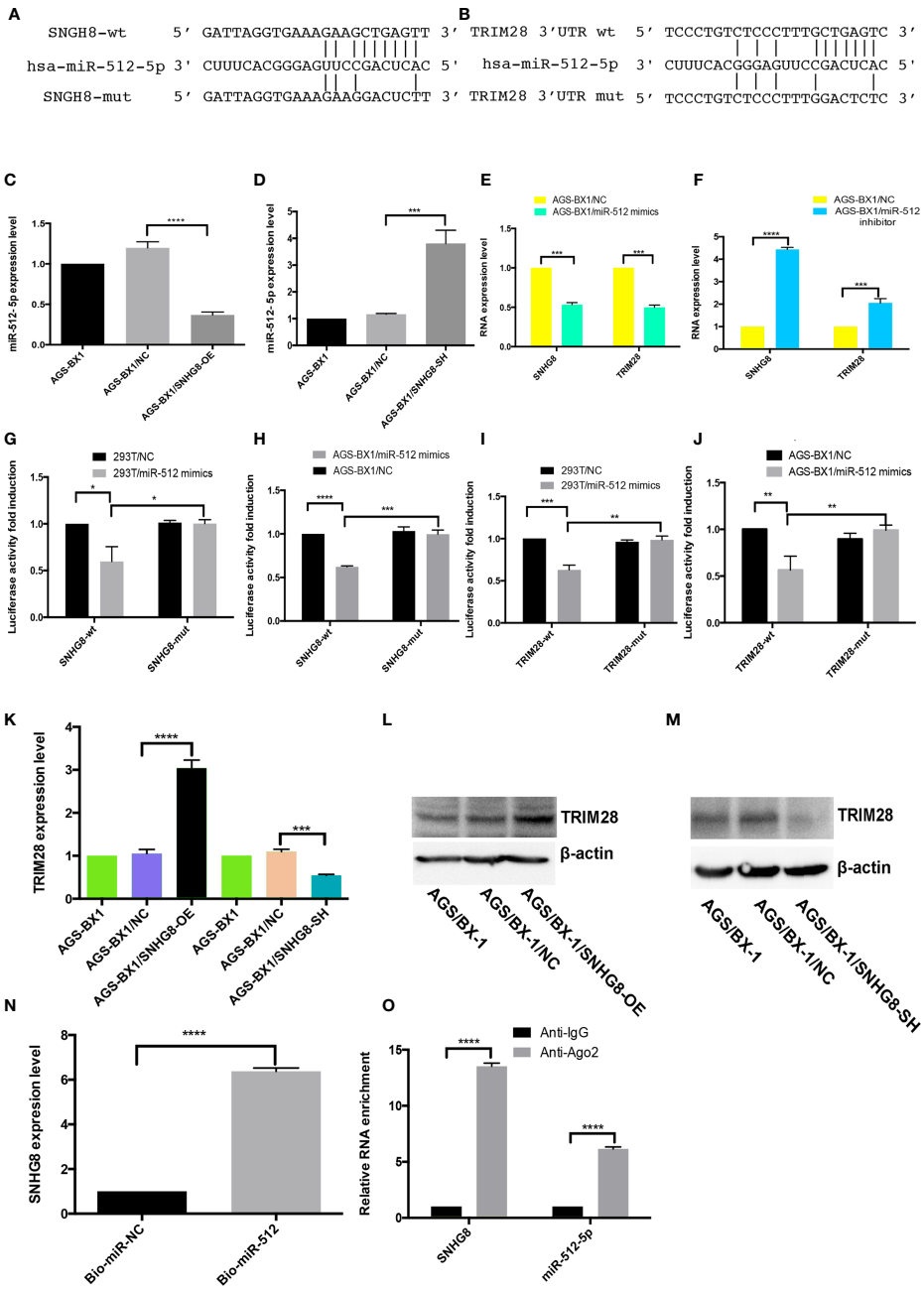

FIGURE 5 | SNHG8 exerted its function through sponging hsa-miR-512-5p and upregulating of TRIM28. **(A, B)** Sequence alignment of hsa-miR-512-5p with the putative binding sites in the wild-type and mutant regions of SNHG8 and TRIM28. **(C, D)** Hsa-miR-512-5p expression was decreased in AGS-BX1/SNHG8-OE cells and increased in AGS-BX1/SNHG8-SH cells tested with qRT-PCR. **(E, F)** The expression of SNHG8 and *TRIM28* was reduced in AGS-BX1/miR-512-5p mimic cells tested with qRT-PCR. **(G–J)** Dual-luciferase reporter assay showed that hsa-miR-512-5p mimics reduced the intensity of fluorescence in HEK293T or AGS-BX1 cells transfected with SNHG8-Wt or TRIM28-Wt, but not in the controls of SNHG8-Mut or TRIM28-Mut vector. **(K–M)** TRIM28 expression was increased in AGS-BX1/SNHG8-OE cells and decreased in AGS-BX1/SNHG8-SH cells tested with qRT-PCR and Western blot analysis. **(N)** SNHG8 expression was measured with qRT-PCR after RNA pull-down assay using Bio-miR-NC and Bio-miR-512-5p. **(O)** SNHG8 and miR-512-5p levels were determined by qRT-PCR after Ago 2 or IgG RIP assay. $^{*}p < 0.05$; $^{**}p < 0.01$; $^{***}p < 0.001$; $^{****}p < 0.0001$.

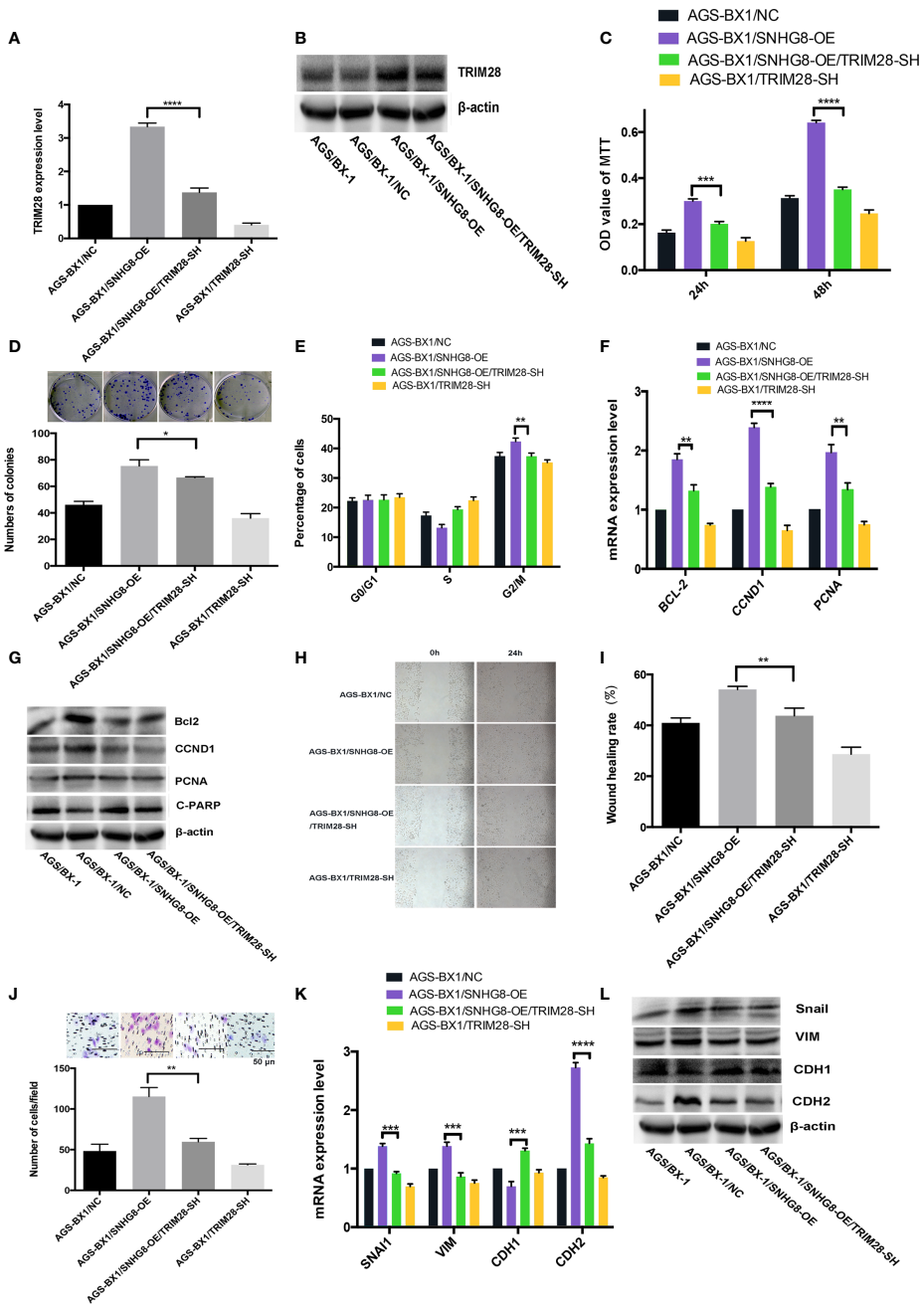

FIGURE 6 | Enhancing of *TRIM28* was critical for SNHG8-mediated malignant behaviors. **(A, B)** *TRIM28* expression was increased in AGS-BX1/SNHG8-OE cells and reduced by silencing of *TRIM28* tested by RT- PCR and Western blot. **(C)** SNHG8 enhanced cell proliferation could be reduced by silencing of *TRIM28* tested with MTS assay. **(D)** SNHG8 enhanced colony formation could be reduced by silencing of *TRIM28*. **(E)** SNHG8-enhanced cell cycle stopping at G2/M could be reduced by silencing of *TRIM28* as detected by flow cytometry. **(F, G)** SNHG8-enhanced expression of *BCL-2*, *CCND1*, *C-PARP*, and *PCNA* could be reduced by silencing of *TRIM28* tested with qRT-PCR and Western Blot. **(H, I)** SNHG8-enhanced cell migration could be reduced by silencing of *TRIM28* tested with wound healing assay. **(J)** SNHG8-enhanced cell invasion could be reduced by silencing of *TRIM28* tested with transwell assay. **(K, L)** SNHG8-enhanced expressions of invasion/metastasis-related-genes of *VIM* and *CDH2* could be reduced by silencing of *TRIM28* tested with qRT-PCR and Western blot. $^{*}p < 0.05$; $^{**}p < 0.01$; $^{***}p < 0.001$; $^{****}p < 0.0001$.

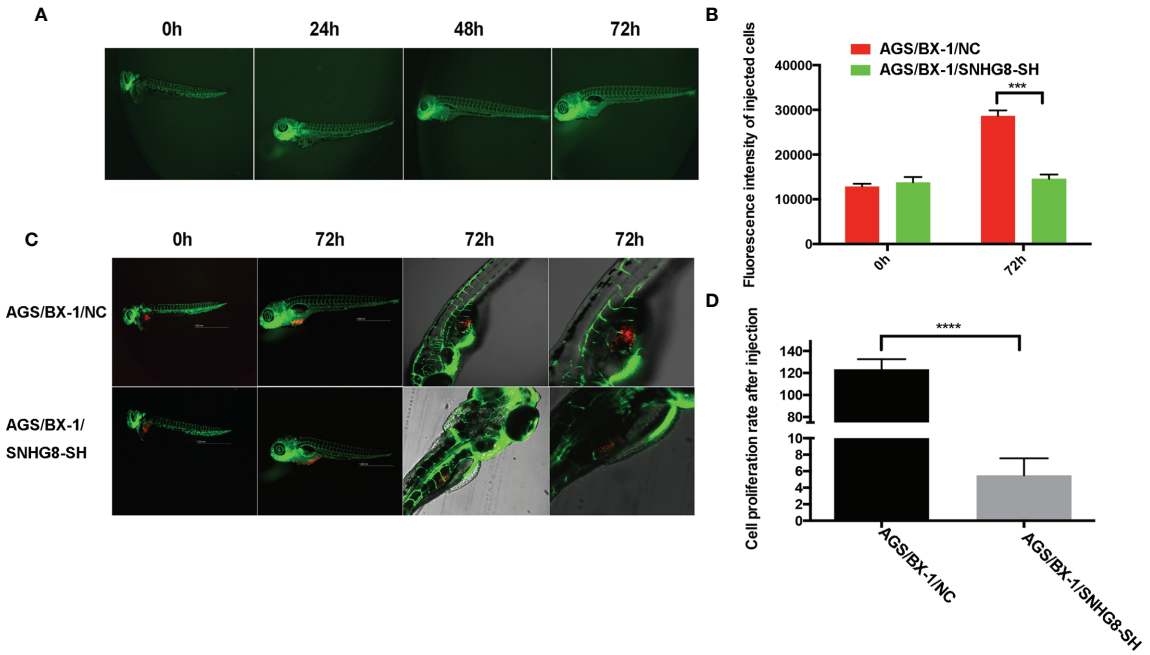

FIGURE 7 | SNHG8 promoted the growth of EBVaGC tumor in zebrafish. **(A)** The growth of zebrafish was not affected by the injection of AGS-BX1 cells in 3 days. **(B)** Representative images of zebrafish from the control (AGS-BX1-NC) and AGS-BX1-SNHG8-SH groups with zoom-in of cancer cells. **(C, D)** Analysis of cancer cell numbers of each group in zebrafish assay. AGS-BX1 cells transfected with red florescence gene (AGS-BX1-NC, AGS-BX1-SNHG8-SH) could form tumor in zebrafish, which could be reduced by silencing of SNHG8 as determined by red fluorescence integral density and cancer cells in zebrafish abdominal cavity. ***$p < 0.001$; ****$p < 0.0001$.

dual-luciferase reporter assay indeed confirmed that SNHG8 functions as a ceRNA in the miR-512-5p/TRIM28 axis as SNHG8 bound to miR-512-5p, while *TRIM28* bound to miR-152-5p. Furthermore, subsequent biotinylated miRNA pull-down assays confirmed the competitive binding between SNHG8 and *TRIM28* to miR-512-5p. Moreover, the rescue experiment showed that SNHG8 significantly reduced the effects of miR-512-5p on *TRIM28*.

TRIM28, a member of a conserved family of transcription co-factors, has diverse functions for the regulation of cell proliferation, DNA repair, and differentiation (40–43). *TRIM28* regulated E-cadherin and N-cadherin, resulting in EMT in lung cancer cells (44). *TRIM28* prevented *TRIM24* from SPOP-mediated degradation, promoting the progression of prostate cancer (42). *TRIM28* also affected the mTOR signaling pathway, resulting in the growth of cervical cancer (45). Reduction of *TRIM28* could reduce the malignant behaviors triggered by BHRF1-SNHG8.

Taken together, our *in vitro* and *in vivo* data showed that *BHRF1* upregulated SNHG8, which sponged miR-512-5p, leading to a high level of *TRIM28*, carrying out the malignant behaviors. On the other hand, the silencing of SNHG8 would lead to miR-512-5p upregulation and reduction of TRIM28. This process of BHRF1^{+}/SNHG8 ^{high}/miR-512-5p ^{low}/TRIM28^{high} in EBVaGC directly enhances the activation of a set of tumor-promoting factors, such as proliferation-related genes (*BCL-2*, *CCND1*, *PCNA*, *PARP1*) and metastasis-related genes (*Snail*, *VIM*, *CDH1*, and *CDH2*).

Therefore, silencing of SNHG8 would greatly reduce the malignant behaviors of EBVaGC, which might pave a new road to overcome EBVaGC.

CONCLUSION

Our findings demonstrated that *BHRF1* triggered the expression of SNHG8, which sponged miR-512-5p and upregulated *TRIM28* and a set of effectors (such as *BCL-2*, *CCND1*, PCNA, *CDH1*, *CDH2*, *Snail*, and *VIM*) to promote the EBVaGC tumorigenesis and invasion. SNHG8 could be an independent prognostic factor for EBVaGC and sever as target for the therapy.

DATA AVAILABILITY STATEMENT

The original contributions presented in the study are included in the article/supplementary material. Further inquiries can be directed to the corresponding authors.

ETHICS STATEMENT

The studies involving human participants were reviewed and approved by the Ethics Committee of the Fujian University Cancer Hospital, Fujian Cancer Hospital (Fuzhou, China). The patients/participants provided their written informed consent to participate in this study.

AUTHOR CONTRIBUTIONS

XGL and TH designed the research. CZ, JL, DH, HL, and KL performed the experiments. YS, XGL, LZ, and TH analyzed the data. DH, XZ, LZ, and XDL conducted the histological/pathological analysis. XDL, JL, and CZ wrote the paper. LZ and TH edited the paper. All authors contributed to the article and approved the submitted version.

FUNDING

This study was supported by the Natural Science Foundation of Fujian Province (No. 2019J01196, 2020J011109), Fujian Provincial Clinlical Research Center for Cancer Radiotherapy and Immunotherapy (NO. 2020Y2012), the Joint Funds for the Innovation of Science and Technology, Fujian province (No. 2018Y9113), Medical Innovation Program of Fujian Province (No. 2019-CX-5), Strategic Priority Research Program of Chinese Academy of Sciences (XDB38050200, XDA26040304), National Key R&D Program of China (2018YFC0910403, 2017YFC1201200), and Shanghai Municipal Science and Technology Major Project (2017SHZDZX01).

ACKNOWLEDGMENTS

The authors thank Dr. Shimin Zhang for his helpful comments.

REFERENCES

1. Farrell PJ. Epstein-Barr Virus and Cancer. *Annu Rev Pathol* (2019) 14:29–53. doi: 10.1146/annurev-pathmechdis-012418-013023
2. Ayee R, Ofori MEO, Wright E, Quaye O. Epstein Barr Virus Associated Lymphomas and Epithelia Cancers in Humans. *J Cancer* (2020) 11(7):1737–50. doi: 10.7150/jca.37282
3. Hui KF, Chiang AK. Suberoylanilide Hydroxamic Acid Induces Viral Lytic Cycle in Epstein-Barr Virus-Positive Epithelial Malignancies and Mediates Enhanced Cell Death. *Int J Cancer* (2010) 126(10):2479–89. doi: 10.1002/ijc.24945
4. Shannon-Lowe C, Rickinson A. The Global Landscape of EBV-Associated Tumors. *Front Oncol* (2019) 9:713. doi: 10.3389/fonc.2019.00713
5. Sun K, Jia K, Lv H, Wang SQ, Wu Y, Lei H, et al. EBV-Positive Gastric Cancer: Current Knowledge and Future Perspectives. *Front Oncol* (2020) 10:583463. doi: 10.3389/fonc.2020.583463
6. Burke AP, Yen TS, Shekitka KM, Sobin LH. Lymphoepithelial Carcinoma of the Stomach With Epstein-Barr Virus Demonstrated by Polymerase Chain Reaction. *Mod Pathol* (1990) 3(3):377–80.
7. Nogueira C, Mota M, Gradiz R, Cipriano MA, Caramelo F, Cruz H, et al. Prevalence and Characteristics of Epstein-Barr Virus-Associated Gastric Carcinomas in Portugal. *Infect Agent Cancer* (2017) 12:41. doi: 10.1186/s13027-017-0151-8
8. Wapinski O, Chang HY. Long Noncoding RNAs and Human Disease. *Trends Cell Biol* (2011) 21(6):354–61. doi: 10.1016/j.tcb.2011.04.001
9. Peng WX, Koirala P, Mo YY. LncRNA-Mediated Regulation of Cell Signaling in Cancer. *Oncogene* (2017) 36(41):5661–7. doi: 10.1038/onc.2017.184
10. Li J, Meng H, Bai Y, Kai W. Regulation of lncRNA and Its Role in Cancer Metastasis. *Oncol Res* (2016) 23(5):205–17. doi: 10.3727/096504016X14549667334007
11. Schmitt AM, Chang HY. Long Noncoding RNAs in Cancer Pathways. *Cancer Cell* (2016) 29(4):452–63. doi: 10.1016/j.ccell.2016.03.010
12. Bhan A, Soleimani M, Mandal S. Long Noncoding RNA and Cancer: A New Paradigm. *Cancer Res* (2017) 77(15):3965–81. doi: 10.1016/j.eururo.2014.01.032
13. Sültmann H, Diederichs S. Long Noncoding RNA: "LNCs" to Cancer. *Eur Urol* (2014) 65(6):1152–3. doi: 10.1016/j.eururo.2014.01.032.
14. Liang H, Yu T, Han Y, Jiang H, Wang C, You T, et al. LncRNA PTAR Promotes EMT and Invasion-Metastasis in Serous Ovarian Cancer by Competitively Binding miR-101-3p to Regulate ZEB1 Expression. *Mol Cancer* (2018) 17(1):119. doi: 10.1186/s12943-018-0870-5
15. Chen C, Zhang Z, Li J, Sun Y. SNHG8 is Identified as a Key Regulator in non-Small-Cell Lung Cancer Progression Sponging to miR-542-3p by Targeting CCND1/CDK6. *Onco Targets Ther* (2018) 11:6081–90. doi: 10.2147/OTT.S170482
16. Song Y, Zou L, Li J, Shen Z-P, Cai Y-L, Wu X-D. LncRNA SNHG8 Promotes the Development and Chemo-Resistance of Pancreatic Adenocarcinoma. *Eur Rev Med Pharmacol Sci* (2018) 22(23):8161–8. doi: 10.26355/eurrev_201812_16508
17. Jin S, Yang X, Li J, Yang W, Ma H, Zhang Z, et al. P53-Targeted LincRNA-p21 Acts as a Tumor Suppressor by Inhibiting JAK2/STAT3 Signaling Pathways in Head and Neck Squamous Cell Carcinoma. *Mol Cancer* (2016) 18(1):38–52. doi: 10.1186/s12943-019-0993-3
18. Tang Y, Song G, Liu H, Yang S, Yu X, Shi L, et al. Silencing of Long Non-Coding RNA HOTAIR Alleviates Epithelial-Mesenchymal Transition in Pancreatic Cancer via the Wnt/β-Catenin Signaling Pathway. *Cancer Manag Res* (2021) 13(2):3247–57. doi: 10.2147/CMAR.S265578
19. Zhang L, Kang W, Lu X, Ma S, Dong L, Zou B. LncRNA CASC11 Promoted Gastric Cancer Cell Proliferation, Migration and Invasion *In Vitro* by Regulating Cell Cycle Pathway. *Cell Cycle* (2018) 17(15):1886–900. doi: 10.1080/15384101.2018.1502574
20. Deng W, Zhang Y, Cai J, Zhang J, Liu X, Yin J, et al. LncRNA-ANRIL Promotes Gastric Cancer Progression by Enhancing NF-kB Signaling. *Exp Biol Med (Maywood)* (2019) 244(12):953–9. doi: 10.1177/1535370219860207
21. Huang T, Ji Y, Hu D, Chen B, Zhang H, Li C, et al. SNHG8 is Identified as a Key Regulator of Epstein-Barr Virus(EBV)-Associated Gastric Cancer by an Integrative Analysis of lncRNA and mRNA Expression. *Oncotarget* (2016) 7(49):80990–1002. doi: 10.18632/oncotarget.13167
22. Shibata D, Weiss LM. Epstein-Barr Virus-Associated Gastric Adenocarcinoma. *Am J Pathol* (1992) 140(4):769–74.
23. Huang J, Liao G, Chen H, Wu F, Hutt-Fletcher L, Hayward G, et al. Contribution of C/EBP Proteins to Epstein-Barr Virus Lytic Gene Expression and Replication in Epithelial Cells. *J Virol* (2006) 80(3):1098–109. doi: 10.1128/JVI.80.3.1098-1109.2006
24. Bavelloni A, Focaccia E, Piazzi M, Errani C, Blalock W, Faenza I. Cell Cycle Arrest and Apoptosis Induced by Kinamycin F in Human Osteosarcoma Cells. *Anticancer Res* (2017) 37(8):4103–9. doi: 10.21873/anticanres.11797
25. Grywalska E, Rolinski J. Epstein-Barr Virus-Associated Lymphomas. *Semin Oncol* (2015) 42(2):291–303. doi: 10.1053/j.seminoncol.2014.12.030
26. Yau TO, Tang CM, Yu J. Epigenetic Dysregulation in Epstein-Barr Virus-Associated Gastric Carcinoma: Disease and Treatments. *World J Gastroenterol* (2014) 20(21):6448–56. doi: 10.3748/wjg.v20.i21.6448
27. Wang J, Zheng X, Qin Z, Wei L, Lu Y, Peng Q, et al. Epstein-Barr Virus miR-BART3-3p Promotes Tumorigenesis by Regulating the Senescence Pathway in Gastric Cancer. *J Biol Chem* (2019) 294(13):4854–66. doi: 10.1074/jbc.RA118.006853
28. Zhang J, Li X, Hu J, Cao P, Yan Q, Zhang S, et al. Long Noncoding RNAs Involvement in Epstein-Barr Virus Infection and Tumorigenesis. *Virol J* (2020) 17(1):51. doi: 10.1186/s12985-020-01308-y
29. Liu Y, Hu Z, Zhang Y, Wang C. Long Non-Coding RNAs in Epstein-Barr Virus-Related Cancer. *Cancer Cell Int* (2021) 21(1):278. doi: 10.1186/s12935-021-01986-w
30. Notarte KI, Senanayake S, Macaranas I, Albano PM, Mundo L, Fennell E, et al. MicroRNA and Other Non-Coding RNAs in Epstein-Barr Virus-Associated Cancers. *Cancers* (2021) 13(15):3909–35. doi: 10.3390/cancers13153909
31. Dong J, Teng F, Guo W, Yang J, Ding G, Fu Z. lncRNA SNHG8 Promotes the Tumorigenesis and Metastasis by Sponging miR-149-5p and Predicts Tumor

Recurrence in Hepatocellular Carcinoma. *Cell Physiol Biochem* (2018) 51 (5):2262–74. doi: 10.1159/000495871
32. Yang H, Jiang Z, Wang S, Zhao Y, Song X, Yufeng X, et al. Long Non-Coding Small Nucleolar RNA Host Genes in Digestive Cancers. *Cancer Med* (2019) 8 (18):7693–704. doi: 10.1002/cam4.2622
33. Hen YY, Ye H, Wang Z, Xia Z, Wang B, Yi W, et al. Knockdown of SNHG8 Repressed the Growth, Migration, and Invasion of Colorectal Cancer Cells by Directly Sponging With miR-663. *BioMed Pharmacother* (2019) 116:109000. doi: 10.1016/j.biopha.2019.109000
34. Shi Z, Zhang H, Jie S, Yang X, Huang Q, Mao Y, et al. Long Non-Coding RNA SNHG8 Promotes Prostate Cancer Progression Through Repressing miR-384 and Up-Regulating HOXB7. *J Gene Med* (2021) 23(3):e3309. doi: 10.1002/jgm.3309
35. Xuan L, Sun Z, Wang J, Gao S. lncRNA SNHG8 Promotes Ovarian Cancer Progression Through Serving as Sponge for miR-1270 to Regulate S100A11 Expression. *J Gene Med* (2021) e3315. doi: 10.1002/jgm.3315
36. Chi Y, Wang D, Wang J, Yu W, Yang J. Long Non-Coding RNA in the Pathogenesis of Cancers. *Cells* (2019) 8(9):1015–59. doi: 10.3390/cells8091015
37. Wang H, Huo X, Yang XR, He J, Cheng L, Wang N, et al. STAT3-Mediated Upregulation of lncRNA HOXD-AS1 as a ceRNA Facilitates Liver Cancer Metastasis by Regulating SOX4. *Mol Cancer* (2017) 16(1):136. doi: 10.1186/s12943-017-0680-1
38. Le K, Guo H, Zhang Q, Huang X, Xu M, Huang Z, et al. Gene and lncRNA Co-Expression Network Analysis Reveals Novel ceRNA Network for Triple-Negative Breast Cancer. *Sci Rep* (2019) 9(1):15122. doi: 10.1038/s41598-019-51626-7
39. Wang L, Cho KB, Li Y, Tao G, Xie Z, Guo B. Long Noncoding RNA (lncRNA)-Mediated Competing Endogenous RNA Networks Provide Novel Potential Biomarkers and Therapeutic Targets for Colorectal Cancer. *Int J Mol Sci* (2019) 20(22):5758–84. doi: 10.3390/ijms20225758
40. Zhou RS, Zhang EX, Sun QF, Ye Z, Liu J, Zhou D, et al. Integrated Analysis of lncRNA-miRNA-mRNA ceRNA Network in Squamous Cell Carcinoma of Tongue. *BMC Cancer* (2019) 19(1):779. doi: 10.1186/s12885-019-5983-8
41. Czerwińska P, Mazurek S, Wiznerowicz M. The Complexity of TRIM28 Contribution to Cancer. *J BioMed Sci* (2017) 24(1):63. doi: 10.1186/s12929-017-0374-4
42. Fong KW, Zhao JC, Song B, Zheng B, Yu J. TRIM28 Protects TRIM24 From SPOP-Mediated Degradation and Promotes Prostate Cancer Progression. *Nat Commun* (2018) 9(1):5007. doi: 10.1038/s41467-018-07475-5
43. Jin JO, Lee GD, Nam SH, Lee TH, Kang DH, Yun JK, et al. Sequential Ubiquitination of P53 by TRIM28, RLIM, and MDM2 in Lung Tumorigenesis. *Cell Death Differ* (2021) 28(6):1790–803. doi: 10.1038/s41418-020-00701-y
44. Chen L, Muñoz-Antonia T, Cress WD. Trim28 Contributes to EMT *via* Regulation of E-Cadherin and N-Cadherin in Lung Cancer Cell Lines. *PloS One* (2014) 9(7):e101040. doi: 10.1371/journal.pone.0101040
45. Li F, Wang Z, Lu G. TRIM28 Promotes Cervical Cancer Growth Through the mTOR Signaling Pathway. *Oncol Rep* (2018) 39(4):1860–6. doi: 10.3892/or.2018.6235

Conflict of Interest: The authors declare that the research was conducted in the absence of any commercial or financial relationships that could be construed as a potential conflict of interest.

Publisher's Note: All claims expressed in this article are solely those of the authors and do not necessarily represent those of their affiliated organizations, or those of the publisher, the editors and the reviewers. Any product that may be evaluated in this article, or claim that may be made by its manufacturer, is not guaranteed or endorsed by the publisher.

frontiers in Oncology

ORIGINAL RESEARCH
published: 16 December 2021
doi: 10.3389/fonc.2021.737986

MicroRNA-20a Suppresses Tumor Proliferation and Metastasis in Hepatocellular Carcinoma by Directly Targeting EZH1

Qianqian Zhang[3†], *Xiaohong Deng*[1,2,4†], *Xiuxin Tang*[1,2,4,5], *Ying You*[1,2,4,5], *Meihua Mei*[1,2,4,5], *Danping Liu*[1,2,4,5], *Lian Gui*[1,2,4], *Yan Cai*[1,2,4,5], *Xiaoping Xin*[1,2,4], *Xiaoshun He*[1,2,4] *and Junqi Huang*[1,2,4,5*]

[1] Organ Transplant Center, The First Affiliated Hospital, Sun Yat-sen University, Guangzhou, China, [2] Guangdong Provincial Key Laboratory of Organ Donation and Transplant Immunology, The First Affiliated Hospital, Sun Yat-sen University, Guangzhou, China, [3] Guangdong Provincial Key Laboratory of Biomedical Imaging and Guangdong Provincial Engineering Research Center of Molecular Imaging, The Fifth Affiliated Hospital, Sun Yat-sen University, Zhuhai, China, [4] Guangdong Provincial International Cooperation Base of Science and Technology (Organ Transplantation), The First Affiliated Hospital, Sun Yat-sen University, Guangzhou, China, [5] Department of Laboratory Medicine, The First Affiliated Hospital, Sun Yat-sen University, Guangzhou, China

OPEN ACCESS

Edited by:
Divya P. Kumar,
JSS Academy of Higher Education and Research, India

Reviewed by:
Anjali Devi,
JSS Academy of Higher Education and Research, India
Lei Zheng,
Southern Medical University, China

***Correspondence:**
Junqi Huang
huangjq@mail.sysu.edu.cn

[†]*These authors have contributed equally to this work*

Specialty section:
This article was submitted to Gastrointestinal Cancers: Hepato Pancreatic Biliary Cancers, a section of the journal Frontiers in Oncology

Received: *08 July 2021*
Accepted: *12 October 2021*
Published: *16 December 2021*

Citation:
Zhang Q, Deng X, Tang X, You Y, Mei M, Liu D, Gui L, Cai Y, Xin X, He X and Huang J (2021) MicroRNA-20a Suppresses Tumor Proliferation and Metastasis in Hepatocellular Carcinoma by Directly Targeting EZH1. Front. Oncol. 11:737986. doi: 10.3389/fonc.2021.737986

Purpose: Hepatocellular carcinoma (HCC), a worldwide leading cause of morbidity and mortality, is the most frequent primary liver tumor. Most HCC patients are diagnosed with advanced liver cancer, resulting in a very low 5-year survival rate. Thus, there is an urgent need for the development of targeted therapies. In this study, we aimed to investigate the effect and mechanism of the miR-20a/EZH1 axis on the proliferation and metastasis of HCC and the inhibitory effect of the EZH1/EZH2 inhibitor UNC1999 on HCC.

Materials and Methods: The expression of miR-20a in human HCC tissues and cell lines was detected using quantitative real-time PCR (qRT-PCR). The expressions of proteins were analyzed with immunohistochemistry and Western blotting. Luciferase assay was used to verify whether miR-20a targets EZH1 or EZH2. The effect of miR-20a on HCC progression was studied *in vivo* and *in vitro*. The tumor inhibitory effect of UNC1999 was confirmed in vivo. CCK8 assay, wound healing assay, cell migration and invasion assay were used to evaluate the synergistic effect of UNC1999 with sorafenib. RNA sequencing (RNA-seq) was performed to screen the differentially expressed genes in the Huh7 and SMMC7721 cell lines after UNC1999, sorafenib, and combination treatments.

Results: In this study, miR-20a showed a lower expression in both HCC tissues and cell lines. MiR-20a inhibited the proliferation and migration of SMMC7721 and Huh7 cells. The results of the luciferase assay and Western blot analysis revealed that miR-20a directly targeted EZH1, a histone methyltransferase. We demonstrated that miR-20a negatively regulated the expression of EZH1 and inhibited the proliferation and metastasis of HCC by reducing H3K27 methylation. We found UNC1999 inhibited tumor cells proliferation and enhanced the inhibitory effect of sorafenib.

Conclusion: We demonstrated that miR-20a suppresses the tumor proliferation and metastasis in HCC by directly targeting EZH1. UNC1999 can inhibit tumor proliferation *in vivo* and increase the sensitivity of hepatoma cell lines to sorafenib.

Keywords: hepatocellular carcinoma, microRNA-20a, EZH1, metastasis, epigenetics

INTRODUCTION

Hepatocellular carcinoma (HCC), ranking seventh globally in incidence among malignant tumors, is characterized by a poor therapeutic effect and a high mortality rate, which makes it the third leading cause of cancer-related deaths in the world (1). Despite some advances in early detection and the recent improvements in treatment, the prognosis of patients with HCC remain poor. The current challenges are to identify new therapeutic targets and strategies and to incorporate these strategies into existing treatment regimens in order to improve treatment outcomes.

Over the past decade, mounting evidence implicates that microRNAs (miRNAs) have a well-recognized role in tumorigenesis (2–4). Currently, the understanding of the tumor-related role of miRNAs is divided into two main aspects: on one hand, the highly expressed miRNAs promote tumor progression by downregulating the expression of tumor suppressor genes; on the other hand, the low expression of miRNAs inhibits tumor formation by upregulating the expression of oncogenes (5). The altered expressions of several miRNAs (i.e., miR-18, miR-20a, miR-21, miR-34, miR-17-92, let-7a, let-7c, miR-92, miR-122, miR-195, miR-199a, miR-200a, miR-341, and miR-370) have been associated with HCC in mice and/or humans, but experimental evidence establishing a causal relationship between the abnormal expressions of these miRNAs and HCC is generally lacking (6). MiR-20a is one of the members of the miR-17-92 cluster that is located on chromosome 13 (13q31.3) (7). Downregulation of miR-20a was observed in primary HCC of patients following liver transplantation (6). Fan et al. reported that the decreased expression of miR-20a in HCC is related to its recurrence and prognosis (7), and new research has confirmed that miR-20a overexpression can inhibit liver cancer *in vivo* (8); however, the downstream mechanism of miR-20a remains unclear and merits further study.

Enhancer of zeste homologue 1 (EZH1) is a member of the Polycomb group (PcG) protein family that plays a crucial role in gene silencing (9, 10). Being one of the catalytic subunits of Polycomb repressive complex 2 (PRC2), EZH1 can repress the transcription of target genes by triggering the trimethylation of H3K27 (H3K27me3) (11). According to reports, EZH1 participates in the pathogenesis of many cancers (12–17), such as breast cancer, lung cancer, prostatic cancer, and hematologic malignancies.

However, the relationship between miR-20a and EZH1 and their functions in HCC remain undiscovered. Recent studies have revealed that several tumor suppressor miRNAs (i.e., miR-200c and miR-26a) are identified as the direct targets of EZH2 (18, 19). The role of EZH1 in HCC is far from clear. Exploring the miRNA/EZH1-associated signaling network in HCC development may provide novel therapeutic strategies for HCC treatment.

In this research, we identified that the expression of miR-20a is impaired in HCC tissues and cell lines, in a subcutaneous xenograft tumor model of HCC, due to EZH1-mediated epigenetic repression.

MATERIALS AND METHODS

Patients and HCC Samples

Cancer and matched paracancerous tissues were obtained intraoperatively from 32 HCC patients in The First Affiliated Hospital, Sun Yat-sen University (Guangzhou, China), in 2015. Patients were included in this experiment upon giving informed consent. The present study met the approval of the Ethical Committee of the hospital. Details of the samples are summarized in **Table 1**.

Reagents

UNC1999 and sorafenib were purchased from AbMole Bioscience (Houston, TX, USA). For cell culture experiments, UNC1999 was diluted in dimethyl sulfoxide (DMSO) to a stock of 10 mM, while sorafenib was diluted in DMSO to stocks of 100 μM.

Cell Culture and Cell Transfection

In this study, we used human HCC cell lines, such as Huh7, Bel-7402, QGY-7703, SMMC7721, PLC8024, H2M, and H2P, and the human immortalized normal hepatocellular cell line MIHA, which were gifted by Professor Zhu Xiaofeng's laboratory, Sun Yat-sen University Cancer Center. The HCC cells were cultured using

TABLE 1 | Clinicopathologic characteristics of HCC patients.

Feature	miR-20a: NO. of cases	EZH1: NO. of cases
Sex		
Female	2	3
Male	19	29
Age (years)		
<60	13	19
≥60	8	13
Tumor size (cm)		
<5	7	9
≥5	14	23
TNM stage		
I, II	11	16
III, IV	10	16
Portal vein tumor thrombus		
Yes	6	10
No	15	22
Cirrhosis		
Yes	6	5
No	16	27

Dulbecco's modified Eagles' medium (DMEM) (Gibco, Big Cabin, UK) supplemented with 10% fetal bovine serum (FBS), 100 μg/ml streptomycin, and 100 IU/ml penicillin at 37°C with 5% CO_2. For cell transfection, the miRNA mimic, micrONTM mimic negative control (cy3), and siEZH1 were produced by RiboBio (Guangdong, China). The transfection buffer and reagent were also purchased from RiboBio. The miRNA mimic was transfected for 24 h and siEZH1 was transfected for 48 h in six-well plates with 3×10^5 cells per well.

Murine Subcutaneous Xenograft Tumor Model of HCC

Four-week-old male Balb/c nude mice were purchased from Nanjing Biomedical Research Institute of Nanjing University. A volume of 100 μl SMMC-7721 suspension cells, which contained 5×10^6 cells, were injected subcutaneously into the flank region. In study of miR-20a, when the tumor reached a size of 5 mm × 5 mm, the mice were intratumorally injected with agomiR-20a or agomiR NC (both from RiboBio) twice a week. After 6 weeks, the gross morphology and tumor metastasis were assessed after euthanasia by macroscopically measuring the total size of the tumor nodules, conducted with hematoxylin and eosin (HE) staining of the tumor, liver, and lung. In the study of UNC1999, when the tumor reached a size of $100mm^3$, the mice were administered with DMSO as control or 150mg/kg UNC1999 once a day for 17 days. The tumor size was calculated with the following formula: volume (mm^3) = [$width^2$ × length]/2. All animal experiments were approved by the Ethics Committee for Clinical Research and Experimental Animals of the First Affiliated Hospital, Sun Yat-sen University.

Quantitative Real-Time Polymerase Chain Reaction

RNA was extracted from cells and tissue samples with the Total RNA Kit (Omega Bio-Tek, Norcross, GA, USA) according to the manufacturer's protocol. Reverse transcription was done with the Superscript III Kit (Invitrogen, Carlsbad, CA, USA). The expression level of mRNA was detected by quantitative real-time PCR (qRT-PCR) with an SYBR Green PCR Master Mix kit using a CFX96 System. The primers are shown in **Table 2**.

Cell Counting Kit-8 Assay

Cells were inoculated in a 96-well plate at 5×10^3 cells/100 μl per well. Then, the cells were incubated with increasing concentrations of miR-20a (25, 50, and 100 μM), sorafenib, sorafenib combined with UNC1999 for 12, 24, or 48 h, respectively. The supernatant was removed and 10 μl Cell Counting Kit-8 (CCK-8) solution was added into each well containing 100 μl medium. After incubation for 3 h at 37°C, the absorbance of each group at 450 nm was detected (n = 3) using an absorbance microplate reader (Sunrise, Tecan, Grödingen, Austria).

Colony Forming Assay

After miR-20a transfection, 500 cells were seeded into a six-well plate and allowed to grow for 10 days, during which period the medium was refreshed every 3 days. Then, the colonies were visualized with crystal violet staining.

Cell Migration and Invasion Assay

After transfection with small interfering RNAs (siRNAs) or miRNAs or treated with sorafenib, and the combination of sorafenib and UNC1999, the cell concentration was adjusted to a value of 3×10^5/ml in serum-free medium. In the migration assay, 200 μl of the suspended cells was plated into the upper chamber of the Transwell insert (Corning, Shanghai, China). Then, 600 μl culture medium with 15% FBS was added to the outside of the Transwell inserts. After 24 h, microscopic observations were performed. In the invasion assay, the Transwell inserts were treated with a Matrigel matrix (BD Biosciences, Franklin Lakes, NJ, USA) at 37°C for 2 h. Then, 200 μl of the suspended cells was seeded and incubated for 24 h. The rest of the procedures were similar to those in the migration assay.

Wound Healing Assay for Migration

In the study of miR-20a, suspension cells (2×10^4 cells/well) were inoculated into a 96-well plate for subsequent treatment and incubation. In the study of UNC1999, suspention cells (5×10^4 cells/well) were incubated into a 6-well plate. Then, three parallel lines were slightly scratched. The cells were washed with PBS three times to remove the deciduous cells and incubated at 37°C for 24 h or 72 h.

Western Blot Assay

SMMC7721 and Huh7 cells were lysed with RIPA (CWBio, Beijing, China) on ice. Cell protein lysates were separated by 10% SDS-PAGE, electrotransfered to polyvinylidene fluoride (PVDF) membrane (Roche, Basel, Switzerland), and blocked in 5% bovine serum albumin (BSA) for 1 h at room temperature. The membranes were incubated with primary antibody overnight at 4°C. The next day, the membranes were incubated with a secondary antibody for 1 h at room temperature. The bands were detected with an electrochemiluminescence (ECL) chromogenic substrate (Advansta, San Jose, CA, USA) and exposed using a fluorescence chemiluminescence imaging analysis system.

Dual-Luciferase Reporter Assay

293T cells were plated into a 24-well plate for 24 h. The cells were then transfected with miRNA mimics and plasmids. After

TABLE 2 | Primers.

Primer	Sequence
GAPDH-F	GGGAAACTGTGGCGTGAT
GAPDH-R	GAGTGGGTGTCGCTGTTGA
EZH1-F	GCTTCCTTCACCCTTTTCATGCCACCC
EZH1-R	CGACGACCAGAGCACTTGGAG
EZH2-F	CCCTGACCTCTGTCTTACTTGTGGA
EZH2-R	ACGTCAGATGGTGCCAGCAATA
VEGFR-2-F	GTGATCGGAAATGACACTGGAG
VEGFR-2-R	CATGTTGGTCACTAACAGAAGCA
FGF21-F	GCCTTGAAGCCGGGAGTTATT
FGF21-R	GTGGAGCGATCCATACAGGG
SIRT1-F	AAGTTGACTGTGAAGCTGTACG
SIRT1-R	TGCTACTGGTCTTACTTTGAGGG
FGFR1-F	GGCTACAAGGTCCGTTATGCC
FGFR1-R	GATGCTGCCGTACTCATTCTC

transfection for 48 h, the luciferase activities were measured with a dual-luciferase assay (Promega, Madison, WI, USA).

Immunohistochemical Staining

The tumor tissues were deparaffinized, rehydrated, and blocked with 3% BSA. After blocking with BSA, the slices were incubated with primary antibodies against EZH1 (1:200), EZH2 (1:1,000), H3K27me (1:200), H3K27me2 (1:200), and H3K27me3 (1:500; all from Abcam, Cambridge, UK) overnight at 4°C. Then, the secondary antibody goat anti-rabbit horseradish peroxidase (HRP) was added and the slices incubated for 1 h at room temperature. A DAB reagent was added for the development of a brown color. Finally, the cell nucleases were stained with hematoxylin.

In Situ Hybridization for miRNA

Paraffin-embedded tissue sections were cut and the paraffin removed. Then, the slices were placed in a boiling antigen repair reagent for antigen retrieval. Protease K was added to digest the slices for 15–25 min after cooling. After washing, the slices were incubated with a pre-hybridization reagent and then with a hybridization reagent. BSA was added to block the washed slices. Anti-digoxin-labeled alkaline phosphatase was added and incubated for 30 min after BSA was removed. The slices were then washed with Tris-buffered saline (TBS), after which 5-bromo-4-chloro-3-indolyl phosphate (BCIP)/nitro blue tetrazolium (NBT) was added. Finally, the cell nucleus was stained with a Nuclear Fast Red solution.

RNA-Seq Analysis

SMMC7721 and Huh7 cells were treated with DMSO (control), 15 μM UNC1999 or sorafenib, or a combination of UNC1999 and sorafenib. RNA was extracted from the treated cells, and then the Illumina high-throughput sequencing platform was used for transcriptome sequencing. The edgeR algorithm was used to analyze the differentially expressed genes (DEGs) in each group after obtaining the sequence expression data. The Benjamini–Hochberg (BH) method was used to correct *p*-values for the multiple hypothesis test. Genes with $p \leq 0.05$ and a fold-change (treated/untreated) cutoff >1 were considered as candidate DEGs. Both Gene Ontology (GO) annotation classification and Kyoto Encyclopedia of Genes and Genomes (KEGG) enrichment analysis were performed on the DEGs.

Statistical Analysis

Each experiment was repeated at least three times. Quantitative data were presented as the mean ± SD. Statistical analysis was performed with SPSS 16.0 and GraphPad Prism 6.0 software. Student's *t*-test and Pearson's correlation analysis were adopted to evaluate statistical significance. A $p < 0.05$ was considered statistically significant.

RESULTS

MiR-20a Expression Was Decreased in Human HCC Tissues

To explore the role of miR-20a in HCC, we collected tissue samples from HCC patients. qRT-PCR and miRNA *in situ* hybridization were performed to detect the expression of miR-20a in HCC and paratumorous tissues, which showed that the expression of miR-20a in HCC was significantly decreased compared with that in paratumorous tissues (**Figures 1A, B**).

MiR-20a Expression and Its Inhibitory Function in the Proliferation and Metastasis of HCC Cells

We examined the expression levels of miR-20a in seven HCC cell lines (Huh7, Bel-7402, QGY-7703, SMMC7721, PLC-8024, H2M, and H2P) and in normal liver cells (MIHA). Compared with MIHA, the expression of miR-20a was lower in HCC cell lines, with a statistically significant difference (**Figure 2A**). Among them, SMMC7721 and Huh7 cells were the two strains with the lowest levels of miR-20a expression. Therefore, we selected SMMC7721 and Huh7 cells to conduct subsequent experiments in order to further study the function of miR-20a in HCC tumorigenesis. We transfected SMMC7721 and Huh7 cells with an miRNA mimic (miR-20a mimic) and found that the expression of miR-20a significantly increased (**Supplementary Figures S1** and **S2**). The results of the CCK-8 and colony

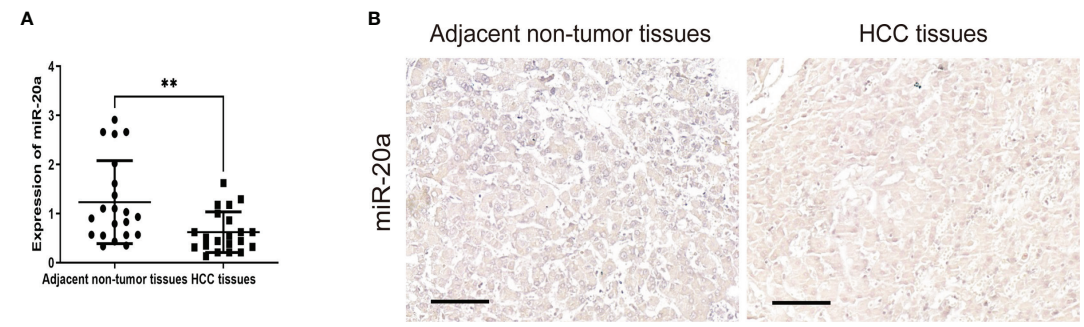

FIGURE 1 | MiR-20a expression in human hepatocellular carcinoma (HCC) tissues. Quantitative real-time PCR (qRT-PCR) **(A)** and *in situ* hybridization **(B)** of miR-20a were used to detect the expression of miR-20a in HCC and its adjacent tissues. *Scale bar*, 100 μm ($n = 21$). $^{**}p < 0.01$.

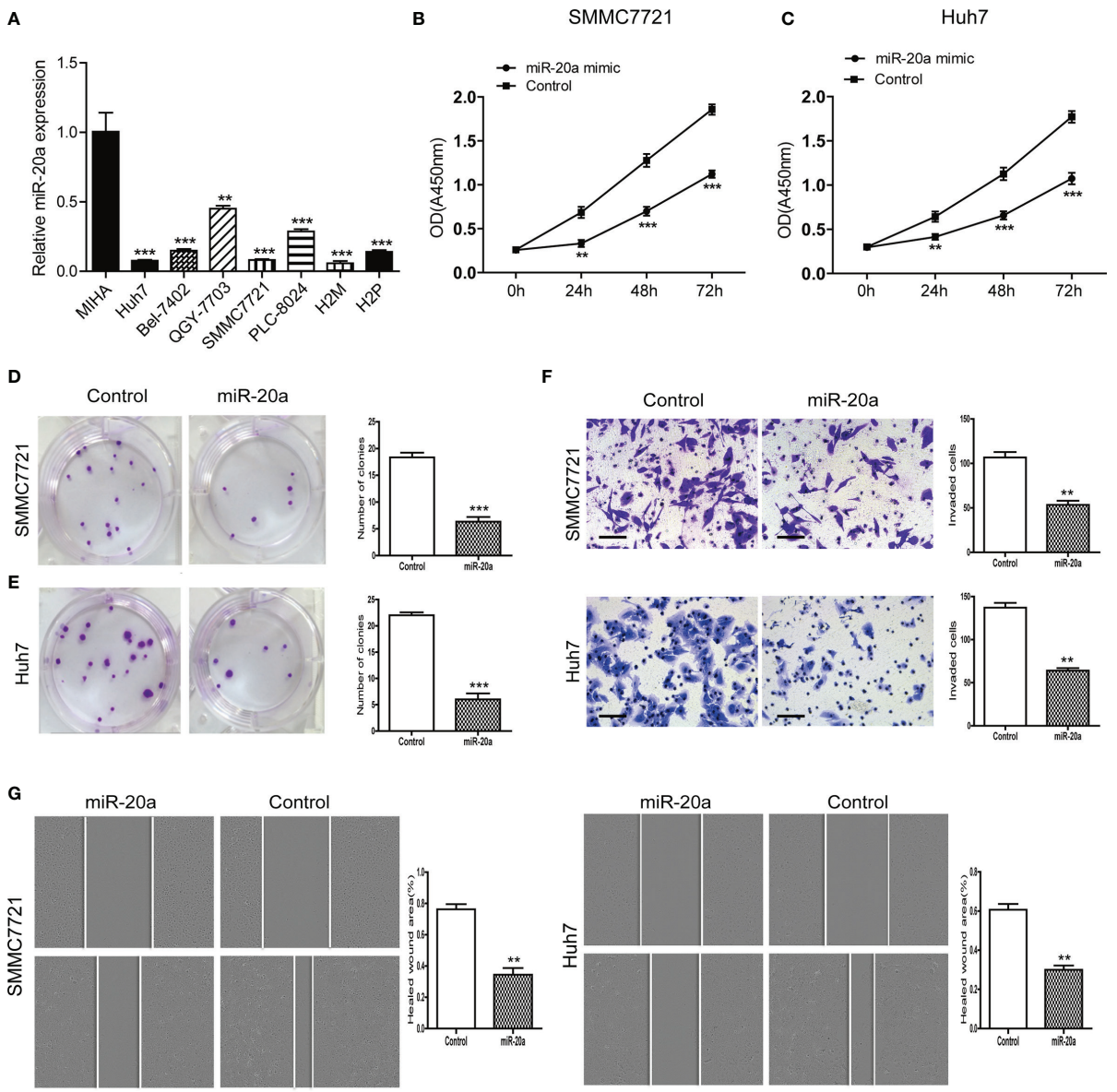

FIGURE 2 | MiR-20a expression in hepatocellular carcinoma (HCC) cells and its inhibitory function in the proliferation and metastasis of HCC. **(A)** Expression level of miR-20a in seven HCC cell lines (MIHA as the normal liver cells) (n = 3). $^{**}p < 0.01$, $^{***}p < 0.001$. **(B, C)** The proliferation of SMMC7721 and Huh7 cells was measured with the CCK-8 assay (n = 3). $^{**}p < 0.01$, $^{***}p < 0.001$. **(D, E)** Colony formation assay in SMMC7721 and Huh7 cells transfected with miR-20a and its control. Representative pictures (*left*) and statistical data (*right*) are shown (n = 3). $^{***}p < 0.001$. **(F)** Cell invasion was analyzed using the Transwell system in SMMC7721 and Huh7 cells transfected with miR-20a and its control. *Scale bar*, 100 μm (n = 3). $^{**}p < 0.01$. **(G)** Wound healing assay was used to establish the migration ability of the HCC cell lines SMMC7721 (*left*) and Huh7 (*right*) (n = 3). $^{**}p < 0.01$.

formation assays revealed that there was a reduction in cell proliferation after transfection with miR-20a (**Figures 2B–E**). Subsequently, we found that, after transfection for 24 h, there were fewer cells invading the other side of the Transwell membrane (**Figure 2F**). Moreover, the healed wound area was smaller in the miR-20a transfection group, showing that miR-20a inhibited the migration capacity of SMMC7721 and Huh7 (**Figure 2G**). Therefore, miR-20a was downregulated in the HCC cell lines, and an upregulated miR-20a inhibited the proliferation and metastasis of the HCC cell lines.

MiR-20a Directly Targeted EZH1

To explore the potential regulatory mechanisms of miR-20a in HCC migration and proliferation, we analyzed the target genes associated with miR-20a using the software TargetScan (http://www.targetscan.org/vert_71/), miRWalk (http://mirwalk.umm.

uni-heidelberg.de/), and miRDB (http://mirdb.org/). The results of the bioinformatics analysis showed that miR-20a may target the histone methyltransferase, the enhancer of zeste homologs 1 and 2 (EZH1 and EZH2). To verify the direct binding of miR-20a to the 3′UTR of EZH1/EZH2, we used the dual-luciferase reporter assay. The results showed that miR-20a could directly target EZH1, but not EZH2. MiR-20a overexpression markedly decreased the luciferase activities in the EZH1 wild-type (WT) group, but not in the EZH1 mutant group, indicating that miR-20a directly targeted the 3′UTR of EZH1 (**Figure 3A**). However, there was no direct binding between miR-20a and EZH2 (**Figure 3B**). Similarly, the inhibitory ability of miR-20a in the expression of the EZH1 protein was verified by Western blotting (**Figures 3C, D**). The results suggested that *EZH1* is a direct target gene of miR-20a in HCC.

Expression of EZH1 and H3K27 Methylation in Human HCC Tissues

EZH1 expression was significantly increased in HCC tissues (**Figure 4A**). EZH1 was positively expressed in HCC, but negatively expressed in paratumorous tissues (**Figure 4C**). Thus, there was a negative correlation between miR-20a and EZH1 in HCC tissues (**Figure 4B**). MiR-20a might affect HCC progression by regulating EZH1, which is one of the core

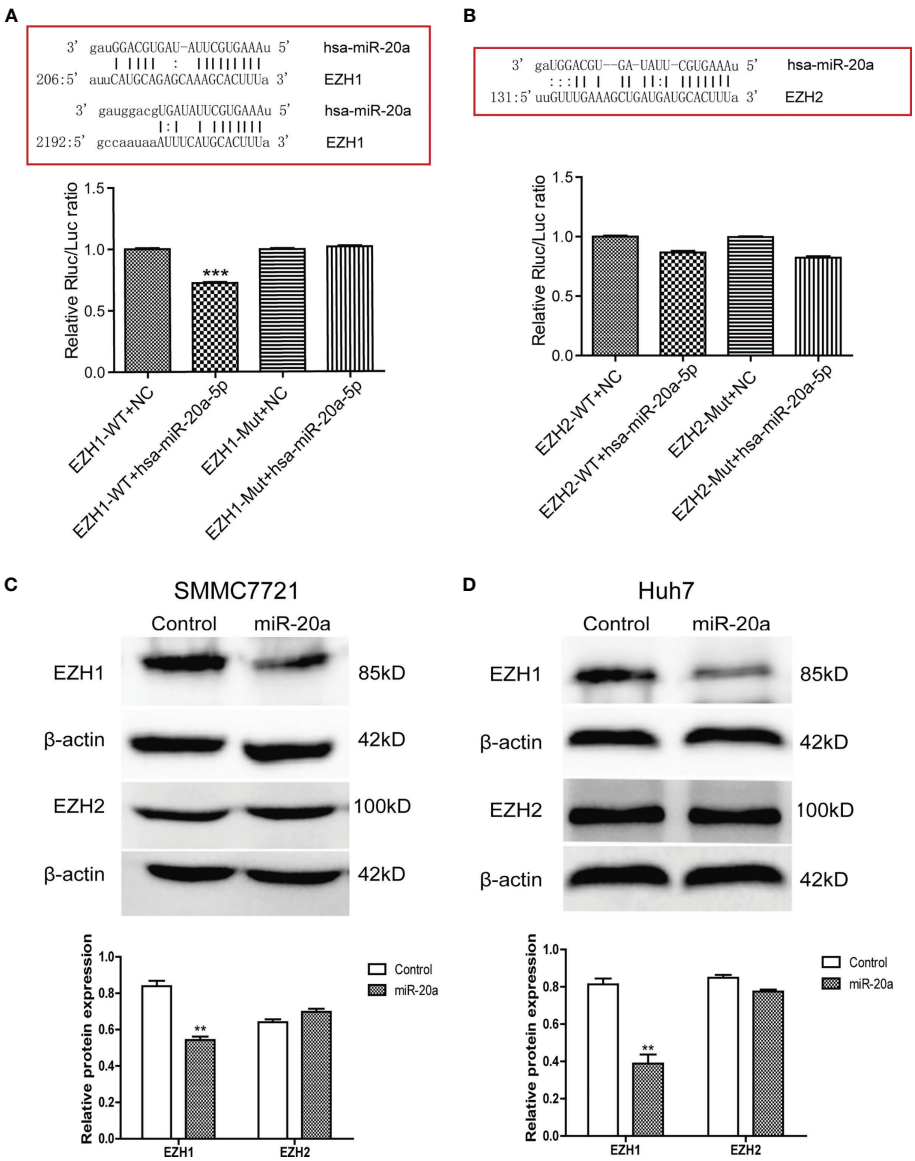

FIGURE 3 | MiR-20a directly targeted EZH1. **(A, B)** Bioinformatics analysis and luciferase assay were performed to detect the interaction of miR-20a with EZH1 and EZH2 ($n = 3$). ***$p < 0.001$. **(C, D)** After transfection of miR-20a and its control, the protein levels of EZH1 and EZH2 in SMMC7721 and Huh7 cells were detected using specific antibodies ($n = 3$). **$p < 0.01$.

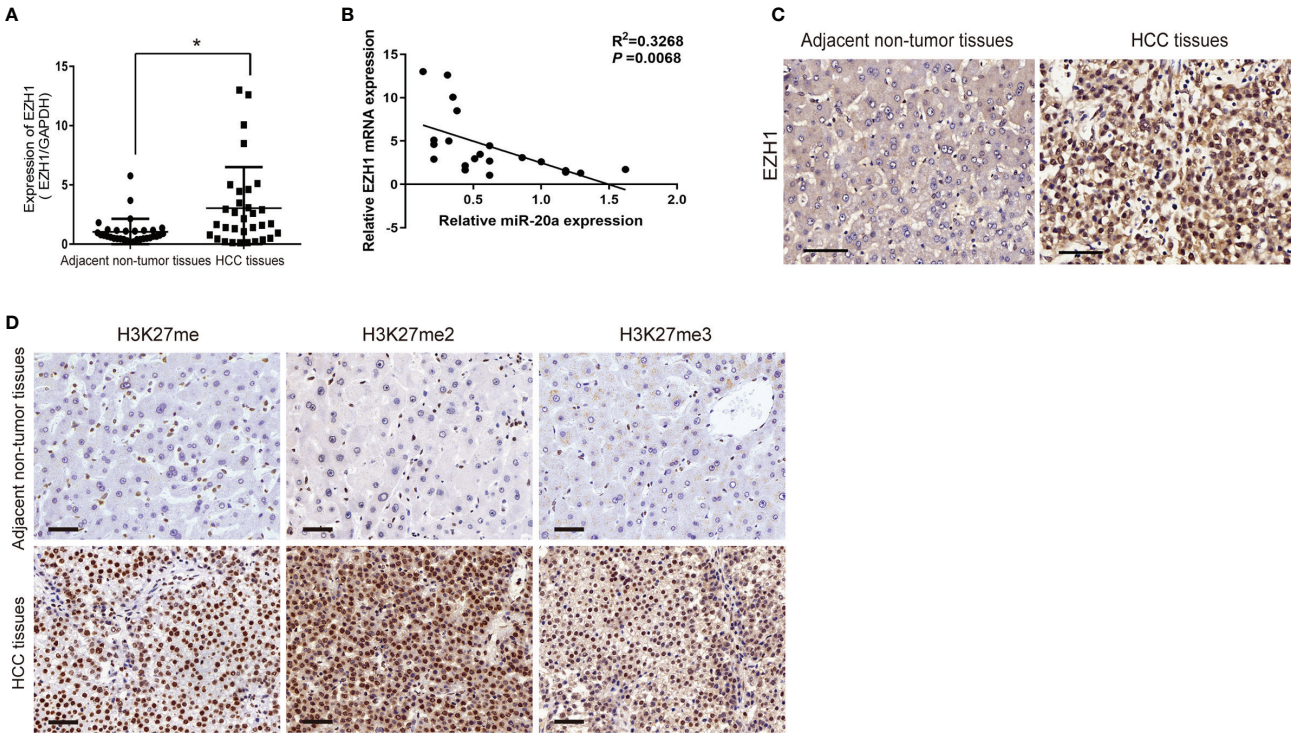

FIGURE 4 | Expression of EZH1 in human hepatocellular carcinoma (HCC) tissues. **(A, C)** Quantitative real-time PCR (qRT-PCR) and immunohistochemistry were employed to measure the expression of EZH1 in hepatocellular carcinoma and its adjacent tissues. *Scale bar*, 50 μm (n = 32). *p < 0.05. **(B)** An inverse correlation between the expression levels of miR-20a and EZH1 was obvious in HCC tissues. p=0.0068. **(D)** The expressions of H3K27me, H3K27me2, and H3K27me3 in HCC and its adjacent tissues were detected by immunohistochemistry. *Scale bar*, 50 μm.

members of PRC2 and has histone methyltransferase activity. Using immunohistochemistry, we found that histone H3 lysine 27 methylation (H3K27me) occurred in HCC tissues and that the expressions of H3K27me, H3K27me2, and H3K27me3 were upregulated (**Figure 4D**). Therefore, EZH1 might inhibit the target gene expression through modifications in H3K27 methylation, eventually leading to tumorigenesis.

Knockdown of EZH1 Inhibited HCC Proliferation and Metastasis

MiR-20a could directly regulate EZH1, but the function of EZH1 in HCC is unclear. We used the Kaplan–Meier plot (20) to determine the prognostic value of EZH1 in HCC, with the results indicating that patients with a low EZH1 expression show better overall survival (OS) compared to those with a high EZH1 expression (p< 0.05) (**Figure 5A**). To further elucidate the role of EZH1, SMMC7721 cells were transfected with three types of siEZH1 for 48 h to confirm the reduction of EZH1 expression. The results of Western blot analysis revealed that the expression level of EZH1 was significantly decreased (**Figure 5B**). Therefore, we selected siEZH1-1 for further experiments. The results of both the CCK-8 assay (**Figure 5C**) and the colony formation assay (**Figure 5D**) showed that the proliferation ability of SMMC7721 was markedly inhibited in the siEZH1-1 group. Moreover, siEZH1 also significantly suppressed the migration and invasion ability of SMMC7721 (**Figures 5E, F**).

MiR-20a Inhibited HCC Formation and Metastasis by Directly Targeting EZH1 *In Vivo*

To determine the effect of miR-20a on HCC tumorigenicity, we performed tumorigenesis experiments in nude mice. SMMC7721 cells were subcutaneously injected into nude mice. After tumor formation (more than 5 mm × 5 mm), the mice were divided into two groups. The miR-20a agonist (agomiR-20a) and its control were continuously injected for 6 weeks. The tumor growth inhibitory rate and the tumor volume decrease rate were calculated. There was no significant change in the body weight of the mice in the two groups (**Figure 6B**). However, the tumor volume in the mice of the agomiR-20a group decreased to some degree (**Figure 6C**). These results indicated that miR-20a inhibited the growth of HCC. Subsequently, we examined the expressions of miR-20a, EZH1, and EZH2 in nude mice using qRT-PCR, *in situ* hybridization, and immunohistochemistry. Compared with that in the control group, the expression of miR-20a increased in the agomiR-20a group (p < 0.05), whereas that of EZH1 decreased (p < 0.01), the expression of EZH2 showed no significant change (p > 0.05) (**Figures 6D–I**). Then,

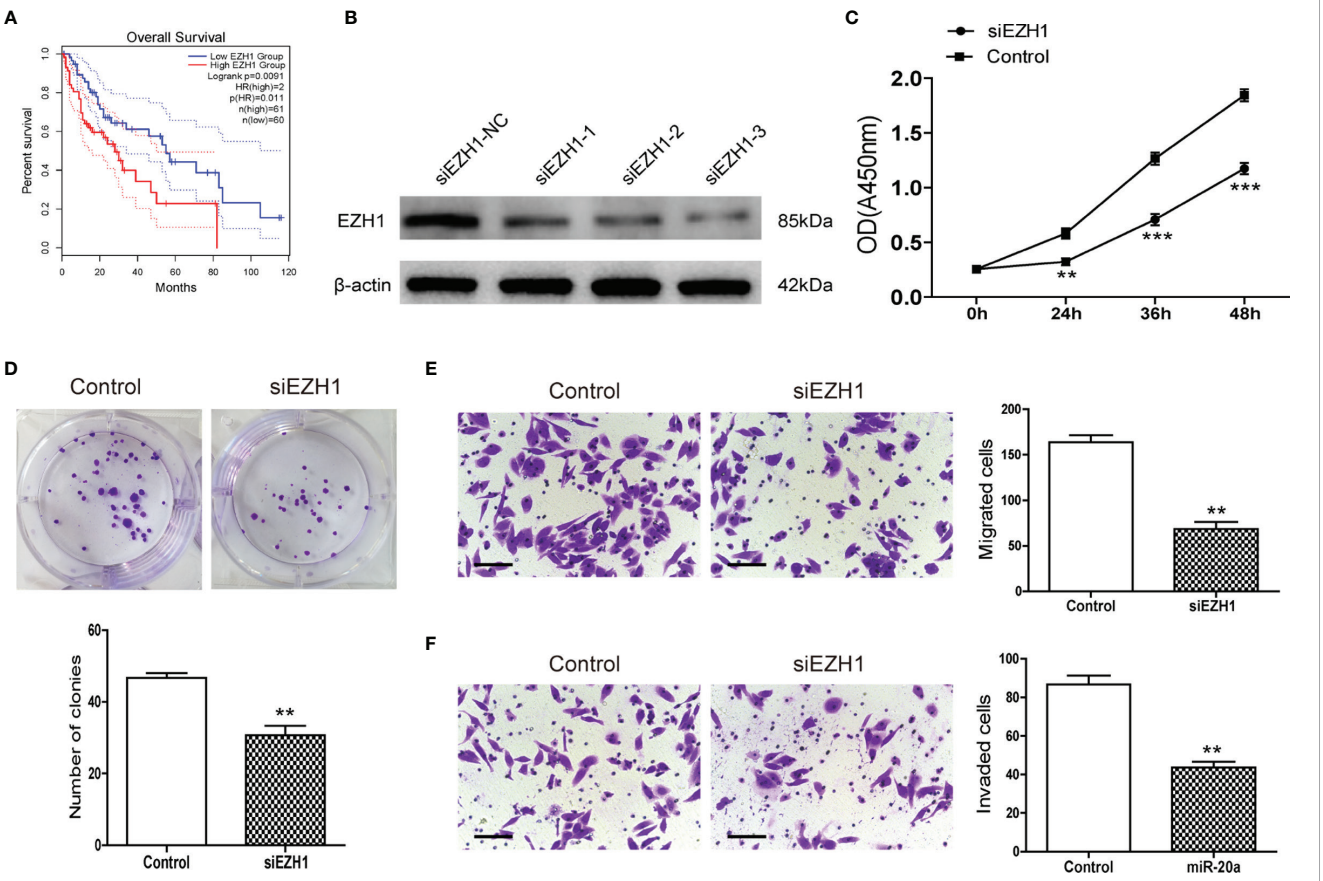

FIGURE 5 | Knockdown of EZH1 inhibited the proliferation and metastasis of hepatocellular carcinoma (HCC). **(A)** Kaplan–Meier survival curves show the overall survival (OS) rate of HCC patients with high (n = 180) and low (n = 181) protein expression levels of EZH1 from the GEPIA database. **(B)** Transfection of siEZH1 in the HCC cell line SMMC7721 inhibited the expression of EZH1. **(C)** The proliferation of SMMC7721 was measured using the CCK-8 assay (n = 3). $^{**}p < 0.01$, $^{***}p < 0.001$. **(D)** Colony formation assay in SMMC7721 transfected with siEZH1 and its control. Representative pictures (*top*) and statistical data (*bottom*) are shown (n = 3). $^{**}p < 0.01$. **(E)** Transwell assay analysis of SMMC7721 was performed after transfection with siEZH1 and its control to determine the migration capacity. *Scale bar*, 100 μm (n = 3). $^{**}p < 0.01$. **(F)** Transwell assay analysis of SMMC7721 was performed after transfection with siEZH1 and its control to determine the invasion capacity. *Scale bar*, 100 μm (n = 3). $^{**}p < 0.01$.

we dissected the mice and detected visible liver metastasis in the control group. The HE staining results clearly showed the presence of tumor cells; the structure of the hepatic lobules disappeared and an obvious necrosis of the liver cells around the tumor was observed. However, there was no liver metastasis in the agomiR-20a group (**Figure 6J**). An increased number of cells was found in the lungs of nude mice, as well as a large number of infiltrated inflammatory cells in the control group, but not in the agomiR-20a group (**Figure 6K**).

UNC1999, an Oral EZH1/EZH2 Inhibitor, Inhibited HCC Formation *In Vivo*

UNC1999 was developed as the first oral EZH1/EZH2 inhibitor in 2013 (21). We have found that UNC1999 had inhibitory effect in HCC cells in our previous study (22). We used murine subcutaneous xenograft tumor model to evaluate the curative effect and safety of UNC1999 in HCC. There were no statistical significant changes in body weight and the tumor volume in the two groups (**Figures 7A–C**).

However, they decreased to some degree in the UNC1999 group. The number of white blood cells (WBC), neutrophils (NE), lymphocytes (LYM) and monocytes (MNC) in peripheral blood was higher in the UNC1999 group (**Figure 7D**), but still in the normal reference range. There was no significant difference in plasma creatinine (CREA), alanine aminotransferase (ALT) and aspartate aminotransferase (AST) (**Figure 7E**) between the two groups, suggesting that UNC1999 had a very finite liver and renal toxicity. Blood glucose and triglycerides were significantly lower in UNC1999 group (**Figure 7E**), which suggests that UNC1999 may affect glucose and lipid metabolism.

UNC1999 Enhanced the Inhibitory Effects of Sorafenib in HCC Cells

Sorafenib is a tyrosine kinase inhibitor that shows antitumour effects against various cancers (23). However, the clinical application of

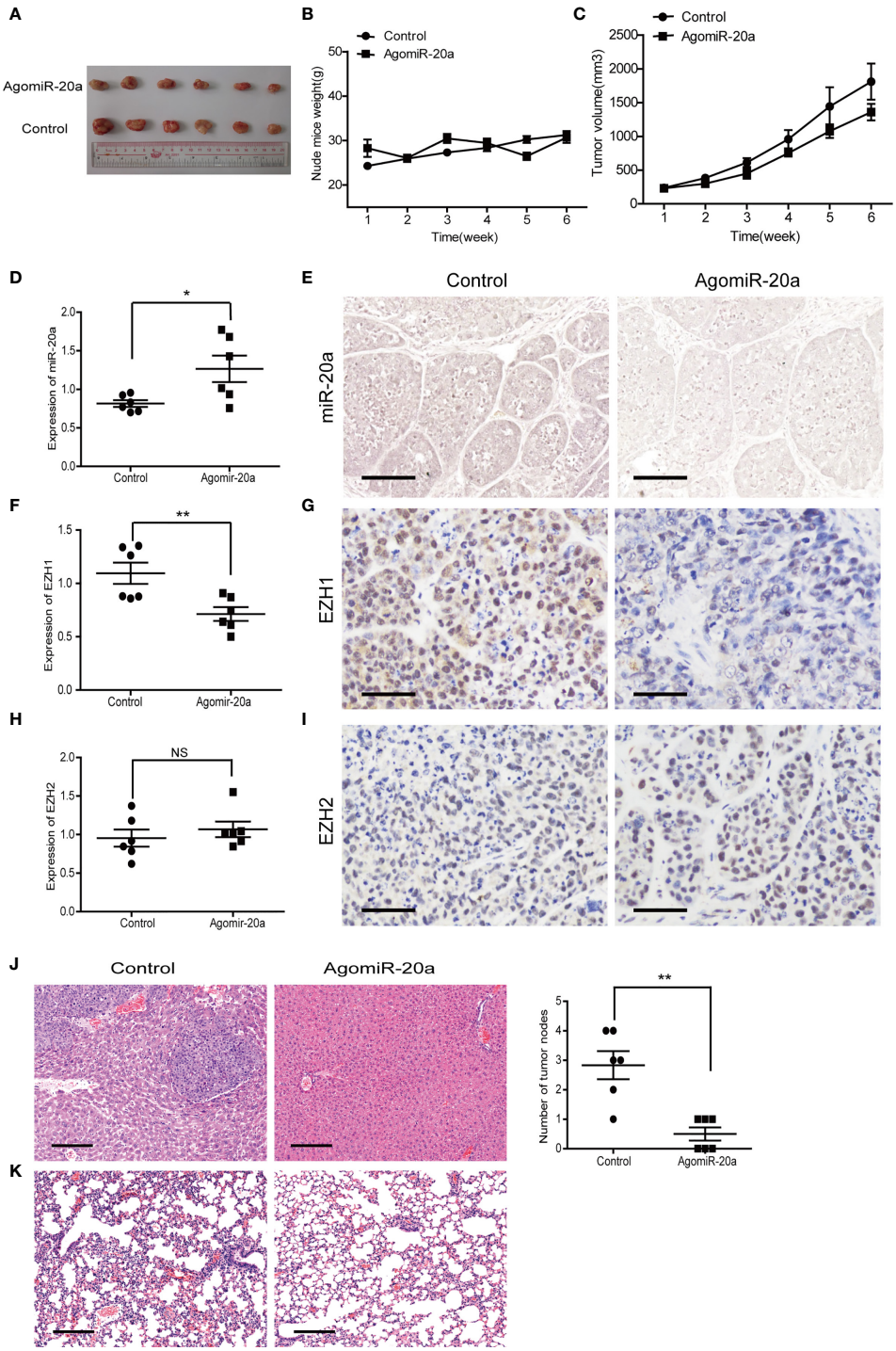

FIGURE 6 | MiR-20a inhibited tumorigenicity *in vivo*. **(A–C)** Tumors formed in nude mice. SMMC7721 cells were injected into the flanks of nude mice by subcutaneous injection. Mice were killed after 6 weeks. Representative pictures of solid tumors **(A)**, tumor weight **(B)**, and tumor volume **(C)** are presented (n = 6). **(D, F, H)** Expressions of miR-20a **(D)**, EZH1 **(F)**, and EZH2 **(H)** in subcutaneous tumors of nude mice detected by quantitative real-time PCR (qRT-PCR) (n = 6). $^{*}p < 0.05$, $^{**}p < 0.01$, (NS denotes the absence of significant difference). **(E)** MicroRNA *in situ* hybridization was employed to detect the expression of miR-20a in subcutaneous tumors of nude mice. *Scale bar*, 100 μm. **(G)** EZH1 expression in subcutaneous tumors of nude mice detected by immunohistochemistry. EZH1 expression in the nucleus: positive expression is shown in *brown* and negative in *blue*. *Scale bar*, 50 μm. **(I)** EZH2 expression in subcutaneous tumors of nude mice detected by immunohistochemistry. EZH2 expressed in the nucleus: positive expression is shown in *brown* and negative in *blue*. *Scale bar*, 50 μm. **(J, K)** Liver and lung metastases of the miR-20a agonist group and its control shown using hematoxylin–eosin (HE). *Scale bar*, 200 μm.

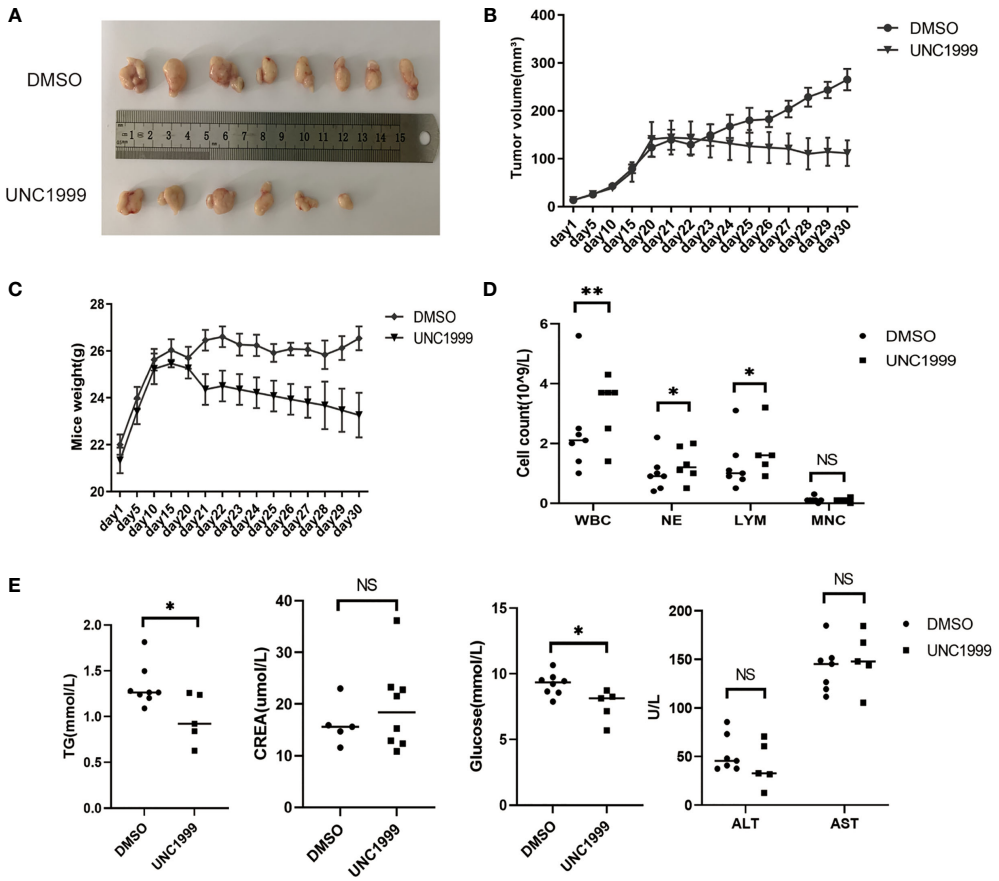

FIGURE 7 | UNC1999 inhibited tumorigenicity *in vivo*. **(A–C)** Tumors formed in nude mice. SMMC7721 cells were injected into nude mice by subcutaneous injection. On day 20 after injection, mice with tumor were randomly divided into two groups and were given DMSO as control or UNC1999 (150mg/kg) separately by gavage once a day. After 17 days, mice were euthanized. **(A)** Representative pictures of solid tumors (DMSO group n=8, UNC1999 group n=6). **(B)** Tumor volume. **(C)** Mice weight. **(D)** The numbers of white blood cells (WBC), neutrophils (NE), lymphocytes (LYM) and monocytes (MNC) in peripheral blood of mice in DMSO group and UNC1999 group. *$p < 0.05$, **$p <$ 0.01, NS denotes the absence of significant difference. **(E)** The levels of triglyceride (TG), creatinine (CREA), glucose, ALT and AST in plasma of mice in DMSO group and UNC1999 group. (*$p < 0.05$, NS denotes the absence of significant difference).

sorafenib is often hampered by drug resistance (23). To explore synergistic effect of UNC1999 with sorafenib in HCC, we used sorafenib and combination of sorafenib and UNC1999 in SMMC7721 and Huh7 cells. CCK8 assay results showed that the optimal dosage was 15 μM for 12 h (**Figures 8A, B**). RNA-seq analysis was performed to seek out DEGs in SMMC7721 and Huh7 cells. We identified up-regulated and down-regulated DEGs by using volcano plots (**Figures 8C, D**). Heatmap of DEGs revealed the related genes may have synergistic effect in HCC cells (**Figures 8E, F**). Results of wound healing assay and Transwell experiment showed that UNC1999 significantly enhanced sorafenib inhibitory ability in HCC cells (**Figures 8G, H**). Bioinformatics (RNA-seq) analysis indicated that, compared with sorafenib group, the transcription level of *FGF21* in the combination group decreased significantly and was verified by qRT-PCR. FGF21 can promote cell proliferation, vascular proliferation, and wound repair. It participates in maintaining the balance of energy metabolism and is closely related to liver diseases. In patients with liver tumors, the levels of FGF21 in hepatocytes were invariably elevated compared to those in healthy controls (24). Therefore, we used qRT-PCR to verify the receptor of FGF21 (*FGFR1*), the targets of sorafenib (*VEGFR2*) (23) and upstream gene of FGF21 (*SIRT1*). These genes were all down-regulated in the combination group (**Figure 8I**). We found a pathway related to FGF21 (**Figure 8J**) in KEGG website (https://www.kegg.jp/), which showed FGF21-FGFR1 binding targeted the cell proliferation, cell survival and translation via PI3K-Akt and MAPK signaling pathways. The plasma level of FGF21 was reduced in sorafenib-treated HCC patients (25), which suggested that FGF21 might be related with sorafenib treatment in HCC. Finally, we took a diagram to show our work (**Figure 9**), miR-20a and UNC1999 inhibited tumor proliferation and metastasis by inhibiting EZH1. At the same time, UNC1999 could increase the sensitivity of hepatoma cell lines to sorafenib by down regulating *SIRT1*, *FGF21*, *FGF21* and *VEGFR2*.

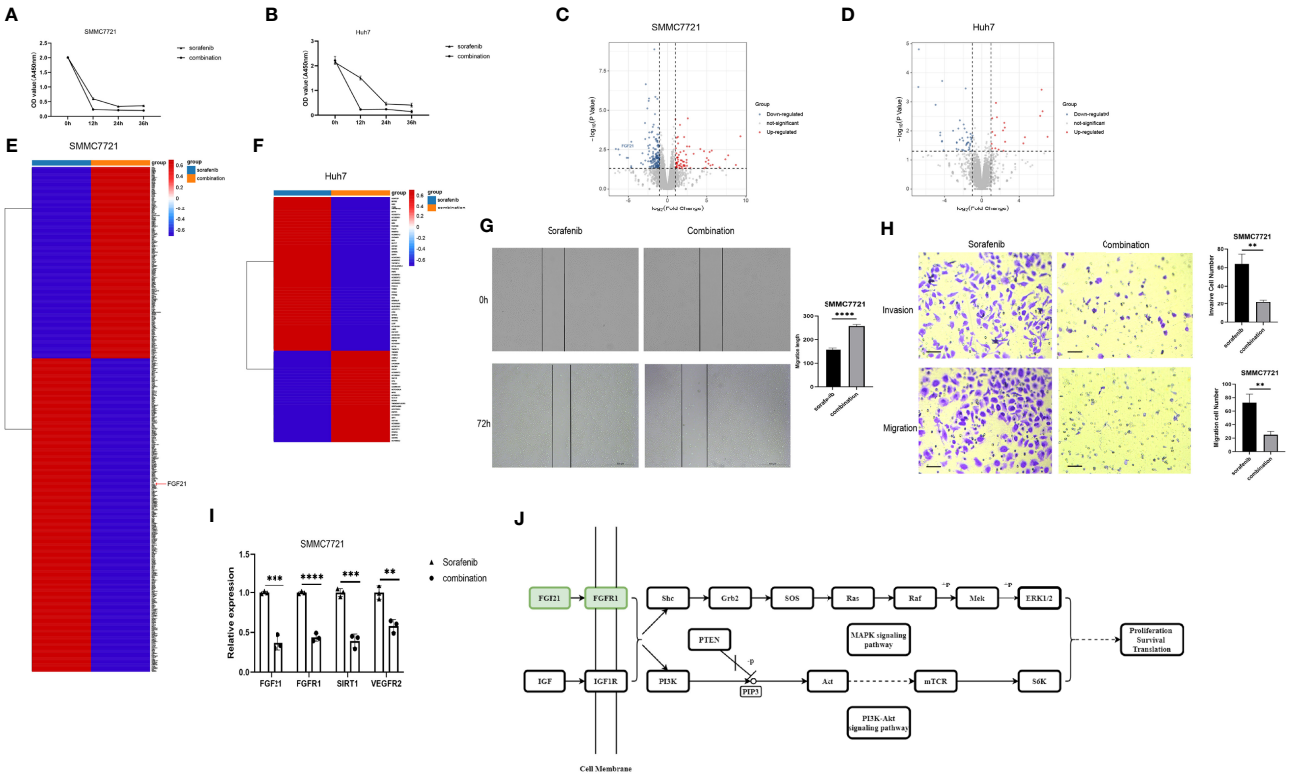

FIGURE 8 | UNC1999 enhanced sorafenib inhibitory effects in hepatocellular carcinoma cell lines. **(A, B)** Proliferation of SMMC7721 **(A)** and Huh7 **(B)** was measured by using CCK8 assay. **(C, D)** Volcano plots of DEGs between sorafenib and combination group of SMMC7721 **(C)** and Huh7 **(D)**. **(E, F)** Expression of up-regulated and downregulated DEGs that were related to HCC proliferation and metastasis of sorafenib group and combination group in SMMC7721 **(E)** and Huh7 **(F)** were presented in heatmaps. **(G)** Wound healing assay was used to establish the migration ability of SMMC7721 (n=3, $^{****}P < 0.0001$). **(H)** Cell invasion and migration in SMMC7721 were analyzed using the Transwell assay. Scale bar, 500μm (n=3, $^{**}P < 0.01$). **(I)** The expression of FGF21, FGFR1, SIRT1 and VEGFR2 in SMMC7721 was measured by qRTPCR. $^{**}p < 0.01$, $^{***}p < 0.001$, $^{****}p < 0.0001$. **(J)** Diagram of FGF21-related KEGG pathway. sorafenib group: 15μM sorafenib; combination group: 15μM sorafenib and 15μM UNC1999.

DISCUSSION

In the current study, we found that miR-20a was suppressed in HCC tissues (**Figures 1A, B**) and that its overexpression inhibited the growth of HCC cells, as shown by the results of the CCK-8 and colony formation assays (**Figures 2A–E**). We speculated that miR-20a played an inhibitory regulation role in HCC and that its low expression could accelerate the development of HCC. The results of the Transwell and wound healing assays of SMMC7721 and Huh7 cells showed that miR-20a inhibited the invasion and migration of HCC (**Figures 2F, G**). In addition, we also verified our findings in animals. With animal studies *in vivo*, we observed that there were no significant changes in the tumor size and body weight of the animals in the two groups (**Figures 6A–C**). Interestingly, there was obvious tumor metastasis in the liver of mice in the control group. However, the miR-20a overexpression group showed no appearance of metastases (**Figure 6J**). Inflammation was detected in the lungs of the control group of animals, which was absent in the miR-20a group (**Figure 6K**). In summary, we found that miR-20a overexpression inhibited HCC cell proliferation, invasion, and migration *in vitro* and *in vivo*.

MiR-20a is critically involved in the proliferation and metastasis of HCC cells, but its specific regulatory mechanism has not been elucidated yet. Based on these results and the data from the bioinformatics analysis, we speculated that miR-20a played indirect regulatory functions in the pathogenesis of HCC. An earlier study revealed that miR-17-5p inhibited EZH1 and that the downregulation of miR-17-5p was associated with drug resistance in lung cancer cells by targeting EZH1 (26). Through bioinformatics analysis and luciferase assays, we discovered that miR-20a, which is located in the same gene cluster as miR-17-5p, can directly target EZH1, but not EZH2, an EZH1 homolog (**Figures 3A, B**). The Western blot results further validated our speculation that the overexpression of miR-20a inhibited the protein levels of EZH1 (**Figures 3C, D**). EZH1 is a vital member of the polyclonal family PcG, which can elicit epigenetic silencing by regulating the remodeling of chromatin. The PcG gene forms two Polycomb inhibitory complexes (PRC1 and PRC2) by complex coding different proteins. The PRC1 complex consists of CBX, PHC, BMI1, and RING1A, and RING1B (27). On the other hand, the PRC2 complex consists of EZH1, EZH2, SUZ12, EED, RBBP2, and AEBP2 (28). EZH1 is an important catalytic subunit of the PRC2 complex. EZH1 could methylate lysine 27 of

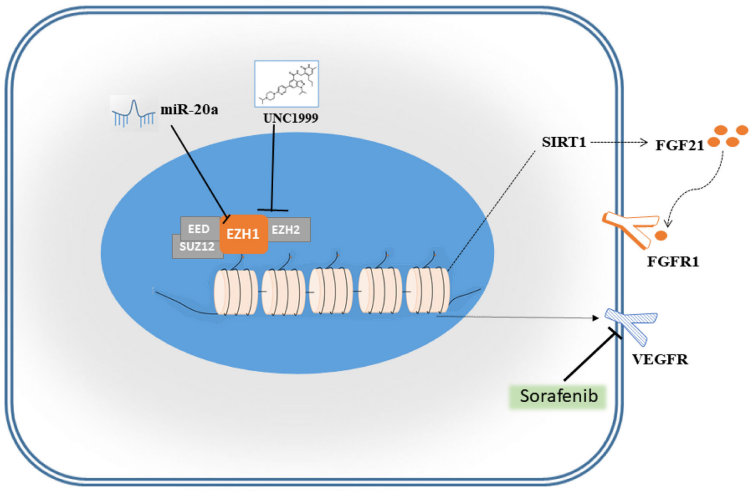

FIGURE 9 | Schematic diagram of miR-20a and EZH1.

histone H3 methylation, and the PRC1 complex recognizes and binds to specific gene loci, leading to the repression of gene transcription (29, 30). Currently, the high expression of EZH1 in some tumors, such as in lung cancer, breast cancer, and prostate cancer, suggests that it is closely related to tumorigenesis. Our group found that the expression of EZH1 in HCC was significantly upregulated (**Figures 4A, C**). We also established that the expressions of H3K27me, H3K27me2, and H3K27me3 were upregulated in HCC patients (**Figure 4D**), indicating that EZH1 may participate in H3K27 methylation, causing cell proliferation and gene transcription inhibition and ultimately leading to the occurrence of tumors.

Our results showed that EZH1/2 inhibitor UNC1999 had a tendency to inhibit the prolifeation of liver cancer *in vivo*, then we performed RNA-seq on the SMMC7721 and Huh7 cell lines treated with sorafenib and a combination of sorafenib and UNC1999. UNC1999 is an orally bioavailable selective dual EZH1/EZH2 inhibitor that works in competition with the cofactor *S*-adenosyl-L-methionine (SAM) (21). UNC1999 has shown inhibitory effects on a variety of tumors, such as mixed lineage leukemia (MLL), rearranged leukemia, and multiple myeloma (31). Sorafenib is an orally bioavailable multi-kinase inhibitor that was approved by the Food and Drug Administration (FDA) for clinical use in the treatment of HCC in 2007 and can block tumor angiogenesis by inhibiting VEGFR and platelet-derived growth factor receptor (PDGFR) (32). Many patients treated with sorafenib eventually developed resistance to the drug. Our results showed that UNC1999 could reduce the expression of VEGFR-2 and achieve maximum inhibition in combination with sorafenib. Therefore, VEGFR-2 is one of the effective targets of UNC1999. On the other hand, in the sorafenib group and the combination group, FGF21, one of the fibroblast growth factors, and its relative genes *FGFRl* and *SIRT1* were down-regulated. Studies (33, 34) have shown that FGF21 is an important activator of the PI3K signaling pathway, one of the signaling pathways in initiating and promoting HCC. Our KEGG analysis results showed that the PI3K/Akt signaling pathway was significantly down-regulated, which exactly confirmed that the target of UNC1999 may be the FGF21/PI3K/Akt signaling pathway. Consequently, VEGFR-2, FGF21, and its downstream PI3K/Akt signaling pathway may explain the inhibition and synergistic effects of UNC1999.

The present study has several limitations. Firstly, we did not have enough tissue samples from HCC patients to examine the expressions of miR-20a and EZH1. Secondly, the results of the RNA-seq analysis were not validated using qRT-PCR and Western blot assay globally. Finally, further in-depth analysis is required to study the roles of miR-20a and EZH1 in HCC tumorigenesis and to explore miR-20a as a potential prognostic target.

CONCLUSION

In summary, miR-20a negatively regulates the expression of EZH1 and reduces the methylation of H3K27. The EZH1/EZH2 inhibitor UNC1999 has inhibitory effects on the metastasis, invasion, and migration of HCC. However, the specific role of EZH1 in HCC remains to be further studied.

DATA AVAILABILITY STATEMENT

The datasets presented in this study can be found in online repositories. The names of the repository/repositories and accession number(s) can be found below: http://www.ncbi.nlm.nih.gov/bioproject/765866.

ETHICS STATEMENT

The studies involving human participants were reviewed and approved by the Ethics Committee for Clinical Research and Experimental Animals of the First Affiliated Hospital, Sun Yat-sen University. The patients/participants provided written informed consent to participate in this study. The animal study was reviewed and approved by the Ethics Committee for Clinical Research and Experimental Animals of the First Affiliated Hospital, Sun Yat-sen University.

AUTHOR CONTRIBUTIONS

JH conceived and designed the experiments. QZ and XD performed research, analyzed the data, and wrote the paper. XT, YY, MM, and DL performed research, analyzed the data, and wrote part of the paper related to EZH1 inhibitor UNC1999 function. LG, YC, and XX analyzed the results and improved the manuscript. XH provided clinical samples. All authors supervised the research, analyzed the results, and improved the manuscript. All authors contributed to the article and approved the submitted version.

FUNDING

This work was supported by the National Natural Science Foundation of China (NO. 31370870 and NO. 81871238), the Natural Science Foundation of Guangdong Province (NO. S2013020013000 and NO. 2021A1515010435), the Science and Technology Program of Guangdong, China (NO. 2013A020229003, NO. 2015B050501002, NO. 2020A0505020003, and NO. 2020B1212060026), and the Science and Technology Program of Guangzhou, China (NO. 201604020083 and no. 202103000007).

SUPPLEMENTARY MATERIAL

The Supplementary Material for this article can be found online at: https://www.frontiersin.org/articles/10.3389/fonc.2021.737986/full#supplementary-material

Supplementary Figure 1 | Cy3-miRNA mimic NC can effectively transfect hepatocellular carcinoma cells SMMC7721. **(A)** Cy3-labeled mimic NC was observed under a fluorescence microscope to preliminary assess transfection efficiency in SMMC7721. **(B)** The expression of miR-20a in SMMC7721 hepatocellular carcinoma cells was detected by qRT-PCR 24h, 36h and 48h after transfection. (MiR-20a mimic *vs* miR-20a mimic NC, $n = 3$, $^{***}p < 0.001$, $^{**}p < 0.01$).

Supplementary Figure 2 | Cy3-miRNA mimic NC can effectively transfect liver cancer cells Huh7. **(A)** Cy3-labeled mimic NCs were observed under a fluorescence microscope to initially assess transfection efficiency in Huh7. **(B)** The expression of miR-20a in Huh7 cells was detected by qRT-PCR 24h, 36h and 48h after transfection. (MiR-20a mimic *vs* miR-20a mimic NC, n = 3, $^{***}p < 0.001$).

REFERENCES

1. Sung H, Ferlay J, Siegel RL, Laversanne M, Soerjomataram I, Jemal A, et al. Global Cancer Statistics 2020: GLOBOCAN Estimates of Incidence and Mortality Worldwide for 36 Cancers in 185 Countries. *CA Cancer J Clin* (2021) 71(3):209–49. doi: 10.3322/caac.21660
2. Tsuchida A, Ohno S, Wu W, Borjigin N, Fujita K, Aoki T, et al. miR-92 Is a Key Oncogenic Component of the miR-17-92 Cluster in Colon Cancer. *Cancer Sci* (2011) 102(12):2264–71. doi: 10.1111/j.1349-7006.2011.02081.x
3. Li X, Zhang Z, Yu M, Li L, Du G, Xiao W, et al. Involvement of miR-20a in Promoting Gastric Cancer Progression by Targeting Early Growth Response 2 (EGR2). *Int J Mol Sci* (2013) 14(8):16226–39. doi: 10.3390/ijms140816226
4. Li S, Qiang Q, Shan H, Shi M, Gan G, Ma F, et al. MiR-20a and miR-20b Negatively Regulate Autophagy by Targeting RB1CC1/FIP200 in Breast Cancer Cells. *Life Sci* (2016) 147:143–52. doi: 10.1016/j.lfs.2016.01.044
5. Goodall GJ, Wickramasinghe VO. RNA in Cancer. *Nat Rev Cancer* (2021) 21 (1):22–36. doi: 10.1038/s41568-020-00306-0
6. Yu Z, Wang C, Wang M, Li Z, Casimiro MC, Liu M, et al. A Cyclin D1/ microRNA 17/20 Regulatory Feedback Loop in Control of Breast Cancer Cell Proliferation. *J Cell Biol* (2008) 182(3):509–17. doi: 10.1083/jcb.200801079
7. Fan M-Q, Huang C-B, Gu Y, Xiao Y, Sheng J-X, Zhong L. Decrease Expression of microRNA-20a Promotes Cancer Cell Proliferation and Predicts Poor Survival of Hepatocellular Carcinoma. *J Exp Clin Cancer Res* (2013) 32(1):21. doi: 10.1186/1756-9966-32-21
8. Tipanee J, Di Matteo M, Tulalamba W, Samara-Kuko E, Keirsse J, Van Ginderachter JA, et al. Validation of miR-20a as a Tumor Suppressor Gene in Liver Carcinoma Using Hepatocyte-Specific Hyperactive Piggybac Transposons. *Mol Ther Nucleic Acids* (2020) 19:1309–29. doi: 10.1016/ j.omtn.2020.01.015
9. Margueron R, Reinberg D. The Polycomb Complex PRC2 and Its Mark in Life. *Nature* (2011) 469(7330):343–9. doi: 10.1038/nature09784
10. Laugesen A, Hojfeldt JW, Helin K. Molecular Mechanisms Directing PRC2 Recruitment and H3K27 Methylation. *Mol Cell* (2019) 74(1):8–18. doi: 10.1016/j.molcel.2019.03.011
11. Lavarone E, Barbieri CM, Pasini D. Dissecting the Role of H3K27 Acetylation and Methylation in PRC2 Mediated Control of Cellular Identity. *Nat Commun* (2019) 10(1):1679. doi: 10.1038/s41467-019-09624-w
12. Mochizuki-Kashio M, Aoyama K, Sashida G, Oshima M, Tomioka T, Muto T, et al. Ezh2 Loss in Hematopoietic Stem Cells Predisposes Mice to Develop Heterogeneous Malignancies in an Ezh1-Dependent Manner. *Blood* (2015) 126(10):1172–83. doi: 10.1182/blood-2015-03-634428
13. Rizq O, Mimura N, Oshima M, Saraya A, Koide S, Kato Y, et al. Dual Inhibition of EZH2 and EZH1 Sensitizes PRC2-Dependent Tumors to Proteasome Inhibition. *Clin Cancer Res* (2017) 23(16):4817–30. doi: 10.1158/1078-0432.Ccr-16-2735
14. Sun Y, Zhou Y, Bai Y, Wang Q, Bao J, Luo Y, et al. A Long Non-Coding RNA HOTTIP Expression Is Associated With Disease Progression and Predicts Outcome in Small Cell Lung Cancer Patients. *Mol Cancer* (2017) 16(1):162. doi: 10.1186/s12943-017-0729-1
15. Rizk M, Rizq O, Oshima M, Nakajima-Takagi Y, Koide S, Saraya A, et al. Akt Inhibition Synergizes With Polycomb Repressive Complex 2 Inhibition in the Treatment of Multiple Myeloma. *Cancer Sci* (2019) 110(12):3695–707. doi: 10.1111/cas.14207
16. Yamagishi M, Hori M, Fujikawa D, Ohsugi T, Honma D, Adachi N, et al. Targeting Excessive EZH1 and EZH2 Activities for Abnormal Histone Methylation and Transcription Network in Malignant Lymphomas. *Cell Rep* (2019) 29(8):2321–37.e2327. doi: 10.1016/j.celrep.2019.10.083
17. Zeng Z, Yang Y, Wu H. MicroRNA-765 Alleviates the Malignant Progression of Breast Cancer *via* Interacting With EZH1. *Am J Trans Res* (2019) 11 (7):4500–7.
18. Zhang X, Zhang X, Wang T, Wang L, Tan Z, Wei W, et al. MicroRNA-26a Is a Key Regulon That Inhibits Progression and Metastasis of C-Myc/EZH2 Double High Advanced Hepatocellular Carcinoma. *Cancer Lett* (2018) 426:98–108. doi: 10.1016/j.canlet.2018.04.005
19. Xu L, Lin J, Deng W, Luo W, Huang Y, Liu CQ, et al. EZH2 Facilitates BMI1-Dependent Hepatocarcinogenesis Through Epigenetically Silencing microRNA-200c. *Oncogenesis* (2020) 9(11):101. doi: 10.1038/s41389-020-00284-w

20. Tang Z, Kang B, Li C, Chen T, Zhang Z. GEPIA2: An Enhanced Web Server for Large-Scale Expression Profiling and Interactive Analysis. *Nucleic Acids Res* (2019) 47(W1):W556–60. doi: 10.1093/nar/gkz430
21. Konze KD, Ma A, Li F, Barsyte-Lovejoy D, Parton T, Macnevin CJ, et al. An Orally Bioavailable Chemical Probe of the Lysine Methyltransferases EZH2 and EZH1. *ACS Chem Biol* (2013) 8(6):1324–34. doi: 10.1021/cb400133j
22. Tang X, Deng X, Xin X, Li J, He X, Huang J. Effect and Mechanism of EZH1/2 Inhibitor UNC1999 on Hepatocellular Carcinoma Cell: A Preliminary Study. *J Sun Yat sen University Med Sci* (2019) 40(6):821–32. doi: 10.13471/j.cnki.j.sun.yat-sen.univ(med.sci).2019.0115
23. Horwitz E, Stein I, Andreozzi M, Nemeth J, Shoham A, Pappo O, et al. Human and Mouse VEGFA-Amplified Hepatocellular Carcinomas Are Highly Sensitive to Sorafenib Treatment. *Cancer Discov* (2014) 4(6):730–43. doi: 10.1158/2159-8290.Cd-13-0782
24. Yang CF, Lu WQ, Lin T, You P, Ye M, Huang YQ, et al. Activation of Liver FGF21 in Hepatocarcinogenesis and During Hepatic Stress. *BMC Gastroenterol* (2013) 13:14. doi: 10.1186/1471-230x-13-67
25. Liu M, Zhou R, Wu X, Xu X, Su M, Yang B. Clinicopathologic Characterization of Sorafenib-Induced Endoplasmic Reticulum Stress in Human Liver Cancer CELLS. *J Physiol Pharmacol* (2018) 69(4):5. doi: 10.26402/jpp.2018.4.08
26. Zhang WH, Lin J, Wang P, Sun J. miR-17-5p Down-Regulation Contributes to Erlotinib Resistance in Non-Small Cell Lung Cancer Cells. *J Drug Targeting* (2017) 25(2):125–31. doi: 10.1080/1061186x.2016.1207647
27. Fitieh A, Locke AJ, Motamedi M, Ismail IH. The Role of Polycomb Group Protein BMI1 in DNA Repair and Genomic Stability. *Int J Mol Sci* (2021) 22 (6):2976. doi: 10.3390/ijms22062976
28. Kouznetsova VL, Tchekanov A, Li X, Yan X, Tsigelny IF. Polycomb Repressive 2 Complex-Molecular Mechanisms of Function. *Protein Sci* (2019) 28(8):1387–99. doi: 10.1002/pro.3647
29. Margueron R, Li GH, Sarma K, Blais A, Zavadil J, Woodcock CL, et al. Ezh1 and Ezh2 Maintain Repressive Chromatin Through Different Mechanisms. *Mol Cell* (2008) 32(4):503–18. doi: 10.1016/j.molcel.2008.11.004
30. Shen XH, Liu YC, Hsu YJ, Fujiwara Y, Kim J, Mao XH, et al. EZH1 Mediates Methylation on Histone H3 Lysine 27 and Complements EZH2 in Maintaining Stem Cell Identity and Executing Pluripotency. *Mol Cell* (2008) 32(4):491–502. doi: 10.1016/j.molcel.2008.10.016
31. Xu B, On DM, Ma A, Parton T, Konze KD, Pattenden SG, et al. Selective Inhibition of EZH2 and EZH1 Enzymatic Activity by a Small Molecule Suppresses MLL-Rearranged Leukemia. *Blood* (2015) 125(2):346–57. doi: 10.1182/blood-2014-06-581082
32. Brunetti O, Gnoni A, Licchetta A, Longo V, Calabrese A, Argentiero A, et al. Predictive and Prognostic Factors in HCC Patients Treated With Sorafenib. *Medicina-Lithuania* (2019) 55(10):16. doi: 10.3390/medicina55100707
33. Dai H, Hu W, Zhang L, Jiang F, Mao X, Yang G, et al. FGF21 Facilitates Autophagy in Prostate Cancer Cells by Inhibiting the PI3K-Akt-mTOR Signaling Pathway. *Cell Death Dis* (2021) 12(4):303. doi: 10.1038/s41419-021-03588-w
34. Yu X, Li Y, Jiang G, Fang J, You Z, Shao G, et al. FGF21 Promotes Non-Small Cell Lung Cancer Progression by SIRT1/PI3K/AKT Signaling. *Life Sci* (2021) 269:118875. doi: 10.1016/j.lfs.2020.118875

Conflict of Interest: The authors declare that the research was conducted in the absence of any commercial or financial relationships that could be construed as a potential conflict of interest.

frontiers in Oncology

ORIGINAL RESEARCH
published: 03 January 2022
doi: 10.3389/fonc.2021.812785

Aerial View of the Association Between m6A-Related LncRNAs and Clinicopathological Characteristics of Pancreatic Cancer

*Bowen Huang[1], Jianzhou Liu[1], Jun Lu[1], Wenyan Gao[2], Li Zhou[1], Feng Tian[1], Yizhi Wang[1], Mingjie Luo[1], Dong Liu[3], Congyong Xie[3], Ziyu Xun[4], Chengxi Liu[1], Yu Wang[1], Haibo Ma[1] and Junchao Guo[1]**

[1] Department of General Surgery, State Key Laboratory of Complex Severe and Rare Diseases, Peking Union Medical College Hospital, Chinese Academy of Medical Sciences and Peking Union Medical College, Beijing, China, [2] State Key Laboratory of Molecular Oncology, National Cancer Center/National Clinical Research Center for Cancer/Cancer Hospital, Chinese Academy of Medical Sciences and Peking Union Medical College, Beijing, China, [3] Department of Mathematics, Jinan University, Guangzhou, China, [4] Department of Liver Surgery, State Key Laboratory of Complex Severe and Rare Diseases, Peking Union Medical College Hospital, Chinese Academy of Medical Science and Peking Union Medical College, Beijing, China

OPEN ACCESS

Edited by:
Kanjoormana Aryan Manu,
Amala Cancer Research Centre, India

Reviewed by:
Chenyu Lin,
The Ohio State University, United States
Xin Li,
Sun Yat-sen University, China

***Correspondence:**
Junchao Guo
gjcpumch@163.com

Specialty section:
This article was submitted to Gastrointestinal Cancers: Hepato Pancreatic Biliary Cancers, a section of the journal Frontiers in Oncology

Received: 10 November 2021
Accepted: 09 December 2021
Published: 03 January 2022

Citation:
Huang B, Liu J, Lu J, Gao W, Zhou L, Tian F, Wang Y, Luo M, Liu D, Xie C, Xun Z, Liu C, Wang Y, Ma H and Guo J (2022) Aerial View of the Association Between m6A-Related LncRNAs and Clinicopathological Characteristics of Pancreatic Cancer. Front. Oncol. 11:812785. doi: 10.3389/fonc.2021.812785

Pancreatic cancer is a highly malignant tumor with a poor survival prognosis. We attempted to establish a robust prognostic model to elucidate the clinicopathological association between lncRNA, which may lead to poor prognosis by influencing m6A modification, and pancreatic cancer. We investigated the lncRNAs expression level and the prognostic value in 440 PDAC patients and 171 normal tissues from GTEx, TCGA, and ICGC databases. The bioinformatic analysis and statistical analysis were used to illustrate the relationship. We implemented Pearson correlation analysis to explore the m6A-related lncRNAs, univariate Cox regression and Kaplan-Meier methods were performed to identify the seven prognostic lncRNAs signatures. We inputted them in the LASSO Cox regression to establish a prognostic model in the TCGA database, verified in the ICGC database. The AUC of the ROC curve of the training set is 0.887, while the validation set is 0.711. Each patient has calculated a risk score and divided it into low-risk and high-risk subgroups by the median value. Moreover, the model showed a robust prognostic ability in the stratification analysis of different risk subgroups, pathological grades, and recurrence events. We established a ceRNA network between lncRNAs and m6A regulators. Enrichment analysis indicated that malignancy-associated biological function and signaling pathways were enriched in the high-risk subgroup and m6A-related lncRNAs target mRNA. We have even identified small molecule drugs, such as Thapsigargin, Mepacrine, and Ellipticine, that may affect pancreatic cancer progression. We found that seven lncRNAs were highly expressed in tumor patients in the GTEx-TCGA database, and LncRNA CASC19/UCA1/LINC01094/LINC02323 were confirmed in both pancreatic cell lines and FISH relative quantity. We provided a comprehensive aerial view between m6A-related lncRNAs and pancreatic cancer's clinicopathological characteristics, and performed experiments to verify the robustness of the prognostic model.

Keywords: pancreatic cancer, m6A, lncRNA, prognostic model, clinicopathological characteristics

INTRODUCTION

Of all the primary human cancers, pancreatic cancer has the worst prognosis. In the United States, approximately 57,600 people are diagnosed with pancreatic cancer each year, and 47,000 people die from this disease, ranking as the third leading cause of cancer death after lung cancer and colorectal cancer (1), with a 5-year survival rate of 6% (2). After decades of fighting pancreatic cancer, surgical resection remains the only possible cure. Unfortunately, due to the late onset of clinical symptoms in pancreatic cancer patients, only 15%-20% of patients have the opportunity to undergo pancreatic resection, and the postoperative 5-year survival rate is only 18% (3). Patients who can't receive surgical treatment also can't benefit from chemical drugs, possibly because most patients with chemotherapy already have locally advanced or metastatic nidus. There is also the difficulty in diagnosing pancreatic cancer, often delayed due to the early stage's lack of symptoms. Therefore, it is imperative to have sensitive and accurate molecular markers in the early diagnosis, prognosis judgment, and treatment strategy selection of pancreatic cancer (4).

Most studies have suggested that N6-methyladenosine(m6A) methylation, one of the most common RNA modifications, can affect the complexity of cancer progression by regulating biological functions related to cancer. m6A modification of noncoding RNAs regulates cleavage, transport, stability, and degradation (5). The m6A regulators can be divided into three types: writers (methyltransferases), readers (signal transducers), and erasers (demethylases) (6). Recent research has demonstrated that m6A modification could regulate tumorigenesis and progression in pancreatic cancer. For instance, The writer METTL3 promotes pancreatic cancer cell proliferation, invasion, chemoresistance, and radioresistance (7, 8). The upregulation of reader HNRNPC was associated with rs7495G, which confer a higher risk of PDAC through a miRNA-mediated manner (9). The eraser ALKBH5 prevents pancreatic cancer progression by posttranscriptional activation of PER1 through m6A abolishment, decreasing WIF-1 RNA methylation and mediating Wnt signaling (10, 11).

It's well known that long non-coding RNAs' (lncRNAs) abnormal expression is closely connected with the degree of tumor malignancy. Very little research found that m6A modification can affect pancreatic cancer progression by interfering with the expression of lncRNAs so far (12, 13). Our team hoped to identify the prognostic significance of m6A-related lncRNAs by bioinformatics and statistical analysis of data from patients with PDAC based on Genotype-Tissue Expression(GTEx), The Cancer Genome Atlas(TCGA), and International Cancer Genome Consortium(ICGC) databases. Furthermore, we constructed an m6A-related lncRNAs prognostic model to predict the overall survival of PDAC patients. Meanwhile, the stratified analysis was carried out with PDAC patients in different risk and clinicopathological subgroups, categorized based on the lncRNAs prognostic model. Furthermore, we built a competing endogenous RNA (ceRNA) network to search the target miRNAs and m6A regulators of these m6A-related prognostic lncRNAs. Besides, we identified small molecule drugs that may interfere with pancreatic cancer progression by targeting mRNA expression levels. Ultimately, we also explored whether critical lncRNAs were differentially expressed between tumor and normal samples in the GTEx-TCGA database, cell lines, and tissue microarray. In a word, we have drawn a bird-eye view of the relationship between m6A-related lncRNAs and clinicopathological characteristics of pancreatic cancer.

MATERIALS AND METHODS

Databases and m6A Regulatory Genes

We merge the GTEx and TCGA databases as the training set, Fragments Per Kilobase of transcript per Million mapped reads (FPKM) normalized RNA-seq and the corresponding clinicopathological data were acquired from the University of California, Santa Cruz (UCSC) website (https://xenabrowser.net/datapages/). To obtain an ICGC validation set, we downloaded standardized RNA-seq data and related clinicopathological profiles from the ICGC website (https://daco.icgc.org/). We got a GTEx-TCGA training set involving 178 patients and 171 normal samples and an ICGC-CA validation dataset involving 262 patients. Patients with missing critical lncRNAs expression profiles, survival data, and clinicopathological features were excluded in clinical data analysis.

To include m6A regulatory genes that have been experimentally confirmed as much as possible, we searched PubMed for all literature associated with m6A modification. Several reviews comprehensively summarized that all the m6A regulatory genes were adopted (6, 14–17). Finally, twenty-six genes were included in subsequent studies, including ten writers, fourteen readers, and two erasers (**Table 1**).

Annotation of LncRNAs

The lncRNA annotation file of Genome Reference Consortium Human Build 38 (GRCh38) release 102 was acquired from the Ensembl website (http://asia.ensembl.org/index.html) for annotation of the lncRNAs in the GTEx-TCGA and ICGC databases. By recognizing the genes' Ensemble IDs, We could identify the lncRNAs in the GTEx-TCGA and the ICGC databases.

Cell Culture

Six human PDAC cell lines, AsPC-1, BxPC-3, Capan-1, CFPAC-1, MIA PaCa-2, SW1990, and one normal pancreatic duct epithelium cell line, HPNE, were obtained from the American Type Culture Collection (ATCC) (Manassas, VA, USA). Capan-1 and CFPAC-1 were cultured in Iscove's Modified Dulbecco Medium (IMDM) (HyClone, Logan, UT, USA), SW1990 was cultured in Roswell Park Memorial Institute (RPMI) 1640 Medium (HyClone, Logan, UT, USA), and the rest of cell lines were cultured in Dulbecco's Modified Eagle Medium (DMEM) (HyClone, Logan, UT, USA). The Capan-1 was supplemented with 20% fetal bovine serum (FBS) (Gibco, CA, USA), and the rest of the cell lines were supplemented with 10% FBS. All of them were at 37°C in a 5% CO2 cell culture incubator.

TABLE 1 | The list of the 26 m6A-related methylation regulative factors from publications.

m6A Type	Regulator	Gene Synonyms	Ensembl ID
Writer	METTL3	M6A, MT-A70, Spo8	ENSG00000165819
	METTL14	KIAA1627	ENSG00000145388
	METTL16	METT10D, MGC3329	ENSG00000127804
	ZCCHC4	FLJ23024, HSPC052, ZGRF4	ENSG00000168228
	WTAP	KIAA0105, MGC3925, Mum2	ENSG00000146457
	VIRMA	DKFZP434I116, KIAA1429, fSAP121	ENSG00000164944
	RBM15	OTT, OTT1	ENSG00000162775
	RBM15B	HUMAGCGB, OTT3	ENSG00000259956
	ZC3H13	DKFZp434D1812, KIAA0853, Xio	ENSG00000123200
	CBLL1	FLJ23109, HAKAI, RNF188	ENSG00000105879
Reader	YTHDF1	C20orf21, FLJ20391	ENSG00000149658
	YTHDF2	CAHL, HGRG8, NY-REN-2	ENSG00000198492
	YTHDF3	FLJ31657	ENSG00000185728
	YTHDC1	KIAA1966, YT521, YT521-B	ENSG00000083896
	YTHDC2	DKFZp564A186, FLJ10053, FLJ2194	ENSG00000047188
	IGF2BP1	IMP-1	ENSG00000159217
	IGF2BP2	IMP-2	ENSG00000073792
	IGF2BP3	CT98, IMP-3, IMP3	ENSG00000136231
	HNRNPC	HNRPC	ENSG00000092199
	RBMX	HNRNPG, RNMX, hnRNP-G	ENSG00000147274
	HNRNPA2B1	HNRPA2B1	ENSG00000122566
	EIF3A	EIF3, EIF3S10, KIAA0139, TIF32	ENSG00000107581
	FMR1	FMRP, FRAXA, MGC87458, POF, POF1	ENSG00000102081
	PRRC2A	BAT2, D6S51E, G2	ENSG00000204469
Eraser	FTO	ALKBH9, KIAA1752, MGC5149	ENSG00000140718
	ALKBH5	FLJ20308, OFOXD1	ENSG00000091542

RNA Reverse Transcription and Quantitative Real-Time Polymerase Chain Reaction(qRT-PCR)

Cells were plated in 6-well plates at 5×10^5 cells/well and total RNA was extracted from the cell lines with TRIzol™ Reagent (15596026; Life Technologies Corporation, Carlsbad, CA, USA) and total RNA was reverse transcribed using a riboSCRIPT™ mRNA/lncRNA qRT-PCR Kit (Ribobio, Guangzhou, China) to synthesize cDNA. The obtained cDNAs were quantified by RT-PCR using a Veriti® 96-Well Thermal Cycler (4375786; Applied Biosystems, Foster City, CA, USA). All steps were according to the manufacturer's instructions. Glyceraldehyde-3-phosphate dehydrogenase (GAPDH) was used as endogenous controls for lncRNAs. All samples were normalized to internal controls, and the fold changes were calculated using a relative quantification method ($2^{-\Delta\Delta Ct}$). qRT-PCR reactions were performed in triplicate. The primer sequences were listed in **Supplementary Table 1**.

Tissue Microarray Construction and Fluorescence *In Situ* Hybridization (FISH)

The tissue microarray (Outdo, Shanghai, China) was established to detect the expression level of lncRNAs in PDAC tissues and paracancer tissues by processing formalin-fixed and paraffin-embedded blocks. FISH staining was performed using primers (Tsingke, Beijing, China) at 500nM. Two experienced pathologists independently performed the staining evaluation. FISH relative quantity was applied to evaluate the expression level of LncRNAs according to the staining intensity and proportion score among positive-stained cells using a scale of quartering. Tissues without FISH staining were not included in the statistics.

Bioinformatic Analyses

The Pearson correlation analysis was applied to mining m6A-related lncRNAs. We defined the $|\text{Pearson R}| > 0.6$ and $p < 0.001$ as the criteria to extract m6A-related lncRNAs. Then univariate Cox regression and Kaplan-Meier (K-M) analyses were implemented to filtrate the prognostic m6A-related lncRNAs in the two databases. We use the Venn diagram to extract the pivotal lncRNAs that can satisfy the screening of two databases and two methods. The correlational relationships among the m6A related-lncRNAs in PDAC were analyzed based on Spearman's correction coefficient calculation. Moreover, using the R package "glmnet" to conduct Least Absolute Shrinkage and Selection Operator (LASSO) Cox regression (18), we could establish an m6A-related lncRNA prognostic model for the pancreatic cancer patients. The risk score calculating equation is:

$$Riskscore = \sum_{k=1}^{n} Coef_k \times x_k$$

Which $Coef_k$ means the coefficients, x_k is the FPKM value of each prognostic lncRNAs. Risk scores were calculated for all PDAC patients involved in our project. Using the GTEx-TCGA cohort, Differentially Expressed Genes (DEG) in the high-risk subgroup PDAC patients in contrast to the low-risk subgroup were identified based on the standards of $|\log2(\text{fold change})| > 0.5$ and $p < 0.05$ using the R package "limma" (19). The DEG of the tumor and normal tissues in different subgroups according to the criterion of $|\log2(\text{fold change})| > 2$ and $p < 0.01$ in GETx-TCGA databases were shown used by the R package "limma" too. The R packages "clusterProfiler" and "org.Hs.eg.db" were library to Gene Ontology (GO) and Kyoto Encyclopedia of Genes and

Genomes (KEGG) Pathway analyses. Python language was employed to predict the target miRNAs of the m6A-related lncRNAs in the miRcode (http://www.mircode.org/) and Starbase (http://starbase.sysu.edu.cn/) databases. What's more, we searched for the target mRNAs of these miRNAs in miRDB (http://mirdb.org/), miRTarBase (http://mirtarbase.cuhk.edu.cn/php/index.php), and Starbase databases. The ceRNA network was plotted using the software of "Cytoscape" (20). Lastly, we used the Connectivity Map (CMAP) database (https://portals.broadinstitute.org/cmap/) to find out the small molecule drugs that might be related to PDAC following the genes that were distinctly different between tumor and normal samples mentioned above (21).

Statistical Analyses

The K-M curves and the log-rank test were utilized to compare all genes' overall survival and extract the m6a-related prognostic lncRNAs. The prognostic ability of the model for 1/3/5-year overall survival was evaluated by receiver operating characteristic (ROC) curves and the area under the curve (AUC) values (22). The Kruskal-Wallis test was used to compare the risk scores between different subgroups in the TCGA database based on the following clinicopathological features: age, gender, smoking, drinking, diabetes, pancreatitis, grade, stage, TNM classification, location, recurrence, outcome, new tumor, multi-malignancies. The student's t-test was used to compare the seven lncRNAs expression among six PDAC cell lines and one normal pancreatic duct epithelium cell line. Univariate and multivariate Cox regression analyses were employed to assess the independent prognostic value of the m6A-related lncRNAs prognostic model regarding overall survival in two cohorts. The Mann-Whitney test was used to evaluate the lncRNAs relative quantity between PDAC tissue and paracancer normal tissues. All statistical data and figures were analyzed by R (version 4.0.3) and GraphPad Prism 8.0 to ensure aesthetics and editability. All statistical results with a p-value <0.05 were considered significant.

RESULTS

Identification of m6A-Related LncRNAs in PDAC Patients

Firstly, using the downloaded profile from the "Ensembl" website, we identified 4441 lncRNAs in the GTEx-TCGA database and 14181 lncRNAs in the ICGC-CA database based on recognizing the Ensemble IDs of the genes for the following analysis. In addition, we extracted the expression matrixes of 26 m6A regulatory genes from the GTEx-TCGA and the ICGC-CA databases. A lncRNAs whose expression value was correlated with one of the 26 m6A regulatory genes, with $|\text{Pearson R}| > 0.6$ and $p < 0.001$ as the criterion, was defined as an m6A-related lncRNA. We obtained 762 lncRNAs significantly correlated with m6A regulatory genes in the GTEx-TCGA database, while 1370 lncRNAs in the ICGC database. Combined with the survival information, univariate Cox regression and Log-rank test were executed to screen seven m6A-related prognostic lncRNAs in both databases (**Figure 1A**).

Establish the m6a-Related LncRNAs Prognostic Model in the TCGA Database

All m6A-related lncRNAs showed positive co-expression, which presented an extensive synergy effect (**Figures 1B, C**). The lncRNA CASC19 and LINC02323 possessed the most significant correlation coefficient (0.68) in the GTEx-TCGA database, while the lncRNA ITGB1-DT and LINC02323, NRAV and PRECSIT had the largest correlation coefficient (0.68) in the ICGC database. In order to build the m6A-related lncRNAs prognostic model for forecasting the overall survival of PDAC patients, at the same time, avoid the expression overfitting possibility brought by high correlation, we performed a LASSO regression analysis based on the seven m6A-related prognostic lncRNAs in the TCGA cohort. Moreover, it generated the prognostic model containing seven m6A-related lncRNAs and each lncRNA coefficient (**Figure 1D** and **Supplementary Figures 1A, B**). For each patient in the TCGA database, a risk score was calculated based on the coefficient for each lncRNAs. Patients in the TCGA training cohort were divided into low-risk and high-risk subgroups based on the median value of risk scores. K-M curves demonstrated that PDAC patients with higher risk scores had worse outcomes (**Figure 1E**). The ROC curves illustrated that the lncRNAs prognostic model has an excellent predictive ability to predict overall survival in the TCGA training cohort (1-year AUC = 0.710, 3-year AUC = 0.803, 5-year AUC = 0.887; **Figure 1G**). Risk score and survival status distributions are plotted in **Figure 1I**.

Validation of the LncRNAs Prognostic Model in the ICGC Database

To validate the lncRNAs prognostic model's predictive ability based on the TCGA training set, we calculated risk scores for patients in the ICGC cohort using the same equation. PDAC patients in the ICGC database were assigned to low-risk and high-risk subgroups according to the median risk score. The results were consistent with the TCGA database findings: PDAC patients with higher risk scores had lower overall survival rates and a shorter overall survival time in the ICGC dataset (**Figure 1F**). The ROC curves also demonstrated that m6A-related lncRNAs prognostic model had a robust prognostic value for PDAC patients in the ICGC database (1-year AUC = 0.641, 3-year AUC = 0.698, 5-year AUC = 0.711; **Figure 1H**). Risk score and survival status distributions are shown in **Figure 1J**, and it showed that patients with higher risk scores had shorter overall survival time and more death status. These results showed that the lncRNAs prognostic model was a robust and stable overall survival predictive tool.

Prognostic Analysis of the Seven m6A-Related LncRNAs

Univariate Cox regression analysis was employed to evaluate seven m6A-related lncRNAs in the prognostic model and their prognostic roles. The forest plot shows that all of them are risk

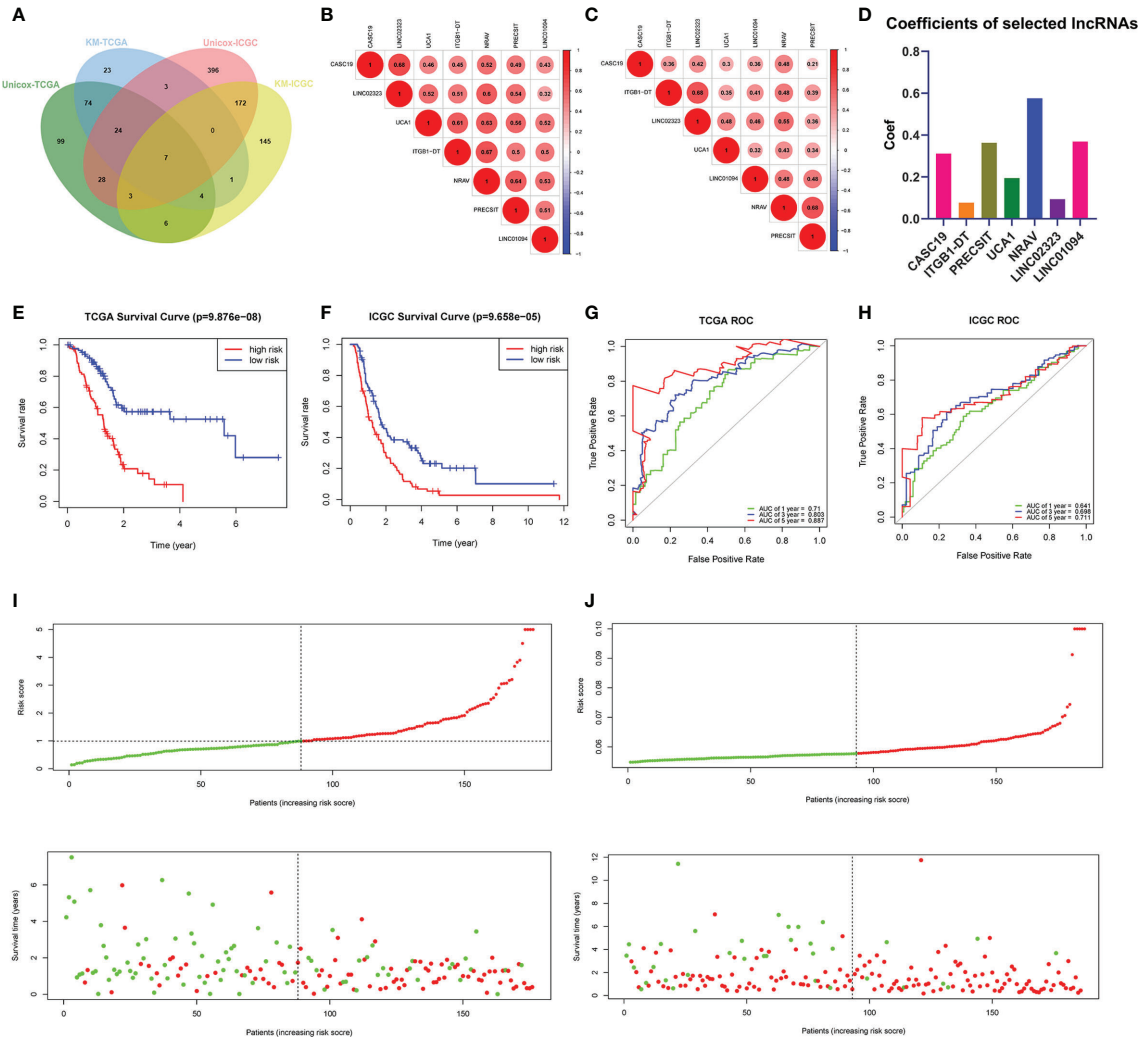

FIGURE 1 | **(A)** Venn's diagram screened the critical prognostic lncRNA-signatures in GTEx-TCGA and ICGC databases. **(B, C)** The correlation heatmap of the GTEx-TCGA database **(B)** and ICGC database **(C)**. **(D)** Used the LASSO regression to calculate the coefficients. **(E, F)** K-M curves showed that the high-risk subgroup had worse overall survival than the low-risk subgroup in TCGA **(E)** and ICGC **(F)** databases. **(G, H)** ROC curves of lncRNA-signatures for predicting the 1/3/5-year survival in the TCGA **(G)** and ICGC **(H)** databases. **(I, J)** The risk scores and survival status of PDAC patients were distributed in the TCGA **(I)** and ICGC **(J)** databases.

factors with Hazard Ratio (HR) >1 in PDAC patients (**Figure 2A**). The K-M survival curves confirmed that higher expression of CASC19, ITGB1-DT, LINC01094, LINC02323, NRAV, PRECSIT, and UCA1 were associated with worse overall survival in the TCGA database (**Figures 2B–H**).

Pathway and Process Enrichment Analysis of Different Risk Subgroups

For investigating the potential biological process and pathway involved in the molecular heterogeneity between the low-risk and high-risk subgroups, we identified 1107 differential expression genes (DEGs) between the low-risk and high-risk subgroups in the TCGA cohort with the filter criteria $|\log2\ (\text{fold change})| > 0.5$ and $p < 0.05$ (**Figure 2I**). These DEGs were primarily enriched in these GO terms: the biological process (BP) included the leukocyte migration, epidermis development, cell junction assembly, skin development, positive regulation of cell adhesion, etc.; the cell component (CC) contains cell-cell junction, collagen-containing extracellular matrix, apical part of the cell, external side of the plasma membrane, apical plasma membrane, etc.; the molecular function (MF) included cell adhesion molecule binding, receptor-ligand activity, actin binding, cadherin binding, cell adhesion mediator activity, etc. (**Figure 2J**). The KEGG analyses revealed that 16 malignant characteristics were enriched in the high-risk subgroup, such as hematopoietic cell lineage, cell adhesion molecules, insulin secretion, malaria, axon guidance, etc. (**Figure 2K**). These results may disclose some perspectives into the cellular biological effects related to the m6A-related lncRNAs prognostic model.

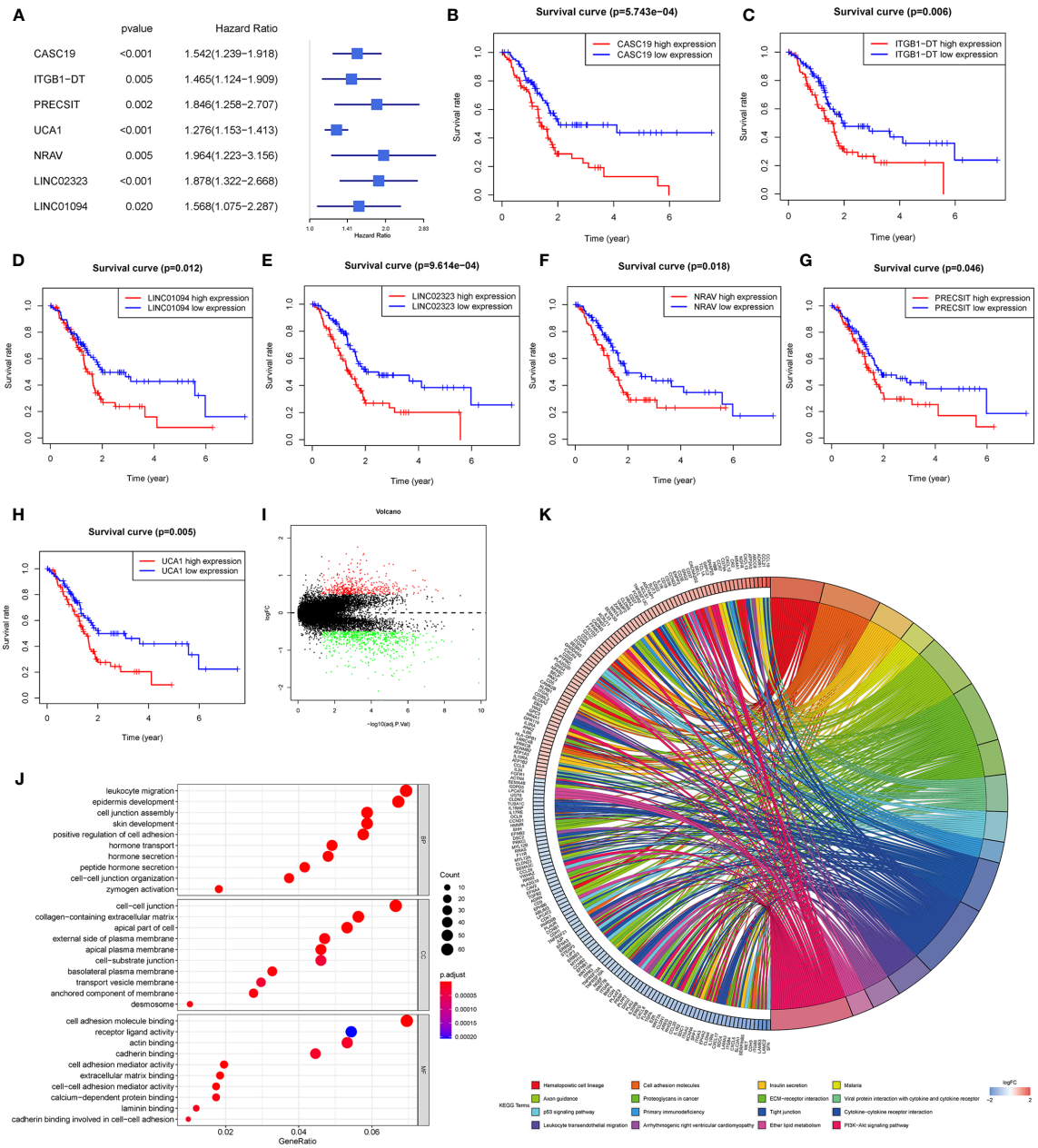

FIGURE 2 | **(A)** Forest plot of the prognostic ability of the seven lncRNAs signatures. **(B–H)** K-M curves showed that patients with high expression levels of the seven lncRNAs signatures had worsened overall survival. **(I)** Differential genes were extracted from patients with different risk subgroups. **(J, K)** GO **(J)** and KEGG **(K)** analyses were performed for different risk subgroups.

Stratification Analysis of the m6A-Related LncRNAs Prognostic Model

The heatmap exhibited LINC01094, CASC19, LINC02323, PRECSIT, UCA1, ITGB1-DT, and NRAV were enriched in the high-risk subgroup and showed the association between each m6A-related lncRNAs expression and the clinicopathological features of PDAC patients (**Figure 3A**). We attempted to identify whether clinicopathological characteristics were connected with the risk score (**Figures 3B–D** and **Supplementary Figures 2A–N**). The results revealed that the PDAC patients with a higher risk score, the tumor issue have a worse pathological differentiation and showed a strictly increasing relationship (P<0.05). Besides, we found that the PDAC patients with higher risk scores were also more likely to have tumor recurrence after treatment (P<0.05). The patients with distant metastasis had the highest risk score, followed by the locoregional recurrence. The new primary tumor had the lowest risk

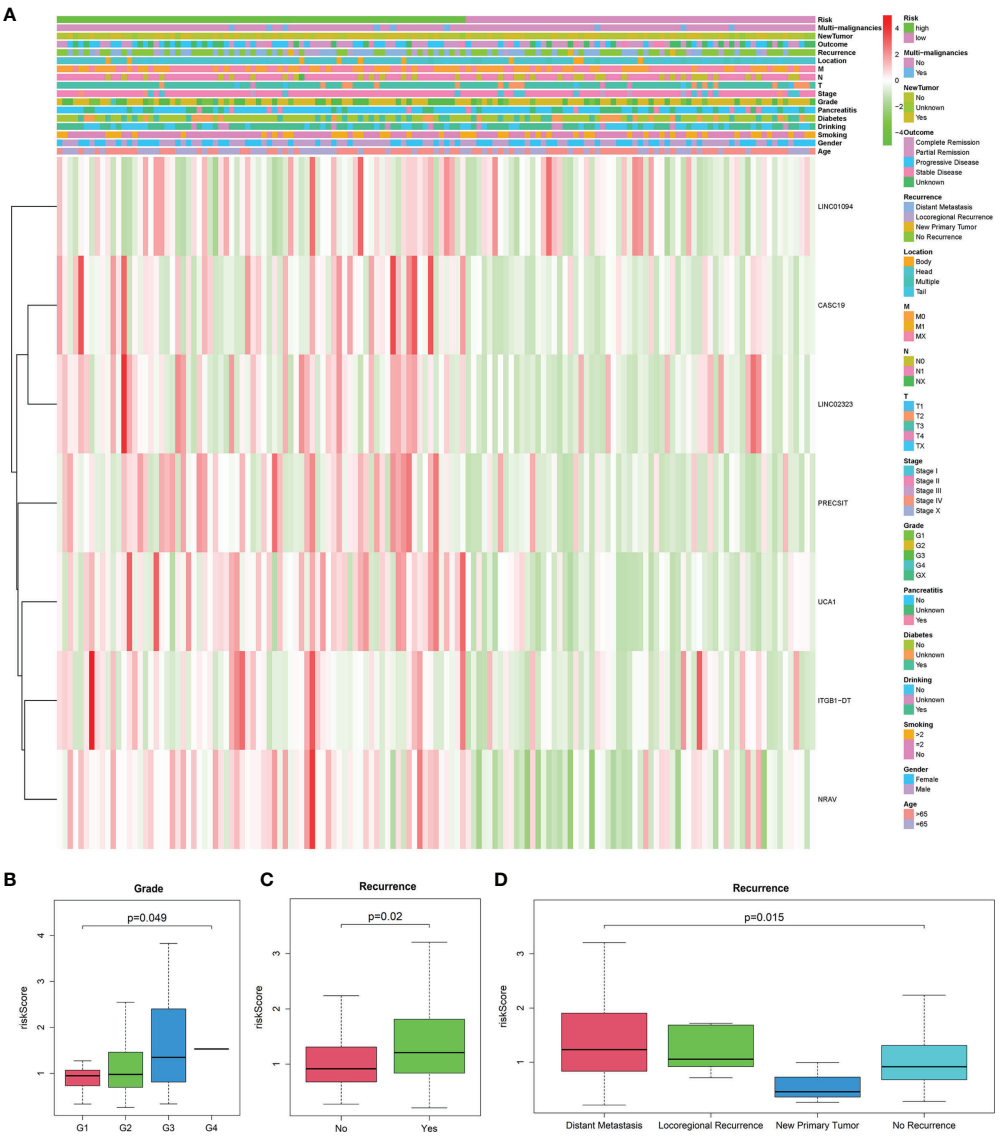

FIGURE 3 | **(A)** Heatmap of the connections between the expression levels of the seven lncRNAs signatures and clinicopathological features in the TCGA database (n=141). **(B–D)** Patients with different clinicopathological features, including pathology grade (G1 = 18, G2 = 82, G3 = 39, G4 = 1, GX=1) and recurrence event (Distant Metastasis=51, Locoregional Recurrence=16, New Primary Tumor=3, No Recurrence=71), had different levels of risk scores, calculated based on the seven lncRNAs signatures.

score with only three samples. To better assess the m6A-related lncRNAs prognostic model's prognostic capacity, we carried out a stratification analysis to verify whether it can forecast overall survival in various subgroups. We performed K-M curves for subgroups with more than five people's risk stratification according to the clinicopathological characteristics. In contrast with lower risk score patients, higher risk PDAC patients had worse overall survival in both the pathological G2 and G3 grades (**Figures 4A, B**), while there was no significant difference in the G1 stratification (**Supplementary Figure 3A**). Likewise, we confirmed that the m6A-related lncRNAs prognostic model retained its capacity to predict overall survival for whether PDAC patients have recurrence events or not (P<0.05, **Figure 4C, D**). Moreover, the further detailed stratification was performed, we detected that the PDAC patients with distant metastasis had a shorter survival time(P<0.05, **Figure 4E**). On the contrary, the locoregional recurrence patients had no significant difference (**Supplementary Figure 3B**).

LncRNAs Prognostic Model Was an Independent Prognostic Factor for PDAC Patients

We used univariate and multivariate Cox analyses to assess whether the m6A-related lncRNAs prognostic model was an

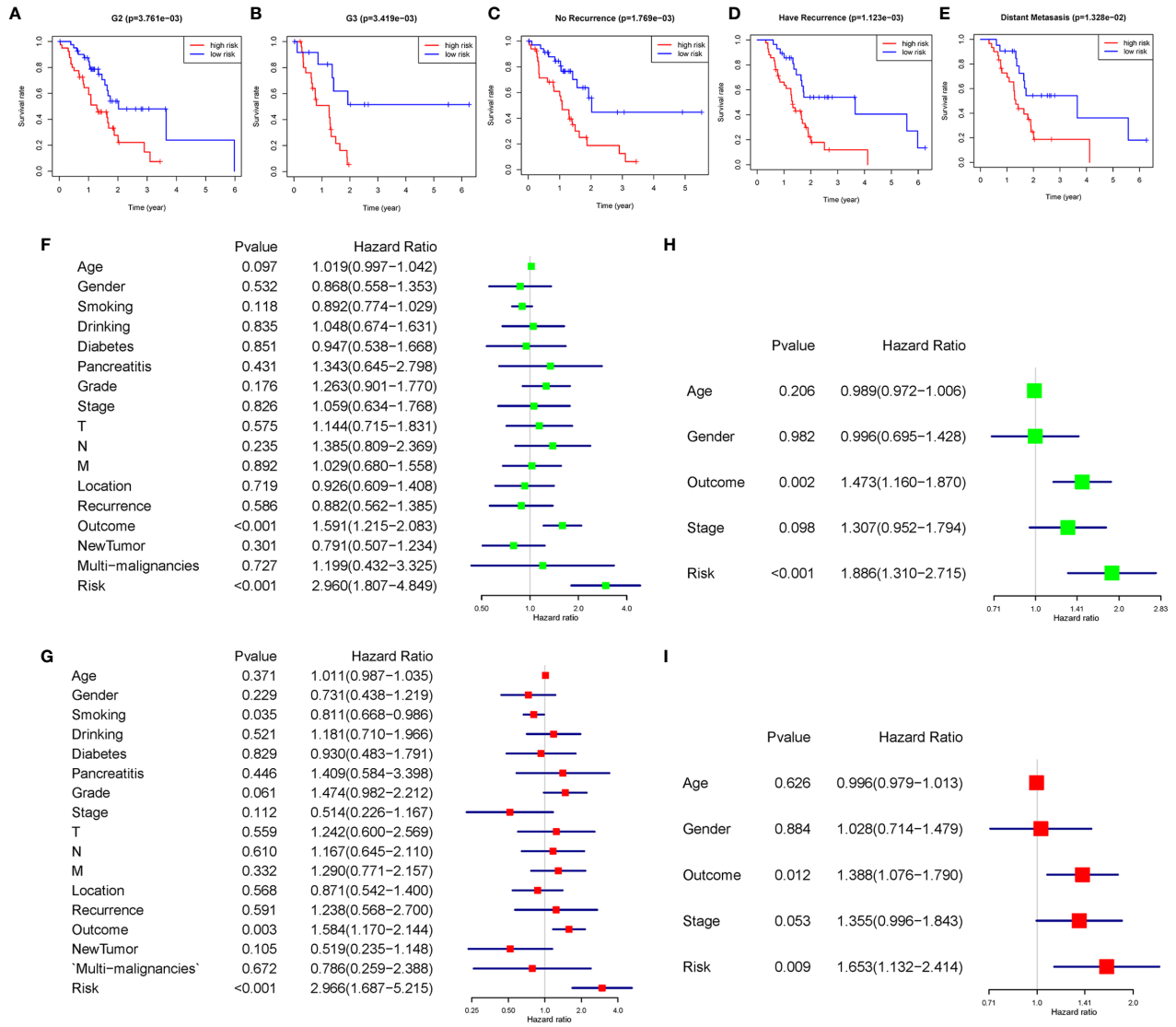

FIGURE 4 | **(A–E)** The seven lncRNA-signatures retained their prognostic value in multiple subgroups of PDAC patients, including patients with pathology grade two, pathology grade three, no recurrence event, have recurrence event, and distant metastasis. **(F–I)** Univariate and multivariate analyses revealed that risk stratification was an independent prognostic predictor in the TCGA **(F, G)** and ICGC **(H, I)** databases.

independent prognostic factor for patients with PDAC. Based on the data of PDAC patients in the TCGA database, univariate Cox analysis indicated that lncRNAs prognostic model was remarkably associated with overall survival [the hazard ratio (HR): 2.960, 95% confidence interval (CI): 1.807-4.849, $p < 0.001$; **Figure 4F**] and multivariate Cox analysis further showed that lncRNAs prognostic model was an independent predictor of overall survival, with the HR(95%CI) was 2.966(1.687-5.215) ($p < 0.001$, **Figure 4G**). The same results were verified in the ICGC database with less clinicopathological characteristics abundance (**Figures 4H, I**). These results indicated that the m6A-related lncRNAs prognostic model might avail clinical prognosis evaluation as an independent prognostic indicator.

Construction of the ceRNA Network and Functional Enrichment Analysis

To further understand how the critical lncRNAs act on N6-methyladenosine regulators by sponging miRNAs in PDAC patients, we constructed a ceRNA network to explore the mechanism of m6A-related lncRNAs. Six lncRNAs were extracted from the Starbase and miRcode databases, and 162 pairs of interactions between the 6 lncRNAs and 153 miRNAs were identified. Then we excavated three databases (Starbase, miRDB, and miRTarBase) to search target N6-methyladenosine regulators based on the 153 miRNAs and a total of 890 pairs of interactions between the 153 miRNAs and 26 m6A regulators were identified in all three databases. Finally, 6 lncRNAs, 153

miRNAs, and 26 m6A regulators were included in the ceRNA network (**Figure 5A**). Furthermore, there are 17288 mRNAs we extract from the three databases the 153 miRNAs target, and we affirmed 1145 DEGs from the GTEx-TCGA database with the filter criteria |log2 (fold change)| > 2 and p < 0.01. These DEGs were wielded to implement functional enrichment analysis, and we found that these genes were enriched in the BP included extracellular matrix organization, extracellular structure organization, neutrophil activation, etc.; the CC contains collagen-containing extracellular matrix, cell-substrate junction, focal adhesion, etc.; the MF included cell adhesion molecule binding, extracellular matrix structural constituent, glycosaminoglycan binding, etc. (**Figure 5B**). KEGG analysis showed that 31 signaling pathways were enriched in pancreatic cancer, some of which had tumor characteristics, including protein digestion and absorption, ECM-receptor interaction, focal adhesion, etc (**Figure 5C**). These data may provide medical workers clues for finding the potential pathways of these m6A-related lncRNAs in PDAC.

Exploration of Small Molecule Drugs Related to Pancreatic Cancer

We put the 1145 DEGs mentioned above into the CMAP database for analysis. We set P< 0.01,|mean|> 0.6 as the filter criteria, and extracted twelve small molecule drugs related to PDAC. The Thapsigargin, Adiphenine, Viomycin, and Nadolol negative control the m6A-related lncRNAs targeted mRNA expression. While the Mepacrine, Ellipticine, 8-azaguanine, DL-thiorphan, Proscillaridin, Trazodone, Bisacodyl, and Riboflavin positive regulated the targeted mRNA expression level (**Figure 5D**).

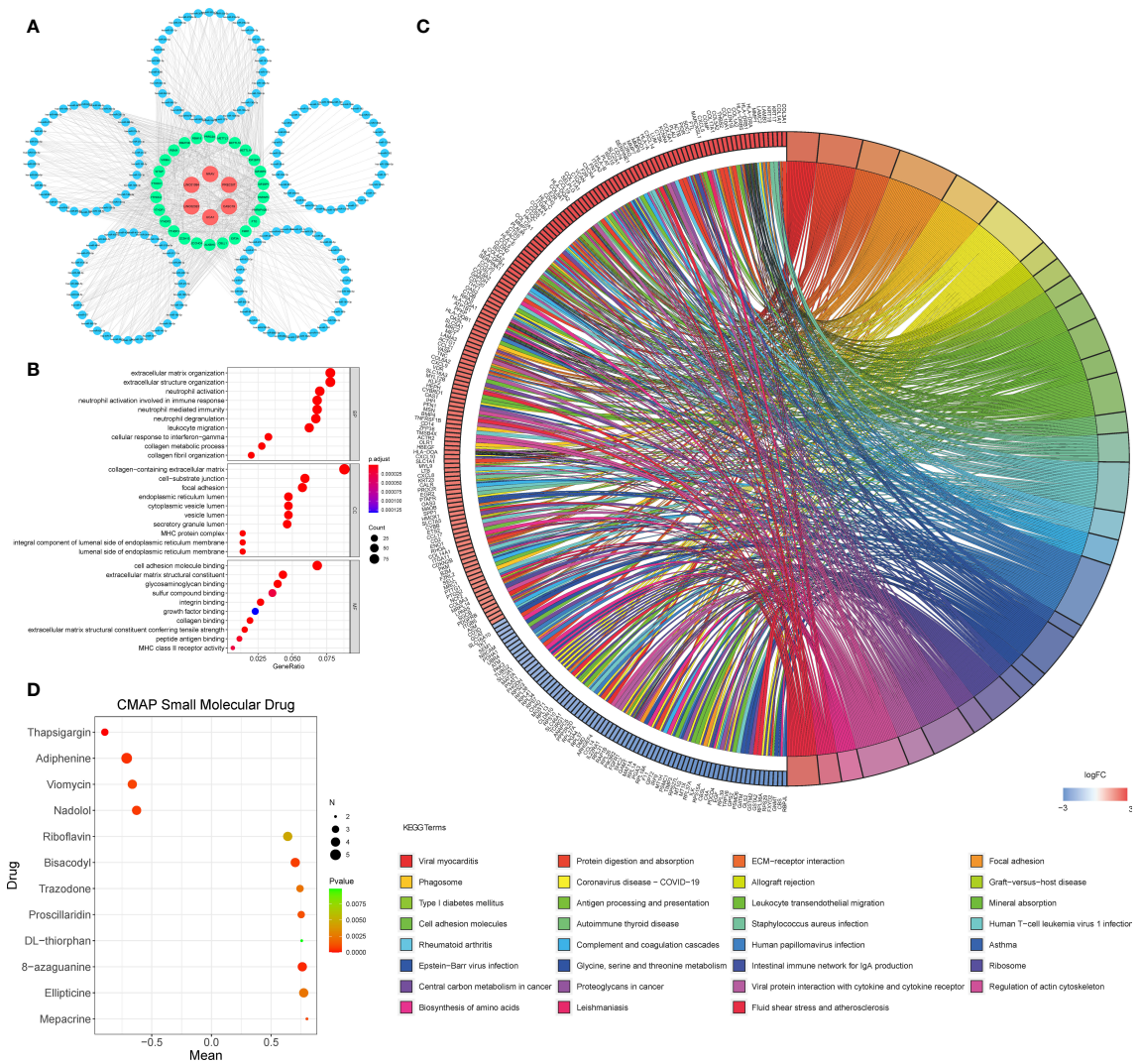

FIGURE 5 | **(A)** The ceRNA network of the six m6A-related lncRNAs (red) and their target miRNAs (blue) and m6A-related methylation regulative mRNAs (green). **(B, C)** GO **(B)** and KEGG **(C)** analyses were performed for differential target mRNA expression. **(D)** CMAP was used to explore the potential drug to cure PDAC according to the expression level of targeted mRNA in the ceRNA network in the GTEx-TCGA database (P< 0.01,|mean|> 0.6).

The Differential Expression Level of Pivotal m6A-Related LncRNAs

We analyzed the expression of each m6A-related lncRNAs in PDAC patients compared to normal pancreas tissues in the GTEx-TCGA database using the R package "limma." Based on the Bayesian algorithm, we generated boxplots for seven critical lncRNAs and observed a statistically significant increased expression in tumor samples for all m6A-related lncRNAs ($p < 0.001$, **Figures 6A–G**). We used six PDAC cell lines and one normal pancreatic duct epithelium cell line to explore seven lncRNAs expression. Significant differences existed among these cell lines in LncRNAs CASC19/UCA1/LINC01094/LINC02323/NRAV based on the student's t-test, which were following the bioinformatic analysis (**Figures 6H–L**). In contrast, the results about LncRNA PRECSIT and ITGB1-DT were not consistent with the above (**Supplementary Figures 3C, D**). FISH staining was performed on tissue microarray to confirm whether critical lncRNAs also differ in human tissues. The results showed that the LncRNA CASC19/UCA1/LINC01094/LINC02323 relative quantity of PDAC was higher than paracancer normal tissues based on the Mann-Whitney test($p < 0.001$, **Figures 7A–D**). The LncRNA NRAV FISH relative quantity was slightly higher in PDAC tissues than in paracancer normal tissues, but there was no statistical difference (**Figure 7E**).

DISCUSSION

A total of 440 PDAC tumor samples and 171 normal tissues from the GTEx-TCGA and ICGC cohorts were included in our study to exploit the prognostic significance of m6A-related lncRNAs. Seven pivotal lncRNAs were confirmed to have prognostic value in both the TCGA and ICGC databases, and were used to establish an m6A-related lncRNAs prognostic model for predicting the overall survival of PDAC patients. Based on each cohort's median risk score, PDAC patients were divided into the low-risk and high-risk subgroups, and the high-risk group had worse clinical outcomes and enrichment of neoplasm characteristics and specific malignant-related pathways. The higher patients' risk score, the worse the pathological grade and the more recurrent events. Multivariate Cox regression analysis showed that the m6A-related lncRNAs prognostic model and initial treatment outcome were the independent risk factors for overall survival. A ceRNA network consisted of 6 m6A-related lncRNAs, 153 miRNAs, and 26 m6A regulators to view this lncRNAs prognostic model's potential functions. Simultaneously, we analyzed the targeted mRNA's enrichment analysis to discover its potential biological function and signal pathway based on the m6A-related lncRNAs prognostic model. Moreover, we found that Thapsigargin, Adiphenine, Viomycin, and Nadolol negative control the m6A-related lncRNAs targeted mRNA expression. Besides, the Mepacrine, Ellipticine, 8-azaguanine, DL-thiorphan, Proscillaridin, Trazodone, Bisacodyl, and Riboflavin positive regulated the targeted mRNA expression level. These tiny molecular drugs may cure pancreatic cancer by intervening in the m6A-related ceRNA network expression. Meanwhile, we found that seven lncRNAs were highly expressed in tumor samples in the GTEx-TCGA database. In order to confirm the robustness of the prognostic model and strive for application to clinical translational, we performed experimental validation of critical lncRNAs. The cell experiments confirmed that the five m6A-related lncRNAs in PDAC samples was overexpressed than the normal pancreas tissues and seven cell lines, and the FISH staining further demonstrated that the lncRNAs CASC19/UCA1/LINC01094/LINC02323 highly expressed in the tissue microarray, which is good for clinical workers to screen and diagnose PDAC patients.

Multiple projects have suggested that m6A modification might function as a regulator in oncogenicity, but it is still unclear how it acts in a lncRNA-dependent pattern during PDAC progression. To date, m6A regulators can maintain the malignancy of PDAC by modifying specific lncRNAs has only been mentioned in a few articles. He et al. have found ALKBH5 inhibits pancreatic cancer motility by demethylating lncRNA KCNK15-AS1 (13). The research may be the earliest experimental exploration of how lncRNA affects pancreatic cancer through m6A modification. Shortly after that, Hu et al. demonstrated that lncRNA DANCR targets IGF2BP2 through m6A modification, and IGF2BP2 and DANCR work together to promote cancer stemness-like properties and pancreatic cancer pathogenesis (12). Meng et al. revealed N6-Methyladenosine was highly enriched within LINC00857 and enhanced its RNA stability. Meanwhile, LINC00857 modulates E2F3 expression by binding to miR-150-5p, ultimately promoting tumorigenesis in pancreatic cancer (23). Studies had disclosed that m6A modification of lncRNAs could influence pancreatic cancer tumorigenesis, and lncRNAs might serve as competing endogenous RNAs, targeting m6A regulators and influencing aggressive tumor progression. Based on the above considerations, we believe that lncRNAs participated in m6A modification, and we ought to pay more attention to the interactions and functions of lncRNAs and m6A modifications to identify prognostic markers and therapeutic targets of pancreatic cancer.

We identified seven m6A-related prognostic lncRNAs from three databases and 611 samples. The lncRNA CASC19 developed pancreatic cancer with CASC19/miR-148b/E2F7 axis (24). Multiple studies have indicated that UCA1 acts as a ceRNA in developing and progressing pancreatic cancer in multiple axes (25–27). LINC02323 sponged miR-1343-3p to upregulate the TGFBR1 expression and promote the epithelial-mesenchymal transition and metastasis in lung adenocarcinoma (28). PRECSIT promotes the progression of cutaneous squamous cell carcinoma *via* STAT3 signaling (29). LINC01094 facilitates clear cell renal cell carcinoma radioresistance by targeting the miR-577/CHEK2/FOXM1 axis (30). NRAV has a certain suggestive effect in predicting the prognosis of hepatocellular carcinoma (31). ITGB1-DT could form a positive feedback loop with ITGB1/Wnt/β-Catenin/MYC to facilitate lung adenocarcinoma progression (32). Seven lncRNAs were reported to be associated with oncogenesis, but there have been few reports regarding pancreatic cancer and no reports

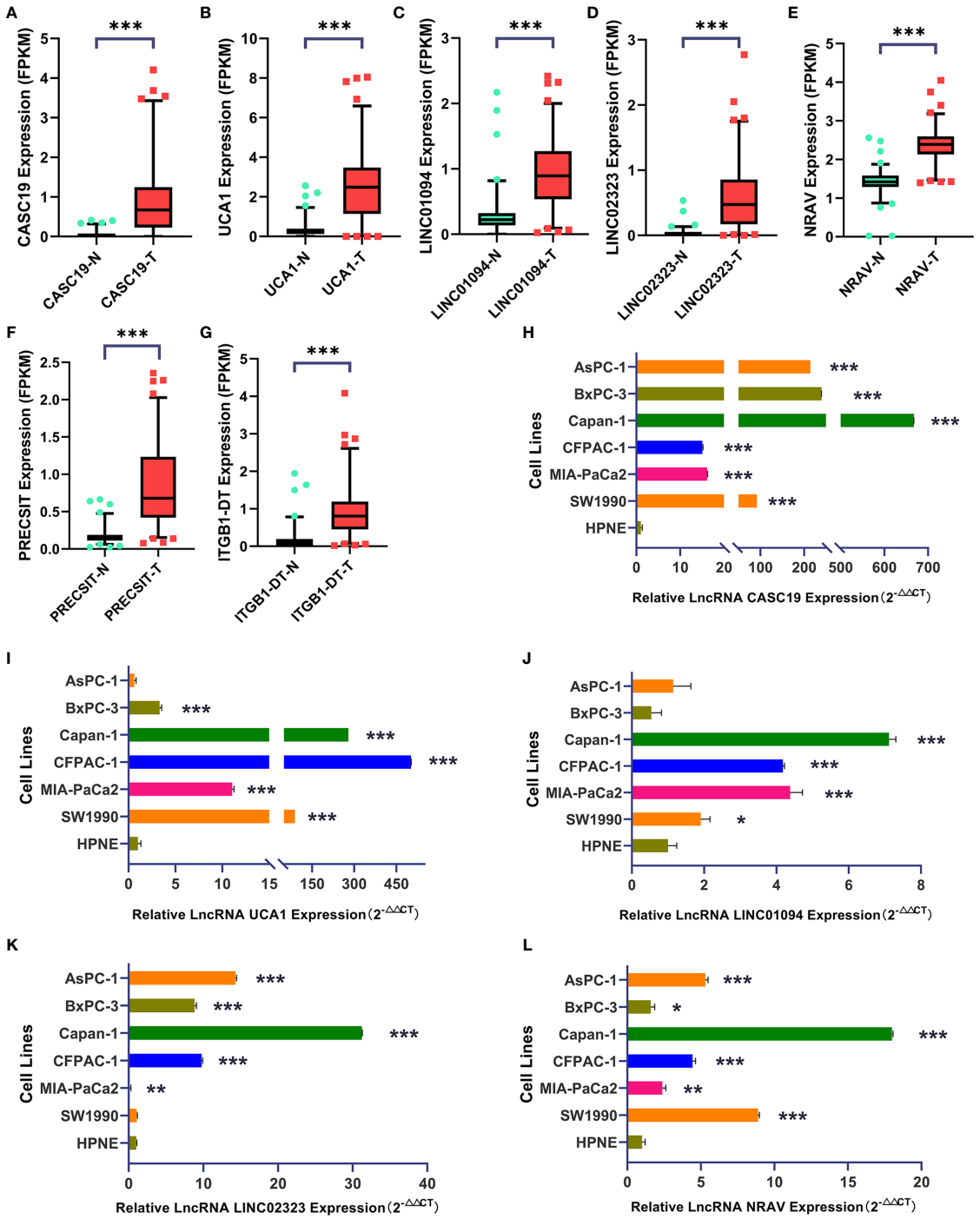

FIGURE 6 | **(A–G)** Seven lncRNAs signatures were quantified in tumor and normal tissues using the GTEx-TCGA database (T=178, N=171). **(H–L)** LncRNA CASC19/UCA1/LINC01094/LINC02323/NRAV expression in six PDAC cell lines and one pancreatic duct epithelial cell line (Triplicate). The symbol * means $P < 0.05$, ** means $P < 0.01$, *** means $P < 0.001$.

on how the lncRNAs interact with the m6A regulator so far. Our study identified the seven pivotal m6A-related prognostic lncRNAs, thereby providing insights into their potential roles in PDAC tumorigenesis and progression.

In our research, pathological grades and recurrent events were associated with higher risk scores, indicating a poor prognosis. Histopathological grading of PDAC is an important prognostic factor that has become the consensus of surgeons (33). Besides,

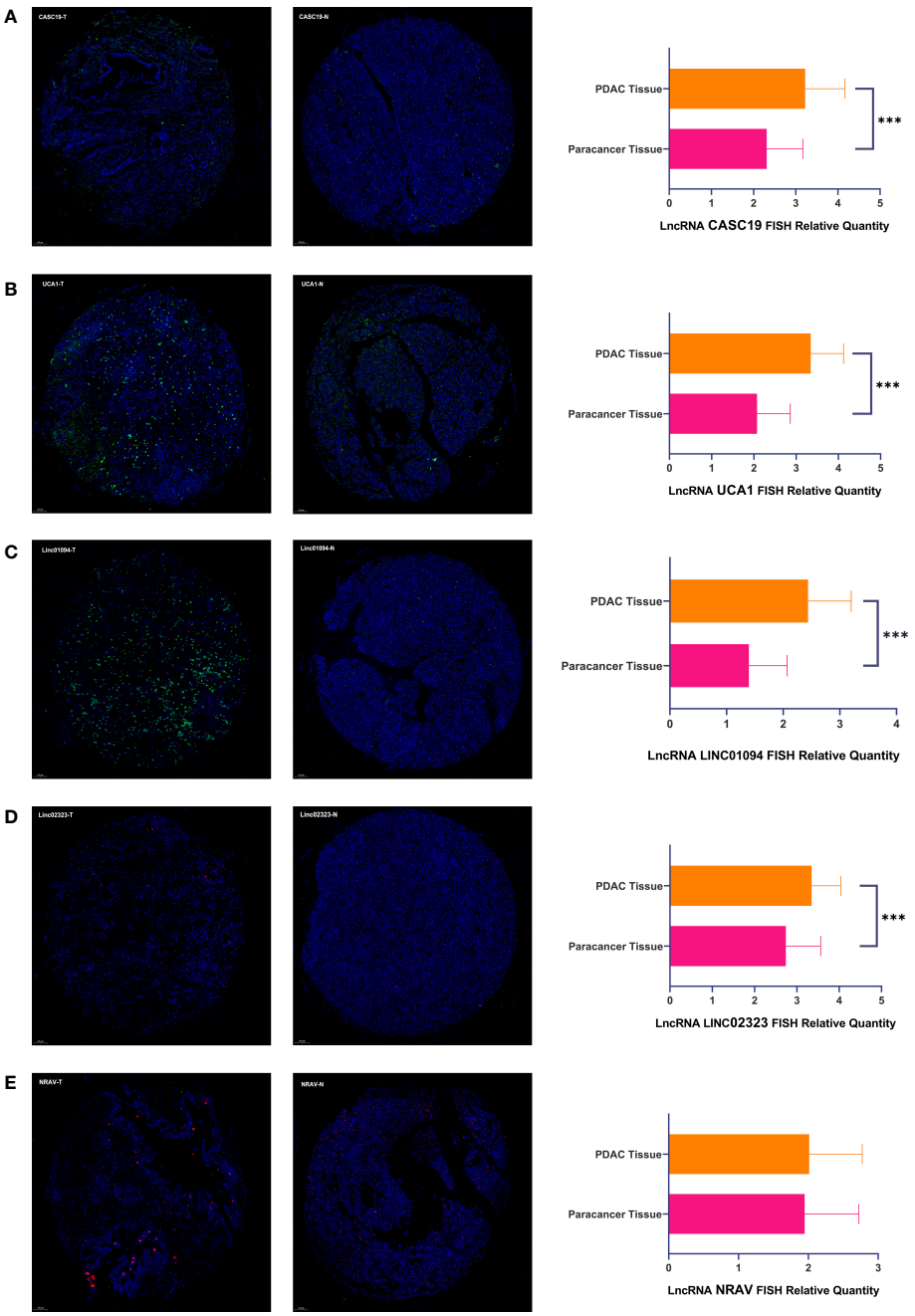

FIGURE 7 | **(A–E)** There were representative microphotographs and relative quantity of PDAC tissues and paracancer normal tissues using tissue microarray-based on FISH about five pivotal lncRNAs (PDAC Tissue=90, Paracancer Tissue=90). The symbol *** means $P < 0.001$.

metastasis causes more significant than 90% of cancer death, although recent therapeutic advances in cancer treatment (34). Fortunately, we have access to some small molecule drugs with therapeutic potential through the CMAP database. We found that the positively regulated drug mepacrine has been initially used as an antimalarial. Moreover, a growing body of reports suggested that mepacrine was associated with gynecologic and breast cancer treatment (35). Recent research shows that treatment of pancreatic cancer by carefully packaged nanoparticles enhances the activity of Mepacrine and minimizes their associated hepatotoxicity (36, 37). Ellipticine and its derivatives were isolated from the wood of Ochrosia elliptica, which showed clinical responses in AML, thyroid cancer, renal cancer, and bone metastases from advanced breast cancer and soft−tissue sarcoma in clinical trials (38).

The novel immunomodulatory drug 8-azaguanine significantly increased the cytotoxicity of NK cells and developed as an antineoplastic agent (39). On the other hand, the negative control group molecule thapsigargin could induce apoptosis by inhibiting the sarcoplasmic/endoplasmic reticulum Ca^{2+} ATPase pump, which can treat as a novel antineoplastic agent. However, the high toxicity of this compound to normal cells is a significant impediment (40). Adiphenine is an anticholinergic drug, but there is no reported use in the treatment of cancer currently. Viomycin is a tuberactinomycin antibiotic that could inhibit bacterial protein synthesis by blocking elongation factor G catalyzed translocation of mRNA on the ribosome. It is essential for treating multi-drug-resistant tuberculosis, but there is no literature on cancer treatment at present (41). Ultimately, we demonstrated that four pivotal lncRNAs were overexpressed coherently in patients, cell lines, and tissue microarray, which means that these four markers can be specifically screened for pancreatic cancer in clinical applications.

Although we built a robust and reliable model, there were several limitations in our study. First, the K-M curves of patients with G1 and G3 pathologic grades intersect between half and one year because most patients received surgical treatment. In the short term, surgical treatment patients are at risk of complications that lead to death after surgery, resulting in a bias. In the long term, low-risk patients had longer survival times across all pathological stratifications. Another hand, Pancreatic cancer is relatively rare compared to other cancers, and the lack of data to analyze may also lead to bias. Moreover, the lncRNAs' role and their interactions with m6A regulators should be confirmed through experiments, which is the next step for our team to explore. Lastly, the staining method of qRT-PCR has some limitations in clinical application because of its low detection sensitivity, which may be why PRECSIT and ITGB1-DT cannot be consistent with the results from the GTEx-TCGA database. Furthermore, the abundance of lncRNA in peripheral blood is lower than that in cells, so it is necessary to improve the sensitivity of detection methods for better application in clinical detection. What's more, the FISH staining showed that the lncRNA NRAV had no significant difference between PDAC and paracancer tissues, the poor quality of tissue microarray and insufficient sample quantity may be the main reasons.

There are few studies on how lncRNAs affect the progression of pancreatic cancer through the m6A modification. First of all, our project has filled the gap in predicting clinical prognosis based on m6A-related lncRNAs. We established a robust and effective m6A-related lncRNAs prognostic model for pancreatic cancer in multiple databases. Secondly, we analyzed the relationship between risk score and abundant clinicopathological characteristics based on the prognostic model. Moreover, we analyzed the possible biological mechanism and signaling pathway of the pivotal m6A-related lncRNAs and found its ceRNA network between lncRNAs and m6A-regulators through miRNAs. Thus, we could find out small molecule drugs that may treat pancreatic cancer by targeting the ceRNA network, providing more attractive clues for researchers studying pancreatic cancer. In the end, we used cell experiments and FISH staining to confirm that the expression of key lncRNA in the prognostic model was significantly higher in PDAC than the normal sample, thus providing compelling evidence for clinical translation, which is also ahead of similar studies in the field. Considering that our team will apply this result to clinical trials later, we will use the probe method to accurately detect critical m6a-related lncRNA in blood for clinical application of pancreatic cancer in the future.

CONCLUSION

We developed a robust m6A-related lncRNA prognostic model for clinical workers to predict PDAC overall survival. Moreover, the stratification analysis demonstrated that the higher risk score was associated with the worse pathological grade and the more recurrent events. Furthermore, the enrichment analysis indicated that malignancy-associated biological function and signaling pathways were enriched in the high-risk subgroup and m6A-related ceRNA network. Besides, the small molecule drugs that may affect the progression of PDAC were identified. Ultimately, we confirmed that the LncRNA CASC19/UCA1/LINC01094/LINC02323 were overexpressed in the GTEx-TCGA database, pancreatic cell lines, and tissue microarray. In conclusion, we provided a comprehensive aerial view between m6A-related lncRNAs and pancreatic cancer's clinicopathological characteristics and performed experiments to verify the robustness of the prognostic model.

DATA AVAILABILITY STATEMENT

Publicly available datasets were analyzed in this study. This data can be found here: the University of California, Santa Cruz (UCSC) website (https://xenabrowser.net/datapages/), The Cancer Genome Atlas (https://portal.gdc.cancer.gov/), and International Cancer Genome Consortium (https://icgc.org).

ETHICS STATEMENT

The studies involving human participants were reviewed and approved by The Ethics Committee of Peking Union Medical College Hospital. The patients/participants provided their written informed consent to participate in this study.

AUTHOR CONTRIBUTIONS

BWH conceived the study. BWH, JZL, and JL wrote the manuscript. WYG, LZ, FT, and YZW applied to guide suggestions. MJL, DL, CYX, and ZYX analyzed the data. CXL, YW, and HBM prepared the dataset. JCG obtained financial support. All authors contributed to the article and approved the submitted version.

FUNDING

This study was supported by the National Natural Science Foundation of China (Grant No. 81972324), the Chinese

Academy of Medical Sciences Innovation Fund for Medical Sciences (Grant No. 2016-I2M-3-019), and the non-profit Central Research Institute Fund of Chinese Academy of Medical Sciences (Grant No. 2018PT32014). The funder bodies were not involved in the study design, collection, analysis, interpretation of data, the writing of this article or the decision to submit it for publication.

ACKNOWLEDGMENTS

Thanks to all who have contributed to the process of writing this article.

SUPPLEMENTARY MATERIAL

The Supplementary Material for this article can be found online at: https://www.frontiersin.org/articles/10.3389/fonc.2021.812785/full#supplementary-material

Supplementary Figure 1 | (A, B) Used the LASSO regression to calculate the minimum value of lambda.

Supplementary Figure 2 | (A–N) Patients with different clinicopathological features had different levels of risk scores, but there was no statistically significant difference.

Supplementary Figure 3 | (A) The K-M curve of the G1 subgroup. **(B)** The K-M curve of the locoregional recurrence subgroup. **(C, D)** LncRNA PRECSIT/ITGB1-DT expression in six PDAC cell lines and one pancreatic duct epithelial cell line.

REFERENCES

1. Siegel RL, Miller KD, Jemal A. Cancer Statistics, 2020. *CA: Cancer J Clin* (2020) 70(1):7–30. doi: 10.3322/caac.21590
2. Kamisawa T, Wood LD, Itoi T, Takaori K. Pancreatic Cancer. *Lancet* (2016) 388(10039):73–85. doi: 10.1016/S0140-6736(16)00141-0
3. Mayo SC, Nathan H, Cameron JL, Olino K, Edil BH, Herman JM, et al. Conditional Survival in Patients With Pancreatic Ductal Adenocarcinoma Resected With Curative Intent. *Cancer-Am Cancer Soc* (2012) 118(10):2674–81. doi: 10.1002/cncr.26553
4. Fesler A, Ju J. Development of microRNA-Based Therapy for Pancreatic Cancer. *J Pancreatology (Online).* (2019) 2(4):147–51. doi: 10.1097/JP9.0000000000000029
5. Ma S, Chen C, Ji X, Liu J, Zhou Q, Wang G, et al. The Interplay Between M6a RNA Methylation and Noncoding RNA in Cancer. *J Hematol Oncol* (2019) 12 (1):121. doi: 10.1186/s13045-019-0805-7
6. He L, Li H, Wu A, Peng Y, Shu G, Yin G. Functions of N6-Methyladenosine and its Role in Cancer. *Mol Cancer.* (2019) 18(1):176. doi: 10.1186/s12943-019-1109-9
7. Xia T, Wu X, Cao M, Zhang P, Shi G, Zhang J, et al. The RNA M6a Methyltransferase METTL3 Promotes Pancreatic Cancer Cell Proliferation and Invasion. *Pathol - Res Pract* (2019) 215(11):152666. doi: 10.1016/j.prp.2019.152666
8. Taketo K, Konno M, Asai A, Koseki J, Toratani M, Satoh T, et al. The Epitranscriptome M6a Writer METTL3 Promotes Chemo- and Radioresistance in Pancreatic Cancer Cells. *Int J Oncol* (2018) 52(2):621–9. doi: 10.3892/ijo.2017.4219
9. Ying P, Li Y, Yang N, Wang X, Wang H, He H, et al. Identification of Genetic Variants in M6a Modification Genes Associated With Pancreatic Cancer Risk in the Chinese Population. *Arch Toxicol* (2021) 95(3):1117–28. doi: 10.1007/s00204-021-02978-5
10. Guo X, Li K, Jiang W, Hu Y, Xiao W, Huang Y, et al. RNA Demethylase ALKBH5 Prevents Pancreatic Cancer Progression by Posttranscriptional Activation of PER1 in an M6a-YTHDF2-Dependent Manner. *Mol Cancer* (2020) 19(1):91. doi: 10.1186/s12943-020-01158-w
11. Tang B, Yang Y, Kang M, Wang Y, Wang Y, Bi Y, et al. M6a Demethylase ALKBH5 Inhibits Pancreatic Cancer Tumorigenesis by Decreasing WIF-1 RNA Methylation and Mediating Wnt Signaling. *Mol Cancer* (2020) 19(1):3. doi: 10.1186/s12943-019-1128-6
12. Hu X, Peng W, Zhou H, Jiang J, Zhou X, Huang D, et al. IGF2BP2 Regulates DANCR by Serving as an N6-Methyladenosine Reader. *Cell Death Differentiation* (2020) 27(6):1782–94. doi: 10.1038/s41418-019-0461-z
13. He Y, Hu H, Wang Y, Yuan H, Lu Z, Wu P, et al. ALKBH5 Inhibits Pancreatic Cancer Motility by Decreasing Long Non-Coding RNA KCNK15-AS1 Methylation. *Cell Physiol Biochem* (2018) 48(2):838–46. doi: 10.1159/000491915
14. Huang H, Weng H, Chen J. M(6)A Modification in Coding and Non-Coding RNAs: Roles and Therapeutic Implications in Cancer. *Cancer Cell* (2020) 37 (3):270–88. doi: 10.1016/j.ccell.2020.02.004
15. Zaccara S, Ries RJ, Jaffrey SR. Reading, Writing and Erasing mRNA Methylation. *Nat Rev Mol Cell Biol* (2019) 20(10):608–24. doi: 10.1038/s41580-019-0168-5
16. Huang H, Weng H, Chen J. The Biogenesis and Precise Control of RNA M(6)A Methylation. *Trends Genet* (2020) 36(1):44–52. doi: 10.1016/j.tig.2019.10.011
17. Livneh I, Moshitch-Moshkovitz S, Amariglio N, Rechavi G, Dominissini D. The M(6)A Epitranscriptome: Transcriptome Plasticity in Brain Development and Function. *Nat Rev Neurosci* (2020) 21(1):36–51. doi: 10.1038/s41583-019-0244-z
18. Friedman J, Hastie T, Tibshirani R. Regularization Paths for Generalized Linear Models *via* Coordinate Descent. *J Stat Software* (2010) 33(1):1–22. doi: 10.18637/jss.v033.i01
19. Ritchie ME, Phipson B, Wu D, Hu Y, Law CW, Shi W, et al. Limma Powers Differential Expression Analyses for RNA-Sequencing and Microarray Studies. *Nucleic Acids Res* (2015) 43(7):e47. doi: 10.1093/nar/gkv007
20. Shannon P, Markiel A, Ozier O, Baliga NS, Wang JT, Ramage D, et al. Cytoscape: A Software Environment for Integrated Models of Biomolecular Interaction Networks. *Genome Res* (2003) 13(11):2498–504. doi: 10.1101/gr.1239303
21. Lamb J, Crawford ED, Peck D, Modell JW, Blat IC, Wrobel MJ, et al. The Connectivity Map: Using Gene-Expression Signatures to Connect Small Molecules, Genes, and Disease. *Sci (American Assoc Advancement Science).* (2006) 313(5795):1929–35. doi: 10.1126/science.1132939
22. Blanche P, Dartigues J, Jacqmin-Gadda H. Estimating and Comparing Time-Dependent Areas Under Receiver Operating Characteristic Curves for Censored Event Times With Competing Risks. *Stat Med* (2013) 32 (30):5381–97. doi: 10.1002/sim.5958
23. Meng X, Deng Y, He S, Niu L, Zhu H. M(6)A-Mediated Upregulation of LINC00857 Promotes Pancreatic Cancer Tumorigenesis by Regulating the miR-150-5p/E2F3 Axis. *Front Oncol* (2021) 11:629947. doi: 10.3389/fonc.2021.629947
24. Lu T, Wei GH, Wang J, Shen J. LncRNA CASC19 Contributed to the Progression of Pancreatic Cancer Through Modulating miR-148b/E2F7 Axis. *Eur Rev Med Pharmacol Sci* (2020) 24(20):10462–71. doi: 10.26355/eurrev_202010_23399
25. Gong J, Lu X, Xu J, Xiong W, Zhang H, Yu X. Coexpression of UCA1 Anditga2in Pancreatic Cancer Cells Target the Expression of miR-107 Through Focal Adhesion Pathway. *J Cell Physiol* (2019) 234(8):12884–96. doi: 10.1002/jcp.27953
26. Guo Z, Wang X, Yang Y, Chen W, Zhang K, Teng B, et al. Hypoxic Tumor-Derived Exosomal Long Noncoding RNA UCA1 Promotes Angiogenesis *via* miR-96-5p/AMOTL2 in Pancreatic Cancer. *Mol Ther Nucleic Acids* (2020) 22:179–95. doi: 10.1016/j.omtn.2020.08.021
27. Liu Y, Feng W, Gu S, Wang H, Zhang Y, Chen W, et al. The UCA1/KRAS Axis Promotes Human Pancreatic Ductal Adenocarcinoma Stem Cell Properties and Tumor Growth. *Am J Cancer Res* (2019) 9(3):496–510.
28. Zhang X, Du L, Han J, Li X, Wang H, Zheng G, et al. Novel Long non-Coding RNA LINC02323 Promotes Epithelial-Mesenchymal Transition and Metastasis *via* Sponging miR-1343-3p in Lung Adenocarcinoma. *Thorac Cancer* (2020) 11(9):2506–16. doi: 10.1111/1759-7714.13562

29. Piipponen M, Nissinen L, Riihila P, Farshchian M, Kallajoki M, Peltonen J, et al. P53-Regulated Long Noncoding RNA PRECSIT Promotes Progression of Cutaneous Squamous Cell Carcinoma *via* STAT3 Signaling. *Am J Pathol* (2020) 190(2):503–17. doi: 10.1016/j.ajpath.2019.10.019
30. Jiang Y, Li W, Yan Y, Yao X, Gu W, Zhang H. LINC01094 Triggers Radio-Resistance in Clear Cell Renal Cell Carcinoma *via* miR-577/CHEK2/FOXM1 Axis. *Cancer Cell Int* (2020) 20(1):274. doi: 10.1186/s12935-020-01306-8
31. Xu Q, Wang Y, Huang W. Identification of Immune-Related lncRNA Signature for Predicting Immune Checkpoint Blockade and Prognosis in Hepatocellular Carcinoma. *Int Immunopharmacol* (2021) 92:107333. doi: 10.1016/j.intimp.2020.107333
32. Chang R, Xiao X, Fu Y, Zhang C, Zhu X, Gao Y. ITGB1-DT Facilitates Lung Adenocarcinoma Progression via Forming a Positive Feedback Loop With ITGB1/Wnt/β-Catenin/MYC. *Front Cell Dev Biol* (2021) 9. doi: 10.3389/fcell.2021.631259
33. Haeberle L, Esposito I. Pathology of Pancreatic Cancer. *Trans Gastroenterol Hepatol* (2019) 4:50. doi: 10.21037/tgh.2019.06.02
34. Ganesh K, Massagué J. Targeting Metastatic Cancer. *Nat Med* (2021) 27 (1):34–44. doi: 10.1038/s41591-020-01195-4
35. Oien DB, Pathoulas CL, Ray U, Thirusangu P, Kalogera E, Shridhar V. Repurposing Quinacrine for Treatment-Refractory Cancer. *Semin Cancer Biol* (2021) 68:21–30. doi: 10.1016/j.semcancer.2019.09.021
36. Etman SM, Abdallah OY, Mehanna RA, Elnaggar Y. Lactoferrin/Hyaluronic Acid Double-Coated Lignosulfonate Nanoparticles of Quinacrine as a Controlled Release Biodegradable Nanomedicine Targeting Pancreatic Cancer. *Int J Pharm* (2020) 578:119097. doi: 10.1016/j.ijpharm.2020.119097
37. Etman SM, Mehanna RA, Bary AA, Elnaggar YSR, Abdallah OY. Undaria Pinnatifida Fucoidan Nanoparticles Loaded With Quinacrine Attenuate Growth and Metastasis of Pancreatic Cancer. *Int J Biol Macromol* (2021) 170:284–97. doi: 10.1016/j.ijbiomac.2020.12.109
38. Isah T. Anticancer Alkaloids From Trees: Development Into Drugs. *Pharmacognosy Rev* (2016) 10(20):90. doi: 10.4103/0973-7847.194047
39. Kim N, Choi J, Song AY, Choi WS, Park H, Park S, et al. Direct Potentiation of NK Cell Cytotoxicity by 8-Azaguanine With Potential Antineoplastic Activity. *Int Immunopharmacol* (2019) 67:152–9. doi: 10.1016/j.intimp.2018.12.020
40. Jaskulska A, Janecka AE, Gach-Janczak K. Thapsigargin—From Traditional Medicine to Anticancer Drug. *Int J Mol Sci* (2021) 22(1):4. doi: 10.3390/ijms22010004
41. Holm M, Borg A, Ehrenberg M, Sanyal S. Molecular Mechanism of Viomycin Inhibition of Peptide Elongation in Bacteria. *Proc Natl Acad Sci* (2016) 113 (4):978–83. doi: 10.1073/pnas.1517541113

Conflict of Interest: The authors declare that the research was conducted in the absence of any commercial or financial relationships that could be construed as a potential conflict of interest.

Publisher's Note: All claims expressed in this article are solely those of the authors and do not necessarily represent those of their affiliated organizations, or those of the publisher, the editors and the reviewers. Any product that may be evaluated in this article, or claim that may be made by its manufacturer, is not guaranteed or endorsed by the publisher.

frontiers in Oncology

REVIEW
published: 26 January 2022
doi: 10.3389/fonc.2021.822745

Interaction of ncRNA and Epigenetic Modifications in Gastric Cancer: Focus on Histone Modification

Qingfan Yang[1,2†], Yu Chen[2,3,4†], Rui Guo[1†], Yalan Dai[1,2], Liyao Tang[3,4], Yueshui Zhao[2,3,4], Xu Wu[2,3,4], Mingxing Li[2,3,4], Fukuan Du[2,3,4], Jing Shen[2,3,4], Tao Yi[5], Zhangang Xiao[2,3,4*] and Qinglian Wen[1,2*]*

[1] Department of Oncology, The Affiliated Hospital of Southwest Medical University, Southwest Medical University, Luzhou, China, [2] South Sichuan Institute of Translational Medicine, Luzhou, China, [3] Laboratory of Molecular Pharmacology, Department of Pharmacology, School of Pharmacy, Southwest Medical University, Luzhou, China, [4] Cell Therapy & Cell Drugs of Luzhou Key Laboratory, Luzhou, China, [5] School of Chinese Medicine, Hong Kong Baptist University, Hong Kong, Hong Kong SAR, China

OPEN ACCESS

Edited by:
Muzafar Ahmad Macha,
Islamic University of Science and Technology, India

Reviewed by:
Qi Shengcai,
Shanghai Stomatology Prevention Hospital, China
Marina V. Nemtsova,
I.M. Sechenov First Moscow State Medical University, Russia

***Correspondence:**
Tao Yi
yitao@hkbu.edu.hk
Zhangang Xiao
zhangangxiao@swmu.edu.cn
Qinglian Wen
wql73115@163.com

[†]These authors have contributed equally to this work

Specialty section:
This article was submitted to Gastrointestinal Cancers: Gastric & Esophageal Cancers, a section of the journal Frontiers in Oncology

Received: 26 November 2021
Accepted: 28 December 2021
Published: 26 January 2022

Citation:
Yang Q, Chen Y, Guo R, Dai Y, Tang L, Zhao Y, Wu X, Li M, Du F, Shen J, Yi T, Xiao Z and Wen Q (2022) Interaction of ncRNA and Epigenetic Modifications in Gastric Cancer : Focus on Histone Modification. Front. Oncol. 11:822745. doi: 10.3389/fonc.2021.822745

Gastric cancer has developed as a very common gastrointestinal tumors, with recent effective advancements in the diagnosis and treatment of early gastric cancer. However, the prognosis for gastric cancer remains poor. As a result, there is in sore need of better understanding the mechanisms of gastric cancer development and progression to improve existing diagnostic and treatment options. In recent years, epigenetics has been recognized as an important contributor on tumor progression. Epigenetic changes in cancer include chromatin remodeling, DNA methylation and histone modifications. An increasing number of studies demonstrated that noncoding RNAs (ncRNAs) are associated with epigenetic changes in gastric cancer. Herein, we describe the molecular interactions of histone modifications and ncRNAs in epigenetics. We focus on ncRNA-mediated histone modifications of gene expression associated with tumorigenesis and progression in gastric cancer. This molecular mechanism will contribute to our deeper understanding of gastric carcinogenesis and progression, thus providing innovations in gastric cancer diagnosis and treatment strategies.

Keywords: ncRNA, histone modification, gastric cancer, epigenetic modifications, mechanisms

1 INTRODUCTION

Gastric cancer (GC) is ranking the fifth most common cancer in the world, with over one million cases in 2018, nearly two-thirds of which occur in developing countries. GC remains the third leading cause of tumor-related death, just behind lung cancers and colorectal cancers (1–3). GC is a highly heterogeneous disease, and according to Lauren's classification, it can be classified into two histological subtypes: the intestinal type and the diffuse type. High-throughput technologies have been well developed, and a new molecular classification is proposed by The Cancer Genome Atlas (TCGA), which subdivided GC into chromosomal instability (CIN)、genomic stability (GS)、microsatellite instability (MSI) and Epstein-Barr-Virus positivity (EBV) (4). There are four subtypes according to the WHO classification system, including papillary, tubular, signet ring, and mucinous (5).

GC is a heterogeneous cancer with multifactorial and unique epigenetic and genetic events, but the pathogenesis and molecular mechanisms remain elusive (6, 7). Both genetic and environmental factors are able to participate in the development and progression of GC (8). Genetic mutations have been considered as driving force for cancer development. However, current research data show substantial evidence that epigenetic alterations play an essential role in the development and progression of cancers, including GC (9, 10). Epigenetics refers to alterations in the process of gene expression without changes in DNA sequence, which are heritable, transient and reversible in gene expression (11). Epigenetic changes in cancer include DNA methylation, histone modifications and chromatin remodeling. The occurrence as well as progression of GC can be partially ascribed to environmental factors, including age, high salt intake, a diet low in fruits/vegetables and H. pylori infection (1).. However, environmental effects on GC are controllable, and only by exploring epigenetic regulation in depth can epigenetic alterations be controlled and managed. Histone modification occupies an important place in the regulatory mechanisms of epigenetics, and it is detected mainly in amino acids and carbohydrates, which also plays an essential role in cancer development (12). Recently, a large amount of literature indicates that noncoding RNAs (ncRNAs) are closely related to histone modifications in GC. In this review, the epigenetic alterations of histone post-transcriptional modifications associated with ncRNAs in gastric cancer have been intensively discussed.

2 A BRIEF DESCRIPTION OF HISTONE POST-TRANSCRIPTIONAL MODIFICATIONS

Chromatin is a linearly arranged structure composed of millions of nucleosomes consisting mainly of DNA, RNA and histones (13). The fundamental unit of human genetic material is the nucleosome and consists of a histone octamer wrapped by a double-stranded DNA, this octamer contains two copies of histones H2A, H2B, H3 and H4 (14). Post-translational modifications of histones, including multiple covalent modifications such as methylation, acetylation, phosphorylation, ubiquitination, sumoylation, etc. They largely regulate DNA accessibility and gene expression (15). Currently, aberrant regulation of histone modifications has now been investigated in many kinds of cancers, and the role of histone modifications is being extensively studied. In this paper, we briefly describe the various types of histone post-transcriptional modifications and focus on the interaction between ncRNAs and histone acetylation/methylation in GC.

2.1 The Role of Histone Acetylation in Cancer

Histone acetylation, a reversible and dynamic process, is inversely regulated by deacetylases (HDACs) and histone acetyltransferases (HATs) (16). Acetylation neutralizes the positively charged lysine side chains to make the DNA structure more open and make it easier for transcription factors to combine with other proteins, which in turn promotes gene expression. In recent years, three major families of HATs have been identified, including MYST family (MOZ, Ybf2, Sas2, TIP60), Gcn5-related N-acetyltransferase family (GNAT) and orphan family (CBP/EP300 and nuclear receptors) (17). HDACs can be classified into four categories: Class I HDACs, consisting of HDACs 1, 2, 3 and 8; Class II HDACs, consisting of HDACs 4, 5, 6, 7, 9 and 10; Class III HDACs, consisting of seven silencing regulatory proteins, including NAD-dependent protein deacetylases and ADP ribosylases, also known as Sirtuins; Class IV HDACs, containing only HDAC11, has sequence similarity compared to class I and II proteins (16). HATs relax chromatin structure and promote transcription through transferring the acetyl group from acetyl coenzyme A to histone amino acid terminus. In contrast, HDACs make the chromatin structure more compact by removing the acetyl group from the lysine terminus, thereby inhibiting transcription. Altered overall levels of histone acetylation have been shown to be connected with many tumor phenotypes (18). In general, hyperacetylation leads to increased gene expression, especially when proto-oncogenes are involved, and gene expression might be activated. Hypoacetylation of oncogenes is usually localized to the promoter simultaneously with DNA methylation, resulting in suppression of gene expression (19).

2.2 The Mechanisms of Histone Methylation

Histone methylation plays an important role in cell biological fate, such as DNA recombination and damage repair, gene expression and cell differentiation, and so forth (20). Histone methylation, catalyzed by histone methyltransferases (HMTs), occurs mainly on lysine and arginine residues located at histone tails. Arginine can be mono- or dimethylated, while for lysine, apart from mono- and dimethylated, it is able to be trimethylated (21). Histone methylation regulatory genes include protein arginine methyltransferases PRMTs, lysine methyltransferases KMTs (e.g. EZH2 and DOT1L), and histone demethylases HDMs (e.g. LSD1 and KDMs). The function of all KMTs is to bind s-adenosylmethionine (SAM) methyl donors to lysine methyl acceptors and facilitates methyl transfer from SAM to the telomeres (22). Protein arginine methylation reactions are mainly catalyzed by the protein arginine methyltransferase family, including PRMT1-9. These enzymes catalyze the reaction of transferring a methyl group from S-adenosylmethionine (AdoMet) to a guanidino nitrogen of arginine, which results in the formation of methylarginine and S-adenosylhomocysteine (AdoHcy) (23). Lysine methylation occurs mainly on histone H3 and H4, for example, six lysine residues, H3K4, H3K9, H3K27, H3K36, H3K79, and H4K20, are proven to be methylated in histones H3 and H4, respectively. Among them, acetylation can take place in histone H3 for H3K9 and H3K27. Lots of other lysine residues, H3K14, H3K18, H3K23 and H4K5, H4K8, H4K12 and H4K16, can only be acetylated rather than methylated. Methylation/acetylation in H3K9 and H3K27

performs different physiological functions, for instance, acetylation of H3K9 and H3K27 leads to gene transcriptional activation, whereas methylation of H3K9 and H3K27 represses transcription (14).

2.3 The Mechanisms of Histone Phosphorylation in Cancer

Histone phosphorylation occurs mainly at serine, tyrosine and threonine residues in the histone tails, which is regulated by various kinases and phosphatases, mediating biological fate such as DNA damage repair, chromatin remodeling, transcriptional activation and apoptosis (24). During mitosis, histone phosphorylation disrupts the balance of interactions between histones and DNA, resulting in an unstable chromatin structure, which ultimately allows the chromatin structure to remodel into homologous chromosomes (21). It is worth noting that histone phosphorylation mediates the transcriptional regulation of genes, particularly those that regulate the cell cycle and cell proliferation. For example, H3Ser10p and H2BSer32p are involved in epidermal growth factor (EGF)-mediated gene transcriptional activation (25, 26). In addition, H3ser10p mediates the transcriptional activation of proto-oncogenes such as c-myc and c-fos (26, 27). Histone H3 threonine 45 (H3T45) is phosphorylated with the participation of protein kinase C1, which promotes acetylation of H3K56 and ultimately regulates apoptosis and DNA replication (28, 29). A growing number of studies have shown that histone phosphorylation is involved in tumorigenesis and progression. For example, histone H4 phosphorylation is closely associated with liver regeneration and hepatocellular carcinoma (30). Increased levels of histone H3S10 phosphorylation is involved in the proliferation of gastric cancer cells and can be an independent prognostic indicator of vascular infiltration in gastric cancer (31, 32).

2.4 A Brief Description of Histone Ubiquitination

In post-transcriptional modifications, protein ubiquitination is a common process in cells (33, 34). Ubiquitination is a cascade reaction that relies on Adenosine Triphosphate (ATP) to link ubiquitin to a substrate protein. Ubiquitin activated by ubiquitin activating enzymes E1s is transferred to the ubiquitin binding enzymes E2s and ultimately transferred to the substrate protein by the ubiquitin ligases E3s (35). Among them, the ubiquitin ligases E3s are key enzymes in the ubiquitination process because of their specific recognition of the substrate protein (36). Histone ubiquitination is also involved in DNA damage repair, gene transcriptional regulation and genomic stability (37). Protein deubiquitination is catalyzed by deubiquitinating enzymes (DUB) and the dynamic balance of ubiquitination and deubiquitination plays an important role in cellular homeostasis. Therefore, their aberrant expression has been shown to be involved in the development and progression of many cancers (38–40).

2.5 A Novel Histone Modification: Sumoylation

Sumoylation has the same mechanism compared with ubiquitination, allowing for the covalent attachment of small ubiquitin-like modifiers (SUMO) to lysine residues of the substrate protein, which is a reversible post-transcriptional modification (41). Sumoylation acts as a negative regulator involved in the regulation of protein stability, gene transcription and ultimately repression of gene transcription (42, 43). Most of the substrate proteins for sumoylation are nuclear proteins. For example, the sumoylation of transcription factor can recruit chromatin-modifying enzymes to repress gene expression (44). In addition, sumoylation regulates the expression and activity of histone-modifying enzymes, suggesting a close relationship between sumoylation and epigenetic regulation (24). For instance, sumoylation of the transcription factor E2F1 promotes EZH2 transcription by increasing the binding of E2F1 to the EZH2 promoter (45). It has been shown that SUMO-1 is involved in the proliferation and apoptosis of endometrial cancer cells by increasing the level of histone H4 sumoylation (46). Another study shows that the sumoylation of transcription factor ETV1 promotes prostate cancer development (47), suggesting that sumoylation is involved in tumorigenesis and progression.

3 THE ROLE OF NCRNAS IN GC

3.1 Overview of Noncoding RNAs in Cancer

Noncoding RNAs (ncRNAs) are a unique kind of RNA transcripts that are intensively recognized in eukaryotic genomes (48). Although over 75% of the human genome can be transcribed, among them, only *ca.* 2% of the transcription products are translated into proteins, and the remaining transcripts (which cannot encode proteins) are initially treated as junk transcription products (49). Transformed from junk transcription products to functional molecules that regulate cellular processes, ncRNAs regulate gene expression at different levels during physiological development, including signal transduction, chromatin remodeling, gene transcription and post-transcriptional modifications (50). Through their regulatory networks, ncRNAs can modulate many downstream targets to mediate specific cell biological fate (51). Growing evidence indicates that ncRNAs influence normal cell function and disease progression, especially in cancer development, which are considered as tumor suppressors and oncogenic factors (52, 53). Meanwhile, high-throughput sequencing technologies developed a lot, and increasing studies are showing that a little bit of ncRNAs have small open reading frames (sORFs), which can encode peptides or proteins (48). It has been demonstrated that HOXB-AS3, encoded by lncRNA, is shown to regulate tumor energy metabolism. FBXW7-185aa 18 and PINT-87aa 20, encoded by circRNA, can block tumor cell cycle and inhibit cell expansion. SHPRH-146aa 19, encoded by circRNA, can suppress tumor cell expansion and malignant phenotype. miPEP-200a and miPEP-200b, encoded by miRNAs, regulate epithelial-mesenchymal transition (EMT), leading to tumorigenesis and progression. According to transcription length, ncRNAs are mainly classified as long noncoding RNA (lncRNAs, linear, >200 nucleotides), circular RNA (circRNAs,

covalently closed continuous loops), and short ncRNAs (linear, <200 nucleotides) (54).

3.2 A Brief Description of miRNAs and Their Role in GC

miRNAs are considered as a class of highly conserved tissue-specific small molecule non-protein-coding RNAs. Mature miRNAs are generated from primary miRNAs (pri-miRNAs) by two consecutive enzymatic reactions and loaded into RNA-induced silencing complexes (RISCs) containing Argonaute 2 (AGO2) (55, 56), which repress messenger RNAs (mRNAs) translation and promote mRNA degradation by directly combining with mRNA, and ultimately inhibit gene expression at the post-transcriptional stage to maintain intracellular homeostasis (57, 58). They are powerful regulatory factors of various biologically important activities such as cell growth and development (59). Regulatory mechanisms of miRNAs action include gene polymorphism, miRNA promoter methylation, interactions with RNA binding proteins (RBPs) or other RNAs, nucleotide modification of miRNA sequences at different stages of maturation, and unsymmetric miRNA strand selection (60) (36). miRNAs can repress the expression and activity of target RNAs at the post-transcriptional level, and the mechanism is the recognition of miRNA response elements (MREs) of target RNAs. MREs are usually located in the 3' untranslated region (3'UTR) of the RNA, and can also be located in the 5' untranslated region (5'UTR) and in the coding sequence (CDS). miRNAs recognize and bind sequence-complementary MREs at the 3'UTR of the target transcription product, and their inhibition of protein synthesis mechanism is not fully understood (56). When RNA transcripts have identical MREs on their 3'UTR, they can act as competing endogenous RNAs (ceRNAs), influencing each other's expression by competing and combining with miRNAs from the same library. Each miRNA can target multiple RNAs, and at the same time, each RNA can be a target of multiple miRNAs. Ultimately, miRNAs can form a complex ceRNET with their associated transcripts (**Figure 1A**) (61). Herein, we highlight a few example from each category, with **Figure 1B** providing visual representations of the ceRNA network (62–64). Many physiological and pathological processes, including cardiovascular/metabolic diseases and cancers, are proven to be heavily dependent on miRNAs (65). Therefore, tumor development, such as cell proliferation, motility, apoptosis and angiogenesis, can be affected by aberrant expression of miRNAs (66). Recently, growing studies have demonstrated that deregulation of miRNAs expression is related to gastric cancer by acting as oncogenes and tumor suppressors, which can contribute to the diagnosis and treatment of GC (67–69). What's more, there is growing evidence suggesting that circulating plasma and serum miRNAs can act as potential biomarkers for non-invasive tumor diagnosis, cancer therapy and prognosis (70–72).

3.3 The Mechanisms of lncRNAs in GC

lncRNA is defined as a transcript greater than 200 nt in length, and typically lacks the capability of encoding proteins (73). lncRNAs exert a variety of biological functions at the epigenetic level by regulating gene expression. As a result, tumorigenesis and progression are highly dependent on the dysfunctional lncRNAs (74). Recent studies disclose that a lot of lncRNAs are aberrantly regulated in GC, and altered lncRNA expression participates in cancer pathological processes, such as cell proliferation, metastasis, EMT, apoptosis, tumor stemness, drug resistance, etc. Therefore, it has the potential to act as a biomarker and therapeutic target for GC (75–78). Furthermore, it has been shown that the broad expression pattern in cancer, stability in circulating body fluids (plasma and urine) and tumor specificity of lncRNAs imply that subtype/tissue-specific expression of lncRNAs is important for the discovery of novel diagnostic, prognostic and therapeutic targets (79–81).

3.4 circRNAs: A Rising Star in GC Research Field

Circular RNAs (circRNAs) are covalent closed-loop structures formed by post-sniping of precursor mRNAs without 5' caps or 3' polyA tails, and they are also a class of endogenous RNAs without function of encoding proteins or peptides (82). Unlike linear RNA, circRNA has a special cyclic covalent bond structure, which makes them evolutionarily conserved and highly stable. Thus, they are inherently resistant to RNA exonucleases as well as RNaseR activity and are widely expressed in complex tissues and cell types at specific stages (83). Literature demonstrates that circRNAs have many biological functions, such as microRNA sponges, transcriptional regulation, regulation of mRNA stability, encoding functional proteins, and binding to RNA-binding proteins (84). Therefore, circRNAs have obvious impacts on many human diseases, such as diabetes, neurological/cardiovascular diseases, and cancers, thus exhibiting great potential as diagnostic and therapeutic targets (85, 86). In the case of GC, the importance of dysregulated circRNAs in gastric carcinogenesis, progression and clinicopathology has been demonstrated, thus showing the value of biomarkers for diagnosis and treatment (87, 88).

4 NCRNAS REGULATE HISTONE MODIFICATION IN GC

Firstly, ncRNAs specify the histone modification pattern of target genes by recruiting tissue modification complexes directed to specific gene loci and might repress *cis* or *trans* transcription of target genes (**Figure 2**); Secondly, ncRNAs regulate target genes by participating in ceRNET as miRNA sponges (**Figure 3**); Thirdly, they can directly target histone modifiers and affect the alteration of histone or non-histone modifications pattern (**Figure 4**). Through these mechanisms, they drive the malignant biological behaviors of GC cells and ultimately promote tumor formation and progression (**Table 1** and **Table 2**).

4.1 miRNAs Regulate Histone Modification in GC

4.1.1 miRNAs Regulate the Expression of Target Genes by Recruiting Histone-Modifying Complexes

The expression of miR-584-3p is decreased in GC. miR-584-3p inhibits MMP-14 transcription by recruiting euchromatic histone lysine methyltransferase 2 (EHMT2) and enhancer of

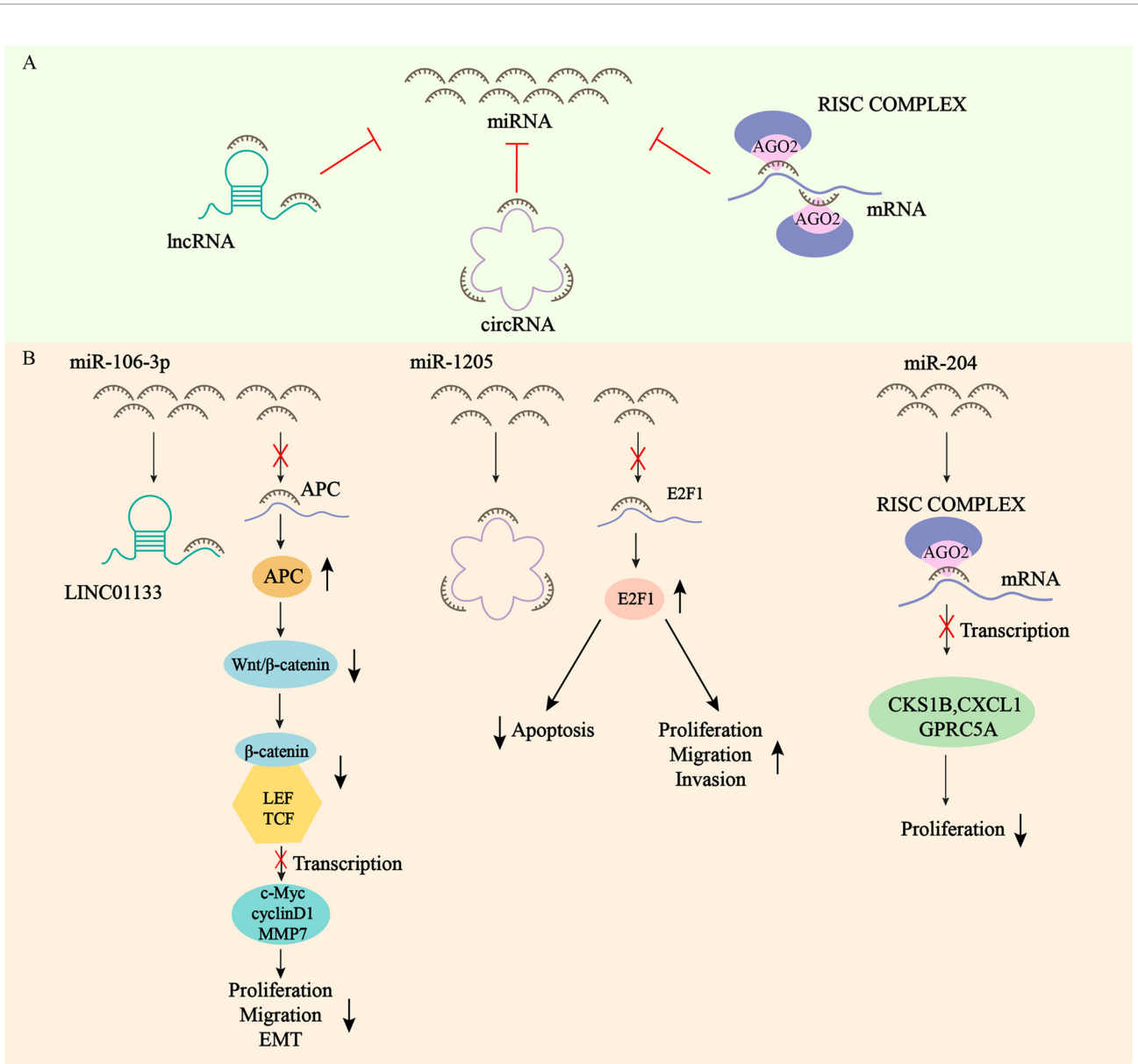

FIGURE 1 | Network of competitive endogenous RNAs. **(A)** mRNAs, lncRNAs, and circRNAs all contain microRNA (miRNA) response elements (MREs) that can bind to miRNAs and regulate the expression of RNA targets at the post-transcriptional level. **(B)** LINC01133 exerts oncogenic effect by acting as a sponge for miR-106-3p, which regulates the expression of APC and inactivates the Wnt/β-catenin signaling pathway. circCYFIP2 exerts oncogenic effect by acting as a sponge for miR-1205, which regulates the expression of E2F1. miRNA-204 inhibits the transcription of CKS1B, CXCL1 and GPRC5A mRNAs by binding to AGO2 to form the RISC complex, which ultimately inhibits the proliferation of GC.

zeste homolog 2 (EZH2) to interact with AGO2, leading to enrichment of repressive epigenetic markers and reduced binding of YY1 to the MMP-14 promoter. YY1 (one member of the GLI-Krüppel protein family) directly targets the matrix metalloproteinase 14 (MMP-14) to promote MMP-14 expression in GC cells and tissues, resulting in tumorigenesis and invasion. miR-584-3p ultimately inhibits GC cell growth, metastasis and angiogenesis by suppressing the expression of MMP14 (90).

4.1.2 miRNAs Regulate Histone Acetylation in GC

In GC cells, miR543 expression is upregulated, promoting cell cycle and proliferation, and thus positively correlates with the clinical phenotype of GC patients. By directly targeting the SIRT1 3 '-UTR, miR-543 can inhibit the expression of SIRT1 mRNA, thereby promoting GC cell proliferation and cell cycle progression. SIRT1, a class III histone deacetylase, is downregulated in GC and can inhibit gastric carcinogenesis and progression (90).

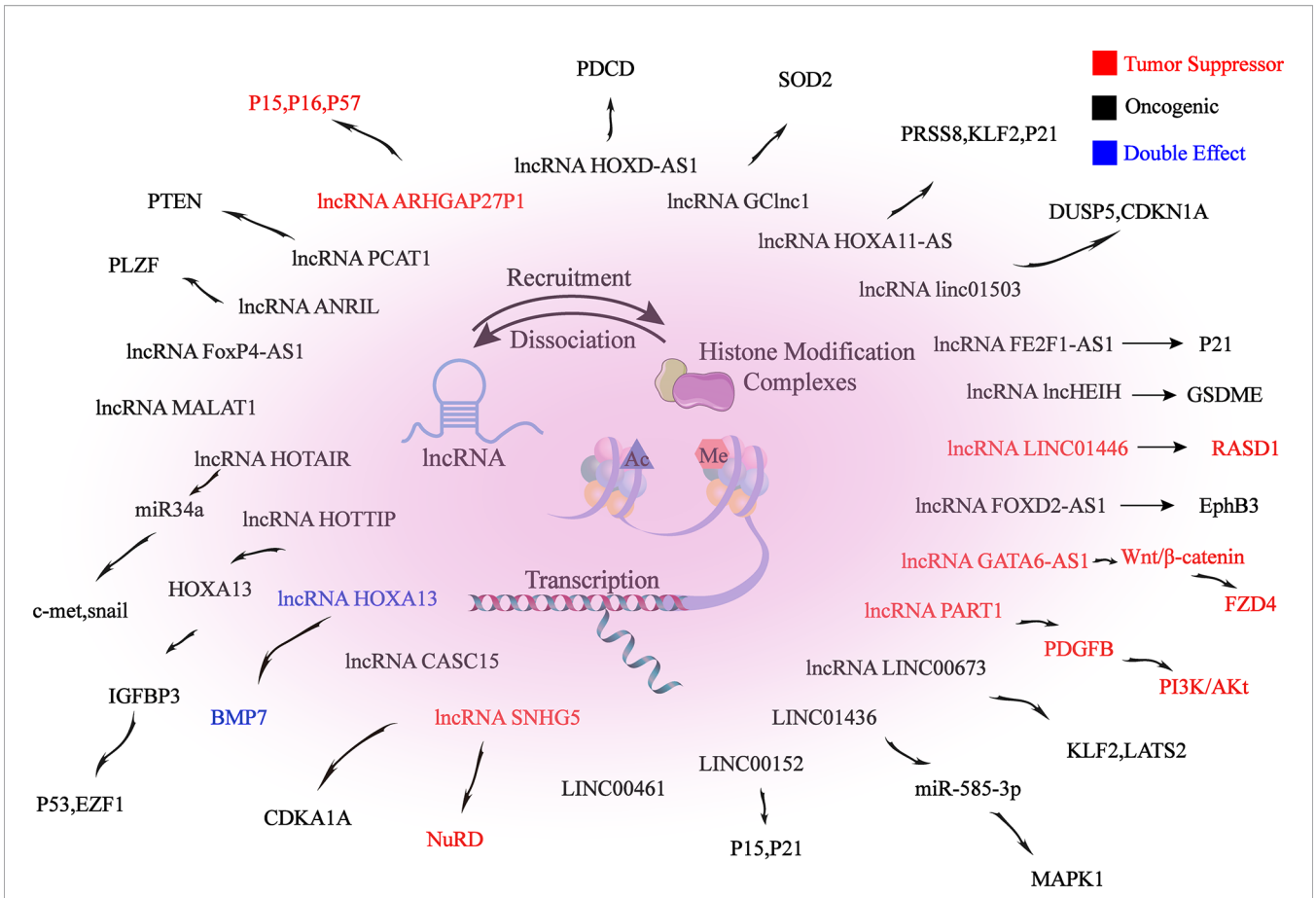

FIGURE 2 | lncRNAs mediate histone modifications of target genes. lncRNAs induce changes in promoter histone modification patterns by recruiting histone modification complexes to target gene promoter-associated binding sites, thereby epigenetically regulating target gene expression, which ultimately alters the biological behaviors of GC.

miR-489 is significantly downregulated in GC cells and tissues, and the downregulation can promote GC cell proliferation, invasion and migration, which is positively correlated with the prognosis of GC patients. Knockdown of HDAC7, a direct target of miR-489, can inhibit GC development as well as antagonize the effects of miR-489 inhibitors on GC cells. Taken together, by targeting HDAC7 and blocking the PI3K/AKT pathway, miR-489 exerts tumor suppressive effects in GC cell growth (99).

The overexpression of miR-31, which is aberrantly downregulated in GC cell lines, might inhibit proliferation and migration of GC cells, as well as induce apoptosis. miR-31 expression in GC is epigenetically regulated, and down-regulation of miR-31 is related to DNA methylation of promoter. In addition, HDAC2 can act as a direct target of miR-31 through combining with MREs in the 3'-UTR, and its expression is negatively regulated by miR-31. HDAC2 inactivation restores the activity of p16 ^{INK4a}, which has anti-tumor effects in gastric cancer (91).

miR-383-5p expression is downregulated in GC cells and tissues. Therefore, miR-383-5p overexpression inhibits proliferation, induces apoptosis, as well as suppresses tumor growth in GC cell lines. HDAC9 is a direct target of miR-383-5p, which can be upregulated in GC cell lines. Therefore, it is closely associated with malignant development of GC. As a result, knockdown of HDAC9 in GC cell lines promotes apoptosis and inhibits proliferation, and microRNA-383-5p can suppress GC development through targeting HDAC9 expression (92).

4.1.3 miRNAs Regulate Histone Methylation in GC

miRNA-329 expression is reduced in GC. miRNA-329 overexpression in GC cells promotes apoptosis and inhibits the malignant biological behaviors of GC cells. miRNA-329 mimics and siRNAs targeting KDM1A, a downstream target of miRNA-329, reduce the expression of KDM1A and increase the levels of H3K4me1 and H3K4me2. As a result, patient with high expression of miRNA-329 or low expression of KDM1A has a longer overall survival. In summary, microRNA-329 promotes apoptosis and inhibits proliferation, metastasis and growth by negatively regulating KDM1A in GC cells (93).

miR-448 is overexpressed in GC, promotes glycolysis and growth of GC, and is associated with poorer survival. The

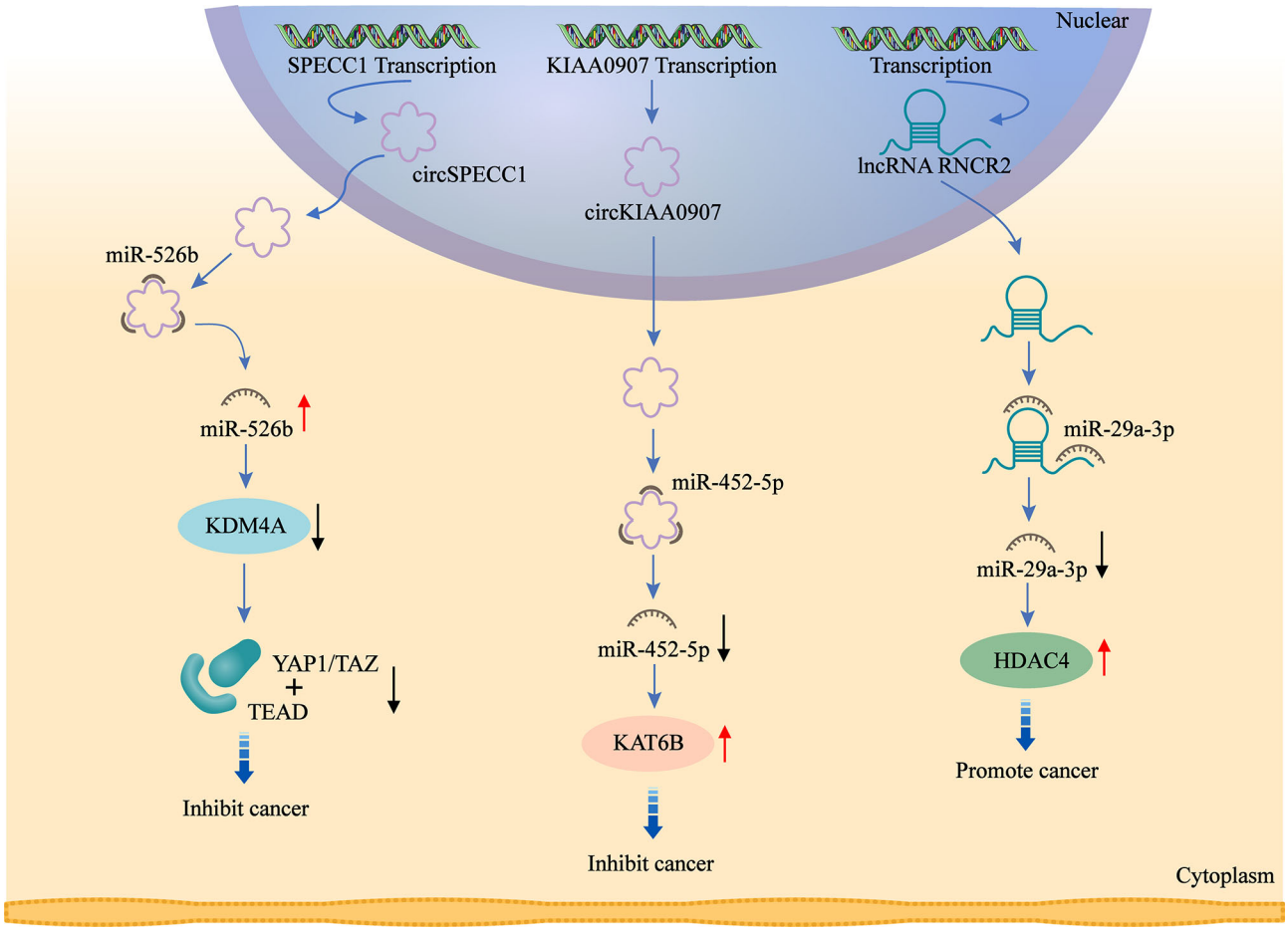

FIGURE 3 | ceRNAs are involved in the regulation of histone modifiers. circ_0000745 acts as a sponge for miR-526b and promotes KDM4A expression. circKIAA0907 acts as a sponge of miR-452-5P and promotes KAT6B expression. lncRNA MIAT acts as a sponge for miR-29a-3p and promotes HDAC4 expression. ceRNAs alter histone and non-histone modifications by regulating the expression of histone modifiers, which affects downstream signaling targets and ultimately exerts their oncogenic or anti-tumor effects.

mechanism is that miR-448 expression is increased in GC, and the increasing expression of miR-448 upregulates the expression of the rate-limiting enzyme of glycolysis, Myc, through directly inhibiting KDM2B, which ultimately stimulates glycolysis (94).

miR-212 expression is aberrantly reduced in human GC cells and tissues. miR-212 is found to inhibit RBP2 expression through directly combining with the 3'UTR site of Retinoblastoma binding protein 2 (RBP2). RBP2, a newly identified histone demethylase, is overexpressed in GC. miR-212 exerts oncogenic effects in gastric cancer by suppressing RBP2 expression and increasing the expression of P21 ^{CIP1} and P27 ^{kip1} to arrest the cell cycle and inhibit cell colony formation (100).

miR-192/215 expression is significantly increased in GC cells and tissues. miR-192/215 can directly combine with the 3'UTR of SET8 to facilitate proliferation and metastasis of GC cells. Histone methyltransferase SET8 (KMT5A), one of the members of SET domain-containing methyltransferase family, is responsible for catalyzing monomethylation of H4K20me. And the expression of SET8 is downregulated in GC cells and tissues. Furthermore, in GC cells, SET8 triggers oncogene-induced senescence (OIS) and induces senescence through p53-dependent DNA damage induced oncogenes. Thus, by inhibiting the senescence signaling pathway, miR-192/215-SET8-p53 axis exacerbates GC development (95).

RUNX3 is a transcription factor that binds directly to the region of miR-29b promoter and cooperates with Smad3, leading to higher activity of miR-29b promoter. Both miR-29b and RUNX3 are decreased in GC tissues, with positively correlated expression. miR-29b directly binds to KDM2A 3′-UTR and negatively regulates the expression of KDM2A, serving as a target of miR-29b. Through this mechanism, the proliferation and migration of GC cells are inhibited (101).

As miR-491-5p is decreased in GC cells, tissues and serum, its high expression can inhibit proliferation and invasion in GC. By targeting JMJD2B (KDM4B), miRNA-491-5p can inhibit malignant biological behaviors in GC cell lines, exhibiting the potential as a gastric cancer-associated marker (96).

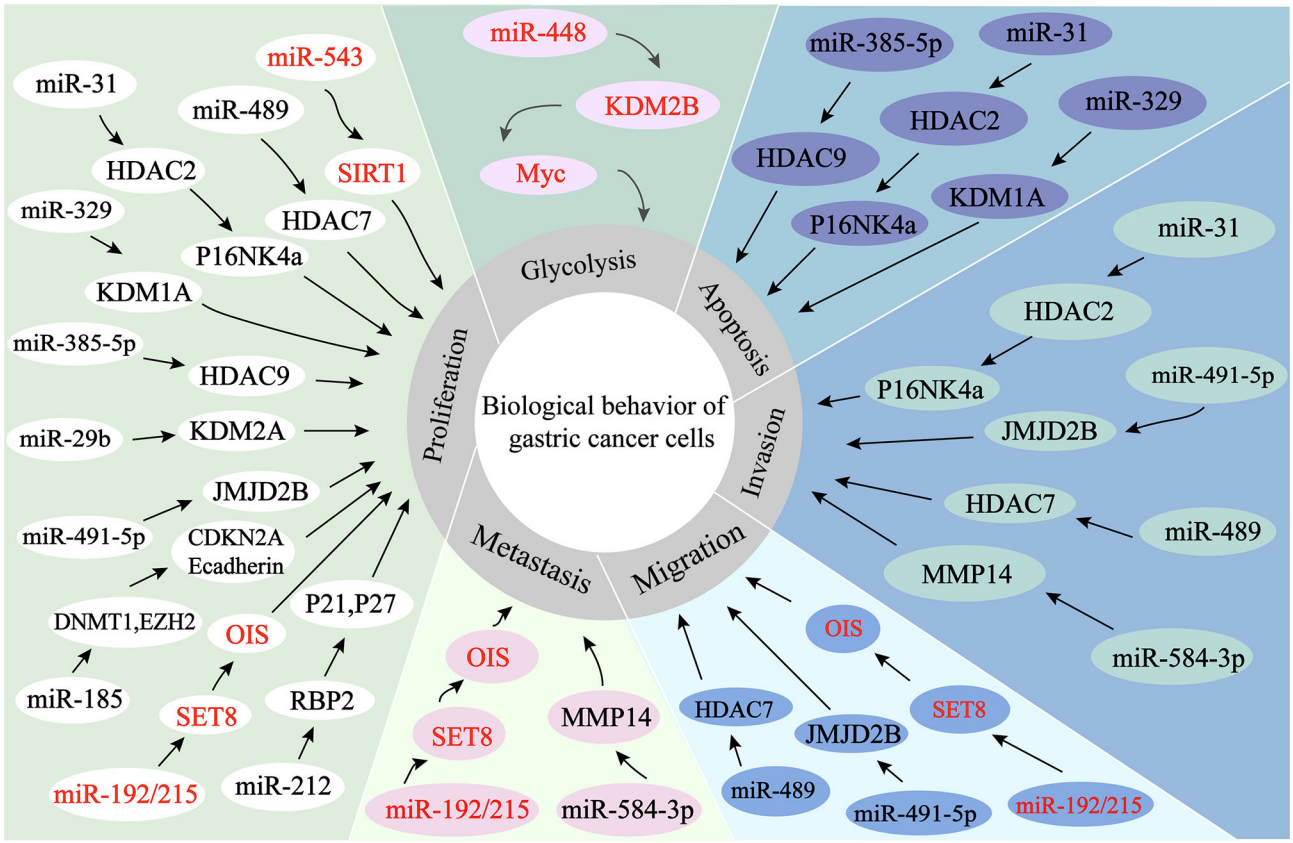

FIGURE 4 | miRNAs regulate histone modification in GC. 1. miR-584-3P recruits EZH2 and EHMT2 to the MMP-14 promoter, thereby inhibiting the expression of MMP-14 and ultimately exerting its oncogenic effects. 2. miRNAs directly target histone modifiers and affect the alteration of histone or non-histone modifications patterns, ultimately leading to changes in the biological behaviors of gastric cancer cells.

4.1.4 miRNAs Regulate Histone Acetylation and Methylation in GC

The GKN1-miR-185-DNMT1 axis exerts oncogenic effects in gastric cancer through mediating epigenetic alterations and cell cycle. Gastrokine 1 (GKN1) reduces GC cell proliferation, viability, and colony formation, as well as blocks cell cycle. The mechanisms are as follows: 1. GKN1 inhibits DNMT1 and EZH2 expression through upregulation of miR-185 expression. miR-185 negatively regulates the inhibitory actions of GKN1 on tumorigenicity, expression of DNMT1 and EZH2, as well as DNMT1 activity; 2. GKN1-induced miR-185 leads to CDKN2A and E-cadherin re-expression through demethylation of CDKN2A and E-cadherin promoter regions; 3. GKN1 negatively regulates DNMT1 through repressing HDAC1 and inducing Tip60 in a miR-185-free manner (97).

4.2 lncRNAs Regulate Histone Modification in GC

4.2.1 lncRNAs Regulate Histone Acetylation in GC

lncRNA SNHG5 is a transcript consisting of six exons of U50HG, which has been reported to be the host gene of snoRNAs U50 and U50'. SNHG5 expression is aberrantly decreased in GC cells and tissues, inhibiting metastasis and proliferation in GC cells. The NuRD complex participates in chromatin remodeling and histone deacetylase with subunits, including MTA1, MTA2, HDAC1 and HDAC2. The mechanism is that the overexpression of SNHG5 affects the formation of the NuRD complex by blocking the transference of MTA2 from the cytoplasm to the nucleus, resulting in significant upregulation of histone H3 and non-histone p53 acetylation levels, which interferes with nucleosome remodeling and the formation of the histone deacetylation complex. As a result, the metastasis and growth of GC cells are suppressed (98).

The expression of lncRNA MALAT1 is aberrantly upregulated in GC cells and tissues. MALAT1 induces EGFL7 protein expression by altering H3 histone acetylation at the region of EGFL7 promoter. Epidermal growth factor-like domain-containing protein 7 (EGFL7), also known as vascular endothelial statin, is encoded by the EGFL7 gene and involved in regulating the formation of vascular ducts and the progression of many cancers. MALAT1 stimulates migration and invasion of GC cell lines through the above mechanism (102).

MIAT expression is significantly increased in GC. Knockdown of lncMIAT inhibits the malignant biological behaviors of GC cells.

TABLE 1 | miRNAs regulate histone modification in GC.

miRNA	Expression	Target	Function	Reference
miR-584-3p	Downregulation	MMP-14 promoter	Tumor suppressor	(89)
miR-489	Downregulation	HKDC7	Tumor suppressor	(91)
miR-31	Downregulation	HDAC2	Tumor suppressor	(92)
miR-383-5p	Downregulation	HDAC9	Tumor suppressor	(93)
miR-329	Downregulation	KDM1A	Tumor suppressor	(94)
miR-212	Downregulation	RBP2	Tumor suppressor	(95)
miR-29b	Downregulation	KDM2A	Tumor suppressor	(96)
miR-491-5p	Downregulation	JMJD2B	Tumor suppressor	(97)
miR-185	Downregulation	DNMT1, EZH2	Tumor suppressor	(98)
miR-543	Upregulation	SIRT1	Oncogenic	(99)
miR-448	Upregulation	KDM2B	Oncogenic	(100)
miR-192/215	Upregulation	SET8	Oncogenic	(101)

lncMIAT competitively combines with miR-29a-3p through serving as a sponge for miR-29a-3p, thereby increasing HDAC4 expression and ultimately exerting an oncogenic effect in GC (103).

4.2.2 lncRNAs Regulate Histone Methylation in GC

lncRNA HOXA11-AS is specifically increased in GC, promoting GC cell proliferation, migration and invasion, with apoptosis inhibition. HOXA11-AS is thought to bind directly to LSD1, EZH2, WDR5, STAU1, DNMT1 and AGO2 in tumor cells, acting as a frame for EZH2 and LSD1/DNMT1 to downregulate PRSS8, KLF2 and P21 expression, thus promoting GC. EZH2 can recognize and bind to PRSS8, KLF2 and P21 promoters, which in turn drives H3K27me3 modification. While LSD1 contributes to H3K4 demethylation by binding directly to the PRSS8 promoter. Moreover, HOXA11-AS can also serve as a miR-1297 sponge by binding to miR-1297, releasing repressive effect on EZH2 mRNA. In addition, EZH2 is further recruited by HOXA11-AS to epigenetically inhibit the expression of KLF2 and PRSS8 (104, 109).

lncRNA FEZF1-AS1 is located at chromosome 7, which is a transcript of 2564 bp in length. The transcription factor SP1 specifically recognizes and binds to the FEZF1-AS1 promoter binding site, increasing the expression of FEZF1-AS1 in GC. GC cells are proliferated through the following mechanisms: Firstly, FEZF1-AS1 causes G1-S cell cycle arrest; Secondly, FEZF1-AS1 binds to LSD1, causing p21 promoter H3K4me2 demethylation and inhibiting the expression of the downstream target p21 (110).

In GC, Linc01503 is regulated by the transcription factor 1 (EGR1) and its expression is upregulated. Linc01503 epigenetically represses the expression of cyclin-dependent kinase inhibitor 1A (CDKN1A) and dual-specificity phosphatase 5 (DUSP5) by recruiting LSD1 and EZH2. EZH2

TABLE 2 | lncRNAs regulate histone modification in GC.

lncRNA	Expression	Mechanism	Target	Function	Reference
lncRNA SNHG5	Downregulation	Histone acetylation	MTA2, NuRD	Tumor suppressor	(102)
lncRNA MALAT1	Upregulation		EGFL7	Oncogenic	(103)
lncRNA MIAT	Upregulation		MiR-29a-3p, HDAC4	Oncogenic	(104)
lncRNA GATA6-AS1	Downregulation	Histone methylation	FZD4	Tumor suppressor	(105)
LINC01446	Downregulation		RASD1	Tumor suppressor	(106)
lncRNA PART1	Downregulation		PLZF, PDGFB	Tumor suppressor	(107)
lncRNA ARHGAP27P1	Downregulation		P15, P16, P57	Tumor suppressor	(108)
lncRNA HOXD-AS1	Upregulation		PDCD	Oncogenic	(109)
lncRNA HOXA11-AS	Upregulation		PRSS8, KLF2, P21	Oncogenic	(110)
lncRNA FEZF1-AS1	Upregulation		P21	Oncogenic	(111)
lncRNA linc01503	Upregulation		DUSP5, CDKN1A	Oncogenic	(112)
lncRNA FOXP4-AS1	Upregulation		EZH2, LSD1	Oncogenic	(108)
LINC00461	Upregulation		LSD1	Oncogenic	(113)
lncRNA PCAT1	Upregulation		PTEN	Oncogenic	(114)
lncRNA ANR1L	Upregulation		PLZF	Oncogenic	(115)
lncRNA HOTTIP	Upregulation		IGFBP3	Oncogenic	(116)
lncRNA HOTAIR	Upregulation		miR34a	Oncogenic	(117)
lncRNA HOXA13	Upregulation		BMP7	Oncogenic	(118)
lncRNA CASC15	Upregulation		CDKN1A	Oncogenic	(119)
LINC00673	Upregulation		KLF2, LAST2	Oncogenic	(120)
LINC01436	Upregulation		miR-585-3P	Oncogenic	(121)
lncRNA FOXD2-AS1	Upregulation		EphB3	Oncogenic	(122)
lncRNA lncHEIH	Upregulation		GSDME	Oncogenic	(123)
LINC00152	Upregulation		P15, P21	Oncogenic	(124)
lncRNA GClnc1	Upregulation	Histone acetylation, methylation	SOD2	Oncogenic	(125)

binds to CDKN1A and DUSP5 promoters, driving histone 3 lysine 4 trimethylation (H3K4me3). While LSD1 binds to DUSP5 and CDKN1A promoters, mediating H3K4me2 demethylation. Ultimately, GC cell cycle progression and proliferation can be promoted by Linc01503, with apoptosis inhibited (111).

The expression of HOXD-AS1 is increased in DDP-resistant GC patients. DDP sensitivity of GC cells can be promoted by knockdown of HOXD-AS1, which can promote cisplatin resistance in GC through recruiting EZH2 and upregulating H3K27me3 levels on the region of PDCD4 promoter in GC cells to epigenetically silence PDCD4 (104).

The expression of lncRNA GATA6 antisense RNA 1 (GATA6-AS1) was decreased in GC cells, which promotes the malignant development of GC cells, such as proliferation, metastasis and invasion. Its overexpression can inhibit tumor growth as well as lymph node metastasis (LNM) in GC. GATA6-AS1 can downregulate the expression of FZD4 by specifically recruiting and binding with EZH2 to increase the enrichment of H3K27me3 in the region FZD4 promoter, which in turn inhibits the Wnt/β-catemin downstream pathway, ultimately leading to the blockage of GC progression (112).

lncRNA 01446 (LINC01446), a 3484-bp ncRNA, is located at chromosome 7p12.1. LINC01446 is downregulated in GC, which is correlates with metastasis and poor prognosis in GC patients. This lncRNA can epigenetically repress Ras-related dexamethasone inducible 1 (RASD1) by recruiting LSD1 to the region of RASD1 promoter, ultimately promoting malignant behaviors of tumor cells (105).

lncRNA PART1 is locate at chromosome 5q12.1. PART1 is decreased in tumor cells and tissues, which is closely related to poor prognosis of GC patients. PART1 overexpression inhibits invasion and metastasis of GC cells. Mechanistically, PART1 acts as a role of tumor suppressor by interacting with androgen receptor (AR) and stimulating the PLZF gene expression in GC cells. Then, co-occupancy of EZH2 and PLZF on the PDGFB promoter region enable histone 3 lysine 27 trimethylation (H3K27me3) to epigenetically silence PDGFB and suppress the PI3K/Akt pathway (106).

Rho GTPase-activating protein (ARHGAP) is a family of Rho homologous GTPase activating proteins that exert oncogenic effects by aberrant regulation of Rho/Rac/Cdc42-like GTPases (107). ARHGAP20 gene is confirmed to be located at chromosome 17q24.1, which is decreased in GC cells, tissues and plasma. Low expression of ARHGAP27P1 is related to adverse clinical features, suggesting a poor prognosis for GC patients. Mechanistic investigations showed that ARHGAP27P1 inhibits proliferation and blocks the cell cycle through combining with Jumonji-domain containing 3 (JMJD3), leading to a significant downregulation of H3K27me3 levels, which ultimately epigenetically induces transcription of p15, p16 and p57 genes (126). Highly expressed FOXP4-AS1 can promote proliferation, migration as well as metastasis of GC cells by interacting with EZH2/LSD1 (127).

LINC00461 is upregulated in GC tissues, which is positively correlated to TNM staging and lymphatic metastasis, mediating cell proliferation and apoptosis in GC through interacting with LSD1, thereby aggravating the progression of GC (108).

lncRNA prostate cancer–associated transcript 1 (PCAT-1) is upregulated in CDDP-resistant GC cell lines and tissues. Mechanistically, PCAT-1 epigenetically silences PTEN gene by recruiting EZH2 to the region of PTEN promoter, resulting in H3K27 trimethylation in the PTEN gene promoter region, ultimately leading to the progress of cisplatin resistance in GC cells. Trough inhibiting of PCAT-1 and upregulating PTEN expression, cisplatin sensitivity of CDDP-resistant GC cells can be enhanced (113).

Tumor suppressor PLZF inhibits proliferation, metastasis and invasion of GC cells. The expression of PLZF is downregulated and negatively correlates with the expression level of lncRNA ANRIL in GC. This lncRNA recruits EZH2, a core member of PRC2, in turn catalyzes H3K27 trimethylation, which then drives PLZF gene silencing by increasing DNA methylation of PLZF. In summary, lncRNA ANRIL suppresses EMT as well as cell proliferation through epigenetic regulation of the tumor suppressor PLZF (114).

lncRNA HOTTIP causes hypomethylation of the HoxA13 promoter E1 site and elevates levels of H3K4me3 by decreasing the recruitment of DNA methyltransferases DNMT1 and DNMT3b at the HoxA13 promoter E1 site, increasing the binding of WDR5 and MLL complexes, which ultimately epigenetically activates HoxA13 expression. Meanwhile, IGFBP3 and HOTTIP are shown to be downstream targets of HoxA13 in GC cells. The expression of HoxA13 and HOTTIP shows positive feedback. HoxA13 trans-activated the expression of IGFBP-3 gene by binding to the Hox binding element at the IGFBP-3 promoter region. IGFBP-3 has been reported to inhibit migration, invasion and EMT in GC through inhibiting invasion factors, such as MMP14 and urokinase-type fibrinogen activator (115). However, IGFBP-3 might enhance division and metastasis in GC CS12 cell line, and knockdown of IGFBP-3 inhibits the poor biological behaviors of GC cells (128).

lncRNA HOTAIR is highly upregulated in GC, which promotes metastasis and invasion of GC cells by inducing EMT, and its overexpression predicts poor prognosis. HOTAIR epigenetically represses miR34a and activates the expression of its downstream targets C-Met (HGF/C-Met/Snail pathway) and Snail by recruiting the multiple sparing repressor complex 2 (PRC2, including EZH2, SUZ12, etc.) to bind directly to the region of miR34a promoter and induce H3K27 trimethylation. Thereby GC cell EMT process and tumor metastasis are accelerated (116).

Another study shows that the expression level of the epithelial marker E-cadherin (CDH1) is increased in HOTAIR knockdown GC. By contrast, the expression levels of mesenchymal markers are downregulated in HOTAIR knockdown GC cells, such as Snail, Slug, Twist, N-cadherin and β-catenin. HOTAIR knockdown derepresses the histone marker H3K27me3 for E-cadherin and induces conversion of the E-cadherin promoter to the active marker acetylated H3K27. In addition, the loss of SUZ12 with the involvement of the active acetyltransferase CBP leads to an increase in acetylation of H3K27 (129). In summary,

in the region of E-cadherin promoter, HOTAIR can epigenetically repress E-cadherin by turning acetylation of histone H3 lysine 27 into methylation, which ultimately promotes EMT of GC (130).

Reprogramming of cancer cells into induced pluripotent stem cells (iPSCs) might be a novel method to suppress tumorigenesis. Another research reported the successful reprogramming of the human gastric cell lines (CS12s) into induced pluripotent stem cell–like cell lines (CS12iPSLCs) by utilizing Jun dimerization protein 2 (JDP2) and octamer-binding protein 4 (OCT4). The study shows that CS12iPSLCs exhibit reduced tumorigenicity *in vivo* and reduce colony formation, proliferation, invasion, migration, and drug resistance *in vitro*. The oncogenic function of Bone morphogenetic protein 7 (BMP7) is switched by lncRNA HOXA13 axis and loses in CS12iPSLCs. H3K4me3 can be increased by recruiting HOXA13, MLL1, WDR5 and HOTTIP at the BMP7 promoter S1 site, thereby activating the expression of BMP7 and promoting the process of GC in CS12. H3K27me3 can be enhanced by recruiting HOXA13, ZEH2, JARID2 and HOTAIR at the BMP7 promoter S2 site, thereby epigenetically suppressing BMP7 expression and inhibiting the progression of GC in CS12iPSLC. In summary, the HOXA13-HOTAIR and HOXA13-HOTTIP axis are recruited to different sites of the BMP7 promoter, leading to different outcomes of GC (117).

lncRNA CASC15 (cancer susceptibility candidate 15) is located at chromosome 6p22.3, which regulates GC cell biological behaviors and is involved in tumorigenesis and progression. The mechanisms are as follows: Firstly, CASC15 regulates GC cell growth partially by serving as a bridge between EZH2 and WDR5 in nucleus, epigenetically silencing CDKN1A. Moreover, in cytoplasm, CASC15 mediates GC cell migration in part by serving as a ceRNA for miR-33a-5p, which competitively binds to ZEB1 (118).

lncRNA LINC00673, an intergenic lncRNA, is located at chromosome 17q25.1. The expression of LINC00673 is aberrantly increased in GC cells. Knockdown of LINC00673 suppresses invasion as well as proliferation, with promoted apoptosis. LINC00673, activated by transcription factor SP1, exerts its oncogenic effects partly through serving as a frame for EZH2 and LSD1 to epigenetically suppress KLF2 and LATS2 genes, promoting the progression of GC (119).

LINC01436 is highly expressed in gastric cancer tissues and cells. High LINC01436 level is associated with poor patient prognosis. In addition, knockdown of LINC01436 inhibits migration and proliferation, with apoptosis promoted. Mechanistically, LINC01436 mediates trimethylation of H3K27 at the miR-585-3p promoter through enhancing EZH2, epigenetically silencing miR-585-3p expression, which in turn upregulates mitogen-activated protein kinase 1 (MAPK1) expression, ultimately promoting GC progression (120).

lncRNA FOXD2-AS1 expression is significantly increased in GC and positively related to the tumor size, later pathological stage as well as poor prognosis. Overexpression of FOXD2-AS1 can accelerate tumor development and predict poor prognosis in GC patients by EZH2 binding to the region of EphB3 promoter and inducing H3K27me3 modification, or LSD1 combining with the region of EphB3 promoter and inducing demethylation of H3K4, ultimately epigenetically silencing of EphB3 (121).

Overexpression of lncHEIH in GC promotes proliferation, migration, tumorigenesis, and expansion of GC stem cells, leading to tumor malignant transformation. lncHEIH can upregulate EZH2 expression, while recruiting and binding EZH2 in the GSDME promoter region and inducing H3K27me3 modification in this region to epigenetically silence GSDME expression, thereby promoting GC progression (122).

lncRNAs 152 (LINC00152) expression is significantly increased in gastric cancer cells and tissues, which is correlated with lymph node metastasis, depth of tumor invasion, higher TNM stage as well as poor prognosis. LINC00152 epigenetically silences the expression of p15 and p21 through combining with EZH2, ultimately accelerating cell cycle progression and proliferation in GC (123).

4.2.3 lncRNAs Regulate Histone Acetylation and Methylation in GC

lncRNA BC041951, named gastric cancer-associated lncRNA 1 (GClnc1), is upregulated in GC and closely associated with poor prognosis of patients. Mechanistically, lncRNA GClnc1 might serve as a modular scaffold to recruit WD repeat protein 5 (WDR5) and histone acetyltransferase KAT2A to the region of the superoxide dismutase 2 mitochondria (SOD2) gene promoter (one of the target genes of the WDR5/KAT2A complex), increasing the levels of H3K4 trimethylation and H3K9 acetylation in the promoter region of SOD2, thereby epigenetically promoting the expression of SOD2. As a result, GC cell proliferation, invasion, tumor growth can be promoted, in addition, chemotherapy resistance can be controlled (124).

4.3 circRNAs Regulate Histone Modification in GC

4.3.1 circRNAs Regulate Histone Acetylation in GC

circMRPS35 suppresses GC development through recruiting KAT7 to mediate histone modification. This study shows that circMRPS35 expression is significantly decreased in GC and related to the clinicopathological features and better prognosis of patients. circMRPS35 exerts oncogenic effect by inhibiting invasion and proliferation of GC cells *in vitro* and *in vivo*. The mechanism is that circMRPS35 enriches H4K5 acetylation at the regions of FOXO1 and FOXO3a promoters by recruiting the histone acetyltransferase KAT7, which ultimately epigenetically activates the expression of FOXO1 and FOXO3a, and induces subsequent responses in their downstream targets, including upregulation of p21, p27 and E-calmodulin, with downregulation of Twist1 expression, ultimately inhibiting cell proliferation and invasion (125).

Another study showed that circKIAA0907 is downregulated in GC. Upregulation of circKIAA0907 induces cell cycle arrest, proliferation and apoptosis, as well as inhibits autophagy. Mechanistically, circKIAA0907 serves as a sponge of miR-452-5p to increase lysine acetyltransferase 6B (KAT6B) expression in GC. KAT6B is a target gene of miR-452-5p, which has been found to play an regulatory role in many cancers. Shi et al.

demonstrates that microRNA-4513 induces EMT and cell proliferation by targeting KAT6B (131). circKIAA0907 inhibits GC development and progression through downregulating miR-452-5p and upregulating KAT6B. This study demonstrates the potential diagnostic and therapeutic value of circKIAA0907, which can serve as a tumor suppressor in GC *via* the miR-452-5p/KAT6B axis (132).

4.3.2 circRNAs Regulate Histone Methylation in GC

circ_0000745 (circ_SPECC1), transcribed from the SPECC1 gene, is downregulated in GC tissues and blood. It exerts anti-tumor effects by significantly inhibiting metastasis and proliferation of GC cells, with apoptosis promoted. circ_SPECC1 is shown to bind directly to miR-526b, which in turn affects miR-526b downstream signaling targets. miR-526b is downregulated in GC cells and tissues, inhibiting invasion and proliferation, with apoptosis promoted. Lysine demethylase 4A (KDM4A, also known as JMJD2A), a member of the histone demethylase family, is also an important target of miR-526b, whose expression is shown to be increased in various cancers. Huang et al. (133) demonstrates that KDM4A expression is aberrantly increased in GC tissues and correlated with clinicopathological features. Inhibition of KDM4A expression weakens transformation and growth of GC cells, with apoptosis promoted. In GC, YAP1/TAZ serve as downstream target genes of KDM4A, promoting transcription through binding to the transcription factor TEAD, ultimately leading to tumor formation (134). In summary, circ_SPECC1 can improve the inhibiting effect of miR-526b at the downstream signaling target YAP1/KDM4A, with invasion and growth of GC cells inhibited (135).

5 NCRNAS ARE REGULATED BY HISTONE MODIFICATION IN GC

Altering the ncRNA histone modification pattern by recruiting histone modifiers into the ncRNA promoter epigenetically regulates ncRNA expression, which in turn changes downstream signaling pathways and target genes. This mechanism ultimately plays an essential role in GC (**Table 3**).

5.1 miRNAs Are Regulated by Histone Modification in GC

5.1.1 miRNAs Are Regulated by Histone Acetylation in GC

miR-155 expression is increased in GC and exhibits pro-carcinogenic effects. MRTF-A (MKL1) promotes miR-155 expression by inducing the acetylation of histones and the recruitment of RNA polymerase II in the region of miR-155 promoter through the Wnt-β-catenin pathway. MRTF-A can act as a coactivator of serum response factor (SRF), participating in cell apoptosis, differentiation, proliferation and migration. miR-155 inhibits SOX1 expression through combining with the 3'UTR of SOX1, promoting migration of tumor cells. In summary, MRTF-A/miR-155/SOX1 axis can mediate metastasis of GC (146).

miR-34a and miR-34b/c, derived from miR-34 family, participate in cell cycle arrest, senescence and apoptosis in tumor. Mechanistically, Sirt7 can epigenetically inhibit miR-34a expression by deacetylating H3K18ac, ultimately preventing apoptosis in gastric cancer cells. The expression of Sirt7, a family member of NAD^+-dependent protein deacetylases, is significantly upregulated in GC, and its knockdown promotes apoptosis and reduces the growth of tumor (137).

miR-330-3p expression is downregulated in GC. However, the ectopic expression of miR-330-3p decreases migration, proliferation, colony formation, and EMT in tumor cells. Treatment of GC cells with the histone deacetylase inhibitor trichostatin A (TSA) and the DNA methylation inhibitor 5-aza-CdR (AZA) enhances the expression of miR-330-3p. This indicates that the downregulation of miR-330-3p is partially mediated through hypermethylation in the region of the gene promoter. In addition, MSI1 is a target gene of miR-330-3p in GC cells. MSI1, an RNA binding protein (RBP), is upregulated in GC cell lines and tissues through combining with the mRNA 3'UTR sequences, leading to translational repression. Moreover, its expression is negatively related to the expression of miR-330-3p in GC tissues (139).

miR-375 expression is downregulated in GC due to methylation of its promoter and histone deacetylation, which is related to poor prognosis and lymph node metastasis. While miR-375 ectopic expression inhibits cell proliferation and

TABLE 3 | ncRNAs regulated by histone modification in EC.

ncRNA	Expression	Mechanism	Target	Function	Reference
miR-142-5p	Upregulation	Histone demethylation	CD9	Oncogenic	(136)
miR-155	Upregulation	Histone acetylation	SOX1	Oncogenic	(137)
miR-454	Upregulation	Histone deacetylation	CHD5	Oncogenic	(138)
miR-34a	Downregulation	Histone deacetylation	CD44	Tumor suppressor	(139, 140)
miR-330-3p	Downregulation	Histone deacetylation	MSI1	Tumor suppressor	(141)
miR-375	Downregulation	Histone deacetylation	YAP1, TEAD4, CTGF	Tumor suppressor	(142)
miR-454	Upregulation	Histone deacetylation	CHD5	Oncogenic	(138)
miR-133	Downregulation	Histone deacetylation,	mcl-1, Bcl-xL	Tumor suppressor	(143)
HOXC-AS3	Upregulation	Histone methylation, Histone acetylation	MMP7, WNT10B, HDAC5	Oncogenic	(144)
lncRNA FENDRR	Downregulation	Histone deacetylation	FN1, MMP2, MMP9	Tumor suppressor	(145)
lncRNA HRCEG	Downregulation	Histone deacetylation	–	Tumor suppressor	(145)

tumorgrowth. miR-375 specifically and directly inhibits the expression of YAP1, TEAD4 and CTGF through combining with their 3'UTRs. YAP1, a co-activator of transcription, is a crucial downstream signaling molecule of the Hippo pathway. It mainly combines with the transcription factor TEAD and exerts oncogenic effects. The expression of CTGF is mediated by YAP1 and TEAD in GC cells. Overall, miR-375 is downregulated in GC cells due to its promoter methylation, which results in the co-activation of YAP1/TEADs-CTGF in the Hippo signaling pathway to promote gastric carcinogenesis (141).

Histone deacetylase 3 (HDAC3) is significantly upregulated in GC tissues and cells. However, knockdown of HDAC3 inhibits the growth of GC cells. HDAC3 overexpression upregulates miR-454 expression, which is significantly related to malignant clinical features in GC patients, implying that it can act as a biomarker for poor prognosis. Moreover, CHD5 is suggested to be a target of miR-454. The ectopic expression of CHD5 inhibits cell proliferation and tumorigenicity, as well as leads to cellular senescence. CHD5 expression is downregulated in GC and negatively associated with miR-454 levels. In summary, HDAC3 targets CHD5 through miR-454 to regulate the growth of GC cells (142).

Histone modification of the miR-133 family at the promoter region leads to a significant decrease of miR-133 expression in GC. Restoration of miR-133b/a-3p expression can target the anti-apoptotic molecules Bcl-xL and Mcl-1 to inhibit proliferation and induce apoptosis in GC cells, thereby suppressing GC growth. In summary, miR-133b/a-3p is regulated by histone modifications, exerting oncogenic effects in GC through targeting Bcl-xL and Mcl-1 (138).

Histone deacetylase 1 (HDAC1) knockdown inhibits cell metastasis and adhesion in GC cells through upregulating miR-34a. The mechanism is that the HDAC1/miR-34a axis regulates CD44 expression, activation as well as its downstream factors, including LIM domain kinase 1 (LIMK-1), matrix metalloproteinase (MMP)-2, ras homolog family member A (RhoA), and Bcl-2. The former three proteins participate in the organization of the microtubulin and actin cytoskeletons as well as the formation of cellular pseudopods. Thus, the depletion of HDAC1 can decreases the metastatic ability of GC cells through the miR-34a/CD44 axis (143).

5.1.2 miRNAs Are Regulated by Histone Methylation in GC

LSD1 is thought to be a demethylase of H3K4me1/2, H3K9me1/2 and several non-histone proteins, which is extensively expressed in GC tissues. LSD1 deletion leads to upregulation of the migration inhibitory factor CD9 through decreasing intracellular miR-142-5p expression, which ultimately inhibits GC migration (140).

5.2 lncRNAs Are Regulated by Histone Acetylation in GC

lncRNA HOXC-AS3, located at chromosome 12q13.13, is defined as an antisense transcript of HOXC10. Gaining of H3K27ac and H3K4me3 activation of the promoter contributes to driving HOXC-AS3 gene in GC cells and tissues. By binding to YBX1, HOXC-AS3 transcriptionally regulates genes, such as MMP7, WNT10B and HDAC5. They are related to the biological behaviors of GC cells, ultimately inducing migration and proliferation in GC. In addition, HDAC5 gene is a member of the histone deacetylase (HDAC) family. Therefore, this study suggests that HOXC-AS3 is regulated by histone modifications, which in turn regulates HDAC5 to promote GC (136).

The lncRNA FENDRR is a gene of length 3099nts and located at Chr3q13.31. The expression of FENDRR is reduced in GC, which is correlated with poor prognosis and clinicopathological characteristics in GC patients. The histone deacetylase 3 (HDAC3) drives metastasis of GC cells through epigenetic silencing of FENDRR, induction of fibronectin1 (FN1) expression, and activation of MMP2/MMP9 (144).

lncRNA HRCEG is decreased in GC cells, which is an HDAC1-regulated RNA affecting GC cell proliferation and EMT transformation. HRCEG expression is negatively regulated by histone deacetylase 1 (HDAC1). The overexpression of HRCEG inhibits GC cells proliferation and EMT process (145).

6 CONCLUSIONS AND FUTURE PERSPECTIVES

Recently, growing evidence indicates that epigenetic alteration is a critical factor involved in tumorigenesis and progression. Research progress has been achieved in the use of epigenetic methods to treat cancer. For instance, numerous drugs targeting epigenetic pathways have achieved clinical efficacy, including inhibitors of DNMTs and HDACs. However, the mechanisms of epigenetic alterations in tumorigenesis and progression have not been fully explored. In this review, we attempt to comprehensively describe the important role of ncRNA and histone modification interactions in the pathogenesis of GC, thus providing a solid basis for identifying more specific and effective epigenetic therapeutic agonists/inhibitors. As the field of ncRNAs continues to evolve, there are many technologies that support the feasibility of ncRNA-based therapies. For ncRNAs with down-regulated expression, their expression levels can be enhanced by liposomes/nanoparticles from virus- or plasmid-based expression vectors. For ncRNAs with up-regulated expression, RNAi/shRNAs can be constructed or CRISPR-Cas9 can be used to suppress their expression levels. However, efforts are still needed in ncRNA-based therapy for tumors. Moreover, considering the limited efficacy of monotherapies and the possibility of serious adverse effects, we should achieve more progress in the field of epigenetic drugs combined with other anti-tumor drugs for cancer treatment, which will be a boon for GC patients.

AUTHOR CONTRIBUTIONS

QY and YD were responsible for the review of the literature. QY and YC wrote the manuscript. YC and RG edited the

manuscript. QY and YD drew the tables and pictures. TY, QW, and ZX designed the study and made valuable discussions and revisions to the manuscript. All authors contributed to the article and approved the submitted version.

ACKNOWLEDGMENTS

ZX is thankful to the National Natural Science Foundation of China (Grants 81503093, 81972643, and 81672444) for the financial supports.

REFERENCES

1. Smyth EC, Nilsson M, Grabsch HI, van Grieken NC, Lordick F. Gastric Cancer. *Lancet* (2020) 396(10251):635–48. doi: 10.1016/S0140-6736(20)31288-5
2. Bray F, Ferlay J, Soerjomataram I, Siegel RL, Torre LA, Jemal A. Global Cancer Statistics 2018: GLOBOCAN Estimates of Incidence and Mortality Worldwide for 36 Cancers in 185 Countries. *CA Cancer J Clin* (2018) 68(6):394–424. doi: 10.3322/caac.21492
3. Eusebi LH, Telese A, Marasco G, Bazzoli F, Zagari RM. Gastric Cancer Prevention Strategies: A Global Perspective. *J Gastroenterol Hepatol* (2020) 35(9):1495–502. doi: 10.1111/jgh.15037
4. Link A, Kupcinskas J. MicroRNAs as non-Invasive Diagnostic Biomarkers for Gastric Cancer: Current Insights and Future Perspectives. *World J Gastroenterol* (2018) 24(30):3313–29. doi: 10.3748/wjg.v24.i30.3313
5. Sexton RE, Al Hallak MN, Diab M, Azmi AS. Gastric Cancer: A Comprehensive Review of Current and Future Treatment Strategies. *Cancer Metastasis Rev* (2020) 39(4):1179–203. doi: 10.1007/s10555-020-09925-3
6. Sterea AM, Egom EE, El Hiani Y. TRP Channels in Gastric Cancer: New Hopes and Clinical Perspectives. *Cell Calcium* (2019) 82:102053. doi: 10.1016/j.ceca.2019.06.007
7. Guggenheim DE, Shah MA. Gastric Cancer Epidemiology and Risk Factors. *J Surg Oncol* (2013) 107(3):230–6. doi: 10.1002/jso.23262
8. Correa P. Gastric Cancer: Overview. *Gastroenterol Clin North Am* (2013) 42(2):211–7. doi: 10.1016/j.gtc.2013.01.002
9. Karimi P, Islami F, Anandasabapathy S, Freedman ND, Kamangar F. Gastric Cancer: Descriptive Epidemiology, Risk Factors, Screening, and Prevention. *Cancer Epidemiol Biomarkers Prev* (2014) 23(5):700–13. doi: 10.1158/1055-9965.EPI-13-1057
10. Feng W, Ding Y, Zong W, Ju S. Non-Coding RNAs in Regulating Gastric Cancer Metastasis. *Clin Chim Acta* (2019) 496:125–33. doi: 10.1016/j.cca.2019.07.003
11. Puneet, Kazmi HR, Kumari S, Tiwari S, Khanna A, Narayan G. Epigenetic Mechanisms and Events in Gastric Cancer-Emerging Novel Biomarkers. *Pathol Oncol Res* (2018) 24(4):757–70. doi: 10.1007/s12253-018-0410-z
12. Werner RJ, Kelly AD, Issa JJ. Epigenetics and Precision Oncology. *Cancer J* (2017) 23(5):262–9. doi: 10.1097/PPO.0000000000000281
13. Michalak EM, Burr ML, Bannister AJ, Dawson MA. The Roles of DNA, RNA and Histone Methylation in Ageing and Cancer. *Nat Rev Mol Cell Biol* (2019) 20(10):573–89. doi: 10.1038/s41580-019-0143-1
14. Song Y, Wu F, Wu J. Targeting Histone Methylation for Cancer Therapy: Enzymes, Inhibitors, Biological Activity and Perspectives. *J Hematol Oncol* (2016) 9(1):49. doi: 10.1186/s13045-016-0279-9
15. Zhou Z, Lin Z, Pang X, Tariq MA, Ao X, Li P, et al. Epigenetic Regulation of Long non-Coding RNAs in Gastric Cancer. *Oncotarget* (2018) 9(27):19443–58. doi: 10.18632/oncotarget.23821
16. Li Y, Seto E. HDACs and HDAC Inhibitors in Cancer Development and Therapy. *Cold Spring Harb Perspect Med* (2016) 6(10):634. doi: 10.1101/cshperspect.a026831
17. Audia JE, Campbell RM. Histone Modifications and Cancer. *Cold Spring Harb Perspect Biol* (2016) 8(4):a019521. doi: 10.1101/cshperspect.a019521
18. Fraga MF, Ballestar E, Villar-Garea A, Boix-Chornet M, Espada J, Schotta G, et al. Loss of Acetylation at Lys16 and Trimethylation at Lys20 of Histone H4 is a Common Hallmark of Human Cancer. *Nat Genet* (2005) 37(4):391–400. doi: 10.1038/ng1531
19. Baylin SB, Jones PA. Epigenetic Determinants of Cancer. *Cold Spring Harb Perspect Biol* (2016) 8(9):a019505. doi: 10.1101/cshperspect.a019505
20. Black JC, Van Rechem C, Whetstine JR. Histone Lysine Methylation Dynamics: Establishment, Regulation, and Biological Impact. *Mol Cell* (2012) 48(4):491–507. doi: 10.1016/j.molcel.2012.11.006
21. Qin J, Wen B, Liang Y, Yu W, Li H. Histone Modifications and Their Role in Colorectal Cancer (Review). *Pathol Oncol Res* (2020) 26(4):2023–33. doi: 10.1007/s12253-019-00663-8
22. McCabe MT, Mohammad HP, Barbash O, Kruger RG. Targeting Histone Methylation in Cancer. *Cancer J* (2017) 23(5):292–301. doi: 10.1097/PPO.0000000000000283
23. Di Lorenzo A, Bedford MT. Histone Arginine Methylation. *FEBS Lett* (2011) 585(13):2024–31. doi: 10.1016/j.febslet.2010.11.010
24. Shanmugam MK, Arfuso F, Arumugam S, Chinnathambi A, Jinsong B, Warrier S, et al. Role of Novel Histone Modifications in Cancer. *Oncotarget* (2018) 9(13):11414–26. doi: 10.18632/oncotarget.23356
25. Lau AT, Lee SY, Xu YM, Zheng D, Cho YY, Zhu F, et al. Phosphorylation of Histone H2B Serine 32 is Linked to Cell Transformation. *J Biol Chem* (2011) 286(30):26628–37. doi: 10.1074/jbc.M110.215590
26. Choi HS, Choi BY, Cho YY, Mizuno H, Kang BS, Bode AM, et al. Phosphorylation of Histone H3 at Serine 10 is Indispensable for Neoplastic Cell Transformation. *Cancer Res* (2005) 65(13):5818–27. doi: 10.1158/0008-5472.CAN-05-0197
27. Chadee DN, Hendzel MJ, Tylipski CP, Allis CD, Bazett-Jones DP, Wright JA, et al. Increased Ser-10 Phosphorylation of Histone H3 in Mitogen-Stimulated and Oncogene-Transformed Mouse Fibroblasts. *J Biol Chem* (1999) 274(35):24914–20. doi: 10.1074/jbc.274.35.24914
28. Darieva Z, Webber A, Warwood S, Sharrocks AD. Protein Kinase C Coordinates Histone H3 Phosphorylation and Acetylation. *Elife* (2015) 4:e09886. doi: 10.7554/eLife.09886
29. Trevino LS, Wang Q, Walker CL. Phosphorylation of Epigenetic "Readers, Writers and Erasers": Implications for Developmental Reprogramming and the Epigenetic Basis for Health and Disease. *Prog Biophys Mol Biol* (2015) 118(1-2):8–13. doi: 10.1016/j.pbiomolbio.2015.02.013
30. Besant PG, Attwood PV. Histone H4 Histidine Phosphorylation: Kinases, Phosphatases, Liver Regeneration and Cancer. *Biochem Soc Trans* (2012) 40(1):290–3. doi: 10.1042/BST20110605
31. Takahashi H, Murai Y, Tsuneyama K, Nomoto K, Okada E, Fujita H, et al. Overexpression of Phosphorylated Histone H3 is an Indicator of Poor Prognosis in Gastric Adenocarcinoma Patients. *Appl Immunohistochem Mol Morphol* (2006) 14(3):296–302. doi: 10.1097/00129039-200609000-00007
32. Uguen A, Conq G, Doucet L, Talagas M, Costa S, De Braekeleer M, et al. Immunostaining of Phospho-Histone H3 and Ki-67 Improves Reproducibility of Recurrence Risk Assessment of Gastrointestinal Stromal Tumors. *Virchows Arch* (2015) 467(1):47–54. doi: 10.1007/s00428-015-1763-2
33. Park HB, Kim JW, Baek KH. Regulation of Wnt Signaling Through Ubiquitination and Deubiquitination in Cancers. *Int J Mol Sci* (2020) 21(11):3904. doi: 10.3390/ijms21113904
34. Antao AM, Tyagi A, Kim KS, Ramakrishna S. Advances in Deubiquitinating Enzyme Inhibition and Applications in Cancer Therapeutics. *Cancers (Basel)* (2020) 12(6):1579. doi: 10.3390/cancers12061579
35. Sun T, Liu Z, Yang Q. The Role of Ubiquitination and Deubiquitination in Cancer Metabolism. *Mol Cancer* (2020) 19(1):146. doi: 10.1186/s12943-020-01262-x
36. Tang R, Langdon WY, Zhang J. Regulation of Immune Responses by E3 Ubiquitin Ligase Cbl-B. *Cell Immunol* (2019) 340:103878. doi: 10.1016/j.cellimm.2018.11.002
37. Thompson LL, Guppy BJ, Sawchuk L, Davie JR, McManus KJ. Regulation of Chromatin Structure *via* Histone Post-Translational Modification and the Link to Carcinogenesis. *Cancer Metastasis Rev* (2013) 32(3-4):363–76. doi: 10.1007/s10555-013-9434-8
38. Popovic D, Vucic D, Dikic I. Ubiquitination in Disease Pathogenesis and Treatment. *Nat Med* (2014) 20(11):1242–53. doi: 10.1038/nm.3739
39. Hahn MA, Dickson KA, Jackson S, Clarkson A, Gill AJ, Marsh DJ. The Tumor Suppressor CDC73 Interacts With the Ring Finger Proteins RNF20

and RNF40 and is Required for the Maintenance of Histone 2B Monoubiquitination. *Hum Mol Genet* (2012) 21(3):559–68. doi: 10.1093/hmg/ddr490
40. Prenzel T, Begus-Nahrmann Y, Kramer F, Hennion M, Hsu C, Gorsler T, et al. Estrogen-Dependent Gene Transcription in Human Breast Cancer Cells Relies Upon Proteasome-Dependent Monoubiquitination of Histone H2B. *Cancer Res* (2011) 71(17):5739–53. doi: 10.1158/0008-5472.CAN-11-1896
41. Hay RT. SUMO: A History of Modification. *Mol Cell* (2005) 18(1):1–12. doi: 10.1016/j.molcel.2005.03.012
42. Gill G. Post-Translational Modification by the Small Ubiquitin-Related Modifier SUMO has Big Effects on Transcription Factor Activity. *Curr Opin Genet Dev* (2003) 13(2):108–13. doi: 10.1016/s0959-437x(03)00021-2
43. Shiio Y, Eisenman RN. Histone Sumoylation is Associated With Transcriptional Repression. *Proc Natl Acad Sci U S A* (2003) 100 (23):13225–30. doi: 10.1073/pnas.1735528100
44. Wotton D, Pemberton LF, Merrill-Schools J. SUMO and Chromatin Remodeling. *Adv Exp Med Biol* (2017) 963:35–50. doi: 10.1007/978-3-319-50044-7_3
45. Du L, Fakih MG, Rosen ST, Chen Y. SUMOylation of E2F1 Regulates Expression of EZH2. *Cancer Res* (2020) 80(19):4212–23. doi: 10.1158/0008-5472.CAN-20-1259
46. Zheng J, Liu L, Wang S, Huang X. SUMO-1 Promotes Ishikawa Cell Proliferation and Apoptosis in Endometrial Cancer by Increasing Sumoylation of Histone H4. *Int J Gynecol Cancer* (2015) 25(8):1364–8. doi: 10.1097/IGC.0000000000000501
47. Oh S, Shin S, Janknecht R. Sumoylation of Transcription Factor ETV1 Modulates its Oncogenic Potential in Prostate Cancer. *Int J Clin Exp Pathol* (2021) 14(7):795–810. doi: 10.1038/s41598-019-44685-3
48. Wang J, Zhu S, Meng N, He Y, Lu R, Yan GR. ncRNA-Encoded Peptides or Proteins and Cancer. *Mol Ther* (2019) 27(10):1718–25. doi: 10.1016/j.ymthe.2019.09.001
49. Peschansky VJ, Wahlestedt C. Non-Coding RNAs as Direct and Indirect Modulators of Epigenetic Regulation. *Epigenetics* (2014) 9(1):3–12. doi: 10.4161/epi.27473
50. Mattick JS, Makunin IV. Non-Coding RNA. *Hum Mol Genet* (2006) 15 Spec No 1:R17–29. doi: 10.1093/hmg/ddl046
51. Anastasiadou E, Jacob LS, Slack FJ. Non-Coding RNA Networks in Cancer. *Nat Rev Cancer* (2018) 18(1):5–18. doi: 10.1038/nrc.2017.99
52. Zhang P, Wu W, Chen Q, Chen M. Non-Coding RNAs and Their Integrated Networks. *J Integr Bioinform* (2019) 16(3):20190027. doi: 10.1515/jib-2019-0027
53. Pavet V, Portal MM, Moulin JC, Herbrecht R, Gronemeyer H. Towards Novel Paradigms for Cancer Therapy. *Oncogene* (2011) 30(1):1–20. doi: 10.1038/onc.2010.460
54. Li D, Zhang J, Li J. Role of miRNA Sponges in Hepatocellular Carcinoma. *Clin Chim Acta* (2020) 500:10–9. doi: 10.1016/j.cca.2019.09.013
55. Slack FJ, Chinnaiyan AM. The Role of Non-Coding RNAs in Oncology. *Cell* (2019) 179(5):1033–55. doi: 10.1016/j.cell.2019.10.017
56. Abdollahzadeh R, Daraei A, Mansoori Y, Sepahvand M, Amoli MM, Tavakkoly-Bazzaz J. Competing Endogenous RNA (ceRNA) Cross Talk and Language in ceRNA Regulatory Networks: A New Look at Hallmarks of Breast Cancer. *J Cell Physiol* (2019) 234(7):10080–100. doi: 10.1002/jcp.27941
57. Mishra S, Yadav T, Rani V. Exploring miRNA Based Approaches in Cancer Diagnostics and Therapeutics. *Crit Rev Oncol Hematol* (2016) 98:12–23. doi: 10.1016/j.critrevonc.2015.10.003
58. Lu TX, Rothenberg ME. MicroRNA. *J Allergy Clin Immunol* (2018) 141 (4):1202–7. doi: 10.1016/j.jaci.2017.08.034
59. Saliminejad K, Khorram Khorshid HR, Soleymani Fard S, Ghaffari SH. An Overview of microRNAs: Biology, Functions, Therapeutics, and Analysis Methods. *J Cell Physiol* (2019) 234(5):5451–65. doi: 10.1002/jcp.27486
60. Correia de Sousa M, Gjorgjieva M, Dolicka D, Sobolewski C, Foti M. Deciphering Mirnas' Action Through miRNA Editing. *Int J Mol Sci* (2019) 20(24):6249. doi: 10.3390/ijms20246249
61. Qi X, Zhang DH, Wu N, Xiao JH, Wang X, Ma W. ceRNA in Cancer: Possible Functions and Clinical Implications. *J Med Genet* (2015) 52 (10):710–8. doi: 10.1136/jmedgenet-2015-103334
62. Yang XZ, Cheng TT, He QJ, Lei ZY, Chi J, Tang Z, et al. LINC01133 as ceRNA Inhibits Gastric Cancer Progression by Sponging miR-106a-3p to Regulate APC Expression and the Wnt/beta-Catenin Pathway. *Mol Cancer* (2018) 17(1):126. doi: 10.1186/s12943-018-0874-1
63. Lin J, Liao S, Li E, Liu Z, Zheng R, Wu X, et al. Circcyfip2 Acts as a Sponge of miR-1205 and Affects the Expression of Its Target Gene E2F1 to Regulate Gastric Cancer Metastasis. *Mol Ther Nucleic Acids* (2020) 21:121–32. doi: 10.1016/j.omtn.2020.05.007
64. Shrestha S, Yang CD, Hong HC, Chou CH, Tai CS, Chiew MY, et al. Integrated MicroRNA-mRNA Analysis Reveals miR-204 Inhibits Cell Proliferation in Gastric Cancer by Targeting CKS1B, CXCL1 and GPRC5A. *Int J Mol Sci* (2017) 19(1):87. doi: 10.3390/ijms19010087
65. Rupaimoole R, Slack FJ. MicroRNA Therapeutics: Towards a New Era for the Management of Cancer and Other Diseases. *Nat Rev Drug Discovery* (2017) 16(3):203–22. doi: 10.1038/nrd.2016.246
66. Han TS, Hur K, Cho HS, Ban HS. Epigenetic Associations Between lncRNA/circRNA and miRNA in Hepatocellular Carcinoma. *Cancers (Basel)* (2020) 12(9):2622. doi: 10.3390/cancers12092622
67. Shin VY, Chu KM. MiRNA as Potential Biomarkers and Therapeutic Targets for Gastric Cancer. *World J Gastroenterol* (2014) 20(30):10432–9. doi: 10.3748/wjg.v20.i30.10432
68. Lin J, Shen J, Yue H, Cao Z. Mirna1835p.1 Promotes the Migration and Invasion of Gastric Cancer AGS Cells by Targeting TPM1. *Oncol Rep* (2019) 42(6):2371–81. doi: 10.3892/or.2019.7354
69. Zheng P, Chen L, Yuan X, Luo Q, Liu Y, Xie G, et al. Exosomal Transfer of Tumor-Associated Macrophage-Derived miR-21 Confers Cisplatin Resistance in Gastric Cancer Cells. *J Exp Clin Cancer Res* (2017) 36(1):53. doi: 10.1186/s13046-017-0528-y
70. Zhang Z, Dong Y, Hua J, Xue H, Hu J, Jiang T, et al. A five-miRNA Signature Predicts Survival in Gastric Cancer Using Bioinformatics Analysis. *Gene* (2019) 699:125–34. doi: 10.1016/j.gene.2019.02.058
71. Smirnov A, Fishman V, Yunusova A, Korablev A, Serova I, Skryabin BV, et al. DNA Barcoding Reveals That Injected Transgenes are Predominantly Processed by Homologous Recombination in Mouse Zygote. *Nucleic Acids Res* (2020) 48(2):719–35. doi: 10.1093/nar/gkz1085
72. Han TS, Hur K, Xu G, Choi B, Okugawa Y, Toiyama Y, et al. MicroRNA-29c Mediates Initiation of Gastric Carcinogenesis by Directly Targeting ITGB1. *Gut* (2015) 64(2):203–14. doi: 10.1136/gutjnl-2013-306640
73. Chan JJ, Tay Y. Noncoding RNA:RNA Regulatory Networks in Cancer. *Int J Mol Sci* (2018) 19(5):1310. doi: 10.3390/ijms19051310
74. Chi Y, Wang D, Wang J, Yu W, Yang J. Long Non-Coding RNA in the Pathogenesis of Cancers. *Cells* (2019) 8(9):1015. doi: 10.3390/cells8091015
75. Hu G, Niu F, Humburg BA, Liao K, Bendi S, Callen S, et al. Molecular Mechanisms of Long Noncoding RNAs and Their Role in Disease Pathogenesis. *Oncotarget* (2018) 9(26):18648–63. doi: 10.18632/oncotarget.24307
76. Wu Q, Ma J, Wei J, Meng W, Wang Y, Shi M. lncRNA SNHG11 Promotes Gastric Cancer Progression by Activating the Wnt/beta-Catenin Pathway and Oncogenic Autophagy. *Mol Ther* (2021) 29(3):1258–78. doi: 10.1016/j.ymthe.2020.10.011
77. Wei GH, Wang X. lncRNA MEG3 Inhibit Proliferation and Metastasis of Gastric Cancer *via* P53 Signaling Pathway. *Eur Rev Med Pharmacol Sci* (2017) 21(17):3850–6.
78. Zhu L, Zhu Y, Han S, Chen M, Song P, Dai D, et al. Impaired Autophagic Degradation of lncRNA ARHGAP5-AS1 Promotes Chemoresistance in Gastric Cancer. *Cell Death Dis* (2019) 10(6):383. doi: 10.1038/s41419-019-1585-2
79. Bhan A, Soleimani M, Mandal SS. Long Noncoding RNA and Cancer: A New Paradigm. *Cancer Res* (2017) 77(15):3965–81. doi: 10.1158/0008-5472.CAN-16-2634
80. Sheng Y, Han C, Yang Y, Wang J, Gu Y, Li W, et al. Correlation Between LncRNA-LINC00659 and Clinical Prognosis in Gastric Cancer and Study on its Biological Mechanism. *J Cell Mol Med* (2020) 24(24):14467–80. doi: 10.1111/jcmm.16069
81. Li X, Du Y, Wang Y. The Value of LncRNA SNHG5 as a Marker for the Diagnosis and Prognosis of Gastric Cancer. *Am J Transl Res* (2021) 13 (5):5420–7.
82. Verduci L, Strano S, Yarden Y, Blandino G. The circRNA-microRNA Code: Emerging Implications for Cancer Diagnosis and Treatment. *Mol Oncol* (2019) 13(4):669–80. doi: 10.1002/1878-0261.12468

83. Lei M, Zheng G, Ning Q, Zheng J, Dong D. Translation and Functional Roles of Circular RNAs in Human Cancer. *Mol Cancer* (2020) 19(1):30. doi: 10.1186/s12943-020-1135-7
84. Meng S, Zhou H, Feng Z, Xu Z, Tang Y, Li P, et al. CircRNA: Functions and Properties of a Novel Potential Biomarker for Cancer. *Mol Cancer* (2017) 16 (1):94. doi: 10.1186/s12943-017-0663-2
85. Yin Y, Long J, He Q, Li Y, Liao Y, He P, et al. Emerging Roles of circRNA in Formation and Progression of Cancer. *J Cancer* (2019) 10(21):5015–21. doi: 10.7150/jca.30828
86. Kristensen LS, Andersen MS, Stagsted LVW, Ebbesen KK, Hansen TB, Kjems J. The Biogenesis, Biology and Characterization of Circular RNAs. *Nat Rev Genet* (2019) 20(11):675–91. doi: 10.1038/s41576-019-0158-7
87. Zhang Y, Liu H, Li W, Yu J, Li J, Shen Z, et al. CircRNA_100269 is Downregulated in Gastric Cancer and Suppresses Tumor Cell Growth by Targeting miR-630. *Aging (Albany NY)* (2017) 9(6):1585–94. doi: 10.18632/aging.101254
88. Huang M, He YR, Liang LC, Huang Q, Zhu ZQ. Circular RNA Hsa_Circ_0000745 may Serve as a Diagnostic Marker for Gastric Cancer. *World J Gastroenterol* (2017) 23(34):6330–8. doi: 10.3748/wjg.v23.i34.6330
89. Zheng L, Chen Y, Ye L, Jiao W, Song H, Mei H, et al. miRNA-584-3p Inhibits Gastric Cancer Progression by Repressing Yin Yang 1- Facilitated MMP-14 Expression. *JSci Rep* (2017) 7(1):8967. doi: 10.1038/s41598-017-09271-5
90. Li J, Dong G, Wang B, Gao W, Yang Q. miR-543 Promotes Gastric Cancer Cell Proliferation by Targeting SIRT1. *Biochem Biophys Res Commun* (2016) 469(1):15–21. doi: 10.1016/j.bbrc.2015.11.062
91. Wei J, Wang Z, Wang Z, Yang Y, Fu C, Zhu J, et al. MicroRNA-31 Function as a Suppressor Was Regulated by Epigenetic Mechanisms in Gastric Cancer. *BioMed Res Int* (2017) 2017:5348490. doi: 10.1155/2017/5348490
92. Xu G, Li N, Zhang Y, Zhang J, Xu R, Wu Y. MicroRNA-383-5p Inhibits the Progression of Gastric Carcinoma *via* Targeting HDAC9 Expression. *Braz J Med Biol Res* (2019) 52(8):e8341. doi: 10.1590/1414-431X20198341
93. Cai L, Chen Q, Fang S, Lian M, Cai M. MicroRNA-329 Inhibits Cell Proliferation and Tumor Growth While Facilitates Apoptosis *via* Negative Regulation of KDM1A in Gastric Cancer. *J Cell Biochem* (2018) 119 (4):3338–51. doi: 10.1002/jcb.26497
94. Hong X, Xu Y, Qiu X, Zhu Y, Feng X, Ding Z, et al. MiR-448 Promotes Glycolytic Metabolism of Gastric Cancer by Downregulating KDM2B. *Oncotarget* (2016) 7(16):22092–102. doi: 10.18632/oncotarget.8020
95. Zhang X, Peng Y, Yuan Y, Gao Y, Hu F, Wang J, et al. Histone Methyltransferase SET8 is Regulated by miR-192/215 and Induces Oncogene-Induced Senescence *via* P53-Dependent DNA Damage in Human Gastric Carcinoma Cells. *Cell Death Dis* (2020) 11(10):937. doi: 10.1038/s41419-020-03130-4
96. Zhang J, Ren J, Hao S, Ma F, Xin Y, Jia W, et al. MiRNA-491-5p Inhibits Cell Proliferation, Invasion and Migration *via* Targeting JMJD2B and Serves as a Potential Biomarker in Gastric Cancer. *Am J Transl Res* (2018) 10(2):525–34.
97. Yoon JH, Choi YJ, Choi WS, Ashktorab H, Smoot DT, Nam SW, et al. GKN1-miR-185-DNMT1 Axis Suppresses Gastric Carcinogenesis Through Regulation of Epigenetic Alteration and Cell Cycle. *Clin Cancer Res* (2013) 19(17):4599–610. doi: 10.1158/1078-0432.CCR-12-3675
98. Zhao L, Guo H, Zhou B, Feng J, Li Y, Han T, et al. Long non-Coding RNA SNHG5 Suppresses Gastric Cancer Progression by Trapping MTA2 in the Cytosol. *Oncogene* (2016) 35(44):5770–80. doi: 10.1038/onc.2016.110
99. Zhang H, Li L, Yuan C, Wang C, Gao T, Zheng Z. MiR-489 Inhibited the Development of Gastric Cancer *via* Regulating HDAC7 and PI3K/AKT Pathway. *World J Surg Oncol* (2020) 18(1):73. doi: 10.1186/s12957-020-01846-3
100. Jiping Z, Ming F, Lixiang W, Xiuming L, Yuqun S, Han Y, et al. MicroRNA-212 Inhibits Proliferation of Gastric Cancer by Directly Repressing Retinoblastoma Binding Protein 2. *J Cell Biochem* (2013) 114(12):2666–72. doi: 10.1002/jcb.24613
101. Kong Y, Zou S, Yang F, Xu X, Bu W, Jia J, et al. RUNX3-Mediated Up-Regulation of miR-29b Suppresses the Proliferation and Migration of Gastric Cancer Cells by Targeting KDM2A. *Cancer Lett* (2016) 381(1):138–48. doi: 10.1016/j.canlet.2016.07.038
102. Deng QJ, Xie LQ, Li H. Overexpressed MALAT1 Promotes Invasion and Metastasis of Gastric Cancer Cells *via* Increasing EGFL7 Expression. *Life Sci* (2016) 157:38–44. doi: 10.1016/j.lfs.2016.05.041
103. Li Y, Wang K, Wei Y, Yao Q, Zhang Q, Qu H, et al. lncRNA-MIAT Regulates Cell Biological Behaviors in Gastric Cancer Through a Mechanism Involving the miR-29a-3p/HDAC4 Axis. *Oncol Rep* (2017) 38(6):3465–72. doi: 10.3892/or.2017.6020
104. Sun M, Nie F, Wang Y, Zhang Z, Hou J, He D, et al. LncRNA HOXA11-AS Promotes Proliferation and Invasion of Gastric Cancer by Scaffolding the Chromatin Modification Factors PRC2, LSD1, and DNMT1. *Cancer Res* (2016) 76(21):6299–310. doi: 10.1158/0008-5472.CAN-16-0356
105. Lian Y, Yan C, Lian Y, Yang R, Chen Q, Ma D, et al. Long Intergenic non-Protein-Coding RNA 01446 Facilitates the Proliferation and Metastasis of Gastric Cancer Cells Through Interacting With the Histone Lysine-Specific Demethylase LSD1. *Cell Death Dis* (2020) 11(7):522. doi: 10.1038/s41419-020-2729-0
106. Han H, Wang S, Meng J, Lyu G, Ding G, Hu Y, et al. Long Noncoding RNA PART1 Restrains Aggressive Gastric Cancer Through the Epigenetic Silencing of PDGFB *via* the PLZF-Mediated Recruitment of EZH2. *Oncogene* (2020) 39(42):6513–28. doi: 10.1038/s41388-020-01442-5
107. Nakamura F. FilGAP and its Close Relatives: A Mediator of Rho-Rac Antagonism That Regulates Cell Morphology and Migration. *Biochem J* (2013) 453(1):17–25. doi: 10.1042/BJ20130290
108. Shi X, You X, Zeng WC, Deng YJ, Hong HL, Huang OX, et al. Knockdown of LINC00461 Inhibits Cell Proliferation and Induces Apoptosis in Gastric Cancer by Targeting LSD1. *Eur Rev Med Pharmacol Sci* (2019) 23 (24):10769–75. doi: 10.26355/eurrev_201912_19779
109. Liu Z, Chen Z, Fan R, Jiang B, Chen X, Chen Q, et al. Over-Expressed Long Noncoding RNA HOXA11-AS Promotes Cell Cycle Progression and Metastasis in Gastric Cancer. *Mol Cancer* (2017) 16(1):82. doi: 10.1186/s12943-017-0651-6
110. Liu YW, Xia R, Lu K, Xie M, Yang F, Sun M, et al. LincRNAFEZF1-AS1 Represses P21 Expression to Promote Gastric Cancer Proliferation Through LSD1-Mediated H3K4me2 Demethylation. *Mol Cancer* (2017) 16(1):39. doi: 10.1186/s12943-017-0588-9
111. Ma Z, Gao X, Shuai Y, Wu X, Yan Y, Xing X, et al. EGR1-Mediated Linc01503 Promotes Cell Cycle Progression and Tumorigenesis in Gastric Cancer. *Cell Prolif* (2021) 54(1):e12922. doi: 10.1111/cpr.12922
112. Li ZT, Zhang X, Wang DW, Xu J, Kou KJ, Wang ZW, et al. Overexpressed lncRNA GATA6-AS1 Inhibits LNM and EMT *via* FZD4 Through the Wnt/beta-Catenin Signaling Pathway in GC. *Mol Ther Nucleic Acids* (2020) 19:827–40. doi: 10.1016/j.omtn.2019.09.034
113. Li H, Ma X, Yang D, Suo Z, Dai R, Liu C. PCAT-1 Contributes to Cisplatin Resistance in Gastric Cancer Through Epigenetically Silencing PTEN *via* Recruiting EZH2. *J Cell Biochem* (2020) 121(2):1353–61. doi: 10.1002/jcb.29370
114. Wang JB, Jin Y, Wu P, Liu Y, Zhao WJ, Chen JF, et al. Tumor Suppressor PLZF Regulated by lncRNA ANRIL Suppresses Proliferation and Epithelial Mesenchymal Transformation of Gastric Cancer Cells. *Oncol Rep* (2019) 41 (2):1007–18. doi: 10.3892/or.2018.6866
115. Roy R, Yang J, Moses MA. Matrix Metalloproteinases as Novel Biomarkers and Potential Therapeutic Targets in Human Cancer. *J Clin Oncol* (2009) 27 (31):5287–97. doi: 10.1200/JCO.2009.23.5556
116. Liu YW, Sun M, Xia R, Zhang EB, Liu XH, Zhang ZH, et al. LincHOTAIR Epigenetically Silences Mir34a by Binding to PRC2 to Promote the Epithelial-to-Mesenchymal Transition in Human Gastric Cancer. *Cell Death Dis* (2015) 6:e1802. doi: 10.1038/cddis.2015.150
117. Wu DC, Wang SSW, Liu CJ, Wuputra K, Kato K, Lee YL, et al. Reprogramming Antagonizes the Oncogenicity of HOXA13-Long Noncoding RNA HOTTIP Axis in Gastric Cancer Cells. *Stem Cells* (2017) 35(10):2115–28. doi: 10.1002/stem.2674
118. Wu Q, Xiang S, Ma J, Hui P, Wang T, Meng W, et al. Long non-Coding RNA CASC15 Regulates Gastric Cancer Cell Proliferation, Migration and Epithelial Mesenchymal Transition by Targeting CDKN1A and ZEB1. *Mol Oncol* (2018) 12(6):799–813. doi: 10.1002/1878-0261.12187
119. Huang M, Hou J, Wang Y, Xie M, Wei C, Nie F, et al. Long Noncoding RNA LINC00673 Is Activated by SP1 and Exerts Oncogenic Properties by Interacting With LSD1 and EZH2 in Gastric Cancer. *Mol Ther* (2017) 25 (4):1014–26. doi: 10.1016/j.ymthe.2017.01.017
120. Xu Y, Dong M, Wang J, Zhao W, Jiao M. LINC01436 Inhibited miR-585-3p Expression and Upregulated MAPK1 Expression to Promote Gastric Cancer Progression. *Dig Dis Sci* (2021) 66(6):1885–94. doi: 10.1007/s10620-020-06487-w

121. Xu TP, Wang WY, Ma P, Shuai Y, Zhao K, Wang YF, et al. Upregulation of the Long Noncoding RNA FOXD2-AS1 Promotes Carcinogenesis by Epigenetically Silencing EphB3 Through EZH2 and LSD1, and Predicts Poor Prognosis in Gastric Cancer. *Oncogene* (2018) 37(36):5020–36. doi: 10.1038/s41388-018-0308-y
122. Lu Y, Hou K, Li M, Wu X, Yuan S. Exosome-Delivered LncHEIH Promotes Gastric Cancer Progression by Upregulating EZH2 and Stimulating Methylation of the GSDME Promoter. *Front Cell Dev Biol* (2020) 8:571297. doi: 10.3389/fcell.2020.571297
123. Chen WM, Huang MD, Sun DP, Kong R, Xu TP, Xia R, et al. Long Intergenic non-Coding RNA 00152 Promotes Tumor Cell Cycle Progression by Binding to EZH2 and Repressing P15 and P21 in Gastric Cancer. *Oncotarget* (2016) 7 (9):9773–87. doi: 10.18632/oncotarget.6949
124. Sun TT, He J, Liang Q, Ren LL, Yan TT, Yu TC, et al. LncRNA GClnc1 Promotes Gastric Carcinogenesis and May Act as a Modular Scaffold of WDR5 and KAT2A Complexes to Specify the Histone Modification Pattern. *Cancer Discovery* (2016) 6(7):784–801. doi: 10.1158/2159-8290.CD-15-0921
125. Jie M, Wu Y, Gao M, Li X, Liu C, Ouyang Q, et al. CircMRPS35 Suppresses Gastric Cancer Progression *via* Recruiting KAT7 to Govern Histone Modification. *Mol Cancer* (2020) 19(1):56. doi: 10.1186/s12943-020-01160-2
126. Zhang G, Xu Y, Zou C, Tang Y, Lu J, Gong Z, et al. Long Noncoding RNA ARHGAP27P1 Inhibits Gastric Cancer Cell Proliferation and Cell Cycle Progression Through Epigenetically Regulating P15 and P16. *Aging (Albany NY)* (2019) 11(20):9090–110. doi: 10.18632/aging.102377
127. Chen RY, Ju Q, Feng LM, Yuan Q, Zhang L. The Carcinogenic Complex lncRNA FOXP4-AS1/EZH2/LSD1 Accelerates Proliferation, Migration and Invasion of Gastric Cancer. *Eur Rev Med Pharmacol Sci* (2019) 23(19):8371–6. doi: 10.26355/eurrev_201910_19148
128. Wang SS, Wuputra K, Liu CJ, Lin YC, Chen YT, Chai CY, et al. Oncogenic Function of the Homeobox A13-Long Noncoding RNA HOTTIP-Insulin Growth Factor-Binding Protein 3 Axis in Human Gastric Cancer. *Oncotarget* (2016) 7(24):36049–64. doi: 10.18632/oncotarget.9102
129. Tie F, Banerjee R, Stratton CA, Prasad-Sinha J, Stepanik V, Zlobin A, et al. CBP-Mediated Acetylation of Histone H3 Lysine 27 Antagonizes Drosophila Polycomb Silencing. *Development* (2009) 136(18):3131–41. doi: 10.1242/dev.037127
130. Song Y, Wang R, Li LW, Liu X, Wang YF, Wang QX, et al. Long non-Coding RNA HOTAIR Mediates the Switching of Histone H3 Lysine 27 Acetylation to Methylation to Promote Epithelial-to-Mesenchymal Transition in Gastric Cancer. *Int J Oncol* (2019) 54(1):77–86. doi: 10.3892/ijo.2018.4625
131. Ding H, Shi Y, Liu X, Qiu A. MicroRNA-4513 Promotes Gastric Cancer Cell Proliferation and Epithelial-Mesenchymal Transition Through Targeting KAT6B. *Hum Gene Ther Clin Dev* (2019) 30(3):142–8. doi: 10.1089/humc.2019.094
132. Zhu L, Wang C, Lin S, Zong L. CircKIAA0907 Retards Cell Growth, Cell Cycle, and Autophagy of Gastric Cancer *In Vitro* and Inhibits Tumorigenesis *In Vivo via* the miR-452-5p/KAT6B Axis. *Med Sci Monit* (2020) 26:e924160. doi: 10.12659/MSM.924160
133. Hu CE, Liu YC, Zhang HD, Huang GJ. JMJD2A Predicts Prognosis and Regulates Cell Growth in Human Gastric Cancer. *Biochem Biophys Res Commun* (2014) 449(1):1–7. doi: 10.1016/j.bbrc.2014.04.126
134. Zhang J, Zhou Y, Tang PMK, Cheng ASL, Yu J, To KF, et al. Mechanotransduction and Cytoskeleton Remodeling Shaping YAP1 in Gastric Tumorigenesis. *Int J Mol Sci* (2019) 20(7):1576. doi: 10.3390/ijms20071576
135. Chen LH, Wang LP, Ma XQ. Circ_SPECC1 Enhances the Inhibition of miR-526b on Downstream KDM4A/YAP1 Pathway to Regulate the Growth and Invasion of Gastric Cancer Cells. *Biochem Biophys Res Commun* (2019) 517 (2):253–9. doi: 10.1016/j.bbrc.2019.07.065
136. Zhang E, He X, Zhang C, Su J, Lu X, Si X, et al. A Novel Long Noncoding RNA HOXC-AS3 Mediates Tumorigenesis of Gastric Cancer by Binding to YBX1. *Genome Biol* (2018) 19(1):154. doi: 10.1186/s13059-018-1523-0
137. Zhang S, Chen P, Huang Z, Hu X, Chen M, Hu S, et al. Sirt7 Promotes Gastric Cancer Growth and Inhibits Apoptosis by Epigenetically Inhibiting miR-34a. *Sci Rep* (2015) 5:9787. doi: 10.1038/srep09787
138. Liu Y, Zhang X, Zhang Y, Hu Z, Yang D, Wang C, et al. Identification of Mirnomes in Human Stomach and Gastric Carcinoma Reveals miR-133b/a-3p as Therapeutic Target for Gastric Cancer. *Cancer Lett* (2015) 369(1):58–66. doi: 10.1016/j.canlet.2015.06.028
139. Guan A, Wang H, Li X, Xie H, Wang R, Zhu Y, et al. MiR-330-3p Inhibits Gastric Cancer Progression Through Targeting MSI1. *Am J Transl Res* (2016) 8(11):4802–11.
140. Zhao LJ, Fan QQ, Li YY, Ren HM, Zhang T, Liu S, et al. LSD1 Deletion Represses Gastric Cancer Migration by Upregulating a Novel miR-142-5p Target Protein CD9. *Pharmacol Res* (2020) 159:104991. doi: 10.1016/j.phrs.2020.104991
141. Kang W, Huang T, Zhou Y, Zhang J, Lung RWM, Tong JHM, et al. miR-375 is Involved in Hippo Pathway by Targeting YAP1/TEAD4-CTGF Axis in Gastric Carcinogenesis. *Cell Death Dis* (2018) 9(2):92. doi: 10.1038/s41419-017-0134-0
142. Xu G, Zhu H, Zhang M, Xu J. Histone Deacetylase 3 is Associated With Gastric Cancer Cell Growth *via* the miR-454-Mediated Targeting of CHD5. *Int J Mol Med* (2018) 41(1):155–63. doi: 10.3892/ijmm.2017.3225
143. Lin L, Jiang H, Huang M, Hou X, Sun X, Jiang X, et al. Depletion of Histone Deacetylase 1 Inhibits Metastatic Abilities of Gastric Cancer Cells by Regulating the miR-34a/CD44 Pathway. *Oncol Rep* (2015) 34(2):663–72. doi: 10.3892/or.2015.4010
144. Xu TP, Huang MD, Xia R, Liu XX, Sun M, Yin L, et al. Decreased Expression of the Long non-Coding RNA FENDRR is Associated With Poor Prognosis in Gastric Cancer and FENDRR Regulates Gastric Cancer Cell Metastasis by Affecting Fibronectin1 Expression. *J Hematol Oncol* (2014) 7:63. doi: 10.1186/s13045-014-0063-7
145. Wu S, Wu E, Wang D, Niu Y, Yue H, Zhang D, et al. LncRNA HRCEG, Regulated by HDAC1, Inhibits Cells Proliferation and Epithelial-Mesenchymal-Transition in Gastric Cancer. *Cancer Genet* (2020) 241:25–33. doi: 10.1016/j.cancergen.2019.12.007
146. Yin L, Liu T, Li C, Yan G, Li C, Zhang J, et al. The MRTF-A/miR-155/SOX1 Pathway Mediates Gastric Cancer Migration and Invasion. *Cancer Cell Int* (2020) 20:303. doi: 10.1186/s12935-020-01395-5

Conflict of Interest: The authors declare that the research was conducted in the absence of any commercial or financial relationships that could be construed as a potential conflict of interest.

Publisher's Note: All claims expressed in this article are solely those of the authors and do not necessarily represent those of their affiliated organizations, or those of the publisher, the editors and the reviewers. Any product that may be evaluated in this article, or claim that may be made by its manufacturer, is not guaranteed or endorsed by the publisher.

frontiers in Oncology

REVIEW
published: 02 February 2022
doi: 10.3389/fonc.2022.783079

Non-Coding RNAs in Colorectal Cancer: Their Functions and Mechanisms

Zimo Jia[1], *Jiaqi An*[1], *Ziyuan Liu*[2] *and Fan Zhang*[1,3]*

[1] Department of Biochemistry and Molecular Biology, Hebei Medical University, Shijiazhuang, China, [2] School of Medicine, Shihezi University, Shihezi, China, [3] The Key Laboratory of Neural and Vascular Biology, Ministry of Education, Shijiazhuang, China

Colorectal cancer (CRC) is a common malignancy with high mortality. However, the molecular mechanisms underlying CRC remain unclear. Controversies over the exact functions of non-coding RNAs (ncRNAs) in the progression of CRC have been prevailing for multiple years. Recently, accumulating evidence has demonstrated the regulatory roles of ncRNAs in various human cancers, including CRC. The intracellular signaling pathways by which ncRNAs act on tumor cells have been explored, and in CRC, various studies have identified numerous dysregulated ncRNAs that serve as oncogenes or tumor suppressors in the process of tumorigenesis through diverse mechanisms. In this review, we have summarized the functions and mechanisms of ncRNAs (mainly lncRNAs, miRNAs, and circRNAs) in the tumorigenesis of CRC. We also discuss the potential applications of ncRNAs as diagnostic and prognostic tools, as well as therapeutic targets in CRC. This review details strategies that trigger the recognition of CRC-related ncRNAs, as well as the methodologies and challenges of studying these molecules, and the forthcoming clinical applications of these findings.

Keywords: ncRNAs, colorectal cancer, function, mechanism, tumorigenesis

OPEN ACCESS

Edited by:
Kanjoormana Aryan Manu, Amala Cancer Research Centre, India

Reviewed by:
Xiangying Deng, Central South University, China
Christos K. Kontos, National and Kapodistrian University of Athens, Greece

***Correspondence:**
Fan Zhang
zhangfan86@hebmu.edu.cn

Specialty section:
This article was submitted to Gastrointestinal Cancers: Colorectal Cancer, a section of the journal Frontiers in Oncology

Received: *25 September 2021*
Accepted: *12 January 2022*
Published: *02 February 2022*

Citation:
Jia Z, An J, Liu Z and Zhang F (2022) Non-Coding RNAs in Colorectal Cancer: Their Functions and Mechanisms. Front. Oncol. 12:783079. doi: 10.3389/fonc.2022.783079

INTRODUCTION

Colorectal cancer (CRC), with a high incidence and mortality rate, is the third most prevalent malignant tumor and the second leading cause of cancer-related death worldwide (1). Globally, there are two main distinct pathways of precursor lesions: the conventional adenomatous carcinoma pathway (also known as the chromosomal instability sequence) leading to 70%-90% of CRC, and the serrated neoplasia pathway leading to 10%-20% of CRC (2). These pathways represent a diverse multiplicity of genetic and epigenetic events in a fairly consistent sequence (3). The chromosomal instability phenotype typically develops after a genomic event triggered by an APC mutation, followed by RAS activation or function loss of TP53. In contrast, the serrated neoplasia pathway is associated with RAS and RAF mutations and epigenetic instability characterized by a CpG island methylation phenotype, leading to microsatellite stable and unstable cancers (2). Due to the lack of distinctively incipient symptoms and the limitations of early detection, most CRC patients are diagnosed at advanced stages. Metastatic disease accounts for the vast majority of cancer-associated deaths. And the liver is the most frequent site of distant metastasis from CRC, with over 50% of CRC deaths being attributed to metastasis (4). Despite advances in the diagnosis and treatment of CRC,

such as some practical chemotherapeutic drugs and immunotherapy, the genetic background and underlying molecular mechanisms mediating this disease are still unclear (5). Although the increased risk of toxicity and cost, new therapeutic agents have exactly improved survival in advanced disease settings. However, the long-term prognosis for metastatic disease remains poor due to late diagnosis and treatment failure (6). To improve CRC therapy, novel potent drugs require identification, and therapeutic strategies need to be appraised and developed.

The result of the human genome project shows that protein-coding genes represent less than 2% of the total human genome, whereas, more than 90% of the human genome is composed of non-coding RNAs (ncRNAs), which are actively transcribed from the human genome but cannot encode proteins (7, 8). ncRNA families are habitually divided into two broad categories. One is housekeeping ncRNA, including highly abundant ribosomal RNAs (rRNAs) and transfer RNAs (tRNAs). The other is regulatory ncRNAs, including long ncRNAs (lncRNAs), microRNAs (miRNAs), circular RNAs (circRNAs), PIWI-interacting RNA, tRNA-derived small RNA (tRFs), small nucleolar RNA (snoRNAs), siRNAs, and so on (9). Among the most studied classes of ncRNAs are lncRNAs, miRNAs, and circRNAs.

As one of several types of ncRNAs, lncRNAs are larger transcripts with more than 200 nucleotides (nt) in length, and a considerable portion of lncRNAs species are transcribed by polymerase II. Similarly, most have 5'-end m^7G caps and 3'-end poly(A) tails, and they are presumed to be transcribed and synthesized in the same way as mRNAs, but cannot translate into protein (10). There are two types of functional elements in lncRNAs, one is the interactor element that directly interacts physical with other molecules, and proteins, and the other is the structural element, which leads to the formation of secondary and/or tertiary 3D RNA structures and regulates their functional interactions (11). It is the ability to interact with RNA and proteins through rigorous base pairing or chemical interactions in secondary structures that enables lncRNAs to function in various ways. Many lncRNAs have been identified to play a role in gene regulation, for instance, by affecting transcription factor targeting or epigenetic modification. In addition, interactions with mRNAs might cause the alteration of their transcriptional speed and stability. As such, the interaction between lncRNAs and proteins may affect protein activity, stability, or localization (12, 13).

miRNAs are highly conserved, small, 21–22 nts in length, single-stranded ncRNAs, regulating a wide range of biological processes, including cell proliferation, differentiation, and apoptosis (14). The biogenesis of miRNAs is a multistep process (**Figure 1**). First, the miRNA gene is generally transcribed by RNA polymerase II and III as primary miRNA (pri-miRNA), which is dissected into 70 nts long precursor miRNA (pre-miRNA) by nuclear ribonuclease Drosha, and then exported to the cytoplasm by exportin-5 (15). Finally, the pre-miRNA is cleaved by Dicer into the double-stranded miRNA, of which the passenger strand is degraded. The mature miRNA strand is integrated into Argonaute (AGO) protein in the RNA-induced silencing complex (RISC) to mediate translational repression by targeting mRNAs. Moreover, in addition to interacting with mRNAs, miRNAs can also target lncRNAs and circRNAs, and competing endogenous RNAs (ceRNAs) manipulate other RNA transcripts by competing for shared miRNAs (16, 17).

As a novel class of endogenous ncRNAs, circRNAs were initially considered as non-functional by-products of alternative splicing (18). Subsequent reports have elucidated that circRNAs can serve as miRNAs sponges, mediate alternative splicing, and regulate the expression of parental genes (19).

Most recently, since the widespread implementation of tiled microarray and high-throughput sequencing techniques across the entire genome and transcript, ncRNAs have gained extensive attention as a promising tool for curing cancer. Multiple studies have uncovered that ncRNAs are involved in multiple biological processes, for example, cell proliferation, apoptosis, differentiation, and transcription (8, 20). Subsequent investigations indicate that ncRNAs are indispensable for the modulation of a variety of cancers, for example, hepatocellular carcinoma, esophageal squamous cell carcinoma, gastric cancer, and so on (21). Moreover, studies focusing on the functions of ncRNAs in CRC have increased in recent years. Numerous ncRNAs have been demonstrated to be involved in CRC development and progression (**Figure 2**). For instance, an isolated report showed that lncRNA KCNQ1OT1 was significantly overexpressed in CRC tissue. By combining with miR-216b-5p, KCNQ1OT1 could elevate the expression of ZNF146, thereby leading to an acceleration of CRC proliferation, migration, and invasion (22). Additionally, evidence is accumulating that ncRNAs can provide the possibility for exploring molecular targeted therapy and novel drug development for healing CRC patients. And these ncRNAs are relevant to the diagnosis and prognosis of CRC; therefore, the expression of ncRNAs is regarded as a regulatory factor crucial for the progression of CRC. Because the investigation of ncRNAs and cancer hallmarks, as well as tumorigenesis in CRC, has grown impressively over the last decade, making it impossible to cover each published paper. In this review, we focus on the role of prominent ncRNAs, such as lncRNAs and miRNAs, and recently emerging circRNAs in CRC development, tumorigenesis, and metastasis, as well as their clinical significance, hoping to offer a novel approach to the treatment of CRC. Other ncRNAs such as piRNAs, snoRNAs, and siRNAs will be explored in a subsequent paper.

NCRNAS AND CRC

lncRNAs and CRC

Deregulation of lncRNA transcripts has been associated with CRC investigation to date and influences primary cancer hallmarks such as proliferation, apoptosis, metastasis, invasion, and angiogenesis (23). Additionally, lncRNAs have been

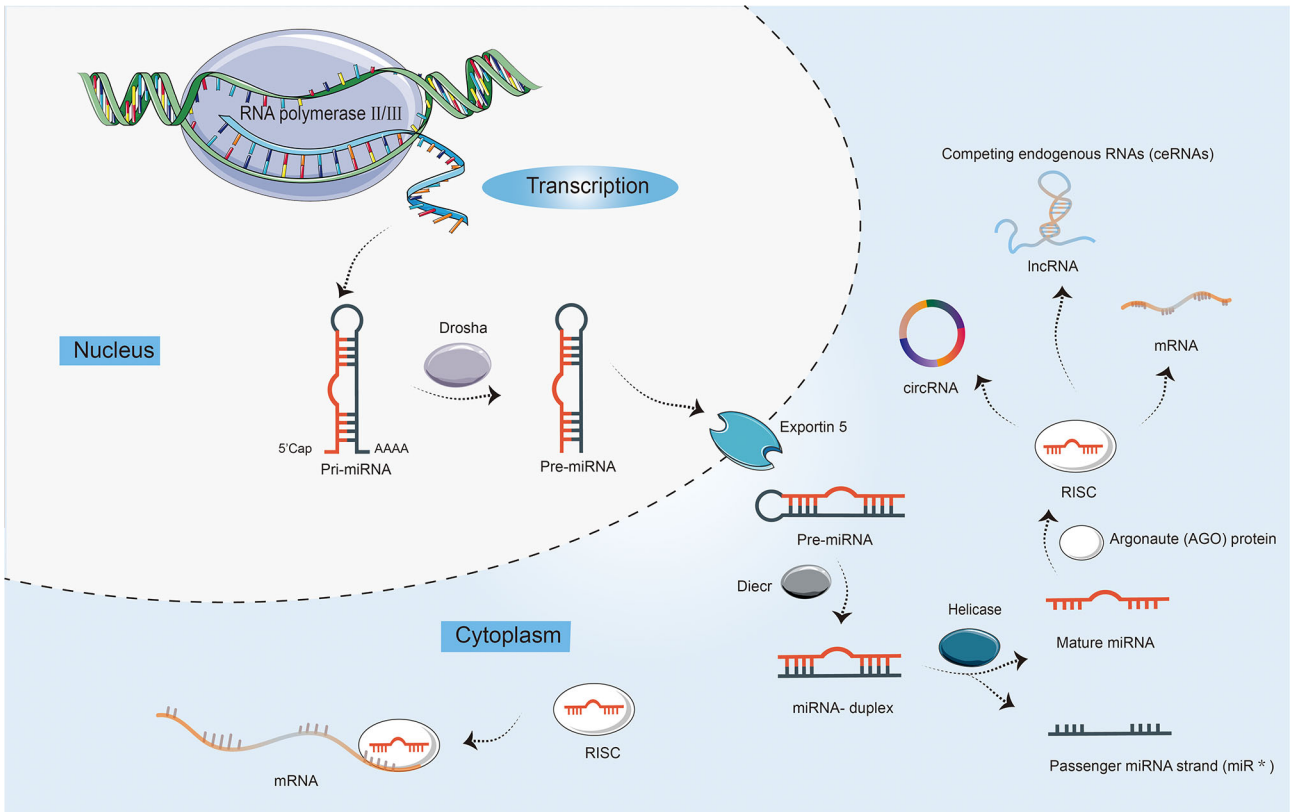

FIGURE 1 | The biogenesis and characteristics of microRNAs (miRNAs). First, the transcription of a primary miRNA transcript (pri-miRNA) by RNA polymerases II and III. Second, the production of pri-miRNA by the nuclear ribonuclease Drosha into a precursor miRNA (pre-miRNA) with a stem-loop structure. Third, nuclear export of pre-miRNAs by exportin 5. Fourth, the cleavage of pre-miRNAs by enzyme Dicer to yield double-stranded miRNA and its helicase-mediated unwinding. Finally, the passenger strand is degraded, while the mature miRNA strand is integrated into Argonaute (AGO) protein in the RNA-induced silencing complex (RISC). miRNAs not only can mediate translational repression by interacting with mRNAs, but also target long ncRNAs (lncRNAs) and circular RNAs (circRNAs). In addition, competing endogenous RNAs (ceRNAs) can regulate other RNA transcripts by competing for shared miRNAs.

associated with other biological processes such as metabolic disorders and drug resistance (**Table 1**).

The ability of carefully selected lncRNAs to target multiple pathways that are altered in CRC makes these molecules interesting candidates for therapeutics or targets of therapeutics. HOTAIR is a well-studied lncRNA that has been widely reported as an oncogenic molecule in CRC. Previous studies had disclosed that HOTAIR knockdown inhibited cell proliferation, invasion and migration, while promoting apoptosis and enhancing cell radiosensitivity in CRC (44). A recent study showed that knockdown of HOTAIR decreased cell viability, promoted apoptosis, and inhibited cellular autophagy in CRC through upregulation of miR-93 and downregulation of autophagy-associated 12 (ATG12) (45). Furthermore, deletion of HOTAIR enhanced radiosensitivity by regulating the miR-93/ATG12 axis in CRC cells and CRC xenograft tumor models. lncRNA HOTTIP expression levels of CRC patients are identified to be elevated and intimately relative to the clinical stage and distant metastasis. Knockdown HOTTIP markedly attenuates the proliferative and migratory capability of CRC cells (46). Interestingly, another study has found that SGK1 is dramatically downregulated compared with control when HOTTIP is knocked down in HCT116 and SW620 cells. Furthermore, the decreased SKG1 can promote the expression of GSK3β and inhibit the expression of FOXO3a, which is consistent with the result of knockdown HOTTIP (47). It is worth noting that whether knockdown HPTTIP is associated with SKG1 downregulation in CRC needs further experimental verification. To prioritize all RAMS in metastatic CRC (mCRC), Silva-Fisher et al. studied whether the expression of lncRNAs is related to patient outcome (48). Notably, they found that lncRNA RAMS11 is a top upregulated lncRNA and can promote CRC growth and metastasis. And its abnormal expression also predicted unfavorable outcomes in CRC patients, suggesting the great role of RAMS11 expression as a biomarker for identifying high-risk patients (48). Another study showed that downregulation of RAMS11 significantly represses proliferation, autophagy, metastasis, and invasion of HCT-116 and SW480 cells *in vitro*. More importantly, the crucial pathway investigation suggests that Dsi-RAMS11 potentially promotes apoptosis and autophagy *via* phosphorylation of AMPK and suppression of AKT and mTOR signaling pathways (49). As a

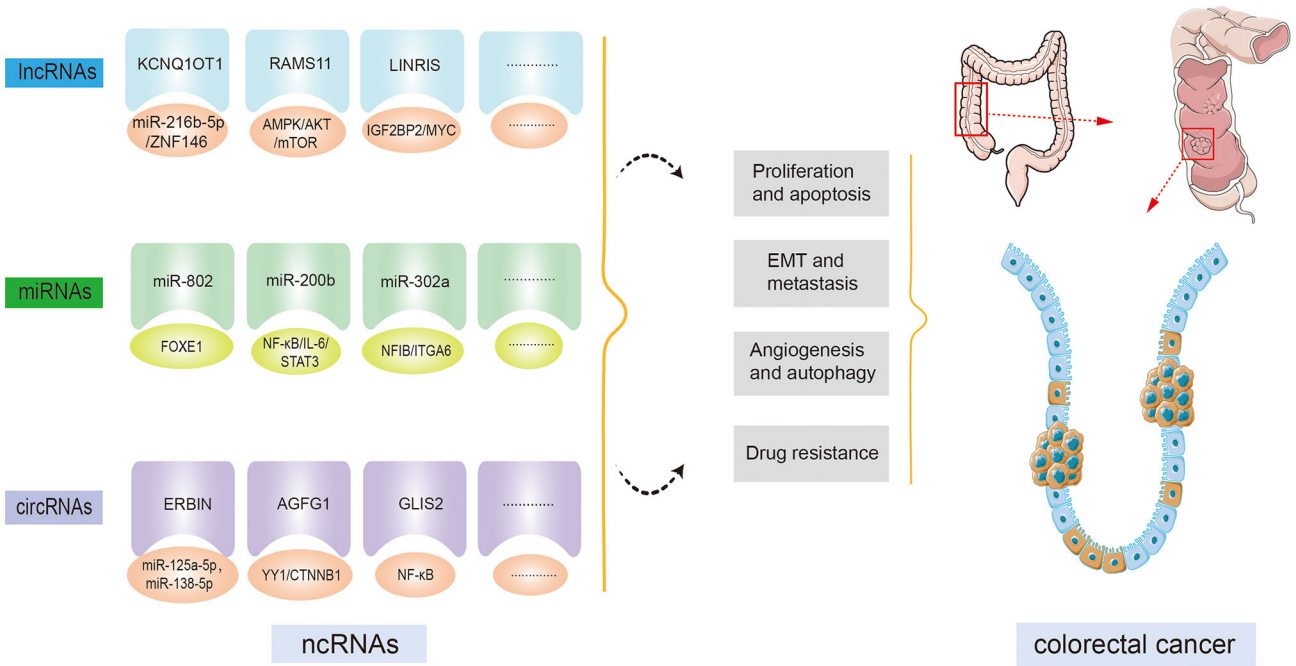

FIGURE 2 | Non-coding RNAs (ncRNAs) regulatory functions in colorectal cancer (CRC) initiation and progression. By targeting downstream molecules or signaling pathways, ncRNAs are involved in CRC cell proliferation, apoptosis, epithelial-mesenchymal transition (EMT), metastasis, angiogenesis, autophagy, drug resistance, and other CRC processes.

consequence, through autophagy, apoptosis and AKT/AMPKα/mTOR signaling pathways, RAMS11 downregulation is negatively associated with proliferation and metastasis of CRC cells. However, an important limitation of this study is the absence of *in vivo* demonstration, which may further confirm the conclusions. These results above support the view that cell death by lncRNA RAMS11 may occur *via* more than one regulatory mechanism and fundamental differences may exist between the AKT and mTOR pathways. Several additional lncRNAs have been implicated in CRC progression. Pharmacological screens reveal that RAMS11 enhances CRC resistance to topoisomerase inhibitors and provides mechanistic insight into the RAMS11-dependent TOP2 regulation that promotes mCRC promotion.

miRNAs and CRC

At the beginning of the 21th century, Michael et al. found the expression of miR-143 and miR-145 were downregulated in CRC, firstly associating miRNA with CRC development (50). To date, among all types of ncRNAs, miRNAs are the best understood, which have been well studied in the occurrence and progression of CRC (5, 51). Accordingly, these molecular changes stimulate proliferation, apoptosis, metastasis, angiogenesis, and drug resistance of CRC. Particularly, the distribution of miRNAs in tumors has characteristics related to CRC diagnosis, prognosis, and response to treatment. Hence, we have summarized the functions and mechanisms of key miRNAs (**Table 2**).

miR-124, a repressive miRNA downregulated in CRC tissues, mainly through upregulating and downregulating the expression of related target genes and thus modulating molecular signaling pathways, affecting the development and treatment of CRC. On one hand, aberrantly methylated miR-124 is capable of elevating the expression of DNMT3B to promote CRC proliferation, invasion and migration (69). 5-Aza-CdR can reverse the expression level of miR-124 in Hct-116 cells by inhibiting methylation, thus reducing the expression of DNMT3B and decreasing cell proliferation, migration and invasion. On the other hand, miR-124 can target a specific region in PD-L1 3' untranslated region (UTR) to reduce PD-L1 mRNA, protein, and cell surface expression, therefore inhibiting Tregs induction and CRC immunosuppression. As a result, the viability and proliferation of CRC cells are significantly diminished (70). Besides, miR-124 overexpression inhibits CRC proliferation and arrests the cell cycle at the G1 phase by downregulating c-Myc and induces apoptosis in CRC cells *via* upregulation of both intrinsic and extrinsic pathways. The underlying mechanism is that miR-124 downregulates Bcl-2 expression and increases the level of Bax pro-apoptotic gene, which subsequently may lead to the induction of apoptosis. miR-200 family, which modulates the expression of proteins involved in tumor metastasis and angiogenesis, is another causative collection of miRNAs downregulated in CRC. miR200 family is categorized into two groups: miR200a/b/429 and miR200c/141, which are located on chromosomes 1 and 12, respectively (71). Despite the different chromosomal locations and differences in expression patterns

TABLE 1 | Selected examples of regulatory lncRNAs.

lncRNAs	Expression	Potential biomarker	Therapeutic value	Function	Target/ signaling pathway	Ref
LINRIS	↑	Prognosis	NA	Promote aerobic glycolysis and autophagy while inhibiting proliferation	IGF2BP2/Myc	(24)
TCONS_00012883	↑	Prognosis, tumor size and TNM stage	NA	Promote proliferation and metastasis	DDX3/YY1/ MMP1	(25)
BLACAT1	↑	Prognosis, TNM stage and distant metastasis	OXA-resistance and therapeutic target	Promote proliferation, migration, and invasion while inhibiting apoptosis	miR-519d-3p/ CREB1	(26)
PiHL	↑	Prognosis	5-FU resistance and therapeutic target	Promote proliferation, and colorectal xenograft tumors	p53, GRWD1/ RPL11/MDM2	(27)
ITGB8-AS1	↑	Diagnosis	Therapeutic target	Promote cell proliferation and migration	Integrin-mediated focal adhesion	(28)
AC010789.1	↑	Prognosis and lymphatic metastasis	NA	Promote proliferation, migration, invasion, and EMT	miR-432-3p/ ZEB1, Wnt/β-Catenin	(29)
DNAJC3-AS1	↑	Prognosis and TNM stage	NA	Promote proliferation, migration and invasion, and lipid accumulation	EGFR/PI3K/AKT/ NF-Kb/SREBP1	(30)
HOTAIR	↑	Prognosis and diagnosis	5-FU resistance and therapeutic target	Promote viability, migration, invasion and EMT	SNAIL/ HNF4α, miR-218, NF-κB/ TS	(31, 32)
GAS5	↓	Diagnosis	NA	Inhibit migration and invasion while promoting apoptosis, autophagy, and AVO activities	miR-222-3p/ GAS5/PTEN	(33, 34)
KCNQ1OT1	↑	Diagnosis	Cisplatin resistance and therapeutic target	Promote cell motility and proliferation while inhibit apoptosis	miR-216b-5p/ ZNF14,miR-497/ Bcl-2	(22, 35)
FLANC	↑	Prognosis	Therapeutic target	Promote proliferation, migration, and angiogenesis while inhibiting apoptosis	STAT3/ VEGFA	(36)
NEAT1	↑	Prognosis	NA	Promote proliferation, migration, metastasis and invasion	DDX5/Wnt/β-catenin	(37)
TPT1-AS1	↑	Prognosis TNM stage, tumor size, lymphatic metastasis, and distant metastasis	NA	Promote invasion, metastasis and angiogenesis	NF90/VEGFA	(38)
H19	↑	Prognosis	5-FU resistance and therapeutic target	Promote autophagy	SIRT1	(39)
MCF2L-AS1	↑	Prognosis	NA	Promote proliferation, invasion, and glycolysis	miR-874-3p/ FOXM1	(40, 41)
RAD51-AS1	↓	Prognosis	NA	Inhibit proliferation, migration, invasion, and glycolysis	miR-29b/c-3p/ NDRG2	(42)
ZNF667-AS1	↓	Prognosis	NA	Inhibit proliferation, migration, and invasion	ANK2/JAK2	(43)

↑, up-regulate; ↓, down-regulate; EMT, epithelial-mesenchymal transition; TNM, tumor node metastasis; 5-FU, 5-fluorouracil; OXA, oxaliplatin; NA, not available.

between the two parts, there is a significant overlap in their targets and biological functions, mainly involving components that play a role in epithelial-mesenchymal transition (EMT). And the EMT program in cancer cells is associated with an increase in cancer metastasis. Additionally, miR-200 directly inhibits the transcriptional inhibitor zinc finger E-box-binding homeobox 1, a known transcriptional suppressor of the cytoskeletal rearrangement protein E-cadherin, thus inducing EMT during CRC metastasis. Deng et al. reported that the direct target of miR-200b was the 3'-UTR of AKT2 and miR-200b induces inflammation through the AKT2-mediated NF-κB/IL-6/ STAT3 signaling pathway. miR-200b regulated the expression of E-cadherin and N-cadherin that engaged in EMT (72).

EGFR (also known as Her1) is a human epidermal growth factor receptor belonging to a family of HER-related proteins that can be selectively activated by some different ligands (73). Once the ligand binds to EGFR, the receptor forms a dimer that initiates autophosphorylation of the receptor *via* tyrosine kinase activity within the receptor. Autophosphorylation triggers a series of signaling events, mainly through the RAS/RAF/MEK/ MAPK and PI3K/AKT pathways (74). These pathways are responsible for cancer cell proliferation, activation of invasion and metastasis, blockade of apoptosis, and promotion of angiogenesis. Dysregulation of the EGFR pathway has been validated as a relevant procedure in CRC, and it has been identified as a target of several miRNAs. RASA1 is a member of RAS GTPase activating proteins (RAS-GAP) family (75). While the oncoprotein RAS can be inactivated by binding to the RAS-GAP members. miR-21 directly modulates RASA1 expression by targeting its 3'-UTR, and mutation or loss of function of RASA1 in CRC leads to activation of the RAS-MAPK cascade, promoting CRC progression (76). Furthermore, there is a link between EGFR and Wnt signaling. In APC-mutant CRC cells, elevated EGFR signaling boosts Wnt activity, which supports the notion that Wnt signaling is further regulated in the presence of impaired β-catenin degradation complexes. In a

TABLE 2 | Selected examples of regulatory miRNAs.

miRNAs	Expression	Potential biomarker	Therapeutic value	Function	Target/signaling pathway	Ref
miR-30b-5p	↓	Liver metastasis	NA	Inhibit invasion and migration, EMT, adhesion, and motility	Rap1b	(52)
miR-133b	↓	NA	OXA and 5-FU resistance	Inhibit migration, invasion, stemness, and drug resistance	DOT1L/H3K79me2, LUCAT1/EZH2	(53, 54)
miR-450a-5p	↑	Prognosis	NA	Promote stemness and angiogenesis	SOX2	(55)
miR-25-3p	↑	Diagnosis	NA	Promote metastasis and angiogenesis	KLF2, KLF4	(56)
miR –34a	↓	Lymphatic metastasis	OXA resistance and therapeutic target	Inhibit autophagy while promoting apoptosis	SIRT1, TGF-β/Smad4	(57)
miR-106b-3p	↑	Prognosis	NA	Promoted migration, invasion, and EMT	DLC-1	(58)
miR-302a	↓	Prognosis	NA	Inhibit migration, and invasion	NFIB/ITGA6	(59)
miR-138-5p	↓	Lymphatic metastasis	Fluorouracil, doxorubicin, and cisplatin resistance	Inhibit migration and chemotherapy resistance	NFIB-Snail1	(60)
miR-146a	↓	Prognosis and liver metastasis	Cetuximab resistance and therapeutic target	Inhibit proliferation and metastasis	c-met, Snail/β-catenin	(61, 62)
miR-195b-5p	↓	Prognosis	5-FU resistance	Inhibit proliferation, migration, invasion, EMT, stemness, and M2-like TAM polarization	NOTCH2/GATA3/IL-4	(63, 64)
miR-196b-5p	↑	NA	NA	Promote proliferation, cell cycle, migration and invasion while inhibiting apoptosis	ING5	(65)
miR-214-3p	↓	Lymphatic metastasis and tumor size	NA	Inhibit proliferation and metastasis	PLAGL2/MYH9	(66)
miR-1224-5p	↓	Prognosis	NA	Inhibit metastasis, invasion and EMT	SP1-Mediated NF-κB	(67)
miR-875-3p	↓	Prognosis and distant metastasis	NA	Inhibit proliferation and migration	PLK1	(68)

↑, up-regulate; ↓, down-regulate; EMT, epithelial-mesenchymal transition; OXA, oxaliplatin; 5-FU, 5-fluorouracil; NA, not available.

reciprocal manner, Wnt ligands lead to EGFR transcription through metalloproteinase-dependent binding of the cell surface EGFR ligand epitope domain to its GPCR Frizzled receptor (77). For example, miR-139-5p is a novel regulator of crosstalk between the EGFR and Wnt signaling pathways in CRC. miR-139-5p, a KRAS-responsive miRNA, is significantly downregulated in KRAS-mutated CRC tissues and cells, and its transcription is repressed by Wnt/β-catenin signaling in mutant CRC cells (78). miR-139-5p inhibits CRC cell proliferation and metastasis by targeting multiple regulators of the RAS and Wnt signaling pathways and EMT.

Nowadays, numerous lines of reports show that miRNAs serve as oncogenes or tumor suppressors in CRC evolvement (79). The critical roles of miRNAs in the pathogenesis of CRC confirm their suitability for therapeutic development.

circRNAs and CRC

Currently, there are numerous lines of studies focusing on the mechanisms of lncRNAs and miRNAs. Compared to them, the investigation of circRNAs in the progression of human disease is still in its infancy (80, 81). Although the role of circRNAs is less well characterized in other human disorders, most studies have focused on the role of circRNAs in cancers.

ciRS-7, as a type of endogenous circRNA with a closed circular structure, was first identified by Hansen in 2011 (82). ciRS-7 plays a vital role in the transcription of RNA, the expression of downstream genes, and the synthesis of protein. Furthermore, ciRS-7 functions as an oncogene and stimulates tumor progression by competitively repressing miR-7 in various types of cancers, including CRC (82). Another study found that miR-7-mediated inhibition of the EGFR/RAF1/MAPK pathway could be alleviated by overexpression of ciRS-7 in CRC (83). Despite the mutational status of KRAS or BRAF oncogenes, miR-7 could effectively inhibit this pathway in CRC cell lines. This is due to the fact that miR-7 was able to suppress the expression of not only EGFR but also another key MAPK member, RAF1 (84). Interestingly, ciRS-7 resulted in sustained activation of the EGFR/RAF1/MAPK pathway in CRC cells regardless of treatment with low or high concentrations of miR-7 precursors. Thus, dual targeting of ciRS-7 and miR-7 could provide CRC patients with a novel therapeutic strategy to inhibit this oncogenic pathway. In addition, high ciRS-7 expression was linked to a number of clinic-pathological factors, including advanced T-stage, lymphatic and distant metastases, and consequently, patients with higher expression of ciRS-7 had a poor prognosis (83).

Most recently, an increasing number of circRNAs have been observed to be aberrantly expressed in CRC (85). More specifically, their functions in tumorigenesis and metastasis have been reported, where individual circRNAs are considered to be carcinogens or tumor suppressors. For example, Chen et al. discovered that treating RKO and HCT116 cells with cobalt chloride (Cocl2, a hypoxia mimic) or TGF-β increased circERBIN expression, implying that ERBIN may be involved

in cancer progression (86). They also found that ERBIN was highly expressed in CRC cells, and the overexpression of ERBIN facilitated metastasis of CRC cells *in vitro* and *in vivo*. ERBIN exerts its oncogenic effects through regulating multiple cellular pathways, including those involved in CRC angiogenesis, proliferation, invasion, and migration. Mechanistically, ERBIN is known to directly sponge miR-125a-5p and miR-138-5p, accelerate the cap-independent protein translation of HIF-1α, and target eukaryotic translation initiation factor 4E binding protein (86).

Moreover, some studies have unveiled the great potential of circRNAs as promising prognostic markers or biomarkers in patients with CRC (87). Unlike linear RNA molecules, circRNAs possess a covalent closed-loop structure with high stability, preventing degradation induced by the exonuclease RNaseR. Furthermore, circRNAs with cell-specific or stage-specific expression patterns can be found in tissue samples, saliva, or plasma (18). These features could partially explain the possible application of circRNAs as prospective biomarkers. circ002144 expression is dramatically increased in CRC and is positively correlated with cell proliferation, migration, and invasion. The abnormal expression of circ002144 is also closely relevant to poor prognosis, which implies that circ002144 may become a promising biomarker in the prognostic evaluation of CRC (88). It is worth noting that a high level of serum circ0004771 can distinguish CRC patients from healthy individuals (89). The serum circ0004771 may become a prospective non-invasive biomarker for CRC patients. Recent progress in the circRNAs research field has unveiled central aspects of circRNA biogenesis and biology, but more needs to be known about the regulation and functions of these molecules in human disease, especially tumors. Here, we have briefly epitomized the action of important circRNAs in the progression of CRC (**Table 3**). These studies have illustrated the large diversity of strategies by which ncRNAs could modulate oncogenes or tumor suppressors to influence CRC progression.

THE FUNCTIONS AND MECHANISMS OF NCRNAS IN CRC

ncRNAs Modulate CRC Proliferation and Apoptosis

Arguably, the most fundamental feature of malignant cells involves their ability to sustain chronic proliferation (111). The proliferation process of normal cells is induced by cell cycle alternation and receptor tyrosine kinases (PTKs) activation. Interestingly, the procedure can be restricted by themselves, whereas both cell cycle checkpoints ignorance and constituent activation of RTKs failure will lead to tumorigenesis (112). At the same time, proliferation must be tolerated by tumor cells, or tumor growth will be hindered and the cells will enter senescence. Apoptosis, as a programmed cell death that occurs during the advancement or aging process of normal cells, is a kind of homeostatic mechanism to maintain the stabilization of the cell population. There are several main apoptotic pathways: the endogenous or mitochondrial pathway and the exogenous or death receptor pathway, as well as the perforin/enzyme pathway. Several of the aforementioned pathways converge at the same execution pathways or terminals, which are initiated by caspase-3 cleavage (113). Apoptosis is activated in case of extrinsic or intrinsic stressors, exerting an antitumorigenic role. In conclusion, apoptosis is a promising target for the treatment of tumors.

Recent studies indicated that several typical ncRNAs play indispensable roles in CRC proliferation and apoptosis (**Figures 3A, B**) (94, 97). It has been identified that lncRNA SLCO4A1-AS1 is highly expressed in CRC cells, and there is a strong link between higher SLCO4A1-AS1 abundance and proliferation and apoptosis, as observed in CRC. By affecting activation of Wnt/β-catenin signaling, SLCO4A1-AS1 can mediate many cellular processes, such as cell proliferation, migration, differentiation, and apoptosis (114, 115). Consequently, elevated SLCO4A1-AS1 induces the hyper-activation of the Wnt/β-catenin signaling, thus leading to sustained proliferative ability and attenuated apoptotic behavior of CRC cells (116). Further analysis shows that SLCO4A1-AS1 knockdown severely reduced protein levels of β-catenin but not mRNA levels by the mechanism that SLCO4A1-AS1 represses phosphorylation of β-catenin, which in turn inhibits ubiquitination-mediated degradation. The more significant findings to emerge from this study is that SLCO4A1-AS1 modulated β-catenin stability by weakening the link between β-catenin and GSK3β, thereby influencing tumor progression (116). Another way that SLCO4A1-AS1 may modulate tumorigenesis is by sponging miR-508-3p, thus upregulating PARD3 and promoting CRC cell proliferation (117). Ectopic expression of circSPARC is detected in both CRC patients' tissues and plasma. It has been unveiled that SPARC could manipulate STAT3 expression to stimulate CRC proliferation by elevating the level of c-Myc. The process mainly involves two different pathways. On the one hand, SPARC functions as a miR-485-3p decoy to enhance JAK2 activation. On the other hand, it can interact with FUS to stimulate the nuclear translocation of activated p-STAT3 (118). Another study uncovered that miR-485-3p is detected to be extensively downregulated in CRC tissues. The dysregulation of miR-485-3p is positively correlated with P21 expression and negatively correlated with TPX2 expression (119). Since the underlying mechanism has not been discussed yet, more work is needed to definitively identify the specific regulation of miR-485-3p.

It is widely believed that genetic mutations promote the uncontrolled growth and proliferation of tumor cells. However, the situation may be more complex than that. A recent study showed that there are more than 100 mutated tumor suppressor genes that do not act directly on cancer cells (120). The mechanism that drives cancer cell growth is to prevent the immune system from recognizing and destroying tumor tissue, which is the real cause of the uncontrolled spread of cancer cells. Interestingly, these mutated genes are instructing the cancer cells how to evade the immune system, rather than simply saying "grow, grow". This may broaden our understanding of the

TABLE 3 | Selected examples of regulatory circRNAs.

circRNAs	Expression	Potential biomarker	Therapeutic value	Function	Target/ signaling pathway	Ref
0001946	↑	Prognosis	NA	Inhibit growth, migration, and invasion while promoting EMT	miR-135a-5p/ EMT	(90)
ciRS-122	↑	NA	OXA resistant and therapeutic target	Promote glycolysis and ATP production	miR-122/PKM2	(91)
100290	↑	Prognosis	NA	Promote proliferation, migration and invasion while inhibit apoptosis	miR-516b/FZD4/ Wnt/β -catenin	(92)
AGFG1	↑	Liver metastasis	NA	Promote proliferation, migration, invasion and stemness while inhibiting apoptosis	YY1/CTNNB1	(93)
103809	↓	Lymphatic metastasis and clinical stage	NA	Promote proliferation and migration	miR-532-3P/ FOXO4	(94)
102209	↑	Histological grade and liver metastasis	NA	Promote proliferation, migration, invasion and EMT while inhibiting cell cycle arrest and apoptosis	miR-761/RIN1	(95)
102958	↑	Prognosis and clinical stage, lymphatic metastasis	NA	Promote proliferation, migration and invasion	miR-585/ CDC25B	(96)
001680		NA	Irinotecan resistance and therapeutic target	Promote proliferation, migration, and stemness	miR-340 /BMI1	(97)
0060745	↑	Lymphatic and liver metastasis, and advanced clinical stage	NA	Promote proliferation and metastasis	miR-4736/CSE1L	(98)
002144	↑	Prognosis, tumor size, lymphatic and distant metastasis, and TNM stage	NA	Promote viability, proliferation, migration, and invasion while inhibiting apoptosis	miR-615-5p/ LARP1/mTOR	(88)
0000392	↑	Diagnosis, pathological stage, lymphatic and distant metastasis	NA	Promote proliferation and motility while inhibiting apoptosis	miR-193a-5p/ PIK3R3/AKT	(99)
ITGA7	↓	Lymphatic metastasis, tumor size, and TNM stage	NA	Inhibit proliferation and metastasis	RAS	(100
CCDC66	↑	Hypoxia	NA	Promote viability, migration, and invasion while inhibiting apoptosis	miR–3140/ autophagy	(101)
circ-133	↑	Hypoxia and TNM stage	NA	Promote metastasis	GEF-H1/RhoA	(102)
circ5615	↑	Prognosis and TNM stage	NA	Promote proliferation and cell cycle	TNKS, Wnt/β-catenin	(103)
FBXW7	↓	Tumor size	NA	Inhibit proliferation, migration and invasion	NEK2, mTOR, and PTEN	(104)
PACRGL	↑	Prognosis	NA	Promote proliferation, migration, invasion, and N1-N2 neutrophils differentiation	miR-142-3p, miR-506-3p/ TGF-β1	(105)
FNDC3B	↓	Prognosis	NA	Inhibit proliferation, invasion, migration, EMT and angiogenesis	miR-97-5p/ TIMP3	(106)
001971	↑	Tumor size, TNM stage, and lymphatic metastasis	NA	Promote proliferation, invasion, and angiogenesis	miR-29c-3p/ VEGFA	(107)
ZNF609	↓	Diagnosis and tumor size	NA	Promote apoptosis	p53	(108)
0026344	↓	Prognosis, diagnosis, and lymphatic metastasis	NA	Inhibit proliferation and invasion while promoting apoptosis	miR-21, miR-31	(109)
RAE1	↑	Lymphatic metastasis, and tumor size	NA	Promote migration and invasion	miR-338-3p/ TYRO3	(110)

↑, *up-regulate;* ↓, *down-regulate; EMT, epithelial-mesenchymal transition; TNM, tumor node metastasis; OXA, oxaliplatin; NA, not available.*

changing traditional concept of proliferation and provide new insights for future research.

ncRNAs Regulate CRC Metastasis

The metastatic establishment of CRC at distant organs is largely incurable and primarily contributes to the deaths of CRC patients. EMT represents the first step of metastasis and is intimately linked with the acquisition of a migratory phenotype in CRC cells (121). EMT is characterized by the loss of epithelial polarity and breakdown of tissue architecture, including the cell adhesion, the acquisition of N-cadherin and E-cadherin expression, thereby leading to the destabilized adherens junctions and increased cell mobility (122). Invasion-metastasis involves EMT and its reverse counterpart, the mesenchymal-epithelial transition, both of which are normally activated during embryonic development and tissue homeostasis, contributing to proper morphogenesis of tissues and organs (123).

Molecular underpinnings for dissemination of mCRC have been uncovered by accumulating novel paradigms in the study of mCRC (124). For instance, recent studies have illustrated the novel function of lncRNA MALAT1 in accelerating CRC metastasis through two intercellular signal transductions (125). One is MALAT1 restricting the influence of miR-15 on the

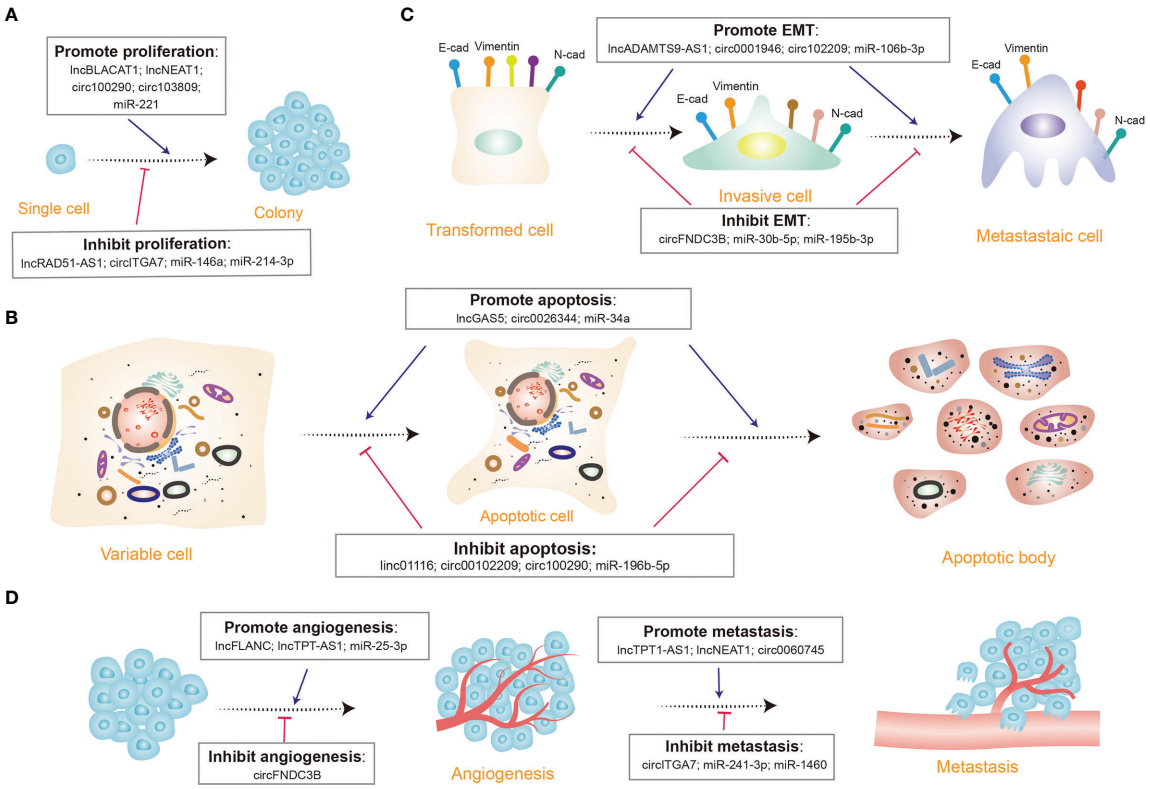

FIGURE 3 | Diverse functions of non-coding RNAs (ncRNAs) in colorectal cancer. **(A)** A few ncRNAs regulate cell proliferation by promoting (e.g., lncBLACT1) or inhibiting cell proliferation progression (e.g., circITGA7). **(B)** Many ncRNAs modulate cell apoptosis *via* triggering (e.g., lncGAS5) or curbing (e.g., miR-196b-5p) cell apoptosis. **(C)** Several ncRNAs control the epithelial-mesenchymal transition (EMT) process through inducing (e.g., circ102209) or repressing (e.g., miR-30b-5p) EMT; E-cad, E-cadherin; N-cad, N-cadherin. **(D)** Certain ncRNAs manipulate tumor angiogenesis and metastasis procedure, some appear to facilitate tumor angiogenesis (e.g., lncFLANC), while others restrain (e.g., circFNDC3B) the process; some promote metastasis (e.g., lncTPT1-AS1), while others inhibit (e.g., miR-1460) the process.

transcriptional levels of LRP6 by sponging miR-15 family members, which expedites β-catenin signaling, while the other is MALAT1 binding SFPQ and interacting with the IRES domain in the 5'-UTR of the corresponding RUNX2 mRNA. As a result of both functional mechanisms, the downstream target gene RUNX2 is elevated at the transcriptional level, which is eventually linked to CRC metastasis (125). The results of another study have revealed that circAGFG1 is upregulated with a significant increase in CRC metastasis (93). circAGFG1 directly binds to miR-4262 and miR-185-5p to enhance YY1 expression and CTNNB1 transcription, contributing to an acceleration of CRC metastasis (93). Consistently, the expression of lncRNA H19 is higher in mesenchymal subtypes of CRC cells than in epithelial subtypes. In CRC, H19 is found to be specifically overexpressed clones capable of seeding metastases, while short hairpin RNA (shRNA)-mediated knockdown of H19 in metastasis-capable clones abrogates the development of distant metastases (126). Based on this study, H19 acts as a ceRNA against miR-200b and miR-200c, resulting in derepression of ZEB1 and GIT2 in primary tumors and distant metastases. Nonetheless, GIT2 is shown to facilitate colonization at metastatic sites (127). An important strength of this study is relying on endogenous AGO pulldown, which provides biochemical support rather than nucleic acid sequence analysis or indirect measures of ceRNA activity, as well as targeted mutagenesis to verify the feature of H19 as ceRNA, despite the controversy regarding ceRNAs in general. Furthermore, miRNAs also exert an important role during CRC metastasis. Compared to normal tissues, the expression of miR-302a is substantially decreased in CRC tissues, especially in patient-derived xenografts and CTX-resistant cells. miR-302a overexpression inhibits metastasis in CRC cells and restores CTX responsiveness (59). miR-302a has also been observed to repress metastasis-promoting effect of NFIB that physiologically stimulates ITGA6 transcription. By decreasing CD44-induced cancer stem cell-like properties, EGFR-mediated MAPK, and AKT activation, miR-302a restores CTX responsiveness. Many ncRNAs have been demonstrated to be involved in EMT and metastasis of CRC (**Figures 3C, D**). Emerging evidence has depicted the specific functions and mechanisms of ncRNAs in CRC cells during their metastatic journey, which may be exploited to possibly halt metastatic growth and even prevent successful dissemination. Additionally, it would be interesting to see how these ncRNAs function during other steps in the

invasion-metastasis cascade. Future work will be designed to substantiate the mechanisms of these ncRNAs in contributing to EMT and metastasis and to find potential novel therapeutic approaches for the diagnosis and treatment of CRC.

ncRNAs Manipulate CRC Angiogenesis

Despite their physiological and morphological homogeneity, tumors display a wide range of morphological and phenotypic differences, including the expression of receptors on the surface of cells and their angiogenic capabilities (128). Angiogenesis is identified as an important hallmark of malignant tumors because quantities of blood vessels are needed to feed cancer cells (129). A number of ncRNAs have recently been demonstrated to be auxiliary diagnostic biomarkers for a range of cancers, and their expression varies among them. Likewise, the most recent research indicated that ncRNAs were heterogeneous in their regulation of tumor angiogenesis.

There are some frequently dysregulated ncRNAs involved in angiogenesis (**Figure 3D**). In clinical samples, miR-450a-5p is negatively correlated with SOX2 (55). An isolated study has discovered that miR-450a-5p induces angiogenesis *via* directly targeting the 3'-UTR regions of SOX2 in CRC (130). In addition, many miRNAs are packaged within tumor cell-derived exosomes, emerging as vital contributors to the complicated modulation and balance of pro-and anti-angiogenic molecules. Exosomal miR-25-3p-derived from CRC cells has been shown to be associated with angiogenesis (56). Exosomal miR-25-3p disrupts endothelial barrier integrity, increases vascular permeability, and simultaneously triggers angiogenesis. circ001971 expression is dramatically elevated in CRC tissues. Knockdown of circ001971 in CRC cells significantly interrupts HUVEC tube formation, consequently reducing the angiogenesis and tumor growth of SW620 cell-derived cancer *in vitro* (107).

VEGFA, a member of the growth factor family, has a strong capacity to activate the angiogenic milieu by increasing microvascular density and vascular permeability, which promotes tumor angiogenesis and metastasis and leads to tumors resistant to antiangiogenic therapy. The Krüppel-like factor (KLF) factor family is composed of zinc finger-containing transcription factors that regulate a variety of biological processes (131). miR-25-3p is recently been demonstrated to induce vascular permeability and angiogenesis in vascular endothelial cells by downregulating KLF2 and KLF4. Additionally, both KLF2 and KLF4 are downregulated in CRC (56). Specifically, KLF2 negatively regulates angiogenesis by inhibiting VEGFR221, whereas KLF4 maintains the integrity of endothelial barrier function by promoting tight junction-related proteins including ZO-1 and ocludin5 (132). Furthermore, cir001971 acts as a ceRNA to relieve miR-29c-3p-induced VEGFA inhibition, which contributes to the aggravation of angiogenesis in CRC (107). An additional study indicated that lncRNA FLANC was involved in CRC angiogenesis *via* the STAT3/VEGFA pathway (36). Western-blot data confirmed that the overexpression of FLANC leads to a higher level of the phosphorylated STAT3, which acts as the active form triggering VEGFA (36). In conclusion, these findings lead to the determination that different ncRNAs exert multifaceted and even contradictory roles in regulating CRC angiogenesis through several distinct mechanisms, thereafter proving the heterogeneity of ncRNAs. Hence, we speculate that future research will focus on angiogenesis inhibitors and, how ncRNAs serve their roles in effective targeted therapies to repress angiogenesis will be studies focus.

ncRNAs Regulate CRC Autophagy

Autophagy is a cellular catabolic and evolutionarily conserved process, which removes redundant or dysfunctional components by dissociating the defective or malfunctioning organelles inside the cells (133, 134). Autophagy has a complex and context-dependent role in carcinogenesis. In addition to removing damaged organelles and aggregated proteins, autophagy serves as a surveillance mechanism to protect normal cells from the transformation into cancerous cells by reducing DNA damage, reactive oxygen species, and damaged mitochondria (135). Multiple lines of evidence have established that ncRNAs, as important regulatory molecules in CRC, are also involved in the autophagy of tumor cells (136). Once cancer occurs, autophagy is upregulated to ensure the survival of tumor cells in crisis circumstances such as hypoxia and growth factor deprivation. Inhibition or promotion of ncRNAs could decrease autophagy, allowing therapeutic strategies and treatment agents more effective (137). Through their ability to influence autophagy in CRC cells, miRNAs play a crucial role in the occurrence and development of CRC. The precise processes through which miRNAs influence autophagy and regulate cancer occurrence and progression have not been established. Inhibition of protective autophagy by miR-27b-3p may lead to increased sensitivity of CRC cells to chemotherapy, as ectopic expression of miR-27b-3p is downregulated in oxaliplatin-resistant CRC cells (HCT116-OxRS and W480-OxR) versus the corresponding parental cells. Impairing autophagy in CRC cells by reducing ATG10 expression can make them more susceptible to chemotherapeutic agents *in vitro* and *in vivo*, which is consistent with the report that miR-27b-3p levels positively correlate with disease-free survival time in CRC patients (138). Besides, lncRNAs also affect autophagy by modulating the expression of ATG genes, which are key regulators in the autophagy process (139). HOTAIR-mediated autophagy was reported to be a crucial event in the development and progression of CRC. As a molecular sponge of miR-93, lncRNA HOTAIR could modulate the expression of ATG12 to induce CRC autophagy (45). Through downregulation of miR-34a, lncRNA NEAT1 promoted autophagy in CRC cell lines. An in-depth study of its molecular mechanism revealed that NEAT1 targeted miR-34a, while miR-34a was shown to target putative binding sites in the 3'-UTR, ATG9A, and ATG4B of HMGB1, which were involved in autophagy activation (140). And inhibition of the putative targets of miR-34a involved in autophagy revealed a new pathway for NEAT1 to regulate chemoresistance. Moreover, a recent study revealed that dysregulation of lncRNA GAS5 expression could induce autophagy in CRC (33). GAS5 facilitated the formation of vesicle-like structures and autolysosome structures in cells. lncRNAs frequently function as ceRNAs for modulating

autophagy-related miRNAs. A detailed cellular mechanism explained that GAS5 enhanced PTEN expression by acting as a ceRNA of miR-222-3p, which subsequently promoted CRC cell autophagy (33). It was reported that modulation of miR-20a was substantially lower under hypoxia that facilitated hypoxia-induced autophagy in CRC cells (141). Also, research showed that the ectopic expression of circCCDC66 could interact with miR-3140 in autophagy (101).

Given that aberrant autophagy is implicated in the pathogenesis of CRC, deliberate manipulation of autophagy may be effective in treating CRC. A precise determination of autophagy activity is essential to downstream autophagy-based therapy for CRC since autophagy dynamics vary greatly within different cellular statuses, and both an increase and a decrease in autophagy can contribute to CRC pathogenesis. Consequently, the importance of tailoring interventions with autophagy regulators in CRC of particular situations rather than applying a 'one size fits all' approach is vital for favorable treatment outcomes.

THE CLINICAL SIGNIFICANCE OF NCRNAS IN CRC

The clinical significance of ncRNAs in CRC explains their capability for diagnosis, treatment, chemotherapeutic resistance, and prognosis. To date, the diagnosis of CRC is mainly dependent on colonoscopy, which is deemed as the gold standard for the diagnosis of CRC (142). Furthermore, this approach has the disadvantage of requiring intestinal preparation and the risk of intestinal rupture, and it is not suitable for patients with anorectal stenosis, peritoneal irritation, severe cardiopulmonary function, and other conditions (143). Therefore, novel biomarkers for diagnosis and effective therapeutic targets are urgently required to improve the current situation.

ncRNAs as Potential Biomarkers for CRC Diagnosis and Prognosis

A competent biomarker should be sensitive, specific, repeatable, stable, and useful in clinical settings. ncRNAs are attractive candidates for biomarkers due to their expression patterns and properties (universality, conservation, tissue/cell selectivity, and stability). Besides, ncRNAs are enriched in human bodily fluids, such as plasma and saliva, facilitating their detection and making them suitable markers for cancer detection, particularly in liquid biopsies. These studies suggest that ncRNAs can serve as biomarkers for improving current detection and diagnostic methods of CRC. The abnormal expression of ncRNAs in CRC should be the prerequisite for them as biomarkers in clinical practice. Furthermore, ncRNAs as a non-invasive technology thereby being an ideal diagnostic approach have attracted much attention. Research has shown that miR-29a and miR-224 could be informative biomarkers for screening and early diagnosis of CRC *via* a noninvasive way (144). Survival of patients with metastatic cancer is still unfavorable, and resistance to therapy remains a major barrier to effective treatment. One intriguing approach to improving cancer treatment is leveraging cancer- and tissue-specific expression profiles to develop prognostic and diagnostic markers for the progression from primary to metastatic diseases.

Ling et al. found that patients with higher miR-224 levels appeared to have unfavorable overall survival in the five CRC cohorts (145). More interestingly, the incorporated analysis with CDH1 dramatically enhanced the predictive power of miR-224 for survival evaluation instead of appraising miR-224 alone (145). In addition to the diagnostic value of miR-224, it might also become a potential prognostic marker in CRC. Another research discovered that miR-224 mediates CRC tumorigenesis through regulating Wnt/β-catenin signaling, further proving that miR-224 was a prognostic biomarker (146). Assessment of miR-203 in serum could be an attractive and promising clinical tool for identifying patients with mCRC. Serum miR-203 was significantly correlated with the metastatic phenotype of CRC and was an independent prognostic biomarker for liver, lymph node, and peritoneal metastases of CRC, respectively (147). Moreover, serum miR-203 levels were significantly upregulated in a stage-dependent manner, and higher miR-203 expression was associated with poor survival in CRC patients, which suggested that miR-203 in serum was an independent prognostic marker.

A recent study illustrated that circ0004771 expression was exceptionally up-regulated in CRC patients, implying circ0004771 could provide a novel biomarker for the diagnosis of CRC (89). Recently, evidence is accumulating that ncRNAs can be not only clinical biomarkers for the early diagnosis and detection, as well as prognosis of cancer, but also potential therapeutic targets to enhance anti-tumor responses by regulating ncRNAs.

ncRNAs as Promising CRC Therapeutic Targets

Chemotherapy, radiotherapy, and excision are the main therapeutic strategies for clinical CRC (148). Although the clinical treatment has been improved, patients tend to have an unfavorable prognosis, and their 5-year survival rates remain low, which seems to be relevant to the chemotherapeutic resistance of CRC cells (149). Of note, recent studies have shown that ncRNAs can affect chemo-resistance in CRC therapy (150, 151). Therefore, identifying novel therapeutic targets for optimizing CRC therapy can be achieved through understanding the regulatory mechanisms of ncRNAs involved in chemotherapy and radiotherapy resistance.

On the one hand, it is well known that 5-Fu is a commonly used chemotherapeutic agent in curing CRC, and it obstructs DNA replication by inhibiting thymidylate synthase, hence leading to cell cycle arrest and apoptosis to induce DNA damage (152). lncRNA H19 level is found to increase in CRC, and it strongly enhances the resistance of CRC cells to 5-Fu. Moreover, molecular mechanism suggests that H19 induces chemotherapy resistance by binding to the downstream target gene SIRT1 (39). On the other hand, cancer stem cells (CSC),

as one of the subpopulations of chemo-resistant cells, play a crucial role in disease recurrence after chemotherapy. miR-133b is rich in CSCs and associated with stem cell-like characteristics, mainly elevated surface markers of CSCs and enhanced chemotherapeutic resistance (53). Furthermore, miR-133b overexpression reduces stem cell gene DOT1L-mediated H3K79me2 modification, which is consistent with down-regulation of stem cell gene transcription (53). Recovery of DOT1L eliminates the inhibitory effect of miR-133b on stem cell and CRC chemoresistance (54). miR-27a is observed to be overexpressed in the progress of anti-therapy of CRC. More importantly, miR-27a can act as a key regulatory factor engaging in metabolism reprogramming that might stimulate the mechanism concerning the chemical resistance of CRC (153).

The features of ncRNAs in CRC elucidate they act as promising treatment candidates for new therapeutic interventions. It is noticeable that circRNA PTK2 interacting with vimentin exerts a catalytic role during CRC growth and metastasis (154). In addition, vein injection of shRNA distinctively targeting circPTK2 immensely blunts CRC metastasis among the patient-derived xenograft models (154). Therefore, circPTK2 might afford an unrealized therapeutic target for the remedy of CRC metastasis. The ability to manipulate ncRNA expression and activity *in vivo* through anti-ncRNAs or ncRNA mimics provides an opportunity for developing innovative therapeutic approaches to CRC. miRNA dysregulation is causal in many cancer cases. miRNA mimics and molecules capable of targeting miRNAs have shown promise in preclinical development. Numerous strategies have been investigated to complement miRNAs with tumor suppressor functions by using miRNA mimics, which are synthetic oligonucleotide duplexes that mimic the function of their naturally occurring miRNA counterparts. Such miRNA mimics can be chemically modified to be more stable or capable of targeted delivery to tumors. miR−34a mimics can be encapsulated into TCP1-CD-QD nanoparticles and transferred into CRC cells, which contributes to the suppression of the proliferation and migration of CRC cells *in vitro* and inhibition of tumor growth in a tumor xenograft model derived from CRC cells (155). Moreover, the obtained indicates that co-delivery of miR-34a mimics and 5-FU could achieve synergistic effects for CRC treatment.

Although only a few typical ncRNAs related to chemoresistance are included in this review, more ncRNAs regulating CRC radiotherapy and chemoresistance need to be further explored. On the other hand, explaining the underlying capacities of ncRNAs in predicting treatment responses and managing individualized treatment choices appears to be another interesting aspect. Particularly, the combination of ncRNAs and chemotherapeutic agents to sensitize CRC seems promising and worthy of clinical trials. Future studies focusing on the regulation of ncRNAs in CRC chemo-resistance may contribute to certifying ncRNAs as encouraging therapeutic candidates. With the increasing involvement of ncRNAs revealed by the studies of chemoradiation resistance in CRC cells, as novel biomarkers, ncRNAs have great potential not only for predicting the efficiency of chemoradiation and prognosis, but for interfering with chemo-radiation resistance as targets in clinical CRC therapies.

Other Clinical Significance of ncRNAs in CRC

In addition to being potentially applied as diagnostic or prognostic biomarkers and therapeutic targets of CRC, the dysregulation of ncRNAs is correlated with the TNM stage, lymphatic metastasis, tumor size, and differentiation grade. For example, circ103809 participates in TNM staging of CRC and can be used as a biomarker (94). The expression of lncRNA DANCR is highly upregulated in CRC, which is associated with the TNM stage (156). Statistical analysis has demonstrated that lncRNA RPPH1 is positively associated with advanced TNM (157). Furthermore, *in situ* hybridization showed that high expression of RPPH1 in advanced TNM stage was associated with poor metastasis and overall survival (157). Overexpression of circCAMSAP1 is tightly linked with stage and clinical stage (158). Zhang et al. have discovered that lncRNA CASC11 expression is positively associated with tumor size, lymph node metastasis, and TNM stage in CRC (159). These ncRNAs mentioned above can provide a basis for the diagnosis and grading of clinical diseases and clues for predicting the prognostic outcomes.

CONCLUSION AND PROSPECT

CRC-related ncRNAs are increasingly becoming one of the most scorching topics in RNA biology and oncology. To date, lncRNAs, miRNAs, and circRNAs are the most commonly investigated ncRNAs that are involved in CRC progression. Of note, the functions and mechanisms of other types of ncRNAs are still unclear but are currently emerging. For instance, it has been revealed that piRNA-54265 is extensively upregulated in CRC and the elevated expression of piRNA-54265 in tumor or serum is significantly correlated with an unfavorable prognosis. Functional assays have revealed that piRNA-54265 targets PIWIL2 protein and this is essential for the formation of PIWIL2/STAT3/phosphorylated-SRC complex, which facilitates STAT3 signaling and enhances proliferation, metastasis as well as chemo-resistance of CRC cells (160). Several recent studies have independently unveiled that snoRNAs are involved in various cancers progression. SNORD126 is observed to be upregulated in CRC clinical samples, and it can promote tumor growth by modulating the PI3K/AKT signaling pathway rather than functioning as a miRNA (161).

The tRNA-derived fragments (tRFs) are generated through endo-nucleolytic cleavage of corresponding tRNAs and have been shown to be potential biomarkers for tumor diagnosis and treatment in several studies (162). For example, tRF levels in breast cancer cells significantly increased under hypoxia, which is consistent with their potential roles in stress response. Goodarzi et al. found that endogenous tRFs destabilize oncogenic transcripts by binding directly to YBX1 (163). Overexpression of YBX1 is associated with tumorigenic

phenotypes and has been shown to facilitate cancer metastasis (164). Furthermore, there is a high correlation between increased expression of multiple tRF-YBX1 targets (EIF4G1, EIF4EBP1 and EIF3B) and reduced recurrence-free survival. Transcripts of these oncogenes function in various aspects of cellular function, including translation and cellular signaling, and are repressed by tRFs in breast cancer cells (163). Recently, studies on the impact of CRC-related tRFs or key tRFs on CRC progression and related mechanisms are emerging. After hypoxic treatment, a total of 14 tRFs were differentially expressed in hypoxia-induced CRC RKO cells by performing tRF sequencing and real-time PCR assays. Among them, tRF-20-M0NK5Y93 might be a promising target for exploration, as its expression was significantly lower under hypoxic conditions than control conditions, and tRF-20-M0NK5Y93 inhibited CRC cell invasion and migration by targeting the EMT-related molecule Claudin-1 (165). Another study showed that tRF/miR-1280, a 17 bp fragment derived from $tRNA^{Leu}$ and pre-miRNA, was low expression in CRC specimens. Mechanistic investigations indicated that the Notch ligand JAG2 was a direct target of tRF/miR-1280 binding and that tRF/miR-1280 inhibited colorectal cancer growth and metastasis by suppressing the Notch signaling pathway that supported the CSC phenotype (166). As for the other ncRNAs, such as eRNAs and paRNAs, no study has reported any strong connections between the ectopic expression of these ncRNAs and human cancers.

In recent years, a limited number of proteins or peptides encoded by ncRNAs have been demonstrated to exhibit significant biological and pathological functions in the tumorigenesis and progression of CRC. For example, it has been reported that lncRNA HOXB-AS3 encodes a conserved 53-aa peptide that inhibits CRC growth by regulating the reprogramming of tumor metabolism and alternative splicing of pyruvate kinase (167). Additionally, function experiments have revealed that circMAPK14-175aa (a 175 amino acid peptide) encoded by circRNA MAPK14 can suppress the CRC malignant phenotype, thus affecting CRC progression and metastasis (168). Currently, some lncRNAs and circRNAs have been shown to encode proteins or peptides, and studies on the coding functions of miRNAs are emerging. A protein and a peptide (miPEP-200a and miPEP-200b) encoded by pri-miRNA (miR-200a and miR-200b) suppress the migration of prostate cancer cells by inhibiting the EMT process (8). These findings broaden the understanding of ncRNA and provide further insight into the function of ncRNAs.

The intestinal microbiota, composed of a considerable population of microorganisms, is maintained by dynamic host-microbiota interactions (169). Numerous studies have shown a link between intestinal dysbiosis and CRC (170). The roles of intestinal microorganisms in initiating and facilitating the CRC process are being increasingly understood. However, few studies focus on ncRNAs in the modulation of dynamic host-microbiota interactions, and the molecular regulators of ncRNAs in intestinal microbiota are still not fully understood. The existence of thousands of ncRNAs involved in the intracellular network regulation obtains essential implications for our understanding of CRC, which in turn forces us to develop our unique view of the disorder, from its causative origins to available treatment options and additional treatment strategies.

The contribution of ncRNAs in the genesis and progression of human illnesses is gaining popularity, but more research is needed to identify the entire extent of this contribution and the processes by which ncRNAs exert their pathological effects. Consequently, what comes to the first is a more pronounced understanding of ncRNAs function and mechanisms, both in CRC physiological and pathological conditions. In this review, we have summarized the latest research on ncRNAs that operate as promotors or tumor suppressors participating in CRC proliferation, apoptosis, invasion, metastasis, angiogenesis, autophagy, and chemo-resistance. Recent research has improved our conception of ncRNAs: not only do they perform fundamental operations in the normal physiological management processes, but also take part in abnormal pathologic regulatory processes. Although the research on ncRNAs has made great progress in recent years, the molecular mechanisms of administering aspects in CRC are still not clear, and further detailed mechanism research is urgently needed. Therefore, more pioneering studies are required for further exploration of the diagnostic and therapeutic opportunities that ncRNAs offer.

AUTHOR CONTRIBUTIONS

FZ collected the related paper. ZJ wrote the draft and revised it. JA and ZL collected the tables and designed them. All authors contributed to the article and approved the submitted version.

ACKNOWLEDGMENTS

We thank Yang Yang for making grammatical corrections to the manuscript.

REFERENCES

1. Yamashita R, Long J, Longacre T, Peng L, Berry G, Martin B, et al. Deep Learning Model for the Prediction of Microsatellite Instability in Colorectal Cancer: A Diagnostic Study. *Lancet Oncol* (2021) 22(1):132–41. doi: 10.1016/S1470-2045(20)30535-0
2. Dekker E, Tanis PJ, Vleugels JLA, Kasi PM, Wallace MB. Colorectal Cancer. *Lancet (London England)* (2019) 394(10207):1467–80. doi: 10.1016/S0140-6736(19)32319-0
3. Muzny DM, Bainbridge MN, Chang K, Dinh HH, Drummond JA, Fowler G, et al. Comprehensive Molecular Characterization of Human Colon and Rectal Cancer. *Nature* (2012) 487(7407):330–7. doi: 10.1038/nature11252
4. Zhou XY, Luo B, Jiang ZK, Xie YK, Wu FC, Huang JQ, et al. Non-Coding RNAS and Colorectal Cancer Liver Metastasis. *Mol Cell Biochem* (2020) 475 (1-2):151–9. doi: 10.1007/s11010-020-03867-8
5. Balacescu O, Sur D, Cainap C, Visan S, Cruceriu D, Manzat-Saplacan R, et al. The Impact of miRNA in Colorectal Cancer Progression and Its Liver Metastases. *Int J Mol Sci* (2018) 19(12). doi: 10.3390/ijms19123711

6. Ogunwobi OO, Mahmood F, Akingboye A. Biomarkers in Colorectal Cancer: Current Research and Future Prospects. *Int J Mol Sci* (2020) 21 (15). doi: 10.3390/ijms21155311
7. Anastasiadou E, Jacob LS, Slack FJ. Non-Coding RNA Networks in Cancer. *Nat Rev Cancer* (2018) 18(1):5–18. doi: 10.1038/nrc.2017.99
8. Wang J, Zhu S, Meng N, He Y, Lu R, Yan GR. ncRNA-Encoded Peptides or Proteins and Cancer. *Mol Ther* (2019) 27(10):1718–25. doi: 10.1016/j.ymthe.2019.09.001
9. Lei B, Tian Z, Fan W, Ni B. Circular RNA: A Novel Biomarker and Therapeutic Target for Human Cancers. *Int J Med Sci* (2019) 16(2):292–301. doi: 10.7150/ijms.28047
10. Statello L, Guo C-J, Chen L-L, Huarte M. Gene Regulation by Long Non-Coding RNAs and Its Biological Functions. *Nat Rev Mol Cell Biol* (2021) 22 (2):96–118. doi: 10.1038/s41580-020-00315-9
11. Winkle M, El-Daly SM, Fabbri M, Calin GA. Noncoding RNA Therapeutics - Challenges and Potential Solutions. *Nat Rev Drug Discov* (2021) 20(8):629–51. doi: 10.1038/s41573-021-00219-z
12. Peng WX, Koirala P, Mo YY. LncRNA-Mediated Regulation of Cell Signaling in Cancer. *Oncogene* (2017) 36(41):5661–7. doi: 10.1038/onc.2017.184
13. Rinn JL, Chang HY. Genome Regulation by Long Noncoding RNAs. *Annu Rev Biochem* (2012) 81:145–66. doi: 10.1146/annurev-biochem-051410-092902
14. Chen L, Heikkinen L, Wang C, Yang Y, Sun H, Wong G. Trends in the Development of miRNA Bioinformatics Tools. *Brief Bioinform* (2019) 20 (5):1836–52. doi: 10.1093/bib/bby054
15. Liu B, Li J, Cairns MJ. Identifying miRNAs, Targets and Functions. *Brief Bioinform* (2014) 15(1):1–19. doi: 10.1093/bib/bbs075
16. Tay Y, Rinn J, Pandolfi PP. The Multilayered Complexity of ceRNA Crosstalk and Competition. *Nature* (2014) 505(7483):344–52. doi: 10.1038/nature12986
17. Salmena L, Poliseno L, Tay Y, Kats L, Pandolfi PP. A ceRNA Hypothesis: The Rosetta Stone of a Hidden RNA Language? *Cell* (2011) 146(3):353–8. doi: 10.1016/j.cell.2011.07.014
18. Ma Z, Shuai Y, Gao X, Wen X, Ji J. Circular RNAs in the Tumour Microenvironment. *Mol Cancer* (2020) 19(1):8. doi: 10.1186/s12943-019-1113-0
19. Yin Y, Long J, He Q, Li Y, Liao Y, He P, et al. Emerging Roles of circRNA in Formation and Progression of Cancer. *J Cancer* (2019) 10(21):5015–21. doi: 10.7150/jca.30828
20. Esmaeili M, Keshani M, Vakilian M, Esmaeili M, Peymani M, Seyed Forootan F, et al. Role of non-Coding RNAs as Novel Biomarkers for Detection of Colorectal Cancer Progression Through Interaction With the Cell Signaling Pathways. *Gene* (2020) 753:144796. doi: 10.1016/j.gene.2020.144796
21. Dragomir MP, Kopetz S, Ajani JA, Calin GA. Non-Coding RNAs in GI Cancers: From Cancer Hallmarks to Clinical Utility. *Gut* (2020) 69(4):748–63. doi: 10.1136/gutjnl-2019-318279
22. Zhu S, Chen CY, Hao Y. LncRNA KCNQ1OT1 Acts as miR-216b-5p Sponge to Promote Colorectal Cancer Progression *via* Up-Regulating ZNF146. *J Mol Histol* (2021) 52:479–90. doi: 10.1007/s10735-020-09942-0
23. Poursheikhani A, Abbaszadegan MR, Kerachian MA. Mechanisms of Long non-Coding RNA Function in Colorectal Cancer Tumorigenesis. *Asia Pac J Clin Oncol* (2020) 17:7–23. doi: 10.1111/ajco.13452
24. Wang Y, Lu J-H, Wu Q-N, Jin Y, Wang D-S, Chen Y-X, et al. LncRNA LINRIS Stabilizes IGF2BP2 and Promotes the Aerobic Glycolysis in Colorectal Cancer. *Mol Cancer* (2019) 18(1):174. doi: 10.1186/s12943-019-1105-0
25. Yang P, Li J, Peng C, Tan Y, Chen R, Peng W, et al. TCONS_00012883 Promotes Proliferation and Metastasis *via* DDX3/YY1/MMP1/PI3K-AKT Axis in Colorectal Cancer. *Clin Trans Med* (2020) 10(6):e211. doi: 10.1002/ctm2.211
26. Chen R, Zhou S, Chen J, Lin S, Ye F, Jiang P. LncRNA BLACAT1/miR-519d-3p/CREB1 Axis Mediates Proliferation, Apoptosis, Migration, Invasion, and Drug-Resistance in Colorectal Cancer Progression. *Cancer Manag Res* (2020) 12:13137–48. doi: 10.2147/CMAR.S274447
27. Deng X, Li S, Kong F, Ruan H, Xu X, Zhang X, et al. Long Noncoding RNA PiHL Regulates P53 Protein Stability Through GRWD1/RPL11/MDM2 Axis in Colorectal Cancer. *Theranostics* (2020) 10(1):265–80. doi: 10.7150/thno.36045
28. Lin X, Zhuang S, Chen X, Du J, Zhong L, Ding J, et al. lncRNA ITGB8-AS1 Functions as a ceRNA to Promote Colorectal Cancer Growth and Migration Through Integrin-Mediated Focal Adhesion Signaling. *Mol Ther J Am Soc Gene Ther* (2021) 30. doi: 10.1016/j.ymthe.2021.08.011
29. Duan W, Kong X, Li J, Li P, Zhao Y, Liu T, et al. LncRNA AC010789.1 Promotes Colorectal Cancer Progression by Targeting MicroRNA-432-3p/ZEB1 Axis and the Wnt/beta-Catenin Signaling Pathway. *Front Cell Dev Biol* (2020) 8:565355. doi: 10.3389/fcell.2020.565355
30. Tang Y, Tang R, Tang M, Huang P, Liao Z, Zhou J, et al. LncRNA DNAJC3-AS1 Regulates Fatty Acid Synthase *via* the EGFR Pathway to Promote the Progression of Colorectal Cancer. *Front Oncol* (2020) 10:604534. doi: 10.3389/fonc.2020.604534
31. Jin L, Pan YL, Zhang J, Cao PG. LncRNA HOTAIR Recruits SNAIL to Inhibit the Transcription of HNF4alpha and Promote the Viability, Migration, Invasion and EMT of Colorectal Cancer. *Transl Oncol* (2021) 14(4):101036. doi: 10.1016/j.tranon.2021.101036
32. Li P, Zhang X, Wang L, Du L, Yang Y, Liu T, et al. lncRNA HOTAIR Contributes to 5FU Resistance Through Suppressing miR-218 and Activating NF-κb/TS Signaling in Colorectal Cancer. *Mol Ther Nucleic Acids* (2017) 8:356–69. doi: 10.1016/j.omtn.2017.07.007
33. Liu L, Wang H-J, Meng T, Lei C, Yang X-H, Wang Q-S, et al. lncRNA GAS5 Inhibits Cell Migration and Invasion and Promotes Autophagy by Targeting miR-222-3p *via* the GAS5/PTEN-Signaling Pathway in CRC. *Mol Ther Nucleic Acids* (2019) 17:644–56. doi: 10.1016/j.omtn.2019.06.009
34. Liu L, Meng T, Yang X-H, Sayim P, Lei C, Jin B, et al. Prognostic and Predictive Value of Long non-Coding RNA GAS5 and mircoRNA-221 in Colorectal Cancer and Their Effects on Colorectal Cancer Cell Proliferation, Migration and Invasion. *Cancer Biomark* (2018) 22(2):283–99. doi: 10.3233/CBM-171011
35. Zheng ZH, You HY, Feng YJ, Zhang ZT. LncRNA KCNQ1OT1 is a Key Factor in the Reversal Effect of Curcumin on Cisplatin Resistance in the Colorectal Cancer Cells. *Mol Cell Biochem* (2020) 476:2575–85. doi: 10.1007/s11010-020-03856-x
36. Pichler M, Rodriguez-Aguayo C, Nam SY, Dragomir MP, Bayraktar R, Anfossi S, et al. Therapeutic Potential of FLANC, a Novel Primate-Specific Long non-Coding RNA in Colorectal Cancer. *Gut* (2020) 69(10):1818–31. doi: 10.1136/gutjnl-2019-318903
37. Zhang M, Weng W, Zhang Q, Wu Y, Ni S, Tan C, et al. The lncRNA NEAT1 Activates Wnt/β-Catenin Signaling and Promotes Colorectal Cancer Progression *via* Interacting With DDX5. *J Hematol Oncol* (2018) 11 (1):113. doi: 10.1186/s13045-018-0656-7
38. Zhang Y, Sun J, Qi Y, Wang Y, Ding Y, Wang K, et al. Long non-Coding RNA TPT1-AS1 Promotes Angiogenesis and Metastasis of Colorectal Cancer Through TPT1-AS1/NF90/VEGFA Signaling Pathway. *Aging* (2020) 12(7):6191–205. doi: 10.18632/aging.103016
39. Wang M, Han D, Yuan Z, Hu H, Zhao Z, Yang R, et al. Long non-Coding RNA H19 Confers 5-Fu Resistance in Colorectal Cancer by Promoting SIRT1-Mediated Autophagy. *Cell Death Dis* (2018) 9(12):1149. doi: 10.1038/s41419-018-1187-4
40. Zhang Z, Yang W, Li N, Chen X, Ma F, Yang J, et al. LncRNA MCF2L-AS1 Aggravates Proliferation, Invasion and Glycolysis of Colorectal Cancer Cells *via* the Crosstalk With miR-874-3p/FOXM1 Signaling Axis. *Carcinogenesis* (2021) 42(2):263–71. doi: 10.1093/carcin/bgaa093
41. Huang F-K, Zheng C-Y, Huang L-K, Lin C-Q, Zhou J-F, Wang J-X. Long non-Coding RNA MCF2L-AS1 Promotes the Aggressiveness of Colorectal Cancer by Sponging miR-874-3p and Thereby Up-Regulating CCNE1. *J Gene Med* (2021) 23(1):e3285. doi: 10.1002/jgm.3285
42. Li C, Wang P, Du J, Chen J, Liu W, Ye K. LncRNA RAD51-AS1/miR-29b/C-3p/NDRG2 Crosstalk Repressed Proliferation, Invasion and Glycolysis of Colorectal Cancer. *IUBMB Life* (2021) 73(1):286–98. doi: 10.1002/iub.2427
43. Zhuang L, Ding W, Ding W, Zhang Q, Xu X, Xi D. lncRNA ZNF667-AS1 (NR_036521.1) Inhibits the Progression of Colorectal Cancer *via* Regulating ANK2/JAK2 Expression. *J Cell Physiol* (2021) 236(3):2178–93. doi: 10.1002/jcp.30004
44. Yang X-D, Xu H-T, Xu X-H, Ru G, Liu W, Zhu J-J, et al. Knockdown of Long Non-Coding RNA HOTAIR Inhibits Proliferation and Invasiveness and

Improves Radiosensitivity in Colorectal Cancer. *Oncol Rep* (2016) 35 (1):479–87. doi: 10.3892/or.2015.4397
45. Liu Y, Chen X, Chen X, Liu J, Gu H, Fan R, et al. Long non-Coding RNA HOTAIR Knockdown Enhances Radiosensitivity Through Regulating microRNA-93/ATG12 Axis in Colorectal Cancer. *Cell Death Dis* (2020) 11 (3):175. doi: 10.1038/s41419-020-2268-8
46. Liu T, Wang H, Yu H, Bi M, Yan Z, Hong S, et al. The Long Non-Coding RNA HOTTIP Is Highly Expressed in Colorectal Cancer and Enhances Cell Proliferation and Invasion. *Mol Ther Nucleic Acids* (2020) 19:612–8. doi: 10.1016/j.omtn.2019.12.008
47. Liu T, Yu T, Hu H, He K. Knockdown of the Long non-Coding RNA HOTTIP Inhibits Colorectal Cancer Cell Proliferation and Migration and Induces Apoptosis by Targeting SGK1. *Biomed Pharmacother* (2018) 98:286–96. doi: 10.1016/j.biopha.2017.12.064
48. Silva-Fisher JM, Dang HX, White NM, Strand MS, Krasnick BA, Rozycki EB, et al. Long non-Coding RNA RAMS11 Promotes Metastatic Colorectal Cancer Progression. *Nat Commun* (2020) 11(1):2156. doi: 10.1038/s41467-020-15547-8
49. Islam Khan MZ, Law HKW. RAMS11 Promotes CRC Through mTOR-Dependent Inhibition of Autophagy, Suppression of Apoptosis, and Promotion of Epithelial-Mesenchymal Transition. *Cancer Cell Int* (2021) 21(1):321. doi: 10.1186/s12935-021-02023-6
50. Michael MZ, OC SM, van Holst Pellekaan NG, Young GP, James RJ. Reduced Accumulation of Specific microRNAs in Colorectal Neoplasia. *Mol Cancer Res* (2003) 1(12):882–91.
51. Dong Q, Zhou L, Liu F, Ao F, Gong X, Jiang C, et al. Long non-Coding RNAs in the Development, Diagnosis and Prognosis of Nasopharyngeal Carcinoma. *Int J Clin Exp Pathol* (2017) 10(8):8098–105.
52. Fan M, Ma X, Wang F, Zhou Z, Zhang J, Zhou D, et al. MicroRNA-30b-5p Functions as a Metastasis Suppressor in Colorectal Cancer by Targeting Rap1b. *Cancer Lett* (2020) 477:144–56. doi: 10.1016/j.canlet.2020.02.021
53. Ma M, Li L, Long F, Xiao H, Lu M, Lin C. MiR-133b Inhibits Colorectal Cancer Metastasis *via* lncRNA-Lucat1. *Future Oncol (Lond Engl)* (2021) 17 (9):1013–23. doi: 10.2217/fon-2020-0420
54. Lv L, Li Q, Chen S, Zhang X, Tao X, Tang X, et al. miR-133b Suppresses Colorectal Cancer Cell Stemness and Chemoresistance by Targeting Methyltransferase DOT1L. *Exp Cell Res* (2019) 385(1):111597. doi: 10.1016/j.yexcr.2019.111597
55. Chen J, Chen S, Zhuo L, Zhu Y, Zheng H. Regulation of Cancer Stem Cell Properties, Angiogenesis, and Vasculogenic Mimicry by miR-450a-5p/SOX2 Axis in Colorectal Cancer. *Cell Death Dis* (2020) 11(3):173. doi: 10.1038/s41419-020-2361-z
56. Zeng Z, Li Y, Pan Y, Lan X, Song F, Sun J, et al. Cancer-Derived Exosomal miR-25-3p Promotes Pre-Metastatic Niche Formation by Inducing Vascular Permeability and Angiogenesis. *Nat Commun* (2018) 9(1):5395. doi: 10.1038/s41467-018-07810-w
57. Qiao P-F, Yao L, Zeng Z-L. Catalpol-mediated microRNA-34a Suppresses Autophagy and Malignancy by Regulating SIRT1 in Colorectal Cancer. *Oncol Rep* (2020) 43(4):1053–66. doi: 10.3892/or.2020.7494
58. Liu H, Liu Y, Sun P, Leng K, Xu Y, Mei L, et al. Colorectal Cancer-Derived Exosomal miR-106b-3p Promotes Metastasis by Down-Regulating DLC-1 Expression. *Clin Sci (Lond Engl 1979)* (2020) 134(4):419–34. doi: 10.1042/CS20191087
59. Sun L, Fang Y, Wang X, Han Y, Du F, Li C, et al. miR-302a Inhibits Metastasis and Cetuximab Resistance in Colorectal Cancer by Targeting NFIB and CD44. *Theranostics* (2019) 9(26):8409–25. doi: 10.7150/thno.36605
60. Xu W, Chen B, Ke D, Chen X. MicroRNA-138-5p Targets the NFIB-Snail1 Axis to Inhibit Colorectal Cancer Cell Migration and Chemoresistance. *Cancer Cell Int* (2020) 20:475. doi: 10.1186/s12935-020-01573-5
61. Bleau A-M, Redrado M, Nistal-Villan E, Villalba M, Exposito F, Redin E, et al. miR-146a Targets C-Met and Abolishes Colorectal Cancer Liver Metastasis. *Cancer Lett* (2018) 414:257–67. doi: 10.1016/j.canlet.2017.11.008
62. Hwang W-L, Jiang J-K, Yang S-H, Huang T-S, Lan H-Y, Teng H-W, et al. MicroRNA-146a Directs the Symmetric Division of Snail-Dominant Colorectal Cancer Stem Cells. *Nat Cell Biol* (2014) 16(3):268–80. doi: 10.1038/ncb2910
63. Lin X, Wang S, Sun M, Zhang C, Wei C, Yang C, et al. miR-195-5p/NOTCH2-Mediated EMT Modulates IL-4 Secretion in Colorectal Cancer to Affect M2-Like TAM Polarization. *J Hematol Oncol* (2019) 12(1):20. doi: 10.1186/s13045-019-0708-7
64. Jin Y, Wang M, Hu H, Huang Q, Chen Y, Wang G. Overcoming Stemness and Chemoresistance in Colorectal Cancer Through miR-195-5p-Modulated Inhibition of Notch Signaling. *Int J Biol Macromol* (2018) 117:445–53. doi: 10.1016/j.ijbiomac.2018.05.151
65. Xin H, Wang C, Chi Y, Liu Z. MicroRNA-196b-5p Promotes Malignant Progression of Colorectal Cancer by Targeting ING5. *Cancer Cell Int* (2020) 20:119. doi: 10.1186/s12935-020-01200-3
66. Zhou Z, Wu L, Liu Z, Zhang X, Han S, Zhao N, et al. MicroRNA-214-3p Targets the PLAGL2-MYH9 Axis to Suppress Tumor Proliferation and Metastasis in Human Colorectal Cancer. *Aging (Albany NY)* (2020) 12 (10):9633–57. doi: 10.18632/aging.103233
67. Li J, Peng W, Yang P, Chen R, Gu Q, Qian W, et al. MicroRNA-1224-5p Inhibits Metastasis and Epithelial-Mesenchymal Transition in Colorectal Cancer by Targeting SP1-Mediated NF-kappaB Signaling Pathways. *Front Oncol* (2020) 10:294. doi: 10.3389/fonc.2020.00294
68. Li SS, Zhu HJ, Li JY, Tian LM, Lv DM. MiRNA-875-3p Alleviates the Progression of Colorectal Cancer *via* Negatively Regulating PLK1 Level. *Eur Rev Med Pharmacol Sci* (2020) 24(3):1126–33. doi: 10.26355/eurrev_202002_20163
69. Shahmohamadnejad S, Nouri Ghonbalani Z, Tahbazlahafi B, Panahi G, Meshkani R, Emami Razavi A, et al. Aberrant Methylation of miR-124 Upregulates DNMT3B in Colorectal Cancer to Accelerate Invasion and Migration. *Arch Physiol Biochem* (2020) 128:1–7. doi: 10.1080/13813455.2020.1779311
70. Roshani Asl E, Rasmi Y, Baradaran B. MicroRNA-124-3p Suppresses PD-L1 Expression and Inhibits Tumorigenesis of Colorectal Cancer Cells *via* Modulating STAT3 Signaling. *J Cell Physiol* (2021) 236(10):7071–87. doi: 10.1002/jcp.30378
71. Rupaimoole R, Slack FJ. MicroRNA Therapeutics: Towards a New Era for the Management of Cancer and Other Diseases. *Nat Rev Drug Discov* (2017) 16(3):203–22. doi: 10.1038/nrd.2016.246
72. Deng S, Wang H, Fan H, Zhang L, Hu J, Tang Q, et al. Over-Expressed miRNA-200b Ameliorates Ulcerative Colitis-Related Colorectal Cancer in Mice Through Orchestrating Epithelial-Mesenchymal Transition and Inflammatory Responses by Channel of AKT2. *Int Immunopharmacol* (2018) 61:346–54. doi: 10.1016/j.intimp.2018.06.024
73. Normanno N, Tejpar S, Morgillo F, De Luca A, Van Cutsem E, Ciardiello F. Implications for KRAS Status and EGFR-Targeted Therapies in Metastatic CRC. *Nat Rev Clin Oncol* (2009) 6(9):519–27. doi: 10.1038/nrclinonc.2009.111
74. Ciardiello F, Tortora G. EGFR Antagonists in Cancer Treatment. *N Engl J Med* (2008) 358(11):1160–74. doi: 10.1056/NEJMra0707704
75. Ohta M, Seto M, Ijichi H, Miyabayashi K, Kudo Y, Mohri D, et al. Decreased Expression of the RAS-GTPase Activating Protein RASAL1 is Associated With Colorectal Tumor Progression. *Gastroenterology* (2009) 136(1):206–16. doi: 10.1053/j.gastro.2008.09.063
76. Yang Y, Weng W, Peng J, Hong L, Yang L, Toiyama Y, et al. Fusobacterium Nucleatum Increases Proliferation of Colorectal Cancer Cells and Tumor Development in Mice by Activating Toll-Like Receptor 4 Signaling to Nuclear Factor-κb, and Up-Regulating Expression of MicroRNA-21. *Gastroenterology* (2017) 152(4):851–66. doi: 10.1053/j.gastro.2016.11.018
77. Civenni G, Holbro T, Hynes NE. Wnt1 and Wnt5a Induce Cyclin D1 Expression Through ErbB1 Transactivation in HC11 Mammary Epithelial Cells. *EMBO Rep* (2003) 4(2):166–71. doi: 10.1038/sj.embor.embor735
78. Du F, Cao T, Xie H, Li T, Sun L, Liu H, et al. KRAS Mutation-Responsive miR-139-5p Inhibits Colorectal Cancer Progression and is Repressed by Wnt Signaling. *Theranostics* (2020) 10(16):7335–50. doi: 10.7150/thno.45971
79. Liu T, Zhang X, Du L, Wang Y, Liu X, Tian H, et al. Exosome-Transmitted miR-128-3p Increase Chemosensitivity of Oxaliplatin-Resistant Colorectal Cancer. *Mol Cancer* (2019) 18(1):43. doi: 10.1186/s12943-019-0981-7
80. Xu D, Wu Y, Wang X, Hu X, Qin W, Li Y, et al. Identification of Functional circRNA/miRNA/mRNA Regulatory Network for Exploring Prospective Therapy Strategy of Colorectal Cancer. *J Cell Biochem* (2020) 121:4785–97. doi: 10.1002/jcb.29703

81. Deng Q, Wang CJ, Hao R, Yang QY. Circ_0001982 Accelerates the Progression of Colorectal Cancer *via* Sponging microRNA-144. *Eur Rev Med Pharmacol Sci* (2020) 24(4):1755–62. doi: 10.26355/eurrev_202002_20352
82. Chen J, Yang J, Fei X, Wang X, Wang K. CircRNA ciRS-7: A Novel Oncogene in Multiple Cancers. *Int J Biol Sci* (2021) 17(1):379–89. doi: 10.7150/ijbs.54292
83. Weng W, Wei Q, Toden S, Yoshida K, Nagasaka T, Fujiwara T, et al. Circular RNA ciRS-7-A Promising Prognostic Biomarker and a Potential Therapeutic Target in Colorectal Cancer. *Clin Cancer Res* (2017) 23(14):3918–28. doi: 10.1158/1078-0432.CCR-16-2541
84. Santarpia L, Lippman SM, El-Naggar AK. Targeting the MAPK-RAS-RAF Signaling Pathway in Cancer Therapy. *Expert Opin Ther Targets* (2012) 16 (1):103–19. doi: 10.1517/14728222.2011.645805
85. Qu S, Yang X, Li X, Wang J, Gao Y, Shang R, et al. Circular RNA: A New Star of Noncoding RNAs. *Cancer Lett* (2015) 365(2):141–8. doi: 10.1016/j.canlet.2015.06.003
86. Chen L-Y, Wang L, Ren Y-X, Pang Z, Liu Y, Sun X-D, et al. The Circular RNA Circ-ERBIN Promotes Growth and Metastasis of Colorectal Cancer by miR-125a-5p and miR-138-5p/4EBP-1 Mediated Cap-Independent HIF-1α Translation. *Mol Cancer* (2020) 19(1):164. doi: 10.1186/s12943-020-01272-9
87. Guo L, Yang G, Kang Y, Li S, Duan R, Shen L, et al. Construction and Analysis of a ceRNA Network Reveals Potential Prognostic Markers in Colorectal Cancer. *Front Genet* (2020) 11:418. doi: 10.3389/fgene.2020.00418
88. Wu M, Kong C, Cai M, Huang W, Chen Y, Wang B, et al. Hsa_circRNA_002144 Promotes Growth and Metastasis of Colorectal Cancer Through Regulating miR-615-5p/LARP1/mTOR Pathway. *Carcinogenesis* (2020) 42:601–10. doi: 10.1093/carcin/bgaa140
89. Pan B, Qin J, Liu X, He B, Wang X, Pan Y, et al. Identification of Serum Exosomal Hsa-Circ-0004771 as a Novel Diagnostic Biomarker of Colorectal Cancer. *Front Genet* (2019) 10:1096. doi: 10.3389/fgene.2019.01096
90. Deng Z, Li X, Wang H, Geng Y, Cai Y, Tang Y, et al. Dysregulation of CircRNA_0001946 Contributes to the Proliferation and Metastasis of Colorectal Cancer Cells by Targeting MicroRNA-135a-5p. *Front Genet* (2020) 11:357. doi: 10.3389/fgene.2020.00357
91. Wang X, Zhang H, Yang H, Bai M, Ning T, Deng T, et al. Exosome-Delivered circRNA Promotes Glycolysis to Induce Chemoresistance Through the miR-122-PKM2 Axis in Colorectal Cancer. *Mol Oncol* (2020) 14(3):539–55. doi: 10.1002/1878-0261.12629
92. Fang G, Ye BL, Hu BR, Ruan XJ, Shi YX. CircRNA_100290 Promotes Colorectal Cancer Progression Through miR-516b-Induced Downregulation of FZD4 Expression and Wnt/beta-Catenin Signaling. *Biochem Biophys Res Commun* (2018) 504(1):184–9. doi: 10.1016/j.bbrc.2018.08.152
93. Zhang L, Dong X, Yan B, Yu W, Shan L. CircAGFG1 Drives Metastasis and Stemness in Colorectal Cancer by Modulating YY1/CTNNB1. *Cell Death Dis* (2020) 11(7):542. doi: 10.1038/s41419-020-2707-6
94. Bian L, Zhi X, Ma L, Zhang J, Chen P, Sun S, et al. Hsa_circRNA_103809 Regulated the Cell Proliferation and Migration in Colorectal Cancer *via* miR-532-3p / FOXO4 Axis. *Biochem Biophys Res Commun* (2018) 505 (2):346–52. doi: 10.1016/j.bbrc.2018.09.073
95. Li C, Zhou H. Circular RNA Hsa_circRNA_102209 Promotes the Growth and Metastasis of Colorectal Cancer Through miR-761-Mediated Ras and Rab Interactor 1 Signaling. *Cancer Med* (2020) 9(18):6710–25. doi: 10.1002/cam4.3332
96. Li R, Wu B, Xia J, Ye L, Yang X. Circular RNA Hsa_circRNA_102958 Promotes Tumorigenesis of Colorectal Cancer *via* miR-585/CDC25B Axis. *Cancer Manag Res* (2019) 11:6887–93. doi: 10.2147/CMAR.S212180
97. Jian X, He H, Zhu J, Zhang Q, Zheng Z, Liang X, et al. Hsa_circ_001680 Affects the Proliferation and Migration of CRC and Mediates its Chemoresistance by Regulating BMI1 Through miR-340. *Mol Cancer* (2020) 19(1):20. doi: 10.1186/s12943-020-1134-8
98. Wang X, Ren Y, Ma S, Wang S. Circular RNA 0060745, a Novel circRNA, Promotes Colorectal Cancer Cell Proliferation and Metastasis Through miR-4736 Sponging. *Onco Targets Ther* (2020) 13:1941–51. doi: 10.2147/OTT.S240642
99. Xu H, Liu Y, Cheng P, Wang C, Liu Y, Zhou W, et al. CircRNA_0000392 Promotes Colorectal Cancer Progression Through the miR-193a-5p/PIK3R3/AKT Axis. *J Exp Clin Cancer Res* (2020) 39(1):283. doi: 10.1186/s13046-020-01799-1
100. Li X, Wang J, Zhang C, Lin C, Zhang J, Zhang W, et al. Circular RNA Circitga7 Inhibits Colorectal Cancer Growth and Metastasis by Modulating the Ras Pathway and Upregulating Transcription of its Host Gene ITGA7. *J Pathol* (2018) 246(2):166–79. doi: 10.1002/path.5125
101. Feng J, Li Z, Li L, Xie H, Lu Q, He X. Hypoxia-induced Circccdc66 Promotes the Tumorigenesis of Colorectal Cancer *via* the Mir-3140/Autophagy Pathway. *Int J Mol Med* (2020) 46(6):1973–82. doi: 10.3892/ijmm.2020.4747
102. Yang H, Zhang H, Yang Y, Wang X, Deng T, Liu R, et al. Hypoxia Induced Exosomal circRNA Promotes Metastasis of Colorectal Cancer *via* Targeting GEF-H1/RhoA Axis. *Theranostics* (2020) 10(18):8211–26. doi: 10.7150/thno.44419
103. Ma Z, Han C, Xia W, Wang S, Li X, Fang P, et al. Circ5615 Functions as a ceRNA to Promote Colorectal Cancer Progression by Upregulating TNKS. *Cell Death Dis* (2020) 11(5):356. doi: 10.1038/s41419-020-2514-0
104. Lu H, Yao B, Wen X, Jia B. FBXW7 Circular RNA Regulates Proliferation, Migration and Invasion of Colorectal Carcinoma Through NEK2, mTOR, and PTEN Signaling Pathways *In Vitro* and *In Vivo*. *BMC Cancer* (2019) 19 (1):918. doi: 10.1186/s12885-019-6028-z
105. Shang A, Gu C, Wang W, Wang X, Sun J, Zeng B, et al. Exosomal circPACRGL Promotes Progression of Colorectal Cancer *via* the miR-142-3p/miR-506-3p- TGF-Beta1 Axis. *Mol Cancer* (2020) 19(1):117. doi: 10.1186/s12943-020-01235-0
106. Zeng W, Liu Y, Li WT, Li Y, Zhu JF. CircFNDC3B Sequestrates miR-937-5p to Derepress TIMP3 and Inhibit Colorectal Cancer Progression. *Mol Oncol* (2020) 14(11):2960–84. doi: 10.1002/1878-0261.12796
107. Chen C, Huang Z, Mo X, Song Y, Li X, Li X, et al. The Circular RNA 001971/miR-29c-3p Axis Modulates Colorectal Cancer Growth, Metastasis, and Angiogenesis Through VEGFA. *J Exp Clin Cancer Res* (2020) 39(1):91. doi: 10.1186/s13046-020-01594-y
108. Zhang X, Zhao Y, Kong P, Han M, Li B. Expression of Circznf609 is Down-Regulated in Colorectal Cancer Tissue and Promotes Apoptosis in Colorectal Cancer Cells by Upregulating P53. *Med Sci Monit* (2019) 25:5977–85. doi: 10.12659/MSM.915926
109. Yuan Y, Liu W, Zhang Y, Zhang Y, Sun S. CircRNA Circ_0026344 as a Prognostic Biomarker Suppresses Colorectal Cancer Progression *via* microRNA-21 and microRNA-31. *Biochem Biophys Res Commun* (2018) 503(2):870–5. doi: 10.1016/j.bbrc.2018.06.089
110. Du J, Xu J, Chen J, Liu W, Wang P, Ye K. Circrae1 Promotes Colorectal Cancer Cell Migration and Invasion by Modulating miR-338-3p/TYRO3 Axis. *Cancer Cell Int* (2020) 20:430. doi: 10.1186/s12935-020-01519-x
111. Hanahan D, Weinberg RA. Hallmarks of Cancer: The Next Generation. *Cell* (2011) 144(5):646–74. doi: 10.1016/j.cell.2011.02.013
112. Li G, Zhou L-N, Yang H, He X, Duan Y, Wu F. Ninjurin 2 Overexpression Promotes Human Colorectal Cancer Cell Growth and. *Aging* (2019) 11 (19):8526–41. doi: 10.18632/aging.102336
113. Pistritto G, Trisciuoglio D, Ceci C, Garufi A, D'Orazi G. Apoptosis as Anticancer Mechanism: Function and Dysfunction of its Modulators and Targeted Therapeutic Strategies. *Aging* (2016) 8(4):603–19. doi: 10.18632/aging.100934
114. Krishnamurthy N, Kurzrock R. Targeting the Wnt/beta-Catenin Pathway in Cancer: Update on Effectors and Inhibitors. *Cancer Treat Rev* (2018) 62:50–60. doi: 10.1016/j.ctrv.2017.11.002
115. Bugter JM, Fenderico N, Maurice MM. Mutations and Mechanisms of WNT Pathway Tumour Suppressors in Cancer. *Nat Rev Cancer* (2021) 21(1):5–21. doi: 10.1038/s41568-020-00307-z
116. Yu J, Han Z, Sun Z, Wang Y, Zheng M, Song C. LncRNA SLCO4A1-AS1 Facilitates Growth and Metastasis of Colorectal Cancer Through β-Catenin-Dependent Wnt Pathway. *J Exp Clin Cancer Res* (2018) 37(1):222. doi: 10.1186/s13046-018-0896-y
117. Wang Z, Jin J. LncRNA SLCO4A1-AS1 Promotes Colorectal Cancer Cell Proliferation by Enhancing Autophagy *via* miR-508-3p/PARD3 Axis. *Aging* (2019) 11(14):4876–89. doi: 10.18632/aging.102081
118. Wang J, Zhang Y, Song H, Yin H, Jiang T, Xu Y, et al. The Circular RNA circSPARC Enhances the Migration and Proliferation of Colorectal Cancer by Regulating the JAK/STAT Pathway. *Mol Cancer* (2021) 20(1):81. doi: 10.1186/s12943-021-01375-x

119. Taherdangkoo K, Kazemi Nezhad SR, Hajjari MR, Tahmasebi Birgani M. miR-485-3p Suppresses Colorectal Cancer *via* Targeting TPX2. *Bratisl Lek Listy* (2020) 121(4):302–7. doi: 10.4149/BLL_2020_048
120. Martin TD, Patel RS, Cook DR, Choi MY, Patil A, Liang AC, et al. The Adaptive Immune System is a Major Driver of Selection for Tumor Suppressor Gene Inactivation. *Science* (2021) 373(6561):1327–35. doi: 10.1126/science.abg5784
121. Catalano V, Turdo A, Di Franco S, Dieli F, Todaro M, Stassi G. Tumor and its Microenvironment: A Synergistic Interplay. *Semin Cancer Biol* (2013) 23 (6 Pt B):522–32. doi: 10.1016/j.semcancer.2013.08.007
122. Vu T, Datta PK. Regulation of EMT in Colorectal Cancer: A Culprit in Metastasis. *Cancers* (2017) 9(12). doi: 10.3390/cancers9120171
123. Klein CA. Cancer Progression and the Invisible Phase of Metastatic Colonization. *Nat Rev Cancer* (2020) 20(11):681–94. doi: 10.1038/s41568-020-00300-6
124. Fares J, Fares MY, Khachfe HH, Salhab HA, Fares Y. Molecular Principles of Metastasis: A Hallmark of Cancer Revisited. *Signal Transduct Target Ther* (2020) 5(1):28. doi: 10.1038/s41392-020-0134-x
125. Ji Q, Cai G, Liu X, Zhang Y, Wang Y, Zhou L, et al. MALAT1 Regulates the Transcriptional and Translational Levels of Proto-Oncogene RUNX2 in Colorectal Cancer Metastasis. *Cell Death Dis* (2019) 10(6):378. doi: 10.1038/s41419-019-1598-x
126. Zhou W, Ye XL, Xu J, Cao MG, Fang ZY, Li LY, et al. The lncRNA H19 Mediates Breast Cancer Cell Plasticity During EMT and MET Plasticity by Differentially Sponging miR-200b/C and Let-7b. *Sci Signal* (2017) 10(483). doi: 10.1126/scisignal.aak9557
127. Liu SJ, Dang HX, Lim DA, Feng FY, Maher CA. Long Noncoding RNAs in Cancer Metastasis. *Nat Rev Cancer* (2021) 21(7):446–60. doi: 10.1038/s41568-021-00353-1
128. Pan M, Chen Q, Lu Y, Wei F, Chen C, Tang G, et al. MiR-106b-5p Regulates the Migration and Invasion of Colorectal Cancer Cells by Targeting FAT4. *Biosci Rep* (2020) 40(11). doi: 10.1042/BSR20200098
129. Shang A, Wang X, Gu C, Liu W, Sun J, Zeng B, et al. Exosomal miR-183-5p Promotes Angiogenesis in Colorectal Cancer by Regulation of FOXO1. *Aging (Albany NY)* (2020) 12(9):8352–71. doi: 10.18632/aging.103145
130. Herrera-Solorio AM, Peralta-Arrieta I, Armas Lopez L, Hernandez-Cigala N, Mendoza Milla C, Ortiz Quintero B, et al. LncRNA SOX2-OT Regulates AKT/ERK and SOX2/GLI-1 Expression, Hinders Therapy, and Worsens Clinical Prognosis in Malignant Lung Diseases. *Mol Oncol* (2021) 15 (4):1110–29. doi: 10.1002/1878-0261.12875
131. Tetreault M-P, Yang Y, Katz JP. Krüppel-Like Factors in Cancer. *Nat Rev Cancer* (2013) 13(10):701–13. doi: 10.1038/nrc3582
132. Bhattacharya R, Senbanerjee S, Lin Z, Mir S, Hamik A, Wang P, et al. Inhibition of Vascular Permeability Factor/Vascular Endothelial Growth Factor-Mediated Angiogenesis by the Kruppel-Like Factor KLF2. *J Biol Chem* (2005) 280(32):28848–51. doi: 10.1074/jbc.C500200200
133. Zhang Y, Li C, Liu X, Wang Y, Zhao R, Yang Y, et al. Circhipk3 Promotes Oxaliplatin-Resistance in Colorectal Cancer Through Autophagy by Sponging miR-637. *EBioMedicine* (2019) 48:277–88. doi: 10.1016/j.ebiom.2019.09.051
134. Glick D, Barth S, Macleod KF. Autophagy: Cellular and Molecular Mechanisms. *J Pathol* (2010) 221(1):3–12. doi: 10.1002/path.2697
135. Singh SS, Vats S, Chia AY, Tan TZ, Deng S, Ong MS, et al. Dual Role of Autophagy in Hallmarks of Cancer. *Oncogene* (2018) 37(9):1142–58. doi: 10.1038/s41388-017-0046-6
136. Chen L, He M, Zhang M, Sun Q, Zeng S, Zhao H, et al. The Role of Non-Coding RNAs in Colorectal Cancer, With a Focus on Its Autophagy. *Pharmacol Ther* (2021) 226:107868. doi: 10.1016/j.pharmthera.2021.107868
137. Pentimalli F. Autophagy in Disease: Hunger for Translation. *Cell Death Dis* (2019) 10(3):247. doi: 10.1038/s41419-019-1419-2
138. Sun W, Li J, Zhou L, Han J, Liu R, Zhang H, et al. The C-Myc/miR-27b-3p/ATG10 Regulatory Axis Regulates Chemoresistance in Colorectal Cancer. *Theranostics* (2020) 10(5):1981–96. doi: 10.7150/thno.37621
139. Liu P-F, Farooqi AA, Peng S-Y, Yu T-J, Dahms H-U, Lee C-H, et al. Regulatory Effects of Noncoding RNAs on the Interplay of Oxidative Stress and Autophagy in Cancer Malignancy and Therapy. *Semin Cancer Biol* (2020). doi: 10.1016/j.semcancer.2020.10.009
140. Liu F, Ai FY, Zhang DC, Tian L, Yang ZY, Liu SJ. LncRNA NEAT1 Knockdown Attenuates Autophagy to Elevate 5-FU Sensitivity in Colorectal Cancer *via* Targeting miR-34a. *Cancer Med-Us* (2019) 9 (3):1079–91. doi: 10.1002/cam4.2746
141. Che J, Wang W, Huang Y, Zhang L, Zhao J, Zhang P, et al. miR-20a Inhibits Hypoxia-Induced Autophagy by Targeting ATG5/FIP200 in Colorectal Cancer. *Mol Carcinog* (2019) 58(7):1234–47. doi: 10.1002/mc.23006
142. Cotton PB, Durkalski VL, Pineau BC, Palesch YY, Mauldin PD, Hoffman B, et al. Computed Tomographic Colonography (Virtual Colonoscopy): A Multicenter Comparison With Standard Colonoscopy for Detection of Colorectal Neoplasia. *JAMA* (2004) 291(14):1713–9. doi: 10.1001/jama.291.14.1713
143. Moss S, Mathews C, Day TJ, Smith S, Seaman HE, Snowball J, et al. Increased Uptake and Improved Outcomes of Bowel Cancer Screening With a Faecal Immunochemical Test: Results From a Pilot Study Within the National Screening Programme in England. *Gut* (2017) 66(9):1631–44. doi: 10.1136/gutjnl-2015-310691
144. Zhu YX, Xu AD, Li JM, Fu JH, Wang GH, Yang YL, et al. Fecal miR-29a and miR-224 as the Noninvasive Biomarkers for Colorectal Cancer. *Cancer Biomark* (2016) 16(2):259–64. doi: 10.3233/Cbm-150563
145. Ling H, Pickard K, Ivan C, Isella C, Ikuo M, Mitter R, et al. The Clinical and Biological Significance of MIR-224 Expression in Colorectal Cancer Metastasis. *Gut* (2016) 65(6):977–89. doi: 10.1136/gutjnl-2015-309372
146. Li T, Lai Q, Wang S, Cai J, Xiao Z, Deng D, et al. MicroRNA-224 Sustains Wnt/beta-Catenin Signaling and Promotes Aggressive Phenotype of Colorectal Cancer. *J Exp Clin Cancer Res* (2016) 35:21. doi: 10.1186/s13046-016-0287-1
147. Hur K, Toiyama Y, Okugawa Y, Ide S, Imaoka H, Boland CR, et al. Circulating microRNA-203 Predicts Prognosis and Metastasis in Human Colorectal Cancer. *Gut* (2017) 66(4):654–65. doi: 10.1136/gutjnl-2014-308737
148. Pidikova P, Reis R, Herichova I. miRNA Clusters With Down-Regulated Expression in Human Colorectal Cancer and Their Regulation. *Int J Mol Sci* (2020) 21(13). doi: 10.3390/ijms21134633
149. Micallef I, Baron B. The Mechanistic Roles of ncRNAs in Promoting and Supporting Chemoresistance of Colorectal Cancer. *Noncoding RNA* (2021) 7 (2). doi: 10.3390/ncrna7020024
150. Li P, Zhang X, Wang H, Wang L, Liu T, Du L, et al. MALAT1 Is Associated With Poor Response to Oxaliplatin-Based Chemotherapy in Colorectal Cancer Patients and Promotes Chemoresistance Through EZH2. *Mol Cancer Ther* (2017) 16(4):739–51. doi: 10.1158/1535-7163.MCT-16-0591
151. Fanale D, Castiglia M, Bazan V, Russo A. Involvement of Non-Coding RNAs in Chemo- and Radioresistance of Colorectal Cancer. *Adv Exp Med Biol* (2016) 937:207–28. doi: 10.1007/978-3-319-42059-2_11
152. Wei L, Wang X, Lv L, Zheng Y, Zhang N, Yang M. The Emerging Role of Noncoding RNAs in Colorectal Cancer Chemoresistance. *Cell Oncol (Dordr)* (2019) 42(6):757–68. doi: 10.1007/s13402-019-00466-8
153. Barisciano G, Colangelo T, Rosato V, Muccillo L, Taddei ML, Ippolito L, et al. miR-27a is a Master Regulator of Metabolic Reprogramming and Chemoresistance in Colorectal Cancer. *Br J Cancer* (2020) 122(9):1354–66. doi: 10.1038/s41416-020-0773-2
154. Yang H, Li X, Meng Q, Sun H, Wu S, Hu W, et al. CircPTK2 (Hsa_Circ_0005273) as a Novel Therapeutic Target for Metastatic Colorectal Cancer. *Mol Cancer* (2020) 19(1):13. doi: 10.1186/s12943-020-1139-3
155. Xu J, Zhang G, Luo X, Wang D, Zhou W, Zhang Y, et al. Co-Delivery of 5-Fluorouracil and miRNA-34a Mimics by Host-Guest Self-Assembly Nanocarriers for Efficacious Targeted Therapy in Colorectal Cancer Patient-Derived Tumor Xenografts. *Theranostics* (2021) 11(5):2475–89. doi: 10.7150/thno.52076
156. Liu Y, Zhang M, Liang L, Li J, Chen YX. Over-Expression of lncRNA DANCR is Associated With Advanced Tumor Progression and Poor Prognosis in Patients With Colorectal Cancer. *Int J Clin Exp Pathol* (2015) 8(9):11480–4.
157. Liang ZX, Liu HS, Wang FW, Xiong L, Zhou C, Hu T, et al. LncRNA RPPH1 Promotes Colorectal Cancer Metastasis by Interacting With TUBB3 and by Promoting Exosomes-Mediated Macrophage M2 Polarization. *Cell Death Dis* (2019) 10(11):829. doi: 10.1038/s41419-019-2077-0

158. Zhou C, Liu HS, Wang FW, Hu T, Liang ZX, Lan N, et al. Circcamsap1 Promotes Tumor Growth in Colorectal Cancer *via* the miR-328-5p/E2F1 Axis. *Mol Ther* (2020) 28(3):914–28. doi: 10.1016/j.ymthe.2019.12.008
159. Zhang Z, Zhou C, Chang Y, Zhang Z, Hu Y, Zhang F, et al. Long non-Coding RNA CASC11 Interacts With hnRNP-K and Activates the WNT/beta-Catenin Pathway to Promote Growth and Metastasis in Colorectal Cancer. *Cancer Lett* (2016) 376(1):62–73. doi: 10.1016/j.canlet.2016.03.022
160. Mai D, Ding P, Tan L, Zhang J, Pan Z, Bai R, et al. PIWI-Interacting RNA-54265 is Oncogenic and a Potential Therapeutic Target in Colorectal Adenocarcinoma. *Theranostics* (2018) 8(19):5213–30. doi: 10.7150/thno.28001
161. Fang X, Yang D, Luo H, Wu S, Dong W, Xiao J, et al. SNORD126 Promotes HCC and CRC Cell Growth by Activating the PI3K-AKT Pathway Through FGFR2. *J Mol Cell Biol* (2017) 9(3):243–55. doi: 10.1093/jmcb/mjw048
162. Thompson DM, Parker R. Stressing Out Over tRNA Cleavage. *Cell* (2009) 138(2):215–9. doi: 10.1016/j.cell.2009.07.001
163. Goodarzi H, Liu X, Nguyen HCB, Zhang S, Fish L, Tavazoie SF. Endogenous tRNA-Derived Fragments Suppress Breast Cancer Progression *via* YBX1 Displacement. *Cell* (2015) 161(4):790–802. doi: 10.1016/j.cell.2015.02.053
164. Jürchott K, Kuban R-J, Krech T, Blüthgen N, Stein U, Walther W, et al. Identification of Y-Box Binding Protein 1 as a Core Regulator of MEK/ERK Pathway-Dependent Gene Signatures in Colorectal Cancer Cells. *PloS Genet* (2010) 6(12):e1001231. doi: 10.1371/journal.pgen.1001231
165. Luan N, Chen Y, Li Q, Mu Y, Zhou Q, Ye X, et al. TRF-20-M0NK5Y93 Suppresses the Metastasis of Colon Cancer Cells by Impairing the Epithelial-to-Mesenchymal Transition Through Targeting Claudin-1. *Am J Trans Res* (2021) 13(1):124–42.
166. Huang B, Yang H, Cheng X, Wang D, Fu S, Shen W, et al. tRF/miR-1280 Suppresses Stem Cell-Like Cells and Metastasis in Colorectal Cancer. *Cancer Res* (2017) 77(12):3194–206. doi: 10.1158/0008-5472.CAN-16-3146
167. Huang J-Z, Chen M, Chen D, Gao X-C, Zhu S, Huang H, et al. A Peptide Encoded by a Putative lncRNA HOXB-AS3 Suppresses Colon Cancer Growth. *Mol Cell* (2017) 68(1):171–84. doi: 10.1016/j.molcel.2017.09.015
168. Wang L, Zhou J, Zhang C, Chen R, Sun Q, Yang P, et al. A Novel Tumour Suppressor Protein Encoded by Circmapk14 Inhibits Progression and Metastasis of Colorectal Cancer by Competitively Binding to MKK6. *Clin Trans Med* (2021) 11(10):e613. doi: 10.1002/ctm2.613
169. Dong J, Tai JW, Lu L-F. miRNA-Microbiota Interaction in Gut Homeostasis and Colorectal Cancer. *Trends Cancer* (2019) 5(11):666–9. doi: 10.1016/j.trecan.2019.08.003
170. Tilg H, Adolph TE, Gerner RR, Moschen AR. The Intestinal Microbiota in Colorectal Cancer. *Cancer Cell* (2018) 33(6):954–64. doi: 10.1016/j.ccell.2018.03.004

Conflict of Interest: The authors declare that the research was conducted in the absence of any commercial or financial relationships that could be construed as a potential conflict of interest.

Publisher's Note: All claims expressed in this article are solely those of the authors and do not necessarily represent those of their affiliated organizations, or those of the publisher, the editors and the reviewers. Any product that may be evaluated in this article, or claim that may be made by its manufacturer, is not guaranteed or endorsed by the publisher.

frontiers in Oncology

ORIGINAL RESEARCH
published: 24 February 2022
doi: 10.3389/fonc.2022.816884

Identification of circRNA–miRNA–Immune-Related mRNA Regulatory Network in Gastric Cancer

Zhenhai Wu[1], *Pengyuan Liu*[2] *and Ganlu Zhang*[1]*

[1] Department of Oncology, Zhejiang Hospital, Hangzhou, China, [2] The Second School of Clinical Medicine, Zhejiang Chinese Medical University, Hangzhou, China

The pathogenesis of gastric cancer (GC) is still not fully understood. We aimed to find the potential regulatory network for ceRNA (circRNA–miRNA–immune-related mRNA) to uncover the pathological molecular mechanisms of GC. The expression profiles of circRNA, miRNA, and mRNA in gastric tissue from GC patients were downloaded from the Gene Expression Omnibus (GEO) datasets. Differentially expressed circRNAs, miRNAs, and immune-related mRNAs were filtered, followed by the construction of the ceRNA (circRNA–miRNA–immune-related mRNA) network. Functional annotation and protein–protein interaction (PPI) analysis of immune-related mRNAs in the network were performed. Expression validation of circRNAs and immune-related mRNAs was performed in the new GEO and TCGA datasets and *in-vitro* experiment. A total of 144 differentially expressed circRNAs, 216 differentially expressed miRNAs, and 2,392 differentially expressed mRNAs were identified in GC. Some regulatory pairs of circRNA–miRNA–immune-related mRNA were obtained, including hsa_circ_0050102–hsa-miR-4537–NRAS–Tgd cells, hsa_circ_0001013–hsa-miR-485-3p–MAP2K1–Tgd cells, hsa_circ_0003763–hsa-miR-145-5p–FGF10–StromaScore, hsa_circ_0001789–hsa-miR-1269b–MET–adipocytes, hsa_circ_0040573–hsa-miR-3686–RAC1–Tgd cells, and hsa_circ_0006089–hsa-miR-5584-3p–LYN–neurons. Interestingly, FGF10, MET, NRAS, RAC1, MAP2K1, and LYN had potential diagnostic value for GC patients. In the KEGG analysis, some signaling pathways were identified, such as Rap1 and Ras signaling pathways (involved NRAS and FGF10), Fc gamma R-mediated phagocytosis and cAMP signaling pathway (involved RAC1), proteoglycans in cancer (involved MET), T-cell receptor signaling pathway (involved MAP2K1), and chemokine signaling pathway (involved LYN). The expression validation of hsa_circ_0003763, hsa_circ_0004928, hsa_circ_0040573, FGF10, MET, NRAS, RAC1, MAP2K1, and LYN was consistent with the integrated analysis. In conclusion, the identified ceRNA (circRNA–miRNA–immune-related mRNA) regulatory network may be associated with the development of GC.

Keywords: gastric cancer, circRNA, miRNAs, mRNAs, diagnosis, immune, signaling pathway, protein–protein interaction

OPEN ACCESS

Edited by:
Divya P. Kumar, JSS Academy of Higher Education and Research, India

Reviewed by:
Sajjad Sisakhtnezhad, Razi University, Iran
Adenilson Leão Pereira Federal University of Pará, Brazil

***Correspondence:**
Ganlu Zhang
ZGLoncology@163.com

Specialty section:
This article was submitted to Gastrointestinal Cancers: Gastric & Esophageal Cancers, a section of the journal Frontiers in Oncology

Received: *17 November 2021*
Accepted: *24 January 2022*
Published: *24 February 2022*

Citation:
Wu Z, Liu P and Zhang G (2022) Identification of circRNA–miRNA–Immune-Related mRNA Regulatory Network in Gastric Cancer. Front. Oncol. 12:816884. doi: 10.3389/fonc.2022.816884

INTRODUCTION

Gastric cancer (GC) is one of the most serious malignant tumors (1). According to the GLOBOCAN Estimates of Incidence and Mortality Worldwide for 36 Cancers in 185 Countries, the incidence of GC is 7.7% (2). In addition, with 2.26 million new cases estimated in 2020, GC (0.77 million) has become the most commonly diagnosed cancer worldwide, ranking only second to female breast cancer (3). Recurrence is the main cause of GC-related death. Although mortality is steadily decreasing, GC still leads to a poor diagnosis and prognosis for patients (4). In addition, the 5-year survival rate of patients is still very low in serious GC patients. It has been shown that obesity, active tobacco smoking, high meat and salt intake, low vegetable/fruit intake, *Helicobacter pylori* infection, and gut microbiota have been shown to be associated with an increased risk of GC (5–8). In addition, epigenetic alterations are associated with the processes of gastric carcinogenesis and metastasis (9). Clinically, surgery is the only curative treatment; however, some patients have inoperable disease at diagnosis (10). Hence, there is a need to elucidate the potential molecular mechanisms in the development of GC and to look for new molecular markers and therapeutic targets.

circRNAs usually result from splicing/back-splicing events *via* exon or intron circularization (11). circRNA can act as a molecular sponge of miRNA to regulate mRNA expression. It was reported that sponge circRNAs are part of a complex RNA-binding protein–circRNA–miRNA–mRNA interaction network and are involved in the establishment, chemoresistance, and progression of GC (12). hsa_circ_LARP4 can inhibit cell invasion of GC by sponging hsa-miR-424-5p and regulating large tumor suppressor kinase 1 (LATS1) expression (13). hsa_circ_NRIP1 can act as an hsa-miR-149-5p sponge to promote GC progression *via* the AKT serine/threonine kinase 1 (AKT1)/mechanistic target of rapamycin kinase (mTOR) pathway (14). hsa_circ_NHSL1 can promote GC progression through the hsa-miR-1306-3p/SIX homeobox 1 (SIX1)/vimentin axis (15). hsa_circ_CACTIN can promote GC progression by sponging hsa-miR-331-3p and regulating transforming growth factor beta receptor 1 (TGFBR1) expression (16). hsa_circ_0026359 can enhance cisplatin resistance in GC *via* targeting the hsa-miR-1200/DNA polymerase delta 4, accessory subunit (POLD4) pathway (17). In addition, it is believed that the pathogenies and progression of GC are influenced by the cross-talk between tumor cells and the host immune system (18–20). In view of this, we tried to find the potential differentially expressed circRNAs, miRNAs, and immune-related mRNAs in GC.

MATERIALS AND METHODS

Data Retrieval and Analysis

In this study, the expression profiles of circRNA, miRNA, and mRNA were downloaded from the Gene Expression Omnibus (GEO) datasets by searching keywords ["gastric cancer" (All Fields) AND "Homo sapiens"(porgn) AND "gse"(Filter)]. The following datasets were selected: 1) dataset must be genome-wide transcriptome data of mRNA/miRNA/circRNA; 2) data were obtained from tumor tissues of the GC group and paracancer control group; and 3) both standardized and raw datasets were considered. Finally, two circRNA expression datasets (GSE83521 and GSE89143), two miRNA expression datasets (GSE93415 and GSE158315), and two mRNA expression datasets (GSE66229 and GSE65801) were selected (**Table 1**).

Screening of Differentially Expressed circRNAs, miRNAs, and Immune-Related mRNAs

The probe and ID of circRNA/miRNA/mRNA were mapped one by one. After scale standardization, the dataset was merged and batch effects were removed *via* the ComBat function of sva package (R-4.0.5). The metaMA and limma packages were used to identify circRNAs/miRNAs/mRNAs. The default parameter of the Pvalcombination command of the metaMA package was used to make the difference. *p*-values and effect sizes (ES, the effectSize obtained from the metaMA package) from data were calculated either from classical or moderated *t*-tests. These *p*-values were combined by the inverse normal method. The Benjamini–Hochberg threshold was used to calculate the false discovery rate (FDR). |Combined.ES| >1 and FDR <0.05 were the screening criteria for circRNAs/miRNAs/mRNAs. In

TABLE 1 | Detailed information of selected datasets of circRNA, miRNA, and mRNA expression datasets.

	GEO accession	Author	Platform	Samples (N:GC)	Year	Tissue
circRNA	GSE83521	Yan Zhang	GPL19978 Agilent-069978 Arraystar Human CircRNA microarray V1	6:6	2017	Gastric tissue
	GSE89143	Junming Guo	GPL19978 Agilent-069978 Arraystar Human CircRNA microarray V1	3:3	2017	Gastric tissue
miRNA	GSE93415	Marek Sierżęga	GPL19071 Exiqon miRCURY LNA microRNA array; 7th generation REV - hsa, mmu, and rno; batch 208520-22; lot 35101-35101 (miRBase 19.0)	20:20	2017	Gastric tissue
	GSE158315	Yuping Wang	GPL18058 Exiqon miRCURY LNA microRNA array, 7th generation (miRBase v18, condensed Probe_ID version)	5:5	2021	Gastric tissue
mRNA	GSE66229	Michael Nebozhyn	GPL570 (HG-U133_Plus_2) Affymetrix Human Genome U133 Plus 2.0 Array	100:300	2015	Gastric tissue
	GSE65801	Hao Li	GPL14550 Agilent-028004 SurePrint G3 Human GE 8 × 60K Microarray (Probe Name Version)	32:32	2015	Gastric tissue

N, paracancer control group; GC, gastric cancer group.

addition, immune-related mRNAs were downloaded from the ImmPort database (https://www.immport.org/shared/home). Those immune-related mRNAs were obtained by intersection of differentially expressed mRNAs and immune-related mRNAs in the ImmPort database. xCell (21) was used to calculate the distribution of immune cells in each sample based on the ssGSEA method. xCell score was organized into immune cell infiltration matrix to calculate the types of immune cells that differed between the GC group and the normal control group. The Pearson correlation coefficient method was used to calculate the correlation between mRNAs and differential immune cells.

Construction of the ceRNA (circRNA–miRNA–Immune-Related mRNA) Regulatory Network

The TargetScan (http://www.targetscan.org/vert_71/) software was utilized to predict targeted relationship between differentially expressed circRNAs and differentially expressed miRNAs. In addition, the miRWalk software (http://mirwalk.umm.uni-heidelberg.de/interactions/) was applied to predict targeted relationship between miRNAs and mRNAs. The relationship pairs of miRNA–mRNA verified in at least one database (TargetScan, miRDB, and MiRTarBase) were selected. The overlapping mRNAs were obtained between predicted mRNAs (in the miRNA–mRNA relationship pairs) and immune-related differential expression mRNAs. The ceRNA (circRNA–miRNA–immune-related mRNA) regulatory network was constructed by fusing with the circRNA–miRNA relationship pairs and miRNA–immune-related mRNA relationship pairs.

Functional Annotation of Immune-Related mRNAs in the ceRNA Regulatory Network

To investigate the function of immune-related mRNAs in the regulatory ceRNA network, Gene Ontology (GO) and Kyoto Encyclopedia of Genes and Genomes (KEGG) analyses were performed by using the DAVID database (https://david.ncifcrf.gov/tools.jsp). FDR <0.05 was considered as statistical significance.

Protein–Protein Interaction Network of Immune-Related mRNAs in the ceRNA Regulatory Network

To further explore the interaction between immune-related mRNAs in the ceRNA regulatory network, protein–protein interaction (PPI) was performed by using the STRING database. The results were imported using the Cytoscape software (http://www.cytoscape.org/). The CytoHubba plug-in was used to filter core immune-related mRNAs by intersecting the first 10 mRNAs of each algorithm (degree, MNC, MCC, and EPC). In addition, the ROC analysis was carried out to assess the diagnostic value of core immune-related mRNAs in the PPI network.

Expression Validation of Differentially Expressed circRNAs and Immune-Related mRNAs

In order to further validate the expression of identified circRNAs and immune-related mRNAs, electronic validation was performed. The GSE93541 dataset (involving tumor tissues from three cases and three normal controls) and the GSE141977 dataset (involving plasma from three cases and three normal controls) were used for expression validation of identified circRNAs. Additionally, the Cancer Genome Atlas (TCGA) dataset (involved tumor tissues from 375 cases and 32 normal controls) was used to validate the expression of identified mRNAs. The expression result of these circRNAs and mRNAs was shown by the box plots. Statistical significance was ascribed to p-value <0.05.

In addition, qRT-PCR was used to further validate the expression of identified circRNAs and immune-related mRNAs. Five GC patients and five normal controls were enrolled. The blood sample of these individuals was collected. All participating individuals provided informed consent with the approval of the Ethics Committee of Zhejiang Hospital (2021-164K). Total RNA of the blood sample was extracted and DNA was synthesized using FastQuant cDNA first-strand synthesis kit. qRT-PCR was performed in the SuperReal PreMix Plus (SYBR Green). Relative circRNA/mRNA expression was analyzed by the $2^{-\triangle\triangle CT}$ method. $2^{-\triangle\triangle CT}$ >1 and $2^{-\triangle\triangle CT}$ <1 represented upregulation and downregulation, respectively.

RESULTS

Differentially Expressed circRNAs, miRNAs, and Immune-Related mRNAs

A total of 144 differentially expressed (55 upregulated and 89 downregulated) circRNAs, 216 differentially expressed (105 upregulated and 111 downregulated) miRNAs, and 2,392 differentially expressed (1,329 upregulated and 1,063 downregulated) mRNAs were identified in GC. The top 10 differentially expressed circRNAs were identified, such as hsa_circ_0045602 (upregulation), hsa_circ_0006089 (upregulation), hsa_circ_0001789 (upregulation), hsa_circ_0018004 (downregulation), and hsa_circ_0003763 (downregulation) (**Table 2**). hsa-miR-4537 was one of top 10 downregulated miRNAs (**Table 3**). The top 10 differentially expressed mRNAs are listed in **Table 4**. The heat map of the top 100 differentially expressed circRNAs, miRNAs, and mRNAs is shown in **Figures 1A–C**, respectively. In addition, 1,793 immune-related mRNAs were obtained from the ImmPort database. It was noted that 159 immune-related mRNAs were also differentially expressed mRNAs in GC (**Figure 2**).

ceRNA (circRNA–miRNA–Immune-Related mRNA) Regulatory Network

A total of 2,037 negatively regulated targeting relationship pairs of circRNA–miRNA (involving 143 circRNAs and 198 miRNAs) and 142 negatively regulated targeting relationship pairs of miRNA–immune-related mRNA (involving 97 miRNAs and 58 immune-related mRNAs) were identified *via* the TargetScan software and miRWalk, respectively. The ceRNA (circRNA–miRNA–immune-related mRNA) regulatory network (involving 137 circRNAs, 96 miRNAs,

TABLE 2 | The top 10 upregulated and downregulated circRNAs in GC.

ID	Symbol	Combined.ES	*p*-value	FDR	Up/down
hsa_circRNA_102191	hsa_circ_0045602	3.118562462	1.07E–06	0.000830662	Up
hsa_circRNA_104947	hsa_circ_0007613	3.076836769	1.43E–06	0.000830662	Up
hsa_circRNA_101882	hsa_circ_0040573	3.859880212	1.82E–06	0.000830662	Up
hsa_circRNA_102592	hsa_circ_0052001	3.180131272	2.28E–06	0.000830662	Up
hsa_circRNA_101471	hsa_circ_0034398	2.865182594	3.78E–06	0.000836756	Up
hsa_circRNA_102614	hsa_circ_0006089	2.831849087	3.94E–06	0.000836756	Up
hsa_circRNA_104589	hsa_circ_0001789	3.306599675	4.20E–06	0.000836756	Up
hsa_circRNA_100641	hsa_circ_0019054	2.89673611	4.77E–06	0.00087084	Up
hsa_circRNA_101875	hsa_circ_0040481	2.642927097	9.51E–06	0.001488245	Up
hsa_circRNA_102777	hsa_circ_0055521	2.42548772	2.78E–05	0.003039928	Up
hsa_circRNA_100571	hsa_circ_0018004	–3.196809378	9.51E–07	0.000830662	Down
hsa_circRNA_104599	hsa_circ_0001793	–3.624031186	2.17E–06	0.000830662	Down
hsa_circRNA_400066	hsa_circ_0092330	–2.876804101	3.17E–06	0.000836756	Down
hsa_circRNA_101651	hsa_circ_0036941	–2.829679697	3.88E–06	0.000836756	Down
hsa_circRNA_001914	hsa_circ_0000902	–2.987023494	7.15E–06	0.001204509	Down
hsa_circRNA_101965	hsa_circ_0000740	–2.632340492	1.05E–05	0.001531677	Down
hsa_circRNA_103442	hsa_circ_0003763	–2.780691514	1.88E–05	0.00256875	Down
hsa_circRNA_400056	hsa_circ_0092297	–2.597537412	2.21E–05	0.00275069	Down
hsa_circRNA_100382	hsa_circ_0007277	–2.696712581	2.26E–05	0.00275069	Down
hsa_circRNA_104661	hsa_circ_0004366	–2.495771422	2.39E–05	0.00275519	Down

ES, effect size; FDR, false discovery rate.

and 58 immune-related mRNAs) was obtained by fusing with the circRNA–miRNA relationship pairs and miRNA–immune-related mRNA relationship pairs (**Figure 3**). Some ceRNA relationship pairs were identified, such as hsa_circ_0045602–hsa-miR-4538–WNT5A and hsa_circ_0018004–hsa-miR-199a-5p–KL.

Enrichment Analysis of Immune-Related mRNAs in the ceRNA Regulatory Network

Fifty-eight immune-related mRNAs in the regulatory ceRNA network were used for functional enrichment analysis. GO analysis showed that signal transduction, extracellular space, and growth factor activity were the most significantly enriched biological process, cytological component, and molecular function, respectively (**Figure 4**). According to the KEGG analysis, Rap1 and Ras signaling pathways [involved NRAS proto-oncogene, GTPase (NRAS), and fibroblast growth factor 10 (FGF10)], Fc gamma R-mediated phagocytosis and cAMP signaling pathway [involved Rac family small GTPase 1 (RAC1)], proteoglycans in cancer [involved MET proto-oncogene, receptor tyrosine kinase (MET)], T-cell receptor signaling pathway [involved mitogen-activated protein kinase

TABLE 3 | The top 10 upregulated and downregulated miRNAs in GC.

Symbol	Combined.ES	*p*-value	FDR	Up/down
hsa-miR-181a-5p	2.621880675	8.01E–13	6.84E–10	Up
hsa-miR-181b-5p	2.541945488	4.05E–12	1.15E–09	Up
hsa-miR-23a-3p	2.283816919	1.17E–10	1.11E–08	Up
hsa-miR-331-3p	2.121044968	1.04E–09	6.82E–08	Up
hsa-miR-320c	2.029389583	1.53E–09	8.73E–08	Up
hsa-miR-25-3p	1.94259155	4.78E–09	2.55E–07	Up
hsa-miR-320d	1.961475455	6.29E–09	2.98E–07	Up
hsa-miR-92a-3p	1.928060578	7.06E–09	3.02E–07	Up
hsa-miR-21-3p	1.858793042	1.58E–08	5.18E–07	Up
hsa-miR-320e	1.904827788	1.72E–08	5.44E–07	Up
hsa-miR-4279	–2.564714404	1.76E–12	7.51E–10	Down
hsa-miR-3124-3p	–2.474608778	5.60E–12	1.19E–09	Down
hsa-miR-4728-3p	–2.455455298	1.21E–11	2.07E–09	Down
hsa-miR-4635	–2.393092709	1.54E–11	2.19E–09	Down
hsa-miR-4537	–2.418295745	5.96E–11	7.27E–09	Down
hsa-miR-642b-5p	–2.298345262	8.63E–11	9.21E–09	Down
hsa-miR-5196-3p	–2.172908344	3.75E–10	3.20E–08	Down
hsa-miR-877-3p	–2.202854847	4.82E–10	3.51E–08	Down
hsa-miR-4290	–2.27123672	4.93E–10	3.51E–08	Down
hsa-miR-4268	–2.219462893	1.40E–09	8.54E–08	Down

ES, effect size; FDR, false discovery rate.

TABLE 4 | The top 10 upregulated and downregulated mRNAs in GC.

ID	Symbol	Combined.ES	*p*-value	FDR	Up/down
9997	SCO2	1.400471	<0.001	<0.001	Up
9991	ROD1	1.325606	<0.001	<0.001	Up
9966	TNFSF15	1.160469	<0.001	<0.001	Up
995	CDC25C	1.639835	<0.001	<0.001	Up
994	CDC25B	1.62622	<0.001	<0.001	Up
993	CDC25A	1.407589	<0.001	<0.001	Up
9928	KIF14	2.287231	<0.001	<0.001	Up
9926	LPGAT1	1.19746	<0.001	<0.001	Up
9918	NCAPD2	1.645622	<0.001	<0.001	Up
991	CDC20	1.774075	<0.001	<0.001	Up
9992	KCNE2	−1.72329	<0.001	<0.001	Down
9934	P2RY14	−1.90515	<0.001	<0.001	Down
9905	SGSM2	−1.00543	<0.001	<0.001	Down
9892	SNAP91	−1.27282	<0.001	<0.001	Down
9886	RHOBTB1	−1.07693	<0.001	<0.001	Down
9874	TLK1	−1.11589	<0.001	<0.001	Down
9867	PJA2	−1.7726	<0.001	<0.001	Down
9832	JAKMIP2	−1.09529	<0.001	<0.001	Down
9829	DNAJC6	−1.03815	<0.001	<0.001	Down
9783	RIMS3	−1.64884	<0.001	<0.001	Down

ES, effect size; FDR, false discovery rate.

kinase 1 (MAP2K1)], and chemokine signaling pathway [involved LYN proto-oncogene, Src family tyrosine kinase (LYN)] were significantly enriched signaling pathways (**Figure 4** and **Table 5**).

PPI Network of Immune-Related mRNAs in the ceRNA Regulatory Network

In order to further explore the interaction between immune-related mRNAs in the regulatory ceRNA network, the PPI network was established (**Figure 5**). Six core immune-related mRNAs were identified by four algorithms, namely, FGF10, MET, NRAS, RAC1, MAP2K1, and LYN (**Figure 6**). It is worth mentioning that FGF10 (AUC = 0.764), MET (AUC = 0.829), NRAS (AUC = 0.840), RAC1 (AUC = 0.797), MAP2K1 (AUC = 0.813), and LYN (AUC = 0.817) had a potential diagnostic value for GC (**Figure 7**). It was indicated that these mRNAs had a diagnostic potential for GC. In addition, the ceRNA subnetwork (involving 59 circRNAs and 10 miRNAs) based on the above six mRNAs was constructed (**Figure 8**). The ceRNA subnetwork contains 75 nodes and 124 edges. Some ceRNA relationship pairs were identified, such as hsa_circ_0050102–hsa-miR-4537–NRAS, hsa_circ_0001013–hsa-miR-485-3p–MAP2K1, hsa_circ_0003763–hsa-miR-145-5p–FGF10, hsa_circ_0001789–hsa-miR-1269b–MET, hsa_circ_0040573–hsa-miR-3686–RAC1, and hsa_circ_0006089–hsa-miR-5584-3p–LYN. In addition, xCell was used to calculate the distribution of immune cells in each sample based on the ssGSEA method. The types of immune cells were different in the GC group from those in the normal control group. For example, Tgd cells and adipocytes were the most upregulated and downregulated types of immune cells in GC (**Figure 9**). The Pearson correlation coefficient method was used to calculate the correlation between above six mRNAs of differential immune cells (**Figure 10**). The result showed that NRAS, RAC1, and MAP2K1 were positively correlated with Tgd cells. FGF10 was positively correlated with StromaScore. LYN and MET were negatively correlated with neurons and adipocytes, respectively.

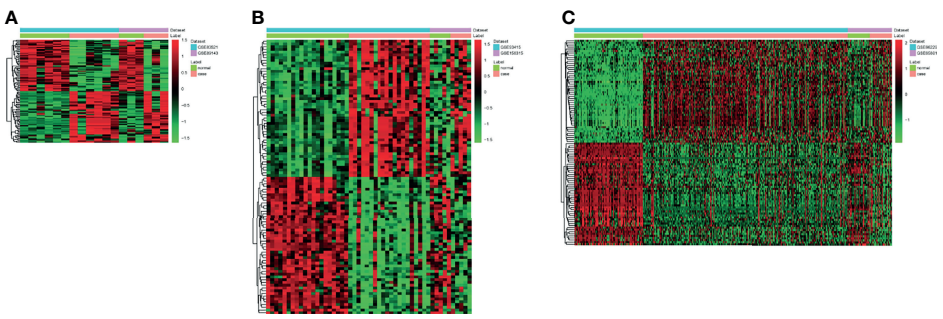

FIGURE 1 | The heat map of the top 100 differentially expressed circRNAs **(A)**, miRNAs **(B)**, and mRNAs **(C)** in gastric cancer (GC).

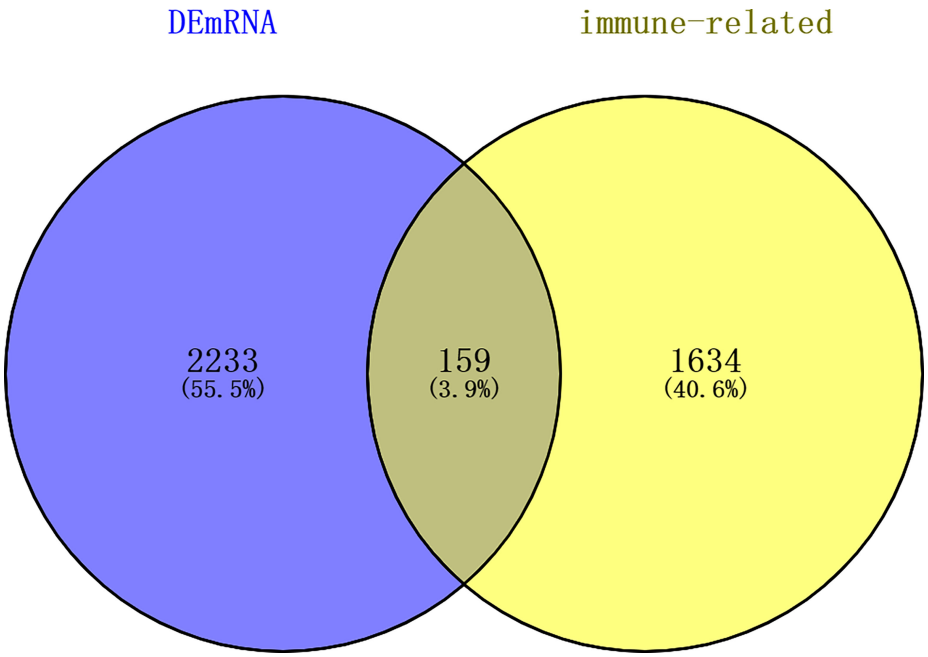

FIGURE 2 | Venn diagram of differentially expressed mRNAs in GC and immune-related mRNAs in the ImmPort database. dEmRNA, differentially expressed mRNA.

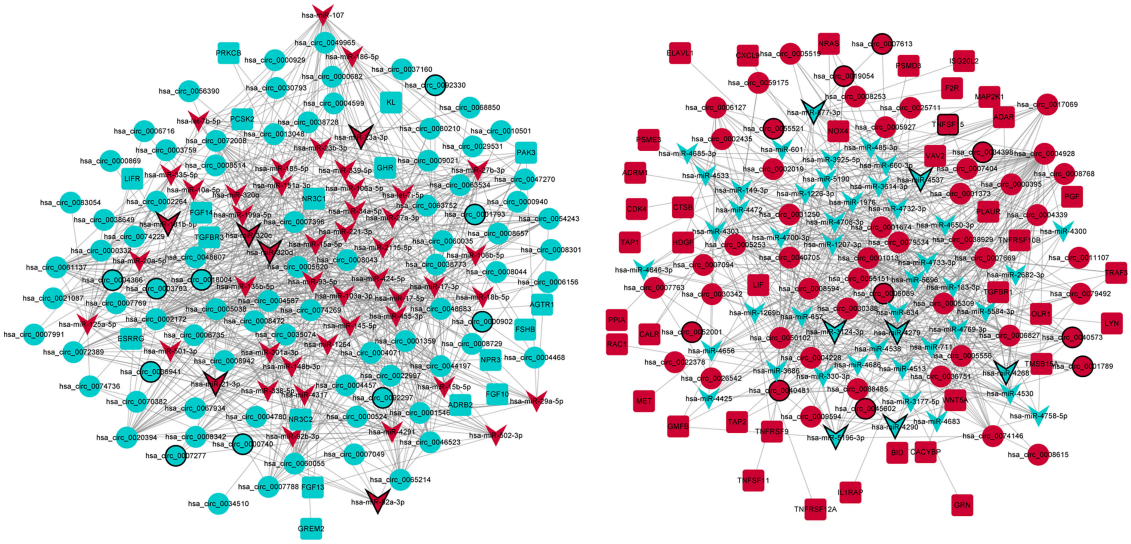

FIGURE 3 | The ceRNA (circRNA–miRNA–immune-related mRNA) regulatory network in GC. Circle, V shape, and rectangle represent differentially expressed circRNA, miRNA, and mRNA, respectively. Red and green represent upregulation and downregulation, respectively. The black border represents the top 10 up/downregulated circRNAs/miRNAs/mRNAs.

Expression Validation of Differentially Expressed circRNAs and Immune-Related mRNAs

To further validate the expression of identified circRNAs and immune-related mRNAs, electronic validation was performed. The GSE93541 dataset (**Figure 11A**) and the GSE141977 dataset (**Figure 11B**) were used for expression validation of hsa_circ_0003763, hsa_circ_0004928, and hsa_circ_0040573. The result showed that hsa_circ_0003763 was downregulated and hsa_circ_0004928 and hsa_circ_0040573 were upregulated

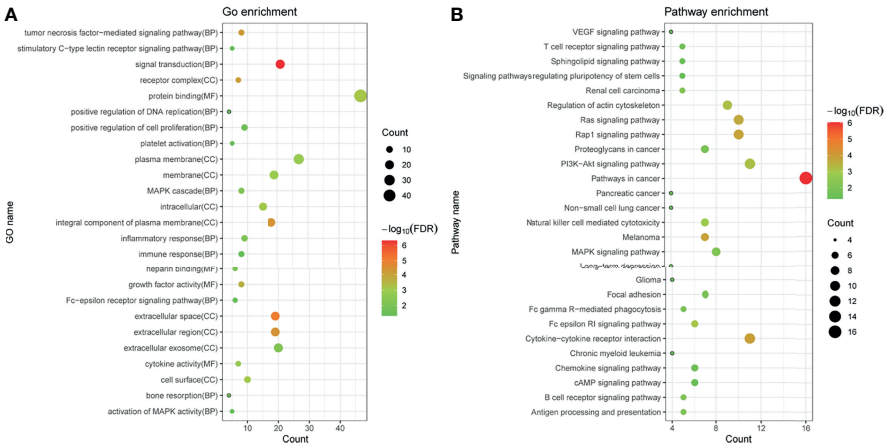

FIGURE 4 | GO **(A)** and KEGG **(B)** enrichment analyses of immune-related mRNAs in the regulatory ceRNA network in GC. BP, biological process; CC, cytological component; MF, molecular function.

TABLE 5 | KEGG enrichment analysis of immune-related mRNAs in the ceRNA regulatory network in GC.

Term	Count	*p*-value	FDR	mRNAs
hsa05200:Pathways in cancer	16	8.65E−09	9.34E−07	MAP2K1, PRKCB, F2R, WNT5A, TGFBR1, PGF, NRAS, FGF14, TRAF3, CDK4, AGTR1, RAC1, FGF13, BID, MET, FGF10
hsa04060:Cytokine–cytokine receptor interaction	11	2.17E−06	1.17E−04	GHR, CXCL9, TNFRSF12A, TNFSF15, TNFRSF9, LIF, TNFSF11, TNFRSF10B, LIFR, IL1RAP, TGFBR1
hsa05218:Melanoma	7	5.05E−06	1.47E−04	MAP2K1, NRAS, FGF14, CDK4, FGF13, MET, FGF10
hsa04015:Rap1 signaling pathway	10	5.43E−06	1.47E−04	MAP2K1, NRAS, FGF14, PRKCB, F2R, RAC1, FGF13, MET, PGF, FGF10
hsa04014:Ras signaling pathway	10	9.89E−06	2.14E−04	MAP2K1, NRAS, FGF14, PRKCB, RAC1, FGF13, PAK3, MET, PGF, FGF10
hsa04810:Regulation of actin cytoskeleton	9	4.54E−05	7.33E−04	MAP2K1, NRAS, FGF14, F2R, RAC1, FGF13, PAK3, VAV2, FGF10
hsa04151:PI3K–Akt signaling pathway	11	4.75E−05	7.33E−04	GHR, MAP2K1, NRAS, FGF14, CDK4, F2R, RAC1, FGF13, MET, PGF, FGF10
hsa04664:Fc epsilon RI signaling pathway	6	6.55E−05	8.85E−04	LYN, MAP2K1, NRAS, PRKCB, RAC1, VAV2
hsa04650:Natural killer cell mediated cytotoxicity	7	1.12E−04	0.001343	MAP2K1, NRAS, PRKCB, TNFRSF10B, RAC1, BID, VAV2
hsa05211:Renal cell carcinoma	5	7.86E−04	0.008494	MAP2K1, NRAS, RAC1, PAK3, MET
hsa04662:B-cell receptor signaling pathway	5	9.30E−04	0.009003	LYN, MAP2K1, NRAS, RAC1, VAV2
hsa04010:MAPK signaling pathway	8	0.001	0.009003	MAP2K1, NRAS, FGF14, PRKCB, RAC1, FGF13, TGFBR1, FGF10
hsa04612:Antigen processing and presentation	5	0.001337	0.011104	PSME3, TAP2, TAP1, CALR, CTSB
hsa05205:Proteoglycans in cancer	7	0.001573	0.012138	MAP2K1, NRAS, PRKCB, WNT5A, PLAUR, RAC1, MET
hsa04510:Focal adhesion	7	0.00183	0.013074	MAP2K1, PRKCB, RAC1, PAK3, MET, PGF, VAV2
hsa04666:Fc gamma R-mediated phagocytosis	5	0.001937	0.013074	LYN, MAP2K1, PRKCB, RAC1, VAV2
hsa04660:T-cell receptor signaling pathway	5	0.003655	0.023221	MAP2K1, NRAS, CDK4, PAK3, VAV2
hsa05223:Non-small cell lung cancer	4	0.005345	0.032068	MAP2K1, NRAS, PRKCB, CDK4
hsa04062:Chemokine signaling pathway	6	0.006326	0.034272	LYN, MAP2K1, CXCL9, NRAS, RAC1, VAV2
hsa04730:Long-term depression	4	0.006482	0.034272	LYN, MAP2K1, NRAS, PRKCB
hsa04370:VEGF signaling pathway	4	0.006787	0.034272	MAP2K1, NRAS, PRKCB, RAC1
hsa04071:Sphingolipid signaling pathway	5	0.006981	0.034272	MAP2K1, NRAS, PRKCB, RAC1, BID
hsa05214:Glioma	4	0.008093	0.035418	MAP2K1, NRAS, PRKCB, CDK4
hsa05212:Pancreatic cancer	4	0.008093	0.035418	MAP2K1, CDK4, RAC1, TGFBR1
hsa04024:cAMP signaling pathway	6	0.008199	0.035418	MAP2K1, FSHB, F2R, RAC1, ADRB2, VAV2
hsa05220:Chronic myeloid leukemia	4	0.010713	0.044498	MAP2K1, NRAS, CDK4, TGFBR1
hsa04550:Signaling pathways regulating pluripotency of stem cells	5	0.01188	0.047521	MAP2K1, NRAS, WNT5A, LIF, LIFR

FDR, false discovery rate.

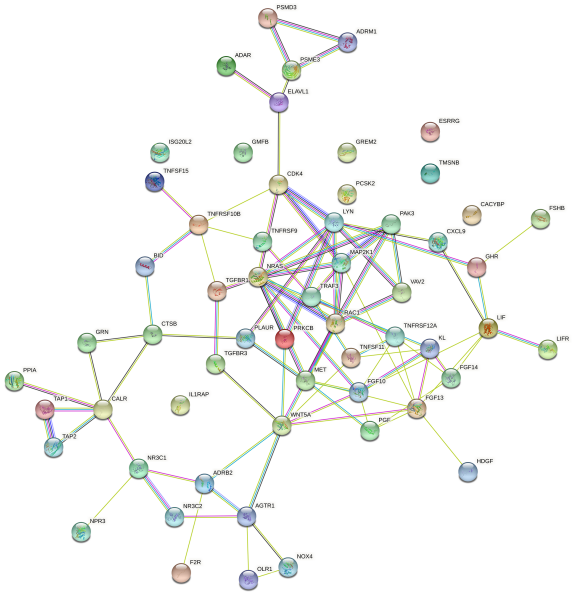

FIGURE 5 | The PPI network of immune-related mRNAs in the regulatory ceRNA network in GC.

in GC. Although there was no significant difference (may be caused by the small sample size), the expression trend was consistent with the integrated analysis results. In addition, the TCGA dataset was used to validate the expression of FGF10, MET, NRAS, RAC1, MAP2K1, and LYN (**Figure 12**). The result showed that FGF10 was significantly downregulated. MET, NRAS, RAC1, MAP2K1, and LYN were remarkably upregulated in GC, which is in line with the integrated analysis results.

To validate the expression of two circRNAs (hsa_circ_0003763 and hsa_circ_0004928) and four immune-related mRNAs (FGF10, MET, RAC1, and LYN), blood samples from five GC patients and five normal controls were collected for qRT-PCR (**Figure 13**). The clinical information of these individuals is listed in **Table 6**. The qRT-PCR result showed that RAC1 and LYN were significantly upregulated in GC, which was consistent with the integrated analysis results, while the expression trends of hsa_circ_0004928, MET, hsa_circ_0003763, and FGF10 were the same with the integrated analysis results without statistical significance.

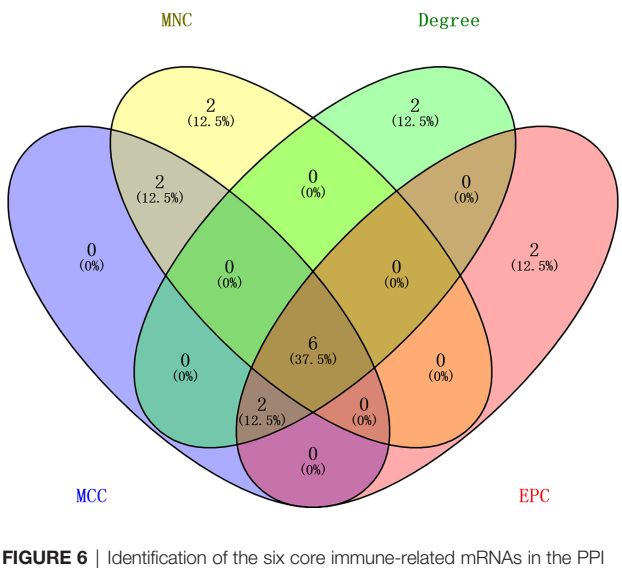

FIGURE 6 | Identification of the six core immune-related mRNAs in the PPI network *via* four algorithms in GC.

DISCUSSION

Up to now, no articles about hsa_circ_0050102 have been reported in any diseases. hsa_circ_0003763 was associated with pancreatic ductal adenocarcinoma (22). hsa_circ_0003763 was upregulated in hepatocellular carcinoma tissues and facilitated the invasion of hepatocellular carcinoma cells (23). hsa-miR-4537 was associated with vitreoretinal lymphoma (24). hsa-miR-145-5p played key roles in GC epithelial cells and affected cell invasion and migration of GC cells (25). In GC cells, hsa-miR-145-5p has been verified as the direct target of has_circ_0000376 (26). It has been demonstrated that hsa_circ_DLST can act as the sponge of has-miR-502-5p to regulate the NRAS/MAP kinase/ERK kinase 1/2 signaling pathways in GC cells (27). FGF10, a secreted factor, stimulated the proliferation of lung cancer cells (28). In GC, FGF10 was involved in several signaling pathways (29). Tgd cells were related to the prognosis of patients with stomach adenocarcinoma (30). In this study, we found regulatory pairs of hsa_circ_0050102–hsa-miR-4537–NRAS–Tgd cells and hsa_circ_0003763–hsa-miR-145-5p–FGF10–StromaScore in GC, among which, NRAS and FGF10 had potential diagnostic value for patients. In addition, NRAS and FGF10 were involved in both Rap1 and Ras signaling pathways in GC. Rap1 played important roles in the metastasis and invasion of various tumor cells by regulating cytoskeleton remodeling. In GC, some differentially expressed angiogenesis-related genes were associated with the Rap1 signaling pathway (31). Genes involved in the Ras signaling pathway were found in approximately 40% of GC patients (32). It has been suggested that regulatory networks of hsa_circ_0050102–hsa-miR-4537–NRAS–Tgd cells and hsa_circ_0003763–hsa-miR-145-5p–FGF10–StromaScore may play important roles in the proliferation, migration, and invasion of GC by involving signaling pathways of Rap1 and Ras.

hsa_circ_0040573 was found in human umbilical vein endothelial cell line (33). It was shown that RAC1 was an essential effector of GC malignant transformation and metastasis (34, 35). In gastric cancer tissues, the expression of RAC1 was increased, which was significantly related to TNM

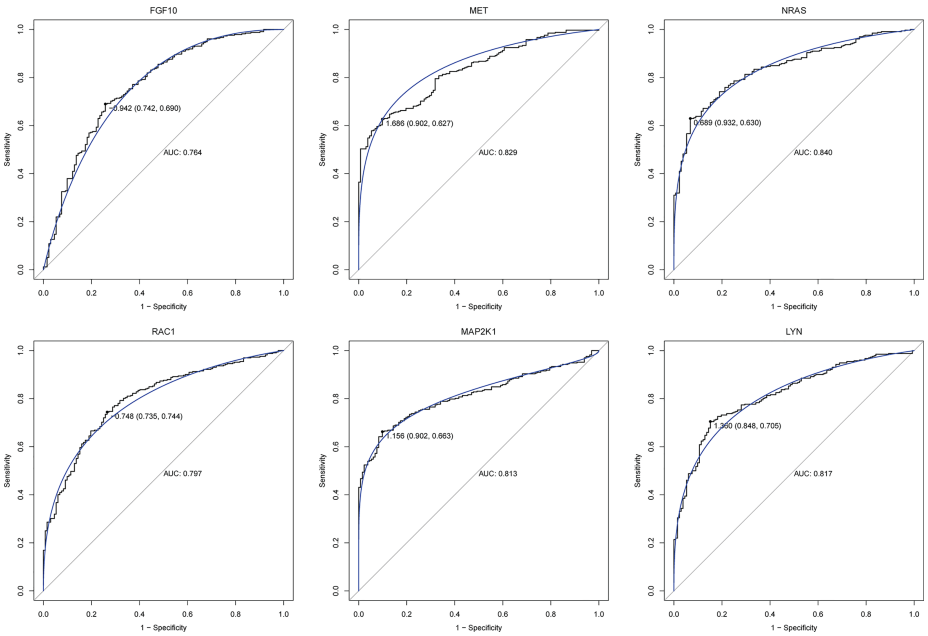

FIGURE 7 | ROC analysis of six core immune-related mRNAs in the PPI network in GC.

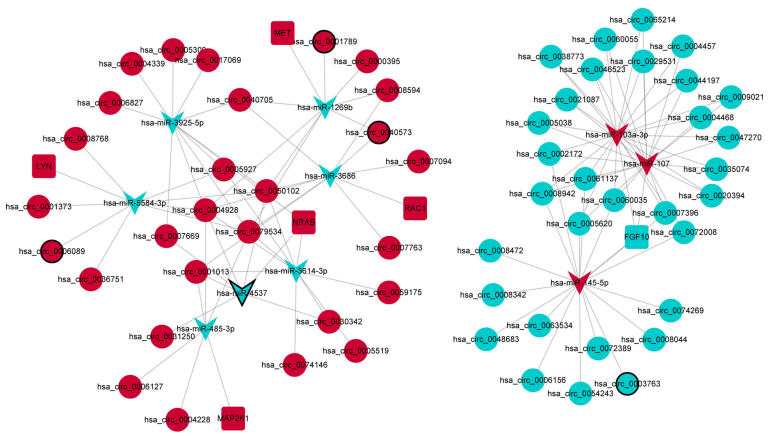

FIGURE 8 | The ceRNA subnetwork based on six core immune-related mRNAs in the PPI network in GC. Circle, V shape, and rectangle represent differentially expressed circRNA, miRNA, and mRNA, respectively. Red and green represent upregulation and downregulation, respectively. The black border represents the top 10 up/downregulated circRNAs/miRNAs/mRNAs.

stage (36). Herein, we found the regulatory pairs of hsa_circ_0040573–hsa-miR-3686–RAC1–Tgd cells in GC. It was noted that RAC1 had potential diagnostic value for patients. Moreover, RAC1 was associated with Fc gamma R-mediated phagocytosis and cAMP signaling pathway. Fc gamma R-mediated phagocytosis was found in plasma exosomes from GC patients (37). It has been demonstrated that there was a significant positive correlation between nuclear factor kappa B (NF-κB) and cAMP-regulated phosphoprotein expression level in GC tissues (38). Thus, it can be seen that hsa_circ_0040573, RAC1, and Tgd cells played a crucial role in malignant transformation, metastasis, and TNM stage of GC.

The expression of hsa_circ_0001789 was found in GC (39). hsa-miR-1269b was downregulated in basal cell carcinoma and GC (40, 41). MET can be internalized by macrophages to educate them toward a protumorigenic phenotype (42). In addition, the

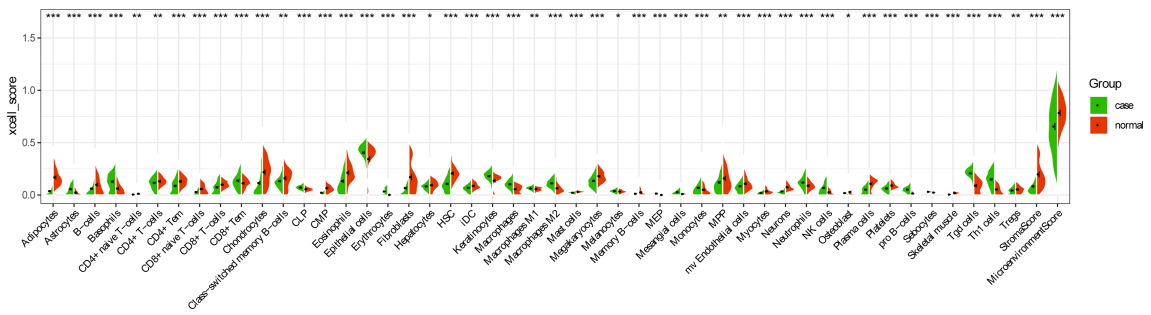

FIGURE 9 | Distribution of immune cell types in GC. *$p < 0.05$; **$p < 0.01$; ***$p < 0.001$.

upregulated paracrine hepatocyte growth factor can bind the c-MET receptor on the migrated GC cells to facilitate the proliferation of metastatic GC cells (43). In fat tissues, adipocytes regulated cancer development by their effects on the microenvironment. A previous report preliminarily showed that omental adipocytes could promote GC cell invasiveness (44). Herein, we found a regulatory pair of hsa_circ_0001789–hsa-miR-1269b–MET–adipocytes in GC. MET had a potential diagnostic value for patients. Furthermore, MET was involved in proteoglycans in cancer in GC. In gastric epithelia, the basal surface of cells was surrounded by the basement membrane, which was mainly composed of glycoproteins (45–47). The proteoglycan signaling pathway has been found in GC (48). It was indicated that the regulatory pair of hsa_circ_0001789–hsa-miR-1269b–MET–adipocytes played roles in cell proliferation and invasiveness of GC.

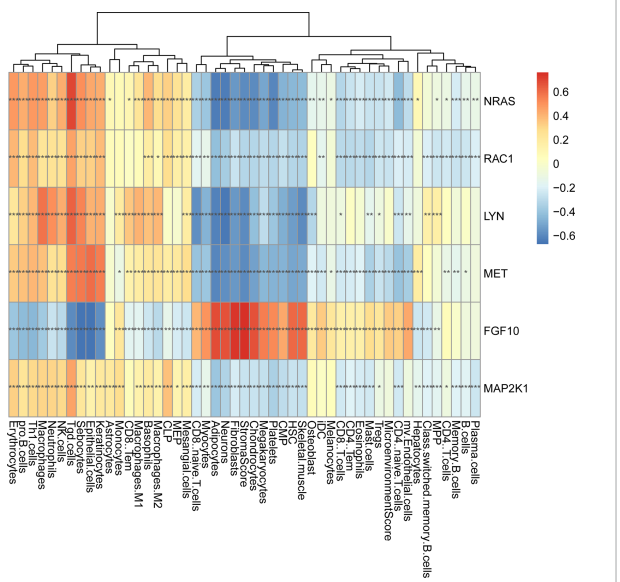

FIGURE 10 | The correlation analysis between six core immune-related mRNAs and immune cells in GC. *$p < 0.05$; **$p < 0.01$; ***$p < 0.001$.

hsa_circ_0001013, upregulated in GC, regulated the expression of fibrillin 1 through competing with miRNA response elements of hsa-miRNA-182-5p, which led to metastasis in GC (49). hsa-miR-485-3p, a key regulator of gastrointestinal stromal tumors, served as a molecular biomarker and potential therapeutic target for this malignant disease (50). The role of hsa-miR-485-3p has been found in GC cells (51). MAP2K1 was involved in the PD-L1 pathway in GC (52). In our study, we found the regulatory network of hsa_circ_0001013–hsa-miR-485-3p–MAP2K1–Tgd cells in GC, among which, MAP2K1 had a potential diagnostic value for GC patients. In addition, MAP2K1 was enriched in T-cell receptor signaling pathway. Our result indicated that hsa_circ_0001013, hsa-miR-485-3p, MAP2K1, and Tgd cells may be associated with tumor metastasis in the development of GC.

hsa-miR-5584-3p played important roles in tongue squamous cell carcinoma by interacting with hsa_circ_087212 (53). LYN was significantly downregulated in gastric gastrointestinal stromal tumors with high-grade malignancy (54). In this study, we found the relationship between hsa_circ_0006089, hsa-miR-5584-3p, and LYN. Moreover, LYN had a potential diagnostic value and was negatively correlated with neurons. In addition, LYN was involved in chemokine signaling pathway. It was suggested that chemokines and their specific receptors can play an important role in GC progression *via* promotion of angiogenesis, invasion, survival, and metastasis (55). This indicated that the regulatory network of hsa_circ_0006089–hsa-miR-5584-3p–LYN–neurons played important roles in angiogenesis, invasion, survival, and metastasis of GC.

Besides the above circRNA–miRNA–immune-related mRNA regulatory network, some other circRNA–miRNA–mRNA regulatory networks were also found in GC, such as hsa_circ_0045602–hsa-miR-4538–WNT5A and hsa_circ_0018004–hsa-miR-199a-5p–KL. hsa_circ_0045602 was upregulated in GC tumor tissues (56). The expression of hsa-miR-4538 was decreased in acute myeloid leukemia (57). hsa-miR-199a-5p level was significantly increased in GC tissues.

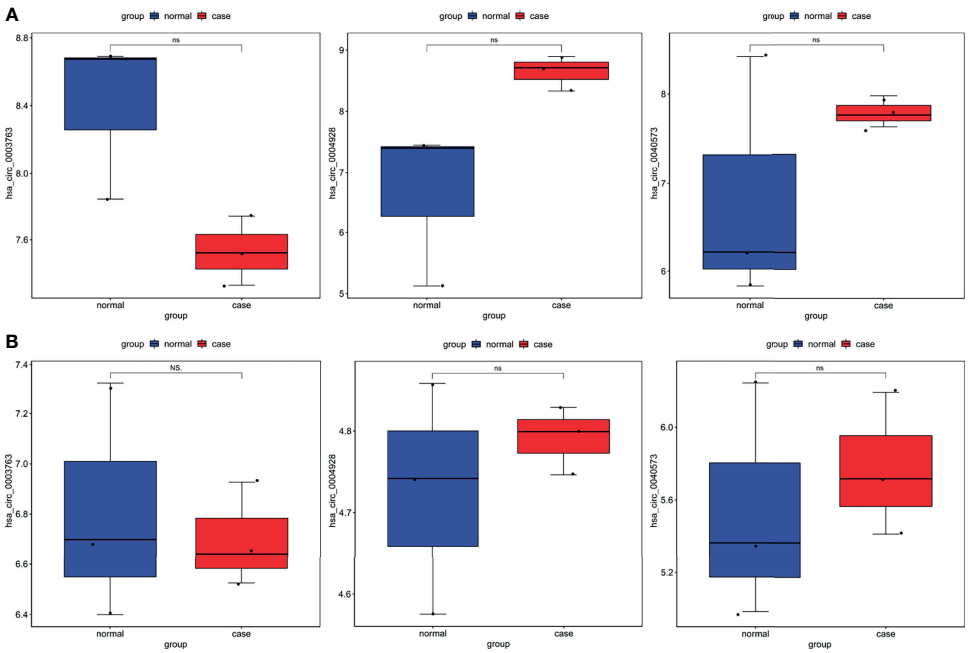

FIGURE 11 | Expression validation of hsa_circ_0003763, hsa_circ_0004928, and hsa_circ_0040573 in the GSE93541 dataset **(A)** and GSE141977 dataset **(B)**. Ns, no significant difference.

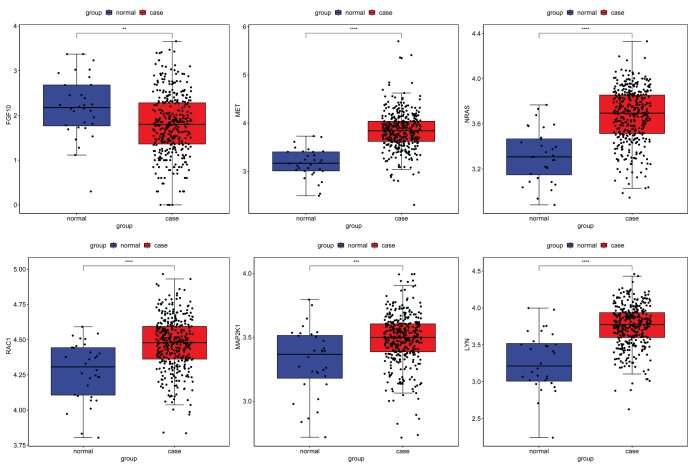

FIGURE 12 | Expression validation of FGF10, MET, NRAS, RAC1, MAP2K1, and LYN in the TCGA dataset. $^{**}p < 0.01$; $^{***}p < 0.001$; $^{****}p < 0.0001$.

Moreover, a higher miR-199a-5p expression level of hsa-miR-199a-5p promoted the invasion of GC cells and was related to increased likelihood of lymph node metastasis (58). Thus, it can be seen that these molecules may be involved in tumor cell invasion and metastasis of GC.

In conclusion, our study found several ceRNA (circRNA–miRNA–immune-related mRNA) regulatory networks including hsa_circ_0050102–hsa-miR-4537–NRAS–Tgd cells, hsa_circ_0001013–hsa-miR-485-3p–MAP2K1–Tgd cells, hsa_circ_0003763–hsa-miR-145-5p–FGF10–StromaScore, hsa_circ_0001789–hsa-miR-1269b–MET–adipocytes, hsa_circ_0040573–hsa-miR-3686–RAC1–Tgd cells, and hsa_circ_0006089–hsa-miR-5584-3p–LYN–neurons in GC, among which FGF10, MET, NRAS, RAC1, MAP2K1, and LYN had a potential diagnostic value for GC patients. In addition, some signaling pathways were identified, such as Rap1 and Ras

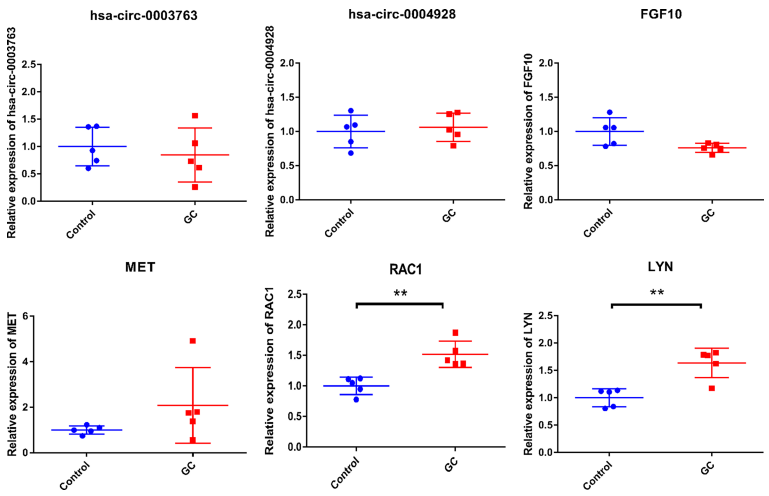

FIGURE 13 | *In-vitro* validation of hsa_circ_0003763, hsa_circ_0004928, FGF10, MET, RAC1, and LYN. ***p*-value < 0.01.

TABLE 6 | Clinical information of individuals in the *in-vitro* experiment.

Group	Age (years)	Gender	Height (cm)	Weight (kg)	Pathological grading	Clinical staging			Differentiated degree	Metastasis	Metastatic site	Smoking history	Drinking history
					Stage I, II, III, IV	T	N	M	(G1, 2, 3, 4)				
Control 1	63	Female	158	52	NA	NA	NA	NA	NA	NA	NA	No	No
Control 2	45	Female	156	54.5	NA	NA	NA	NA	NA	NA	NA	No	No
Control 3	66	Female	161	57	NA	NA	NA	NA	NA	NA	NA	No	No
Control 4	39	Female	159	59	NA	NA	NA	NA	NA	NA	NA	No	No
Control 5	59	Female	153	57	NA	NA	NA	NA	NA	NA	NA	No	No
GC 1	66	Male	170	73.2	IA	pT1a	0	0	G3	No	No	No	No
GC 2	58	Male	173	49	IIIB	pT4a	3a	0	G1	No	No	No	No
GC 3	70	Male	160	48	cIVB	cT4a	x	1	G3	Yes	Cervical lymph node	No	No
GC 4	58	Male	168	63.9	IV	cTx	x	1	Gx	Yes	Liver	Yes	Yes
GC 5	54	Female	158	56.6	IV	cT4	x	1	Gx	Yes	Abdominal cavity, left adnexa, and ascites	Yes	No

NA, not applicable.

signaling pathways (involved NRAS and FGF10), Fc gamma R-mediated phagocytosis and cAMP signaling pathway (involved RAC1), proteoglycans in cancer (involved MET), T-cell receptor signaling pathway (involved MAP2K1), and chemokine signaling pathway (involved LYN). Our study may provide a novel field for understanding the molecular mechanisms of GC at the immunological levels. However, there are limitations to our study. Firstly, larger numbers of samples in qRT-PCR are needed. Secondly, an *in-vitro* gastric cell line experiment in cultures and tissues from healthy and gastric cancer patients is further needed to confirm the results of the *in-silico* analyses. Thirdly, the cell reporter assay for miRNA–circRNA–mRNA interaction is further needed.

DATA AVAILABILITY STATEMENT

The original contributions presented in the study are included in the article/supplementary material. Further inquiries can be directed to the corresponding author.

ETHICS STATEMENT

All participating individuals provided informed consent with the approval of the Ethics Committee of Zhejiang Hospital (2021-164K). The patients/participants provided their written informed consent to participate in this study.

AUTHOR CONTRIBUTIONS

GZ was the major contributor in the subject design. GZ contributed administrative support. PL provided the materials and samples and collected and sorted the data. ZW and GZ contributed to the data analysis and interpretation. All authors read and approved the final manuscript.

REFERENCES

1. Torre LA, Bray F, Siegel RL, Ferlay J, Lortet-Tieulent J, Jemal A. Global Cancer Statistics, 2012. *CA: Cancer J Clin* (2015) 65(2):87–108. doi: 10.3322/caac.21262
2. Sung H, Ferlay J, Siegel RL. Global Cancer Statistics 2020: GLOBOCAN Estimates of Incidence and Mortality Worldwide for 36 Cancers in 185 Countries. *CA Cancer J Clin* (2021) 71: (3):209–49. doi: 10.3322/caac.21660
3. Ferlay J, Colombet M, Soerjomataram I, Parkin DM. Cancer Statistics for the Year 2020: An Overview. *Int J Cancer* (2021). doi: 10.1002/ijc.33588
4. Parkin DM. The Global Health Burden of Infection-Associated Cancers in the Year 2002. *Int J Cancer* (2006) 118(12):3030–44. doi: 10.1002/ijc.21731
5. Al-Mahrouqi H, Parkin L, Sharples K. Incidence of Stomach Cancer in Oman and the Other Gulf Cooperation Council Countries. *Oman Med J* (2011) 26 (4):258–62. doi: 10.5001/omj.2011.62
6. IARC Working Group on the Evaluation of Carcinogenic Risks to Humans. Personal Habits and Indoor Combustions. Volume 100 E. A Review of Human Carcinogens. IARC Monographs on the Evaluation of Carcinogenic Risks to Humans. *IARC Monogr Eval Carcinog Risks Hum* (2012) 100: (Pt E):1–538.
7. Plummer M, Franceschi S, Vignat J, Forman D, de Martel C. Global Burden of Gastric Cancer Attributable to Helicobacter Pylori. *Int J Cancer* (2015) 136 (2):487–90. doi: 10.1002/ijc.28999
8. Moss SF. The Clinical Evidence Linking Helicobacter Pylori to Gastric Cancer. *Cell Mol Gastroenterol Hepatol* (2017) 3(2):183–91. doi: 10.1016/j.jcmgh.2016.12.001
9. Nagini S. Carcinoma of the Stomach: A Review of Epidemiology, Pathogenesis, Molecular Genetics and Chemoprevention. *World J Gastrointest Oncol* (2012) 4(7):156–69. doi: 10.4251/wjgo.v4.i7.156
10. Van Cutsem E, Sagaert X, Topal B, Haustermans K, Prenen H. Gastric Cancer. *Lancet (London England)* (2016) 388(10060):2654–64. doi: 10.1016/S0140-6736(16)30354-3
11. Petkovic S, Müller S. RNA Circularization Strategies *In Vivo* and *In Vitro*. *Nucleic Acids Res* (2015) 43(4):2454–65. doi: 10.1093/nar/gkv045
12. Pereira AL, Magalhães L, Pantoja RP, Araújo G, Ribeiro-Dos-Santos Â, Vidal AF. The Biological Role of Sponge Circular RNAs in Gastric Cancer: Main Players or Coadjuvants? *Cancers (Basel)* (2020) 12 (7):1982. doi: 10.3390/cancers12071982
13. Zhang J, Liu H, Hou L, Wang G, Zhang R, Huang Y, et al. Circular RNA_LARP4 Inhibits Cell Proliferation and Invasion of Gastric Cancer by Sponging miR-424-5p and Regulating LATS1 Expression. *Mol Cancer* (2017) 16(1):151. doi: 10.1186/s12943-017-0719-3
14. Zhang X, Wang S, Wang H, Cao J, Huang X, Chen Z, et al. Circular RNA Circnrip1 Acts as a microRNA-149-5p Sponge to Promote Gastric Cancer Progression *via* the AKT1/mTOR Pathway. *Mol Cancer* (2019) 18(1):20. doi: 10.1186/s12943-018-0935-5
15. Zhu Z, Rong Z, Luo Z, Yu Z, Zhang J, Qiu Z, et al. Circular RNA Circnhsl1 Promotes Gastric Cancer Progression Through the miR-1306-3p/SIX1/vimentin Axis. *Mol Cancer* (2019) 18(1):126. doi: 10.1186/s12943-019-1054-7
16. Zhang L, Song X, Chen X, Wang Q, Zheng X, Wu C, et al. Circular RNA CircCACTIN Promotes Gastric Cancer Progression by Sponging MiR-331-3p and Regulating TGFBR1 Expression. *Int J Biol Sci* (2019) 15(5):1091–103. doi: 10.7150/ijbs.31533
17. Zhang Z, Yu X. Circular RNA Circ_0026359 Enhances Cisplatin Resistance in Gastric Cancer *via* Targeting miR-1200/POLD4 Pathway. *Biomed Res Int* (2020) 2020:. doi: 10.1155/2020/5103272
18. Wang F, Meng W, Wang B, Qiao L. Helicobacter Pylori-Induced Gastric Inflammation and Gastric Cancer. *Cancer Lett* (2014) 345(2):196–202. doi: 10.1016/j.canlet.2013.08.016
19. Yolanda LV, Sergio PD, Hugo ES, Isabel AF, Rafael BZ, Aldo TD, et al. Gastric Cancer Progression Associated With Local Humoral Immune Responses. *BMC Cancer* (2015) 15:924. doi: 10.1186/s12885-015-1858-9
20. Tsujimoto H, Ono S, Ichikura T, Matsumoto Y, Yamamoto J, Hase K. Roles of Inflammatory Cytokines in the Progression of Gastric Cancer: Friends or Foes? *Gastric Cancer* (2010) 13(4):212–21. doi: 10.1007/s10120-010-0568-x
21. Aran D, Hu Z, Butte AJ. Xcell: Digitally Portraying the Tissue Cellular Heterogeneity Landscape. *Genome Biol* (2017) 18(1):220. doi: 10.1186/s13059-017-1349-1
22. Guo X, Zhou Q, Su D, Luo Y, Fu Z, Huang L, et al. Circular RNA circBFAR Promotes the Progression of Pancreatic Ductal Adenocarcinoma *via* the miR-34b-5p/MET/Akt Axis. *Mol Cancer* (2020) 19(1):83. doi: 10.1186/s12943-020-01196-4
23. Li K, Cao J, Zhang Z, Chen K, Ma T, Yang W, et al. Circular RNA Circgsk3b Promotes Cell Proliferation, Migration, and Invasion by Sponging miR-1265 and Regulating CAB39 Expression in Hepatocellular Carcinoma. *Front Oncol* (2020) 10:598256. doi: 10.3389/fonc.2020.598256
24. Minezaki T, Usui Y, Asakage M, Takanashi M, Shimizu H, Nezu N, et al. High-Throughput MicroRNA Profiling of Vitreoretinal Lymphoma: Vitreous and Serum MicroRNA Profiles Distinct From Uveitis. *J Clin Med* (2020) 9 (6):1844. doi: 10.3390/jcm9061844
25. Zhou K, Song B, Wei M, Fang J, Xu Y. MiR-145-5p Suppresses the Proliferation, Migration and Invasion of Gastric Cancer Epithelial Cells *via* the ANGPT2/NOD_LIKE_RECEPTOR Axis. *Cancer Cell Int* (2020) 20:416. doi: 10.1186/s12935-020-01483-6
26. Ju C, Zhou J, Miao H, Chen X, Zhang Q. Bupivacaine Suppresses the Progression of Gastric Cancer Through Regulating Circ_0000376/miR-145-5p Axis. *BMC Anesthesiol* (2020) 20(1):275. doi: 10.1186/s12871-020-01179-4
27. Zhang J, Hou L, Liang R, Chen X, Zhang R, Chen W, et al. CircDLST Promotes the Tumorigenesis and Metastasis of Gastric Cancer by Sponging miR-502-5p and Activating the NRAS/MEK1/ERK1/2 Signaling. *Mol Cancer* (2019) 18(1):80. doi: 10.1186/s12943-019-1015-1
28. Suzuki T, Yasuda H, Funaishi K, Arai D, Ishioka K, Ohgino K, et al. Multiple Roles of Extracellular Fibroblast Growth Factors in Lung Cancer Cells. *Int J Oncol* (2015) 46(1):423–9. doi: 10.3892/ijo.2014.2718
29. Carino A, Graziosi L, Marchianò S, Biagioli M, Marino E, Sepe V, et al. Analysis of Gastric Cancer Transcriptome Allows the Identification of Histotype Specific Molecular Signatures With Prognostic Potential. *Front Oncol* (2021) 11:663771. doi: 10.3389/fonc.2021.663771
30. Hong C, Yang S, Wang Q, Zhang S, Wu W, Chen J, et al. Epigenetic Age Acceleration of Stomach Adenocarcinoma Associated With Tumor Stemness Features, Immunoactivation, and Favorable Prognosis. *Front Genet* (2021) 12:563051. doi: 10.3389/fgene.2021.563051
31. Cai WY, Dong ZN, Fu XT, Lin LY, Wang L, Ye GD, et al. Identification of a Tumor Microenvironment-Relevant Gene Set-Based Prognostic Signature and Related Therapy Targets in Gastric Cancer. *Theranostics* (2020) 10 (19):8633–47. doi: 10.7150/thno.47938
32. Hatakeyama M. Helicobacter Pylori CagA and Gastric Cancer: A Paradigm for Hit-and-Run Carcinogenesis. *Cell Host Microbe* (2014) 15(3):306–16. doi: 10.1016/j.chom.2014.02.008
33. O'Leary VB, Smida J, Matjanovski M, Brockhaus C, Winkler K, Moertl S, et al. The circRNA Interactome-Innovative Hallmarks of the Intra- and Extracellular Radiation Response. *Oncotarget* (2017) 8(45):78397–409. doi: 10.18632/oncotarget.19228
34. Xue Y, Bi F, Zhang X, Pan Y, Liu N, Zheng Y, et al. Inhibition of Endothelial Cell Proliferation by Targeting Rac1 GTPase With Small Interference RNA in Tumor Cells. *Biochem Biophys Res Commun* (2004) 320(4):1309–15. doi: 10.1016/j.bbrc.2004.06.088
35. Xue Y, Bi F, Zhang X, Zhang S, Pan Y, Liu N, et al. Role of Rac1 and Cdc42 in Hypoxia Induced P53 and Von Hippel-Lindau Suppression and HIF1alpha Activation. *Int J Cancer* (2006) 118(12):2965–72. doi: 10.1002/ijc.21763
36. Li P, Chen X, Su L, Li C, Zhi Q, Yu B, et al. Epigenetic Silencing of miR-338-3p Contributes to Tumorigenicity in Gastric Cancer by Targeting SSX2IP. *PloS One* (2013) 8(6):e66782. doi: 10.1371/journal.pone.0066782

37. Rao M, Zhu Y, Qi L, Hu F, Gao P. Circular RNA Profiling in Plasma Exosomes From Patients With Gastric Cancer. *Oncol Lett* (2020) 20(3):2199–208. doi: 10.3892/ol.2020.11800
38. Zhu S, Soutto M, Chen Z, Peng D, Romero-Gallo J, Krishna US, et al. Helicobacter Pylori-Induced Cell Death Is Counteracted by NF-κb-Mediated Transcription of DARPP-32. *Gut* (2017) 66(5):761–2. doi: 10.1136/gutjnl-2016-312141
39. Xia Y, Lv J, Jiang T, Li B, Li Y, He Z, et al. CircFAM73A Promotes the Cancer Stem Cell-Like Properties of Gastric Cancer Through the miR-490-3p/HMGA2 Positive Feedback Loop and HNRNPK-Mediated β-Catenin Stabilization. *J Exp Clin Cancer Res: CR* (2021) 40(1):103. doi: 10.1186/s13046-021-01896-9
40. Wei HP, Zhan S, Zhu QA, Chen ZJ, Feng X, Chen JY, et al. Genome-Wide Expression Difference of MicroRNAs in Basal Cell Carcinoma. *J Immunol Res* (2021) 2021:7223500. doi: 10.1155/2021/7223500
41. Zhang C, Zhang CD, Ma MH, Dai DQ. Three-microRNA Signature Identified by Bioinformatics Analysis Predicts Prognosis of Gastric Cancer Patients. *World J Gastroenterol* (2018) 24(11):1206–15. doi: 10.3748/wjg.v24.i11.1206
42. Che Y, Geng B, Xu Y, Miao X, Chen L, Mu X, et al. Helicobacter Pylori-Induced Exosomal MET Educates Tumour-Associated Macrophages to Promote Gastric Cancer Progression. *J Cell Mol Med* (2018) 22(11):5708–19. doi: 10.1111/jcmm.13847
43. Huang T, Song C, Zheng L, Xia L, Li Y, Zhou Y. The Roles of Extracellular Vesicles in Gastric Cancer Development, Microenvironment, Anti-Cancer Drug Resistance, and Therapy. *Mol Cancer* (2019) 18(1):62. doi: 10.1186/s12943-019-0967-5
44. Xiang F, Wu K, Liu Y, Shi L, Wang D, Li G, et al. Omental Adipocytes Enhance the Invasiveness of Gastric Cancer Cells by Oleic Acid-Induced Activation of the PI3K-Akt Signaling Pathway. *Int J Biochem Cell Biol* (2017) 84:14–21. doi: 10.1016/j.biocel.2016.12.002
45. Frantz C, Stewart KM, Weaver VM. The Extracellular Matrix at a Glance. *J Cell Sci* (2010) 123(Pt 24):4195–200. doi: 10.1242/jcs.023820
46. Egeblad M, Nakasone ES, Werb Z. Tumors as Organs: Complex Tissues That Interface With the Entire Organism. *Dev Cell* (2010) 18(6):884–901. doi: 10.1016/j.devcel.2010.05.012
47. Xu R, Boudreau A, Bissell MJ. Tissue Architecture and Function: Dynamic Reciprocity *via* Extra- and Intra-Cellular Matrices. *Cancer Metastasis Rev* (2009) 28(1-2):167–76. doi: 10.1007/s10555-008-9178-z
48. Sandoval-Bórquez A, Polakovicova I, Carrasco-Véliz N, Lobos-González L, Riquelme I, Carrasco-Avino G, et al. MicroRNA-335-5p Is a Potential Suppressor of Metastasis and Invasion in Gastric Cancer. *Clin Epigenet* (2017) 9:114. doi: 10.1186/s13148-017-0413-8
49. Tian Y, Xing Y, Zhang Z. Bioinformatics Analysis of Key Genes and circRNA-miRNA-mRNA Regulatory Network in Gastric Cancer. *Biomed Res Int* (2020) 2020. doi: 10.1155/2020/2862701
50. Jia N, Tong H, Zhang Y, Katayama H, Wang Y, Lu W, et al. CeRNA Expression Profiling Identifies KIT-Related circRNA-miRNA-mRNA Networks in Gastrointestinal Stromal Tumour. *Front Genet* (2019) 10:825. doi: 10.3389/fgene.2019.00825
51. Sun HD, Xu ZP, Sun ZQ, Zhu B, Wang Q, Zhou J, et al. Down-Regulation of Circpvrl3 Promotes the Proliferation and Migration of Gastric Cancer Cells. *Sci Rep* (2018) 8(1):10111. doi: 10.1038/s41598-018-27837-9
52. Du Z, Yan D, Li Z, Gu J, Tian Y, Cao J, et al. Genes Involved in the PD-L1 Pathway Might Associate With Radiosensitivity of Patients With Gastric Cancer. *J Oncol* (2020) 2020:7314195. doi: 10.1155/2020/7314195
53. Wei T, Ye P, Yu GY, Zhang ZY. Circular RNA Expression Profiling Identifies Specific Circular RNAs in Tongue Squamous Cell Carcinoma. *Mol Med Rep* (2020) 21(4):1727–38. doi: 10.3892/mmr.2020.10980
54. Shen C, Yin Y, Chen H, Wang R, Yin X, Cai Z, et al. Secreted Protein Acidic and Rich in Cysteine-Like 1 Suppresses Metastasis in Gastric Stromal Tumors. *BMC Gastroenterol* (2018) 18(1):105. doi: 10.1186/s12876-018-0833-8
55. Pawluczuk E, Łukaszewicz-Zając M, Mroczko B. The Role of Chemokines in the Development of Gastric Cancer - Diagnostic and Therapeutic Implications. *Int J Mol Sci* (2020) 21(22):8456. doi: 10.3390/ijms21228456
56. Zhang Y, Wang M, Zang X, Mao Z, Chen Y, Mao F, et al. CircHN1 Affects Cell Proliferation and Migration in Gastric Cancer. *J Clin Lab Anal* (2020) 34: (10): e23433. doi: 10.1002/jcla.23433
57. Ma QL, Wang JH, Yang M, Wang HP, Jin J. MiR-362-5p as a Novel Prognostic Predictor of Cytogenetically Normal Acute Myeloid Leukemia. *J Trans Med* (2018) 16(1):68. doi: 10.1186/s12967-018-1445-3
58. He XJ, Ma YY, Yu S, Jiang XT, Lu YD, Tao L, et al. Up-Regulated miR-199a-5p in Gastric Cancer Functions as an Oncogene and Targets Klotho. *BMC Cancer* (2014) 14:218. doi: 10.1186/1471-2407-14-218

Conflict of Interest: The authors declare that the research was conducted in the absence of any commercial or financial relationships that could be construed as a potential conflict of interest.

Publisher's Note: All claims expressed in this article are solely those of the authors and do not necessarily represent those of their affiliated organizations, or those of the publisher, the editors and the reviewers. Any product that may be evaluated in this article, or claim that may be made by its manufacturer, is not guaranteed or endorsed by the publisher.

frontiers | Frontiers in Oncology

TYPE Systematic Review
PUBLISHED 13 September 2022
DOI 10.3389/fonc.2022.828339

OPEN ACCESS

EDITED BY
Kanjoormana Aryan Manu,
Amala Cancer Research Centre, India

REVIEWED BY
Amit Gupta,
All India Institute of Medical Sciences, India
Kin Israel Notarte,
Johns Hopkins Medicinee, United States
Priyanka Sharma,
University of Texas MD Anderson Cancer Center, United States

*CORRESPONDENCE
Yong Yuan
yongyuan@scu.edu.cn

†These authors have contributed equally to this work

SPECIALTY SECTION
This article was submitted to Gastrointestinal Cancers: Gastric and Esophageal Cancers, a section of the journal Frontiers in Oncology

RECEIVED 03 December 2021
ACCEPTED 24 August 2022
PUBLISHED 13 September 2022

CITATION
Fang P, Zhou J, Li X, Luan S, Xiao X, Shang Q, Zhang H, Yang Y, Zeng X and Yuan Y (2022) Prognostic value of micro-RNA 375, 133, 143, 145 in esophageal carcinoma: A systematic review and meta-analysis. *Front. Oncol.* 12:828339. doi: 10.3389/fonc.2022.828339

Prognostic value of micro-RNA 375, 133, 143, 145 in esophageal carcinoma: A systematic review and meta-analysis

Pinhao Fang[1†], Jianfeng Zhou[1†], Xiaokun Li[1†], Siyuan Luan[1], Xin Xiao[1], Qixin Shang[1], Hanlu Zhang[1], Yushang Yang[1], Xiaoxi Zeng[2] and Yong Yuan[1*]

[1]Department of Thoracic Surgery, West China Hospital, Sichuan University, Chengdu, China, [2]West China Biomedical Big Data Center, West China Hospital, Sichuan University, Chengdu, China

Many studies have confirmed that micro-RNA (mir) is related to the prognosis of esophageal carcinoma (EC), suggesting the mir could be used to guide the therapeutic strategy of EC. Some of mir molecules are considered as favorable prognostic factors for EC. The purpose of our study is to evaluate the prognostic potential of mir-375, 133, 143, 145 in primary EC, we summarized all the results from available studies, aiming delineating the prognostic role of mir in EC. Relevant studies were identified by searching databases including Medline, Embase, Web of science, Cochrane Library. The studies which explored the prognostic value of mir-375, 133, 143, 145 expressions on survival outcomes in patients with EC were included in this study. The hazard ratios (HR) and their responding 95% confidence interval (CI) were also extracted. A total of 25 studies were collected, including 1260 patients, and the prognostic values of four mirs in EC were analyzed. Survival outcomes including overall survival (OS), progression-free survival (PFS) and disease-free survival (DFS) were used as the primary endpoint to evaluate the prognostic value of mir. The pooled analysis results showed that up-regulation of mir-375 indicated favorable OS (HR=0.50; 95%CI: 0.37-0.69; P<0.001). In addition, the up-regulation of mir-133 (HR=0.40, 95%CI: 0.24-0.65, P<0.001), 143 (HR=0.40, 95%CI: 0.21-0.76, P < 0.001) and 145 (HR=0.55, 95%CI: 0.34-0.90, P<0.001) are also proved as protected factors in EC. Therefore, our study demonstrated that these mirs may have the potential to be used as prognostic biomarkers for EC in clinical practice.

KEYWORDS

micro-RNA, esophageal carcinoma, prognosis, meta-analysis, biomaker

Introduction

Esophageal carcinoma (EC) is a common and fatal gastrointestinal malignant tumor which is a group of heterogeneous malignancies including squamous cell carcinoma (ESCC) and adenocarcinoma (EAC). Its clinical characters are associated with races, geographical distribution and other risk factors. EC is currently the sixth most common cancer worldwide (1), and is also one of the most deadly malignant tumor (2). According to the latest research, in 2020, there were 604000 cases of EC and 544000 deaths worldwide (3). Since the symptoms of early stage in EC are easy to be neglected, patients with EC are often diagnosed at late stage, and the optimum opportunity for surgery is lost (4). As a result, the five-year survival rate of EC patients is low, only about 30% (5). Although the advancement in therapeutic technologies including surgery, chemotherapy, radiotherapy and other novel treatments for EC has been greatly upgraded (6), it is still essential to find new biological markers to assess the prognosis of EC patients after surgery (7).

Non-coding RNA plays a vital role in cancer biology and provides potential targets for cancer intervention (8, 9). Early studies had indicated that non-coding RNA had the potential clinical utility for diagnosing and prognosticating cancers (10). One type of non-coding RNA is called micro-RNA (mir), which ranges in size from 20-24 nucleotides (11). In recent years, many studies have confirmed that mirs regulate gene expression by targeting mRNA for translational inhibition or cleavage, thereby involving in various biological phenotypes such as cell proliferation, differentiation, and apoptosis (11–13). Some mirs are considered to be related to the occurrence and development of tumors. Meanwhile, some of them were used as biomarkers for cancer detection and prognosis (14, 15). Mir-375 has been confirmed by studies that it is widely present in various tissues, which has been characterized as an important cancer-related mir (16, 17). The expression of mir-375 has been proved significantly reduced in malignant tumor cells (18). Several studies had reported that mir-375 were related to the prognosis of EC with low-expression in cancer tissue (19, 20), but nowadays, some more new researches were conducted to detect the mechanism of mir-375 may involve in EC, especially in prognosis, we collected entire of these data to make an update. On the other side, no published meta-analysis had investigated the impact of mir-133, 143, 145 on EC prognosis. In order to comprehensively and systematically investigate these mirs in EC prognosis, we conducted this meta-analysis to investigate the prognostic value of mir-375, 133, 143 and 145 while discussing the therapeutic potentialities of these mirs.

Materials and methods

Literature retrieval strategy

In order to obtain potentially eligible documents, we carefully searched the Medline, Embase, Web of science, Cochrane Library databases using the following search strategies and terms: (((((((esophageal cancer [Title/Abstract]) OR esophageal carcinoma [Title/Abstract]) OR esophageal squamous cell carcinoma [Title/Abstract]) OR esophageal esophageal adenocarcinoma [Title/Abstract])) AND (((MicroRNA [Title/Abstract]) OR miRNAs[Title/Abstract]) OR RNA, Micro [Title/Abstract])) AND (((prognostic [Title/Abstract]) OR prognosis [Title/Abstract]) OR survival [Title/Abstract])) updated until July 1, 2022. The retrieved related reviews and meta-analysis lists are also manually checked to identify more relevant information.

Inclusion and exclusion criteria

The eligible studies included in this meta-analysis meet the following criteria (1): studies have reported specific methods of collecting mirs through surgical resection or blood collection and measuring their expression (2); the patients in studies had received treatment options such as surgery, radiotherapy or chemotherapy; (3) studies clearly illustrate the correlation between mir expression and survival outcomes of patients such as overall survival (OS), disease-free survival (DFS), progression-free survival (PFS), et al; (4) the patients were grouped according to the level of mir expression; (5) sufficient data are reported, and the hazard ratio (HR) and 95% confidence interval (CI) of mir expression can be retrieved based on the data in the article. The exclusion criteria are: (1) non-esophageal carcinoma patients; (2) duplicated studies; (3) studies using only *in vitro* cell lines; (4) animal experiments; (5) reviews, letters, case reports and expert opinions; (6) data could not be extracted or original data was lost.

Data extraction and quality assessment

All eligible research data and information are independently extracted by two independent researchers (Fang and Zhou). The collected data information of various studies including: author, publication year, race, cancer type, patient number, sample type, mir detection method, survival outcomes, cut-off value and its 95% confidence interval. Based on the study population, intervention, comparison and outcome (PICO) format, the PICO of this study is defined bellow: P: patients with EC; I: patients with high mirs expression level; C: patients with low mirs expression level; O: survival outcomes. To reduce the bias of data extraction, the survival curve data was evaluated by other independent individual (Li), and the Engauge Digitizer version 4.1 software was used to analyze the survival curve. The original data and additional information needed for this study were obtained by contacting the authors of the included studies. The Newcastle-Ottawa Scale (NOS) was applied to assess the quality of all included studies (S1). The NOS scores including selection,

comparability, and outcome, the score ≥6 was considered as study with high quality (21).

Statistical analysis

The high or low expression of mir is defined according to the cut-off value provided by the author. The pooled HR and the corresponding 95% confidence interval were used to assess the correlation between mir expression and prognosis. All statistical analyses of this Meta-analysis are performed using Stata12.0 software (StataCorp, College Station, TX, USA) in accordance with PRISMA (S2) guidelines. The heterogeneity among the included studies was determined by the chi-square-based Q test and the I^2 statistics; the *P* value of the Q test was ≤0.05; the I^2 value ≥50% considered that the study had significant heterogeneity, the random-effects model was used to pool the effect size ($P_Q \leq 0.05$, $I^2 \geq 50\%$). If the *P* value of the Q test was >0.05; the I^2 value <50%, we considered that the research heterogeneity is acceptable ($P_Q > 0.05$, $I^2 < 50\%$), and the fixed-effects model was used to analysis. To reduce the heterogeneity among studies and understand the prognostic value of mir-375, basing on multiple criteria we conducted a subgroup analysis of cancer type, sample type, race. To test the reliability of the main outcomes in our analysis, we conducted a sensitivity analysis of the included studies by removing one single study in turn and estimated whether there was publication bias among the studies using Begg's test by assessing the asymmetry of an inverted funnel plot.

Results

According to the mentioned criteria above, we have identified 25 studies from the preliminary literature search from databases shown in the flow diagram (Figure 1). Exclude duplicate documents 560 articles. After screening the research title and abstract, 231 articles that are not related to the research content are excluded. We read the full text of 55 articles, and further excluded 32 articles because relevant data could not be extracted or couldn't meet the inclusion criteria. A total of 25 published studies met the inclusion criteria for our meta-analysis which had analyzed the correlation between mir and EC survival outcomes. There are a total of 13 studies reported the prognosis of mir-375 and EC (16, 22–31), 12 articles reported mir-133 (32–34), mir-143 (35–37) and mir-145 (38–43), and all of these studies discussed the prognosis of EC. The total number of patients included in the study was 1260, ranging from 22-249. The category of cancer is ESCC or EAC and quantitative real-time PCR (qRT-PCR), microarray et al, were used to detect the

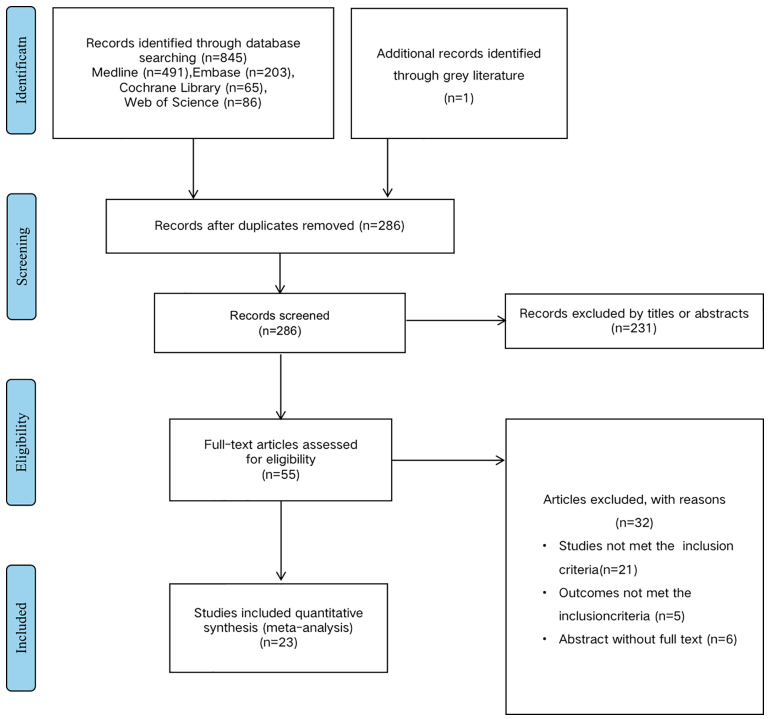

FIGURE 1
Methodological flow chart of the review.

expression of mir in tissue or blood. The cut-off values of mir expression varied in different studies, 20 studies reported the cut-off value of mir, including the mean, median, percentile, and fixed value. For mir-375, 9 studies were conducted in Asian populations, and 4 were conducted in Western. The study populations of mir-143 and mir-133 were only Asian race, as for mir-145, both patients in Asia and Western countries were included. More detailed information is summarized in (Table 1).

To evaluate the OS for mir-375, a random-effects model was applied since there was heterogeneity among (I^2 = 61.2%, P=0.002), pooled HR was 0.50 (95%CI: 0.37-0.69, P<0.001), in addition, the high expression of mir-375 showed no correlation with PFS the pooled HR was 0.88 (95%CI:0.37-2.06, P>0.05) (Figure 2), indicating that up-regulated mir-375 may be associated with better OS in EC. As for mir-143 (I^2 = 0.0%, P=0.795) and mir-133 (I^2 = 0.0%, P=0.823) studies evaluating OS were of no statistical heterogeneity, we use a fixed model to pool the HR. The results showed that up-regulated mir-143 and mir-133 was significantly associated with good OS outcome in ESCC with the pooled HR were 0.40 (95%CI: 0.21-0.76, P<0.001) and 0.40 (95%CI: 0.24-0.65, P<0.001) (Figure 3). On the other hand, to evaluate the prognosis of mir-145, we use fixed model to pool the HR, because there were no statistical heterogeneity found in the OS (I^2 = 0.0%, P=0.592) and DFS (I^2 = 0.0%, P=0.901) of mir-145, the results showed that high expression of mir-145 was associated with good OS in EC pooled HR was 0.55 (95%CI:0.34-0.90, P<0.001) but no correction was found in DFS because the pooled HR was 1.27 (95%CI: 0.41-3.98, P>0.05) (Figure 4). As shown in the figure, we have performed a sensitivity analysis picture of mir-375 to see if a single study could have significant impact on the pooled HR for survival, the results were not significant altered by removing anyone of the included studies, and Begg's funnel chart (Figure 5) shows that no significant publication bias has been found (P=0.142). Based on the NOS assessment, the scores of these studies were from 6 to 7, indicating that the quality of the included studies is high, therefor all studies could be used in the subsequent analysis.

Because the heterogeneity among the effect size of mir-375, we conducted a subgroup analysis to find more information. The subgroups were stratified based on following criteria: cancer type, sample type, race. In the subgroup of patient race, we found that up-regulation of mir-375 significantly related to good prognosis in Asian patients (HR: 0.44, 95%CI: 0.32-0.60, P<0.01; random) but not in western patients (HR: 0.68, 95% CI: 0.35-1.31, P>0.05; random) and there was heterogeneity in the data, so we use random-effects model to analysis (Figure 6). In cancer type subgroup, higher mir-375 expression related to good prognosis in ESCC (HR:0.48, 95%CI: 0.34-0.67, P<0.01; random), no correlation was found in patients with EAC (HR: 0.68, 95%CI: 0.13-3.45, P>0.05; random) (Figure 7). The association between higher mir-375 expression and good OS outcomes was statistically significant in sample type from patients' tissue (HR: 0.51, 95%CI: 0.36-0.71, P<0.01; random) but not from plasma (HR: 0.47, 95%CI: 0.16-1.39, P>0.05; random) (Figure 8). The pooled HR value and their 95%CI in each subgroup are demonstrated in figures above. By conducting such subgroup analysis could we find the impact of higher mir-375 expression on prognosis of EC patients with different clinical characteristics.

Discussion

In recent years, various mirs have been confirmed to exhibit prognostic value in a variety of human cancers, and a great many of mirs have also been proved acting as a co-effector with other elements in tumor progression such as: cellular proliferation, survival, migration, and immune evasion. Thus, the mirs play an important role in the field of malignant tumor (10). The study by Zhao et al (44), showed that mir-375 not only reduced the

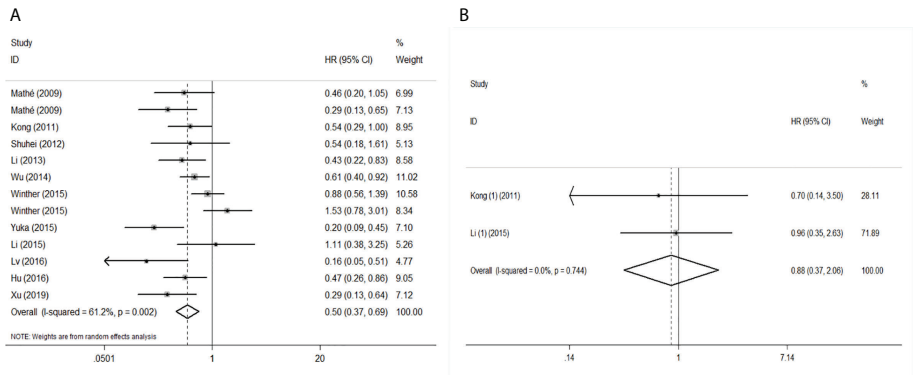

FIGURE 2
Forest plot of pooled HR of mir-375 in predicting survival outcomes in EC. **(A)** mir-375 and OS. **(B)** mir-375 and PFS.

TABLE 1 The main characteristics of all included studies in this meta-analysis.

Micro-RNA	Name	Year	Population	Sample	Cancer type	Treatment	N	HR source	Cut-off	Age	Method	RESULT	NOS score
Mir-375	Mathé	2009	American	Tissue	ESCC	Surgery and chemoradiation	70	Multi	Median	<62: 28; ≥62: 42	Microarray and qRT-PCR	OS	6
	Mathé	2009	American	Tissue	EAC	Surgery and chemoradiation	62	Multi	Median	NA	Microarray and qRT-PCR	OS	6
	Li	2013	Chinese	Tissue	ESCC	Surgery	249	NA	NA	<60: 105; ≥60: 144	ISH	OS	7
	Wu	2014	Chinese	Tissue	ESCC	Surgery	194	Multi	Mean	<60: 106; ≥60: 88	qRT-PCR	OS	7
	Lv	2016	Chinese	Plasma	ESCC	Surgery	126	NA	Median	Mean 59.3	Microarray	OS	7
	Hu	2016	Chinese	Tissue	EC	Surgery	88	Multi	Mean	≥65: 57; <65: 31	qRT-PCR	OS	6
	Winther	2015	Danish	Tissue	ESCC	nCRT and surgery	129	NA	Median	36–81, mean 63	qRT-PCR	OS	7
	Winther	2015	Danish	Tissue	EAC	nCRT and surgery	66	NA	Median	32–86, mean 64	qRT-PCR	OS	7
	Xu	2019	Chinese	Tissue	ESCC	Surgery	43	Multi	The 75th percentile	41-79	qRT-PCR	OS	6
	Kong	2011	Chinese	Tissue	ESCC	Surgery	60	NA	NA	≤66:23; >66: 37	qRT-PCR	OS	6
	Kong (1)	2011	Chinese	Tissue	ESCC	Surgery	60	NA	NA	≤66:23; >66: 37	qRT-PCR	PFS	6
	Shuhei	2012	Japanese	Plasma	ESCC	Surgery	50	Multi	ROC curves	≤65: 25; >65: 25	qRT-PCR	OS	7
	Yuka	2015	Japanese	Tissue	ESCC	Surgery	85	NA	NA	≤65:37; >65: 48	qRT-PCR	OS	7
	Li	2015	Chinese	Plasma	ESCC	Radiotherapy and surgery	38	NA	Median	<65: 17; ≥65: 21	qRT-PCR	OS	6
	Li (1)	2015	Chinese	Plasma	ESCC	Radiotherapy and surgery	38	NA	Median	<65: 17; ≥65: 21	qRT-PCR	PFS	6
Mir-133	Lin	2017	Chinese	Tissue	ESCC	NA	58	Multi	NA	<65: 34; ≥65: 24	ISH	OS	6
	Gao	2016	Chinese	Tissue	ESCC	Surgery	126	Multi	Median	<55: 57; ≥55: 69	qRT-PCR	OS	7
	Akanuma	2014	Japanese	Tissue	ESCC	Surgery	140	Uni	Normal pair	<65: 81; ≥65: 59	qRT-PCR	OS	7
Mir-143	Liu	2019	Chinese	Tissue	ESCC	Surgery	44	Uni	Normal pair	<50: 19; ≥50: 25	qRT-PCR	OS	6
	He	2016	Chinese	Tissue	ESCC	Surgery	80	Multi	50-fold change	Mean 60	qRT-PCR	OS	6
	Zhang	2016	Chinese	Tissue	ESCC	Chemotherapy and surgery	31	Uni	NA	18–75	qRT-PCR	OS	6
Mir-145	Tanaka	2013	Japanese	Tissue	ESCC	nCRT and surgery	64	Uni	Median	45–80, median 67.5	qRT-PCR	DFS	6
	Augustine	2012	Canadian	Tissue	EC	Surgery and chemoradiation	25	NA	Median	NA	Microarray	DFS	6
	Feber	2011	British	Tissue	EAC	Surgery	45	Uni	Median	NA	Microarray	OS	6
	Jin	2019	Chinese	Tissue	ESCC	Surgery	126	Multi	Median	≥60, 57; <60, 69	qRT-PCR	OS	7

(Continued)

TABLE 1 Continued

Micro-RNA	Name	Year	Population	Sample	Cancer type	Treatment	N	HR source	Cut-off	Age	Method	RESULT	NOS score
	Shimonosono	2018	Japanese	Tissue	ESCC	Surgery	22	NA	Median	52-84	qRT-PCR	OS	6
	Hamano	2015	Japanese	Tissue	EC	Surgery and chemotherapy	98	Multi	Median	63.2 ± 8.5	qRT-PCR	OS	7

Tissue, including patients'samples from frozen tissues and formalin-fixed paraffin-embedded; ESCC, esophageal squamous cell cancer; EAC, esophageal adenocarcinoma; EC, esophageal carcinoma; nCRT, neoadjuvant chemoradiation therapy; ISH, in situ hybridization; qRT-PCR, quantitative real-time PCR; NA, information not afforded; OS, overall survival; DFS, disease-free survival; PFS, progression-free survival; (1), the same study conducted by same author, and the author use PFS as the survival outcome to analyze.

stemness, but also decreased adriamycin resistance of breast cancer cells, indicating that mir-375 may inhibit the stemness breast cancer cells by targeting JAK2. Xie et al (45), have proved that low expression of mir-375 are significantly correlated with the occurrence and development of liver cancer. Furthermore, Zhang et al (46), found that mir-133 could inhibit the growth of triple-negative breast cancer by targeting YES1. In general, mir-143 and 145 were also clarified that they played a crucial role in suppressing tumor developing in other human cancer (47, 48). Beyond that, Yi et al (49), proved in their study that mir-375 could suppresses ESCC cells invasion and metastasis by direct targeting of SHOX2 and the interaction of mir-375 and SHOX2 could still affect EMT phenotypes. In addition, the down-regulated level of mir-375 was detected in primary ESCC, and was significantly associated with advanced stage and distant metastasis. The results of the study conducted by Osako et al (50), showed that mir-375 markedly inhibits cancer cell migration and invasion by regulation of MMP13 in ESCC, demonstrating that mir-375 may involve in MMP13 axis and affect the occurrence and development of EC.

Mirs played a key role in tumor pathology, that might partly clarify the association between their expression and EC prognosis and made mirs become a hotspot in oncology researching field. Considering the high mortality rates of EC may partly due to the lack of accurate prognostic biomarkers, in recent years, growing number of researchers had investigated the prognostic value of mirs in EC. Gao et al (51), conducted a meta-analysis focusing on mirs affecting EC prognosis. In their study, the number of literatures investigating these mirs was only 12 which was dated up to 2018. In our study, we made an upgradation of data focusing on mir-375,133,143 and 145 (the specific number of included studies is double to Gao's) published up to November 20, 2021. Importantly, we included 15 studies which investigated the correlation between mir-375 expression and clinical survival outcomes of EC patients. With sufficient studies amount, we could achieve subgroup analysis to comprehensively and systematically investigate these mirs in EC prognosis and to make the conclusion more convincing. Up-regulations of mir-375,133,143 and 145 are associated with favorable prognosis. In addition, according to recent reports, mir was also used as a potential therapeutic targeted molecule in tumor. Many researches had tested the mechanism mirs involving in therapy to anti various human cancers. A study conducted by Campayo showed that up-regulation of mir-375 can increase the sensitivity of rectal cancer cells to chemoradiotherapy (52). On the other hand, Xu et al (53), showed mir-375 could enhance chemosensitivity to 5-fluorouracil in colorectal cancer. Fu et al (54), demonstrated that mir-375 could degrade HOXB3 and inhibit tamoxifen resistance in human breast cancer. Furthermore, Weidle et al (55), showed in their study that mir-133 had a negative impact on regulating cell-cycle and apotosis in gastric carcinoma.

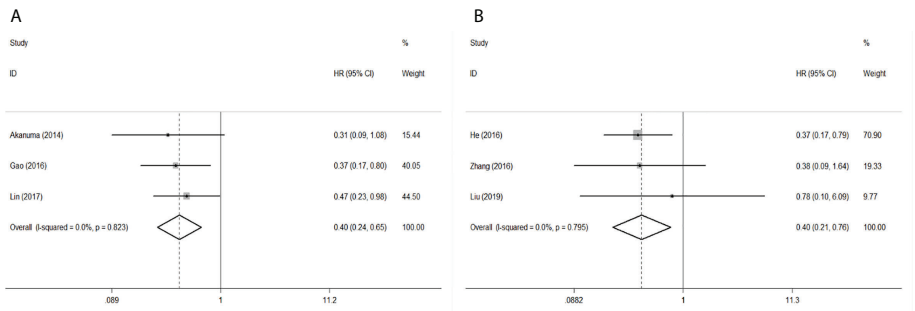

FIGURE 3
Forest plot of pooled HR of mir-133 and mir-143 in predicting survival outcomes OS in EC. **(A)** mir-133. **(B)** mir-143.

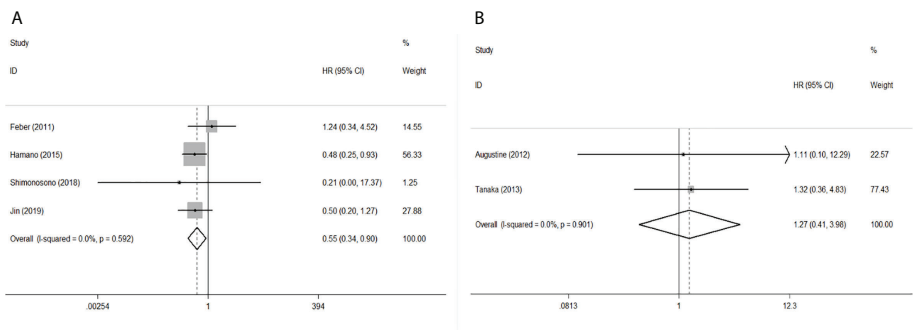

FIGURE 4
Forest plot of pooled HR of mir-145 in predicting survival outcomes in EC. **(A)** mir-145 and OS. **(B)** mir-145 and DFS.

Záveský et al (56), illustrated that mir-143 were capable to inhibit the proliferation of ovarian cancer cells by *in vitro* experiment. Liu et al (57), found that up-regulation of mir-145 could perform as a tumor suppressor inhibiting the growth of non-small-cell lung cancer by targeting RIOK2 and NOB1. Nowadays, molecular-targeted therapy is becoming a vital treatment for malignant tumors and has attracted comprehensive attention worldwide. Therefore, these mirs may also have the potential to be used as targeted molecules for EC treatment in clinic practice.

Although the prognostic value of mir-375 was proved by our study statistically, it should be prudently comprehended because of the following reasons. First, according to the results of subgroups analysis, the pooled HR value showed no significant correlation in EAC which indicated that in different EC types mir-375 may involve in different mechanism which are still unclear to us. Similarly, Mathe et al,[14] also found down-regulation of mir-375 significantly associated with poor EC prognosis only in EAC patients with Barrett' s esophagus. Considering of such discrepancy, more well-designed clinical researches with EAC samples should be conducted in the future to elucidate the relationship from different cancer types. Second, subgroups analysis also showed that sample types also affected a lot, when sample from plasma, the pooled HR showed no association in mir-375 expression and EC prognosis, contradicting to the sample from tissue which indicated the blood mir-375 may not be used as biomarker to detect the tumorigenesis and monitor tumor recurrence. Currently, mir-375 from tissues were more to be used to study. However, circulating biomarkers were more likely to be applied in clinic because they could be easily got and could be monitored through the whole progression of disease. Therefore, deeper clinical studies should be completed to verify whether there is a correlation between mir-375 expression both in tissue and blood. Third, in different races subgroups, up-regulation of mir-375 wasn't related to good prognosis in western patients, this may because of the sample sizes from western countries were small and the conclusion might be biased. Fourth, previous studies had investigated the mirs overexpressed in EC patients. Therefore, in this study, we mainly focused on those mirs down-regulated in EC. According to the pooled HRs results, the included four mirs all act as protective factors, and the result might be different from the reality to a certain extent.

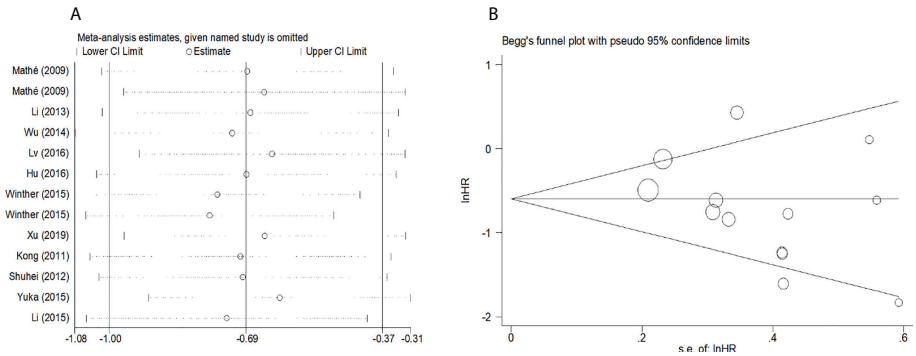

FIGURE 5
(A) Sensitivity analysis for meta-analysis of mir-375. **(B)**Funnel plots of publication bias for meta-analysis of mir-375.

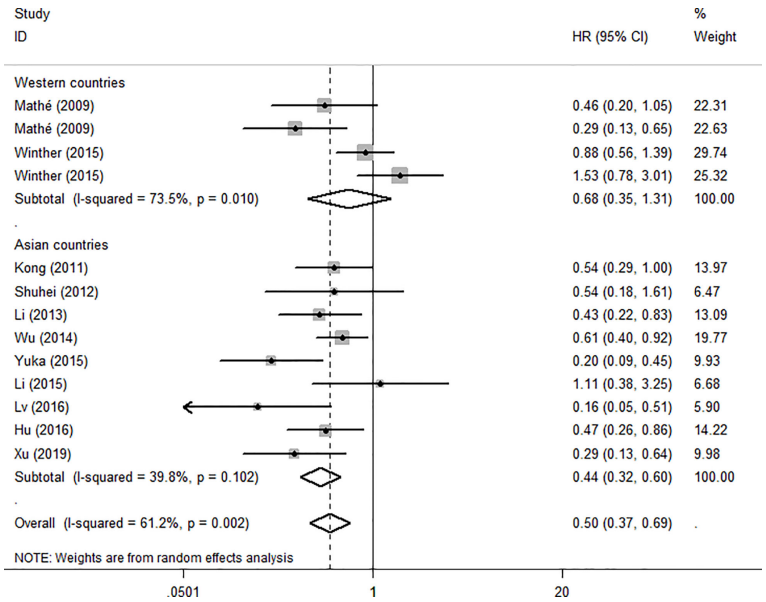

FIGURE 6
Forest plot showing subgroup analysis of the selected studies about the prognostic significance of mir-375 in patients with different races.

Though our meta-analysis proved that mir-375 has an association on the prognosis of patients with EC, there are still some limitations in this study. First, EC is a series of malignant tumor, ESCC and EAC consisted of the most common histological subtypes, but some of studies included in our research did not strictly distinguish the subtypes of EC, leading to a bias in the classification of cancer types. Second, most researchers have used the median or average as the cut-off

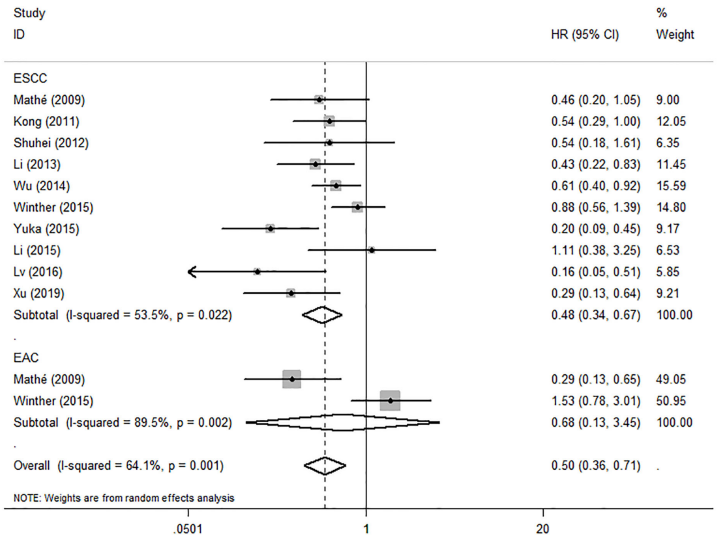

FIGURE 7
Forest plot showing subgroup analysis of the selected studies about the prognostic significance of mir-375 in patients with different cancer types.

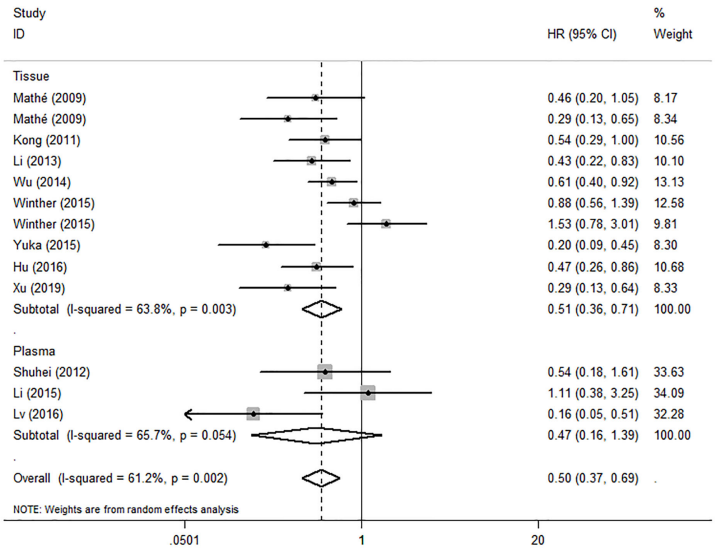

FIGURE 8
Forest plot showing subgroup analysis of the selected studies about the prognostic significance of mir-375 in patients with different sample types.

value in their studies, lacking uniform standards for the cut-off value of mir expression in different studies, the pooled survival outcomes may deviate from the true value. Third, some HR values in this study were calculated by using software Engauge Digitizer to extract data from the survival curve which may bring minor deviations to the outcome. Fourth, there is significant methodological heterogeneity in clinical and baseline demographic characteristics, especially tumor stage, treatment methods which are most likely to affect prognosis in patents. Detailed staging statistics are not provided on patients in the included studies, and many studies have not described the treatment of patients with EC in detail, so subgroup analysis cannot fully reflect the sources of heterogeneity between studies and may lead to bias in patients' homogeneity. Finally, our meta-analysis only collected perspective mirs evidence from databases but have no specific basic research to verify the exact mechanism mirs involving in EC, so the conclusion was less convincing. Hence, more necessary basic research based on EC patients' tissues and cells should be completed to obtain accurate results and conclusions.

Conclusion

The results of this meta-analysis show that high expression of mir-375, mir-143, mir-133 and mir-145 is significantly associated with a better prognosis in EC, indicating that these mirs could be used as prognostic factors for EC. Meanwhile, the recurrence of EC whether could be early detected by monitoring these mirs are still unknown. Furthermore, these novel mirs may also be utilized as potential therapeutic targets for EC treatment. For ESCC in Asian population, high expression of mir-375 is a significantly favorable factor, implying a potential therapeutic target for ESCC. Therefore, more high quality clinical researches are needed to investigate the prognostic and therapeutic value of mir-375.

Data availability statement

The original contributions presented in the study are included in the article/Supplementary Material. Further inquiries can be directed to the corresponding author.

Author contributions

YYu conceptualized the study, revise and proof the manuscript. PF, JZ and XL conceptualized the study and drafted the manuscript. SL, XX, QS, HZ, YYa and XZ collected

the literature. All authors contributed to the manuscript revision and read and approved the submitted version.

Funding

This study was supported by the National Natural Science Foundation of China (Grant No. 81970481)

Conflict of interest

The authors declare that the research was conducted in the absence of any commercial or financial relationships that could be construed as a potential conflict of interest.

Publisher's note

Supplementary material

The Supplementary Material for this article can be found online at: https://www.frontiersin.org/articles/10.3389/fonc.2022.828339/full#supplementary-material

References

1. Enzinger PC, Mayer RJ. Esophageal cancer. *New Engl J Med* (2003) 349 (23):2241–52. doi: 10.1056/NEJMra035010

2. Karamanou M, Markatos K, Papaioannou TG, Zografos G, Androutsos G. Hallmarks in history of esophageal carcinoma. *J BUON: Off J Balkan Union Oncol* (2017) 22(4):1088–91.

3. Sung H, Ferlay J, Siegel RL, Laversanne M, Soerjomataram I, Jemal A, et al. Global cancer statistics 2020: Globocan estimates of incidence and mortality worldwide for 36 cancers in 185 countries. *CA: Cancer J Clin* (2021) 71(3):209–49. doi: 10.3322/caac.21660

4. Malhotra GK, Yanala U, Ravipati A, Follet M, Vijayakumar M, Are C. Global trends in esophageal cancer. *J Surg Oncol* (2017) 115(5):564–79. doi: 10.1002/jso.24592

5. McCann J. Esophageal cancers: Changing character, increasing incidence. *J Natl Cancer Inst* (1999) 91(6):497–8. doi: 10.1093/jnci/91.6.497

6. Li X, Chen L, Luan S, Zhou J, Xiao X, Yang Y, et al. The development and progress of nanomedicine for esophageal cancer diagnosis and treatment. *Semin Cancer Biol* (2022) S1044-579X(22)00013-X. doi: 10.1016/j.semcancer.2022.01.007

7. Orringer MB. Multimodality therapy for esophageal carcinoma–update. *Chest* (1993) 103(4 Suppl):406s–9s. doi: 10.1378/chest.103.4_supplement.406s

8. Kent OA, Mendell JT. A small piece in the cancer puzzle: Micrornas as tumor suppressors and oncogenes. *Oncogene* (2006) 25(46):6188–96. doi: 10.1038/sj.onc.1209913

9. Calin GA, Sevignani C, Dumitru CD, Hyslop T, Noch E, Yendamuri S, et al. Human microrna genes are frequently located at fragile sites and genomic regions involved in cancers. *Proc Natl Acad Sci USA* (2004) 101(9):2999–3004. doi: 10.1073/pnas.0307323101

10. Notarte KI, Senanayake S, Macaranas I, Albano PM, Mundo L, Fennell E, et al. Microrna and other non-coding rnas in Epstein-Barr virus-associated cancers. *Cancers (Basel)* (2021) 13(15):3909. doi: 10.3390/cancers13153909

11. Bartel DP. Micrornas: Genomics, biogenesis, mechanism, and function. *Cell* (2004) 116(2):281–97. doi: 10.1016/s0092-8674(04)00045-5

12. Gao W, Zhang C, Li W, Li H, Sang J, Zhao Q, et al. Promoter methylation-regulated mir-145-5p inhibits laryngeal squamous cell carcinoma progression by targeting Fscn1. *Mol Therapy: J Am Soc Gene Ther* (2019) 27(2):365–79. doi: 10.1016/j.ymthe.2018.09.018

13. Winter J, Jung S, Keller S, Gregory RI, Diederichs S. Many roads to maturity: Microrna biogenesis pathways and their regulation. *Nat Cell Biol* (2009) 11(3):228–34. doi: 10.1038/ncb0309-228

14. Volinia S, Calin GA, Liu CG, Ambs S, Cimmino A, Petrocca F, et al. A microrna expression signature of human solid tumors defines cancer gene targets. *Proc Natl Acad Sci USA* (2006) 103(7):2257–61. doi: 10.1073/pnas.0510565103

15. Trang P, Medina PP, Wiggins JF, Ruffino L, Kelnar K, Omotola M, et al. Regression of murine lung tumors by the let-7 microrna. *Oncogene* (2010) 29 (11):1580–7. doi: 10.1038/onc.2009.445

16. Mathé EA, Nguyen GH, Bowman ED, Zhao Y, Budhu A, Schetter AJ, et al. Microrna expression in squamous cell carcinoma and adenocarcinoma of the esophagus: Associations with survival. *Clin Cancer Research: An Off J Am Assoc Cancer Res* (2009) 15(19):6192–200. doi: 10.1158/1078-0432.Ccr-09-1467

17. Meng XR, Lu P, Mei JZ, Liu GJ, Fan QX. Expression analysis of mirna and target mrnas in esophageal cancer. *Braz J Med Biol Res = Rev Bras pesquisas medicas e biolog* (2014) 47(9):811–7. doi: 10.1590/1414-431x20143906

18. He XX, Chang Y, Meng FY, Wang MY, Xie QH, Tang F, et al. Microrna-375 targets aeg-1 in hepatocellular carcinoma and suppresses liver cancer cell growth in vitro and in vivo. *Oncogene* (2012) 31(28):3357–69. doi: 10.1038/onc.2011.500

19. Fu C, Dong W, Wang Z, Li H, Qin Q, Li B. The expression of mir-21 and mir-375 predict prognosis of esophageal cancer. *Biochem Biophys Res Commun* (2014) 446(4):1197–203. doi: 10.1016/j.bbrc.2014.03.087

20. Wang P, Xu L, Li L, Ren S, Tang J, Zhang M, et al. The microrna-375 as a potentially promising biomarker to predict the prognosis of patients with head and neck or esophageal squamous cell carcinoma: A meta-analysis. *Eur Arch oto-rhino-laryngol: Off J Eur Fed Oto-Rhino-Laryngol Societies (EUFOS): affiliated German Soc Oto-Rhino-Laryngol - Head Neck Surgery* (2019) 276(4):957–68. doi: 10.1007/s00405-019-05325-8

21. Stang A. Critical evaluation of the Newcastle-Ottawa scale for the assessment of the quality of nonrandomized studies in meta-analyses. *Eur J Epidemiol* (2010) 25(9):603–5. doi: 10.1007/s10654-010-9491-z

22. Li J, Li X, Li Y, Yang H, Wang L, Qin Y, et al. Cell-specific detection of mir-375 downregulation for predicting the prognosis of esophageal squamous cell carcinoma by mirna in situ hybridization. *PLoS One* (2013) 8(1):e53582. doi: 10.1371/journal.pone.0053582

23. Wu C, Li M, Hu C, Duan H. Clinical significance of serum mir-223, mir-25 and mir-375 in patients with esophageal squamous cell carcinoma. *Mol Biol Rep* (2014) 41(3):1257–66. doi: 10.1007/s11033-013-2970-z

24. Lv H, He Z, Wang H, Du T, Pang Z. Differential expression of mir-21 and mir-75 in esophageal carcinoma patients and its clinical implication. *Am J Trans Res* (2016) 8(7):3288–98.

25. He Y, Jin J, Wang L, Hu Y, Liang D, Yang H, et al. Evaluation of mir-21 and mir-375 as prognostic biomarkers in oesophageal cancer in high-risk areas in China. *Clin Exp Metastasis* (2017) 34(1):73–84. doi: 10.1007/s10585-016-9828-4

26. Winther M, Alsner J, Tramm T, Baeksgaard L, Holtved E, Nordsmark M. Evaluation of mir-21 and mir-375 as prognostic biomarkers in esophageal cancer. *Acta Oncol (Stockholm Sweden)* (2015) 54(9):1582–91. doi: 10.3109/0284186x.2015.1064161

27. Xu H, Jiang J, Zhang J, Cheng L, Pan S, Li Y. Microrna-375 inhibits esophageal squamous cell carcinoma proliferation through direct targeting of Sp1. *Exp Ther Med* (2019) 17(3):1509–16. doi: 10.3892/etm.2018.7106

28. Kong KL, Kwong DL, Chan TH, Law SY, Chen L, Li Y, et al. Microrna-375 inhibits tumour growth and metastasis in oesophageal squamous cell carcinoma through repressing insulin-like growth factor 1 receptor. *Gut* (2012) 61(1):33–42. doi: 10.1136/gutjnl-2011-300178

29. Komatsu S, Ichikawa D, Takeshita H, Konishi H, Nagata H, Hirajima S, et al. Prognostic impact of circulating mir-21 and mir-375 in plasma of patients with esophageal squamous cell carcinoma. *Expert Opin Biol Ther* (2012) 12 Suppl 1:S53–9. doi: 10.1517/14712598.2012.681373

30. Isozaki Y, Hoshino I, Akutsu Y, Hanari N, Mori M, Nishimori T, et al. Usefulness of Microrna−375 as a prognostic and therapeutic tool in esophageal squamous cell carcinoma. *Int J Oncol* (2015) 46(3):1059–66. doi: 10.3892/ijo.2014.2789

31. Li BX, Yu Q, Shi ZL, Li P, Fu S. Circulating micrornas in esophageal squamous cell carcinoma: Association with locoregional staging and survival. *Int J Clin Exp Med* (2015) 8(5):7241–50.

32. Lin C, Zhang S, Wang Y, Wang Y, Nice E, Guo C, et al. Functional role of a novel long noncoding rna ttn-As1 in esophageal squamous cell carcinoma progression and metastasis. *Clin Cancer research: an Off J Am Assoc Cancer Res* (2018) 24(2):486–98. doi: 10.1158/1078-0432.Ccr-17-1851

33. Gao SH, Liu J, Zhang HJ, Zhao N, Zhang J. Low mir-133a expression is a predictor of outcome in patients with esophageal squamous cell cancer. *Eur Rev Med Pharmacol Sci* (2016) 20(18):3788–92.

34. Akanuma N, Hoshino I, Akutsu Y, Murakami K, Isozaki Y, Maruyama T, et al. Microrna-133a regulates the mrnas of two invadopodia-related proteins, Fscn1 and Mmp14, in esophageal cancer. *Br J cancer* (2014) 110(1):189–98. doi: 10.1038/bjc.2013.676

35. Liu H, Zheng M, Zhao Y, Zhang S. Mir-143 inhibits migration and invasion through regulating Lasp1 in human esophageal cancer. *Int J Clin Exp pathology* (2019) 12(2):466–76.

36. He Z, Yi J, Liu X, Chen J, Han S, Jin L, et al. Mir-143-3p functions as a tumor suppressor by regulating cell proliferation, invasion and epithelial-mesenchymal transition by targeting qki-5 in esophageal squamous cell carcinoma. *Mol cancer* (2016) 15(1):51. doi: 10.1186/s12943-016-0533-3

37. Zhang B, Li R, Chang CX, Han Y, Shi SB, Tian J. Pemetrexed plus dendritic cells as third-line therapy for metastatic esophageal squamous cell carcinoma. *OncoTar Ther* (2016) 9:3901–6. doi: 10.2147/ott.S107319

38. Tanaka K, Miyata H, Yamasaki M, Sugimura K, Takahashi T, Kurokawa Y, et al. Circulating mir-200c levels significantly predict response to chemotherapy and prognosis of patients undergoing neoadjuvant chemotherapy for esophageal cancer. *Ann Surg Oncol* (2013) 20 Suppl 3:S607–15. doi: 10.1245/s10434-013-3093-4

39. Ko MA, Zehong G, Virtanen C, Guindi M, Waddell TK, Keshavjee S, et al. Microrna expression profiling of esophageal cancer before and after induction chemoradiotherapy. *Ann Thorac surg* (2012) 94(4):1094–102. doi: 10.1016/j.athoracsur.2012.04.145

40. Feber A, Xi L, Pennathur A, Gooding WE, Bandla S, Wu M, et al. Microrna prognostic signature for nodal metastases and survival in esophageal adenocarcinoma. *Ann Thorac Surg* (2011) 91(5):1523–30. doi: 10.1016/j.athoracsur.2011.01.056

41. Jin W, Luo W, Fang W, Wang Y, Wang L, Shen Q, et al. Mir-145 expression level in tissue predicts prognosis of patients with esophageal squamous cell carcinoma. *Pathol Res Practice* (2019) 215(6):152401. doi: 10.1016/j.prp.2019.03.029

42. Shimonosono M, Idichi T, Seki N, Yamada Y, Arai T, Arigami T, et al. Molecular pathogenesis of esophageal squamous cell carcinoma: Identification of the antitumor effects of Mir−145−3p on gene regulation. *Int J Oncol* (2019) 54 (2):673–88. doi: 10.3892/ijo.2018.4657

43. Hamano R, Miyata H, Yamasaki M, Kurokawa Y, Hara J, Moon JH, et al. Overexpression of mir-200c induces chemoresistance in esophageal cancers mediated through activation of the akt signaling pathway. *Clin Cancer Research: An Off J Am Assoc Cancer Res* (2011) 17(9):3029–38. doi: 10.1158/1078-0432.Ccr-10-2532

44. Zhao Q, Liu Y, Wang T, Yang Y, Ni H, Liu H, et al. Mir-375 inhibits the stemness of breast cancer cells by blocking the Jak2/Stat3 signaling. *Eur J Pharmacol* (2020) 884:173359. doi: 10.1016/j.ejphar.2020.173359

45. Xie D, Yuan P, Wang D, Jin H, Chen H. Expression and prognostic significance of mir-375 and mir-221 in liver cancer. *Oncol Letters* (2017) 14 (2):2305–9. doi: 10.3892/ol.2017.6423

46. Zhang G, Wang J, Zheng R, Song B, Huang L, Liu Y, et al. Mir-133 targets Yes1 and inhibits the growth of triple-negative breast cancer cells. *Technol Cancer Res Treat* (2020) 19:1533033820927011. doi: 10.1177/1533033820927011

47. Chen Q, Zhou L, Ye X, Tao M, Wu J. Mir-145-5p suppresses proliferation, metastasis and emt of colorectal cancer by targeting Cdca3. *Pathol Res practice* (2020) 216(4):152872. doi: 10.1016/j.prp.2020.152872

48. Boubaker NS, Spagnuolo M, Trabelsi N, Said R, Gurtner A, Regazzo G, et al. Mir-143 expression profiles in urinary bladder cancer: Correlation with clinical and epidemiological parameters. *Mol Biol Rep* (2020) 47(2):1283–92. doi: 10.1007/s11033-019-05228-1

49. Yi J, Jin L, Chen J, Feng B, He Z, Chen L, et al. Mir-375 suppresses invasion and metastasis by direct targeting of Shox2 in esophageal squamous cell carcinoma. *Acta Biochim Biophys Sinica* (2017) 49(2):159–69. doi: 10.1093/abbs/gmw131

50. Osako Y, Seki N, Kita Y, Yonemori K, Koshizuka K, Kurozumi A, et al. Regulation of Mmp13 by antitumor microrna-375 markedly inhibits cancer cell migration and invasion in esophageal squamous cell carcinoma. *Int J Oncol* (2016) 49(6):2255–64. doi: 10.3892/ijo.2016.3745

51. Gao S, Zhao ZY, Zhang ZY, Zhang Y, Wu R. Prognostic value of micrornas in esophageal carcinoma: A meta-analysis. *Clin Trans Gastroenterol* (2018) 9 (11):203. doi: 10.1038/s41424-018-0070-z

52. Campayo M, Navarro A, Benítez JC, Santasusagna S, Ferrer C, Monzó M, et al. Mir-21, mir-99b and mir-375 combination as predictive response signature for preoperative chemoradiotherapy in rectal cancer. *PLoS One* (2018) 13(11): e0206542. doi: 10.1371/journal.pone.0206542

53. Xu F, Ye ML, Zhang YP, Li WJ, Li MT, Wang HZ, et al. Microrna-375-3p enhances chemosensitivity to 5-fluorouracil by targeting thymidylate synthase in colorectal cancer. *Cancer Science* (2020) 111(5):1528–41. doi: 10.1111/cas.14356

54. Fu H, Fu L, Xie C, Zuo WS, Liu YS, Zheng MZ, et al. Mir-375 inhibits cancer stem cell phenotype and tamoxifen resistance by degrading Hoxb3 in human er-positive breast cancer. *Oncol Rep* (2017) 37(2):1093–9. doi: 10.3892/or.2017.5360

55. Weidle UH, Birzele F, Auslaender S, Brinkmann U. Down-regulated micrornas in gastric carcinoma may be targets for therapeutic intervention and replacement therapy. *Anticancer Res* (2021) 41(9):4185–202. doi: 10.21873/anticanres.15223

56. Záveský L, Jandáková E, Weinberger V, Hanzíková V, Slanař O, Kohoutová M. Ascites in ovarian cancer: Microrna deregulations and their potential roles in ovarian carcinogenesis. *Cancer Biomarkers: Section A Dis Markers* (2022) 33(1):1-16. doi: 10.3233/cbm-210219

57. Liu K, Chen H, You Q, Ye Q, Wang F, Wang S, et al. Mir−145 inhibits human Non−Small-cell lung cancer growth by dual-targeting Riok2 and Nob1. *Int J Oncol* (2018) 53(1):257–65. doi: 10.3892/ijo.2018.4393

Advantages of publishing in Frontiers

OPEN ACCESS
Articles are free to read for greatest visibility and readership

FAST PUBLICATION
Around 90 days from submission to decision

HIGH QUALITY PEER-REVIEW
Rigorous, collaborative, and constructive peer-review

TRANSPARENT PEER-REVIEW
Editors and reviewers acknowledged by name on published articles

Frontiers
Avenue du Tribunal-Fédéral 34
1005 Lausanne | Switzerland

Visit us: www.frontiersin.org
Contact us: frontiersin.org/about/contact

REPRODUCIBILITY OF RESEARCH
Support open data and methods to enhance research reproducibility

DIGITAL PUBLISHING
Articles designed for optimal readership across devices

FOLLOW US
@frontiersin

IMPACT METRICS
Advanced article metrics track visibility across digital media

EXTENSIVE PROMOTION
Marketing and promotion of impactful research

LOOP RESEARCH NETWORK
Our network increases your article's readership